Scientific Activities

Institute for Cosmic Ray Research, The University of Tokyo

Report to the Review Committee

20 December 2018

CONTENTS

OVERVIEW 1

NEUTRINO AND ASTROPARTICLE DIVISION 8

Super-Kamiokande
T2K Experiment
XMASS Experiment
Hyper-Kamiokande (R&D)

HIGH ENERGY COSMIC RAY DIVISION 61

TA: Telescope Array
Tibet AS γ Project
CTA
High Energy Astrophysics Group
Ashra (R&D)
ALPACA (R&D)

ASTROPHYSICS AND GRAVITY DIVISION 109

KAGRA Group
Observational Cosmology Group
Theory Group

FACILITIES 151

Kamioka Observatory
Akeno Observatory
Norikura Observatory
KAGRA Observatory
Research Center for Cosmic Neutrinos
Low-Level Radioisotope Measurement Facility

APPENDIX 170

A.1: Organization
A.2: ICRR Staffs (2018)
A.3: Budget (FY2012–2017)
B.1: Agreements of International Academic Cooperation
B.2: International Meetings
B.3: Inter-University Collaborative Researches
B.4: Educational Activities
B.5: Public Relations
C: Report from the Future Planning Committee (2013 and 2017)

OVERVIEW

The Institute for Cosmic Ray Research (ICRR) has its origin at a lodge for research, called Asahi Hut, built on Mt. Norikura based on Asahi Academic Grant. In 1953, it was established as the Cosmic Ray Observatory of the University of Tokyo. This Observatory was Japan's first research facility for nationwide joint use. In 1976, the Cosmic Ray Observatory was reorganized into the Institute for Cosmic Ray Research (ICRR) of the University of Tokyo. Since the era of Cosmic Ray Observatory, ICRR has been functioning as "Inter University Research Institution", where researchers in Japan in the field of cosmic rays carry out diverse researches using various facilities in ICRR.

In 2004, the Japanese National Universities, including the University of Tokyo, became independent administrative agencies (National University Corporations). The concept was to strengthen the Universities by mutual competition. At that time, the concept of "independent administrative agencies" and "Inter University Research Institution" did not go along well.

This problem was recognized by the Ministry of Education, Culture, Sports, Science and Technology (MEXT) in Japan. A new system, called "Joint Usage / Research Center", was established. ICRR was selected as one of these Centers in 2010. Since then, ICRR's research style as "Inter University Research Institution" has been officially re-recognized by the Japanese government.

In 2018 MEXT established "International Joint Usage / Research Center" which can play a central role in international research activity and promoto world-class research. ICRR was selected as one of the six International Joint Usage / Research Centers.

The external review panel of ICRR has been organized approximately every six years since 1994, the last one having been held on 16-18 January, 2013. This report provides the material prepared for the External Review Panel to be held on 15-17 May, 2019 to examine the research activity of the ICRR. The prime purposes of the present Review are:

(1) to give oversight to the institute's scientific activities between 2012 and 2018, whether they meet the international scientific standard and have given sufficient impacts on the community,

(2) to assess the scientific merits of individual research activities and make recommendations about future support,

(3) to assess technical competence of the proponents and feasibility of the R&D experiments or projects,

(4) to assess the Institute's policy and its role in the scientific community.

At present, ICRR consists of 24 faculties, 1 project professor[1], 1 project associate professor[2], 18 assistant professors, 13 project assistant professors[3], 13 postdoctoral fellows and 13 supporting technical staffs, and consists of three divisions — Neutrino and Astroparticle Division, High-Energy Cosmic Ray Division, and Astrophysics & Gravity Division. They are further subdivided into thirteen research groups. Most of the activities receive participations by other university members that partially offset small numbers of staffs of the ICRR. Most of the faculties are counted as members of the Faculty of Science of the Graduate School and are engaged in the teaching of graduate students of this university, jointly with those who belong to Department of Physics and Department of Astronomy in the Hongo campus.

ICRR runs 10 facilities (4 observatories and a center; 4 overseas) to perform its research projects. The overseas facilities are operated jointly in collaboration with academic institutions of respective countries under memoranda of understanding. The Institute also supports, directly or indirectly, some of cosmic-ray related research activities of research scientists in this country. More information as to the structure of ICRR is given in Appendix A.1.

Divisions

Neutrino and Astroparticle Division

This division is focused on particle and astroparticle physics with primary interests in the physics of neutrinos, proton decay, and dark matter using underground experimental detectors at Kamioka Observatory. The primary detector is the Super-Kamiokande (SK), which is a 50,000 ton water Cherenkov detector studying neutrino physics and proton decay. The Tokai-to-Kamioka (T2K) long-baseline neutrino experiment is also a focus project of this division. A liquid xenon detector (XMASS) has been constructed and aims for a direct

*1 fixed-term professor
*2 fixed-term associate professor
*3 fixed-term assistant professors

detection of dark matter interactions. Further, research and development activities towards a future megaton-sized water Cherenkov detector, Hyper-Kamiokande, are ongoing.

High Energy Cosmic Ray Division

This division is devoted to the study of very high energy cosmic rays and cosmic gamma rays, consisting of three major research activities, TA, Tibet ASγ, and CTA, with one theoretical group and two R&D activities.

Telescope Array (TA) experiment explores extreme phenomena in the universe by measuring energy spectrum, particle composition, and arrival direction distribution of cosmic rays with energies of $10^{18} - 10^{20}$ eV or higher. In May 2008 this experiment started full operation of the largest detector in the northern hemisphere (Utah, USA). The TA Low-Energy extension (TALE) studies the transition from galactic to extra-galactic cosmic rays in the energy range between $10^{15.5}$ eV and $10^{18.5}$ eV. The TA$\times$4 project would quadruple the TA aperture of the highest-energy cosmic rays to accelerate the pace of the data collection.

The Tibet ASγ Collaboration operates a surface air shower array of scintillation detectors, underground water Cherenkov muon detectors and air shower core detectors at high altitude (4300m) in Yangbajing, Tibet, China realizing high statistics studies of cosmic rays with energies $10^{12} - 10^{17}$ eV sensitive for both charged cosmic rays and gamma rays in the northern sky.

CTA is an international effort to construct the next generation large scale imaging atmospheric Cherenkov Telescope array to explore the high energy Universe with an order of magnitude better sensitivity, higher angular resolution and wider energy coverage. CTA-Japan is leading the construction of four large size telescopes (LSTs) in La Palma, Spain.

A theoretical group, High Energy Astrophysics group, aims at revealing violent astrophysical phenomena, in which non-thermal particles are accelerated. The group promotes the theoretical study on the multi-messenger astronomy.

In addition there are two research activities, Ashra and ALPACA. On Mauna Loa (Hawaii, USA), Ashra operates an unconventional optical collector complex with a very wide field of view which is to image air showers caused by neutrinos of energies of $10^{15} - 10^{18}$eV or higher from violent astrophysical sources like gamma ray bursts. ALPACA is a joint research project between Bolivia and Japan to construct a surface air shower array and underground water Cherenkov muon detectors at high altitude in Bolivia.

Astrophysics and Gravity Division

This division consists of the KAGRA Group, the Observational Cosmology Group, and the Theory Group.

The KAGRA Group aims at direct detection of gravitational waves. The KAGRA detector is being built at Kamioka toward joining the next international observation O3 with LIGO and Virgo in 2019.

The Observational Cosmology Group is conducting an optical sky survey with prime interests in cosmology and extragalactic astrophysics. The group participates in the Subaru Hyper Suprime-Cam (HSC) survey under the international collaboration, which is a major contributor of the HSC narrow band (NB) project.

The Theory group is making theoretical studies on phenomenology-oriented particle physics, astro/cosmoparticle physics and cosmology.

Facilities

ICRR has four domestic observatories, one center, one domestic facility and four overseas observatories. These facilities are all open to researchers, and the use will be admitted after a proper review process.

Domestic

- Kamioka Observatory.

  This observatory is located 1000 m underground (2700 m.w.e.) in the Kamiokande Mine, Gifu prefecture. The SK water Cherenkov detector is located in this observatory. The observatory is also used by the XMASS experiment. The observatory offers a well-developed and maintained, low vibration and low radioactivity environment. Therefore, it is used by a number of research groups both inside and outside ICRR, including the CANDLES double beta decay experiment led by Osaka University, the NewAGE dark matter experiment led by Kobe University, a cryogenic test experiment for gravitational wave detection (CLIO: Cryogenic Laser Interferometer Gravitational-Wave Observatory) run by ICRR, as well as seismic and geophysical experiments performed by the Earthquake Research Institute of the University of Tokyo and others.

- Akeno Observatory.

  The Akeno Observatory is located in Akeno of Hokuto in Yamanashi Prefecture. It was used for a giant-air-shower-array experiment, AGASA. Now it is used for small-scale observations, research and development including the multi-color imager (MITSuME) led by Tokyo Institute of Technology, large area muon telescope by

Chubu University et al. and a small atmospheric Cherenkov telescope by ICRR et al. It is also used occasionally for detector assembly including the surface detectors of the Telescope Array extension.

- Norikura Observatory (at 2770m altitude).

  This observatory, located close to the summit of Mt. Norikura, was historically a very important station of ICRR. This is now used for long-term monitors of cosmic ray muons and solar neutrons, mainly by teams from Nagoya University and from Shinshu University. It is occasionally used for various types of research (not necessarily cosmic ray proper) that require the high altitude environment, as it now offers a unique high altitude facility in Japan.

- KAGRA observatory.

  KAGRA observatory was established in 2016 for the operation of the large-scale cryogenic gravitational wave telescope, KAGRA, and the research of gravitational wave physics and astronomy.

- Low-Level Radioisotope Measurement Facility. This is located underground in the Kashiwa building, and is used for measurements of the concentration of natural radioisotope by interested researchers in the country.

- Research Center for Cosmic Neutrinos. This was established in 1999 primarily to promote research of neutrino physics. This center has been organizing neutrino meetings and neutrino public lectures. It also acts as a body for accepting ICRR's inter university programmes related to Low-Level Radioisotope Measurement Facility, and is in charge of the computer system of the institute.

Overseas

ICRR operates four overseas observatories, which play central roles to carry out its research projects, jointly with various academic institutions in respective countries:

- The Tibet ASγ Observatory, Yangbajing, Tibet, China

- Observatory for Highest Energy Cosmic Rays, Utah, U. S. A.

- Chacaltaya Observatory of Cosmic Physics, Mt. Chacaltaya, Bolivia

- International Observatory for High Energy Gamma Rays, La Palma, Spain.

Historical Remarks and Funding Sources

Brief histories are described for each group, including the financial view point. In general there are two channels for funding: the use of Grant-in-Aids from the Japan Society for the Promotion of Science (JSPS) by individual scientists, and the fund from the government revenue directly to the Institute through the University finance. The former applies to short term projects, say for 5 years with no guarantees beyond, and the latter to long-term projects that usually costs more than that defrayed by the former. The square parentheses indicate present institute's personnel of each group. The current status and scientific goals of the projects are summarized in the table.

- Super-Kamiokande

  The detector was constructed from 1991 to 1996, and data acquisition began in April 1996. Construction and operation costs are covered by funds provided by the government. Super-Kamiokande discovered atmospheric neutrino oscillations in 1998 and solar neutrino oscillations in 2001. The K2K (KEK to Kamioka) long-baseline accelerator experiment, operated from 1999 to 2004, confirmed the existence of atmospheric neutrino oscillations. Since full reconstruction work performed in 2005 and 2006, the detector has been running stably and high precision oscillation studies have been performed. The readout electronics and online data acquisition system were updated in 2008 to ensure stable operations over the longterm. The detector has been refurbished in 2018 to be ready for a future upgrade by doping gadolinium. [9 faculties + 7 assistant professors + 6 project assistant professors + 2 post-doctoral fellow]

- T2K

  The Tokai-to-Kamioka (T2K) long-baseline accelerator neutrino experiment started in 2009. The SK detector functions as the far detector of the T2K experiment and ICRR is responsible for operating the far detector. Host institutes of the T2K experiment are KEK and ICRR. Based on data taken up until March 2011, the T2K collaboration announced an indication of electron neutrino appearance, and therefore non-zero θ_{13}, with a statistical significance of 2.5σ in June 2011. After the

recovery of the J-PARC accelerator site from damage sustained in the earthquake, the T2K experiment resumed operations in March 2012. With data taken up until June 2012, the significance of the non-zero θ_{13} measurement has improved to 3.2σ. By the end of 2017, T2K has collected both neutrino and anti-neutrino data. The observed number of electron neutrino candidates is now 90 and the confidence level exceeds 7σ. Also, they found larger number of the electron neutrino candidates but fewer number of the electron anti-neutrino candidates. As a result, they found the indication of CP violation at 2σ level. [8 faculties + 7 assistant professors + 5 project assistant professors]

- XMASS

  The XMASS project started in 2000 and after its R&D study the XMASS-I detector construction started in 2007. It completed in 2010 and the subsequent commissioning run until 2012 enabled us to conduct various dark matter and new physics searches. The detector refurbishment in 2012 succeeded to reduce the impact of surface background by an order of magnitude and data taking with the lower background continues through the end of the fiscal year 2018. A planned future detector, XMASS1.5, became uncompetitive as other large-scale liquid-xenon detector become operational first. Participation in a second generation experiment started by looking for an international cooperation to construct a more sensitive detector. The project is mainly supported by Grant-in-Aids of the Ministry of Education, Culture, Sports, Science and Technology. [4 faculties + 1 project associate professor + 2 assistant professors + 3 project assistant professors + 1 post-doctoral fellow]

- Hyper-Kamiokande R&D

  The Hyper-Kamiokande or Hyper-K will provide major new capabilities to make new discoveries in particle and astroparticle physics. The Hyper-K is a priority project listed in the Roadmap 2017 of the Japanese Ministry of Education, Culture, Sports, Science and Technology (MEXT), and seed funding has been allocated within MEXT budget request for JFY2019. The principal project milestones include: Construction to start in 2020, and Start data taking in 2027. The R&D project is supported by Grant-in-Aids of the MEXT. [9 faculties + 7 assistant professors + 6 project assistant professors + 2 post-doctoral fellow]

- TA

  The TA project received a fund by Grant-in-Aid for Scientific Research in Priority Areas (2003 - 2008) for its construction and commissioning. A continued fund for 5 years of operation (2009-2013) was granted as Grant-in-Aid for the Specially Promoted Research. The TA consists of a ground array of scintillation counters and fluorescence telescopes. The hybrid observation of cosmic ray air showers with TA started in May 2008, and has been maintained by the contributions of Japan, USA, Korea, Russia and Belgium. The TA collaboration confirmed GZK suppression with 3.9σ significance. Mass composition of cosmic rays above $10^{18.2}$ eV is consistent with proton. TA found an evidence for a cluster of cosmic rays that we call the hotspot with 3.4σ. The Grant-in-Aid for the Specially Promoted Research (2015-2019) was obtained for the TA$\times$4 project to quadruple the aperture of the TA surface detector for its construction and commissioning. The TA Low-Energy extension studies the transition from galactic to extra-galactic cosmic rays. Its telescopes were completed in 2013 and have been operational. The deployment of the TALE surface detectors was completed in 2017 and have been in operation. [1.5 faculties + 2.5 assistant professors + 1 project assistant professor + 1 technical specialist + 2 skilled assistants]

- Tibet ASγ

  The Tibet air shower array was constructed with gradual upgrades from 1988 to 2014, by the funds from Grants-in-Aid and from the government. As an upgrade, new air shower core detectors were added for the next-step measurement of the chemical composition in the knee energy region, while large ($\sim$4,000 m^2) muon detectors aiming at higher-sensitivity (by a facto of $\sim$10 improvement) gamma-ray observation in the 100 TeV region were constructed under the Tibet air shower array. The muon detectors also play an important role to measure the chemical composition of cosmic rays in the knee energy region. The hybrid experiment (air shower array + muon detectors + air shower core detectors) started data-taking in 2014. The Tibet ASγ Collaboration found that yearly variation in depth of the Sun shadow in cosmic rays was sensitive to the coronal magnetic field in the Sun in 2013, and that the average in-

terplanetary magnetic field employed in a popular solar magnetic field model was underestimated by approximately 50 % in 2018. [1.5 faculties + 1.5 assistant professors + 1 post-doctral fellow]

- CTA

  CTA R&D program had been financed by a Grant-in-Aid for Specially Promoted Research (2012-2016). Four CTA Large Size Telescopes (LSTs) with a 23m dish on La Palma have been under construction with the budget for the facility development from the Japanese Government MEXT (2016-2018), in the cooperation with Germany, Spain, France and Italy. LST1 was already inaugurated in 2018 October, three more LST2-4 will be completed in the next three years. The array of four LSTs is planned to start the scientific operation in 2022. The significant part of the operation and maintenance of LST1-4 and CTA North site is financed by a Grant-in-Aid for scientific research (S) (2017-2021) and specific research budget from MEXT since 2018. CTA-Japan is planning the LST extension to CTA-South after the completion of CTA-North to make CTA as an all sky observatory. [4 faculties + 3 assistant professor + 1 post-doctral fellow]

- High Energy Astrophysics

  This group was established in December 2009 with one faculty member. From April 2013 a assistant professor joined, but the original faculty member retired March 2016. Until June 2017, only the assistant professor had acted as a permanent member. From July 2017, the group was reconstructed with one faculty member. One assistant professor joined March 2018, which stimulates the activity of the group again. The group is currently pursuing the theoretical study on high-energy astronomical phenomena based on the multi-messenger astronomy, collaborating with the other groups in ICRR. [1 faculty + 1 assistant professor]

- Ashra R&D

  The Ashra R&D and phase-1 construction were funded by the Coordination Fund for Promoting Science and Technology and Grant-in-Aid for Scientific Research since 2003. In 2004, University of Hawaii (UH) joined as a local host institute. After the state of Hawaii permitted the site use, the construction of light collectors in shelters on Mauna Loa was carried out in 2007. Since 2008, optical transient observation has started. Commissioning of astronomical tau neutrino search was performed. In 2011, the 10-year extension of the site use permit was granted. Since 2012, efficient physics observations for tau neutrinos, nucleons and optical transients have been tried to continue with budget support. [1 faculty + 1 technical staff]

- ALPACA R&D

  The ALPACA, a joint project between Bolivia and Japan, will be composed of an 83,000 m^2 surface air shower array and a 5,400 m^2 underground muon detector array to make wide field-of-view (2 sr) high-sensitivity observation of high-energy cosmic rays/cosmic gamma rays (world-best sensitivity for gamma rays around/over 100 TeV) on the Cerro Estuqueria highland, 4,740 m above sea level around Mount Chacaltaya, Bolivia. ALPACA-Japan will make a major contribution to construction of the surface array and the muon detector array. The R&D program is mostly financed by TORAY science foundation. Approximately 20 % of the surface array of ALPACA will be constructed with the grant in cooperation with Bolivia. [1.5 faculties + 1.5 assistant professors + 1 post-doctral fellow]

- KAGRA

  TAMA 300 detector had been built to detect gravitational wave (GW) from nearby our Galaxy and operated at the highest sensitivity with the first stable operation in 2000. In order to realize practical detection of GW events by more sensitive detector, the Large-scale Cryogenic Gravitational wave Telescope (LCGT, nick-named as KAGRA in 2012) was planned for GW events within 200 Mpc and its funding was requested. The first demonstration of cryogenic thermal noise sensitivity by CLIO as of KAGRA prototype in 2010 lead the partial funding under a new category of government revenue funding, “Leading-edge Research Infrastructure Program”, from 2010 to 2012 and the site excavation underground at Kamioka has been started in May, 2012 by another funding of MEXT. Additionally the fund for KAGRA upgrade to replace the core optics (silica mirrors) with sapphire mirrors was approved by MEXT. This project is supported by both KEK and NAOJ. [4 faculties + 3 assistant professor + 3 project professors + 2 project assistant professors + 7 post-doctoral fellows + 6 technical staff(2 tenured + 4 project-oriented)]

- Observational Cosmology

  Japanese Sloan Degital Sky Survey (SDSS) key members moved to ICRR in 1996 with a Grant-in-Aid for Specially Promoted Area, forming the observational cosmology group. SDSS-I and II programs were completed by 2008 with additional supports from JSPS and RESCUE at the Department of Physics. After the completion of the SDSS programs, the group has started new programs mainly with Subaru HSC NBs since July 2010 on the arrival of a new faculty member who wins a Grant-in-Aid for Scientific Research (A) for 2011-2014. Accordingly, the appointment of the new assistant professor was made in April 2012. Adding the Grant-in-Aid for Scientific Research (A) for 2015-2019, the group is leading the HSC-NB project and the related HSC galaxy projects whose observations were started in 2014. The HSC project observations will be completed around 2019, and subsequently the complementary optical spectroscopic observations with PFS will start around 2020. [1 faculty + 1 assistant professor + 1 project researcher + 1 JSPS researcher]

- Theory

  Theory group has a long history, but there was a reset of the group in April 2001 owing to the retirement of the first group leader. A new group was established in 2002 with two faulty members, and one of the member served as the Director of the Institute for three years (2001-2004). Although one faculty member moved in June 2010, the group had a new faculty and recovered its full activity in February 2011. The group is currently studying theories beyond the standard model of particle physics and applying them to the early universe to understand the origin of matter and its fluctuations. [2 faculties + 3 post-doctoral fellows]

Summary of 2012-2018 Activities

Important events related to the ICRR's activity in 2012-2018 since the previous external review in 2012 are summarized below.

- The 4th committee for the planning of the future ICRR research projects was formed in 2012. The report from this committee was released in 2013 (see appendix).
- After the recovery of the J-PARC accelerator site from damage sustained in the earthquake, the T2K experiment resumed operations in 2012.
- The refurbishment of the XMASS detector succeeded to reduce the impact of surface background by an order of magnitude in 2012.
- The SK experiment published the appearance of ν_τ events in the atmospheric neutrino data in 2013.
- The TA experiment published an evidence for a cluster of ultra high energy cosmic rays (the hotspot) in 2014.
- International Observatory for High Energy Gamma Rays, La Palma, Spain was established in 2015.
- The KAGRA observatory was established in 2016.
- The initial KAGRA interferometer was completed, and after commissioning work, the interferometer was operated for the first time in 2016.
- The T2K experiment presented the indication of CP violation at 2σ level in 2017.
- The 5th committee for the planning of the future ICRR research projects was formed in 2016. The report from this committee was released in 2017 (see appendix).
- The University of Tokyo launched Next-Generation Neutrino Science Organization (NNSO), where ICRR, Kavli IPMU, and the School of Science cooperate to promote the project and host the Hyper-Kamiokande construction in 2017.
- The refurbishment of the SK detector for a future upgrade by doping gadolinium started in 2018.
- The Institute for Cosmic Ray Research was certificated as an "International Joint Usage / Research Center" in 2018.

Details of above activities related to the research are described in the following sections.

Project status and main scientific goals

Neutrino and Astroparticle Division

Project	Status	Main Scientific Goals
Super-Kamiokande	running	Study of neutrino oscillations, proton decay, and astrophysical phenomena such as supernova burst
T2K	running	Precise measurement of neutrino oscillation parameters using SK with accelerator neutrino beam
XMASS	data analysis	Direct search for dark matter with a liquid xenon detector
Hyper-Kamiokande	planned / R&D	Study of neutrino CP violation, proton decays and supernova neutrinos with a megaton water Cherenkov detector

High Energy Cosmic Ray Division

Project	Status	Main Scientific Goals
Telescope Array	running	Study of extremely-high energy cosmic rays; their origin, propagation and interaction
Tibet ASγ	running	Study of origin, acceleration mechanism and modulation of high-energy cosmic rays
CTA	under construction	VHE Gamma Ray Astronomy, study of cosmic-ray origin, particle acceleration and indirect search for dark matter
Ashra	R&D	Search for astronomical high-energy neutrino sources
ALPACA	planned / R&D	Study of cosmic-ray origin, Ultra-high energy gamma-astronomy

Astrophysics and Gravity Division

Project name	Status	Main Scientific Goals
KAGRA	under construction	Through detection of gravitational wave, study physics of gravitational waves and open gravitational wave astronomy
Subaru-HSC-NB	running	Uncovering physical processes and history of cosmic reionization and early galaxy formation

NEUTRINO AND ASTROPARTICLE DIVISION

SUPER-KAMIOKANDE

Introduction

Super-Kamiokande(SK, Super-K) is a 50 kton water Cherenkov detector studying the physics of neutrinos, proton decay, and astrophysical phenomena such as supernova. Data taking started in April 1996 and atmospheric neutrino oscillations were discovered in 1998. Solar neutrino oscillations were discovered by a comparison of SK solar neutrino data with SNO charged current data in 2001. The first data phase of Super-K, SK-I, ran until July 2001. Due to an accident in 2001 about 60% of the PMTs in the detector were destroyed and the detector was reconstructed in 2002 using the remaining PMTs. Since the accident, the PMTs have been encased in acrylic and FRP (fiber-reinforced plastic) shells which prevent shock-wave production even if a single PMT implodes. With this setup the second data phase, SK-II, ran from December 2002 to October 2005. The missing PMTs were reproduced and full reconstruction of the detector was performed from October 2005 to July 2006. The third data phase, SK-III, lasted from July 2006 to August 2008. To ensure stable operation over the long term and to improve the sensitivity of the detector, the electronics system was fully upgraded in September 2008. Since this upgrade the fourth data phase, SK-IV, ran until May 2018. The detector has been refurbished from June 2018 in order to repair the leak of the Super-K water tank and to improve water piping in the tank to double the water flow rate.

As described below, high precision neutrino oscillation data were taken using both atmospheric and solar neutrinos during these periods and significant progress in the study of proton decay, supernova physics, and other physics targets has been achieved. In addition, the preparation for a SK-Gd phase, in which gadolinium is dissoved in tank water in order to tag neutrons, has been conducted successfully.

Summary from 2012 to 2018

First of all, here summarized the noticeable achievements during the period of this review, i.e. after 2012.

- Measurements with atmospheric neutrinos have been focused on precision studies of three-flavor effects in neutrino oscillations. With a 328 kiloton-year exposure the SK data favor the NH with a significance of between 91.5% and 94.5% when constrained by T2K data and show a weak indication for $\delta_{CP} \sim 3\pi/2$. The appearance of ν_τ events in the atmospheric data has been confirmed at 4.6σ significance. Searches for exotic oscillations have produced stringent constraints on several extensions to the PMNS (Pontecorvo-Maki-Nakagawa-Sakata) mixing formalism.

- Searches for evidence of dark matter-induced neutrino signals from the galactic center, the sun and the earth have so far yielded null results. Accordingly, limits have been placed on the WIMP self-annihilation cross section as well as on its interaction cross sections with nucleons. Currently SK's limits for masses below several tens GeV/c^2 are among the most stringent in the indirect searches in the world.

- High accuracy solar neutrino measurements are carried out in SK-IV. Improvement of the water circulation system, lowering of energy threshold of data acquisition system, and improvement of analysis software were done. Then, solar neutrino events in 3.49-3.99 MeV in electron kinetic energy are now used in the oscillation analysis. As a result, the global oscillation analysis of solar neutrino experiments and KamLAND experiment provides most accurate oscillation parameters of θ_{12} and Δm^2_{21}. However, there is about 2σ level tension in Δm^2_{21} between solar global analysis and KamLAND measurement.

- The nucleon decay lifetime reached more than or close to 10^{34} years for the major decay modes: $p \to e^+\pi^0$, $p \to \mu^+\pi^0$, and $p \to \nu K^+$, with suppressing background by new technique of neutron tagging. These limits were original goal when the Super-K proposal was written. Searches for other decay modes were also performed and we obtained the most stringent limits on nucleon lifetime in the world.

- SK has been searching for galactic supernovae with the efforts to minimize the dead time. A flux upper limit of supernova relic neutrinos(SRN) was obtained using all data from SK-I to III that has reached within a factor of model predictions. In SK-IV, SRN search by tagging neutron capture on hydrogen was performed. The result shows the world best limit below 16 MeV. This result shows a high potential of neutron tagging techniques, which can be a strong tool for SRN detection.

- Preparation for the next phase of SK with Gadolinium(Gd) loading (SK-Gd) is in progress.

phase	SK-I	SK-II	SK-III	SK-IV
start	Apr. 1996	Sep. 2002	Jul. 2006	Sep. 2008
end	Jul. 2001	Oct. 2005	Aug. 2008	May 2018
ID PMTs	11,146	5,182	11,129	11,129
(photo coverage)	(40%)	(19%)	(40%)	(40%)
OD PMTs	1,885	1,885	1,885	1,885
electronics	ATM	ATM	ATM	QBEE
trigger	hardware	hardware	hardware	software

Table 1. Data taking phases of Super-Kamiokande.

The primary goal for SK-Gd is the first detection of SRNs with neutron tagging. Feasibility of loading Gadolinium into SK has been demonstrated by the EGADS (Evaluating Gadolinium's Action on Detector Systems) project. In addition, we succeeded to develop $Gd_2(SO_4)_3$ powder with low enough radio impurity. A new water system to dissolve Gd and purify Gd loaded water was constructed in a newly excavated hall near SK.

- A major refurbishment work on the SK tank, whose main purpose is to fix the leak for SK-Gd, is underway in FY2018. We are aiming to resume observation with pure water in January 2019, and to start Gd loading Gd within FY2019.

Atmospheric Neutrinos

Super-Kamiokande's atmospheric neutrino data provided the first evidence for neutrino oscillations in 1998 [5] with the observation of a significant deficit of upward-going ν_μ-induced interactions. This deficit is best explained by flavor transitions among predominantly ν_μ and ν_τ. Since that discovery, subsequent observations of neutrinos from the sun, reactors, and accelerator neutrinos have revealed oscillations among all three neutrino flavors and in the span of only 20 years, many aspects of the PMNS mixing paradigm have been revealed. Currently all of its mixing angles and mass splittings have been measured. Despite this success there are several open questions in neutrino oscillation physics, including the nature of the neutrino mass hierarchy, the precise value of the atmospheric mixing angle θ_{23}, and whether or not neutrino oscillations violate CP. The atmospheric neutrino data set at Super-K is sensitive to effects that can resolve these issues but also to exotic oscillation effects predicted models of physics beyond the Standard Model. Over the last six years the Super-K has been focused on detailed studies of the atmospheric neutrino flux and its oscillations to both address these open questions and fully establish its role as a background to searches for dark matter and proton decay.

With the discovery of mixing between the first and third neutrino generations via the mixing angle θ_{13} matter-induced oscillation effects are expected to appear in the flux of atmospheric ν_e and ν_μ. The largest of these effects is a predicted resonant enhancement of the $\nu_\mu \to \nu_e$ oscillation probability of neutrinos traversing the Earth's core at multi-GeV energies. Fortunately this effect is present either for neutrinos if the mass hierarchy is normal or antineutrinos if it is inverted. This enhancement appears as an increase in the upward-going electron-like data at SK, but also affects the spectrum of the muon-like data. The size of this effect is modulated by the precise value of θ_{23} and of the PMNS mixing matrix's CP-violating phase δ_{CP}. These two parameters are also expected to impact the oscillations in the low energy ($E_\nu < 1$ GeV) data such that the entire atmospheric neutrino data set can be used to constrain the most important open questions in oscillation physics.

In order to maximize sensitivity to these effects and those of non-standard oscillation scenarios the atmospheric neutrino data spanning neutrino energies from 100 MeV to TeV and above are analyzed together within a unified framework. Data are divided into three broad categories based on the energy deposition of events in the SK inner and outer detectors. The fully contained (FC) sample features events with primary vertices within the 22.5 kiloton fiducial volume of the inner detector and no particles exiting the inner detector. Events with fiducial vertices but with one or more particles exiting (typically muons) into the OD are termed partially contained (PC). Upward-going muons with vertices within or outside of the outer detector and penetrating into the inner detector form the Up-μ sample.

The FC sample is further divided into 14 subsamples based on visible energy, particle type, and number of rings to improve sensitivity to a wide variety of oscillation phenomena. Though it is not possible to identify neutrino and antineutrino interactions on an event-by-event basis, sensitivity to the mass hierarchy and CP-violating effects is enhanced through statistical separation of these populations. Further, additional in-situ constraints on non-oscillating neutral current and ν_τ background are provided by an additional hierarchy-sensitive multi-ring e-like (other) sample that was introduced into since 2012. Both the PC and Up-μ samples

have average energies above 10 GeV, their lower energy constituents posses hierarchy sensitivity and their higher energy events have exquisite sensitivity to exotic oscillation effects. By 2018 atmospheric neutrino data representing a combined exposure of 328 kiloton-year exposure of the detector have been analyzed. Figure 1 shows the 19 event samples used in these analyses together with the best prediction from the oscillation study presented below.

PMNS Oscillation Analysis

The event selection presented above has been optimized for sensitivity to oscillations characteristic of θ_{13}-induced matter effects. To test for the presence of these effects the SK atmospheric analysis is divided into three parts, each incorporating and increasing amount of external information. Each analysis test both hierarchy hypothesis and the full range of values of the θ_{23}, Δm^2_{32}, and δ_{CP} mixing parameters.

The first analysis is a fully unconstrained test of PMNS mixing and includes a search for the value of θ_{13} itself and relies only on the atmospheric neutrino data. In the second analysis the value of $\sin^2\theta_{13}$ is fixed to 0.0219 according to the average value provided by the Particle Data Group. With this constraint the atmospheric neutrino sensitivity is expected to increase as the data can be used to constrain the other mixing parameters controlling the size of the matter effects. Finally, since it is known that the size of these effects varies with θ_{23}, in particular, a model of the T2K experiment is introduced in the third fit to incorporate their precise constraints on this parameter. To construct the model atmospheric neutrino MC are reweighted to the T2K flux and fit against publicly available binned data to directly incorporate constraints from T2K into the SK analysis.

Table 2 lists the result of each analysis. All fits favor a normal mass hierarchy with θ_{23} in the second octant and δ_{CP} near $3\pi/2$. Constraints on the mixing parameters from the SK only analysis with the θ_{13} constraint appear in Figure 2. The significance of the mass hierarchy result varies based on the assumed values of the mixing parameters and on the analysis under consideration. Over the range of values allowed at 90% C.L. the inverted hierarchy hypothesis is rejected by between 91.5% and 94.5% for analysis constrained by the T2K model and between 80.6% and 96.7% otherwise. Preferences for θ_{23} and δ_{CP} are consistent with other results in the community, with the constraint on the latter improving noticeably when SK is analyzed together with the T2K model [85]. Despite these successes the data are as-yet insufficient to provide solutions for the open questions posed above.

Tau Neutrino Physics

Atmospheric neutrino oscillations are primarily between ν_μ and ν_τ, but the latter is not found in the primary atmospheric flux at energies where such transitions occur. As a result searching for oscillation-induced ν_τ interactions within Super-K is not only important for validation of PMNS-style mixing but can also be used to establish a means of studying its properties. However, the search for ν_τ events is complicated by the large threshold energy for the charged current production of the τ lepton as well as its propensity to decay into several light-producing hadrons. Above the 3.5 GeV production threshold not only is atmospheric neutrino flux reduced by orders of magnitude relative to its peak, but single- and multiple-pion production process become increasingly important at these energies. The latter fact makes charged current ν_e and ν_μ interactions of similar energies become backgrounds.

A neural network-based analysis is used to extract the ν_τ signal from the various backgrounds. However, no cut by neural network analysis is applied and instead it is used with zenith angle information to form probability density functions (PDFs) as part of a two-dimensional unbinned maximum likelihood fit. The PDFs for each event are combinations of that for background and signal:

$$PDFs = PDFs_{bg} + \alpha \times PDFs_{tau} + \sum_i \varepsilon_i \cdot PDFs_{sys}, \quad (1)$$

where the last term represents the change of the PDFs due to systematic error effects. Unlike previous analyses, this likelihood simultaneously incorporates shape and systematic error information to extract the signal.

The fit has been applied to the full detector exposure and indicates the ν_τ normalization factor α is 1.47 ± 0.32(stat+syst.). This corresponds to a statistical significance 4.6σ to reject the no-tau-appearance hypothesis, up from 3.8σ from the previous result. In addition this data has been used for the first time to produce a flux-averaged measurement of the total tau neutrino cross section. For energies between 3.5 GeV and 70 GeV the result is $0.94 \pm 0.20 \times 10^{-38}\text{cm}^2$ as shown in Figure 3. This result is in agreement with both lower-statistics measurements at accelerators and with models at the 1.5σ level.

Exotic Oscillations

Despite the enormous success of the PMNS mixing paradigm in explaining the results of most oscillation experiments there remains room to explore oscillation effects predicted in theories that extend the Standard Model. Indeed, the results of short-baseline oscillation searches do not fit well within the standard three neutrino mixing framework and hint at the possible existence of one or more sterile neutrinos. Further, as an interferrometric effect neutrino oscillations are a sensitive probe of oscillations that deviate from the characteristic pathlength over energy, L/E, dependence of standard oscillations. The SK atmospheric neutrino data have been successfully utilized to address both of these topics.

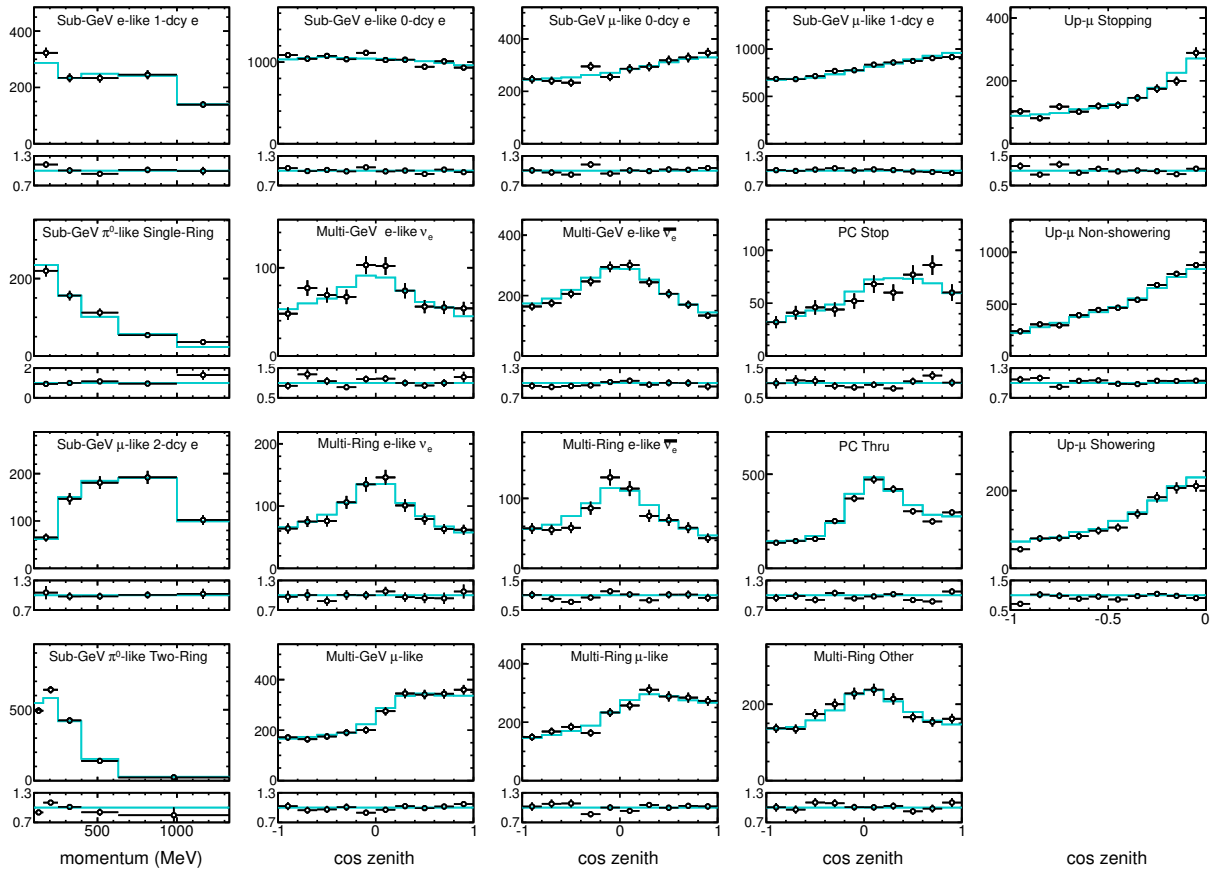

Fig. 1. Zenith angle and lepton momentum distributions for atmospheric neutrino data corresponding to a 328 kiloton-year exposure of Super-Kamiokande spanning its four run periods. The blue histogram denotes the best fit MC expectation and error bars on the data points are statistical. Sub-panels beneath each distribution show the ratio relative to the MC prediction. Upward-going and downward-going events correspond to cosine zenith of -1 and $+1$, respectively.

Fit	Hierarchy	$\sin^2\theta_{13}$	$\sin^2\theta_{23}$	$\lvert\Delta m^2_{32,31}\rvert$ $[\times 10^{-3}$ eV$^2]$	δ_{CP}
SK θ_{13} Free	NH	$0.018^{+0.029}_{-0.013}$	$0.587^{+0.036}_{-0.069}$	$2.50^{+0.13}_{-0.31}$	$4.18^{+1.45}_{-1.66}$
	IH	$0.008^{+0.017}_{-0.007}$	$0.551^{+0.044}_{-0.075}$	$2.20^{+0.33}_{-0.13}$	$3.84^{+2.38}_{-2.12}$
SK θ_{13} Constrained	NH	—	$0.588^{+0.031}_{-0.064}$	$2.50^{+0.13}_{-0.20}$	$4.18^{+1.41}_{-1.61}$
	IH	—	$0.575^{+0.036}_{-0.073}$	$2.50^{+0.08}_{-0.37}$	$4.18^{+1.52}_{-1.66}$
SK+T2K	NH	—	$0.550^{+0.039}_{-0.057}$	$2.50^{+0.05}_{-0.12}$	$4.88^{+0.81}_{-1.48}$
	IH	—	$0.550^{+0.035}_{-0.051}$	$2.40^{+0.13}_{-0.05}$	$4.54^{+1.05}_{-0.97}$

Table 2. Best fit oscillation parameters obtained by the three flavor oscillation analysis. Fits are conducted for both the normal (NH) and inverted (IH) hierarchy assumptions for the atmospheric neutrino data ("SK only") and including constraints from the T2K experiment("SK+T2K"). All fits are performed assuming $\sin^2\theta_{13}$=0.0219, which is taken from PDG.

Short-baseline accelerator experiments suggest that if oscillations into a sterile neutrino exist the characteristic mass splitting is 400 times greater than that seen in atmospheric neutrino oscillations: $\Delta m^2_{14} \sim 1$ eV^2. This splitting would induce an oscillation frequency in the atmospheric neutrino data that is fast enough to produce an oscillation effect that is sensitive only to the size of the mixing angle between the active and sterile states. That is, the SK data are largely insensitive to the details of the mass splitting as well as to the number of sterile neutrino states. Using a 273 kiloton-year subset of the atmospheric neutrino data SK found no evidence for sterile neutrino and established limits on their mixing parameters at the 90% C.L. of $|U_{\mu 4}|^2 < 0.041$ and $|U_{\tau 4}|^2 < 0.18$ [72]. Figure 4 shows the limits from Super-K in comparison with other experiments.

Lorentz invariance violating neutrino oscillations are expected to produce exotic oscillation effects between

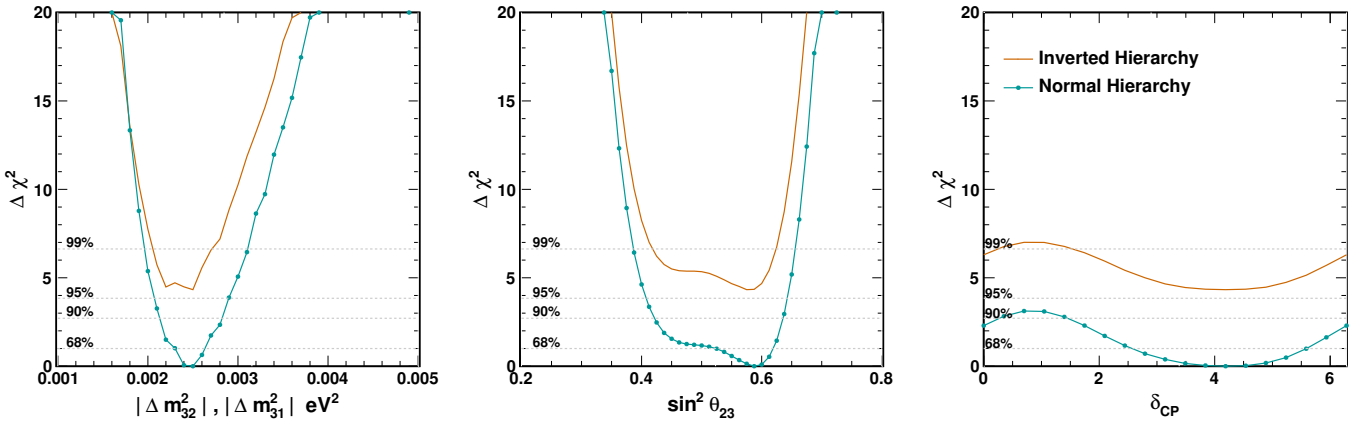

Fig. 2. Constraints on neutrino oscillation parameters from the Super-K atmospheric neutrino data fit assuming $\sin^2\theta_{13} = 0.0219 \pm 0.0012$. Orange lines denote the inverted hierarchy result, which has been offset from the normal hierarchy result, shown in cyan, by the difference in their minimum χ^2 values.

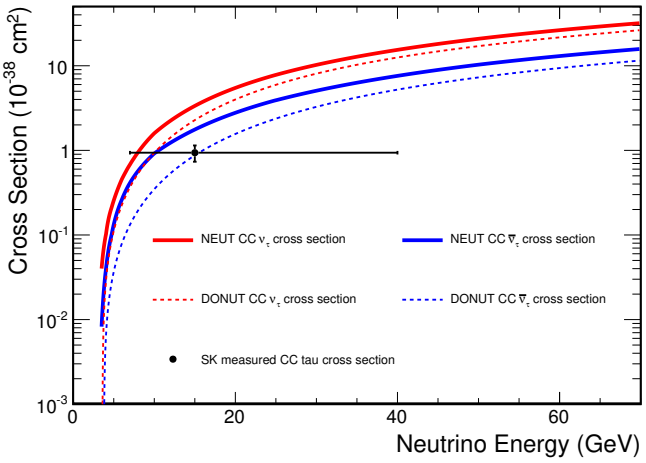

Fig. 3. Flux averaged neutrino cross section measurement from Super-K. Solid lines denote the expected ν_τ (red) and $\bar{\nu}_\tau$ cross sections as a function of energy. Dashed lines denote the cross section based on measurements by the DONuT experiment.

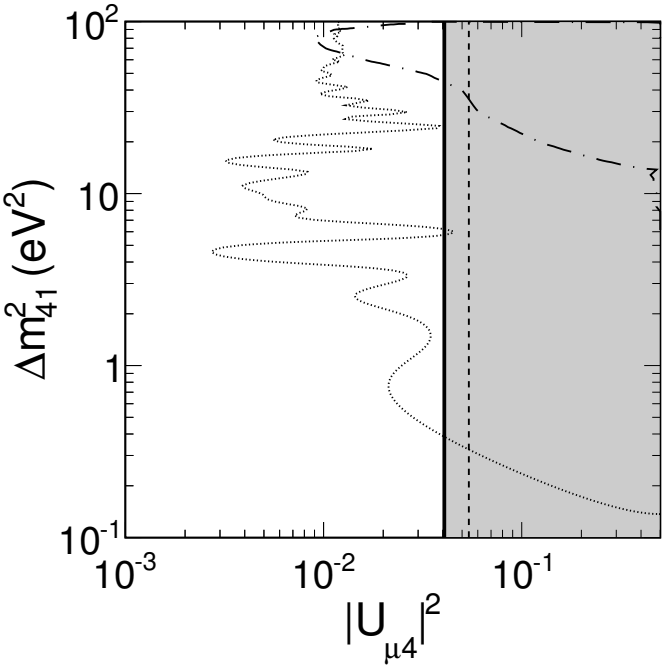

Fig. 4. Super-K limits on mixing into a sterile neutrino in comparison with a combined analysis of MiniBooNE and SciBooNE (dotted) and CCFR (dash-dot). The shaded region shows the 90% C.L. limit from SK.

all neutrino flavors proportional to L or $L \times E$. Due to the wide range of both pathlengths and energies available in the atmospheric sample it is possible to probe such effects in detail. In particular, the high energy upward-going subsets of the atmospheric neutrino data would be subject to large spectral and angular distortions beyond what is seen from PMNS oscillations. Super-K has produced an analysis of atmospheric neutrino data which for the first time makes use of a complete framework for studying Lorentz invariance violation together with standard neutrino oscillations without any simplifying assumptions. This enabled the analysis to make full use of the entire atmospheric neutrino data sample and though no significant departure from the expectations of standard oscillations was observed, new limits have been placed on the presence of Lorentz violating effects and existing limits have been strengthened by the range between three and seven orders of magnitude [71].

Indirect Searches for Dark Matter

The existence of dark matter in the universe is supported by cosmological and astronomical observations, but to date there is no definitive explanation of its nature. One promising hypothesis is that it is a weakly interacting massive particle (WIMP), which can arise in supersymmetic extensions of the Standard Model. If such a particle decays or annihilates into Standard Model particles, their subsequent decay chains would

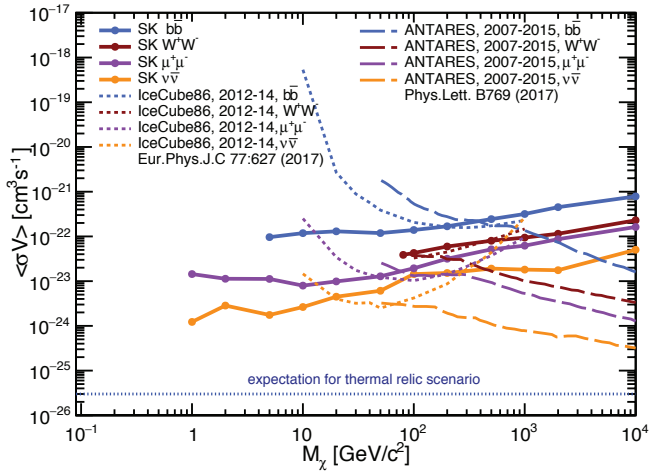

Fig. 5. Super-K limits on the WIMP velocity-averaged self-annihilation cross section in comparison with results from the ANTARES and IceCube experiments.

also produce neutrinos that can be detected at Super-K. Since WIMPs are massive they are expected to accumulate within large gravitational potential wells, such neutrinos would be observed from the center of the galaxy, the sun, or even the Earth. In the last six years Super-K has undergone searches for these neutrinos as a directional excess coming from each of these locations.

While the precise mass of WIMPs is unknown it is possible to search for evidence of such a directional source by assuming a particular mass and that WIMPs decay or annihilate directly into quarks or leptons which subsequently produce a neutrino spectrum based on known Standard Model processes. The Super-K searches use the full data set outlined above, but analyzed in coordinates where the event direction is reconstructed relative to the galactic center or the center of the Earth. Both the reconstructed direction and momentum are used in the analysis, with the latter helping to constrain the WIMP mass via its spectral information. For all searches no evidence of a dark matter signal is found in the Super-K data. Figure 5 shows the derived limit on the velocity-averaged WIMP self-annihilation cross section as a function of mass in comparison with results from other experiments. The power of the Super-K data lies in its low analysis threshold, which has resulted in the most stringent limits below masses of several tens GeV/c^2 regardless of assumed annihilation channel. Similarly, the left panel of Figure 6 shows limits on the WIMP-nucleon spin-independent cross section from the search for events from the center of the Earth. The right panel shows limits on the spin-dependent cross section of WIMPs coming from the sun [73]. In both cases Super-K's constraints are the strongest among the indirect search experiments, though less constraining than limits from direct search experiments.

Other Topics

Over the last six years the Super-K atmospheric analysis has made several other measurements, which support those above or others in the field. As an example of the former, the Super-K produced its first ever measurement of the atmospheric neutrino flux [80] in both the electron and muon channels and demonstrated it is consistent with the expectations of standard models in the field. Regarding the latter, the first direct detection of gravitational waves by the LIGO experiment and several other detections have been made since then. Super-K produced follow-up searches for neutrinos coincident with the first detection of a blackhole-blackhole merger [81] and with a neutron star-neutron star merger [86]. In addition, a search was performed for neutrinos coincident with the astrophysical neutrino data observed at IceCube [84]. Though each of these searches yielded a null result, it is clear that further searches and subsequent detections will advance multi-messenger astronomy and are therefore an important avenue of research at Super-K going forward.

Looking Toward the Future

The pursuit of oscillation physics is among the most important goals for the atmospheric neutrino physics program at Super-Kamiokande and indeed in the community in general. Super-K, especially with constraints from the T2K experiment, has excellent sensitivity to the mass hierarchy and can thereby make contributions to the study of δ_{CP} as well. Currently we aim to introduce several new features into the analysis to further improve this sensitivity, including the introduction of neutron-tagged analysis samples for better neutrino-antineutrino separation, the implementation of an improved reconstruction algorithm that will enable the expansion of the fiducial volume, as well as techniques to improve background suppression and systematic uncertainties. Not only will these be important for addressing the physics goals of the atmospheric sample itself, but will also guide the development of the expected sensitivity of and the future analysis at Hyper-Kamiokande.

Solar Neutrinos

Solar neutrinos are produced by the nuclear fusion reaction, $4p \rightarrow \alpha + 2e^+ + 2\nu_e$, in the core of the Sun. SK detects solar neutrinos through neutrino-electron elastic scattering, $\nu_x + e \rightarrow \nu_x + e$, where the energy, direction, and time of the recoil electron are measured. Thanks to its large (22.5 kiloton) fiducial mass, SK makes precise measurements of ^{8}B solar neutrinos, including precision information on their energy spectrum and its time variation.

Solar neutrino experiments (SK, SNO, Borexino and radio chemical experiments) have provided direct evidence for solar neutrino flavor conversion. Considering

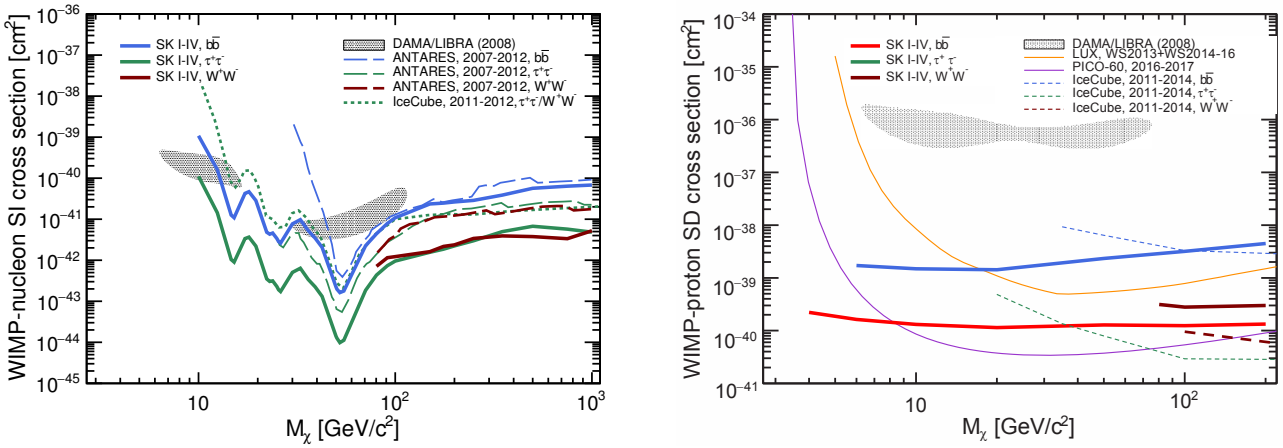

Fig. 6. Limits on the spin-independent WIMP-nucleon interaction cross section for the Super-K search for WIMPS from the center of the Earth (left) and on the spin-dependent cross section for WIMPs from the sun (right). Both analyses assume 100% branching ratios into each of the channels shown.

with the KamLAND reactor experiment, a solar neutrino oscillation scenario is almost established. However, there is still a room for non-standard possibilities in the current experimental results. For example, there is about 2σ tension on Δm^2_{21} oscillation parameter between a global oscillation analysis from solar neutrino experiments and an oscillation analysis from the reactor experiment. Another possible room for new physics would be that the expected transition between vacuum oscillation and matter oscillation in solar neutrino energy spectrum has not been confirmed yet.

The next step of solar neutrino measurements is the precise determination of the oscillation parameters and the role of matter therein. For that purpose, SK has been collecting high statistics solar neutrino data to attempt measurements of a day-night flux difference and a distortion of the energy spectrum.

In this term (after 2012), many efforts continuously made to reduce backgrounds and to increase the precision of the detector calibrations, both of which are crucial for solar neutrino measurements.

The most serious background comes from the beta decay of ^{214}Bi, which is produced in the decays of radon (^{222}Rn) in the air and detector materials as well as from radium in the purified water. In order to reduce the ^{214}Bi background, the SK water system was upgraded again. In 2013-2014, a new heat exchanger was installed to achieve precise control of the water temperature in the detector. This system controls water temperature with 0.1 degree accuracy. It confines high radon remaining water to the very bottom of the SK detector, and then keeps lower radon concentration in the central fiducial volume region.

In order to study energy spectrum in the matter-vacuum transition region, we have lowered the trigger threshold of the data acquisition system from 34 observed PMT hits within 200 nsec to 31 hits since May 2015. The 3 hits corresponds to about 0.5 MeV electron energy. After May 2015, the trigger efficiency between 3.49 MeV and 3.99 MeV electron kinetic energy was improved from ∼86% to ∼100%.

In the analysis software, the energy reconstruction method is improved in April 2018 to consider PMT gain and dark rate variations as a function of time. Preliminary results with this new analysis tools were released at the Neutrino conference held in June 2018.

In 2016, we released a paper about the solar neutrino analysis results until February 2014 (SK-IV 1664 days data set) [79]. Up to now, SK-IV finished data taking. In this report, the updated preliminary results using the data until the end of December 2017 (SK-IV 2860 days data set) are shown. Table 3 shows a summary of solar neutrino observation in each SK phase. The total live time of solar neutrino measurements throughout all phases of SK is 5695 days.

Since SK has observed solar neutrinos for more than 20 years, this long term observation covers nearly 2 solar activity cycles. Figure 7 shows SK yearly flux measurements since SK-I until SK-IV with the sun spot numbers in the same period. From the yearly data in Fig. 7, the χ^2 value is calculated as $\chi^2 = 21.57/21$ d.o.f., which corresponds to a probability of 41%. The SK solar rate measurements are consistent with a constant solar neutrino flux emitted by the Sun.

During the SK-IV 2860 days data set, preliminary number of the observed solar neutrino events are $55810^{+363}_{-361}(stat) \pm 949(syst)$ in 3.49-19.5 MeV electron kinetic energy region. This event rate corresponds to a ^{8}B solar neutrino flux of $(2.289 \pm 0.015(stat) \pm 0.039(syst)) \times 10^6$ /cm^2/sec, assuming a pure ν_e flavor content. A statistically combined flux from all SK phases is $(2.327 \pm 0.044(stat+syst)) \times 10^6$ /cm^2/sec (preliminary).

Figure 8 shows the solar angle distribution in the lowest energy bin of the SK-IV 2860 days data set. The observed number of the solar neutrino events between

Table 3. Summary of the solar neutrino observation in SK. The energy threshold is in electron kinetic energy. The SK-IV information is preliminary.

Phase	Period	Live time (days)	Energy thr. (MeV)
SK-I	April, 1996 - July, 2001	1496	4.49
SK-II	October, 2002 - October, 2005	791	6.49
SK-III	July, 2006 - August, 2008	548	4.49
SK-IV	September, 2008 - May, 2018	2860	3.49

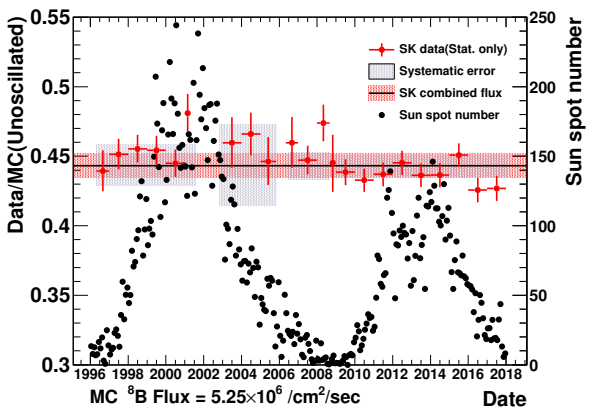

Fig. 7. The measured ^{8}B solar neutrino flux in SK since beginning of SK-I(1996) until end of SK-IV(2018). The vertical axis shows the ratio of the observed flux to the expectation from the unoscillated MC simulation assuming a ^{8}B flux of 5.25×10^6 /cm^2/sec. The red points show the yearly flux measured by SK (statistical uncertainty only). The gray bands show the systematic uncertainties in each SK phase. The black-horizontal line shows the combined measured flux value with uncertainty drawn as the red horizontal band. The back points show the sun spot number provided from the Wold Data Center SILSO, Royal Observatory of Belgium, Brussels (http://www.sidc.be/silso/datafiles/). The results during SK-IV are preliminary.

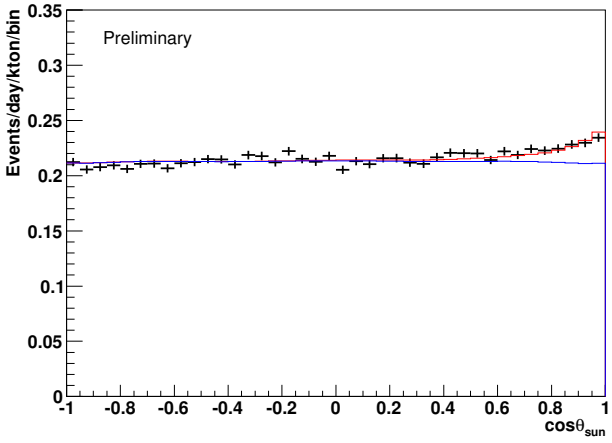

Fig. 8. Solar angle distribution of SK-IV 2860 days data set for events with electron kinetic energies between 3.49 and 3.99 MeV. The black points are data while the red histogram is the best fit to the data. The blue histogram shows the background component of this fit.

3.49 and 3.99 MeV is $1797^{+169}_{-167}(stat)$ (preliminary).

The measured energy spectrum of the SK-IV 2860 days data set is shown in Fig. 9 (top). The vertical axis shows the ratio of the observed energy spectrum to the expectation from the unoscillated MC simulation assuming the ^{8}B flux of 5.25×10^6 /cm^2/sec. Figure 9 (bottom) shows a statistical combination of SK spectra from all phases. The combined energy spectrum is consistent with the standard neutrino oscillation analysis at solar global best-fit Δm^2_{21} parameter within 1σ level, but there are $\sim 2\sigma$ tension with the standard neutrino oscillation analysis at KamLAND best-fit Δm^2_{21} parameter.

Concerning differences in the day and night fluxes, the expected flux asymmetry, defined as $A_{DN} = (day - night)/\frac{1}{2}(day + night)$, is about 2% based on current understanding of neutrino oscillation parameters. Although this is not a large effect, long term observations by SK enable discussion of a finite value of the day-night asymmetry. In 2016, we summarized the day-night asymmetry analysis using all SK data up to SK-IV 1664 days data set. Figure 10 shows the solar zenith angle dependence of the solar neutrino fluxes from the events in 4.49-19.5 MeV from SK-IV 1664 days data set. The obtained $A_{DN}^{fit,SK}$ value using the amplitude fit method was $-3.3 \pm 1.0(stat) \pm 0.5(syst)$%, which was a 2.9σ difference from zero [79]. Currently, the day-night analysis up to SK-IV 2860 days data set is ongoing.

A global solar neutrino oscillation analysis has been performed including all SK data (SK-I [38], SK-II [47], SK-III [54], day-night amplitude fitting from SK-IV 1664 days data set [79], and preliminary energy spectrum from SK-IV 2860 days data set) as well as data from other solar neutrino and reactor experiments, same as Ref. [79].

Figure 11 (top) shows the allowed regions from SK data with the ^{8}B flux constraint of $(5.25 \pm 0.20) \times 10^6$ /cm^2/sec as well as those from KamLAND data. SK data with a flux constraint is significantly contributes to the measurement of θ_{12} and Δm^2_{21} parameters among solar neutrino experiments.

Figure 11 (bottom) shows the allowed regions from

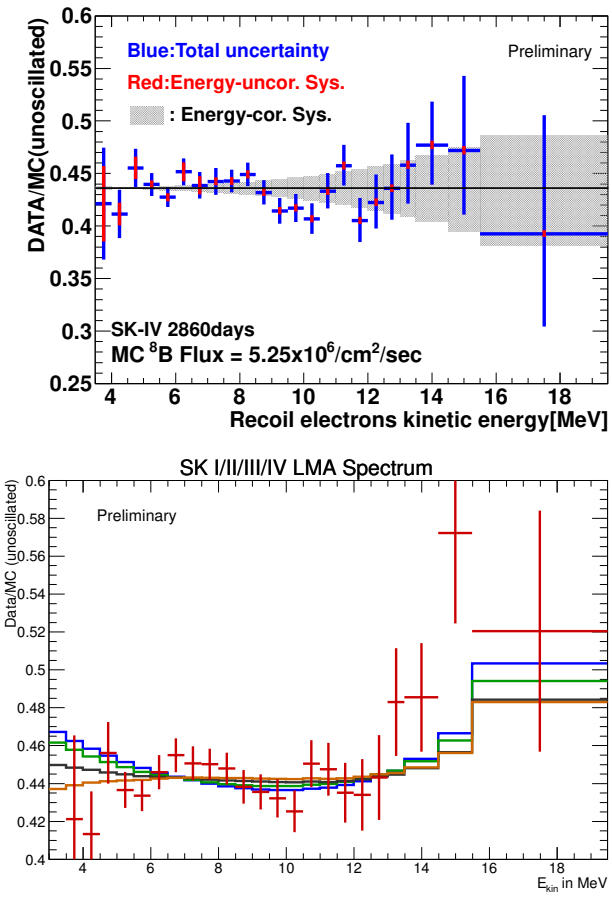

Fig. 9. Solar neutrino energy spectrum in SK-IV (top) and a statistical combination from all phases (bottom). Each point shows the ratio of the data to the expected flux using an unoscillated ^{8}B solar neutrino spectrum. In the bottom plot, blue and green lines are predictions from solar + KamLAND best-fit point and solar global best-fit point. The black and brown lines are best-fit of SK spectrum data with quadratic and exponential functions [79].

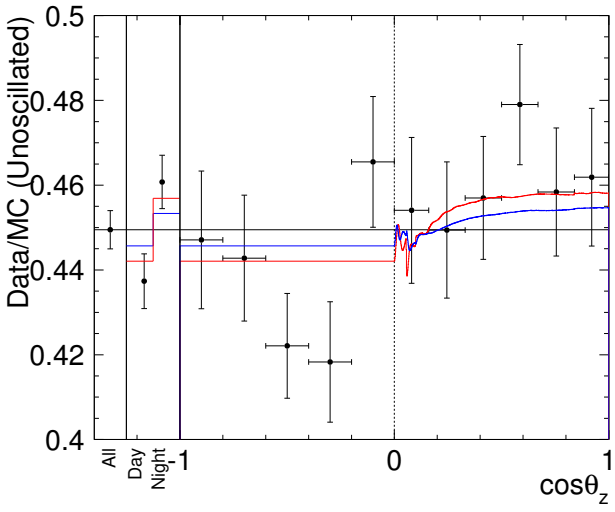

Fig. 10. The solar zenith angle dependence of the solar neutrino flux from the events in 4.49-19.5 MeV from SK-IV 1664 days data set. The black points are observed flux. The red and blue lines are expected flux values at solar global and solar global + KamLAND best-fit parameters, respectively.

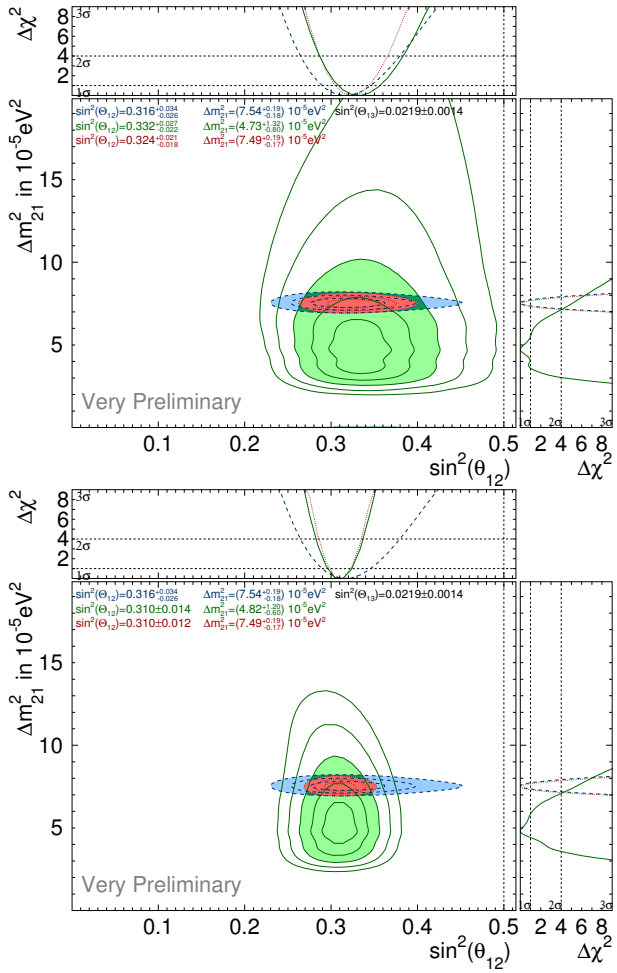

Fig. 11. Allowed regions of neutrino oscillation parameters in the Δm^2_{21} and $\sin^2\theta_{12}$ plane with a constraint of $\sin^2\theta_{13} = 0.0219 \pm 0.0014$. The green, light blue, and red results of the upper figure are obtained from SK data, KamLAND, and SK+KamLAND, respectively. Those of the lower figure are obtained from solar global, KamLAND, and solar global+KamLAND. The curves are drawn for each 1σ step of 1-5σ for SK/solar, and of 1-3σ for the KamLAND and SK/solar+KamLAND results. Contours at 3σ are filled with their colors.

the solar global analysis and solar+KamLAND global analysis. The obtained parameters from the solar global analysis are $\Delta m^2_{21} = (4.82^{+1.20}_{-0.60}) \times 10^{-5}$ eV^2 and $\sin^2\theta_{12} = 0.310 \pm 0.014$. Comparing these values with those from KamLAND ($\Delta m^2_{21} = (7.54^{+0.19}_{-0.18}) \times 10^{-5}$ eV^2 and $\sin^2\theta_{12} = 0.316^{+0.034}_{-0.026}$), there is a 2σ level tension in the Δm^2_{21} results, which is evident in the figure. Combining the solar global analysis with KamLAND analysis, the oscillation parameters become $\Delta m^2_{21} = (7.49^{+0.19}_{-0.17}) \times 10^{-5}$ eV^2 and $\sin^2\theta_{12} = 0.310 \pm 0.012$. These are current most accurate oscillation parameters of θ_{12} and Δm^2_{21}.

Summary and future prospects

High accuracy solar neutrino measurements are carried out in SK-IV. Improvement of the water circulation system, lowering of energy threshold of data acquisi-

tion system, and improvement of analysis software were done. Then, solar neutrino events in 3.49-3.99 MeV in electron kinetic energy are now used in the oscillation analysis.

The combined energy spectrum is consistent with the solar global best-fit within 1σ, but $\sim 2\sigma$ tension with the KamLAND measurement.

The combined day-night asymmetry value until SK-IV 1664 days data set is $-3.3 \pm 1.0(stat) \pm 0.5(syst)\%$, which is a 2.9σ difference from zero. Currently, The day-night analysis up to SK-IV 2860 days data set is ongoing.

The global oscillation analysis of solar neutrino experiments and KamLAND experiment provides most accurate oscillation parameters of θ_{12} and Δm^2_{21}. However, there is about 2σ level tension in Δm^2_{21} between solar global analysis and KamLAND measurement.

The energy spectrum and day-night asymmetry are quite important for understanding the matter effect of the neutrino oscillation. The solar neutrino measurement at SK will continue, and those measurements will be discussed with meaningful statistical significance with further increase of the SK data.

Nucleon Decay Searches

Nucleon decay search gives us a unique window to test Grand Unified Theories (GUTs) of elementary particles. SK is the world's largest detector to search for nucleon decays and it has accumulated data of 91.7 kt·yr (SK-I), 49.2 kt·yr (SK-II), 31.9 kt·yr (SK-III), and 192.1 kt·yr (SK-IV until January 2018), resulting in 365kt·yrs of data in total. Various nucleon decay modes have been searched for in SK, but no significant signal has been seen so far, as is shown in Table 4. The lifetime limits reached more than or close to 10^{34} years in important decay modes, especially, the limits for $p \to e^+\pi^0$ and $p \to \mu^+\pi^0$ have exceeded the original goals written in the SK proposal. The new electronics introduced from SK-IV made improvement in selection efficiency of $p \to \mu^+\pi^0$ and $p \to \bar{\nu}K^+$ [69] by increasing tagging efficiency of Michel electron from muon. The new electronics also enabled to tag neutrons which are accompanied with atmospheric neutrino background[82]. We describe the detail of these important modes.

The proton decays into one charged lepton and one neutral pion ($p \to e^+\pi^0$ and $p \to \mu^+\pi^0$) are the ones that occur in a large number of theoretical models. This decay mode is mediated by super-heavy gauge bosons. Discovery of a signal would give us information about the mass of the gauge bosons, M_X, because the proton lifetime is predicted to be proportional to M_X^4. To discriminate the signal from atmospheric neutrino background, we reconstruct the total visible energy and total momentum corresponding to the parent proton mass and the proton's Fermi momentum in oxygen, respectively.

In SK-IV period, we updated the electronics and it enables tagging of neutrons to separate proton decay signal from atmospheric neutrino background. The signature of the neutron, 2.2 MeV gamma ray emission from the neutron capture on hydrogen with a mean capture time of 200 μsec, is too faint to be triggered by the data acquisition system used in SK-I through SK-III. The upgraded electronics in SK-IV adopt a trigger-less readout scheme to record every hit, including all hits by 2.2 MeV gamma rays. A software trigger is then issued after every fully-contained event to save all hits within a 500 μsec timing window for physics analyses. Neutron tagging can benefit proton decay analyses, providing an additional handle for rejecting the atmospheric neutrino interactions that are the main background to proton decays. Atmospheric neutrino interactions are often accompanied by neutrons, while the probability of a neutron being emitted by deexcitation of a nucleus after proton decay is rather small, and no neutron is produced in the decay of a free proton. Furthermore, these proton decay modes do not produce neutrons in secondary interactions in water because the final state particles in these decay modes are lepton and gammas. Almost a half of atmospheric neutrino background could be rejected by requiring no neutron.

To find 2.2 MeV γ candidates, we search for hit clusters with ≥ 7 hits within a 10 ns sliding time window, after time-of-flight (TOF) subtraction using the vertex of the prompt neutrino interaction. Sixteen variables described in a reference[1] are input to a neural network to distinguish the 2.2 MeV γ signal from background. The efficiency of neutron tagging by this method is estimated to be 20.5±2.1% with a mis-tagging probability of 1.8%. The performance of the neutron tagging was confirmed by introducing a neutron source (Americium-Beryllium) into the SK tank.

Figure 12 shows the number of tagged neutrons for $p \to e^+\pi^0$ (upper) and $p \to \mu^+\pi^0$ (lower) analyses excluding the signal region defined by reconstructed total mass and momentum. These figures show that the neutron multiplicity in the atmospheric neutrino MC (solid histogram) agrees well with data (dots). The dashed histograms show the true number of captured neutrons in the MC, indicating that additional background rejection can be achieved if the neutron tagging efficiency is improved in the future when gadolinium is dissolved in the SK water.

A new analysis technique is applied in these analysis. The signal region is divided into two regions: $P_{tot} < 100$ MeV/c and $100 \leq P_{tot} < 250$ MeV/c. The region below 100 MeV/c is dominated by free protons, and the region $100 \leq P_{tot} < 250$ MeV/c is dominated by bound protons. A reduced systematic error for < 100 MeV/c can be achieved because the initial

*1 Irvine, Tristan James, "Development of Neutron-Tagging Techniques and Application to Atmospheric Neutrino Oscillation Analysis in Super-Kamiokande", Ph. D. Thesis, University of Tokyo, 2014.

mode	exposure ($kt \cdot yr$)	εB_m (%)	observed event	B.G.	τ/B limit ($10^{34} yrs$)
$p \to e^+\pi^0$	365	38-39	0	0.6	2.0
$p \to \mu^+\pi^0$	365	30-38	1	0.7	1.2
$p \to \bar{\nu}K^+$	365				0.8
$-\mu^+$ spec.		31-37	–	–	
– prompt γ		7-9	0	0.4	
$-\pi^+\pi^0$		7-10	0	0.6	

Table 4. Summary of nucleon decay search results in Super-Kamiokande.

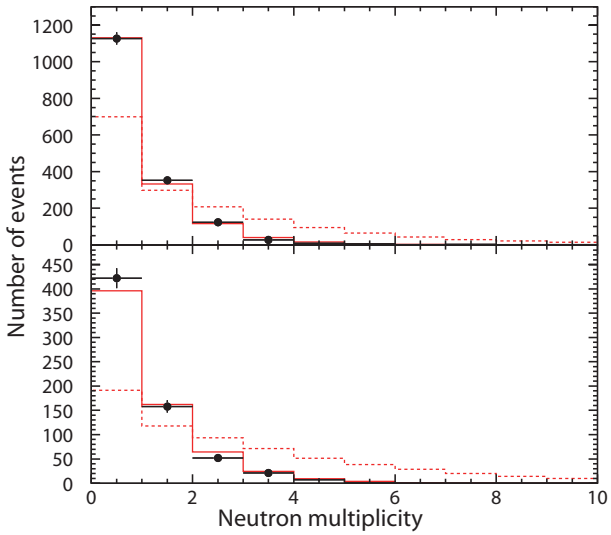

Fig. 12. Distribution of the number of tagged neutrons for $p \to e^+\pi^0$ (top) and $p \to \mu^+\pi^0$ (bottom) analyses excluding the signal region defined by total mass and momentum. Dots show SK-IV data with 133.5 kton·years exposure, the solid histogram shows the multiplicity of tagged neutrons per event in the atmospheric ν MC, and the dashed histogram shows the true multiplicity of neutrons per event.

protons and the products of the proton decay do not suffer from any of the various nuclear interactions. In addition, background contamination from atmospheric neutrinos is concentrated in the $100 \le P_{tot} < 250$ MeV/c, while the region below 100 MeV/c is nearly background free. Figure 13 shows the reconstructed proton mass *vs.* total momentum distribution for signal and atmospheric ν MC, combining all data from SK-I through SK-IV. In the signal MC plots, the light blue dots show the free proton case and the dark blue dots show bound protons.

The new two-box analysis achieves better discovery reach. For example, the 3σ discovery reach in the proton lifetime for $p \to e^+\pi^0$ is 13.3% higher than the conventional single-box analysis for the current exposure, and 20.9% higher for an exposure of 1 megaton·year, which may be achieved by the next generation of detectors.

We analyzed data from SK-I through SK-IV, in total 365kt·years until January 2018. As shown in Table 4, there were no candidate events observed for $p \to e^+\pi^0$ with 0.6 expected background. One event observed for $p \to \mu^+\pi^0$ but it is consistent with expected background (0.7 events). Thus we set lower limit of proton lifetime with 90% confidence level as 2.0×10^{34} and 1.2×10^{34} years for $p \to e^+\pi^0$ and $p \to \mu^+\pi^0$, respectively.

Not only π^0, we studied nucleon decay into charged anti-lepton and other mesons, $p \to (e^+, \mu^+) + (\eta, \rho^0, \omega)$ and $n \to (e^+, \mu^+) + (\pi^-, \rho^-)$ systematically with 316kton·year data. Some candidates were observed but they were consistent with expected background and we got lower limits of nucleon lifetime in range from 3×10^{31} to 1×10^{34} years for these modes.

$p \to \bar{\nu}K^+$ is also important because it is a dominant mode in SUSY-GUTs. In this mode, most of K^+ stops in water and decays into two particles, $\nu\mu^+$ or $\pi^+\pi^0$, which have monochromatic momentum and are back-to-back each other. Thus we looked for single muon ring events with 236 MeV/c. Another important feature is that the remaining nuclei may emit de-excited gamma rays after the proton decay and this γ should be emitted before $K^+ \to \nu\mu^+$ (lifetime: 12 nsec). Thus we looked for the prompt gamma rays in the single muon ring sample. Charged current quasi-elastic scattering ($n\nu_\mu \to p\mu^-$) with nuclear gamma ray, muon below Cherenkov threshold and proton above threshold was one of the dominant background for this search. because the proton ring was reconstructed as muon by shifting vertex largely due to difference of their opening angle of Cherenkov ring. It makes fake time difference between muon and gamma ray. To reject such events, new algorithm which separates proton ring from muon ring by maximum likelihood method based on Cherenkov opening angle and hit pattern. We achieved about 50% background rejection with this method.

For $K^+ \to \pi^+\pi^0$, the momentum of charged pion is just above the Cherenkov threshold and it doesn't make clear Cherenkov ring. We searched for monochromatic π^0s which have PMT activities in the backward. π^0 decays into two γs and this decay mode should have two e-like rings in many cases and we selected two ring sample in the conventional method . However, if energy

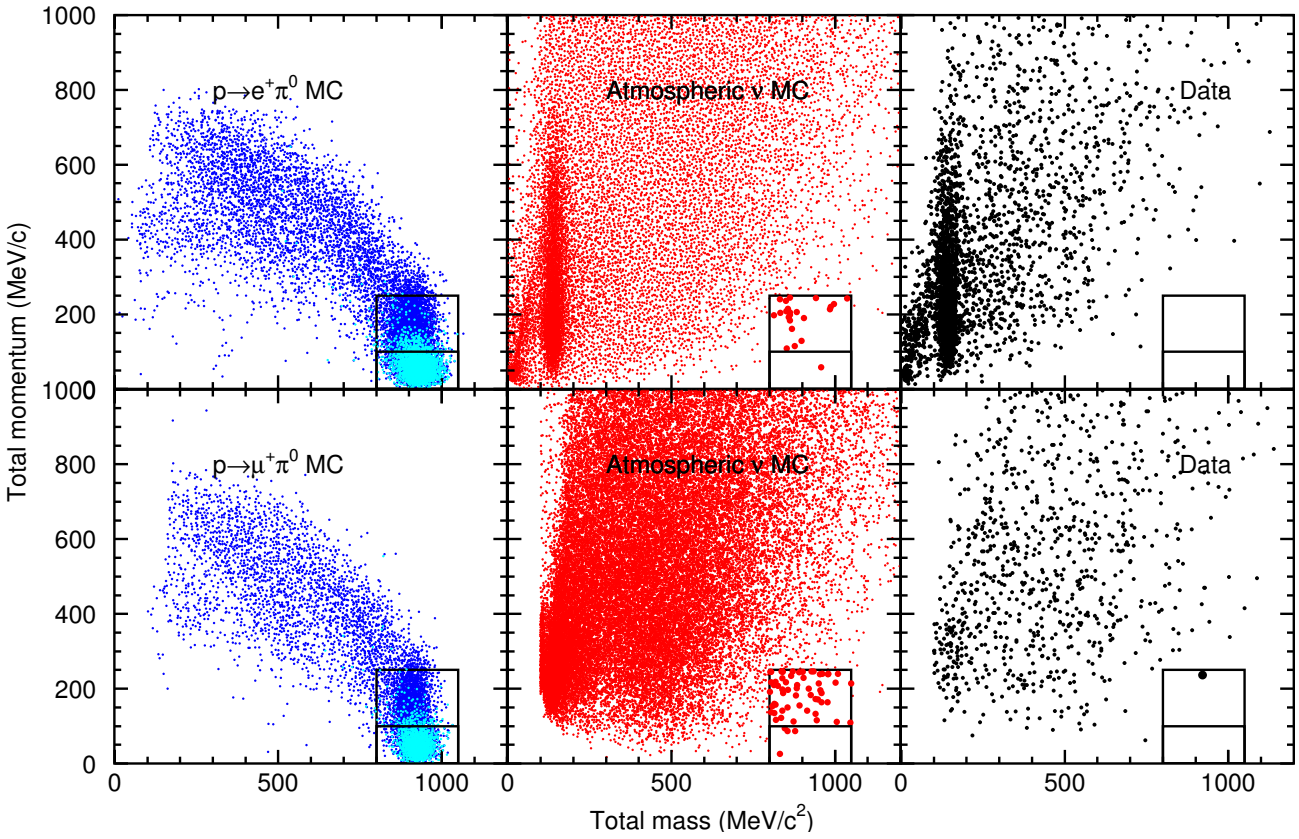

Fig. 13. Reconstructed proton mass *vs.* total momentum for $p \to e^+\pi^0$ (top) and $p \to \mu^+\pi^0$ (bottom). The left panels show signal MC, where light blue corresponds to free protons and dark blue is bound protons. The middle panels show atmospheric ν MC corresponding to 500 years live time of SK, and the right panels show SK-I to SK-IV data. The dot size is enlarged in the signal box. Signal regions defined by total momentum are shown by black boxes. The lower box (P_{tot} <100 MeV/c) is dominated by free protons with less systematic uncertainty in signal MC, while most of events in higher box ($100 <= P_{tot} < 250$ MeV/c) are bound protons affected by nuclear effect. Remaining background events concentrate in the higher box and the lower box is almost background free. Better sensitivity is achieved by separating the signal regions.

of one γ is too small or opening angle of two γ is small, it is identified as one ring sample. To find out one-ring π^0 events, we employed special routine which is used for rejecting background for T2K ν_e analysis. By adding one ring sample, detection efficiency of $K^+ \to \pi^+\pi^0$ was improved by 20%.

Search for $p \to \bar{\nu}K^+$ mode was carried out with improvement described above and neutron tagging only for SK-IV by using 365kt·yrs data. We didn't find any proton decay candidates and calculated partial lifetime limits, taking into account systematic uncertainties. The obtained limits are 8.0×10^{33}years at 90% confidence level.

Super-Kamiokande also looked for the other various nucleon decay modes and Figure 14 shows summary of the lower limit of the nucleon lifetime. We have obtained the world's strongest nucleon lifetime limits for most of the modes.

Future prospect

As seen in this section, the new electronics installed in SK-IV contributes to reduce atmospheric neutrino background by neutron tagging. We achieved to reduce background by almost half for several nucleon decay modes in pure water case, in which neutron tagging efficiency is rather small (about 20%). Figure 15 shows background reduction of $p \to e^+\pi^0$ as a function of efficiency of neutron tagging. We are going to load Gd into water in SK tank and we expect 80% neutron tagging efficiency with 0.1% Gd concentration. In this setup, we are able to achieve further 50% background reduction from SK-IV case. Super-Kamiokande can keep good discovery potential of proton decay with longer exposure by suppressing background low enough.

Supernova Neutrinos

In 1987, the observation of supernova SN1987A by Kamiokande, IMB and BAKSAN opened the neutrino astronomy. This observation confirmed that the en-

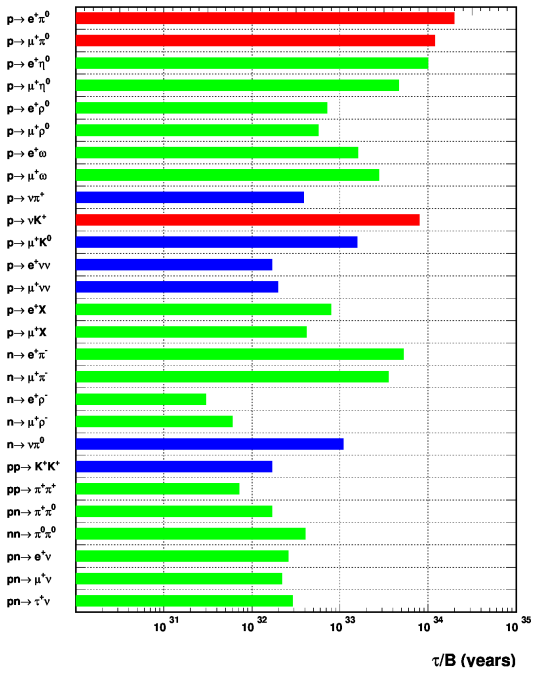

Fig. 14. Summary of lower limits of nucleon with 90% CL studied by Super-Kamiokande. Red and green color shows proton decay modes which were analyzed with 365kt· and 350kt· years data, respectively. Modes in blue color were results of SK I-III data.

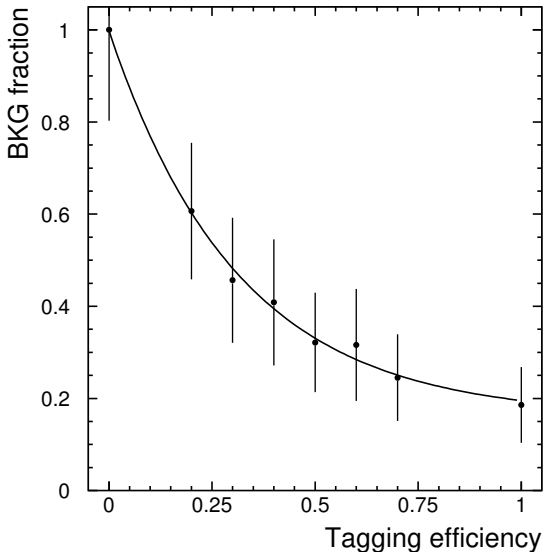

Fig. 15. Background reduction for $p \to e^+\pi^0$ as a function of neutron tagging efficiency. Vertical axis is normalized without neutron tagging case.

ergy released by neutrinos is about several$\times 10^{53}$ergs. However, the core collapse supernova (ccSN) mechanism is not yet fully understood. SK would be able to detect several thousand neutrino events if a ccSN happened near the center of our galaxy. Such an observation would enable us to investigate in detail the mechanics of the ccSN explosion.

On average, 1-2 ccSNe per century are expected in our galaxy. We must be prepared for these events because neutrinos arrive earlier than optical signals. A real-time supernova neutrino burst monitor searches for time clustered events [78]. This online program is called SNWATCH. Events with total energy greater than 7 MeV and vertex position within the 22.5-kton fiducial volume in SK are selected. Cosmic ray muons and their subsequent decay electron events are removed. For each selected event, a 20-second time window is opened backwards in time, and the number of selected events in the window, N_{clus}, is counted. A variable D that identifies the dimension of the vertex distribution is computed. It is an integer number from 0 to 3, corresponding to point-, line-, plane- and volume-like distributions, respectively.

When $N_{clus} \geq 60$ and $D = 3$ a prompt SN warning is generated including automatic phone-calling and emails to experts. Then, the experts check whether it is a real supernova signal or not by looking at various plots which are uploaded to a secured site accessible from the Internet. These alarms are usually due to the accidental coincidence of two cosmic ray induced clusters. So far, no real supernova neutrino burst signal has been observed at SK.

When SNWATCH issues such a warning, first SK shifts call SNWATCH conveners and report the status of SK. Then, SNWATCH conveners and executive committee members meet via TV conference system, and discuss about a prompt announcement to outside researchers and the press. The decision is taken within one hour after the SN warning. In order to train people and test SNWATCH system, there are drills few times in every month. In a drill, a laser-diode light-source flashes to mimic a galactic supernova, and SNWATCH warning notifies SK shifts. Shift takers then call SNWATCH conveners and give a report, and converners actually have to have a meeting. By doing such drills, SK collaboration is ready for a real supernova.

Other searches conducted at SK are those for neutrinos from Supernova Relic Neutrinos (SRNs). The SRN signal is the diffuse supernova neutrino background from all the core collapse supernovae in the past. This signal is expected to be detectable in the 16-30 MeV energy region, which corresponds to the gap between the spectrum of solar and atmospheric neutrinos, however it has never been detected and only upper limit was set by SK [58].

In SK-IV, a new result of the SRN search using the neutron tagging technique was also published [70]. In

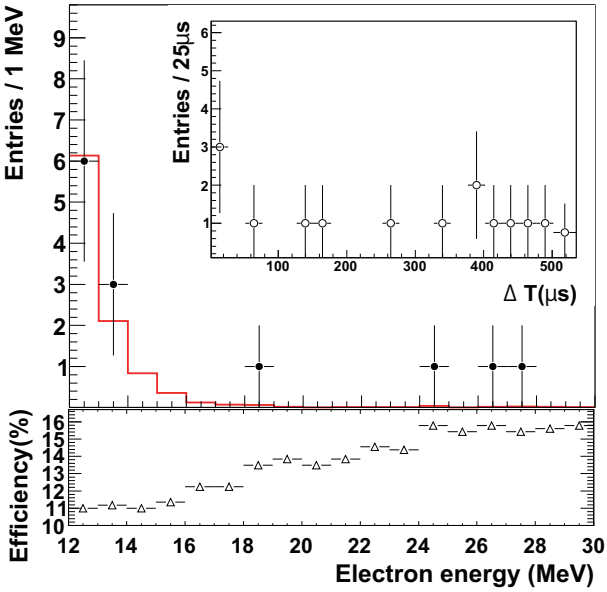

Fig. 16. Energy spectrum of prompt signals (points). The red histogram shows the expected accidental background. The plot embedded in the upper right shows the timing difference for the delayed candidates. The bottom figure shows the detection efficiency of SRN for each energy bin; the jumps at 18 MeV and 24 MeV are due to energy-dependent spallation cuts. Errors are statistical only.

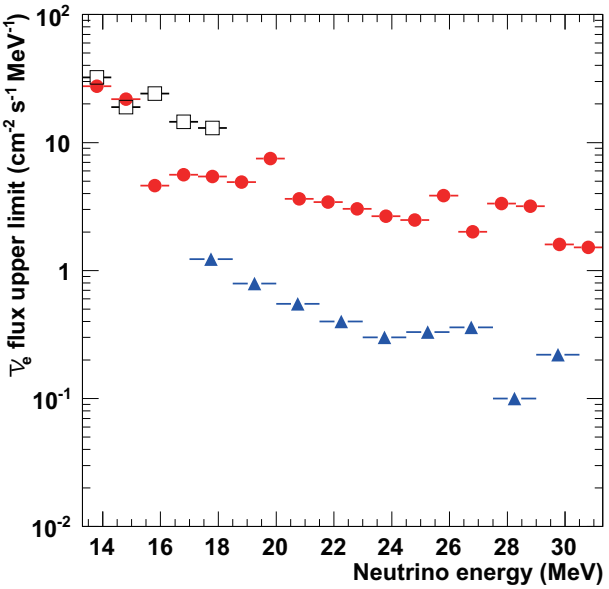

Fig. 17. Model-independent SRN 90% C.L. upper limits as a function of neutrino energy for SK-IV (solid circle). For comparison, both KamLAND result (open square) and previous SK result (solid triangle) are also shown.

this analysis, the neutrons captured on hydrogen from SRN reactions ($\bar{\nu}_e, p \to e^+, n$) are searched. After a neutron is captured, a single 2.2 MeV gamma is emitted. Thus, by detecting the prompt positron signal and the delayed 2.2 MeV gamma signal, we can reduce backgrounds, most of which are not accompanied by neutrons.

Figure 16 shows the energy spectrum of prompt signal, the time difference between a prompt signal and a delayed signal, and the detection efficiency of SRN for each energy bin. Figure 17 shows the obtained flux limit comparing with other results. The neutron detection efficiency is very low because of the low energy of the gamma from the neutron capture on hydrogen (compare the 2.2 MeV gamma with the kinetic energy threshold of 3.5 MeV for solar neutrino analysis). However, with this method we could obtain the world best limit below 16 MeV. This result shows a high potential of neutron tagging techniques, which can be a strong tool for SRN detection.

The Super-Kamiokande Gadolinium Project (SK-Gd)

Supernova relic neutrinos

As described in the previous section, SK obtained flux upper limit of SRNs. The obtained limit is getting closer to the predictions and SRN signals would be detected in the SK-Gd phase. The predicted spectra of SRN[2] are shown in Figure 18.

Since reactor neutrinos and atmospheric neutrinos are dominant background below 10 MeV and above 30 MeV respectively, 10–30 MeV is an open window for the SRN measurement. SK has been searching for SRN as described in the previous section, recently with 2.2MeV gamma tagging. However, it is still limited by background because the detection efficiency of the 2.2 MeV gamma with Cherenkov light is low. By adding 0.2% gadolinium sulfate into the 50 kton water tank, this situation will be significantly improved[3] as shown in Figure 19. Gadolinium has a thermal neutron capture cross section of 49,000 barns (about 5 orders of magnitude larger than that of protons) and emits a gamma cascade of 8 MeV that can be easily detected using Cherenkov light. In order to obtain a 90% efficiency for neutron capture, the Gd concentration should be 0.1% (0.2% if $Gd_2(SO_4)_3$) as illustrated in Figure 19.

Figure 20 shows expected signal spectra for SRN models and conservative background estimation of atmospheric neutrinos with its component. Table 5 shows the expected number of events and background with 10 years observation. Here, we assume the ν_μ CC background events are 1/4 of those of SK, ν_e CC background events are 2/3, and NC background events are 1/3 with neutron tagging, respectively. Topological information of events should allow to reduce the background further, but it is not included in this estimation.

EGADS

In order to study the effect of dissolving Gd in the SK tank, an R&D project called EGADS has been run-

*2 S. Horiuchi et al., Phys. Rev. **D79**, 083013(2009).
*3 J. Beacom and M. Vagins, Phys. Rev. Lett. **93**, 171101 (2004).

Table 5. Expected numbers of SRN signals and backgrounds through SK-Gd 10 years observation

Model	10-16 MeV	16-28 MeV	Total	significance
$T_{eff} = 8$ MeV	11.3	19.9	31.2	5.3σ
$T_{eff} = 6$ MeV	11.3	13.5	24.8	4.3σ
$T_{eff} = 4$ MeV	7.7	4.8	12.5	2.5σ
T_{eff} =SN1987a	5.1	6.8	11.9	2.1σ
BG	10	24	34	–

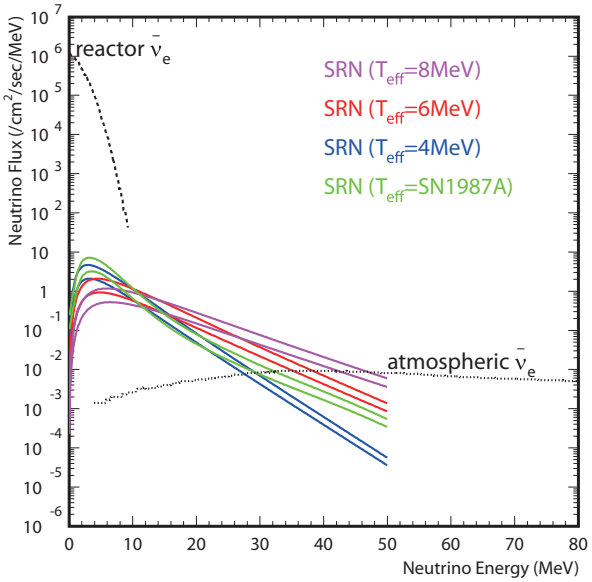

Fig. 18. Expected energy spectra of supernova relic neutrinos (from S. Horiuchi et al., Phys. Rev. **D79**, 083013(2009)). Each color corresponds to an effective neutrino temperature, and each range shows astrophysical uncertainties.

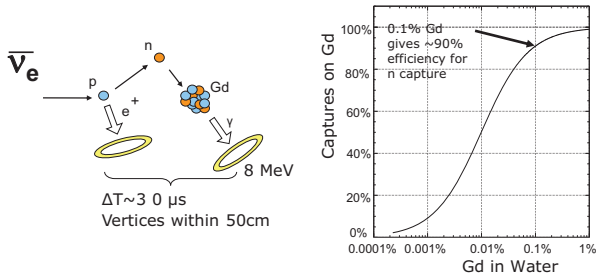

Fig. 19. Neutron tagging with gadolinium (left), and capture efficiency as a function of Gd concentration (right) (M. Vagins' talk in NEUTRINO2010, June 2010, Athens, https://indico.cern.ch/event/73981).

ning in the Kamioka mine since 2014. A new hall was excavated near SK and a 200 m^3 stainless steel tank with ancillary equipment was constructed. The idea is to mimic the SK conditions inside the 200 m^3 tank. The tank is equipped with a selective water filtration system that removes impurities while retaining the Gd and a 15 m^3 Gd premixing and pretreatment plastic tank. It is also instrumented a device to measure the water attenuation length, UDEAL (Underground Device Evaluating Attenuation Length).

Figure 21 shows the history of the measured water transparency in the 200 m^3 tank since October, 2014. The four loadings are clearly identified. It demonstrates that transparencies can be comparable to those achieved at the pure-water SK's phases III and IV, and that in steady operation the measured transparencies are nicely stable at values very appropriate for physics analyses. The $Gd_2(SO_4)_3$ concentration in the 200 m^3 tank is monitored by using an Atomic Absorption Spectrometer (AAS). Water samples are collected by a pump from three points in the detector, at three different height, using the same pipe as the UDEAL sampling. The measured concentration since November 2014 is also shown in Figure 21. The four loadings are clearly seen as steps in the concentration. The concentrations at all three sampling points are: 1) very close to each other, indicating that there is a homogeneous solution in the 200 m^3 tank, and 2) stable between loadings or any other external intervention, demonstrating that there is no significant Gd loss during continuous water recirculation and purification.

In order to see the positive effects of the Gd loading, i.e. the neutron tagging capability, an Am/Be neutron source with BGO crystal was deployed in the EGADS detector. Through the process; $^{241}\mathrm{Am} \rightarrow ^{237}\mathrm{Np} + \alpha$, $^{9}\mathrm{Be} + \alpha \rightarrow ^{12}\mathrm{C} + \gamma(4.4\,\mathrm{MeV}) + n$, the scintillation light from BGO by 4.4 MeV γ can be used as the prompt signal which mimics the Cerenkov light. Figure22 (a) shows the distribution of time differences between prompt and delayed (neutron captured) events after application of several simple analysis cuts. The exponential fit of the distribution indicates a characteristic of 31.32 ± 0.76 (stat.) μs, which is consistent with the expectation for 0.1% Gd concentration. The flat component of the fit function indicates the BG rate in the data. In order to remove the remaining background (BG), a statistical background subtraction method was applied. This method uses data of delayed events rejected by the $\Delta t_{\mathrm{prompt-delayed}} < 500$ μs cut as a background sample. Figure 22 (b) shows the spectrum of the number of hits from a calibration run with the Am/Be source deployed in the center of the detector after background subtraction. The same distribution from a GEANT4 MC simulation is shown. The effi-

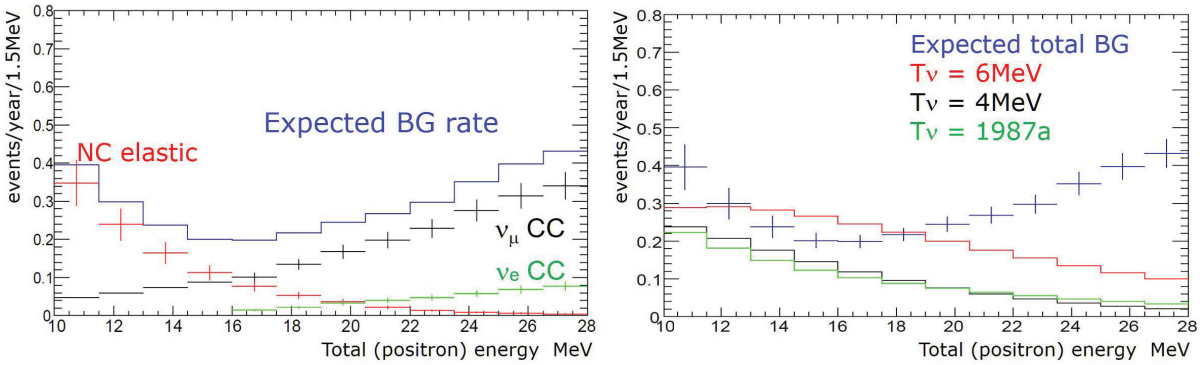

Fig. 20. Expected background components of SK-Gd (left), and expected SRN spectra of some models (right) (from S. Horiuchi et al., Phys. Rev. **D79**, 083013(2009)).

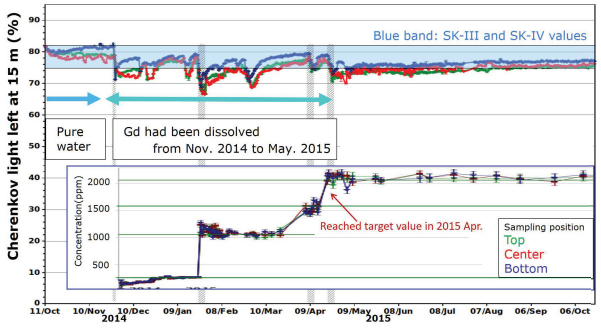

Fig. 21. Percentage of Cherenkov light remaining for water inside the instrumented 200 m^3 EGADS tank for increasing concentrations of gadolinium sulfate. The green, red, and blue lines correspond to data taken from the top, center, and bottom sample points of the 200 m^3 tank, respectively, while the light blue band shows the range of ultra-pure water transparencies during SK-III and SK-IV. The inset is the gadolinium sulfate concentration history, as measured by the AAS, for the three sampling points in the top, center and bottom of the EGADS detector (A. Renshaw, Physics Procedia **37**, 1249 (2012); L. Magro, EPJ Web of Conferences **95**, 04041 (2015)).

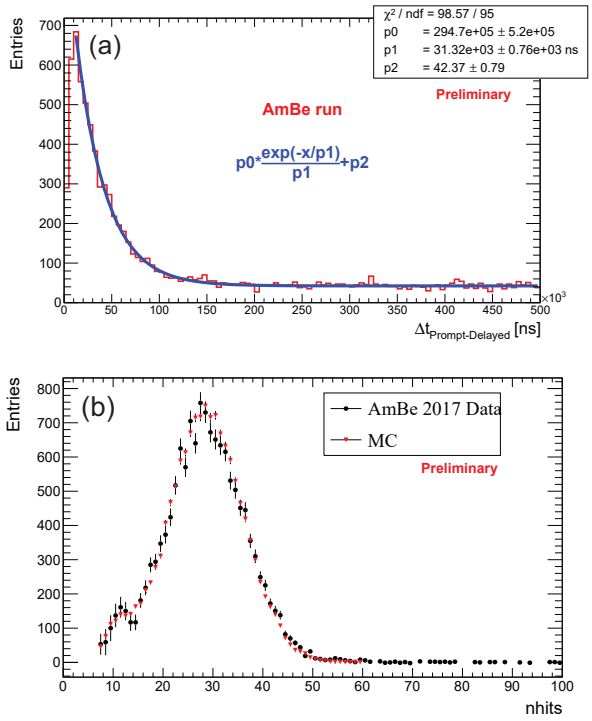

Fig. 22. (a) Distribution of the difference of time between prompt and delayed events in Am/Be run with Am/Be source deployed in the center of the detector. The blue line indicates the fit of the distribution with an exponential + flat component function. (b) Distribution of the number of PMT hits for Am/Be data (black) and MC (red) with Am/Be source deployed in the center of the detector. Statistical background subtraction was applied.

ciency of the Gd neutron capture selection was measured to be $85.3 \pm 0.9\%$ (stat) in data and $84.4 \pm 0.3\%$ (stat) in MC. These results indicate the expected neutron tagging in 0.2% $Gd_2(SO_4)_3$ water.

In summer 2017, the ATM-based electronics that were installed in EGADS were replaced with the front-end electronics used in the current SK. This allows the EGADS DAQ to stand high rates as in case of a close SN. For example, in case of Betelgeuse (about 200 pc) we expect about 3×10^4 events and according to our tests our DAQ could withstand SN bursts up to about 10^6 events. On the other hand, a SN in the opposite side of our galaxy would produce very few events in EGADS. However, because of the clear signature of neutron capture on Gd, the detection of a few inverse beta decay events within 10 seconds would unmistakably allow the detection of such a SN.

Loading Gd into Super-Kamiokande

In order to realize the Gd implementation to SK, we needed additional developments from various view points, such as environmental safety and low energy physics impacts.

New water system

Based on the EGADS results, we designed and constructed "Gd dissolution and purification system" to be used in SK. The system consists of a gadolinium sulfate

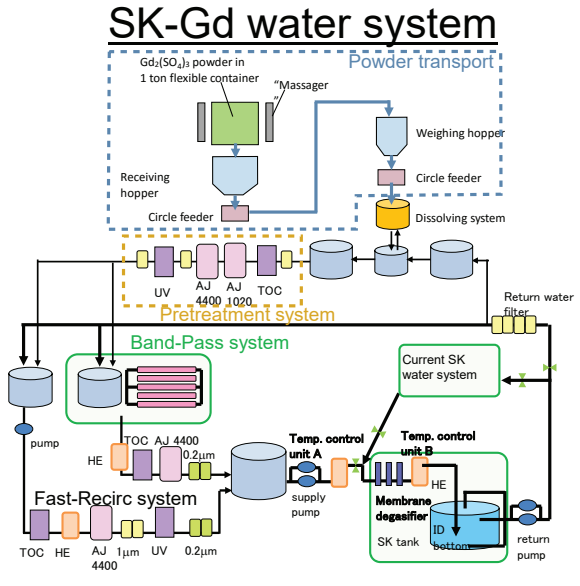

Fig. 23. The SK-Gd water system

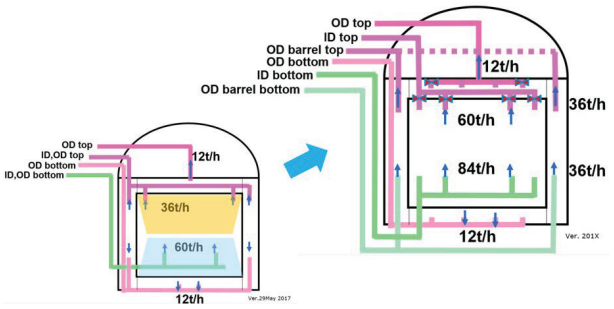

Fig. 24. The water piping modification

transportation unit, a dissolving unit, a pre-treatment unit and a main purification unit in the recirculation loop. The system is installed in Lab. G located approximately 160 m away from the SK tank. The flow diagram of the system is shown in Fig. 23. The system dissolves gadolinium in the SK tank in 17 days (when it is operated with the circulation flow rate of 120 m^3/h) or 35 days (when it is operated with the circulation flow rate of 60 m^3/h) and circulates and purifies gadolinium sulfate solution with the flow rate of 120 m^3/h.

Stopping the leakage

The water tank of SK has a leak that is estimated to be about 1 ton/day. The impact of Gd leakage to the environment is not regulated, therefore it is assumed that the impact is the same as Hg leakage which has the most stringent regulations. Thus, the leakage has to be fixed and the goal is to stop the leak or reduce it by a factor 30 at least. According to previous studies, the main leakage is considered to be at the bottom of the tank. However, to be safer, it was decided to apply sealants to all the welding part of the inner wall of the SK tank that is made of stainless steel (SUS) panels with a thickness of 3-4 mm, height of 2 m and a length of 6 m. The total extension of the weld line is about 6000 m.

MineGuard^{TM} had been considered for the overcoat sealing, however it was found that the original formulation with poly-urethane undergoes hydrolysis. Then a new formulation with poly-urea was developed. It was also found that $CaCO_3$ which is added to MineGuard^{TM} in order to increase its viscosity is contaminated with ^{238}U. To improve the situation, a pure SiO_2 instead of $CaCO_3$ was selected. The newly developed material is named MineGuard C^{TM}. It is estimated that the total Rn emanation from the sealing material will be about one third of that emanated from all the PMTs of the inner detector. Moreover, the sealing material will be present only in the outer detector, so the Rn emanation from the sealing material should be acceptable.

The tank repair work started on May 31st in this year (2018) and is expected to be finished in January 2019.

Upgrade of the water piping in the tank

In this work, the water piping inside the tank is also improved. When dissolving $Gd_2(SO_4)_3$ with the new water system, $Gd_2(SO_4)_3$ is added to the water coming back from the SK tank, and its aqueous solution is supplied to the tank. It is necessary to achieve a uniform Gd concentration inside the tank as soon as all the dissolving process is completed and also to keep a good water transparency. If we scale the flow rate of the EGADS system to SK-Gd system, at least 120 m^3/h of flow is necessary, while SK-IV has circulated and purified water at a flow rate of 60 m^3/h. As already mentioned above, the new water system was designed to process the dissolving and the purification with the recirculation of 120 m^3/h. As a consequence, the piping in the tank should be upgraded for doubled flow rate. In addition, the water flow in the tank has been restricted by the so-called "segmentation Tyvek" which was designed to separate the ID and OD optically but also separate the ID and OD water flow completely. Therefore, to improve the water replacement efficiency, the piping will be modified as shown in Fig. 24

Purification of $Gd_2(SO_4)_3$

The usual $Gd_2(SO_4)_3$ on the market contains radioactive impurities. Since these impurities would be present in the whole detector volume and could mimic several signals, these would be potential background sources for low energy neutrinos including SRN and solar neutrinos. For example, with the ^{238}U contamination in $Gd_2(SO_4)_3$, spontaneous fission would lead to a sizable background for SRN and the solar neutrino analysis would be affected by betas/gammas coming from ^{226}Ra daughters. In order to reduce the radioactive impurities in the $Gd_2(SO_4)_3$, we are currently

working in cooperation with several companies to produce high purity $Gd_2(SO_4)_3$ that could meet the requirements for low energy physics. While these companies provide us with new cleaner samples, we measure them with Ge detectors and an ICP-MS, to determine the U, Th and Ra concentrations. The measurements with Ge detectors are performed in the Canfranc and Boulby laboratories, in Spain and the UK respectively, and the ICP-MS measurements are done in the Kamioka observatory. The results of the measurements of the impurities in $Gd_2(SO_4)_3$ is summarized in Table 6. The company B product achieved the required purity. In FY2018, 1.5 tons of $Gd_2(SO_4)_3$ will be purchased.

Schedule of the SK-Gd

The tank refurbishment work is being carried out for 4 months up to the middle of October, 2018. The pure water supply will be carried out in about two and a half months from the middle of October until the beginning of January 2019 and the neutrino observation and T2K experiment will be resumed with ultra pure water.

Then, it is planned to start measuring the SRN by dissolving 10 tons of $Gd_2(SO_4)_3$ (corresponding to 0.01% of Gd concentration) with adjustment of the schedule of T2K experiment in FY2019. Although the Gd concentration of 0.01% is 1/10 of the final target of 0.1% Gd concentration, the neutron capture efficiency is already 50%. The SK detector will be run at this concentration, then, the remaining $Gd_2(SO_4)_3$ will be added to achieve our full target loading.

Table 6. Physics-based requirements for radioactive impurities in $Gd_2(SO_4)_3$ and the current status of the purification.

unit: $mBq/kg(Gd_2(SO_4)_3)$

Chain	^{238}U			^{232}Th			^{235}U	
	^{238}U		^{226}Ra	^{232}Th	^{228}Ra	^{228}Th	^{235}U	^{227}Ac /^{227}Th
Typical $Gd_2(SO_4)_3$	50		5	100	10	100	30	300
Requirements	< 50		< 0.5	< 0.05	< 0.05	< 0.05	< 3	< 3
Detector	Ge	ICP-MS	Ge	ICP-MS	Ge	Ge	Ge	Ge
Company A	–	< 0.04	–	0.09	–	–	–	–
Company B	< 11	< 0.04	< 0.2	0.02	–	< 0.3	< 0.4	< 1.7
Company C	< 10	< 0.04	< 0.2	0.06	< 0.2	< 0.3	< 0.3	< 1.2

Super-Kamiokande Collaboration

Spokesperson : Masayuki Nakahata (Kamioka Observatory, ICRR, The University of Tokyo)

Institute	Country	(*)
ICRR, Univ. of Tokyo	Japan	35
Boston Univ.	USA	7
California State Univ.	USA	2
Chonnam Univ.	Korea	3
Duke Univ.	USA	3
Ecole Polytechnique	France	5
Fukuoka Institute of Technology	Japan	1
Gifu Univ.	Japan	1
Gwangiu Institute of Science and Technology	Korea	1
Imperial College London	UK	3
INFN Sezione di Bari and Universite Politecnico di Bari	Italy	4
INFN Sezione di Napoli and Universite di Napoli	Italy	3
INFN Sezione di Padova and Universite di Padova	Italy	1
INFN Sezione di Roma and Universite La Sapienza	Italy	3
KEK	Japan	11
Kobe Univ.	Japan	8
Kyoto Univ.	Japan	8
Miyagi Kyoiku Univ.	Japan	1
Nagoya Univ.	Japan	4
National Centre for Nuclear Research	Poland	2
Okayama Univ.	Japan	9
Oxford Univ.	UK	2
Osaka Univ.	Japan	1
Queen Mary University of London	UK	3
Seoul National Univ.	Korea	1
Shizuoka Univ. of Welfare	Japan	1
Stony Brook Univ.	USA	7
SungKyunKwan Univ.	Korea	1
Tokai Univ.	Japan	1
Tokyo Institute of Technology	Japan	3
Tokyo Univ. of Science	Japan	3
TRIUMF.	Canada	1
Tsinghua University	China	2
Univ. of Autonoma Madrid	Spain	2
Univ. of British Columbia	Canada	1
Univ. of California, Irvine	USA	9
Univ. of Hawaii	USA	2
Univ. of Liverpool	UK	3
Univ. of Sheffield	UK	2
Univ. of Tokyo	Japan	2
Univ. of Tokyo, Kavli IPMU	Japan	7
Univ. of Toront	Canada	4
Univ. of Winnipeg	Canada	1
Yokohama National Univ.	Japan	1
Total		175

(*) Number of collaborators.

Members

Staff

Kamioka Observatory

Yoichiro Suzuki, Professor (till Mar. 2014)
Masayuki Nakahata, Professor
Shigetaka Moriyama, Professor
Masato Shiozawa, Professor
Yoshinari Hayato, Assoc. Professor
Yasuhiro Kishimoto, Assoc. Professor
Hiroyuki Sekiya, Assoc. Professor
Shoei Nakayama, Assoc. Professor
Makoto Miura, Research Associate
Yusuke Koshio, Research Associate (till Mar. 2013)
June Kameda, Research Associate
Atsushi Takeda, Research Associate
Kou Abe, Research Associate
Roger Wendell, Research Associate (till Dec. 2015)
Motoyasu Ikeda, Research Associate (from Sep. 2013)
Yasuhiro Nakajima, Research Associate (from Aug. 2016)
Tomonobu Tomura, Project Research Associate (till Mar.2016)
Hidekazu Tanaka, Project Research Associate (from Jun.2012)
Lluis Magro Marti, Project Research Associate (from May, 2016)
Yo Kato, Project Research Associate (from Sep.2016)
Christophe Bronner, Project Research Associate (from May 2017)
Yosuke Kataoka, Project Research Associate (from Dec. 2017)
Takatomi Yano, Project Research Associate (from Dec. 2017)

Research Center for Cosmic Neutrinos

Takaaki Kajita, Professor
Kimihiro Okumura, Assoc. Professor
Yasuhiro Nishimura, Research Associate (from Sep. 2016)
Yasuhiro Nishimura, Project Research Associate (Apr.2012 - Sep. 2016)

Senior Fellows

Kamioka Observatory

Shigeki Tasaka (Aug. 2015 - Mar. 2017)

Postdoctorial Fellows

Kamioka Observatory

Lluis Magro Marti (Apr. 2011 - Mar. 2013)
Yo Kato (Apr. 2016 - Sep. 2016)
Guillaume Pronost (from Mar. 2016)
Yuuki Nakano (from Apr. 2017)

Graduate students

Six students were awarded doctor degrees and six students earned master degrees during 2012–2018, supervised by ICRR staff members.

List of Publications

Before Year 2012

[1] "Measurement of a small atmospheric ν_μ/ν_e ratio", Super-Kamiokande Collaboration (Y. Fukuda et al.), Phys. Lett. B **433**, 9 (1998), **Cited 938 times.**

[2] "Study of the atmospheric neutrino flux in the multi-GeV energy range", Super-Kamiokande Collaboration (Y. Fukuda et al.), Phys. Lett. B **436**, 33 (1998), **Cited 882 times.**

[3] "Measurements of the solar neutrino flux from Super-Kamiokande's first 300 days", Super-Kamiokande Collaboration (Y. Fukuda et al.), Phys. Rev. Lett. **81**, 1158 (1998) [Erratum-ibid. **81**, 4279 (1998)], **Cited 890 times.**

[4] "Search for proton decay via $p \to e^+\pi^0$ in a large water Cherenkov detector", Super-Kamiokande Collaboration (M. Shiozawa et al.), Phys. Rev. Lett. **132**, 3319 (1998), **Cited 190 times.**

[5] "Evidence for oscillation of atmospheric neutrinos", Super-Kamiokande Collaboration (Y. Fukuda et al.), Phys. Rev. Lett. **81**, 1562 (1998), **Cited 5519 times.**

[6] "Calibration of Super-Kamiokande using an electron linac", Super-Kamiokande Collaboration (M. Nakahata et al.), Nucl. Instrum. Meth. A **421**, 113 (1999), **Cited 161 times.**

[7] "Constraints on neutrino oscillation parameters from the measurement of day-night solar neutrino fluxes at Super-Kamiokande", Super-Kamiokande Collaboration (Y. Fukuda et al.), Phys. Rev. Lett. **82**, 1810 (1999), **Cited 507 times.**

[8] "Measurement of the solar neutrino energy spectrum using neutrino electron scattering", Super-Kamiokande Collaboration (Y. Fukuda et al.), Phys. Rev. Lett. **82**, 2430 (1999), **Cited 513 times.**

[9] "Measurement of the flux and zenith-angle distribution of upward through-going muons by Super-Kamiokande", Super-Kamiokande Collaboration (Y. Fukuda et al.), Phys. Rev. Lett. **82**, 2644 (1999), **Cited 827 times.**

[10] "Observation of the east-west anisotropy of the atmospheric neutrino flux", Super-Kamiokande Collaboration (Y. Futagami et al.), Phys. Rev. Lett. **82**, 5194 (1999), **Cited 111 times.**

[11] "Search for proton decay through $p \to \bar{\nu}K^+$ in a large water Cherenkov detector", Super-Kamiokande Collaboration (Y. Hayato et al.), Phys. Rev. Lett. **83**, 1529 (1999), **Cited 176 times.**

[12] "Neutrino-induced upward stopping muons in Super-Kamiokande", Super-Kamiokande Collaboration (Y. Fukuda et al.), Phys. Lett. B **467**, 185 (1999), **Cited 299 times.**

[13] "N-16 as a calibration source for Super-Kamiokande", Super-Kamiokande Collaboration (E. Blaufuss et al.), Nucl. Instrum. Meth. A **458**, 638 (2001), **Cited 38 times.**

[14] "Tau neutrinos favored over sterile neutrinos in atmospheric muon-neutrino oscillations", Super-Kamiokande Collaboration (S. Fukuda et al.), Phys. Rev. Lett. **85**, 3999 (2000), **Cited 935 times.**

[15] "Detection of accelerator produced neutrinos at a distance of 250-km", K2K Collaboration (S.H. Ahn et al.), Phys. Lett. B **511**, 178 (2001), **Cited 296 times.**

[16] "Solar B-8 and hep neutrino measurements from 1258 days of Super-Kamiokande data", Super-Kamiokande Collaboration (S. Fukuda et al.), Phys. Rev. Lett. **86**, 5651 (2001), **Cited 1283 times.**

[17] "Constraints on neutrino oscillations using 1258 days of Super-kamiokande solar neutrino data", Super-Kamiokande Collaboration (S. Fukuda et al.), Phys. Rev. Lett. **86**, 5656 (2001), **Cited 824 times.**

[18] "Search for neutrinos from gamma-ray bursts using Super-Kamiokande", Super-Kamiokande Collaboration (S. Fukuda et al.), Astrophys. J. **578**, 317 (2002), **Cited 35 times.**

[19] "Determination of solar neutrino oscillation parameters using 1496 days of Super-Kamiokande I data", Super-Kamiokande Collaboration (S. Fukuda et al.), Phys. Lett. B **539**, 179 (2002), **Cited 995 times.**

[20] "Search for supernova relic neutrinos at Super-Kamiokande", Super-Kamiokande Collaboration (M. Malek et al.) , Phys. Rev. Lett. **90**, 061101 2003), **Cited 226 times.**

[21] "Indications of neutrino oscillation in a 250 km long baseline experiment", K2K Collaboration (M.H. Ahn et al.), Phys. Rev. Lett. **90**, 041801 (2003), **Cited 928 times.**

[22] "Search for anti-nu(e) from the sun at Super-Kamiokande I", Super-Kamiokande Collaboration (Y. Gando et al.), Phys. Rev. Lett. **90**, 171302 (2003), **Cited 67 times.**

[23] "The Super-Kamiokande detector", Super-Kamiokandecollaboration (Y. Fukuda et al.), Nucl. Instrum. Meth. A **501**, 418 (2003), **Cited 629 times.**

[24] "Development of super-high sensitivity radon detector for the Super-Kamiokande detector", C. Mitsuda, T. Kajita, K. Miyano, S. Moriyama, M. Nakahata, Y. Takeuchi, S. Tasaka, Nucl. Instrum. Meth. A **497**, 414 (2003).

[25] "A search for periodic modulations of the solar neutrino flux in Super-Kamiokande I", Super-Kamiokande Collaboration (J. Yoo et al.), Phys. Rev. D **68**, 092002 (2003), **Cited 74 times.**

[26] "Precise measurement of the solar neutrino day / night and seasonal variation in Super-Kamiokande-1", Super-Kamiokande Collaboration (M.B. Smy et al.), Phys. Rev. D **69**, 011104 (2004), **Cited 282 times.**

[27] "Limits on the neutrino magnetic moment using 1496 days of Super-Kamiokande-I solar neutrino data", Super-Kamiokande Collaboration (D.W. Liu et al.), Phys. Rev. Lett. **93**, 021802 (2004), **Cited 79 times.**

[28] "Search for electron neutrino appearance in a 250 km long baseline experiment", K2K Collaboration (M.H. Ahn et al.), Phys. Rev. Lett. **93**, 051801 (2004), **Cited 69 times.**

[29] "Search for dark matter wimps using upward through-going muons in Super-Kamiokande", Super-Kamiokande Collaboration (S. Desai et al.), Phys. Rev. D **70** 083523 (2004) [Erratum-ibid. D **70** 109901 (2004)], **Cited 382 times.**

[30] "Evidence for an oscillatory signature in atmospheric neutrino oscillation", Super-Kamiokande Collaboration (Y. Ashie et al.), Phys. Rev. Lett. 93: 101801, 2004, **Cited 619 times.**

[31] "Measurement of single pi0 production in neutral current neutrino interactions with water by a 1.3-GeV wide band muon neutrino beam", K2K Collaboration (S. Nakayama et al.), Phys. Lett. B **61**, 255 (2005), **Cited 67 times.**

[32] "Evidence for muon neutrino oscillation in an accelerator-based experiment", K2K Collaboration (E. Aliu et al.), Phys. Rev. Lett. **94** 081802 (2005), **Cited 897 times.**

[33] "A measurement of atmospheric neutrino oscillation parameters by Super-Kamiokande I", Super-Kamiokande Collaboration (Y. Ashie et al.) et al., Phys. Rev. D71: 112005, 2005, **Cited 1060 times.**

[34] "Search for nucleon decay via modes favored by supersymmetric grand unification models in Super-Kamiokande-I", Super-Kamiokande Collaboration (K. Kobayashi et al.), Phys. Rev. D **72**, 052007 (2005), **Cited 137 times.**

[35] "An improved search for $\nu_\mu \to \nu_e$ oscillation in a long-baseline accelerator experiment", K2K Collaboration (S. Yamamoto et al.), Phys. Rev. Lett. **96**, 181801 (2006), **Cited 54 times.**

[36] "Measurement of Neutrino Oscillation by the K2K Experiment", K2K Collaboration (M. H. Ahn et al.), Phys. Rev. D **74** 072003 (2006), **Cited 466 times.**

[37] "Observation of the Anisotropy of 10 TeV Primary Cosmic Ray Nuclei Flux with the Super-Kamiokande-I Detector", The Super-Kamiokande Collaboration (G. Guillian et al.), Phys. Rev. D **75**, 062003 (2007), **Cited 135 times.**

[38] "Solar neutrino measurements in Super-Kamiokande-I", The Super-Kamiokande Collaboration (J. Hosaka et al.), Phys. Rev. D **73**, 112001 (2006), **Cited 551 times.**

[39] "Three flavor neutrino oscillation analysis of atmospheric neutrinos in Super-Kamiokande", The Super-Kamiokande Collaboration (J. Hosaka et al.), Phys. Rev. D **74**, 032002 (2006), **Cited 245 times.**

[40] "Search for Diffuse Astrophysical Neutrino Flux Using Ultra-High Energy Upward-Going Muons in Super-Kamiokande I", The Super-Kamiokande Collaboration (M. E. C. Swanson et al.), Astrophys.J. **652** 206 (2006), **Cited 18 times.**

[41] "High energy neutrino astronomy using upward-going muons in Super-Kamiokande-I", The Super-Kamiokande Collaboration (K. Abe et al.), Astrophys.J. **652**, 198 (2006), **Cited 30 times.**

[42] "A Measurement of Atmospheric Neutrino Flux Consistent with Tau Neutrino Appearance", The Super-Kamiokande Collaboration (K. Abe et al.), Phys. Rev. Lett. **97**, 171801 (2006), **Cited 163 times.**

[43] "Search for Neutral Q-balls in Super-Kamiokande II", The Super-Kamiokande Collaboration (T. Takenaga et al.), Phys. Lett. B **647**, 18 (2007), **Cited 44 times.**

[44] "Search for Supernova Neutrino Bursts at Super-Kamiokande", The Super-Kamiokande Collaboration (M. Ikeda et al.), Astrophys J. **669**, (2007) 519, **Cited 104 times.**

[45] "Study of TeV Neutrinos with Upward Showering Muons in Super-Kamiokande", The Super-Kamiokande Collaboration (S. Desai et al.), Astropart. Phys. **29**, 42 (2008), **Cited 70 times.**

[46] "Search for Matter-Dependent Atmospheric Neutrino Oscillations in Super-Kamiokande", The Super-Kamiokande Collaboration (K. Abe et al.), Phys. Rev. D **77**, 052001 (2008), **Cited 23 times.**

[47] "Solar neutrino measurements in Super-Kamiokande-II", The Super-Kamiokande Collaboration (J. P. Cravens), Phys. Rev. D **78**, 032002 (2008), **Cited 294 times.**

[48] "First Study of Neutron Tagging with a Water Cherenkov Detector", The Super-Kamiokande Collaboration (H. Watanabe et al.), Astropart. Phys. **31**, 320 (2009), **Cited 74 times.**

[49] "Search for Proton Decay via $p \to e^+\pi^0$ and $p \to \mu^+\pi^0$ in a Large Water Cherenkov Detector", The Super-Kamiokande Collaboration (H. Nishino et al.), Phys. Rev. Lett. **102**, 141801 (2009), **Cited 197 times.**

[50] "Kinematic reconstruction of atmospheric neutrino events in a large water Cherenkov detector with proton identification", The Super-Kamiokande Collaboration (M. Fechner et al.), Phys. Rev. D **79**, 112010 (2009), **Cited 23 times.**

[51] "Search for Neutrinos from GRB 080319B at Super-Kamiokande", The Super-Kamiokande Collaboration (E. Thrane et al.), Astophys. J. **697**, 730 (2009), **Cited 6 times.**

[52] "Search for Astrophysical Neutrino Point Sources at Super-Kamiokande", The Super-Kamiokande Collaboration (E. Thrane et al.), Astrophys. J. **704**, 503 (2009), **Cited 37 times.**

[53] "Atmospheric neutrino oscillation analysis with sub-leading effects in Super-Kamiokande I, II and III", The Super-Kamiokande Collaboration (R. Wendell et al.), Phys. Rev. D **81**, 092004 (2010), **Cited 320 times.**

[54] "Solar neutrino results in Super-Kamiokande-III", The Super-Kamiokande Collaboration (K. Abe et al.), Phys. Rev. D **83**, 052010 (2011), **Cited 334 times.**

[55] "Study of Non-Standard Neutrino Interactions with Atmospheric Neutrino Data in Super-Kamiokande I and II", The Super-Kamiokande

Collaboration (G. Mitsuka et al.), Phys. Rev. D **84**, 113008 (2011), **Cited 74 times.**

[56] "An Indirect Search for WIMPs in the Sun using 3109.6 days of upward-going muons in Super-Kamiokande", The Super-Kamiokande Collaboration (T. Tanaka et al.), Astrophys. J. **742**, 78 (2011), **Cited 167 times.**

[57] "Search for Differences in Oscillation Parameters for Atmospheric Neutrinos and Antineutrinos at Super-Kamiokande", The Super-Kamiokande Collaboration (K. Abe et al.), Phys. Rev. Lett. **107**, 241801 (2011), **Cited 95 times.**

[58] "Supernova Relic Neutrino Search at Super-Kamiokande", Super-Kamiokande Collaboration (K. Bays et al.), Phys. Rev. D. **85**, 052007 (2012), **Cited 101 times.**

[59] "Search for Nucleon Decay into Charged Anti-lepton plus Meson in Super-Kamiokande I and II", The Super-Kamiokande Collaboration (H. Nishino et al.), Phys. Rev. D. **85**, 112001 (2012), **Cited 66 times.**

[60] "Search for GUT monopoles at Super-Kamiokande", The Super-Kamiokande Collaboration (K. Ueno et al.), Astropart. Phys. **36**, 121 (2012), **Cited 22 times.**

After Year 2012

[61] "Search for proton decay via $p \to \mu + K^0$ in Super-Kamiokande I, II, and III", Super-Kamiokande Collaboration (C. Regis et al.), Phys. Rev. D. **86**, 012006 (2012), **Cited 51 times.**

[62] "Search for Nucleon Decay into Charged Anti-lepton plus Meson in Super-Kamiokande I and II (H. Nishino et al.)", Phys. Rev. D **85**, 112001 (2012), **Cited 123 times.**

[63] "Evidence for the Appearance of Atmospheric Tau Neutrinos in Super-Kamiokande", Super-Kamiokande Collaboration (K. Abe et al.), Phys. Rev. Lett. **110**, 181802 (2013), **Cited 101 times.**

[64] "Calibration of the Super-Kamiokande Detector", Super-Kamiokande Collaboration (K. Abe et al.), Nucl. Instrum. Meth. A **737**, 253 (2014), **Cited 75 times.**

[65] "First Indication of Terrestrial Matter Effects on Solar Neutrino Oscillation", Super-Kamiokande Collaboration (A. Renshaw et al.), Phys. Rev. Lett. **112**, 091805 (2014), **Cited 76 times.**

[66] "Search for Dinucleon Decay into Kaons in Super-Kamiokande", Super-Kamiokande Collaboration (M. Litos et al.), Phys. Rev. Lett. **112**, 131803 (2014), **Cited 14 times.**

[67] "Search for Nucleon Decay via $n \to \nu\pi^0$ and $p \to \nu\pi^0$ in Super-Kamiokande", Super-Kamiokande Collaboration (K. Abe et al.), Phys. Rev. Lett. **113**, 121802 (2014), **Cited 41 times.**

[68] "Search for Trilepton Nucleon Decay via $p \to e + \nu\nu$ and $p \to \mu + \nu\nu$ in the Super-Kamiokande Experiment", Super-Kamiokande Collaboration (V. Takhistov et al.), Phys. Rev. Lett. **113**, 101801 (2014), **Cited 14 times.**

[69] "Search for proton decay via $p \to \nu K^+$ using using 260 kiloton $\cdot$ year data of Super-Kamiokande", Super-Kamiokande Collaboration (K. Abe et al.), Phys. Rev. D **90**, 072005 (2014), **Cited 88 times.**

[70] "Supernova Relic Neutrino Search with Neutron Tagging at Super-Kamiokande-IV", Super-Kamiokande Collaboration (H. Zhang et al.), Astropart. Phys. **60**, 41 (2015), **Cited 45 times.**

[71] "Test of Lorentz invariance with atmospheric neutrinos", Super-Kamiokande Collaboration (K. Abe et al.), Phys. Rev. D **91**, 052003 (2015), **Cited 33 times.**

[72] "Limits on sterile neutrino mixing using atmospheric neutrinos in Super-Kamiokande", Super-Kamiokande Collaboration (K. Abe et al.), Phys. Rev. D **91**, 052019 (2015), **Cited 76 times.**

[73] "Search for Neutrinos from Annihilation of Captured Low-Mass Dark Matter Particles in the Sun by Super-Kamiokande", Super-Kamiokande Collaboration (K. Choi et al.), Phys. Rev. Lett. **114**, 141301 (2015), **Cited 172 times.**

[74] "Search for n - nbar oscillation in Super-Kamiokande", Super-Kamiokande Collaboration (K. Abe et al.), Phys. Rev. D **91**, 072006 (2015), **Cited 76 times.**

[75] "Search for dinucleon decay into pions at Super-Kamiokande", Super-Kamiokande Collaboration (J. Gustafson et al.), Phys. Rev. D **91**, 072009 (2015), **Cited 18 times.**

[76] "Search for Nucleon and DiNucleon Decays with an Invisible Particle and a Charged Lepton in the Final State at the Super-Kamiokande Experiment", Super-Kamiokande Collaboration (V. Takhistov et al.), Phys. Rev. Lett. **115**, 121803 (2015), **Cited 11 times.**

[77] "First measurement of radioactive isotope production through cosmic-ray muon spallation in Super-Kamiokande IV", Super-Kamiokande Collaboration (Y. Zhang et al.), Phys. Rev. D **93**, 012004 (2016), **Cited 15 times.**

[78] "Real-Time Supernova Neutrino Burst Monitor at Super-Kamiokande", Super-Kamiokande Collaboration (K. Abe et al.), Astropart. Phys. **81**, 39 (2016), **Cited 12 times.**

[79] "Solar Neutrino Measurements in Super-Kamiokande-IV", Super-Kamiokande Collaboration (K. Abe et al.), Phys. Rev. D **94**, 052010 (2016), **Cited 50 times.**

[80] "Measurements of the atmospheric neutrino flux by Super-Kamiokande: Energy spectra, geomagnetic effects, and solar modulation", Super-Kamiokande Collaboration (E. Richard et al.), Phys. Rev. D **94**, 052001 (2016), **Cited 30 times.**

[81] "Search for Neutrinos in Super-Kamiokande associated with Gravitational Wave Events GW150914 and GW151226", Super-Kamiokande Collaboration (K. Abe et al.), Astrophys. J. Lett. **830**, 1 (2016), **Cited 18 times.**

[82] "Search for proton decay via $p \to e + \pi^0$ and $p \to \mu + \pi^0$ in 0.31Megaton·years exposure of the Super-Kamiokande water Cherenkov detector", Super-Kamiokande Collaboration (K. Abe et al.), Phys. Rev. D **95**, 012004 (2017), **Cited 51 times.**

[83] "Search for nucleon decay into charged antilepton plus meson in 0.316 megaton·years exposure of the Super-Kamiokande water Cherenkov detector", Super-Kamiokande Collaboration (K. Abe et al.), Phys. Rev. D **96**, 012003 (2017), **Cited 9 times.**

[84] "Search for an Excess of Events in the Super-Kamiokande Detector in the Directions of the Astrophysical Neutrinos Reported by the IceCube Collaboration", Super-Kamiokande Collaboration (K. Abe et al.), Astrophys. J. **850**, 166 (2017), **Cited 1 times.**

[85] "Atmospheric neutrino oscillation analysis with external constraints in Super-Kamiokande I-IV", Super-Kamiokande Collaboration (K. Abe et al.), Phys. Rev. D **97**, 072001 (2018), **Cited 15 times.**

[86] "Search for Neutrinos in Super-Kamiokande associated with the GW170817 neutron-star merger", Super-Kamiokande Collaboration (K. Abe et al.), Astrophys. J. Lett. **857**, L4 (2018), **Cited 2 times.**

[87] "Search for Boosted Dark Matter Interacting With Electrons in Super-Kamiokande", Super-Kamiokande Collaboration (C. Kachulis et al.), Phys. Rev. Lett. **120**, 221301 (2018), **Cited 7 times.**

T2K EXPERIMENT

Summary from 2012 to 2018

We first summarize the results and achievements obtained during the review period. The most significant ones will be described in more details in the following sections.

- Using the electron candidate events from the first four years of data taking, T2K observed the appearance of electron neutrinos from the oscillation of muon neutrinos with 7.3σ significance [3]. In combination with the measurement of θ_{13} from the disappearance of $\bar{\nu}_e$ by reactor experiments, those data also allowed a first evaluation of the allowed regions for δ_{CP} in T2K.

- After that, T2K started analyzing simultaneously all its samples to measure more precisely δ_{CP} and the atmospheric parameters θ_{23} and Δm^2_{32} while properly accounting for the correlations between the measurements. We first realized a joint analysis of the electron and muon candidate events [4], then a joint analysis of the ν-mode and $\bar{\nu}$-mode data [5] and finally added a new appearance sample, enriched in resonant interactions, to the analysis [6].

- T2K moved to a new, more precise reconstruction algorithm for the far detector for the results presented during the summer 2017 [1]. The additional precision of this new algorithm allowed both to use a new, larger fiducial volume, and to add a new likelihood cut to reduce the main background in disappearance samples. As a result, the number of events in the appearance samples increased by 12% without decreasing purity, and the main background for disappearance samples was reduced by 50%.

- Using the results of the measurement of θ_{13} by reactor experiments, T2K presented more and more precise results on δ_{CP}. Initially only able to exclude some values of δ_{CP} at 90% CL, T2K could later report the exclusion of the conservation of CP symmetry in neutrino oscillations at 90% CL [6] and then with 2σ significance [2]. The precision of the measurement of the atmospheric parameters also increased with the different improvements and additional data, the most recent results [3] yielding $\sin^2(\theta_{23}) = 0.536^{+0.031}_{-0.046}$ and $|\Delta m^2_{32}| = (2.434 \pm 0.064) \times 10^{-3}\mathrm{eV}^2/\mathrm{c}^4$.

- Using data collected in $\bar{\nu}$-mode, T2K could also search for CP violation without using the results of the reactor experiments by comparing directly the oscillations of neutrinos and anti-neutrinos. The favored values of δ_{CP} in this case are similar to the ones obtained with constraints for the reactor experiments, although with lower statistical significance. The anti-neutrino data were also used to compare the disappearance of ν_μ and $\bar{\nu}_\mu$ [7, 8] to search for new physics, and to look for the appearance of $\bar{\nu}_e$ from the oscillations of $\bar{\nu}_\mu$.

- During this period, many cross-section measurements, important for the modelization of neutrino interactions used in oscillation analyses, were done using the near detectors, both on and off-axis. In particular, T2K reported the first measurement of ν_e cross-section at the GeV scale differential as a function of electron kinematics [9]. T2K also presented cross-section measurements for ν_μ, both inclusive and exclusive, for interactions on scintillator (CH) [10, 12, 14, 16, 17], iron [11, 15], and water [13, 18, 19]. T2K presented a first anti-neutrino cross-section measurement [20], and using this time the far detector, a measurement of the neutral current cross-section on oxygen [21].

- T2K also performed searches for physics beyond the standard model: search for oscillations due to sterile neutrinos [22] and violation of Lorentz invariance [23] in the near detectors, as well as measurement of the neutrino time of flight between J-PARC and Super-K [24]. No evidence for new physics was found.

Introduction

The Tokai to Kamioka (T2K) experiment [1] is a long baseline neutrino oscillation experiment: a man-made beam of neutrinos is used to do precise studies of the oscillations of neutrinos. Accelerated protons are used to produce the neutrino beam in the J-PARC center in the Ibaraki prefecture, which then travel 295 km to reach the Super-Kamiokande (Super-K) detector in the Gifu prefecture where neutrinos can be detected after oscillations. A complex of near detectors located 280 meters away from the proton target is used to monitor the neutrino beam, and constrain systematic uncertainties on the neutrino fluxes and interactions. T2K

*1 M. Hartz (on behalf of the T2K collaboration), T2K Neutrino Oscillation Results with Data up to 2017 Summer, KEK special seminar Aug. 4th 2017

*2 ibid.

*3 M. Wascko (on behalf of the T2K collaboration), T2K Status, Results, and Plans, Presentation at the Neutrino 2018 conference

was the first long baseline experiment to use the off-axis beam technique [4]: the beam is not aimed directly at Super-K, but in a direction making a 2.5° angle with the far detector direction. This gives increased sensitivity to neutrino oscillations while reducing the backgrounds by producing a narrow band neutrino beam centered on the energy corresponding to the first maximum of the $\nu_\mu \to \nu_e$ oscillation probability.

The initial physics goal of the experiment is to observe this $\nu_\mu \to \nu_e$ oscillation, by detecting electron neutrinos in a beam of neutrinos produced in the muon flavor. This observation would confirm the paradigm of neutrino oscillations by observing for the first time the appearance of neutrinos of a certain flavor through oscillation, and allow to measure the last unknown mixing angle at the time of the start of the experiment, θ_{13}. At the same time, T2K can produce precise measurements of the atmospheric parameters θ_{23} and Δm^2_{32} through precise study of the pattern of disappearance of the muon neutrinos.

After the appearance of electron neutrinos $\nu_\mu \to \nu_e$ has been observed, the experiment can use its ability to produce a beam of either neutrinos or anti-neutrinos to compare the oscillations of neutrinos and their antiparticles. This allows to study the main remaining open questions in neutrino oscillations (CP symmetry and ordering of the neutrino mass states) by looking at the differences between the oscillations $\nu_\mu \to \nu_e$ and $\bar{\nu}_\mu \to \bar{\nu}_e$. The experiment can also perform searches for physics beyond the standard model (sterile neutrinos, CPT violation). Finally, the near detectors allow to do a wide range of neutrino and anti-neutrino cross-section measurements.

Experimental apparatus

In J-PARC, protons are accelerated to 30 GeV by a series of three accelerators, and hit a 1.9 interaction-length graphite target. The collisions produce hadrons, in particular charged pions and kaons, which are focused by three electromagnetic horns. The hadrons then go through a 96m long decay tunnel where they decay in flight into neutrinos. A beam dump at the end of the decay tunnel stops the remaining hadrons, while high energy muons (5 GeV/c or higher) can pass through this beam dump and are measured to provide a first, indirect monitoring of the neutrino beam. The horns can be used either with a positive current (ν-mode), in which case the beam is mainly made of ν_μ, or with a negative current ($\bar{\nu}$-mode) which gives a mainly $\bar{\nu}_\mu$ beam.

The near detectors are separated into two groups. On the axis of the beam, the INGRID detector, made of fourteen identical modules is used to monitor the beam direction and rate stabilities. Each module is made of a succession of iron plates to provide large target mass (∼7.1 tons per module) and scintillator planes for detection. Using the number of events reconstructed in each module, the beam direction can be measured daily with better than 0.4 mrad accuracy. Located in the direction of Super-K, the off-axis detector ND280 is made of several detectors located inside a 0.2T magnet. The higher precision of those off-axis detectors allow to do more detailed measurements of the unoscillated neutrino beam. In neutrino oscillation analyses, the ND280 is used to provide information on the ν_μ and $\bar{\nu}_\mu$ unoscillated spectra directed at SK, constrain the dominant backgrounds, and constrain the combination of flux and interaction cross sections.

The far detector, Super-K, is a 50 kton water Cherenkov detector, shielded from atmospheric muons by 1000 m of rock, or 2700 meters-water-equivalent (m.w.e.) mean overburden. To select events corresponding to the T2K beam, Super-K is synchronized via GPS to the J-PARC beamline. Hit information within $\pm 500 \mu s$ from the beam arrival timing are used for T2K data analysis. Events where only one ring was reconstructed (corresponding to one charged particle above Cherenkov threshold) are used in oscillation analysis. Those events are separated into muon-like and electron-like events based on the light pattern of this ring, and additional selection cuts are applied to produce samples enriched in charged-current quasi-elastic interactions for which the energy of the neutrino can be better reconstructed.

Experiment status

T2K started collecting physics data in January 2010, and has now completed its 9th run, accumulating a total of 1.51×10^{21} protons on target (POT) in ν-mode and 1.65×10^{21} POT in $\bar{\nu}$-mode. The experiment ran for the first time using anti-neutrino beam in 2014, and has been alternating since between runs in ν-mode and in $\bar{\nu}$-mode. The details of the data used in the far detector analysis (slightly lower due to data quality cuts) can be found in Tab. 1. Over this period, the event rates and the beam direction were found to be consistent with the expectations and stable by the measurements of the muon monitor and the on-axis near detector. In particular, the beam direction remained stable well within the ±1mrad target.

The intensity of the proton beam has been increasing progressively over time, from a few dozens kW in the first runs to stable operation at 485 kW at the end of Run 9. Operation at more than 500 kW was also successfully demonstrated, and the beam intensity is expected to continue increasing in the future. This increase of the beam intensity coupled with improved reliability of the accelerator has allowed to progressively collect larger amounts of data over shorter periods of time as can be seen on Fig. 1.

*4 D. Beavis, A. Carroll, I. Chiang, *et al.*,Long Baseline Neutrino Oscillation Experiment at the AGS (Proposal E889),1995. Physics Design Report, BNL 52459.

Table 1. T2K data taking periods and integrated numbers of protons on target (POT) used in the far detector analysis.

Run Period	Dates	$\times 10^{20}$ POT ν	$\bar{\nu}$
Run 1	Jan.2010 - Jun.2010	0.32	–
Run 2	Nov.2010 - Mar.2011	1.11	–
Run 3	Mar.2012 - Jun.2012	1.60	–
Run 4	Oct.2012 - May.2013	3.60	–
Run 5	May.2014 - Jun.2014	0.24	0.51
Run 6	Oct.2014 - Jun.2015	0.19	3.55
Run 7	Feb.2016 - May.2016	0.48	3.50
Run 8	Oct.2016 - Apr.2017	7.17	–
Run 9	Oct.2017 - May.2018	0.20	8.79
Total	**Jan.2010 - May.2018**	**14.94**	**16.35**

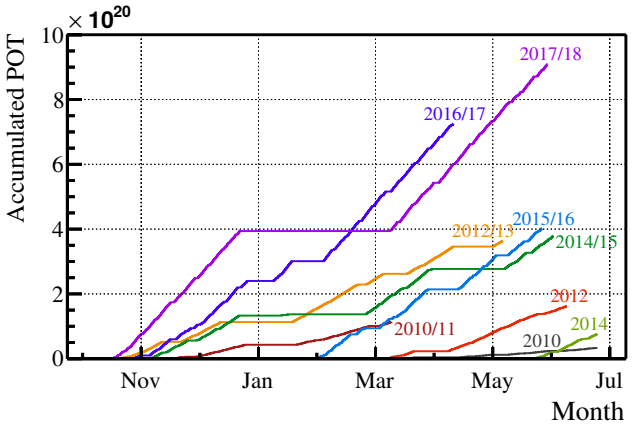

Fig. 1. Protons on target accumulated as a function of time for the nine T2K data taking periods.

Status at the beginning of the review period

At the beginning of the review period in 2012, T2K was fully built and had been collecting data for 3 years (run 1-3), collecting a total of 3.01×10^{20} POT in ν-mode. The experiment had been able to recover in 9 months after the big earthquake on March 11, 2011 and the intensity of the beam had reached 200 kW.

An analysis of the electron-like events collected during this period produced the first evidence of $\nu_\mu \to \nu_e$ appearance driven by nonzero θ_{13}, with a statistical significance of 3.2σ [5]. Using the muon-like events recorded during runs 1 and 2 (corresponding to 1.43×10^{20} POT in ν-mode), T2K had presented the first ν_μ disappearance analysis and measurements of θ_{23} and $|\Delta m^2_{32}|$ by the off-axis beam technique [2]. Assuming two-flavor $\nu_\mu \to \nu_\tau$ oscillations, the best fit values obtained were $\sin^2(2\theta_{23}) = 0.98$ and $|\Delta m^2_{32}| = 2.65 \times 10^{-3}\mathrm{eV}^2/\mathrm{c}^4$. The boundary of the 90% confidence region included the points $(\sin^2(2\theta_{23}), |\Delta m^2_{32}|) = (1.0,\ 3.1 \times 10^{-3}\mathrm{eV}^2)$, $(1.0,\ 2.2 \times 10^{-3}\mathrm{eV}^2)$,and $(0.84,\ 2.65 \times 10^{-3}\mathrm{eV}^2)$, which correspond to the largest of $(|\Delta m^2_{32}|)$, the smallest of $(|\Delta m^2_{32}|)$,and the smallest of $(\sin^2(2\theta_{23}))$ points, respectively.

*5 T. Nakaya (on behalf of the T2K collaboration), "New Results from T2K", presentation at the XXV International Conference on Neutrino Physics and Astrophysics (NEUTRINO 2012).

Neutrino oscillation results

In this section, we describe the general method by which neutrino oscillations are studied in T2K, then present the main results obtained during the review period, and finally look at perspectives for the future.

Analysis method The data observed at the far detector are compared to the predictions of the three-flavor oscillation model to make statistical inferences. To be able to make those predictions, a model of the experiment is constructed using a simulation of the flux of neutrinos reaching the detectors and a model describing the interactions of neutrinos. The predictions from this model are compared to the data observed in the near detectors to tune the predictions for the far detector by constraining the model parameters.

The fluxes of the different flavors of neutrinos reaching the detectors are predicted by a series of simulations. The flux and properties of the proton beam reaching the target are measured by the proton beam line monitors, and used as inputs for the simulations. Interactions of the protons in the graphite target and production of secondary hadrons are then simulated using the FLUKA package [6]. Measurements from hadron production experiments, in particular NA61/SHINE [7], are used to tune this part of the simulation and the out-of-target interactions. The propagation and decay in flight of the hadrons in the decay tunnel are then simulated using the GEANT3 and GCALOR [8] packages. Interactions of ν and $\bar{\nu}$ are modeled using the NEUT Monte Carlo event generator [9].

A binned likelihood fit of the events selected as charged current interactions in the near detectors is used to constrain the flux and neutrino interaction uncertainties. Those events are binned as a function of the momentum and angle of the particle reconstructed as a μ^- or a μ^+ with respect to the axis of the detector, and arranged in different samples based on the topology of the event observed in the detector. The result of this fit provides the initial values and uncertainties of the flux and interaction model parameters used in the far detector analysis to measure parameters describing neutrino oscillations.

*6 T. Bhlen *et al.*, Nucl. Data Sheets **120**, 211 (2014)
*7 N. Abgrall et al. (NA61/SHINE Collaboration), Eur. Phys. J. C **76**, 84 (2016).
*8 C. Zeitnitz and T. A. Gabriel, Proceedings of International Conference on Calorimetry in High Energy Physics (World Scientific, Corpus Christi, Texas, 1992), ISBN 9789810213039, pp. 394–404.
*9 Y. Hayato, Acta Phys. Pol. B **40**, 2477 (2009)

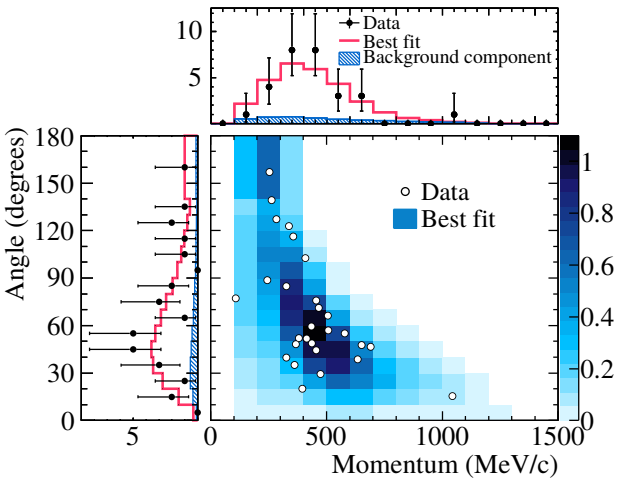

Fig. 2. Distribution of the electron momentum and angle of the ν_e candidate events from T2K run 1-4 with MC predictions at the best fit.

Observation of electron neutrino appearance T2K reported the first observation of the explicit appearance of a different neutrino flavor from neutrinos of another flavor through neutrino oscillations in 2014 [3]. The analysis used the electron-like events observed at the far detector during the runs 1 to 4 to exclude the $\theta_{13} = 0$ hypothesis. After all cuts, the total number of candidate ν_e events selected in the data was 28, which is significantly larger than the 4.92 ± 0.55 expected events for $\theta_{13} = 0$.

The neutrino oscillation parameters were evaluated using a binned extended maximum-likelihood fit. The likelihood consisted of four components: a normalization term (calculated from a Poisson distribution using the mean value from the predicted number of MC events), a term for the spectrum shape (momentum and angle of the particle reconstructed as an electron in the main analysis, reconstructed neutrino energy in the alternative analysis), a systematics term, and a constraint term (present only when results of external measurements are used to constrain the values of some of the oscillation parameters). In the fit, the likelihood was integrated over the nuisance parameters to obtain a marginalized likelihood for the parameters of interest.

The following oscillation parameters were fixed in this analysis: $\sin^2(\theta_{12})$=0.306, $\Delta m^2_{21} = 7.6 \times 10^{-5}$ eV$^2/c^4$ [10], $\sin^2(\theta_{23}) = 0.5$, $\Delta m^2_{32} = 2.4 \times 10^{-3}\mathrm{eV}^2/\mathrm{c}^4$ (from T2K run 1-3 ν_μ disappearance result [25]), and $\delta_{CP} = 0$. For the normal (inverted) hierarchy case, the best-fit value obtained with a 68% C.L. is $\sin^2(2\theta_{13}) = 0.140^{+0.038}_{-0.032}$ ($0.170^{+0.045}_{-0.037}$). Fig. 2 shows the best-fit result, and the 28 observed ν_e candidate events. The alternative analysis using reconstructed energy and a profile likelihood method produced consistent best-fit values and nearly identical confidence regions. The significance for a nonzero θ_{13} was calculated to be 7.3σ, using the difference of log likelihood values between the best-fit θ_{13} value and $\theta_{13} = 0$. An alternative method of calculating the significance, by generating a large number of toy MC experiments assuming $\theta_{13} = 0$, also returned a value of 7.3σ. These significance were calculated using fixed values for θ_{23} and δ_{CP}. For any values of these parameters consistent with their uncertainties, the significance remained above 7σ.

Comparison of the disappearance of muon neutrinos and anti-neutrinos In the standard three flavor oscillation picture, the survival probability in vacuum is identical for muon neutrinos and antineutrinos. For the neutrino energies used by T2K, matter effects do not significantly affect this symmetry. Any difference in the oscillations could therefore be interpreted as possible CPT violation and/or evidence of nonstandard interactions [11] [12]. To look for such effects, we measured separately the values of the parameters describing muon neutrino and anti-neutrino disappearance using the muon-like events collected in ν-mode and $\bar{\nu}$-mode.

In practice, the analysis allowed the antineutrino oscillation parameters for $\overline{\nu}_\mu$ disappearance to vary independently from those describing neutrino oscillations, i.e., $\theta_{23} \neq \overline{\theta}_{23}$ and $\Delta m^2_{32} \neq \Delta\overline{m}^2_{32}$, where the barred parameters govern antineutrino oscillations. All other parameters were assumed to be the same for neutrinos and antineutrinos since the muon like samples cannot constrain them. δ_{CP} was fixed to 0 as it has a negligible impact on the disappearance spectra at T2K, and θ_{13} value was constrained using the measurements by the reactor experiments. Finally, the data from ν-mode and $\bar{\nu}$-mode are analyzed together in a simultaneous fit, as the main uncertainty on the background to measure $\overline{\theta}_{23}$ and $\Delta\overline{m}^2_{32}$ in $\bar{\nu}$-mode is the size of the neutrino background, which depends on the values of θ_{23} and Δm^2_{32}.

Using data corresponding to an exposure of 7.48×10^{20} and 7.47×10^{20} protons on target (POT) for neutrinos and antineutrinos respectively, the best fit values obtained for the parameters describing neutrino oscillations assuming normal hierarchy are $\sin^2(\theta_{23}) = 0.51$ and $\Delta m^2_{32} = 2.53 \times 10^{-3}\mathrm{eV}^2/\mathrm{c}^4$ with 68% confidence intervals of 0.44 – 0.59 and 2.40 – 2.68 ($\times 10^{-3}\mathrm{eV}^2/\mathrm{c}^4$) respectively. For the antineutrino parameters, the best fit values are $\sin^2(\overline{\theta}_{23}) = 0.42$ and $\Delta\overline{m}^2_{32} = 2.55 \times 10^{-3}\mathrm{eV}^2/\mathrm{c}^4$ with 68% confidence intervals of 0.35 – 0.67 and 2.28 – 2.88 ($\times 10^{-3}\mathrm{eV}^2/\mathrm{c}^4$) respectively. In Fig. 3, the 90% confidence regions obtained for the parameters describing the disappearance of muon neutrinos and antineutrinos are compared. The confidence regions obtained in the two cases are compatible, and no

*[10] G. L. Fogli, E. Lisi, A. Marrone, A. Palazzo, and A. M. Rotunno, Phys. Rev. D **84**, 053007 (2011)

*[11] A. Kostelecky and M. Mewes, Phys. Rev. D **85**, 096005 (2012)

*[12] O. G. Miranda and H. Nunokawa, New J. Phys. **17**, 095002 (2015)

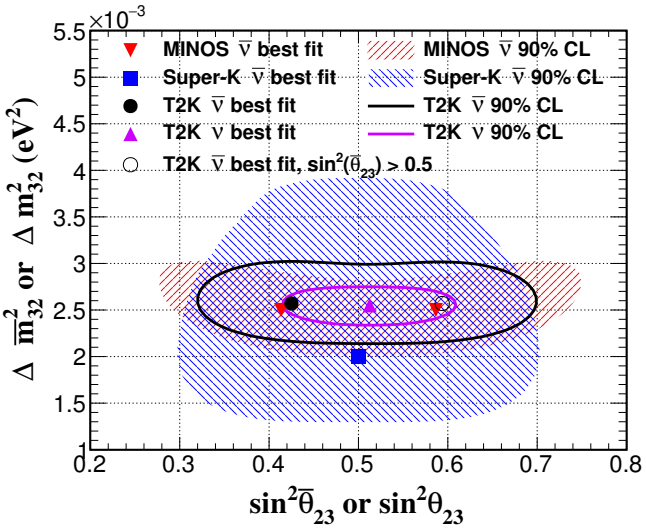

Fig. 3. 90% confidence regions for $\sin^2(\theta_{23})$ and Δm^2_{32} in ν mode (corresponding to 7.482×10^{20} POT) and $\bar{\nu}$-mode (corresponding to 7.471×10^{20} POT). Normal hierarchy is assumed. 90% confidence regions obtained by Super-K and MINOS for $\bar{\nu}$ are also shown. The best fit in the case $\sin^2(\theta_{23}) > 0.5$ is also displayed for comparison with the MINOS result.

evidence for new physics was found in this comparison. This measurement of $\overline{\theta}_{23}$ and $\Delta\overline{m}^2_{32}$ is also consistent with the results obtained by the Super-K [13] and MINOS [14] collaborations.

Exclusion of the conservation of CP symmetry in neutrino oscillations, first at 90% CL and then 2σ In 2017, T2K published results where for the first time the conservation of CP symmetry in neutrino oscillations was excluded with some noticeable statistical significance. First, a joint analysis of the one ring electron-like and muon like events collected in ν-mode and $\bar{\nu}$-mode over the runs 1 to 7 (corresponding to 7.482×10^{20} POT in ν-mode and 7.471×10^{20} POT in $\bar{\nu}$-mode) found a one dimensional 90% CL range for δ_{CP} of (-3.13, -0.39) [5], which did not include the CP-conserving values of 0 and π.

An improved result was then obtained by adding an additional sample to the far detector analysis while still using the data collected from run 1 to 7 [6]. Until that point, for the appearance channel, only the single-ring e-like interactions without additional activity in the detector were used for the oscillation analysis. The new analysis included an additional sample enriched in ν_e interactions in which the e-like ring is accompanied by a delayed Michel electron due to the decay chain $\pi^+ \to \mu^+ \to e^+$ of π^+'s produced in the neutrino interactions. This sample was only used in the ν mode and increased the statistics of the ν_e sample in Super-K by roughly 10%. With this additional sample, the one dimensional 90% CL range for δ_{CP} reduced to (-2.95; -0.44).

In the summer 2017, we presented new results [15] with the additional data collected during run 8 (for a total exposure of 14.7×10^{20} POT in ν-mode and 7.6×10^{20} POT in $\bar{\nu}$-mode) and a number of improvements in the analysis. First, the model describing neutrino interactions was improved both in terms of modelization of the interactions, and of parameterization of their uncertainties. This was in particular the case for the interaction of a neutrino with a pair of correlated nucleons which can lead to significant mis-reconstruction of the neutrino energy in the disappearance analysis. The model was also improved for the nuclear effects affecting charged current quasi-elastic interactions, which is the main interaction type in T2K, and for pion production. The second significant change is a major update of the far detector analysis, with the use of a new event reconstruction algorithm, giving better particle identification capabilities, and improved vertex and momentum resolution. Taking advantage of the increased precision of this new algorithm, the selection cuts for the fiducial volume were optimized to increase sensitivity, and a new likelihood cut was introduced for the disappearance samples to reduce the background coming from neutral current single pion interactions. The expected number of events in the different samples for the new and previous analyses can be seen in Tab. 2. The number of expected events for the e-like samples increased by about 12%, providing better sensitivity to δ_{CP}. In the case of the μ-like samples, the number of expected events slightly decreased, but the purity increased: the number of events for the signal CCQE interaction decreased by 15%, while the number for the single pion neutral current background decreased by 50%, allowing more precise measurements of the atmospheric parameters. With those improvements and additional data, we found a 2σ CL interval of (-2.98, -0.60) for δ_{CP}: the conservation of CP symmetry in neutrino oscillation was excluded with 2σ significance.

At the beginning of the summer 2018, we presented updated results [16] including data collected during the first half of the run 9. The 2σ CL interval for δ_{CP} was found to be of similar size, and slightly shifted: (-2.914, -0.642), confirming the 2σ exclusion of the conservation of CP symmetry obtained the summer before. The results of the data fit for δ_{CP} and the atmospheric parameters can be seen on Fig. 4 and 5 respectively.

Proposal for an extended run of T2K to 20×10^{21} POT (T2K-II) Following the discovery of ν_e appearance and indications that CP symmetry might be

*13 K. Abe et al. (Super-Kamiokande Collaboration), Phys. Rev. Lett. **107**, 241801 (2011)
*14 P. Adamson et al. (MINOS Collaboration), Phys. Rev. Lett. **108**, 191801 (2012)
*15 M. Hartz (on behalf of the T2K collaboration), T2K Neutrino Oscillation Results with Data up to 2017 Summer, KEK special seminar Aug. 4th 2017
*16 M. Wascko (on behalf of the T2K collaboration), T2K Status, Results, and Plans, Presentation at the Neutrino 2018 conference

Table 2. Comparison of the expected number of events in each sample for the run 1-8 exposure, between the new analysis introduced for the summer 2017 results and the previous one.

Sample	New analysis	Previous analysis
ν mode 1R e-like	69.5	56.5
ν mode 1R μ-like	261.6	268.7
ν mode CC1π^+	6.9	5.6
$\bar{\nu}$ mode 1R e-like	7.6	6.1
$\bar{\nu}$ mode 1R μ-like	62.0	65.4

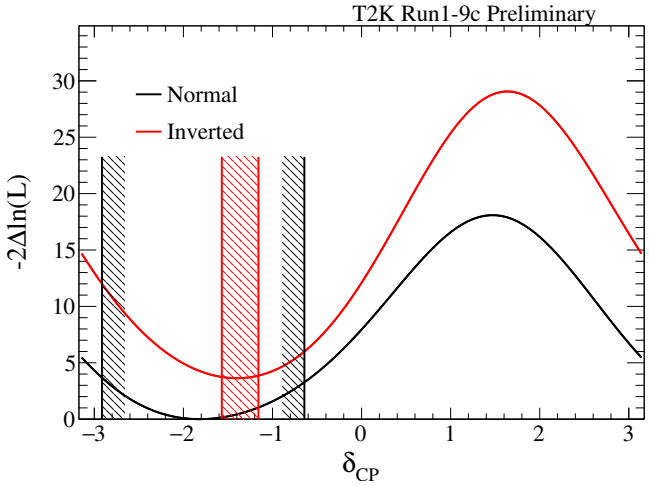

Fig. 4. Results of the fit of T2K run 1-9c data for δ_{CP} with 2σ confidence intervals obtained using the Feldman-Cousins method. The value of θ_{13} was constrained using measurements by reactor experiments.

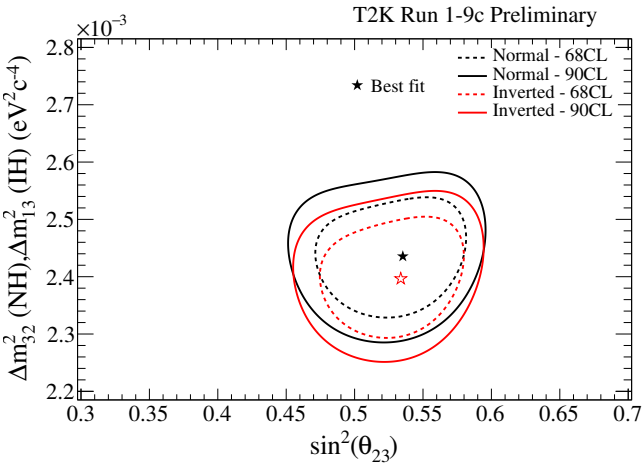

Fig. 5. 68% and 90% CL regions obtained for the atmospheric parameters using T2K run 1-9c data. The value of θ_{13} was constrained using measurements by reactor experiments.

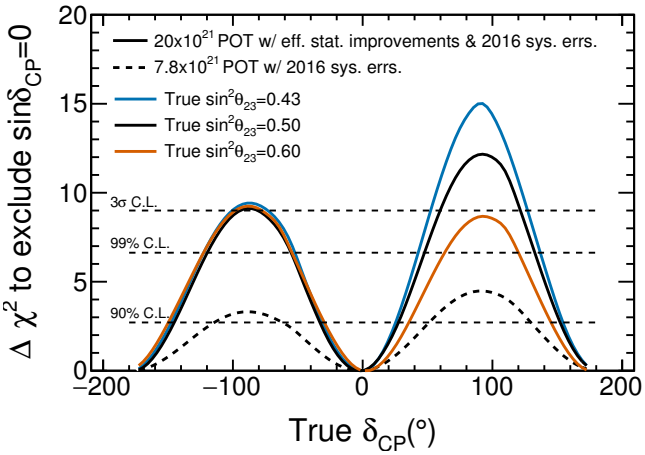

Fig. 6. Sensitivity to CP violation as function of true δ_{CP}, for the approved T2K statistics and a proposed extension of the data taking with analysis improvements. The mass hierarchy is assumed to be normal, and to be known. Sensitivities for different true values of $\sin^2(\theta_{23})$ (0.43, 0.5, 0.63) are compared.

maximally violated in neutrino oscillations, we started studying the future potential of the experiment for the study of CP violation, both with the approved POT and possible extensions of the data taking. Those studies were done with the 2016 version of the analysis, which does not include the improvements of the far detector analysis described in the previous paragraph. We assumed 50% effective statistical improvements (coming from beamline and analysis improvements such as the ones described previously for the far detector) and that the systematic uncertainties could be reduced by 1/3 from their value at the time to reach 4%. We then found that for an exposure of 20×10^{21} POT, the sensitivity to CP violation reached 3σ or higher for the the oscillation parameter region favored by the T2K results at the time (currently favored region is narrower and included in this one): $\delta_{CP}=-\pi/2$, $0.43<\sin^2(\theta_{23})<0.6$ and the mass hierarchy being normal (Fig. 6). In addition the atmospheric parameters, θ_{23} and Δm^2_{32}, can be measured with a precision of 1.7° and 1%, respectively.

As a result we proposed an extension of the T2K run to 20×10^{21} POT, T2K phase 2 [26]. A progressive increase of the intensity of the J-PARC beam, from the current ~500kW to 1.3MW would allow to collect this amount of data by 2026, when the next generation experiments DUNE and Hyper-Kamiokande are expected to start. An upgrade the off-axis near detector ND280 would allow to achieve the reduction of systematic uncertainties needed. A working group was established for this upgrade with members from Europe (including CERN neutrino group), Japan and the US, and produced a reference design for this detector with the goal of installing it in 2021. The proposal for this upgrade was submitted to the CERN SPS committee at the beginning of 2018 [17] and several beam tests are scheduled at CERN during the summer 2018, while a Technical Design Report is expected by the end of the year. In Japan, the proposal for an extended T2K run received

*[17] A. Blondel *et al.*, The T2K-ND280 upgrade proposal, CERN-SPSC-2018-001

stage 1 status at the summer 2016 J-PARC PAC.

Summary

During the review period, T2K has been taking data with an increasingly intense neutrino beam, reaching stable operation at 485 kW and collecting a total of 1.51×10^{21} POT in ν-mode and 1.65×10^{21} POT in $\bar{\nu}$-mode. Using those data, T2K presented the first observation of the appearance of a neutrino flavor through oscillations, the first exclusion of the conservation of CP symmetry in neutrino oscillations with 2σ significance and precise measurements of the atmospheric parameters θ_{23} and Δm^2_{32}. The data recorded in the near detectors were also used to perform cross-section measurements on different target materials, as well as searches for new physics. An extension of the T2K run, with the potential to exclude the conservation of CP symmetry with 3σ significance before the start of the next generation experiments DUNE and Hyper-Kamiokande, was proposed. Work has started on an upgrade of the near detector that would allow to reduce the systematic uncertainties to the level needed to reach this goal.

The Super-K detector is currently being refurbished to allow the Super-Kamiokande experiment to move to its next phase, SK-Gd, where gadolinium sulfate will be dissolved in the ultra pure water to increase the ability of the experiment to detect neutrons. Studies have been performed to evaluate the impact of this upgrade on the T2K operations, and confirmed that the experiment can continue after the upgrade. The good performance of the event reconstruction in the presence of gadolinium was confirmed by simulation based studies, and the change in event selection efficiency will be small. It is also anticipated that the increase in neutron detection efficiency will bring better understanding of the interactions of neutrinos and anti-neutrinos.

T2K collaboration

Spokesperson: Tsuyoshi Nakaya (Kyoto University)
Host institutes of the T2K experiment are the High Energy Accelerator Research Organization(KEK) and ICRR. One of the members of the Executive Committee of the experiment is from ICRR: first Masato Shiozawa until 2017, and Yoshinari Hayato since.

Institute	Country	(*)
ICRR	Japan	25
KEK	Japan	26
Kavli IPMU (WPI), University of Tokyo	Japan	4
Kobe University	Japan	3
Kyoto University	Japan	14
Miyagi University of Education	Japan	1
Okayama University	Japan	4
Osaka City University	Japan	6
Tokyo Institute of Technology	Japan	3
Tokyo Metropolitan University	Japan	2
Tokyo University of Science	Japan	2
University of Tokyo	Japan	8
Yokohama National University	Japan	4
TRIUMF	Canada	19
University of British Columbia	Canada	10
University of Regina	Canada	3

Institute	Country	(*)
University of Toronto	Canada	4
University of Victoria	Canada	1
University of Winnipeg	Canada	4
York University	Canada	5
CEA/DAPNIA Saclay	France	18
LLR Ecole polytechnique (IN2P3)	France	8
LPNHE-Paris	France	9
RWTH Aachen University	Germany	4
INFN Bari	Italy	5
INFN Roma	Italy	3
Napoli University and INFN	Italy	7
Padova University and INFN	Italy	8
IFJ PAN, Cracow	Poland	9
NCBJ, Warsaw	Poland	5
Technical University, Warsaw	Poland	5
University of Silesia, Katowice	Poland	3
Warsaw University	Poland	2
Wroclaw University	Poland	3
INR	Russia	26
IFAE, Barcelona	Spain	8
IFIC, Valencia	Spain	5
UAM, Madrid	Spain	2
Bern	Swiss	6
ETHZ	Swiss	9
University of Geneva	Swiss	12
Imperial College London	UK	15
Lancaster University	UK	12
Oxford University	UK	9
Queen Mary, University of London	UK	8
Royal Holloway, Univ. of London	UK	2
STFC/RAL/Daresbury Laboratory	UK	13
University of Glasgow	UK	4
University of Liverpool	UK	17
University of Sheffield	UK	7
University of Warwick	UK	9
Boston University	USA	2
Colorado State University	USA	8
Duke University	USA	1
Louisiana State University	USA	5
Michigan State University	USA	5
SLAC	USA	1
Stony Brook University	USA	19
University of California, Irvine	USA	3
University of Colorado	USA	5
University of Pittsburgh	USA	3
University of Rochester	USA	2
University of Washington	USA	6
IFIRSE, Quy Nhon/IOP, Hanoi	Vietnam	1

(*): Number of collaborators

Members

Staff

Kamioka Observatory

Yoichiro Suzuki, Professor (till Mar. 2014)
Masayuki Nakahata, Professor
Shigetaka Moriyama, Professor
Masato Shiozawa, Professor
Yoshinari Hayato, Assoc. Professor
Yasuhiro Kishimoto, Assoc. Professor
Hiroyuki Sekiya, Assoc. Professor
Shoei Nakayama, Assoc. Professor
Makoto Miura, Research Associate
Yusuke Koshio, Research Associate (till Mar. 2013)
June Kameda, Research Associate
Atsushi Takeda, Research Associate
Kou Abe, Research Associate
Roger Wendell, Research Associate (till Dec. 2015)
Motoyasu Ikeda, Research Associate (from Sep. 2013)
Yasuhiro Nakajima, Research Associate (from Aug. 2016)
Tomonobu Tomura, Project Research Associate (till Mar.2016)
Hidekazu Tanaka, Project Research Associate (from Jun.2012)
Lluis Magro Marti, Project Research Associate (from May, 2016)
Yo Kato, Project Research Associate (from Sep.2016)
Christophe Bronner, Project Research Associate (from May 2017)
Yosuke Kataoka, Project Research Associate (from Dec. 2017)
Takatomi Yano, Project Research Associate (from Dec. 2017)

Research Center for Cosmic Neutrinos

Takaaki Kajita, Professor
Kimihiro Okumura, Assoc. Professor
Yasuhiro Nishimura, Research Associate (from Sep. 2016)
Yasuhiro Nishimura, Project Research Associate (Apr.2012 - Sep. 2016)

Senior Fellows

Kamioka Observatory

Shigeki Tasaka (Aug. 2015 - Mar. 2017)

Postdoctorial Fellows

Kamioka Observatory

Lluis Magro Marti (Apr. 2011 - Mar. 2013)
Yo Kato (Apr. 2016 - Sep. 2016)
Guillaume Pronost (from Mar. 2016)
Yuuki Nakano (from Apr. 2017)

Graduate students

One student was awarded doctor degree and three

students earned master degrees during 2006–2012, supervised by ICRR staff members.

List of Publications

Before Year 2012

[1] K. Abe *et al.* (T2K Collaboration), "The T2K Experiment," Nucl. Instrum. Meth. A **659**, 106 (2011) doi:10.1016/j.nima.2011.06.067

From Year 2012

[2] K. Abe *et al.* (T2K Collaboration), "First Muon-Neutrino Disappearance Study with an Off-Axis Beam," Phys. Rev. D **85**, 031103 (2012) doi:10.1103/PhysRevD.85.031103. **(152 citations)**

[3] K. Abe *et al.* (T2K Collaboration), "Observation of Electron Neutrino Appearance in a Muon Neutrino Beam," Phys. Rev. Lett. **112**, 061802 (2014). doi:10.1103/PhysRevLett.112.061802. **(487 citations)**

[4] K. Abe *et al.* (T2K Collaboration), "Measurements of neutrino oscillation in appearance and disappearance channels by the T2K experiment with $6.6\text{x}10^{20}$ protons on target," Phys. Rev. D **91**, no. 7, 072010 (2015). doi:10.1103/PhysRevD.91.072010. **(281 citations)**

[5] K. Abe *et al.* (T2K Collaboration), "Combined Analysis of Neutrino and Antineutrino Oscillations at T2K," Phys. Rev. Lett. **118**, no. 15, 151801 (2017) doi:10.1103/PhysRevLett.118.151801. **(115 citations)**

[6] K. Abe *et al.* (T2K Collaboration), "Measurement of neutrino and antineutrino oscillations by the T2K experiment including a new additional sample of ν_e interactions at the far detector," Phys. Rev. D **96**, no. 9, 092006 (2017) Erratum: [Phys. Rev. D **98**, no. 1, 019902 (2018)] doi:10.1103/PhysRevD.96.092006, 10.1103/PhysRevD.98.019902. **(63 citations)**

[7] K. Abe *et al.* (T2K Collaboration), "Precise Measurement of the Neutrino Mixing Parameter θ_{23} from Muon Neutrino Disappearance in an Off-Axis Beam," Phys. Rev. Lett. **112**, no. 18, 181801 (2014) doi:10.1103/PhysRevLett.112.181801. **(255 citations)**

[8] K. Abe *et al.* (T2K Collaboration), "Updated T2K measurements of muon neutrino and antineutrino disappearance using 1.5×10^{21} protons on target," Phys. Rev. D **96**, no. 1, 011102 (2017) doi:10.1103/PhysRevD.96.011102. **(23 citations)**

[9] K. Abe *et al.* (T2K Collaboration), "Measurement of the Inclusive Electron Neutrino Charged Current Cross Section on Carbon with the T2K Near Detector," Phys. Rev. Lett. **113**, no. 24, 241803 (2014) doi:10.1103/PhysRevLett.113.241803. **(68 citations)**

[10] K. Abe *et al.* (T2K Collaboration), "Measurement of the inclusive ν_μ charged current cross section on carbon in the near detector of the T2K experiment," Phys. Rev. D **87**, no. 9, 092003 (2013) doi:10.1103/PhysRevD.87.092003 **(125 citations)**

[11] K. Abe *et al.* (T2K Collaboration), "Measurement of the inclusive ν_μ charged current cross section on iron and hydrocarbon in the T2K on-axis neutrino beam," Phys. Rev. D **90**, no. 5, 052010 (2014) doi:10.1103/PhysRevD.90.052010. **(49 citations)**

[12] K. Abe *et al.* (T2K Collaboration), "Measurement of the ν_μ charged current quasielastic cross section on carbon with the T2K on-axis neutrino beam," Phys. Rev. D **91**, no. 11, 112002 (2015) doi:10.1103/PhysRevD.91.112002. **(40 citations)**

[13] K. Abe *et al.* (T2K Collaboration), "Measurement of the electron neutrino charged-current interaction rate on water with the T2K ND280 π^0 detector," Phys. Rev. D **91**, 112010 (2015) doi:10.1103/PhysRevD.91.112010. **(10 citations)**

[14] K. Abe *et al.* (T2K Collaboration), "Measurement of the ν_μ charged-current quasielastic cross section on carbon with the ND280 detector at T2K," Phys. Rev. D **92**, no. 11, 112003 (2015) doi:10.1103/PhysRevD.92.112003. **(33 citations)**

[15] K. Abe *et al.* (T2K Collaboration), "Measurement of the muon neutrino inclusive charged-current cross section in the energy range of 1-3 GeV with the T2K INGRID detector," Phys. Rev. D **93**, no. 7, 072002 (2016) doi:10.1103/PhysRevD.93.072002. **(13 citations)**

[16] K. Abe *et al.* (T2K Collaboration), "Measurement of double-differential muon neutrino charged-current interactions on C_8H_8 without pions in the final state using the T2K off-axis beam," Phys. Rev. D **93**, no. 11, 112012 (2016) doi:10.1103/PhysRevD.93.112012. **(43 citations)**

[17] K. Abe *et al.* (T2K Collaboration), "Measurement of Coherent π^+ roduction in Low Energy Neutrino-Carbon Scattering," Phys. Rev. Lett. **117**, no. 19, 192501 (2016) doi:10.1103/PhysRevLett.117.192501. **(16 citations)**

[18] K. Abe *et al.* (T2K Collaboration), "First measurement of the muon neutrino charged current

single pion production cross section on water with the T2K near detector," Phys. Rev. D **95**, no. 1, 012010 (2017) doi:10.1103/PhysRevD.95.012010. **(19 citations)**

[19] K. Abe *et al.* (T2K Collaboration), "First measurement of the ν_μ charged-current cross section on a water target without pions in the final state," Phys. Rev. D **97**, no. 1, 012001 (2018) doi:10.1103/PhysRevD.97.012001. **(7 citations)**

[20] K. Abe *et al.* (T2K Collaboration), "Measurement of $\bar{\nu}_\mu$ and ν_μ charged current inclusive cross sections and their ratio with the T2K off-axis near detector," Phys. Rev. D **96**, no. 5, 052001 (2017) doi:10.1103/PhysRevD.96.052001 **(4 citations)**

[21] K. Abe *et al.* (T2K Collaboration), "Measurement of the neutrino-oxygen neutral-current interaction cross section by observing nuclear deexcitation γ rays," Phys. Rev. D **90**, no. 7, 072012 (2014) doi:10.1103/PhysRevD.90.072012. **(21 citations)**

[22] K. Abe *et al.* (T2K Collaboration), "Search for short baseline ν_e disappearance with the T2K near detector," Phys. Rev. D **91**, 051102 (2015) doi:10.1103/PhysRevD.91.051102. **(18 citations)**

[23] K. Abe *et al.* (T2K Collaboration), "Search for Lorentz and CPT violation using sidereal time dependence of neutrino flavor transitions over a short baseline," Phys. Rev. D **95**, no. 11, 111101 (2017) doi:10.1103/PhysRevD.95.111101. **(6 citations)**

[24] K. Abe *et al.* (T2K Collaboration), "Upper bound on neutrino mass based on T2K neutrino timing measurements," Phys. Rev. D **93**, no. 1, 012006 (2016) doi:10.1103/PhysRevD.93.012006. **(4 citations)**

[25] K. Abe *et al.* (T2K Collaboration), "Measurement of Neutrino Oscillation Parameters from Muon Neutrino Disappearance with an Off-axis Beam," Phys. Rev. Lett. **111**, no. 21, 211803 (2013) doi:10.1103/PhysRevLett.111.211803. **(130 citations)**

[26] K. Abe *et al.*, "Proposal for an Extended Run of T2K to 20×10^{21} POT", arXiv:1609.04111 [hep-ex]

XMASS EXPERIMENT

Introduction

XMASS is a multi-purpose experiment using liquid xenon which aims at the detection of cold dark matter, the search for neutrinoless double beta decay, and the detection of low energy solar neutrinos. The name XMASS stands for these three goals: Xenon detector for weakly interacting MASSive particles, Xenon neutrino MASS detector for double beta decay, and Xenon MASsive detector for Solar neutrino.

Astronomical observations suggest that there is dark matter (non-luminous particles with mass) in the universe. One of the most likely candidates for dark matter is a weakly interacting massive particle (WIMP), for example the lightest supersymmetric particle. A recoil of a xenon nucleus from an interaction with dark matter will produce scintillation light in liquid xenon.

The Super-Kamiokande experiment shows that neutrinos have mass. However, we do not yet know the absolute mass of the neutrinos and whether neutrinos are Majorana type or Dirac type. Xenon nuclei with mass number 136 are one of the double beta decay nuclei which are best suited for this research.

The energy spectrum of the higher energy solar neutrinos is measured by Super-Kamiokande, SNO, and Borexino, and that of low energy solar neutrinos (pp neutrinos, etc.) remains important to be measured and monitored. With 10 ton of liquid xenon, one would be able to detect pp neutrinos and ^{7}Be neutrinos by ν+e scattering with a rate of 10 events/day and 5 events/day, respectively.

For all these purposes, background caused by gamma rays which come from outside of the liquid xenon needs to be suppressed. The key idea to reduce this background is that gamma rays can be absorbed by liquid xenon itself (self-shielding) [1]. A sphere of liquid xenon absorbs low energy gamma rays from the outside within 10-20 cm and thus provides for low background in the central volume. WIMPs and neutrinos, however, interact throughout the detector. Therefore, if the vertices of the events can be reconstructed, WIMPs and neutrinos can be observed in a low background environment by extracting only events observed deep inside the detector. Event reconstruction can be accomplished by observing photons with photo multipliers mounted surrounding the liquid xenon. Liquid xenon has the following advantages to realize this idea:

- With the high atomic number ($Z = 54$) and the high density ($\sim 3\,\mathrm{g/cm^3}$) of liquid xenon, external gamma-rays can be absorbed in a short distance from the detector wall (self-shielding).
- Its large light yield of 42,000 photons/MeV, which is as good as that of NaI(Tl) scintillator, enables good event reconstruction as well as the detection of small energy signals like those from dark matter recoil.
- 175 nm scintillation light of liquid xenon can be read out by photomultiplier tubes (PMTs) with a bi-alkaline photocathode and a quartz window.
- Purification is easier than for other materials (e.g. distillation is possible).
- Isotope separation is possible. It is possible to enrich ^{136}Xe for double beta decay or deplete ^{136}Xe for solar neutrino measurements.

We designed and started to construct the first XMASS detector (100 kg FV) for dark matter searches from 2007. The detector started commissioning in 2010 for a commissioning phase. The data consist of calibration data, test runs to understand the detector performance, and normal runs for dark matter searches. Based on the data we found that we could improve the background in the detector by covering parts of its inner surface structures, where natural radioactive contaminations were found. This motivated refurbishment work which started in 2013. After the refurbishment, we started to take data with the improved detector for more than four years, until now.

Summary from 2012 to 2018

Notable achievements in the past six years were:

- Accumulating the largest exposure of a liquid xenon detector for dark matter searches. With the large and stable XMASS-I detector, a total exposure of more than 800 days $\times$ 830 kg is obtained. This is particularly useful to search for annual modulation caused by dark matter particle interactions.
- The highest photoelectron yield among liquid xenon dark matter detectors, $\sim$14 PE/keV electron equivalent. It enables a very low energy threshold necessary for low mass WIMP searches.
- The lowest radon background. A low level of radon background is crucial for future dark matter searches as well as detecting pp-solar neutrino. At $\sim$ 9 μBq/kg-LXe just one order of magnitude improvement on this background would enable XMASS to observe pp-solar neutrinos.

- Particle identification (PID) discriminating between electrons and gammas has been achieved utilizing the difference in scintillation waveform at various electron energies. This is most effective around 60 keV and was used for several important searches of new physics signatures in this energy range.

In addition to improving the detector performance as described above, notable physics results in dark matter, nuclear physics, and astroparticle physics were obtained:

- Dark matter physics
  - We conducted a search for light dark matter with masses below 20 GeV/c^2 using low-threshold data [9] and a search for dark matter with masses in the range from 20 GeV/c^2 to 10 TeV/c^2 using event vertex reconstruction [10]. Our limit 2.2×10^{-44} cm^2 for a 60 GeV/c^2 WIMP. While these results are not the most stringent LXe results, they are the only ones from a single-phase detector and thus complementary to the mainstream ones.
  - Searches for inelastic scattering of dark matter particles on the isotope ^{129}Xe were carried out [11, 12]. We significantly improved the limit to 4.1×10^{-39} cm^2.
  - A searches for dark matter related annual modulation due to the Earth's rotation around the Sun was first published on 1 year of data [13] and improved on 2.5 years of data [14] to examine the signal claimed by DAMA/LIBRA. We did not find any significant modulation amplitude in the data for periodicity with periods between 50 and 600 days. The obtained positive upper limit for the amplitude is $(1.3\text{–}3.2)\times10^{-3}$ /day/kg/keV$_{ee}$ (2–6 keV$_{ee}$), and is the most stringent above 3.0 keV$_{ee}$.
  - Bosonic superweakly interacting massive particles (super-WIMPs) are warm dark matter candidate. They are much lighter than usual WIMPs and may help with some issues in the CDM senario. We published the first experimental search [15] for super-WIMPs and excluded the possibility that such particles constitute all of dark matter. A improved search carried out later set the most stringent upper limit [16].
- Nuclear physics
  - We searched for ^{124}Xe double electron-capture and found no signal [17, 18] . This allowed us to set the most stringent limit to date. Our lifetime limit made some theoretical predictions untenable.
- Astorparticle physics
  - We searched for solar axions produced via $e+\gamma\rightarrow e+a$ [19]. No axion signal was observed and we set the best direct experimental limit on g_{aee}.
  - Axions predicted in some theories with large extra dimensions can be produced in the Sun. Such KK axions were searched for by annual modulation with our distance to the Sun. We thus set the first experimental constraint on KK axion-photon coupling [20].
  - We investigated the possibility to detect galactic supernova neutrinos via coherent elastic neutrino-neucleus scatting in the XMASS-I detector [21]. The total number of events integrated over about 18 s after the explosion of a supernova10 kpc away from the Earth is expected to be 3.5–21.1, while background in the same time window would be negligible.

In the following sections, a description of the XMASS-I detector, its refurbishment, more details of the physics results, and ongoing activities towards future direct dark matter searches are given.

The XMASS-I detector

XMASS-I is a single phase LXe scintillator detector located underground (2700 m water equivalent) at the Kamioka Observatory [7]. Fig. 1 shows a picture of the central part of the XMASS-I detector. It contains ~830 kg of LXe in its active volume. This volume is viewed by 630 hexagonal and 12 cylindrical Hamamatsu R10789 PMTs arranged on an 80 cm diameter pentakisdodecahedral OFHC PMT holder. A total photocathode coverage of more than 62% is achieved. This almost PMT holder is contained in a double-walled vessel also made of oxygen free high conductivity (OFHC) copper. The waveforms in each PMT are recorded by CAEN V1751 waveform digitizers with 1 GHz sampling rate and 10 bit resolution. The detector is calibrated regularly with a ^{57}Co source [8] inserted along the central vertical axis of the detector. By the data taken with the ^{57}Co source at the center of the detector volume, the photoelectron (PE) yield was determined to be ~14 PE/keV. Two different energy scales were used: keVee represents an electron equivalent energy, and keVnr denotes the nuclear recoil energy. In order to shield the LXe detector from external gammas, neutrons, and muon-induced BG, the copper vessel was placed at the center of a ϕ 10 m × 10.5 m cylindrical tank filled with pure water (Fig. 2). The water tank is equipped with 72 Hamamatsu R3600 20-inch PMTs to provide both an active muon veto and passive shielding against those BG sources. XMASS-I was the first direct detection dark matter experiment equipped

Fig. 1. PMT holders and backside of PMTs

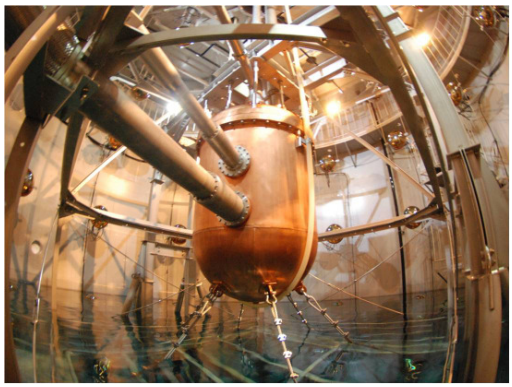

Fig. 2. Detector with copper vessel and an inner view of the water shield

with such an active water Cherenkov shield. The LXe and water Cherenkov detectors are henceforth called the Inner Detector (ID) and the Outer Detector (OD), respectively.

Refurbishment of the detector

During the commissioning data-taking, we found that the majority of events at low energy originated from radioactive contamination in the aluminum seal of the photomultiplier tube (PMT) window. In order to reduce the impact of this BG, and also to understand the origins of the background correctly for future detector design, the detector was refurbished. As we will see in the following section, the background in the fiducial volume caused by the aluminum seal was successfully suppressed and found to be minor after this refurbishment.

In this refurbishment, the contaminated parts of the PMTs were covered with copper rings and plates in order to stop scintillation lights and radiation caused by this contamination. The PMTs were cleaned with acid

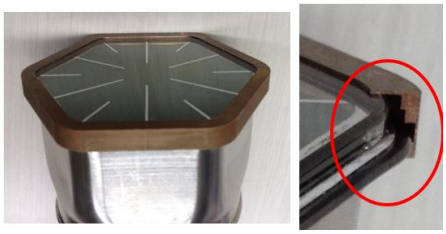

Fig. 3. The PMTs with the copper ring. Right figure shows the edge of PMT window with a half of the copper ring. The aluminum seal of the PMT window is covered by the ring to stop scintillation lights and radiations from the contaminations in the seal.

Fig. 4. The inner surface of the detector before (left) and after (right) of the refurbishment. The thin plates are added to covers the gaps made by the rings. Shadowing effect by gaps around the aluminum seal was the cause of the BGs.

and the copper parts were electropolished in order to remove possible surface contamination. Fig. 3 shows a PMT with a copper ring. The two photos in Fig. 4 show the inner surface of the detector before and after the refurbishment. After a year of refurbishing the detector, data-taking resumed in November 2013. Fig. 5 shows the background energy spectrum before and after refurbishment. The background level was reduced by one order of magnitude as expected from a study before refurbishment.

Search for WIMP dark matter

WIMPs are one of the well-motivated dark matter candidates and are thought to be observable through nuclear recoils produced in their elastic scattering interactions with target nuclei. Although many theories

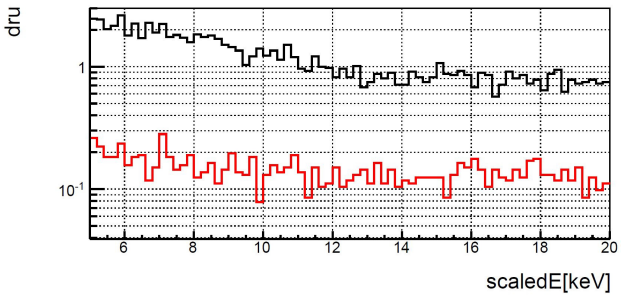

Fig. 5. The observed energy spectrum of background befor (black) and after (red) the refurbishment. One order of magnitude reduction was achieved by the refurbishment.

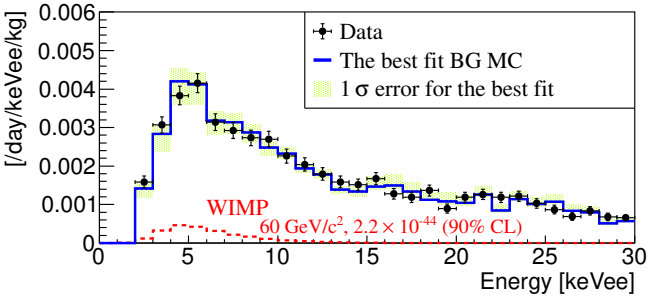

Fig. 6. Observed energy spectrum from 705.9 days of the XMASS fiducial volume data overlaid with the best-fit BG estimate. The expected 60 GeV/c^2 WIMP spectrum at a spin-independent WIMP-nucleon cross section of 2.2×10^{-44} cm^2 is also shown.

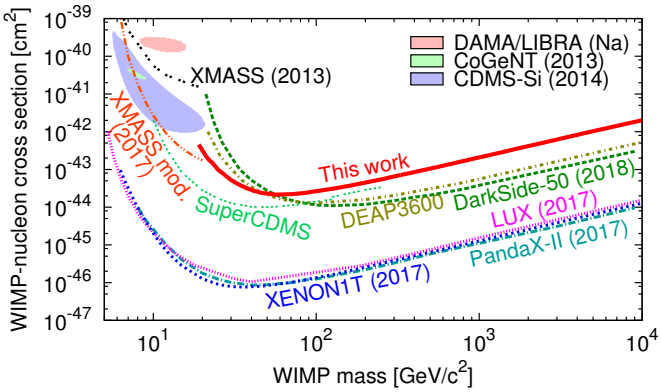

Fig. 7. Spin-independent WIMP-nucleon cross section as a function of the WIMP mass. The red solid curve represents the 90% CL limit obtained from the XMASS fiducial volume data. Our limits derived from the full volume spectrum (black dashed) as well as from the annual modulation search (red dash-dot-dot) are also shown.

beyond the Standard Model of particle physics predict WIMPs with mass larger than 100 GeV/c^2, some experiments indicate a possible WIMP signal with a lighter mass of ∼10 GeV/c^2. Therefore, we first performed a search for low-mass WIMPs using the 6.7 live days of data taken in February 2012 [9]. In order to achieve a low energy threshold of 0.3 keV$_{ee}$, the full LXe volume was analyzed with a simple event selection and without discriminating between nuclear-recoil and electron recoil events. The observed spectrum did not have any feature consistent with WIMP signals, and hence we set a 90% CL upper limits on the spin-independent WIMP-nucleon cross section for WIMPs with masses below 20 GeV/c^2. This result excluded part of the parameter space allowed by other experiments.

We also conducted a search for WIMPs with masses between 20 GeV/c^2 and 10 TeV/c^2 using 705.9 live days of data collected between November 2013 and March 2016 [10]. The event vertex was reconstructed based on the number of PEs in each PMT, and a fiducial volume containing 97 kg of xenon was established by requiring a radial distance from the center of the LXe detector within 20 cm. To search for the WIMP dark matter signal in our fiducial volume data, we performed a chi-square fit of the observed energy spectrum with the expected signal and BG spectra in the 2–15 keV$_{ee}$ energy range. Fig. 6 shows the energy spectrum of the data and the best-fit BG estimate. The event rate in the fiducial volume after data reduction was $(4.2\pm0.2)\times10^{-3}$ /day/kg/keV$_{ee}$ at 5 keV$_{ee}$, with a signal efficiency of 20%. All remaining events are consistent with our background evaluation, most of the "mis-reconstructed events" originated from ^{210}Pb in the copper plates lining the detector's inner surface, but not from the aluminum seal of the PMTs identified before. Hence, the 90% CL upper limit on the spin-independent WIMP-nucleon cross section was derived as a function of mass as shown in Fig. 7. Our lowest limit is 2.2×10^{-44} cm^2 for a 60 GeV/c^2 WIMP, and this is the most stringent constraint from a single-phase LXe detector.

Inelastic scattering that excites low-lying nuclear states in suitable target nuclei provides another avenue to probe WIMP dark matter. The observation of inelastic scattering of WIMPs on nuclei would imply a spin-dependent interaction mechanism as well as that WIMPs have spin. ^{129}Xe has the lowest-lying excited nuclear state at 39.58 keV and almost the highest natural abundance of 26.4% among the xenon isotopes. We searched for such inelastic scattering of WIMPs on ^{129}Xe using 132.0 live days of data collected between December 2010 and May 2012 with a restricted target mass of 41 kg [11]. No significant excess of events was observed, and hence a 90% CL upper limit on the spin-dependent WIMP-neutron cross section was derived (blue dashed in Fig. 8). This limit was the first derived exclusively from data on inelastic scattering. A further search was conducted using new data collected between November 2013 and July 2016 [12]. The total live time in this data set amounts to 800.0 days and the fiducial xenon mass was enlarged to 327 kg. The preliminary result indicated no significant signal for inelastic scattering of WIMPs, and we set a 90% CL upper limit on the cross section with the best limit of 4.1×10^{-39} cm^2 at 200 GeV/c^2 (red solid in Fig. 8). This limit is the most stringent among the WIMP searches via inelastic scattering.

Search for annual modulation

The count rate for a dark matter signal is expected to exhibit annual modulation due to the Earth's motion around the Sun, and this annual modulation would be a strong signature for dark matter. The DAMA/LIBRA experiment observed annual modulation of its event rate at 9.3σ significance in data collected over 14 annual cycles with 100–250 kg of NaI(Tl). However, the interpretation of the result as a dark matter signature is in question because of tension with other

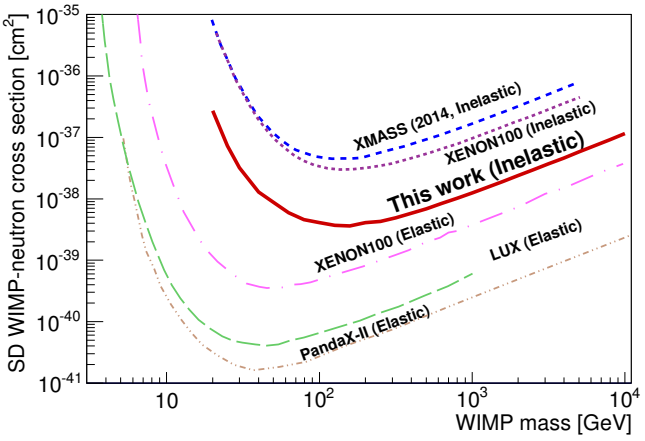

Fig. 8. Spin-dependent WIMP-neutron cross section as a function of the WIMP mass. The blue dashed represents the 90% upper limit using 132.0 days of data, while the red solid shows the preliminary 90%CL upper limits using the 800.0 days of data. The other experimental constraints are derived from elastic scattering data.

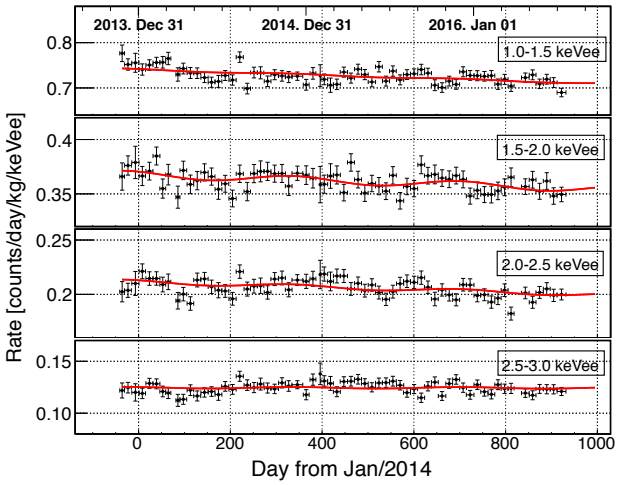

Fig. 9. Observed count rate as a function of time in the 1.0-3.0 keV$_{ee}$ energy range after correcting for relative efficiency. The error bars show the statistical uncertainty. The red solid curves represent the best-fit result for a model-independent analysis.

direct detection experiments. We conducted a search for an annual modulation signal in the full 832 kg LXe volume of XMASS-I using data taken after the detector refurbishment. We analyzed 359.2 live days of data collected between November 2013 and March 2015 in the first publication [13], and we published the second result including more than one year of additional data collected until July 2016, which resulted in a total of 800.0 live days [14].

The observed count rate after cuts as a function of time in the energy region between 1.0 and 3.0 keV$_{ee}$ is shown in Fig. 9. In the figure, the data points are corrected for relative efficiency based on the best-fit parameters. To account for changing BG rates due to long-lived isotopes such as ^{60}Co and ^{210}Pb, we modeled the BG time variation using a linear function.

Fig. 10 shows the best-fit amplitudes as a function of energy after correcting for efficiency. A hypothesis test was done using the χ^2 difference $(\chi^2_0 - \chi^2_1)$ between the modulation hypothesis and the null hypothesis. It gave a p-value of 0.11 for the null hypothesis in the 1.0–20 keV$_{ee}$ energy range. DAMA/LIBRA obtained the modulation amplitude of $\sim 2\times10^{-2}$ /day/kg/keV$_{ee}$ in the 2.0–3.5 keV$_{ee}$ energy range, and XENON100 reported the amplitude of $(1.67\pm0.73)\times 10^{-3}$ /day/kg/keV$_{ee}$ in the 2.0–5.8 keV$_{ee}$ energy range. We obtained a positive upper limits of (1.3–3.2)$\times10^{-3}$ /day/kg/keV$_{ee}$ in the same energy region and obtained the most stringent constraint above 3.0 keV$_{ee}$.

A frequency analysis was also conducted to find any periodicity in the 1–6 keV$_{ee}$ energy range where significant amplitudes were observed by DAMA/LIBRA. We used the χ^2 difference $(\chi^2_0 - \chi^2_1)$ as a test statistics to calculate the significance of the signal for each periodicity, Fig. 11 shows the result from the observed data together with the expected $\pm1\sigma$ and $\pm2\sigma$ local sig-

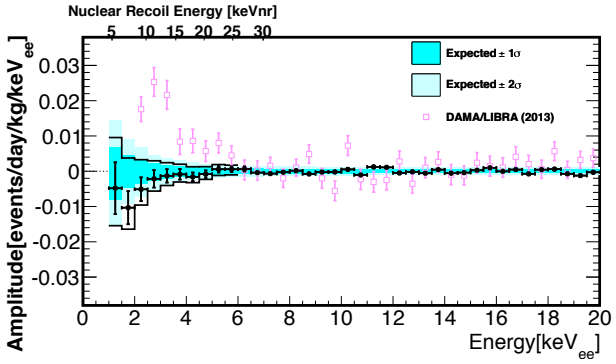

Fig. 10. Observed modulation amplitude as a function of energy for the model independent analysis (circle). The solid lines represent the XMASS 90% positive (negative) upper limits on the modulation amplitude. The $\pm1\sigma$ and $\pm2\sigma$ bands represent the expected sensitivity on the amplitude.

nificance bands from the dummy samples without any modulation signal. Taking into account the "look elsewhere effect," we calculated the global significance as indicated in the figure. No significant periodicity was found between 50 and 600 days.

Search for bosonic super-WIMP dark matter

Although WIMP dark matter is a well-motivated model and fits the cold dark matter paradigm, simulations based on this cold dark matter scenario expect a richer structure on galactic scales than is observed. Furthermore, there is so far no evidence of supersymmetric particles at the LHC, and therefore, it is important to also investigate other dark matter candidates. This leads to an interest in considering lighter and more

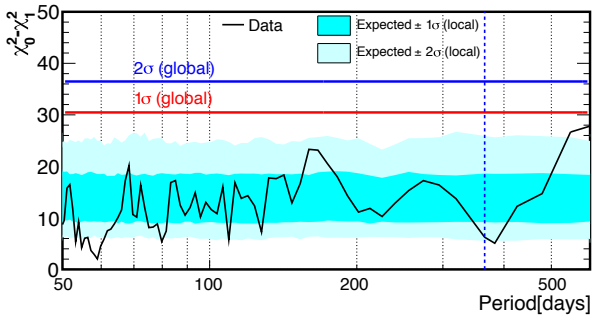

Fig. 11. The χ^2 difference, $\chi^2_0 - \chi^2_1$, as a function of period for the observed data in the 1–6 keV$_{ee}$ energy range. The expected bands for the local $\pm 1\sigma$ and $\pm 2\sigma$ significance and lines for the global 1σ and 2σ significance are also shown.

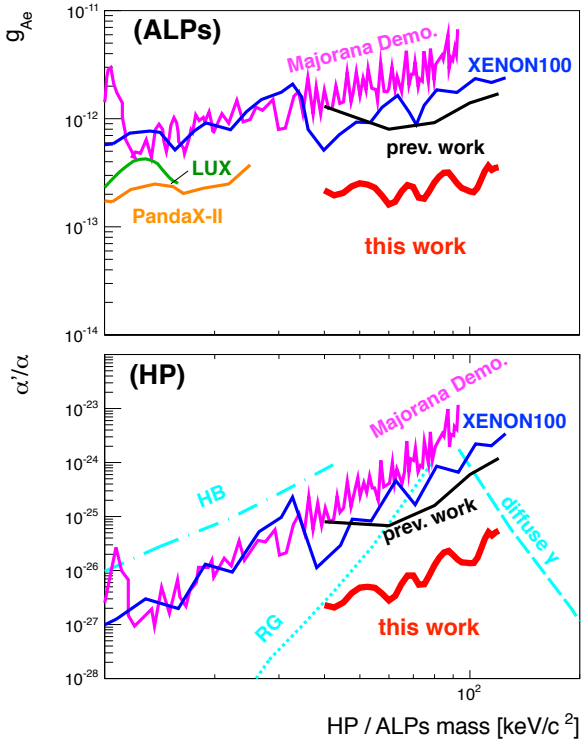

Fig. 12. Obtained 90% C.L. upper limits on coupling constants for electrons and pseudoscalar super-WIMPs (top) and for electrons and vector super-WIMPs (bottom).

weakly interacting particles such as super-WIMPs, a warm dark matter candidate. Bosonic super-WIMPs, namely hidden photons and axion-like particles, are experimentally interesting since their absorption in a target material would deposit an energy essentially equivalent to the super-WIMP's rest mass.

We conducted a search for vector and pseudoscalar super-WIMPs in the 40–120 keV/c^2 mass range first with a 41 kg×132.0 days exposure [15]. No significant excess above background was observed, and hence a 90% CL upper limit on coupling constants for pseudoscalar bosons and vector bosons was obtained (black solid in Fig. 12). This was the first direct detection experiment exploring the vector super-WIMPs and the obtained limit for the vector super-WIMPs excludes the possibility that such particles constitute all of the dark matter. The absence of the signal also provides the most stringent direct constraint on the coupling constant of pseudoscalar dark matter to electrons. This result was published in Physical Review Letters, selected as an Editors' Suggestion. An improved search was then performed with a 327 kg×800.0 days exposure [16]. As a result of fitting the energy spectrum with the expected signal and background, no significant signal was found and the obtained upper limits (red solid in Fig. 12) are the most stringent in both direct and indirect searches to date.

Search for ^{124}Xe double electron capture

Natural xenon contains ^{124}Xe (abundance 0.095%) which undergoes double electron capture: the simultaneous capture of two orbital electrons of the atom in the nucleus. Measurement of its two-neutrino mode would provide a new reference for the calculation of nuclear matrix elements while observation of its neutrinoless mode would be evidence for the Majorana nature of the neutrino. In the case of two-neutrino double K-shell electron capture ($2\nu 2$K) on ^{124}Xe, the total energy deposition is 63.6 keV provided by atomic X-rays and/or Auger electrons. The predicted half-live of ^{124}Xe against $2\nu 2$K is spread over a wide range between 10^{20} and 10^{24} years.

We performed a search for $2\nu 2$K on ^{124}Xe with a fiducial xenon mass of 41 kg (containing 39 g of ^{124}Xe) using 132.0 live days of data [17]. After all cuts, 5 events remained in the signal region while the expected background was 5.3 ± 0.5 events. This allowed us to set the most stringent lower limit on this half-life of $T_{1/2}^{2\nu 2K} > 4.7 \times 10^{21}$ years at 90% CL (magenta dashed in Fig. 13). An improved search was further conducted with an enlarged fiducial xenon mass of 327 kg (containing 311 g of ^{124}Xe) using 800.0 live days of data [18]. We also developed a novel method for discriminating the $2\nu 2$K signal from the β-ray background using LXe scintillation time profiles. As a result of the energy spectrum fitting with the expected signal and background spectra in the 30–200 keV$_{ee}$ energy range, no significant signal was found and we set a 90% CL lower limit on $T_{1/2}^{2\nu 2K}$ of 2.1×10^{22} years. As shown in Fig. 13, the present result gives a lower limit that is stronger by a factor 4.5 over our previous result, and gives the most stringent experimental constraint reported to date.

Search for solar axions

Axion would be produced in the Sun through various mechanisms; here, we focus on Compton scattering of photons on electrons, $e + \gamma \to e + a$, and bremsstrahlung

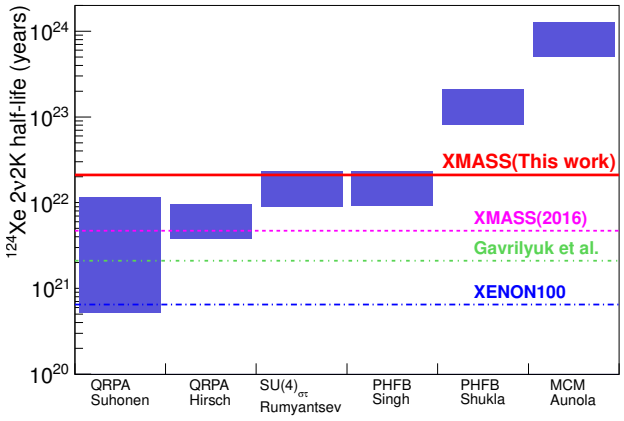

Fig. 13. 90% CL exclusion limits on the ^{124}Xe 2ν2K half-life overlaid with the theoretical calculations. For the theoretical predictions, the reported 2νECEC half-lives are converted to 2ν2K half-lives, divided by the branching ratio for the two electrons being captured from the K-shell, P_{2K}=0.767. The lower and upper edges of the bands correspond to $g_A = 1.26$ and $g_A = 1$, respectively.

of axions from electrons, $e+Z \rightarrow e+a+Z$. We searched for such axions through the axio-electric effect, an analog of the photo-electric effect, using the 6.7 live days of the full LXe volume data [19]. No prominent feature of an axion signal was observed above background and a 90% CL upper limit on the axion-electron coupling constant was derived as $g_{aee} < 5.4 \times 10^{-11}$ for axions with masses below 1 keV/c^2. This was the best direct experimental limit on g_{aee} at that time, and the limit was close to the one obtained theoretically based on consistency between the observed and expected solar neutrino fluxes.

In theories with large extra dimensions, axions could propagate in the extra dimensions beyond the 4-dimensional spacetime and would acquire Kaluza-Klein (KK) excitations, which could be observed as particles with heavier masses in the standard spacetime. The KK axions can be produced in the Sun via the Primakoff effect ($\gamma Z \rightarrow aZ$) and the photon coalescence mechanism ($\gamma\gamma \rightarrow a$). While most of the produced KK axions escape from the solar system, a small fraction can be gravitationally trapped in orbits around the Sun and decay into two photons inside the detector. The event rate of the KK axion decays would modulate annually since the expected number density of the trapped KK axions falls off as r^{-4}, where r is the distance from the Sun. We looked for the decay of these solar KK axions using 832 kg×359.2 days of data by annual modulation [20]. No significant amplitude excess was found, and therefore a 90% confidence level exclusion limit was set on the KK axion-photon coupling constant $g_{a\gamma\gamma}$ as a function of the KK axion number density. This is the first experimental constraint on KK axions.

Other important studies

Detectability of galactic supernova neutrinos

Coherent elastic neutrino-nucleus scattering (CEvNS) is a process in which a neutrino with an energy on the order of MeV interacts with all nucleons in a nucleus coherently, resulting in a large cross section approximately proportional to the square of the number of neutrons in the target nucleus. This interaction is sensitive to all flavors of neutrinos. We investigated the possibility to detect galactic supernova neutrinos via CEvNS in the XMASS-I detector [21]. The total number of events integrated over about 18 s after the explosion of a supernova 10 kpc away from the Earth was expected to be 3.5–21.1, depending on the supernova model used to predict the neutrino flux, while the number of background events in the same time window was measured to be negligible. In case of a supernova explosion as close as Betelgeuse, the total number of observable events can be more than $\sim 10^4$, making it possible to distinguish different supernova models by examining the evolution of the neutrino event rate in XMASS.

Measurement of the LXe scintillation time profile

The time profile of LXe scintillation could potentially be used for particle identification and vertex reconstruction. We measured the scintillation time profile for gamma-ray induced events with ^{55}Fe, ^{241}Am, and ^{57}Co sources [22]. In this analysis two decay components, τ_1 and τ_2, were assumed. The decay constant τ_2 increased from 27.9 ns to 37.0 ns as the gamma-ray energy increased from 5.9 keV to 122 keV. A fast decay component with $\tau_1 \sim 2$ ns was necessary to reproduce the data. Energy dependencies of τ_2 and the fraction of the fast decay component were studied as a function of the kinetic energy of the electrons induced by the gamma-rays. The obtained results were almost consistent with previously reported results and extended them to the lower energy region relevant for direct dark matter searches.

A measurement of the scintillation time profile for nuclear recoil events was also conducted using a ^{252}Cf neutron source [23]. With $\tau_1 = 4.3 \pm 0.6$ ns taken from a prior research, τ_2 was measured to be $26.9^{+0.8}_{-1.2}$ ns with the fast decay componet fraction of $0.252^{+0.028}_{-0.020}$. We also evaluated the performance of pulse shape discrimination between nuclear recoil and electronic events with the aim of reducing the electromagnetic background in WIMP searches. For a 50% nuclear recoil acceptance, the electronic event acceptance was 13.7±1.0% and 4.1±0.7% in the energy ranges of 5–10 keV$_{ee}$ and 10–15 keV$_{ee}$, respectively.

Measurement of ^{210}Pb and ^{210}Po in the copper bulk

Oxygen-free copper (OFC) is a readily available commercial material of low radioisotope (RI) content,

and thus it is often used in recent low-background experiments. There are multiple methods to measure the RI contaminations in materials, however, it is difficult to measure the ^{210}Pb contamination with high precision below $O(100)$ mBq/kg. We established a new method to measure the ^{210}Po and ^{210}Pb contaminations in the copper bulk with a low-background alpha-ray counter [24]. The energy distribution of alpha-rays emerging from the bulk becomes continuous since they lose part of their energy before reaching the surface. In order to determine the ^{210}Pb contamination, we measured ^{210}Po several times over different periods since the ^{210}Pb and ^{210}Po decay equilibrium may be broken. Owing to our measurements's high sensitivity of a few mBq/kg, the ^{210}Pb and ^{210}Po contaminations in the OFC bulk were identified and measured for the first time. The obtained ^{210}Pb contaminations of various OFC samples were 17–40 mBq/kg, though ^{210}Po contamination varied widely. This ^{210}Pb was understood to be a small residual from the electrolysis process based on the investigation of copper samples at various stages in production.

Development of low RI PMT with a dome shape photocathode

For a future detector with a larger volume and smaller background, we developed a new type of three inch PMT; the R13111. To reduce the impact of the detector's inner surface background, which is the main cause of the background for the XMASS-I detector, the photocathode geometry is changed to dome-shaped from flat. As shown in Fig. 14, PMTs with dome-shaped photocathode are more efficient in detecting scintillation photons originating on the surface of the detector than flat PMTs. Our simulation shows that three PMTs surrounding the event vertices on the surface should detect 40%-50% of all photoelectrons. Using this information the background originating from events at the surface can be reduced by three order of magnitudes.

From the performance check of the new PMTs, apart from basic properties such as low dark rate and stable operation inside liquid xenon, the sensitivity for light impinging on the PMT from the side, which is the most important for suppression of the surface background, was confirmed to be as desired: more than 80% of the sensitivity near the center of the photocathode.

Due to careful screening of all components, radioactive impurities in the PMT are drastically reduced. Compared to the R10789 used in the XMASS-I detector, the R13111 manufactured in 2015 achieved a reduction of 69% for the U chain, 59% for the Th chain, larger than 86% for 40K and 84% for ^{60}Co. Fig. 15 summarizes the reduction of the radioactive impurities for from R10789 to R13111.

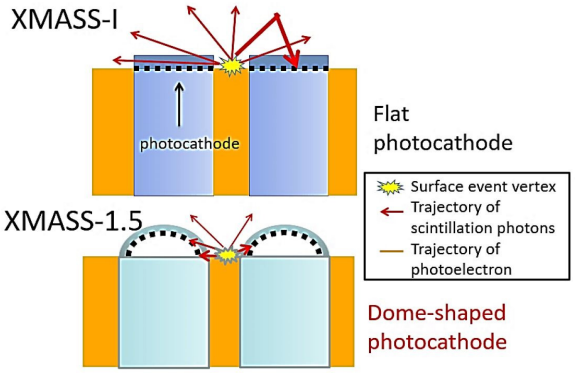

Fig. 14. The schematic view of difference of effectiveness of photon detection for the detector surface event between flat photocathode and dome-shaped photocathode.

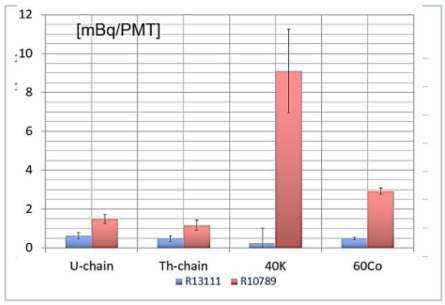

[mBq/PMT]	U chain	Th chain	40K	60Co
Target value	0.15		1.00	0.30
R13111	0.624±0.168	0.478±0.152	<1.24	0.478±0.0567
R10789	1.51±0.243	1.16±0.27	9.10±2.15	2.92±0.161

Fig. 15. The radioactivies of R13111 and R10789 (used in the XMASS-I detector).

Activity towards the future direct dark matter search

Based on the experience with the XMASS-I detector, we planned to construct a larger detector, XMASS-1.5, with five tons fiducial mass of liquid xenon. It was expected to reach a sensitivity of around 10^{-47}cm^2 for WIMPs with a mass of 100 GeV. In 2016, we re-evaluated the plan and concluded that XMASS-1.5 was not competitive any more once one-ton-scale dual-phase liquid-xenon detectors become operational. The primary reason for this decision was that the background due to electron scattering by low energy solar neutrinos is difficult to distinguish from a WIMP signal in single-phase liquid xenon detectors. Though we have some discrimination power between electron and nuclear recoil signals using the scintillation waveforms, it is hard to complete with the particle identification in dual-phase detectors. In addition, dual-phase detectors with similar target size (second generation, G2) were already approved for construction. For these reasons, rather than trying to construct a uncompetitive detector in Kamioka, we aimed for a future, more sensitive, third generation detector (G3) and in the meantime to

collaborate with competitors building their multi-ton G2 detectors.

This future plan was submitted to the future project committee in ICRR and evaluated as shown in a separated report. The committee agreed that the XMASS-1.5 was not competitive with other contemporary projects and accepted this change of our plan for the future. It also recognized participation in the one of G2 experiments, in particular the XENONnT experiment, as appropriate. The XENON collaboration plans to construct the XENONnT detector with $\sim$ five ton liquid xenon target in 2019.

XMASS and the Kamioka Observatory are providing substantial know-how to achieve XENONnT's ambitions. Two areas stand out: xenon purification in the liquid phase, and a newly added neutron veto surrounding the LXe TPC. These address the two of the most serious problems arising with the transition to multi-ton, dual- phase TPC based G2 dark matter direct detection experiments: suppressing electronegative contaminants in the liquid xenon, and tagging fast neutrons emerging in the TPC. These stem from alpha-neutron reactions and in rare cases scatter only once before leaving the TPC, thus mimicking the nuclear recoil signature of a WIMP interaction. From XMASS the new, Japanese members of XENON have expertise with the circulation of LXe and use it in supporting the new liquid purification system for XENONnT. As members also of the Super-Kamiokande collaboration a significant portion of the new Japanese XENON collaborators have knowledge of and access to the water Cherenkov based neutron detection pioneered in Kamioka by EGADS. There is currently a very high chance that we will use this Kamioka technology at Laboratori Nazionali Del Gran Sasso (LNGS) to convert the water Cherenkov muon veto shielding for the TPC into a highly efficient neutron veto with our technology.

Having found our place in our new dark matter detection experiment, we are still planning to use Hall-C for the development of new low background techniques. On our Japanese side this will be directed towards the third generation of LXe based dark matter detectors beyond the upcoming G2 experiments.

Summary

We have achieved following results in the last six years.

- Refurbishment of the XMASS-I detector and reducing the background more than one order of magnitude.
- Operation of the XMASS-I detector for more than four calendar years. This enables us to assess possible annual modulation caused by dark matter particles.
- Understanding the background of the detector inside the fidicual volume well and improve dark matter searches on the basis of this understanding.
- Development of particle discrimination between electrons and gamma rays.
- Various searches and studies of new physics (elastic scattering and inelastic scattering by dark matter particles, and solar KK axions), nuclear physics (double electron captures), and astrophysics (supernovae neutrinos).
- Development of the world's most sensitive alpha-ray counter.

The achievements above already expanded beyond our original physics scope and we developed our own unique approach to new physics. We will conduct more studies using existing large exposure data set.

XMASS Collaboration

Spokesperson : Shigetaka Moriyama (from Dec. 2016) (Kamioka Observatory, ICRR, The University of Tokyo), Yoichiro Suzuki (till Dec. 2016) (Kavli Institute for the Physics and Mathematics of the Universe (WPI), The University of Tokyo)

Institute	Country	(*)
ICRR, Univ. of Tokyo	Japan	16
Kavli IPMU, Univ. of Tokyo	Japan	4
Kobe Univ.	Japan	2
Tokai Univ.	Japan	1
Gifu Univ. (till Mar. 2016)	Japan	1
Yokohama National Univ.	Japan	1
Miyagi Kyoiku Univ.	Japan	1
Nagoya Univ.	Japan	3
Tokushima Univ. (from Oct. 2014)	Japan	1
Nihon Univ. (from Apr. 2018)	Japan	1
Institute for Basic Science	Korea	3
Korea Research Institute of Standards and Science (KRISS)	Korea	2
Total		36

(*) Number of collaborators.

Members

Staff

Yoichiro Suzuki, Professor (till Mar. 2014)
Masayuki Nakahata, Professor
Shigetaka Moriyama, Professor
Yasuhiro Kishimoto, Assoc. Professor
Hiroyuki Sekiya, Assoc. Professor
Atsushi Takeda, Research Associate
Kou Abe, Research Associate
Masaki Yamashita, Project Assoc. Professor

Hiroshi Ogawa, Project Research Associate (till Mar. 2018)
Kazuyoshi Kobayashi, Project Research Associate
Katsuki Hiraide, Project Research Associate
Byeongsu Yang, Project Research Associate (till Apr. 2018)
Koichi Ichimura, Project Research Associate (from Aug. 2013)

Postdoctorial Fellows

Kazufumi Sato, PD Researcher (from Jun. 2015)

Senior Fellows

Shigeki Tasaka (Aug. 2015 - Mar. 2017)

Graduate students

Two students were awarded doctor degrees and six students earned master degrees during 2003–2018, supervised by ICRR staff members.

List of Publications

Before Year 2012

[1] Y. Suzuki, "Low-energy solar neutrino detection by using liquid xenon," hep-ph/0008296.

[2] K. Ueshima *et al.* (XMASS Collaboration), "Scintillation yield of liquid xenon at room temperature," Nucl. Instrum. Meth. A **594** (2008) 148.

[3] K. Abe *et al.* (XMASS Collaboration), "Distillation of Liquid Xenon to Remove Krypton," Astropart. Phys. **31** (2009) 290.

[4] K. Ueshima *et al.* (XMASS Collaboration), "Scintillation-only Based Pulse Shape Discrimination for Nuclear and Electron Recoils in Liquid Xenon," Nucl. Instrum. Meth. A **659** (2011) 161.

[5] A. Minamino *et al.* (XMASS Collaboration), "Self-shielding effect of a single phase liquid xenon detector for direct dark matter search," Astropart. Phys. **35** (2012) 609.

[6] K. Abe et al. (XMASS Collaboration), "Radon Removal from Gaseous Xenon with Activated Charcoal", Nucl. Instrum. Meth. A **661** (2012) 50.

Since Year 2012

[7] K. Abe *et al.* (XMASS Collaboration), "XMASS detector," Nucl. Instrum. Meth. A **716** (2013) 78.

[8] N. Y. Kim *et al.* (XMASS Collaboration), "Micro-source development for XMASS experiment," Nucl. Instrum. Meth. A **784** (2015) 499.

[9] K. Abe *et al.* (XMASS Collaboration), "Light WIMP search in XMASS," Phys. Lett. B **719** (2013) 78.

[10] K. Abe *et al.* (XMASS Collaboration), "A direct dark matter search in XMASS-I," arXiv:1804.02180 [astro-ph.CO], accepted for publication in Phys. Lett. B.

[11] H. Uchida *et al.* (XMASS Collaboration), "Search for inelastic WIMP nucleus scattering on ^{129}Xe in data from the XMASS-I experiment," Prog. Theor. Exp. Phys. **2014** (2014) 063C01.

[12] T. Suzuki *et al.* (XMASS Collaboration), "Search for WIMP-^{129}Xe inelastic scattering with particle identification in XMASS-I," arXiv:1809.05358 [astro-ph.CO].

[13] K. Abe *et al.* (XMASS Collaboration), "Direct dark matter search by annual modulation in XMASS-I," Phys. Lett. B **759** (2016) 272.

[14] K. Abe *et al.* (XMASS Collaboration), "Direct dark matter search by annual modulation with 2.7 years of XMASS-I data," Phys. Rev. D **97** (2018) 102006.

[15] K. Abe *et al.* (XMASS Collaboration), "Search for bosonic superweakly interacting massive dark matter particles with the XMASS-I detector," Phys. Rev. Lett. **113** (2014) 121301 **(Editors' Suggestion)**.

[16] K. Abe *et al.* (XMASS Collaboration), "Search for dark matter in the form of hidden photons and axion-like particles in the XMASS detector," arXiv:1807.08516 [astro-ph.CO], accepted for publication in Phys. Lett. B.

[17] K. Abe *et al.* (XMASS Collaboration), "Search for two-neutrino double electron capture on ^{124}Xe with the XMASS-I detector," Phys. Lett. B **759** (2016) 64.

[18] K. Abe *et al.* (XMASS Collaboration), "Improved search for two-neutrino double electron capture on ^{124}Xe and ^{126}Xe using particle identification in XMASS-I," Prog. Theor. Exp. Phys. **2018** (2018) 053D03.

[19] K. Abe *et al.* (XMASS Collaboration), "Search for solar axions in XMASS, a large liquid-xenon detector," Phys. Lett. B **724** (2013) 46.

[20] N. Oka *et al.* (XMASS Collaboration), "Search for solar Kaluza-Klein axions by annual modulation with the XMASS-I detector," Prog. Theor. Exp. Phys. **2017** (2017) 103C01.

[21] K. Abe *et al.* (XMASS Collaboration), "Detectability of galactic supernova neutrinos coherently scattered on xenon nuclei in XMASS," Astropart. Phys. **89** (2017) 51.

[22] H. Takiya *et al.* (XMASS Collaboration), "A measurement of the time profile of scintillation induced by low energy gamma-rays in liquid xenon with the XMASS-I detector," Nucl. Instrum. Meth. A **834** (2016) 192.

[23] K. Abe *et al.* (XMASS Collaboration), "A measurement of the scintillation decay time constant of nuclear recoils in liquid xenon with the XMASS-I detector," arXiv:1809.05988 [physics.ins-det].

[24] K. Abe *et al.* (XMASS Collaboration), "Identification of ^{210}Pb and ^{210}Po in the bulk of copper samples with a low-background alpha particle counter," Nucl. Instrum. Meth. A **884** (2018) 157.

HYPER-KAMIOKANDE (R&D)

Introduction

The Hyper-Kamiokande or Hyper-K [1, 7] is the ICRR's next main project. The detector, as a straightforward extension of the Super-Kamiokande (Super-K), will provide major new capabilities to make new discoveries in particle and astroparticle physics thanks to an order of magnitude increase in detector mass and improvements in photon-detection system along with the envisioned J-PARC Megawatt-class neutrino beam. Figure 1 shows a schematic view of the Hyper-K cylindrical detector with 60 m in height and 74 m in diameter. The water mass is 0.258 million metric tons, with an order of magnitude larger fiducial mass of 0.187 million metric tons than Super-K. The Hyper-K and J-PARC neutrino beam measurement of neutrino oscillation is more likely to provide a 5-sigma discovery of *CP* violation than any other existing experiment. Hyper-K will also be the world leader for nucleon decay searches. The sensitivity to the partial lifetime of protons for the decay modes of $p \to e^+ + \pi^0$ is expected to exceed 10^{35} years. The astrophysical neutrino program involves precision measurements of solar neutrinos and their matter effects, high-statistical Supernova burst and Supernova relic neutrinos. The Hyper-K is a priority project listed in the Roadmap2017 of the Japanese Ministry of Education, Culture, Sports, Science and Technology (MEXT), and seed funding has been allocated within MEXT budget request for JFY2019. The principal project milestones include: Construction to start in 2020, and Start data taking in $\sim$ 2027.

Summary from 2012 to 2018

List of milestones which we have achieved during this review period through April 2012 to the summer 2018 is shown below.

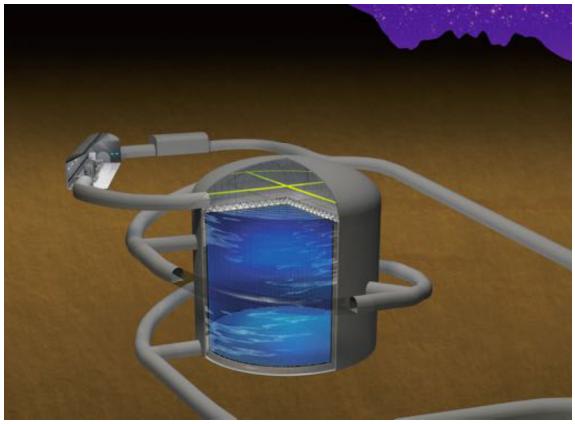

Fig. 1. Schematic view of the Hyper-K water tank.

- 2013.3 Selected as a important large-scale project in Masterplan2013 by Science Council of Japan (SCJ) [1].
- 2015.1 International proto-collaboration has been formed.
- 2015.1 ICRR and the Institute of Particle and Nuclear Studies (IPNS) of KEK signed a memorandum of understanding (MoU) for cooperation on the Hyper-K project.
- 2016.2 Hyper-K Advisory Committee (HKAC) meeting (1st round)
- 2016.2 Hyper-K Design Report [5]
- 2016.6 KEK's Project Implementation Plan (KEK-PIP) set top priority to the J-PARC upgrade for Hyper-Kamiokande [2].
- 2017.2 Selected as a important large-scale project in Masterplan2017 by SCJ [3].
- 2017.3 Recommended as a ICRR's next project by the ICRR future project review committee's report [4].
- 2017.7 Selected in Roadmap2017 by MEXT [5].
- 2017.9 HKAC meeting (2nd round)
- 2017.10 The University of Tokyo launched Next-Generation Neutrino Science Organization (NNSO) [6], where ICRR, Kavli IPMU, and the School of Science cooperate to promote the project and host the detector construction.
- 2018.5 Revised Hyper-K Design Report [7]
- 2018.8 Seed funding has been allocated within MEXT budget request for JFY2019.

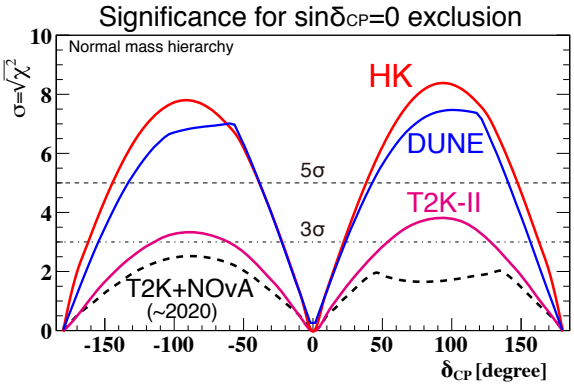

Fig. 2. Significance of the *CP* violation (nonzero $\sin\delta_{CP}$) discovery in lepton sector with a 10-year observation in Hyper-K (HK) as a function of the unknown *CP* phase. The normal hierarchy of neutrino masses is assumed. Ongoing and planned long baseline experiments are superimposed.

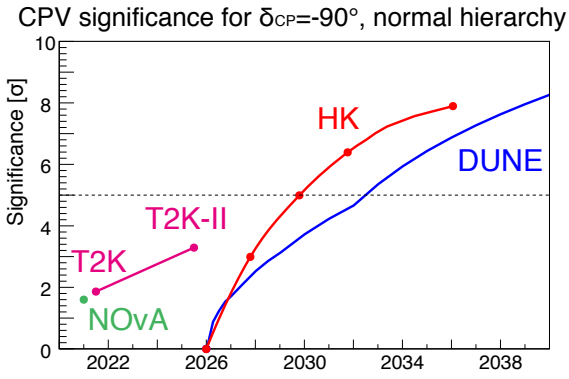

Fig. 3. Discovery potential of the *CP* violation (nonzero $\sin\delta_{CP}$) in lepton sector as a function of year. The normal hierarchy of neutrino masses is assumed. Ongoing and planned long baseline experiments are superimposed.

Physics potentials

Hyper-K will be able to measure the magnitude of the leptonic *CP* violation with high precision, which could explain the baryon asymmetry in the Universe. Figure 2 shows an expected significance of the *CP* violation (nonzero $\sin\delta_{CP}$) discovery by ten years operation. Hyper-K covers the 76% of δ_{CP} parameter space with 3σ or more significance, and 57% of the parameter space with 5σ or more. Hyper-K will go beyond 7σ significance if $\delta_{CP} = -90^\circ$ as suggested by T2K [7] results.

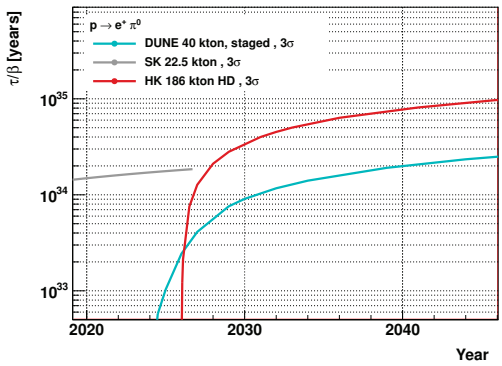

Fig. 4. The $p\to e^+\pi^0$ discovery reach in proton lifetime with 3σ significance as a function of year. It shows Hyper-K (HK) planing to start in 2026, superimposed with the ongoing Super-K (SK) and planned DUNE experiments. The DUNE project assumes 10 kton operation from 2024, toward full 40 kton by increasing 10 kton every year.

Figure 3 shows the discovery significance for the case of $\delta_{CP} = -90^\circ$ as a function of year. The US-based program LBNF/DUNE [8] plans to start its beam in 2026 and it is critical for Hyper-K to start its construction and operation on time.

In Grand Unified Theories, which unify quarks and leptons and unify three forces other than gravity, the decay of proton is one of the most dramatic predictions. A proton decay $p\to e^+\pi^0$ is dominant decay mode mediated by heavy gauge bosons in various models with a prediction close to the current limit of the proton decay life time. Figure 4 shows the 3σ discovery potential for the $p\to e^+\pi^0$ mode as a function of year. Hyper-K is an only realistic proposal which can go beyond the proton lifetime of 1×10^{35} years. Hyper-K will also extend reach to many other decay modes such as SUSY favored $p\to\nu K^+$, decays into heavier mesons, and di-nucleon decays.

High statistics observations of neutrinos from a core collapsed Supernova neutrinos (CCSN) along with gravitational waves are the only way to obtain precious inside information on the dynamics of the CCSN central engine and the explosion mechanism. If a CCSN explosion were to take place near the center of our Galaxy, Hyper-K would observe as many as tens of thousands of neutrino interactions. Furthermore, Hyper-K will have the ability to precisely determine the arrival time of supernova neutrinos, which will help contribute to the understandings of both neutrino and CCSN properties. Moreover the continuous flux of relic supernova neutrinos from all past CCSN explosions in the observable universe will guarantee a steady accumulation of valuable astrophysical data. Figure 5 shows the expected number of relic supernova neutrino events as a function of year.

*1 Master plan 2014 (in Japanese), http://www.scj.go.jp/ja/info/kohyo/pdf/kohyo-22-t188-1.pdf
*2 KEK Roadmap (Project Implementation Plan), https://www.kek.jp/ja/About/OrganizationOverview/Assessment/Roadmap/KEK-PIP.pdf (2016).
*3 Master plan 2017 (in Japanese), http://www.scj.go.jp/ja/info/kohyo/kohyo-23-t241-1.html
*4 Report by ICRR future project committee (in Japanese), http://www.icrr.u-tokyo.ac.jp/public_relation/blog/171026.pdf
*5 MEXT Roadmap2017, http://www.mext.go.jp/component/b_menu/shingi/toushin/___icsFiles/afieldfile/2017/10/18/1388523_002.pdf
*6 Next-Generation Neutrino Science Organization, http://www.nnso.u-tokyo.ac.jp/index-e.html
*7 K. Abe *et al.* [T2K Collaboration], Phys. Rev. Lett. 118, 151801.
*8 R. Acciarri *et al.* [The DUNE Collaboration], arXiv:1601.05471 [physics.ins-det].

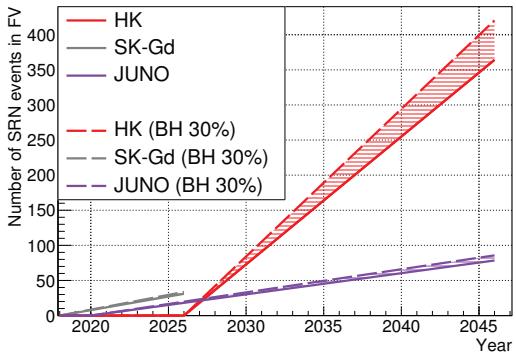

Fig. 5. The accumulated number of supernova relic neutrino events as a function of year. The JUNO experiment and SK-Gd are also plotted. Effective temperature of neutrinos inside supernova is assumed to be 6 MeV. The solid line assumes no black hole formation while the dashed line assumes that 30% of core-collapse stars form a black hole.

Cavern excavation

In order to pin down the candidate place, seismic prospecting by using artificially generated elastic wave was performed at the large area of $(400\,\mathrm{m})^3$. The top panel in Fig. 6 shows the results of reflection imaging overlaid with known faults and fracture zones. The study identified the known faults as expected, while there was no new faults found at the central region. The bottom panel is rock class distribution made by combining the results of seismic tomography, reflection imaging, and the past geological survey. In both figures, the red dashed rectangle denotes a region which has the best rock quality and the least uneven rock over the entire Hyper-K candidate site. We successfully identified the best candidate place that is suitable for the gigantic Hyper-K cavern construction. The cavern excavation is found to be feasible by known technology.

Photosensors

A Cherenkov light in a ultra pure water is detected by 40,000 newly developed photomultiplier tubes (PMTs) shown in Fig. 7 giving 40% photo-coverage of the inner detector surface. Its peak quantum efficiency is about 30%, that is 1.4 times higher than that of the Super-K PMT. By combining with the improved photoelectron collection efficiency the new PMT achieved twice higher single photon detection efficiency. The timing and charge resolutions at single photo-electron also becomes much better as 1.1 ns and 35% which can be compared with 2.1 ns and 53% of the Super-K PMT, respectively. Moreover, pressure tolerance was improved up to the 125 m water depth in order to fit the 60 m depth of the detector water.

To prevent a chain reaction of imploding PMTs caused by single PMT implosion, every PMT in the Hyper-K water tank will be housed in a shock-wave prevention cover. The prototype cover consists of an acrylic front window and a stainless steel backside cover

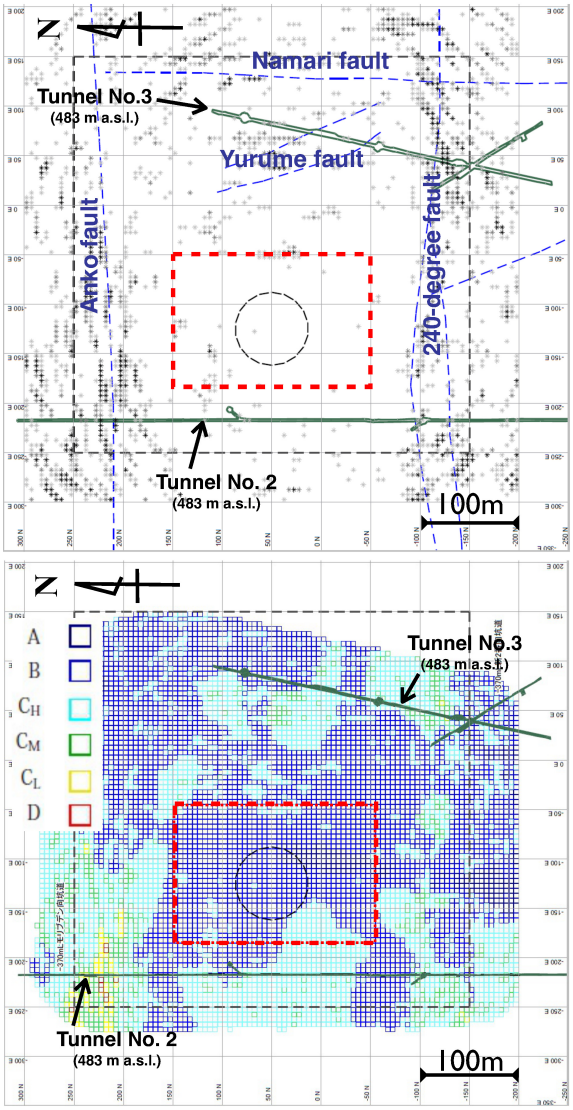

Fig. 6. (Top) Top view of reflection imaging by seismic prospecting at altitude of 483 m above sea level. Asterisks (∗) show identified reflection positions indicating existence of faults, fracture zone, and open cracks in the bedrock. Blue dashed lines indicate the location of known faults. The red dashed rectangles denotes a selected candidate region for Hyper-K cavern and dashed circle indicates the size of the Hyper-K cavern. (Bottom) Rock class distribution obtained by combining the results of seismic tomography, reflection imaging and the geological survey results with bore-hole and the existing tunnels.

with conical shape. A mock test simulating the event of a photo-sensor implosion in Hyper-K was carried out in a deep vertical shaft. It has been demonstrated that the peak amplitude of the pressure shock-wave is significantly reduced and thus does not cause a chain reaction up to 80 m depth. In addition, studies are going on for two alternative designs aiming to reduce weights and / or production costs: one is a stainless steel tube-like-shaped cover, and another is a resin-made monolithic cover.

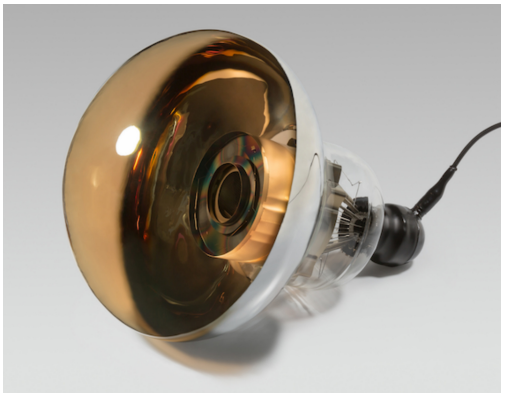

Fig. 7. New 50 cm photomultiplier tube with a box-and-line dynode.

Hyper-Kamiokande Proto-Collaboration

Project Leader : Masato Shiozawa (Kamioka Observatory, ICRR, The University of Tokyo)

Institute	Country	(*)
Kamioka Observatory, ICRR, Univ. of Tokyo	Japan	22
Boston Univ.	USA	4
California State Univ.	USA	3
Chonnam Univ.	Korea	4
Dongshin Univ.	Korea	2
Ecole Polytechnique	France	5
GIST College	Korea	1
Imperial College London	UK	6
INFN Sezione di Bari and Università e Politecnico di Bari	Italy	7
INFN Sezione di Napoli and Università di Napoli	Italy	6
INFN Sezione di Padova and Università di Padova	Italy	6
INFN Sezione di Roma and Università La Sapienza	Italy	2
Institute for Nuclear Research of the Russian Academy of Sciences	Russia	10
Iowa State Univ.	USA	2
IRFU	France	5
KEK	Japan	8
Kobe Univ.	Japan	3
Kyoto Univ.	Japan	7
Kyoto Sangyo Univ.	Japan	1
Laboratory Nuclear and High-Energy Physics	France	3
Lancaster Univ.	UK	6
Los Alamos National Laboratory	USA	1
Louisiana State Univ	USA	3
Michigan State Univ	USA	1
Miyagi Kyoiku Univ.	Japan	1
Nagoya Univ.	Japan	1
Nagoya Univ. Kobayashi-Maskawa Institute for the Origin of Particles and the Universe	Japan	2
Nagoya Univ. Institute for Space-Earth Environmental Research	Japan	2
National Centre for Nuclear Research	Poland	8
Okayama Univ.	Japan	4
Osaka City Univ.	Japan	2
Oxford Univ.	Japan	4
Pennsylvania State Univ.	USA	1
Pontificia Universidade Catolica do Rio de Janeiro	Brazil	2
Queen Mary University of London	UK	12
Rutherford Appleton Laboratory	UK	8
Royal Holloway University of London	UK	7
Seoul National Univ.	Korea	4
Seoyeong Univ.	Korea	1
Stockholm Univ.	Sweden	1
Stony Brook Univ.	USA	5
SungKyunKwan Univ.	Korea	4
Tohoku Univ.	Japan	3
Tokyo Institute of Technology	Japan	4
Tokyo Univ. of Science	Japan	1
TRIUMF.	Canada	7
Univ. of Washington	USA	1
Univ. of Autonoma Madrid	Spain	3
Univ. of British Columbia	Canada	3
Univ. of California, Davis	USA	2
Univ. of California, Irvine	USA	5
Univ. of Edinburgh	UK	7
Univ. of Geneva	Switzerland	7
Univ. of Hawaii	USA	3
Univ. of Liverpool	UK	9
Univ. of Pittsburgh	USA	1

Univ. of Regina	Canada	2
Univ. of Rochester	USA	1
Univ. of Sheffield	UK	8
Univ. of Tokyo	Japan	4
Univ. of Tokyo, Earthquake Research Institute	Japan	2
Univ. of Tokyo, ICRR, RCCN	Japan	6
Univ. of Tokyo, Kavli IPMU	Japan	8
Univ. of Tokyo, NNSO	Japan	(**)
Univ. of Toront	Canada	4
Univ. of Warwick	UK	6
Univ. of Winnipeg	Canada	2
Warsaw Univ.	Poland	1
Warsaw Univ. of Technology	Poland	6
Wroclaw Univ.	Poland	1
Virginia Tech	USA	4
Yerevan Physics Institute	Armenia	1
York Univ.	Canada	5
Kyiv National Univ.	Ukraine	2
Yokohama National Univ.	Japan	1
Total		307

(*) Number of collaborators.
(**) Members also affiliated with ICRR, Kavli IPMU, and the School of Science, University of Tokyo.

Hyper-Kamiokande Working Group

Project leader : Masato Shiozawa
(Kamioka Observatory, ICRR, The University of Tokyo)

Members at ICRR

Staff

Kamioka Observatory
Yoichiro Suzuki, Professor (till Mar. 2014)
Masayuki Nakahata, Professor
Shigetaka Moriyama, Professor
Masato Shiozawa, Professor
Yoshinari Hayato, Assoc. Professor
Yasuhiro Kishimoto, Assoc. Professor
Hiroyuki Sekiya, Assoc. Professor
Shoei Nakayama, Assoc. Professor
Makoto Miura, Research Associate
Yusuke Koshio, Research Associate (till Mar. 2013)
June Kameda, Research Associate
Atsushi Takeda, Research Associate
Kou Abe, Research Associate
Roger Wendell, Research Associate (till Dec. 2015)
Motoyasu Ikeda, Research Associate (from Sep. 2013)
Yasuhiro Nakajima, Research Associate (from Aug. 2016)
Tomonobu Tomura, Project Research Associate (till Mar.2016)
Hidekazu Tanaka, Project Research Associate (from Jun.2012)
Lluis Magro Marti, Project Research Associate (from May, 2016)
Yo Kato, Project Research Associate (from Sep.2016)
Christophe Bronner, Project Research Associate (from May 2017)
Yosuke Kataoka, Project Research Associate (from Dec. 2017)
Takatomi Yano, Project Research Associate (from Dec. 2017)

Research Center for Cosmic Neutrinos
Takaaki Kajita, Professor
Kimihiro Okumura, Assoc. Professor
Yasuhiro Nishimura, Research Associate (from Sep. 2016)
Yasuhiro Nishimura, Project Research Associate (Apr.2012 - Sep. 2016)

Postdoctorial Fellows

Kamioka Observatory
Lluis Magro Marti (Apr. 2011 - Mar. 2013)
Yo Kato (Apr. 2016 - Sep. 2016)
Guillaume Pronost (from Mar. 2016)
Yuuki Nakano (from Apr. 2017)

Graduate students

One student earned master degrees during 2012–2018, supervised by ICRR staff members.

List of Publications

Before Year 2012

[1] K. Abe *et al.*, "Letter of Intent: The Hyper-Kamiokande Experiment — Detector Design and Physics Potential —," arXiv:1109.3262 [hep-ex], **Cited 487 times.**

After Year 2012

[2] E. Kearns *et al.* [Hyper-Kamiokande Working Group], "Hyper-Kamiokande Physics Opportunities," arXiv:1309.0184 [hep-ex], **Cited 65 times.**

[3] K. Abe *et al.* [Hyper-Kamiokande Working Group], "A Long Baseline Neutrino Oscillation Experiment Using J-PARC Neutrino Beam and Hyper-Kamiokande," arXiv:1412.4673 [physics.ins-det], **Cited 91 times.**

[4] K. Abe *et al.* [Hyper-Kamiokande Proto-Collaboration], "Physics potential of a long-baseline neutrino oscillation experiment using a J-PARC neutrino beam and Hyper-Kamiokande," PTEP **2015**, 053C02 (2015)

doi:10.1093/ptep/ptv061 [arXiv:1502.05199 [hep-ex]], **Cited 160 times.**

[5] [Hyper-Kamiokande Proto-Collaboration], "Hyper-Kamiokande Design Report," KEK Preprint 2016-21 / ICRR-Report-701-2016-1, **Cited 40 times.**

[6] K. Abe *et al.* [Hyper-Kamiokande Collaboration], "Physics potentials with the second Hyper-Kamiokande detector in Korea," PTEP **2018**, no. 6, 063C01 (2018) doi:10.1093/ptep/pty044 [arXiv:1611.06118 [hep-ex]], **Cited 62 times.**

[7] [Hyper-Kamiokande Proto-Collaboration], "Hyper-Kamiokande Design Report," arXiv: 1805.04163, **Cited 4 times.**

HIGH ENERGY COSMIC RAY DIVISION

TA: TELESCOPE ARRAY

Introduction of TA and TALE

The Telescope Array (TA) is the largest Ultra-High Energy Cosmic Ray (UHECR) observatory in the northern hemisphere. The main aim of TA is to explore the origin and nature of UHECRs by measuring the energy spectrum, arrival direction distribution and mass composition. The TA collaboration consists of researchers from USA, Russia, Korea, Belgium and Japan.

The TA detector consists of a surface array of 507 plastic scintillator detectors (SDs) and three stations of fluorescence detectors (FDs). It is located in the desert of Utah in USA. The SDs were deployed on a squre grid with 1.2-km spacing, and the SD array covers approximately 700 km^2. Each SD has two layers of 1.2-cm-thick scintillator of 3 m^2. The full operation of SDs started in March 2008. The duty cycle is greater than 95%. The FDs view 3° - 31° or 33° above horizon. All three FD stations started the observation in November 2007, and have duty cycles of approximately 10%.

The TA Low-Energy extension (TALE) enables detailed studies of the energy spectrum and composition from $\sim 10^{16}$ eV upwards. The main aim of TALE is to clarify the expected transition from galactic cosmic rays to extragalactic cosmic rays and the comparison of the data with Monte Carlo simulation that takes into account the results of the LHC experiments. The TALE detector is located north of the TA site. The TALE FD views 31° - 59° in elevation angle. The TALE SD is described later.

Summary from 2012 through 2018

Here we summarize the TA results from 2012 through 2018.

We confirmed the ankle at $10^{18.7}$ eV and the flux suppression above $10^{19.8}$ eV.

The TA $X_{\rm max}$ measurement above $10^{18.2}$ eV is consistent with light composition. We need more statistics to clarify the feature above 10^{19} eV.

We found an indication of a cluster of cosmic rays above 5.7×10^{19} eV (TA hotspot) by oversampling using 20°-radius circles for the first five years of SD data. In order to confirm the TA hotspot and understand its feature, we proposed TAx4, which would quadruple the TA SD aperture with additional two FD sites. We are constructing TAx4, which is in addition expected to explore spectrum anisotropy that TA currently sees at a level of 3σ. And we will measure energy spectrum and $X_{\rm max}$ around the cutoff with more events.

We confirmed the breaks at $10^{16.2}$ eV and $10^{17.0}$ eV with the TALE FD. For the precise $X_{\rm max}$ measurement, the TALE SDs were fully deployed at the TALE site.

Results

Here we present the results more in detail about energy measurement, composition, anisotropy and interdiscplinary research.

Energy Measurement

TA energy spectrum

We published the cosmic-ray energy spectrum for four years of the TA SD data [6]. The preliminary result of cosmic-ray spectrum for nine years of the TA SD data is shown in Fig. 1 [72]. The spectrum shows the ankle at an energy of $10^{18.7}$ eV and the flux suppression above $10^{19.8}$ eV. The statistical significance of having the same spectral index above the ankle (no suppression) is rejected at $\sim 7\sigma$.

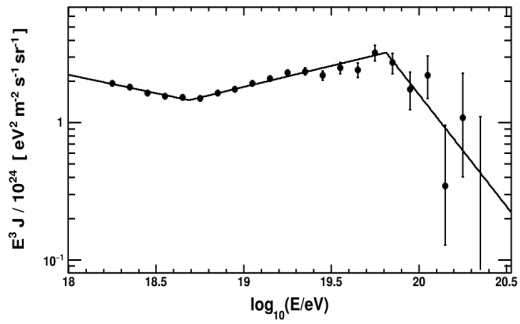

Fig. 1. The preliminary TA cosmic-ray flux multiplied by E^3 for TA SD nine-year data. The solid line shows the fit of the TA data to a broken power law.

Fig. 2 shows the TA and Pierre Auger Observatory (Auger) energy spectra with energy shifts by -5.2% and +5.2%, respectively. Significant discrepancy is seen above around $10^{19.5}$ eV, whereas good agreement is seen below $10^{19.5}$ eV. The TA and Auger collaborations formed a working group, and compared the TA and Auger spectra in the common declination (δ) band (from -15.7° to +24.8°) as shown in Fig. 3a. The cutoff energies agree at 0.5σ level. Based on this study, TA compared TA energy spectra for $\delta > 24.8°$ and $\delta < 24.8°$and found the difference of the cutoff energies as shown in Fig. 3b. The chance probability of obtained this difference is 3.5 σ [30].

TALE energy spectrum

The energy spectrum using the TALE FD data is shown between $\sim$2 PeV and 100 PeV as shown in Fig. 4 [28]. The events observed with the TALE FD are

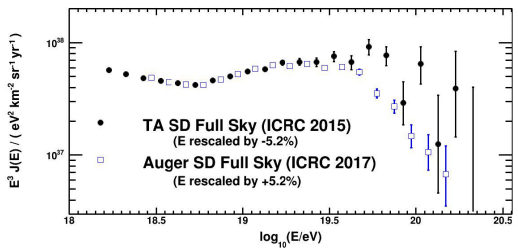

Fig. 2. The TA and Auger energy spectra with energy shifts by -5.2% and +5.2%, respectively.

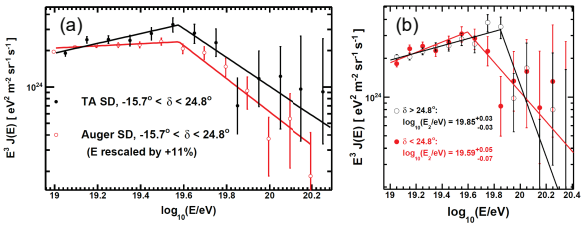

Fig. 3. a) The TA (black) and Auger (red) energy spectra of UHECR events in the common declination band after energy shifts. b) The TA energy spectra for the declination angles below 24.8° in red and above 24.8° in black

placed into three subsets: Cherenkov dominated events, fluoresence dominated events, and mixed signal events. And we see two clear breaks at $10^{16.22}$ eV and $10^{17.04}$ eV in the energy region measured with the TALE FD. We possibly see the knee feature at around $10^{15.6}$ eV. It becomes of great importance to measure the composition precisely using hybrid events by adding the TALE surface detector array to understand this spectral feature. The TALE SD is described later.

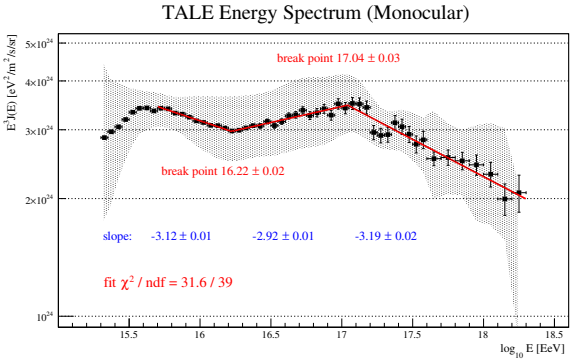

Fig. 4. a) TALE cosmic-ray energy spectrum. The gray band indicates the size of the systematic uncertainties.

Mass Composition

$\mathbf{X_{max}}$

The result of the depth of shower maximum $X_{\rm max}$ result using the first 8.5 years of hybrid events was published [24]. Fig. 5 shows the evolution of the average $X_{\rm max}$ with energy together with MC expectations. The result is in agreement with light composition within systematic uncertainty.

We checked the shape of $X_{\rm max}$ distributions, too. After allowing for systematic shfting of the data $X_{\rm max}$ distributions and performing the likelihood test on the data and MC distributions, we find that we fail to reject QGSJet II-04 protons as being compatible with the data for all energy bins at the 95% confidence level. QGSJet II-04 helium, nitrogen and iron are rejected for $\log_{10}(\mathrm{E}) < 19.0$, 19.2, and 19.4, respectively. For $\log_{10}(\mathrm{E}) > 19.0$, TA has insufficient statistics to distinguish the difference between different composition.

The TA and Auger composition working group reported on a comparison of $X_{\rm max}$ distributions measured by the Auger and TA observatories [78]. A direct comparison of the measured $X_{\rm max}$ distributions is not correct due to different detector acceptances and resolutions as well as different analysis techniques. A set of showers compatible to the composition measured by the Auger detectors was simulated and reconstructed using the official TA software chain. The TA data is within the systematic uncertainties compatible to a mixed composition as the one measured by the Auger detectors.

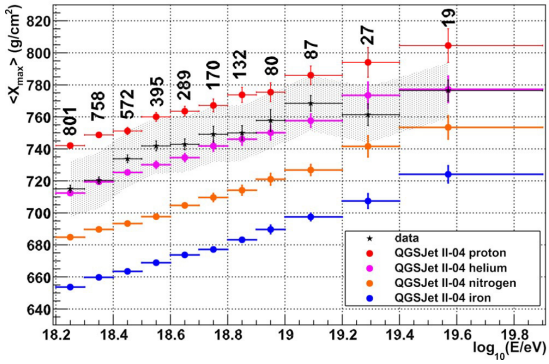

Fig. 5. The average reconstructed $X_{\rm max}$ as a function of energy. The black, red, magenta, orange and blue colors denote the data, pure proton, helium, nitrogen and iron QGSJet II-04 predictions, respectively. The shaded area indicates the size of the total systematic uncertainty.

TA SD composition

The result on UHECR mass composition obtained with the TA SD is presented [31] using the boosted decision tree multivariate analysis based on 14 observables sensitive to the properties of the shower front and the lateral distribution function. The average atomic mass corresponds to $< lnA >= 1.52 \pm 0.08$ (stat.) $\pm$ 0.36 (syst.). The obtained composition is qualitatively consistent with the TA hybrid results.

TA muon studies

The number of muons in inclined air showers observed with water Cherenkov surface detectors at the Pierre Auger Observatory is approximately 1.8 times that of the proton prediction with QGSJet II-03

hadronic model at 10^{19} eV [1]. We studied muons in air showers using seven years of the TA SD data [25, 83]. Air shower events are classified using θ, ϕ and R parameters to search for the condition of high purity of muons. Here θ is the zenith angle of the shower axis, ϕ is the azimuthal angle of the location of a surface detector around the shower core on the ground, and R is the distance of the location of the surface detector from the shower axis. The direction of zero degrees of ϕ is opposite to the cosmic-ray incident direction projected onto the ground. The counterclockwise direction is positive. The condition ($30^\circ < \theta < 45^\circ$ and $150^\circ < |\phi| < 180^\circ$ (the older shower side in an inclined shower), 2000 m $< R <$ 4000 m) gives muon purity of ~65% from the MC expectation at E ~10^{19} eV. Typical ratios of charge densities of the data to those of the MC are 1.72 ± 0.10 (stat) ± 0.40 (syst) at 1910 m $< R <$ 2160 m and 3.14 ± 0.36 (stat) ± 0.72 (syst) at 2760 m $< R <$ 3120 m as shown in Fig. 6. This result is qualitatively consistent with that by Auger. As described above, $X_{\rm max}$ measured with the TA FD is consistent with light composition. So the results of muon studies by Auger and TA make an inquiries about hadronic interaction models used in air shower MC simulations.

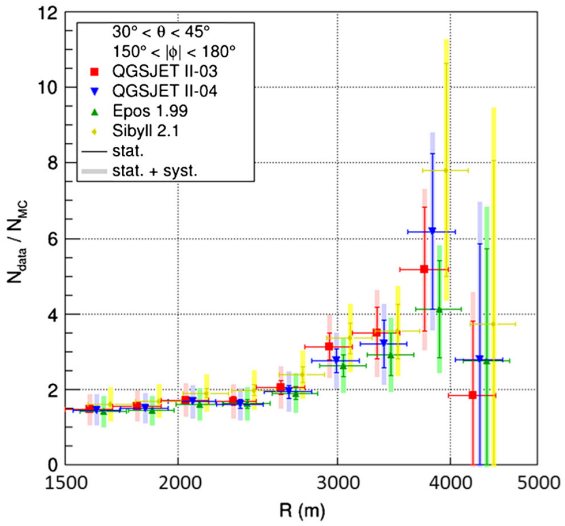

Fig. 6. The ratios of the average charge densities of the data to MC simulations as a function of core distance for $30^\circ < \theta < 45^\circ$, $150^\circ < |\phi| < 180^\circ$ and 1500 m $< R <$ 4500 m. The red, blue , green and yellow represent QGSJET II-03, QGSJET II-04, EPOS1.99 and SIBYLL2.1, respectively.

Search for EeV photons

We present the search for photons with the first nine years of the TA SD data, employing multivariate analysis with the classifier based on the Boosted Decision Tree [79]. There are no photon candidates found in the data set for $10^{18.0}$, $10^{18.5}$, $10^{19.0}$ and $10^{19.5}$ eV, and the diffuse flux limits for photons are obtained.

*1 A. Aab *et al.*, (Pierre Auger Collaboration), Phys. Rev. D 91 032003 (2015).

Arrival Directions of UHECRs

TA hotspot of the highest-energy cosmic rays

We have searched for intermediate-scale anisotropy of 72 cosmic-ray events above 5.7×10^{19} eV using five years of the TA SD data [10]. Fig. 7a shows a sky map of those cosmic rays. The angular resolution of arrival directions of cosmic rays in this energy range is 1.0° to 1.7°. A cluster of events appears in this map centered near right ascension of approximately 150° and declination of approximately 40° with a diameter of aprproximately 30° to 40°. We found a cluster of events that we call the hotspot by oversampling using circles 20° in radius. The Li-Ma significance (pre-trial significance) plot is shown in Fig. 7b. The hotspot has a Li-Ma statistical significance of 5.1σ (the number of observed events = 19 and the number of expected in an isotropic cosmic-ray sky = 4.5). The probability of such a hotspot appearing by chance in an isotropic cosmic-ray sky is estimated to be 3.4σ (post-trial significance). There are no known specific sources behind the hotspot. The hotspot is located near the supergalactic plane, which contains local galaxy clusters. The closest major cluster is the Ursa Major cluster (20 Mpc from Earth). The angular distance between the hotspot the supergalactic plane is approximately 19°. For the first nine years of the TA SD data, 143 events above 5.7×10^{19} eV were observed. The hotspot seems to be larger than originally thought. So we scanned by circles with different radii and obtained the maximum Li-Ma significance of 5σ with oversmpling using circles with a radius of 25° and its chance probability was 3σ [72].

Hot/cold spot

An energy dependent intermediate-scale anisotropy was studied using UHECRs above $10^{19.2}$ eV for seven years of the TA SD data [26]. The energy distributions inside oversampled circles are compared to that outside using the Poisson Likelihood Ratio test. The maximum pre-trial significance was obtained to be 6.17σ at right ascension of 139° and declination of 45°. The energy distribution within the circle at the center of maximum significance shows a deficit of events below $10^{19.75}$ eV and an excess above $10^{19.75}$ eV as shown in Fig. 8. The post-trial probability of this energy anisotropy, appearing by chance anywhere on isotropic sky, is found to be 9×10^{-5} (3.74σ) by MC simulation.

Spectrum anisotropy with respect to the Super-Galactic Plane (SGP)

In the cosmic-ray energy region above 10^{19} eV, the shape of cosmic-ray energy spectrum may carry an imprint of the distribution of the cosmic-ray source density. The SGP consists of local galactic clusters containing more nearby objects. By considering the effect of the loss of UHECRs due to attenuation during the propagation in the universe, the energy spectrum of

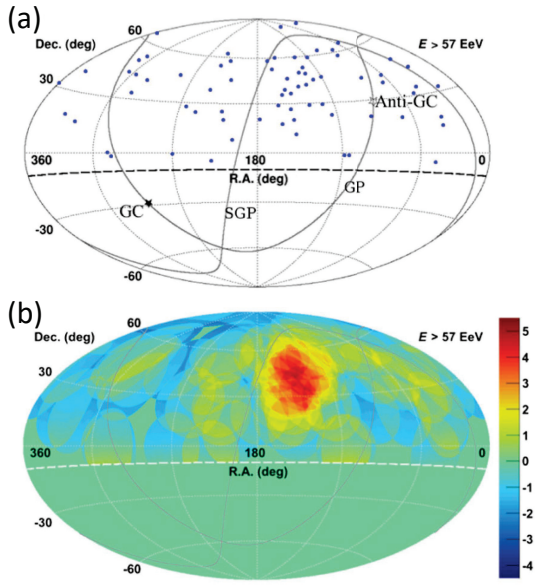

Fig. 7. Preliminary aitoff projection of the UHECR maps for nine years of the TA SD data in equatorial coordinates. (a) The blue data points show the arrival directions of the UHECRs with E $> 5.7\times10^{19}$ eV. The closed and open stars denote the Galactic Center (GC) and the anti-Galactic Center (Anti-GC), respectively. The solid curves indicate the Super-Galactic Plane (SGP) and the Galactic Plane (GP). (b) Li-Ma significance map. Our FoV is defined as the region above the dashed curve at decl. = -10°.

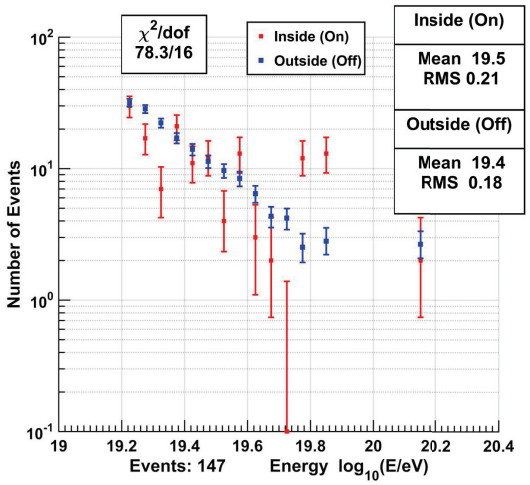

Fig. 8. The histogram of energies of events inside the spherical cap bin of radius 28.43° (red) at the maximum pre-trial significance. It's compared to the histogram of expected (normalized outside) energies (blue).

UHECRs in the area near the SGP (On-source area) is expected to be different from that in the area far from the SGP (Off-source area) containg less nearby objects. Here the On-source area is defined as the area within ±30° from the SGP latitude of 0° and the Off-source area is defined as the area that is the rest in the sky. The dotted broken power law fit line for open squares denotes the Off-source spectrum and the solid broken power law fit line for closed squares denotes the On-source spectrum for the first five years of the TA SD data as shown in Fig. 9. We found that the Off-source spectrum has a break at lower energy than the On-source spectrum. The chance probability of obtaining such or larger difference in statistically equivalent distributions is estimated to be $6.2\pm1.1\times10^{-4}$ (3.2σ) by a MC simulation [29]. The observed difference in the spectra is in a reasonable quantitative agreement with a simplified model assuming that the UHECR sources trace the galaxy distribution from the 2MRS catalogue, primary particles are protons and the magnetic deflections are neglected.

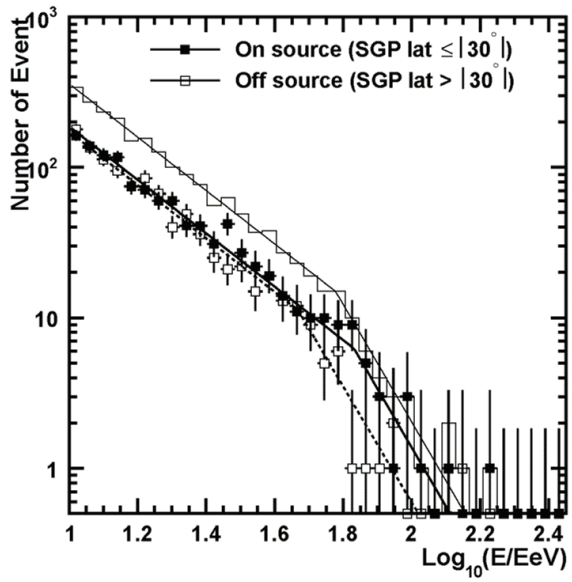

Fig. 9. The energy distributions of UHECR events observed with the TA SDs. The histogram shows the distribution of all events. Closed and open symbols show energy distributions observed in On- and Off-source areas respectively.

Search for EeV protons of galactic origin

Galactic EeV cosmic rays may be seen mostly along the galactic plane, and there may be a shortage of events coming from directions near the galactic anti-center. Guided by models of the galactic magnetic field that indicate that the enhancement along the galactic plane should have a standard deviation of about 20° in galactic latitude, and the deficit in the anti-Galactic Center (Anti-GC) direction should have a standard deviation of about 50°, we use the TA data to search for these effects [20]. Neither an enhancement along the galactic plane nor a deficit in the Anti-GC direction is found. We obtain an upper limit on the fraction of EeV cosmic rays of galactic origin at 1.3% at 95% confidence level.

Search for point-like sources of EeV neutral particles

We searched for steady point-like sources of EeV neutral particles for the first five years of the TA SD data [14]. We found no significant point-like excess

above 0.5 EeV. We also serached for coincidence with the Fermi bright Galactic sources. No significant coincidence was found within the statistical uncertainty.

Interdisciplinary research

TA SD burst events in coincidence with lightning

The TA SD observed several short-time bursts of air shower like events for the first five years. The expectation of chance coincidence is less than 10^{-4}. We found evidence for correlations between these bursts of the TA SD events and powerful lightning data obtained with the National Lightning Detection Network in timing and position [19]. After installting a 3-D lightning mapping array and electric field change instrument at the TA SD site, detailed features were observed [27].

TA extension

TAx4

As mentioned above, TA found evidence for intermediate-scale anisotropy of arrival directions of cosmic rays with greater than 5.7×10^{19} eV. With enhanced statistics, we expect to observe the structure of the hotspot along with other possible excesses and point sources along with the correlations with extreme phenomena in the nearby universe. We proposed to quadruple the area of the TA SD aperture by installing additional 500 counters of the current TA SD design including the existing TA SD array, which will be deployed on a square grid with wider, 2.08-km spacing between each [36]. The new array would need two FD stations overlooking it to increase the number of hybrid events for the confirmation of the energy scale and the measurement of $X_{\rm max}$. These FDs will be formed using additional refurbished HiRes telescopes. The layout of four times TA, which we call TAx4, is shown in Fig. 10 together with TALE.

The proposal of the SD part of TAx4 was approved for the Japan Society for the Promotion of Science through Grant-in-Aid for Scientific Research on Specially Promoted Research in Japan in 2015 as a five-year project. The SD deployment would start in early 2019. The FD part of TAx4 was approved by NSF in the USA in 2016. The TAx4 FD at the northern site was completed and started the stable operation in February of 2018. The TAx4 FD at the southern site is under construction as of summer in 2018.

TALE

The TALE FD operation was commenced in the spring of 2013. We saw two clear breaks in the energy spectrum measured with the TALE FD as shown in Fig. 4. It is of importance to measure $X_{\rm max}$ precisely adding timing information of surface detectors near the shower core on the ground. Therefore we proposed to complete the full TALE surface detector array. The

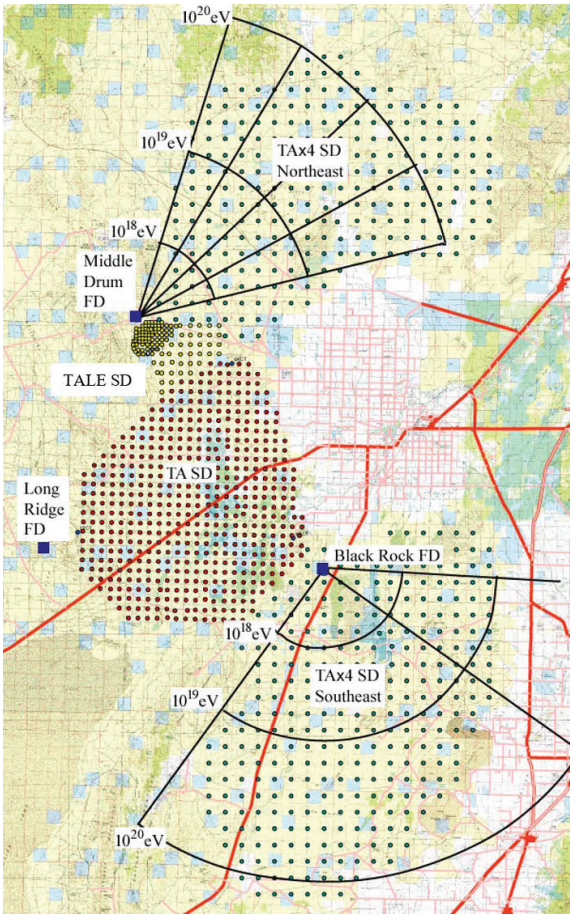

Fig. 10. The layout of the proposed TAx4. The array of 507 SDs (red filled circles on the left) is the current TA SD array. There are three TA FD stations (Middle Drum (MD) to the north, Long Ridge (LR) to the west, and Black Rock (BR) to the east of the TA SD array). The array of surface detectors to the north of the TA SD array is the TALE SD array. Additional two sub-arrays of 500 surface detectors in total (green filled circles) for TAx4 are located to the northeast and southeast of the TA SD array. Additional two FD stations with refurbished HiRes telescopes for the TAx4 are located at the MD and BR FD sites and view to the northeast and southeast as denoted each by the black frame of the fan.

proposal of adding remaining SDs in the TALE SD array was approved for the Japan Society for the Promotion of Science through Grant-in-Aid for Scientific Research (S) in 2015 as a five-year project. The TALE SD array consists of 103 plastic scintillation counters, which are identical to those of the TA SD array. These counters have graded spacings, ranging from 400 m near the TALE FD to 600 m further away, which merge into the TA SD array with 1200-m spacing at its northwestern corner. The 35 TALE surface detectors were firstly deployed in 2013. The full TALE SDs were deployed in February of 2017. The TALE SD array is in stable operation.

The observation of cosmic rays with energies down to 10^{15} eV, called the Non-Imaging CHErenkov (NICHE) array [80], was proposed. The plan is to install an array of simple Cherenkov counters of PMTs

each three inches in diameter on the ground looking upwards within the TALE SD array. The part of the NICHE with 15 PMTs, called jNICHE, was constructed by the Japan Society for the Promotion of Science through Grant-in-Aid for Young Scientists (A) that was approved in 2014.

Associate experiments and prospects

The near future plan is to complete TAx4 and continue data taking of TALE as described above.

The 60 times TA consisting of 10,000 SDs with 2 km spacing (TA2) was proposed to elucidate the origin of UHECRs as a next-generation air-shower ground array experiment [32] in the UHECR2012 symposium. The proposal was reported several times at the Town Meeting hosted by the Cosmic-ray Researchers Congress (CRC) and the ICRR Future Plan Discussion Committee.

The TA site is used worldwidely for R&D of future detectors. The studies of muon detection in air showers are under way with scintillator with absorber and Auger water tanks as an associate experiment at the TA site. Tests of cosmic-ray observations using new types of fluorescence telescopes, which aim at future large and low-cost observations of UHECRs, are being performed as associate experiments at the TA site. One is FAST, which consists of a segmented mirror and four PMTs. Another is CRAFFT, which consists of a 1-m^2 Fresnel lens and an 8-inch PMT.

The JEM-EUSO is the space project to investigate the highest-energy cosmic rays by a wide view UV telescope that will be mounted on the International Space Station (ISS). The prototype (EUSO-TA) of JEM-EUSO has been tested occasionally at the TA site since December, 2012 [2]. K-EUSO consists of Schmidt optics and a multi-anode-photomultiplier array focal surface, covering a field of view of 40 degrees. The advantage is its rather uniform and large aperture (annual exposure is four times TAx4) in the whole sky. It is planned to launch in 2022.

Spokespersons

After December 2011 and before December 2017
Hiroyuki Sagawa, ICRR, Univ. of Tokyo
Gordon Thomson, Dept. of Physics, Univ. of Utah

After December 2017
Shoichi Ogio, Dept. of Physics, Osaka City Univ.
Charles Jui, Dept. of Physics, Univ. of Utah

*2 G. Abdellaoui et al., JEM-EUSO Collaboration, "EUSO-TA - First results from a ground-based EUSO telescope", Astrop. Phys. 102 (2018) 98-111.

Collaboration Name

Institute	Country	(*)
Univ. of Utah	USA	26
Univ. of Yamanashi	Japan	5
Tokyo Insititute of Technology	Japan	7
Hanyang Univ.	Korea	2
Tokyo Univ. of Science	Japan	3
KindaiUniv.	Japan	1
Yonsei Univ.	Korea	1
KEK	Japan	2
Osaka City Univ.	Japan	22
ICRR, Univ. of Tokyo	Japan	17
Kanagawa Univ.	Japan	3
Saitama Univ.	Japan	5
Rutgers Univ.	USA	2
Tokyo City Univ.	Japan	1
Institute for Nuclear Research of the Russian Academy of Sciences	Russia	9
Waseda Univ.	Japan	2
Chiba Univ.	Japan	2
UNIST	Korea	2
Ewha Womans Univ.	Korea	1
IPMU, Univ. of Tokyo	Japan	1
RIKEN	Japan	3
Kochi Univ.	Japan	1
Ritsumeikan Univ.	Japan	1
Univ. Libre de Bruxelles	Belgium	2
Earthquake Research Institute, Univ. of Tokyo	Japan	2
Hiroshima City Univ.	Japan	1
National Institute of Radiological Science	Japan	1
Ehime Univ.	Japan	1
Sungkyunkwan Univ.	Korea	6
Ritsumeikan Univ.	Japan	1
Osaka Electro-Communication Univ.	Japan	1
Shinshu University	Japan	5
Institute of Physics, Czech Academy of Sciences	Czech	1
Total		139

(*) Number of participants as of June 2018.

Members

Staffs
Hiroyuki Sagawa, Assoc. Prof., Feb. 2004 to Nov. 2016; Prof., Nov. 2016 to the present
Takashi Sako, Assoc. Prof. Oct. 2017 to the present
Masahiro Takeda, Assist. Prof., to the present
Toshiyuki Nonaka, Assist. Prof., to the present

Kazumasa Kawata, Project Assist. Prof., Apr. 2012 to Mar. 2014; contd TA in Tibet group, Apr. 2014 to Mar. 2018; Assist. Prof., Apr. 2018 to the present
Masaki Fukushima, Prof., to Sep. 2015

Postdoctoral Fellows

Tatsunobu Shibata, Apr. 2005 to Mar. 2014
Yuichiro Tameda, Apr. 2010 to Mar. 2013
Daisuke Ikeda, Apr. 2010 to Mar. 2018
Eiji Kido, Apr. 2012 to the present
Naoto Sakaki, Apr. 2016 to Mar. 2018
Toshihiro Fujii, Apr. 2016 to the present

Graduate Students

One student was awarded doctor degrees and one student earned master degrees during 2012–2018, supervised by ICRR staff members.

List of Publications

After Year 2012

Papers in Refereed Journals

[1] H. Tokuno *et al.*, "New air fluorescence detectors employed in the Telescope Array experiment", Nucl. Instr. Meth. A676 (2012) 54-65.

[2] S. Kawana *et al.*, "Calibration of photomultiplier tubes for the fluorescence detector of telescope array experiment", Nucl. Instr. Meth. A681 (2012) 68-77.

[3] T. Abu-Zayyad *et al.*, "The Energy Spectrum of Telescope Array's Middle Drum Detector and the Direct Comparision to the High Resolution Fly's Eye Experiment", Astropart. Phys. 39-40 (2012) 109.

[4] T. Abu-Zayyad *et al.*, "The surface detector array of the Telescope Array experiment", Nucl. Instr. Meth. 689 (2012) 109.

[5] T. Abu-Zayyad *et al.*, "Search for anisotropy of ultra-high enenrgy cosmic rays with the Telescope Array experiment", Astrophys. J. 757:26 (2012).

[6] T. Abu-Zayyad *et al.*, "The Cosmic Ray Energy Spectrum Observed with the Surface Detector of the Telescope Array Experiment", Astrophys. J. Lett. 768:L1 (2013).

[7] T. Abu-Zayyad *et al.*, "The energy spectrum of ultra-high-energy cosmic rays measured by the Telescope Array FADC fluorescence detectors in monocular mode", Astropart. Phys. 48 (2013) 16-24.

[8] T. Abu-Zayyad *et al.*, "CORRELATIONS OF THE ARRIVAL DIRECTIONS OF ULTRA-HIGH ENERGY COSMIC RAYS WITH EXTRA-GALACTIC OBJECTS AS OBSERVED BY THE TELESCOPE ARRAY EXPERIMENT", Astrophys. J. 777:88 (8pp), 2013.

[9] T. Abu-Zayyad *et al.*, "Upper limit on the flux of photons with energies above 10^{19} using the Telescope Array surface detector", Phys. Rev. D88, 112005 (2013).

[10] R.U. Abbasi *et al.*, "INDICATIONS OF INTERMEDIATE-SCALE ANISOTROPY OF COSMIC RAYS WITH ENERGY GREATER THAN 57 EeV IN THE NORTHERN SKY MEASURED WITH THE SURFACE DETECTOR OF THE TELESCOPE ARRAY EXPERIMENT", Astrophys. J. Lett. 790:L21 (2014).

[11] P. Tinyakov for the Telescope Array Collaboration, "Latest results from the telescope array", Nucl. Instr. Meth. A742 (2014) 29-34.

[12] B.K. Shin *et al.*, "Gain monitoring of telescope array photomultiplier cameras for the first 4 years of operation", Nucl. Instr. Meth. A768 (2014) 96-103.

[13] A. Aab *et al.*, (Pierre Auger and Telescope Array Collaborations), "SEARCHES FOR LARGE-SCALE ANISOTROPY IN THE ARRIVAL DIRECTIONS OF COSMIC RAYS DETECTED ABOVE ENERGY OF 10^{19} eV AT THE PIERRE AUGER OBSERVATORY AND THE TELESCOPE ARRAY", Astrophys. J., 794:172 (2014).

[14] R.U. Abbasi *et al.*, "A NORTHERN SKY SURVEY FOR POINT-LIKE SOURCES OF EeV NEUTRAL PARTICLES WITH THE TELESCOPE ARRAY EXPERIMENT", Astrophys. J. 804:133 (2015).

[15] R.U. Abbasi *et al.*, "Study of Ultra-High Energy Cosmic Ray composition using Telescope Array's Middle Drum detector and surface array in hybrid mode", Astropart. Phys. 64 (2015) 49-62.

[16] R.U. Abbasi *et al.*, "Measurement of the proton-air cross section with Telescope Array's Middle Drum detector and surface array in hybrid mode", Phys. Rev. D 92, 032007 (2015).

[17] R.U. Abbasi *et al.*, "The energy spectrum of cosmic rays above $10^{17.2}$ eV measured by the fluorescence detectors of the Telescope Array experiment in seven years", Astropart. Phys. 80 (2016) 131-140.

[18] R.U. Abbasi *et al.*, "First upper limits on the radar cross section of cosmic-ray induced extensive air showers", Astropart. Phys. 87 (2017) 1-17.

[19] R.U. Abbasi *et al.* "The bursts of high energy events observed by the telescope array surface detector", Phys. Lett., A381 (2017) 2565-2572.

[20] R.U. Abbasi *et al.*, "Search for EeV protons of galactic origin", Astropart. Phys. 86 (2017) 21-26.

[21] B.R. Dawson, M. Fukushima, P. Sokolsky, "Past, present, and future of UHECR observations", Prog. of Theor. and Exp. Phys., 2017, 12A101.

[22] V. Verzi, D. Ivanov, and Y. Tsunesada, "Measurement of energy spectrum of ultra-high energy cosmic rays", Prog. of Theor. and Exp. Phys., 2017, 12A103.

[23] O. Deligny, K. Kawata, P. Tinyakov, "Measurement of anisotropy and the search for ultra high energy cosmic ray sources", Prog. of Theor. and Exp. Phys. 2017, 12A104.

[24] R.U. Abbasi *et al.*, "Depth of Ultra HIgh Energy Cosmic Ray Induced Air Shower Maxima Measured by the Telescope Array Black Rock and Long Ridge FADC Fluorescence Detectors and Surace Array in Hybrid Mode", Astrophys. J., 858:76 (2018).

[25] R.U. Abbasi *et al.*, "Study of muons from ultra-high energy cosmic ray air showers measured with the Telescope Array experiment", Phys. Rev. D 98, 022002 (2018).

[26] R.U. Abbasi. *et al.*, "Evidence of Intermediate-scale Energy Spectrum Anisotropy of Cosmic Rays $E \geq 10^{19.2}$ eV with the Telescope Array Surface Detector", Astrophys. J. 862:91 (2018).

[27] R.U. Abbasi *et al.*, "Gamma Ray Showers Observed at Ground Level in Coincidence With Downward Lightning Leaders", J. Geophys. Res: Atmos., 123 (2018).

[28] R.U. Abbasi *et al.* "Cosmic-Ray Energy Spectrum between 2 PeV and 2 EeV Observed with the TALE detector in monocular mode", accepted for Astrophys. J., arXiv:1803.01288.

[29] R.U. Abbasi *et al.*, "Search for Anisotropy in the Ultra High Energy Cosmic Ray Spectrum using the Telescope Array Surface Detector", submitted to Phys. Rev. Lett., arXiv:1707.04967.

[30] R.U. Abbasi *et al.*, "Evidence for Declination Dependence of Ultrahigh Energy Cosmic Ray Spectrum in the Northern Hemisphere", submitted to Astrophys. J., arXiv:1801.07820.

[31] R.U. Abassi *et al.*, "Mass composition of ultra-high-energy cosmic rays with the Telescope Array Surface Detector Data", submitted to Phys. Rev. D., arXiv:1808.03680.

Papers in Conference Proceedings

for ICRR TA members and others referred in this report

[32] S. Ogio, "Future plans of the Telescope Array experiment", International Symposium on Future Directions in UHECR Physics (UHECR2012), CERN, Geneva, Switserland, 2012/2/16 (oral).

[33] D. Ikeda, "Recent Results of Energy Spectrum and Mass Composition from Telescope Array Fluorescence Detec", 23rd European Cosmic Ray Symposium (ECRS-2012), Moscow, Russia, 2012/7/3-7/7 (poster).

[34] H. Sagawa, "Detection of the Atmospheric Showers with Telescope Array (TA) experiment", Conference on Calorimetry for the High Energy Frontier (CHEF2014), Paris, France, 2013/4/25 (oral).

[35] H. Sagawa, “Highlights from the Telescope Array Experiment”, 33rd International Cosmic Ray Conference (ICRC2013), Rio de Janeiro, Brazil, 2013/7/4 (invited).

[36] H. Sagawa, “The plan of the Telescope Array Experiment for the Next Five Years”, ICRC2013, 2013/7/2-7/9 (poster).

[37] K. Kawata, “Search for EeV Neutral Particles from the Point-like Sources with the Telescope Array Surface Detector”, ICRC2013, 2013/7/2-7/9 (poster).

[38] K. Kawata, “Search for the Large-Scale Cosmic-Ray Anisotropy at 10^{18} eV with the Telescope Array Surface Detector”, ICRC2013, 2013/7/2-7/9 (poster).

[39] E. Kido, “Constraining UHECR source models by the TA SD energy spectrum”, ICRC2013, 2013/7/4 (oral).

[40] D. Ikeda, ‘Ultra-High Energy Cosmic Ray Spectrum Measured by the Hybrid Analysis in the Telescope Array‘”, ICRC2013, 2013/7/2-7/9 (poster).

[41] T. Shibata, “Absolute energy calibration of the Telescope Array Fluorescence Detector with an Electron Linear Accelerator”, ICRC2013, 2013/7/3 (oral).

[42] D. Ikeda, “Test of Radar Echo Detection using the Electron Beam from the ELS at the Telescope Array Site: A Test for Future Large Scale Extension of the Air Shower Observatory”, ICRC2013, 2013/7/2-7/9 (poster).

[43] T. Nonaka, “Design and prospect of a surface Muon Detector for Telescope Array experiment”, ICRC2013, 2013/7/2-7/9 (poster).

[44] M. Fukushima, “Observation of UHECRs - status and prospects -”, Symposium on Cosmology and Particle Astrophysics (CosPA 2013), Honolulu, USA, , 2013/11/15 (oral).

[45] E. Kido, “Recent Results from the Telescope Array experiment”, High Energy Messengers: Connecting the Non-Thermal Extragalactic Backgrounds (HEM 2014), Chicago, USA, 2014/6/9 (oral).

[46] K. Kawata, “Telescope Array Experiment: Recent Results and Future Plans”, Joint TeV Particle Astrophysics / IDM Conference (TEVPA/IDM), Amsterdam, The Netherlands, 2014/6/23-24 (oral).

[47] M. Fukushima, “TA Recent Results and Prospects”, The XVIII International Symposium on Very High Energy Cosmic Ray Interactons (ISVHECRI 2014), CERN, Geneva, 2014/8/19 (oral).

[48] M. Fukushima, “Observation of UHECRs in the next decade”, 24th European Cosmic Ray Symposium (ECRS 2014), Keil, Germany, 2014/9/1-5 (oral).

[49] H. Sagawa, “TAx4”, Ultra-High-Energy Cosmic-Ray Conference 2014 (UHECR 2014), Springdale, Utah, USA, 2014/10/14 (oral).

[50] E. Kido, “Simulations of Ultra High Energy Cosmic Rays propagation”, UHECR2014, 2014/10/13 (oral).

[51] T. Nonaka, “TA-muon”, UHECR2014, 2014/10/14 (oral).

[52] H. Sagawa, “Recent results from the Telescope Array - studies of ultra-high energy cosmic rays and the prospect -”, International Conference on the Structure and the Interactions of the Phton including the 21th International Wrokshop on Photon-Photon Collisions and the International Workshop on High Energy Photon Colliders (Photon2015), Novosibirsk, Russia, 2015/6/15 (invited).

[53] K. Kawata, “Ultra-High-Energy Cosmic Ray Conference, 34th International Cosmic Ray Conference (ICRC2015), The Hauge, The Netherlands, 2015/7/30 (oral).

[54] R. Takeishi for the Auger and TA Collaborations, “Initial results of a direct comparison between the Surface Detectors of the Pierre Auger Observatory and the Telescope Array”, ICRC2015, 2015/7/30 (poster).

[55] T. Nonaka, “Performance and Operational Status of Muon Detectors in the Telescope Array Experiment”, ICRC2015, 2015/7/30. (poster).

[56] D. Ikeda, “Energy Spectrum and Mass Composition of Ultra-High Energy Cosmic Rays Measured by the hybrid technique in Telescope Array”, ICRC2015, 2015/7/30 (poster).

[57] T. Nonaka, “Anisotropy search in the Ultra High Energy Cosmic Ray Spectrum in the Northern Hemisphere using the Telescope Array surface detector”, ICRC2015, 2015/7/30 (poster).

[58] T. Fujii, “Energy Spectrum and Mass Composition of Ultra-High Energy Cosmic Rays Measured with the Telescope Array Fluorescence Detector Using a Monocular Analysis”, ICRC2015, 2015/7/30 (poster).

[59] E. Kido, ”Interpretation of the energy spectrum observed with the Telescope Array surface detectors”, ICRC2015, 2015/8/4 (oral).

[60] H. Sagawa, “Telescope Array extension: TAx4”, ICRC2015, 2015/8/5 (oral).

[61] H. Sagawa, “Telescope Array Extension”, Cosmic Ray International Seminar 2015 (CRIS2015), Gallipoli, Italy, 2015/9/14 (invited).

[62] T. Fujii, “Energy spectrum measured by the Telescope Array experiment in $10^{15.8}$ eV to $10^{20.3}$ eV range”, TeV Particle Astrophysics 2015 (TEVPA2015), Kashiwa-no-ha Conference Center, Kashiwa, Chiba, 2015/10/26 (oral).

[63] T. Nonaka, “Results from the Telescope Array experiment, Hotspot and anisotropy”, TEVPA2015, 2015/10/26 (invited).

[64] T. Nonaka, “Surface detector for TAx4 expansion and status of Muon measurement at TA site”, Next-Generation Techniques for UHE Astroparticle Physics, Chicago, IL, USA, 2016/2/29 (invited).

[65] D. Ikeda, “Recent Results and Future Prospects from the Telescope Array experiment”, 10th Cosmic Ray International Seminar (CRIS2016), Ischia/Naples, Italy, 2015/7/6 (invited).

[66] E. Kido, “The extension of the Telescope Array experiment”, 38th International Conference on High Energy Physics (ICHEP2016), Chicago, IL, USA, 2016/8/8 (poster).

[67] T. Nonaka,“Anisotropy Search in Energy Distribution in the Northern Hemisphere Using the Telescope Array Surface Detector Data”, 2016 International Conference on Ultra-High Energy Cosmic Rays (UHECR2016), Kyoto Research Park, Kyoto, Kyoto, Japan, 2016/10/11 (oral).

[68] R. Takeishi, “Studies of Muons in Extensive Air Showers from Ultra-High Energy Cosmic Rays Observed with the Telescope Array Surface Detector”, UHECR2016, 2016/10/12 (poster).

[69] E. Kido, “The TAx4 experiment”, UHECR2016, 2016/10/14 (oral).

[70] D. Ikeda, “Recent Results from the Telescope Array Experiment”, Astroparticle Physics Yachay Tech, Quito/Urcuqui,Ecuador, 2016/12/6 (invited).

[71] E. Kido, “The TAx4 experiment”, The 35th International Cosmic Ray Conference (ICRC2017), Busan, Korea, 2017/7/15 (oral).

[72] J.N. Matthews, “Highlights from the Telescope Array”, ICRC2017, 2017/7/17 (invited).

[73] D. Ikeda, “Hybrid Measurement of the Energy Spectrum and Composition of Ultra-High Energy Cosmic Rays by the Telescope Array”, ICRC2017, 2017/7/18 (poster).

[74] T. Fujii,“A systematic uncertainty on the energy scale of the Telescope Array fluorescence detectors”, ICRC2017, 2017/7/18 (poster).

[75] T. Nonaka, “Anisotropy search in Energy distribution in Northern hemisphere using Telescope Array Surface Detector data”, ICRC2017, 2017/7/18 (poster).

[76] R. Takeishi, “Study of muon from ultra-high energy cosmic ray air showers measured with the Telescope Array experiment”, ICRC2017, 2017/7/18 (poster).

[77] E. Kido, “Interpretation of the energy spectrum observed with the Telescope Array detectors”, ICRC2017, 2017/7/18 (poster).

[78] V. de Souza, “Testing the agreement between the X_{max} distributions measured by the Pierre Auger and Telescope Array Observatories”, ICRC2017, 2017/7/18 (oral).

[79] . G. Rubtsov, “Telescope Array search for EeV photons and neutrinos”, ICRC2017, 2017/7/17 (oral).

[80] D. Bergman, “j-NICHE: Prototype detectors of a non-imaging Cherenkov array at the Telescope Array site”, ICRC2017, 2017/7/17 (oral)

[81] H. Sagawa, “Latest results of the Telescope Array experiment on ultra-high energy cosmic rays”, Second KIAA Workshop on Astroparticle Physics, Beijing, China, 2017/8/17 (invited).

[82] R. Takeishi, “Observation of ultra-high energy cosmic rays with the Telescope Array experiment”, 6th International Conference on New Frontiers in Physics (ICNFP2017), Grete, Greek, 2017/8/21 (oral).

Doctor theses

[83] R. Takeishi, ”Study of muons from ultra-high energy cosmic ray air showers measured with the Telescope Array experiment”, University of Tokyo (2016).

Tibet ASγ PROJECT

Introduction

The Tibet air shower experiment has been successfully operated at Yangbajing (90°31' E, 30°06' N; 4300 m above sea level) in Tibet, China since 1990. It has continuously made a wide field-of-view (approximately 2 steradian) observation of cosmic rays and gamma rays in the northern sky.

Summary from 2012 to 2018

Summarized here are the noticeable achievements during the period of this review, i.e., between 2012 and 2018.

- The 2-dimensional anisotropy (0.1 % level) at sidereal time frame in the multi-TeV energy range is characterized by the "Tail-in" (hump) and "Loss-cone" (dip) structures. The Milagro experiment claimed the loss cone ampliture showed a yearly variation. However, we found no such variation in the observed anisotropy.

  We measured the cosmic-ray anisotropy from a 10 TeV to 1 PeV. Above 100 TeV, we found the anisotropy distinct from that at multi-TeV region. The Loss cone and the Tail-in structure becomes less significant and a new component appeared. This result obtained in the northern hemisphere is consistent with the IceCube observation in the southern hemisphere.

- A clear solar-cycle variation of the Sun's shadow in 10 TeV cosmic rays are observed by the Tibet air shower array covering a full solar cycle from 1996 to 2009. Numerical simulations of the Sun's shadow are developed, employing the Potential Field Source Surface (PFSS) model and the Current Sheet Source Surface (CSSS) model for the coronal magnetic field, to interpret the physical implications of the observed solar cycle variation. It is found that the intensity deficit in the simulated Sun's shadow is very sensitive to the coronal magnetic field structure, and the observed variation of the Sun's shadow is better reproduced by the CSSS model than the PFSS model. This is the first successful attempt to evaluate the coronal magnetic field models by means of the Sun's shadow observed in 10 TeV cosmic rays.

  We analyzed the Sun shadow in cosmic rays and found that the shadow center displaced northward (southward) from the optical center of the Sun in the "away" ("toward") interplanetary magnetic field (IMF) sector. We found that the average IMF strength in the away (toward) sector is 1.54 $\pm$ 0.21$_{\rm stat}$ $\pm$ 0.20$_{\rm sys}$ (1.62 $\pm$ 0.15$_{\rm stat}$ $\pm$ 0.22$_{\rm sys}$) times larger than the expected from the numerical simulation assuming the solar magnetic field model. This demonstrates that the obsrvation of the Sun shadow in cosmic rays enables us to make a quantitative evaluation of the average solar magnetic field between the Sun and the Earch, which is difficult by satallite experiments.

- Based on data collected by the Tibet air shower array and the 100 m^2 underground muon detector (MD) during 438 live days, we search for continuous gamma-ray emission from the Crab Nebula above 100 TeV. No significant excess was found, and the most stringent upper limit is obtained above 140 TeV, even with the small 100 m^2 MD.

- As an upgrade, new air shower core detectors (YAC-II) were constructed and started data-taking in 2014 for the next-step measurement of the chemical composition in the knee energy region, while large ($\sim$4,000 m^2) muon detectors (MD) aiming at higher-sensitivity (by a facto of $\sim$10) gamma-ray observation in the 100 TeV region was constructed under the Tibet air shower array and started data-taking in 2014. The MD also plays an important role to measure the chemical composition of cosmic rays in the knee energy region.

Experiment

The Tibet I array was constructed in 1990 and it was gradually upgraded to the Tibet II by 1994 which consisted of 185 fast-timing (FT) scintillation counters placed on a 15 m square grid covering 36,900 m^2, and 36 density (D) counters around the FT-counter array. Each counter has a plastic scintillator plate of 0.5 m^2 in area and 3 cm in thickness. All the FT counters are equipped with a fast-timing 2-inch-in-diameter photomultiplier tube (FT-PMT), and 52 out of 185 FT counters are also equipped with a wide dynamic range 1.5-inch-in-diameter PMT (D-PMT) by which we measure up to 500 particles which saturates FT-PMT output, and all the D-counters have a D-PMT. A 0.5 cm thick lead plate is put on the top of each counter in order to increase the counter sensitivity by converting gamma rays into electron-positron pairs in an electromagnetic shower. The mode energy of the triggered events in Tibet II is 10 TeV.

In 1996, we added 77 FT counters with a 7.5 m lattice interval to a 5,200 m^2 area inside the northern part

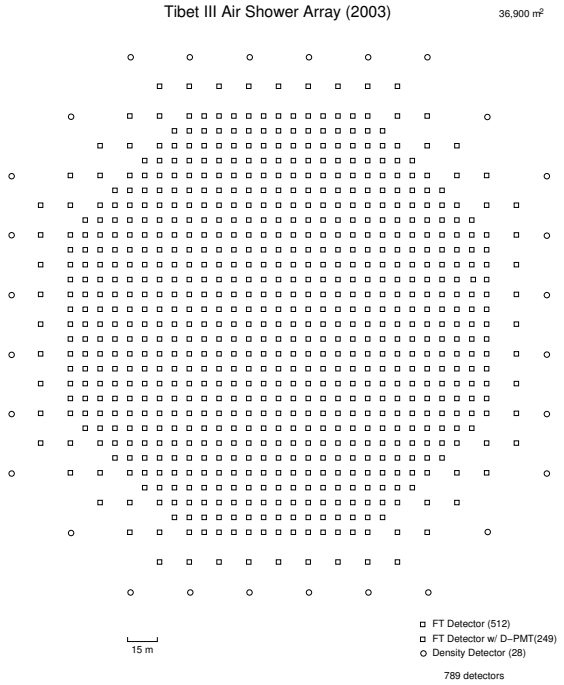

Fig. 1. Schematic view of Tibet III.

of the Tibet II array. We called this high-density array Tibet HD. The mode energy of the triggered events in Tibet HD is a few TeV.

In the late fall of 1999, the array was further upgraded by adding 235 FT-counters so as to enlarge the high-density area from 5,200 m^2 to 22,050 m^2, and we call this array and further upgraded one Tibet III. In 2002, all of the 36,900 m^2 area was covered by the high-density array by adding 200 FT-counters more. Finally we set up 56 FT-counters around the 36,900 m^2 high density array and equipped 8 D-counters with FT-PMT in 2003. At present, the Tibet air shower array consists of 761 FT-counters (249 of which have a D-PMT) and 28 D-counters as in Fig. 1.

The performance of the Tibet air shower array has been well examined by observing the Moon's shadow (approximately 0.5 degrees in diameter) in cosmic rays. The deficit map of cosmic rays around the Moon demonstrates the angular resolution to be around 0.9° at a few TeV for the Tibet III array. The pointing error is estimated to be better than ∼0.01° by the displacement of the shadow's center from the apparent center in the north-south direction, as the east-west component of the geomagnetic field is very small at the experimental site. On the other hand, the shadow center displacement in the east-west direction due to the geomagnetic field enables us to spectroscopically estimate the energy scale uncertainty at ±12 % level.

Physics Results

TeV gamma-ray astrophysics

Gamma rays at TeV energies from the Crab Nebula were first detected by the Whipple collaboration in 1989. Since the detection, the energy spectrum of the Crab Nebula has been measured by many imaging air Cherenkov telescopes as well as air shower arrays; the Tibet ASγ collaboration was the first air shower array which detected gamma rays from the Crab Nebula at multi-TeV energies. The Crab Nebula is now commonly used as a standard candle for gamma-ray experiments. The energy spectrum is reproduced with a mechanism based on the synchrotron self-Compton (SSC) emission of high energy electrons. None of the experiments has detected gamma rays above 100 TeV from the Crab Nebula, and the best upper limits have been given by the CASA-MIA experiment. The observation of the energy spectrum of the Crab Nebula around 100 TeV with higher sensitivity is very important in order to confirm the leptonic origin of the Crab's TeV gamma-ray emission. Therefore, a search is made for gamma rays above ∼100 TeV from the Crab Nebula, using the Tibet air shower (AS) array combined with a 100 m^2 muon detector (MD).

Using the data collected by the 100 m^2 MD from March 2008 to February 2010 (438 live days), we search for continuous gamma-ray emission from the Crab Nebula above 100 TeV. No significant excess is found, and the most stringent upper limit is obtained above 140 TeV, as shown in Fig. 2, even with the small 100 m^2 MD [3].

Cosmic-ray anisotropy in the multi-TeV region with high precision

Galactic cosmic rays at TeV energies reach the Earth almost isotropically, due to strength of the galactic magnetic field disturbing the trajectory of cosmic rays. The Larmor radius of a 1 TeV proton in a lG magnetic field is 0.001 pc, many orders of magnitude shorter than the distance to any potential source of cosmic rays. Numerous experiments including the Tibet air-shower experiment, on the other hand, reported the existence of a small (∼0.1%) galactic cosmic- ray anisotropy at sidereal time frame. They consistently found that there are two distinct large-scale structures in the anisotropy; one is a deficit region in the cosmic-ray flux called the "loss-cone", distributed between 150 degrees and 240 degrees in right ascension, and the other an excess region called the "tail-in", distributed between 40 degrees and 90 degrees in right ascension. The common understanding of the origin of the anisotropy has not been established until now.

The Milagro experiment reported a steady increase in the amplitude of the loss-cone at 6 TeV from July

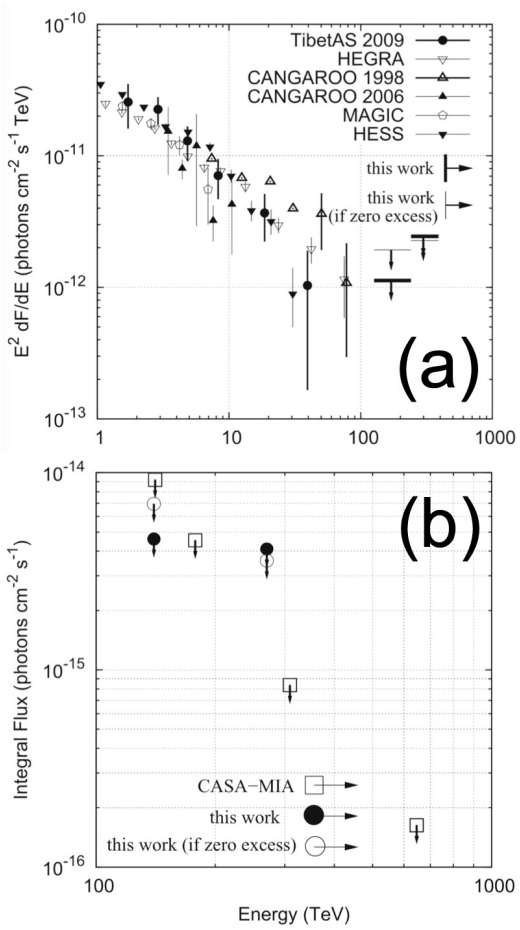

Fig. 2. From Ref. [3] (references therein) . (a) Upper limits on the Crab Nebula's differential flux at the 90% confidence level obtained by this work (thick solid lines with downward arrows). The upper limits obtained by this work assuming zero excess counts are drawn by thin solid lines with downward arrows. The flux points measured by our previous work (closed circles) as well as by HEGRA (open inverse triangles), CANGAROO (filled and open triangles), MAGIC (open pentagons), and H.E.S.S. (filled inverse triangles) are also shown. (b) Upper limits on the Crab Nebula's integral flux at the 90% confidence level obtained by this work (filled circles with downward arrows), along with the upper limits at the 90% confidence level by CASA-MIA (open squares with downward arrows). The upper limits obtained by this work assuming zero excess counts are drawn by open circles with downward arrows.

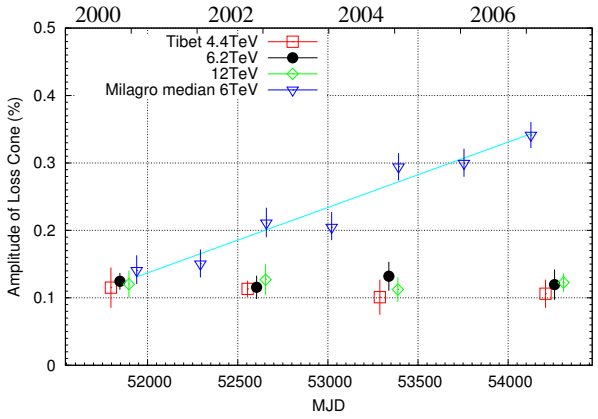

Fig. 3. From Ref. [1]. Time dependence of the loss-cone amplitude observed by the Tibet experiment at 4.4 TeV (open squares), 6.2 TeV (filled circles) and 11 TeV (open diamonds), along with Milagro's data (open inverse triangles) and the best-fit linear function to Milagro's data. The MJDs of our data points correspond to the times at the middle of each period. The upper horizontal axis represents years. All the error bars are the linear sums of the statistical and systematic errors.

2000 to July 2007, in the latter half of the 23rd solar cycle. Milagro was a water Cherenkov detector located in New Mexico at the altitude of 2630 m above sea level, composed of an 80 m × 60 m × 8 m pond surrounded by a 200 m × 200 m array of 175 water tanks. Using a data set consisting of 96 billion cosmic-ray events, which is unprecedentedly large at TeV energies, Milagro significantly claimed the detection of the increase in the loss-cone amplitude at 6 TeV. The Tibet air-shower experiment would be the only experiment that operated during the corresponding period and is capable of examining Milagro's results with comparable statistics at TeV energies. We examined Milagro's claim using the data collected by the Tibet air-shower experiment during 1916 live days from November 1999 through December 2008.

Figure 3 shows the time dependence of the loss-cone amplitude measured at 4.4, 6.2, and 11 TeV by the Tibet experiment in comparison with that measured at 6 TeV by Milagro. It can be clearly seen that, contrary to Milagro's results, the loss-cone amplitude measured by the Tibet experiment is quite stable at 4.4, 6.2, and 11 TeV during the period from 2000 to 2008 [1]. Milagro argued that variations in the heliosphere in relation to solar activities could cause the time dependence of the sidereal cosmic-ray anisotropy. In that case, the same tendency would be seen at sub-TeV energies, where the anisotropy is expected to be much more sensitive to solar activities. Matsushiro underground muon observatory, however, reports that the loss-cone amplitude shows no significant increase at 0.6 TeV during the corresponding period, suggesting that the steady increase in the loss-cone amplitude observed by Milagro at 6 TeV is not caused by the solar modulation effects.

Recently, IceCube reported the anisotropy observed in the southern sky, showing a new phenomenon different from that obtained by EAS-TOP in 2012. A clear deficit with a post-trial significance of -6.3σ at 400 TeV was detected, which was then confirmed by the result from Ice-Top in 2013. The Ice-Top data further revealed the existence of anisotropy at energies up to 1 PeV in 2013. On the other hand, the anisotropy feature above ∼300 TeV observed by the Tibet air shower array in 2006 was found to be different from those in lower energy regions and in agreement with IceCube's result at 400 TeV.

By improving the reconstruction of primary energy, we will also extend the analyzed energy range to two

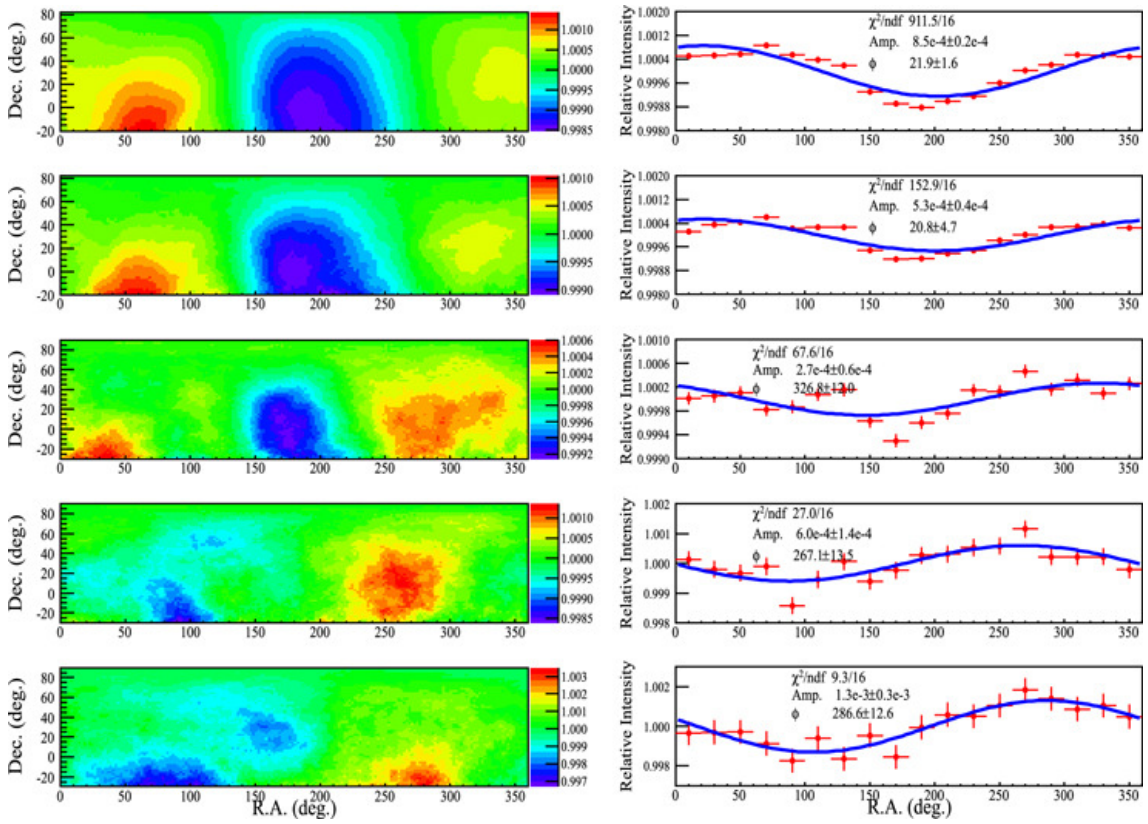

Fig. 4. From Ref. [6]. 2D anisotropy maps in five energy samples (15, 50, 100, 300, and 1000 TeV, from top to bottom). Left panels show the relative intensity maps (with 30° smoothing), while right panels show the 1D projections. The blue curve shows the first harmonic fitting to the data.

decades between 10 TeV and 1 PeV, which is also the widest coverage of such works. Analysis of the 10 - 1000 TeV large-scale sidereal anisotropy of gaalactic cosmic rays was made with the data collected by the Tibet air shower array from 1995 October to 2010 February [6]. In this analysis, we improve the energy estimate and extend the declination range down to -30°. Our result is shown in Fig. 4. We find that the anisotropy maps above 100 TeV are distinct from that at a multi-TeV band. The so-called tail-in and loss-cone features identified at low energies get less significant, and a new component appears at ∼100 TeV. The spatial distribution of the galactic cosmic-ray intensity with an excess (7.2σ pre-trial, 5.2σ post-trial) and a deficit (-5.8σ pre-trial) are observed in the 300 TeV anisotropy map, consistent with IceCube's results at 400 TeV. We further find that the amplitude of the first order anisotropy increases sharply above ∼100 TeV, indicating a new component of the anisotropy. These results will make significant contribution to understanding the origin and propagation of galactic cosmic rays.

Global 3-dimensional structure of the solar and interplanetary magnetic fields by observing the Sun's shadow in cosmic rays

An understanding of the structure of the Sun's magnetic field between it and the Earth is essential if humanity is to venture into space. However, it is extremely difficult to directly observe the coronal magnetic structure within the Earth's orbit, and while spacecraft such as Voyager and Ulysses have carried out some observations, the solar neighborhood is an extremely harsh environment characterized by high temperatures and high levels of radiation. Even the latest spacecraft cannot get close to the Sun, and as a result our understanding of this region is limited.

The Tibet AS γ experiment observed the Sun's shadow of cosmic rays at 10 TeV energies from 1996 to 2009, created when it shields galactic cosmic rays reaching the Earth.

The coronal magnetic field deflects these charged particles as they pass near the Sun, causing variation in the form of the Sun's shadow. The analyzed data were recorded over the 14-year period from 1996 to 2009, and an anti-correlation was discovered between the 11-year solar cycle and this variation, as shown in Fig. 5. The stable size of the Moon's shadow in cosmic rays over the same period demonstrates that the systematic uncertainty is negligible.

We have also developed and performed numerical simulations of the Sun's shadow in galactive cosmic rays, based on two major coronal magnetic field models - the Potential Field Source Surface (PFSS), and the Current Sheet Source Surface (CSSS). The PFSS model leaves out the effect of the electric current in the

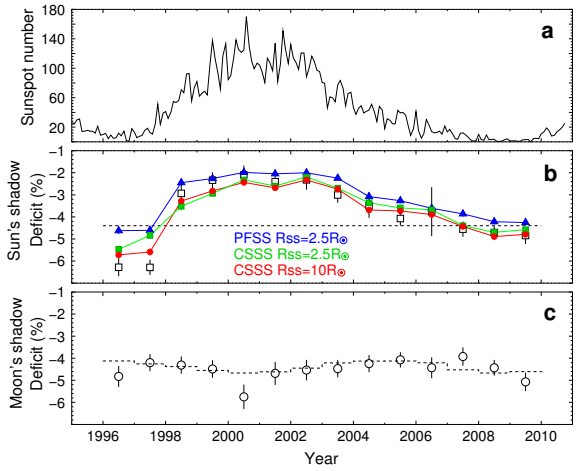

Fig. 5. From Ref. [2]. Temporal variations of (a) the monthly mean sunspot number, (b) the deficit intensity due to the Sun's shadow and (c) the deficit intensity due to the Moon's shadow. The open squares in the panel (b) are the observed central deficit ($D_{\rm obs}$). The blue triangles, green squares and red circles indicate the central deficits ($D_{\rm MC}$) by the MC simulations assuming the PFSS ($R_{\rm ss} = 2.5R_{\odot}$), the CSSS ($R_{\rm ss} = 2.5R_{\odot}$) and the CSSS ($R_{\rm ss} = 10.0R_{\odot}$) models, respectively. $R_{\odot}$ is the solar radius, while $R_{\rm ss}$ is the radius of the source surface (SS) beyond which the magnetic field lines become radial. The dashed lines in the panels (b) and (c) are the deficits expected from the apparent angular size of the Sun and the Moon.

vicinity of the Sun on the structure of the coronal magnetic field, while the CSSS model assumes the effect of the electric current.

The simulation of the trajectories of galactic cosmic rays based on the two models found that the CSSS model better describes the size variation of the Sun's shadow, as shown in Fig. 5.

This is the world's first and most successful analysis of the coronal magnetic structure using the data obtained by the observation of the cosmic ray shadow of the Sun. This research provides a new approach to exploring the Sun's magnetic structure and, with future increased in accuracy, should provide even more detailed knowledge of the magnetic filed between the Sun and the Earth. This research employed the phenomenon that the path of charged cosmic rays is bent when it passes through a magnetic field, and was made possible by the long-term accumulation of cosmic radiation data over a period of 14 years, and is a major step forward in the long-term observation of cosmic radiation. The paper from this result was highlighted as one of the "Editor's Suggestions" in Physical Review Letters (PRL) in 2013[2].

The strong coronal magnetic field affects the cosmic-ray deficit in the shadow, while the interplanetary magnetic field (IMF) between the Sun and the Earth deflects trajectories of TeV cosmic rays a little. The small deflection has actually been observed by some air shower experiments as the North-South displacement of the Sun's shadow center from the optical center of the Sun. We can utilize the observed features of the Sun's shadow as a probe of the solar magnetic field. The solar magnetic field on the photosphere has constantly been monitored by optical measurements employing the Zeeman effect, while the local IMF at the Earth has been directly observed by an near-Earth satellite. However, the observation of the average IMF between the Sun and the Earth is still difficult. As the deflection angle of cosmic rays is proportional to the magnetic field strength, the observed Sun's shadow can be used for evaluating the IMF strength averaged over the distance between the Sun and the Earth.

We use cosmic-ray data recorded during the period between the year 2000 and the year 2009 by the Tibet-III air shower array for the analysis of the Sun's shadow. The observed air shower events are divided into seven energy bins (representative energies: 4.9, 7.7, 13, 22, 43, 90, and 240 TeV), according to the shower size $\Sigma\rho_{\rm FT}$ which is the sum of the number of particles per 1 m^2 as a measure of energy of a primary cosmic-ray particle.

The number of on-source events ($N_{\rm on}$) is defined as the number of air shower events coming from the direction within a circle of Δd radius centered at a given point on the celestial sphere. The number of background, namely, off-source events ($N_{\rm off}$) is calculated by averaging the number of events within each of the eight off-source windows located at the same zenith angle as the on-source one. Subsequently, the flux deficit relative to the number of background events is estimated as $D_{\rm obs} = (N_{\rm on} - N_{\rm off})/N_{\rm off}$ at every 0.1° grid of the Geocentric Solar Ecliptic (GSE) longitude and latitude.

The IMF sector polarity is allocated to each day in reference to the daily-averaged GSE-x and GSE-y components of the IMF (B_x, B_y) observed by the near-Earth satellite and the average $D_{\rm obs}$ in "Away" and "Toward" sectors is separately calculated. The "Away" ("Toward") sector polarity is allocated to a day when the IMF observed two days later satisfies $B_x<0$ and $B_y>0$ ($B_x>0$ and $B_y<0$).

The average N-S and E-W displacement angles in "Away" and "Toward" sectors are calculated for each energy bin and plotted as functions of cosmic ray rigidity in Fig. 6. We convert the representative energy of each energy bin to the average rigidity of the Sun's shadow by considering the energy spectra and chemical composition of primary cosmic rays based on the direct measurements. As expected from the magnetic deflection of charged particles, the observed displacement angles displayed by black solid circles are reasonably fitted by a function $\alpha/(R/10{\rm TV})$ of rigidity R in TV with a fitting parameter α standing for the deflection angle at 10 TV.

In the N-S displacement in Fig. 6(a) and 6(b), we see that the magnitudes of the expected shift (broken curves) are smaller than the magnitudes of the observed one (solid curves) in both sectors, implying an underestimation by the MC simulations. On the other hand, the expected E-W shifts in Figure 2(c) and 2(d), are consistent with the observation, which indi-

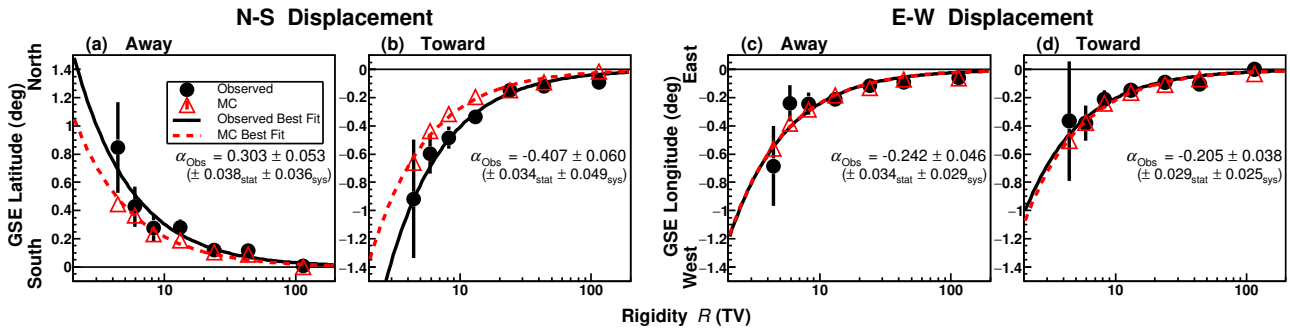

Fig. 6. From Ref. [8]. The rigidity dependence of the N-S [(a), (b)] and E-W [(c), (d)] displacements of the center of the Sun's shadow in away and toward sectors. Black solid circles and red open triangles in each panel show the observed and simulated displacements, respectively, each as a function of the rigidity (R) on the horizontal axis. The error bar of each solid circle indicates the statistical error. Black solid and red broken curves display the function of $\alpha/(R/10\ \mathrm{TV})$ best fitting to black solid circles and red open triangles, respectively. The best-fit parameter α to the observed data is indicated in each panel with systematic errors estimated from the systematic error of the primary energy in our analyses of the Moon's shadow.

cates the E-W shifts are mainly caused by the deflection of cosmic-ray trajectories in the geomagnetic field. It is cofirmed that α in the E-W shifts averaged over "Away" and "Toward" sectors is -0.212 ± 0.034 ($\pm 0.023_{\mathrm{stat}} \pm 0.025_{\mathrm{sys}}$) and consistent with the E-W shiftss in the Moon's shadow. Hence, it is suggested that the underestimation of the N-S shifts in Fig. 6 should be caused by the underestimation of the average field strength between the Sun and the Earth.

For the purpose quantitatively estimating the underestimation, the expected magnetic field strength is simply multiplied by a constant factor f uniformly in the space outside the geomagnetic field. Then, we repeat the MC simulations by changing f and calculate $\alpha(f)$ best fit to each expected shift. The f best fiting the observed shift is evaluated to be $1.54 \pm 0.21_{\mathrm{stat}} \pm 0.20_{\mathrm{sys}}$ ($1.62 \pm 0.15_{\mathrm{stat}} \pm 0.22_{\mathrm{sys}}$) in the "Away" ("Toward") sector, indicating that the model underestimates the IMF strength. This is the first demonstration in the world that the Sun's shadow in cosmic rays allows us to qualitatively evaluate the average IMF strength between the Sun and the Earth[8].

Ongoing Plans

Chemical composition of primary cosmic rays making the knee in the all-particle energy spectrum

We have measured the energy spectra of primary cosmic-ray protons, helium, all particles around the knee energy region. The main component responsible for making the knee structure in the all particle energy spectrum is heavier nuclei than helium. The next step is to identify the chemical component making the knee in the all particle energy spectrum. For the purpose, we constructed Yangbajing Air shower Core detectors II (YAC-II composed of 124 scintillation detectors over $\sim$500m^2 in area), and started data-taking in 2014. YAC-II aims at mainly studying the energy spectra of proton and helium components in the knee energy region.

Gamma-ray astronomy in the 100 TeV region

For the purpose of detecting high-energy cosmic gamma rays with an air shower array, a large underground muon detecter is very effective to reduce cosmic-ray background.

We decided to add a large ($\sim$4,000 m$^2\times$1.5m deep) underground ($\sim$ 2.5 m soil+concrete overburden) water Cherenkov muon detector array (Tibet MD) under the present Tibet air shower array (Tibet AS). By Tibet AS + MD, we aim at background-free detection of celestial point-source gamma rays around 100 TeV with the world-best sensitivity and at locating the origins (PeVatrons) of cosmic rays accelerated up to the knee (PeV) energy region in the northern sky. The measurement of cut off energies in the energy spectra of such gamma rays in the 100 TeV region may contribute significantly to understanding of the cosmic- ray acceleration limit at Supernova Remnants (SNRs). Search for extremely diffuse gamma-ray sources by Tibet AS + MD, for example, from the galactic plane or from the Cygnus region may be very intriguing as well. Above 100 TeV, the angular resolution of Tibet AS with 2-steradian wide field of view is 0.2° and the hadron rejection power of Tibet MD is 1/1000.

In 2014, construction of the $\sim$4,000 m^2 MD was successfully completed and data-taking started. We have accumulated approximately three-year data. Development of Monte Carlo simulation is under way for comparison with real data.Various analysis tools are also extensively being developed. According to the simulation, the sensitivity of the current configuration (Tibet AS + MD) is demonstrated in Fig. 7.

Summary

During the period from 2012 to 2018, the Tibet ASγ experiment contributed significantly to the cosmic-ray physics field in various aspects, thanks to unique features of the Tibet air shower array located at 4300 m

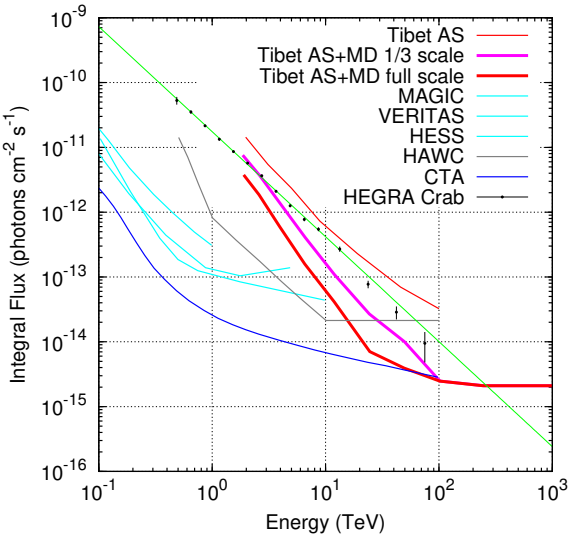

Fig. 7. Sensitivity to point-like gamma-ray sources with Tibet AS+MD (see,Tibet AS+MD 1/3 scale) by pink curve.

above sea level, Yangbajing, Tibet, in China. We are looking forward to new results from the Tibet AS+MD+YAC-II experiment during the forthcoming 6 years.

THE TIBET ASγ COLLABORATION

Institute	Country	(*)
ICRR, Univ. of Tokyo	Japan	4
Hirosaki Univ.	Japan	2
National Astronmomical Observatories	China	2
Institute of High Energy Physics	China	24
Hebei Nornal Univ.	China	2
Tibet Univ.	China	9
Shandong Univ.	China	4
SouthWest Jiaotong Univ.	China	3
Kanagawa Univ.	Japan	4
Utsunomiya Univ.	Japan	1
Konan Univ.	Japan	3
Waseda Univ.	Japan	3
Yokohama National Univ.	Japan	3
Shinshu Univ.	Japan	6
JAXA, ISAS	Japan	1
China Meteorological Administration	China	1
Shandon Arigiculture Univ.	China	1
Saitoma Univ.	Japan	1
National Institute of Informatics	Japan	1
Sakushin Gakuin Univ.	Japan	1
China Univ. of Petroleum	China	1
Tokyo Metropolitan College of Industrial Technology	Japan	1
Max-Planck-Institut für Physik	Germany	1
Yachay Tech	Ecuador	1
Nihon Univ.	Japan	1
Shonan Institute of Technology	Japan	1
JAEA	Japan	1
Total		77

(*) Number of participants as of March 2018.

Members

Staffs

Masato Takita, Associate Professor (February 2001 to November 2016), Professor (November 2016 to the present)
Takashi Sako, Associate Professer (TA/Tibet), October 2017 to the present
Munehiro Ohnishi, Assistant Professor, April 1993 to the present
Kazumasa Kawata, Specially Appointed Assistant Professor (April 2013 to March 2018), Assistant Professor (Tibet/TA, April 2018 to the present) Takahide Kobayashi, Technical Staff, from 1967 to March 2013

Postdoctoral Fellows

Takashi Sako, from April 2010 to March 2017 and from June 2018 to the present

Graduate Students

Three graduate students obtained master degrees during 2012–2018, supervised by ICRR staff members.

List of Publications

After Year 2012

Papers in Refereed Journals

[1] "Is the large-scale sidereal anisotropy of the galactic cosmic-ray intensity really instable at TeV energies?", M. Amenomori *et al.*, Astroparticle Physics, **36** , 237-241 (2012).

[2] "Probe of the Solar Magnetic Field Using the "Cosmic-Ray Shadow of the Sun", M. Amenomori *et al.*, Physical Review Letters, **111** , 011101-1-011101-5 (2013).

[3] "SEARCHE FOR GAMMA RAYS ABOVE 100 TeV FROM THE CRAB NEBULA WITH THE TIBET AIR SHOWER ARRAY AND THE 100m^2 MUON DETECTOR", M. Amenomori *et al.*, THE ASTROPHYSICAL JOURNAL, **813** , 98-1-5 (2015).

[4] "Performance of the Tibet hybrid experiment (YAC-II + Tibet-III + MD) to measure the energy spectra of the light primary cosmic rays at energies 50 - 10,000 TeV", J. Huang *et al.*, Astroparticle Physics, **66** , 18-30 (2015).

[5] "Sensitivity of YAC to measure the light-component spectrum of primary cosmic rays at the 'knee' energies", L. M. . Zhai *et al.*, J. Phys. G Nucl. Part. Phys. , **42** , 045201-1-14 (2015).

[6] "Northern sky Galactic Cosmic Ray anisotropy between 10-1000 TeV with the Tibet Air Shower Array", M. Amenomori *et al.*, THE ASTROPHYSICAL JOURNAL, **836** , 153-1-7 (2016).

[7] "Energy Determination of Gamma-Ray Induced Air Showers Observed by An Extensive Air Shower Array", K. Kawata *et al.*, Experimental Astronomy, **44** , 1-9 (2017).

[8] "Evaluation of the Interplanetary Magnetic Field Strength Using the Cosmic-Ray Shadow of the Sun", M. Amenomori *et al.*, Physical Review Letters, **120** , 031101-1-7 (2018).

Papers in Internatinal Conference Proceedings

[9] "Cosmic-ray shadow" of the Sun at 3 TeV observed by the Tibet Air Shower Array", M. Amenomori et al., Proceedings of The 33rd International Cosmic Ray Conference, Rio de Janeiro, Brazil, July 2 - July 9, 2013, ID=0340.

[10] "A Northern Sky Survey for TeV gamma-ray steady point sources using the Tibet-III air shower array", M. Amenomori et al., Proceedings of The 33rd International Cosmic Ray Conference, Rio de Janeiro, Brazil, July 2 - July 9, 2013, ID=0498.

[11] "Average mass of primary cosmic rays in the knee energy region inferred from Tibet experiment", M. Amenomori et al., Proceedings of The 33rd International Cosmic Ray Conference, Rio de Janeiro, Brazil, July 2 - July 9, 2013, ID=0525.

[12] "Observation of Multi-TeV Gamma Rays from MGRO J2019+37 and MGRO J2031+41 with the Tibet Air Shower Array", M. Amenomori et al., Proceedings of The 33rd International Cosmic Ray Conference, Rio de Janeiro, Brazil, July 2 - July 9, 2013, ID=0513.

[13] "Observation of thundercloud-related charged particles in Tibet", M. Amenomori et al., Proceedings of The 33rd International Cosmic Ray Conference, Rio de Janeiro, Brazil, July 2 - July 9, 2013, ID=0505.

[14] "The TIBET AS+MD Project; progress report 2013", M. Amenomori et al., Proceedings of The 33rd International Cosmic Ray Conference, Rio de Janeiro, Brazil, July 2 - July 9, 2013, ID=0508.

[15] "A Monte Carlo study to measure heavy-component spectra of the primary cosmic-rays at the knee by a new hybrid experiment (YAC-II+Tibet-III+MD)", L. M. Zhai et al., Proceedings of The 33rd International Cosmic Ray Conference, Rio de Janeiro, Brazil, July 2 - July 9, 2013, ID=1049.

[16] "Hadronic interaction and EAS muon investigated with the (YAC + Tibet-III + MD) hybrid experiment", M. Amenomori et al., Proceedings of The 33rd International Cosmic Ray Conference, Rio de Janeiro, Brazil, July 2 - July 9, 2013, ID=1051.

[17] "Observation of the large-scale sidereal anisotropy of the galactic cosmic ray at 300 TeV with the Tibet Air shower Array", M. Amenomori et al., Proceedings of The 33rd International Cosmic Ray Conference, Rio de Janeiro, Brazil, July 2 - July 9, 2013, ID=0256.

[18] "Primary proton and helium spectra at energy range from 50 TeV to 10^{15} eV observed with (YAC+Tibet-III) hybrid experiment", M. Amenomori et al., Proceedings of The 33rd International Cosmic Ray Conference, Rio de Janeiro, Brazil, July 2 - July 9, 2013, ID=1047.

[19] "Progress Report on the MD-A under TIBET III array", M. Amenomori et al., Proceedings of The 33rd International Cosmic Ray Conference, Rio de Janeiro, Brazil, July 2 - July 9, 2013, ID=1018.

[20] "Study on the primary mass sensitivity of muon multiplicity measured with (YAC-II +Tibet-III + MD) experiment", J. S. Liu et al., Proceedings of The 33rd International Cosmic Ray Conference, Rio de Janeiro, Brazil, July 2 - July 9, 2013, ID=1057.

[21] "Test of the hadronic interaction model EPOS-LHC and QGSJETII-04 with Tibet EAS core data", M. Amenomori et al., Proceedings of The 33rd International Cosmic Ray Conference, Rio de Janeiro, Brazil, July 2 - July 9, 2013, ID=1056.

[22] "Progress report on the TIBET AS+MD Project", M. Amenomori et al., Proceedings of the 12th Asia Pacific Physics Conference, Makuhari Messe, Chiba, Japan, July 14 - July 19, 2013, JPS Conf. Proc. 1, 2014, 013124-1-4.

[23] "Observation of intense fluxes of charged particles in association with thundercloud in Tibet", M. Amenomori et al., Proceedings of The 34th International Cosmic Ray Conference, The Hague, The Netherlands, July 30 - August 6, 2015, ID=0246.

[24] "Sidereal anisotropy of Galactic cosmic ray observed by the Tibet Air Shower experiment and the IceCube experiment", M. Amenomori et al., Proceedings of The 34th International Cosmic Ray Conference, The Hague, The Netherlands, July 30 - August 6, 2015, ID=0279.

[25] "Observation of primary cosmic rays with the new Tibet hybrid experiment(YAC-II + Tibet-III + MD)", M. Amenomori et al., Proceedings of The 34th International Cosmic Ray Conference, The Hague, The Netherlands, July 30 - August 6, 2015, ID=0421.

[26] "YAC sensitivity for measuring the light-component spectrum of primary cosmic rays at the "knee energies", L. M. Zai et al., Proceedings of The 34th International Cosmic Ray Conference, The Hague, The Netherlands, July 30 - August 6, 2015, ID=0424.

[27] "Shower reconstruction performance of the new Tibet hybrid experiment consisting of YAC-II, Tibet-III and MD arrays", D. Chen et al., Proceedings of The 34th International Cosmic Ray Conference, The Hague, The Netherlands, July 30 - August 6, 2015, ID=0430.

[28] "Investigation of hadronic interaction models from 10TeV to 1 PeV with the Tibet AS-core", M. Amenomori et al., Proceedings of The 34th International Cosmic Ray Conference, The Hague, The Netherlands, July 30 - August 6, 2015, ID=0431.

[29] "Simulation Study On High Energy Electron and Gamma-ray Detection With the Newly Upgraded

Tibet ASgamma Experiment", Xu Chen et al., Proceedings of The 34th International Cosmic Ray Conference, The Hague, The Netherlands, July 30 - August 6, 2015, ID=0432.

[30] "On the primary model to explain the relation between a rigidity-dependent spectral hardening of proton and helium spectra and a sharp knee of the all-particle spectrum", Ying Zhang et al., Proceedings of The 34th International Cosmic Ray Conference, The Hague, The Netherlands, July 30 - August 6, 2015, ID=0546.

[31] "Search for gamma rays above 100 TeV from the Crab Nebula using the Tibet air shower array and the 100 m^2 muon detector", M. Amenomori et al., Proceedings of The 34th International Cosmic Ray Conference, The Hague, The Netherlands, July 30 - August 6, 2015, ID=0833.

[32] "Energy Determination and Gamma/Hadron Separation using the Lateral Distribution of EAS for the 100 TeV Gamma-Ray Astronomy", K. Kawata et al., Proceedings of The 34th International Cosmic Ray Conference, The Hague, The Netherlands, July 30 - August 6, 2015, ID=0935.

[33] "The TIBET AS+MD Project; progress report 2015", M. Amenomori et al., Proceedings of The 34th International Cosmic Ray Conference, The Hague, The Netherlands, July 30 - August 6, 2015, ID=0969.

[34] "Long term stability analysis on the MD-A under TIBET III array", M. Amenomori et al., Proceedings of The 34th International Cosmic Ray Conference, The Hague, The Netherlands, July 30 - August 6, 2015, ID=1001.

[35] "Northern sky Galactic Cosmic Ray anisotropy between 10 - 1000 TeV with the Tibet Air Shower Array", M. Amenomori et al., Proceedings of The 34th International Cosmic Ray Conference, The Hague, The Netherlands, July 30 - August 6, 2015, ID=0810.

[36] "The Tibet AS+MD Project; status report 2017", M. Amenomori et al., Proceedings of The 35th International Cosmic Ray Conference, Busan, Korea, July 12 - July 20, 2017, ID=831.

[37] "Solar magnetic field strength and the Sun's Shadow observed by the Tibet Air Shower Array", M. Amenomori et al., Proceedings of The 35th International Cosmic Ray Conference, Busan, Korea, July 12 - July 20, 2017, ID=028.

[38] "Interplanetary Coronal Mass Ejection and the Sun's Shadow Observed by the Tibet Air Shower Array", M. Amenomori et al., Proceedings of The 35th International Cosmic Ray Conference, Busan, Korea, July 12 - July 20, 2017, ID=031.

[39] "Measurement of high energy cosmic rays by the new Tibet hybrid experiment", J. Huang et al., Proceedings of The 35th International Cosmic Ray Conference, Busan, Korea, July 12 - July 20, 2017, ID=484.

Presentations in Internatinal Conference Proceedings

[40] "Modeling of the TeV galactic cosmic-ray anisotropy", T. K. Sako, COSPAR2012, Mysore, India, July 14 - July 22, 2012.

[41] " "Cosmic-ray shadow" of the Sun at 3 TeV observed by the Tibet Air Shower Array", T. K. Sako, The 33rd International Cosmic Ray Conference, Rio de Janeiro, Brazil, July 2 - July 9, 2013.

[42] "A Northern Sky Survey for TeV gamma-ray steady point sources using the Tibet-III air shower array", A. Shiomi, The 33rd International Cosmic Ray Conference, Rio de Janeiro, Brazil, July 2 - July 9, 2013.

[43] "Average mass of primary cosmic rays in the knee energy region inferred from Tibet experiment", Y. Katayose, The 33rd International Cosmic Ray Conference, Rio de Janeiro, Brazil, July 2 - July 9, 2013.

[44] "Observation of Multi-TeV Gamma Rays from MGRO J2019+37 and MGRO J2031+41 with the Tibet Air Shower Array", M. Ohnishi, The 33rd International Cosmic Ray Conference, Rio de Janeiro, Brazil, July 2 - July 9, 2013.

[45] "Observation of thundercloud-related charged particles in Tibet", K. Hibino, The 33rd International Cosmic Ray Conference, Rio de Janeiro, Brazil, July 2 - July 9, 2013.

[46] "The TIBET AS+MD Project; progress report 2013", M. Takita, The 33rd International Cosmic Ray Conference, Rio de Janeiro, Brazil, July 2 - July 9, 2013.

[47] "A Monte Carlo study to measure heavy-component spectra of the primary cosmic-rays at the knee by a new hybrid experiment (YAC-II+Tibet-III+MD)", J. Huang, The 33rd International Cosmic Ray Conference, Rio de Janeiro, Brazil, July 2 - July 9, 2013.

[48] "Hadronic interaction and EAS muon investigated with the (YAC + Tibet-III + MD) hybrid experiment", J. Huang, The 33rd International Cosmic Ray Conference, Rio de Janeiro, Brazil, July 2 - July 9, 2013.

[49] "Observation of the large-scale sidereal anisotropy of the galactic cosmic ray at 300 TeV with the Tibet Air shower Array", Z. Y. Feng, The 33rd International Cosmic Ray Conference, Rio de Janeiro, Brazil, July 2 - July 9, 2013.

[50] "Primary proton and helium spectra at energy range from 50 TeV to 10^{15} eV observed with (YAC+Tibet-III) hybrid experiment", J. Huang, The 33rd International Cosmic Ray Conference, Rio de Janeiro, Brazil, July 2 - July 9, 2013.

[51] "Progress Report on the MD-A under TIBET III array", C. Liu, The 33rd International Cosmic Ray Conference, Rio de Janeiro, Brazil, July 2 - July 9, 2013.

[52] "Study on the primary mass sensitivity of muon multiplicity measured with (YAC-II +Tibet-III + MD) experiment", D. Chen et al., The 33rd International Cosmic Ray Conference, Rio de Janeiro, Brazil, July 2 - July 9, 2013.

[53] "Test of the hadronic interaction model EPOS-LHC and QGSJETII-04 with Tibet EAS core data", D. Chen, The 33rd International Cosmic Ray Conference, Rio de Janeiro, Brazil, July 2 - July 9, 2013.

[54] "Progress report on the TIBET AS+MD Project", T. K. Sako, The 12th Asia Pacif, Makuhari Messe, Chiba, Japan, July 14 - July 19, 2013.

[55] "Cosmic-ray shadow of the Sun measured at 3 TeV with the Tibet Air Shower Array" T. K. Sako, COSPAR2014, Moscow, Russia, August 2 - August 10, 2014.

[56] "Observation and modeling of cosmic-ray anisotropy observed with the Tibet air shower array", M. Takita, Cosmic Ray Anisotropies 2015, Bad Honnef, Germany, January 26 - January 30, 2015.

[57] "Observation of intense fluxes of charged particles in association with thundercloud in Tibet", K. Hibino, The 34th International Cosmic Ray Conference, The Hague, The Netherlands, July 30 - August 6, 2015.

[58] "Sidereal anisotropy of Galactic cosmic ray observed by the Tibet Air Shower experiment and the IceCube experiment", Y. Nakamura, The 34th International Cosmic Ray Conference, The Hague, The Netherlands, July 30 - August 6, 2015.

[59] "Observation of primary cosmic rays with the new Tibet hybrid experiment(YAC-II + Tibet-III + MD)", J. Huang, The 34th International Cosmic Ray Conference, The Hague, The Netherlands, July 30 - August 6, 2015.

[60] "YAC sensitivity for measuring the light-component spectrum of primary cosmic rays at the "knee" energies", L. M. Zai, The 34th International Cosmic Ray Conference, The Hague, The Netherlands, July 30 - August 6, 2015.

[61] "Shower reconstruction performance of the new Tibet hybrid experiment consisting of YAC-II, Tibet-III and MD arrays", D. Chen, Proceedings of The 34th International Cosmic Ray Conference, The Hague, The Netherlands, July 30 - August 6, 2015.

[62] "Simulation Study On High Energy Electron and Gamma-ray Detection With the Newly Upgraded Tibet ASgamma Experiment", Xu Chen, The 34th International Cosmic Ray Conference, The Hague, The Netherlands, July 30 - August 6, 2015.

[63] "On the primary model to explain the relation between a rigidity-dependent spectral hardening of proton and helium spectra and a sharp knee of the all-particle spectrum", Ying Zhang, The 34th International Cosmic Ray Conference, The Hague, The Netherlands, July 30 - August 6, 2015, ID=0546.

[64] "Search for gamma rays above 100 TeV from the Crab Nebula using the Tibet air shower array and the 100 m^2 muon detector", T. K. Sako, The 34th International Cosmic Ray Conference, The Hague, The Netherlands, July 30 - August 6, 2015.

[65] "Energy Determination and Gamma/Hadron Separation using the Lateral Distribution of EAS for the 100 TeV Gamma-Ray Astronomy", K. Kawata, The 34th International Cosmic Ray Conference, The Hague, The Netherlands, July 30 - August 6, 2015.

[66] "The TIBET AS+MD Project; progress report 2015", M. Amenomori et al., The 34th International Cosmic Ray Conference, The Hague, The Netherlands, July 30 - August 6, 2015.

[67] "Long term stability analysis on the MD-A under TIBET III array", X. L. Qian, The 34th International Cosmic Ray Conference, The Hague, The Netherlands, July 30 - August 6, 2015.

[68] "Northern sky Galactic Cosmic Ray anisotropy between 10 - 1000 TeV with the Tibet Air Shower Array", Z. Y. Feng, The 34th International Cosmic Ray Conference, The Hague, The Netherlands, July 30 - August 6, 2015.

[69] "The Tibet AS+MD Project; status report 2017", M. Takita, The 35th International Cosmic Ray Conference, Busan, Korea, July 12 - July 20, 2017.

[70] "Solar magnetic field strength and the Sun's Shadow observed by the Tibet Air Shower Array",

Y. Nakamura, The 35th International Cosmic Ray Conference, Busan, Korea, July 12 - July 20, 2017.

[71] "Interplanetary Coronal Mass Ejection and the Sun's Shadow Observed by the Tibet Air Shower Array", K. Kawata, The 35th International Cosmic Ray Conference, Busan, Korea, July 12 - July 20, 2017.

[72] "Measurement of high energy cosmic rays by the new Tibet hybrid experiment", J. Huang, The 35th International Cosmic Ray Conference, Busan, Korea, July 12 - July 20, 2017.

[73] "Study of the Magnetic Field Between the Sun and the Earth by the Sun shadow in Cosmic Rays with the Tibet Air Shower Array", M. Tuang, AOGS2017, Singapore, August 6 - August 10, 2017.

[74] "Sub- and multi-TeV cosmic-ray anisotropies observed with Japanese underground muon detectors and the Tibet Air shower experiment", K. Munakata, Cosmic Ray Anisotropies 2017, Guadalajara, Mexico, October 10 - October 13, 2017.

CTA: CHERENKOV TELESCOPE ARRAY PROJECT

Cherenkov Telescope Array Project (CTA)

[Spokesperson : Masahiro Teshima]

ICRR, Univ. of Tokyo, Kashiwa, Chiba 277-8582

In collaboration with the members of:
Aoyama Gakuin Univ., Kanagawa 252-5258, Japan;
Ibaraki Univ., Mito, Ibaraki 310-8512, Japan;
Osaka Univ., Toyonaka, Osaka 560-0043, Japan;
Kitasato Univ., Kanagawa 252-0373, Japan;
Kyoto Univ., Sakyoku, Kyoto 606-8502, Japan;
Kinki Univ., Osaka, Osaka 577-8502, Japan;
Kumamoto Univ., Chuoku, Kumamoto 860-8555, Japan;
KEK, Tsukuba, Ibaraki 305-0801, Japan;
Konan Univ., Kobe, Hyogo 658-0072, Japan;
Saitama Univ., Saitama, Saitama 338-8570, Japan;
Tokai Univ., Hiratsuka, Kanagawa 259-1292, Japan;
The University of Tokyo, Bunkyo-ku, Tokyo 113-0033;
The University of Tokushima, Tokushima 770-8502;
Nagoya Univ., Nagoya, Aichi 464-8602, Japan;
Hiroshima Univ., Hiroshima 739-8526, Japan;
Miyazaki Univ., Miyazaki, Miyazaki 889-2192, Japan;
Yamagata Univ., Yamagata, Yamagata 990-0021, Japan;
Yamanashi Gakuin Univ., Kofu, Yamamashi 400-8575;
Waseda Univ., Shinjyuku, Tokyo 169-0072, Japan;

Introduction

During the last decades, Very High Energy (VHE) gamma ray astronomy has made spectacular progress and has established itself as a vital branch of astrophysics. To advance this field even further, we propose the Cherenkov Telescope Array (CTA), the next generation VHE gamma ray observatory, in the framework of a worldwide, international collaboration. CTA is the ultimate VHE gamma ray observatory, whose sensitivity and broad energy coverage will attain an order of magnitude improvement above those of current Imaging Atmospheric Cherenkov Telescopes (IACTs). By observing the highest energy photons known, CTA will clarify many aspects of the extreme Universe, including the origin of the highest energy cosmic rays in our Galaxy and beyond, the physics of energetic particle generation in neutron stars and black holes, as well as the star formation history of the Universe. CTA will also address critical issues in fundamental physics, such as the identity of dark matter particles and the nature of quantum gravity.

VHE gamma rays from 100GeV to 10TeV can be observed with current ground-based IACTs. The history of VHE gamma ray astronomy began with the discovery of VHE gamma rays from the Crab Nebula by the Whipple Observatory in 1989. The current generation IACTs featuring new technologies, such as H.E.S.S., MAGIC, and VERITAS, have discovered more than 200 Galactic and extragalactic sources of various types to date.

CTA Project

CTA is designed to achieve superior sensitivity and performance, utilising established technologies and experience gained from the current IACTs. The project is presently in its pre-construction phase, with international efforts from Japan and the EU countries. It will consist of several 10s of IACTs of three different sizes (Large Size Telescopes, Mid Size Telescopes, and Small Size Telescopes). With a factor of 10 increase in sensitivity (1m Crab 10^{-14} erg s^{-1} cm^{-2}), together with much broader energy coverage from 20GeV up to 300TeV, CTA will bring forth further dramatic advances for VHE gamma ray astronomy. The discovery of more than 1000 Galactic and extragalactic sources is anticipated with CTA.

CTA will allow us to explore numerous, diverse topics in physics and astrophysics. The century-old question of the origin of cosmic rays is expected to be finally settled through detailed observations of supernova remnants and other Galactic objects along with the diffuse Galactic gamma ray emission, which will also shed light on the physics of the interstellar medium. Observing pulsars and associated pulsar wind nebulae will clarify physical processes in the vicinity of neutron stars and extreme magnetic fields. The physics of accretion onto supermassive black holes, the long-standing puzzle of the origin of ultrarelativistic jets emanating from them, as well as their cosmological evolution will be addressed by extensive studies of active galactic nuclei (AGN). Through dedicated observing strategies, CTA will also elucidate many aspects of the mysterious nature of gamma ray bursts (GRBs), the most energetic explosions in the Universe. Detailed studies of both AGNs and GRBs can also reveal the origin of the highest energy cosmic rays in the Universe, probe the cosmic history of star formation including the very first stars, as well as provide high precision tests of theories of quantum gravity. For example, the multi-messenger observation with IceCube, Fermi and MAGIC on TXS0506+056 has demonstrated the scientific potential of the next generation telescopes CTA and IceCube Gen2 to identify the sources of Ultra High Energy Cosmic Rays. Finally, CTA will search for

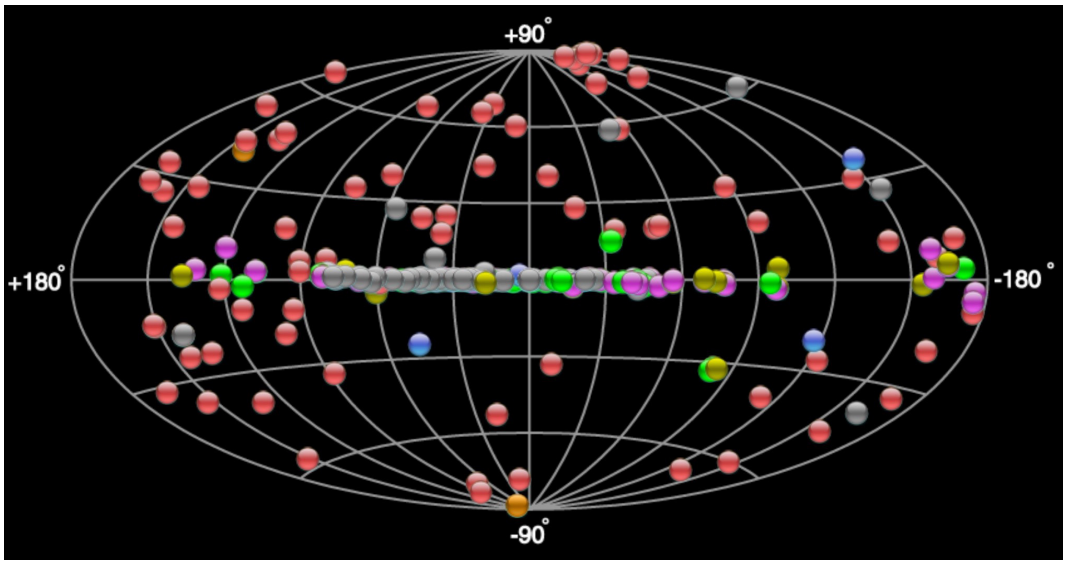

Fig. 1. Very High Energy Gamma Ray Sky (> 100GeV) in the galactic coordinate. More than 200 Galactic and extragalactic sources have been discovered by H.E.S.S., MAGIC and VERITAS. The low latitude sources on the galactic plane are pulsar wind nebulae, super nova remnants, gamma ray binaries and un-known sources, and high latitude sources are mainly Blazars and AGNs.

Fig. 2. Computer graphics of the CTA North observatory. CTA consists of three types of telescopes, Large Size Telescopes (23m diameter), Mid Size Telescopes (12m) and Small Size Telescopes (4m, only in CTA south), and covers the broad energy band from 20GeV to 300TeV.

signatures from elementary particles constituting dark matter with the highest sensitivity so far. The realisation of its rich scientific potential of CTA is very much feasible, thanks to the positive experience gained from the current IACTs.

Structure of the large size telescope (LST)

The structure of the large size telescope (LST) as shown in figure 3 was designed by the MPI Munich group together with MERO-TSK. The major part of the telescope consists of the space frame structure with carbon fiber reinforced plastic (CFRP) tubes. The total weight of the telescope is designed to be about 100 tons and allows the fast rotation of the telescope, 180 degrees in 20 seconds, for fast follow-up observations of gamma ray bursts using the location determined by gamma ray satellites.

The telescope geometry is optimized to maximize the cost performance by Monte Carlo simulations and toy models. The baseline parameters are defined with the dish size of 23m, the focal length of 28m and then F/D = 1.2, and the camera FoV of 4.5 degrees with a pixel size of 0.1 degrees.

The first Large Size Telescope (prototype/LST1) has been successfully built at ORM. The construction was done very smoothly, and we did not find any major problem in the telescope structure and construction.

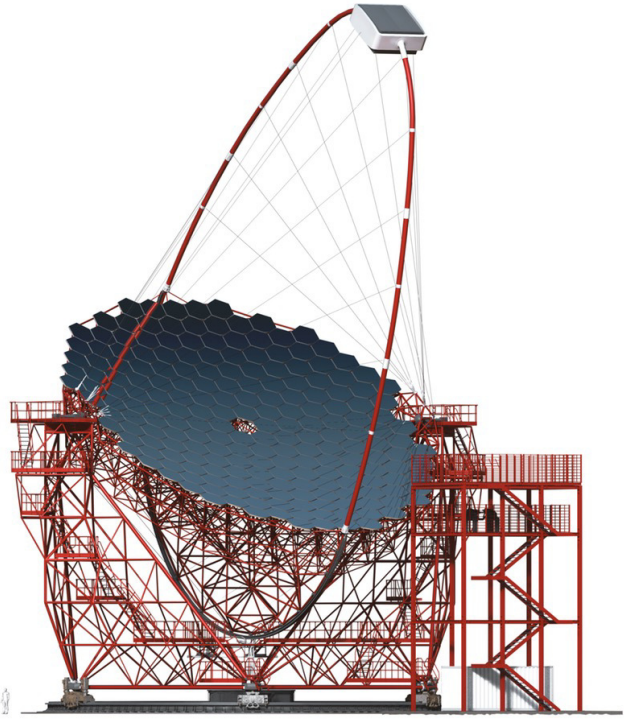

Fig. 3. Large Size Telescope (23m diameter). The telescope mechanical design was done by Max Planck Institute for Physics. CTA Japan has made the contribution to the design and production of the imaging camera at the focal plane, ultrafast readout electronics, and high precision segmented mirrors.

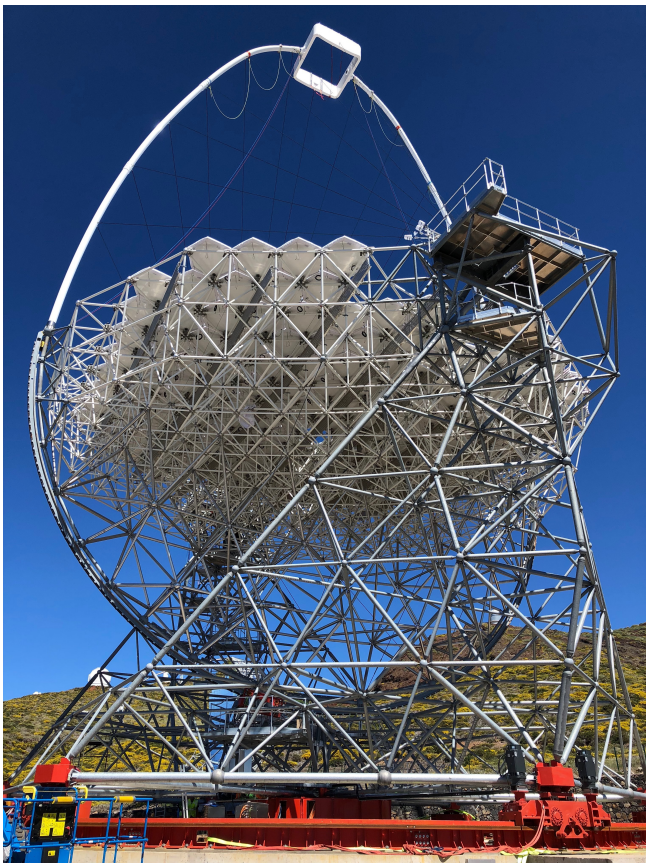

Fig. 4. The first Large Size Telescope LST1 which has a 23m diameter dish erected in the Observatory Roque de los Muchachos. The mirror supporting structure is made of carbon fiber reinforced plastic (CFRP) to make the structure stiff and as light as possible. The camera supporting arch and reinforcing ropes are also made of CFRP.

Activities of CTA Japan

The CTA-Japan consortium is aiming to contribute particularly to the construction of the Large Size Telescopes (LSTs) and has been involved in their development. The LST covers the low energy domain from 20 GeV to 1000 GeV and is especially important for studies of high redshift AGNs and GRBs. The diameter and area of the mirror is respectively 23 m and 400 m^2 to achieve the lowest possible energy threshold of 20 GeV. All optical elements/detectors require high specifications, such as, high reflectivity, high collection efficiency, high quantum efficiency and ultra fast digitization of signals, and etc. For this purpose, CTA-Japan has developed high quantum efficiency photomultipliers, ultrafast readout electronics and high precision segmented mirrors.

Segmented Mirrors for LST

The reflector with its diameter of 23m consists of 198 units of hexagonal shape 1.5m flat to flat segmented mirrors of $2m^2$. The total area of the reflector is about $400m^2$. Each segmented mirror is attached to the knots of the space frame structure through the interface plates with a universal joint and two actuators. The segmented mirrors are of a sandwich structure, consisting of a glass sheet of 2.7mm thickness - aluminum honey-comb of 60mm thickness - and another glass sheet. The weight of a segmented mirror is 45kg. The reflective layer of the mirror is coated with Cr and Al on the surface of the glass sheet with a protective multi-coat layer of SiO_2, HfO_2, and SiO_2. By adjusting the thickness of individual layers with SiO_2 and HfO_2, we can optimize the reflectivity to about 92% due to the interference effect of multi-layers.

Permanent Active Mirror Control

We will define the optical axis (OA) of the LST optics with two infra-red lazers at the center of the dish constantly shining two targets top and bottom of the imaging camera. The individual segmented mirrors have a CMOS Camera at the bottom corner of the HEX mirror which observe the OA lazers at targets near the imaging camera to confirm the direction of the mirror facet relative to the OA lasers (optical axis). The directional offset of the mirror facets will be estimated by taking pictures of OA-laser spots on the targets with a CMOS camera viewing from the individual mirrors. If any significant offsets are found, the direction of the

Fig. 5. Hexagonal shape mirrors of 1510mm size delivered by the University of Tokyo and Sanko LTD. The area is about $2m^2$ and the focal length is tuned between 28m and 29.2m depending on the location of mirror from optical axis. The PSF of individual mirrors is characterised by the parameter D80 within whose circle diameter the light is contained more than 80% of total reflected light, which is less than 16.7mm. Mirrors are produced with the cold slump technique. The mirror surface is protected with the multi-layer coating with SiO^2 and HfO^2 are produced by spattering method. The right picture shows the dish mounted with 198 segmented mirrors during the construction period. They are covered by the light protection covers to avoid accidents with the sun light.

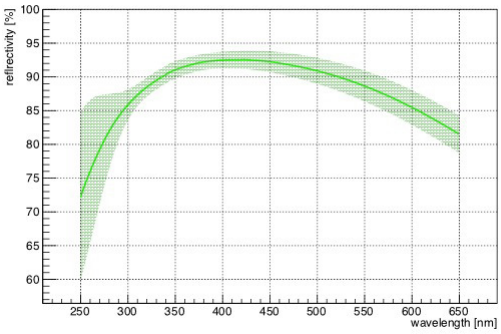

Fig. 6. The average spectral reflectivity and its dispersion of mirrors used in the LST1. The peak reflectivity of 92% is achieved at around 400nm, there is more than 85% reflectivity between 300nm and 600nm. D80 (the diameter containing 80% of total reflected light at 1f position) of all mounted segment mirrors are less than 16.7mm, the averaged D80 is 13.6 mm, which is well smaller than the LST specification of 16.7mm.

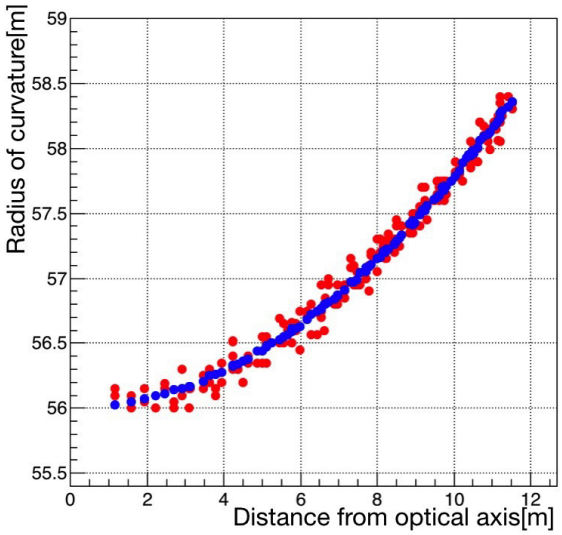

Fig. 7. The radius of curvature of individual segmented mirrors as a function of distance from the optical axis. Red points represent installed mirrors on LST1 and blue ones are ideal values with the isochronous mirror configuration (similar with the parabolic shape).

corresponding mirror facets will be corrected by actuators. The 198 mirrors are divided into 16 groups. The directions of 198 individual mirrors are monitored and controlled by 16 CPUs. The monitoring and control of 12-13 mirrors in each group will be done sequentially and performed typically in 10 seconds. This will be done continuously during the observation. After the first rotation for the GRB follow-up observation, or at the beginning of the observation of any source, we will use the look-up table corresponding to the zenith angle of the target source as the initial value of actuators and then move to the mode of permanent active mirror control loop.

Imaging Camera

The imaging camera has a FOV of 4.5 degrees and a pixel size of 0.1 degrees. The actual size of the image plane will be about 2.3m in diameter. The signals from the photomultipliers will be read with 1G samples/sec speed and be stored in the ring capacitors of 4096 depth, which corresponds to 4 micro-seconds.

The camera will be sealed to resist humidity and dust in the field. The front side (entrance window) of the imaging camera will be covered with uv-transparent plexiglass. The water cooling plate is used to keep

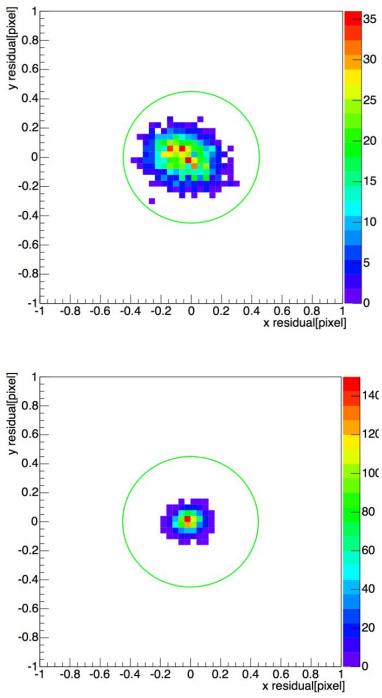

Fig. 8. The precision of the permanent Active Mirror Control (AMC) system examined with the test telescope structure in the MPI backyard. The top picture shows the mirror facet direction after the first adjustment and the bottom one is after the second trial, after reading the position again with CMOS camera. These iteration can be done permanently every 10 seconds even during the observation time. The green radius corresponds to the 14 arc-seconds. We can monitor and control the mirror facet direction with the precision better than 5 arc-seconds.

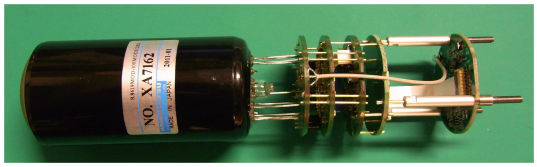

Fig. 9. R11920-100-20 PMT module. This module consists of Hamamatsu Photomultiplier R11920, Cockcroft-Walton HV, and Ultra fast Preamplifier. CTA-Japan has developed this PMT module together with Hamamatsu photonics.

the temperature of the camera and the electronics constant. As a part of the Camera mechanical structure this cooling plate will also serve as a support for the PMT/electronics clusters. The readout electronics and the auxiliary electronics (HV, and amplifiers) will dissipate a heat of 2W/ch. 7-PMTs and readout electronics are mechanically bundled as a PMT/electronics cluster. Since the total number of pixels and clusters are 1855 and 265, the total heat dissipation inside the camera will amount to 4-5kW.

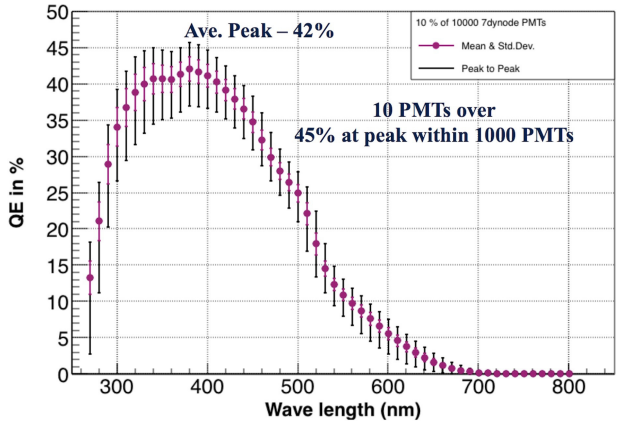

Fig. 10. The averaged Quantum Efficiency of 1000 PMTs produced for LST camera. Q.E. Peak value of 42% is obtained at around 380nm. The best PMTs show the peak value of 45%. We have asked Hamamatsu HPK to measure 10% tubes randomly (1000 among 10,000 produced PMTs) to see the quality of the series of production.

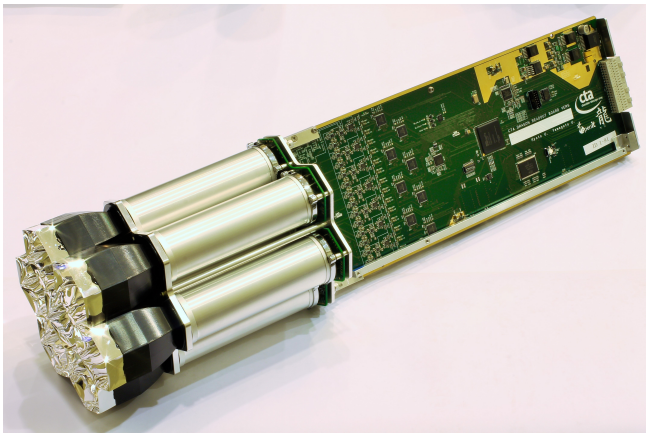

Fig. 11. PMT Cluster, consisting of seven photomultipliers, CW-HVs, Preamplifiers, readout electronics (Dragon card), and trigger system. Signals are digitized in this module and sent to DAQ camera server system via G-bit Ethernet.

DAQ and Data Analysis

The computer cluster with 2000 cores and 3PB disk is installed at the LST1 site. It is designed for the data acquisition of 4 LSTs and 5 MSTs with high speed internet connection with telescopes (40Gbps/LSTs and 20Gbps/MSTs) and for the control of array / telescopes. We will develop the online / on-fly data analysis pipe with this computer cluster and LST1 in the next years.

Time Schedule and Responsibilities

As mentioned above, CTA-Japan has important responsibilities in the production and delivery of many telescope elements, such as segmented mirrors, the active mirror control system, focal plane instruments and

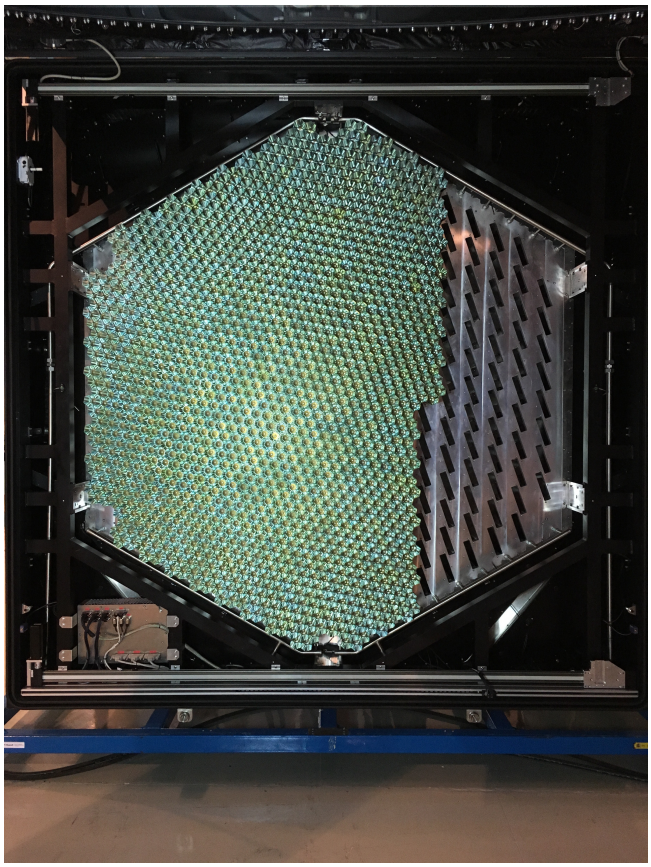

Fig. 12. LST1 Camera under assembling process in August 2018. The camera consists of 265 PMT clusters and 1855 PMTs. PMT clusters with 7 PMTs are inserted through the inclined slots and fixed from the frontal side by three pins and from the rear side by two screws. The apparent green color of the camera is due to the mixture of reflected blue light on the surface of the light guide with UV-blue enhanced coating (95% reflectivity at 350nm) and yellow color direct light from PMT head.

readout electronics of the four Large Size Telescopes installed in CTA North. CTA-Japan delivers these elements after production and procurements with budgets, the JSPS grant in aid research and budget from the Japanese government. The construction and realisation of LSTs in CTA south may be discussed in the coming years.

In 2016 the CTA sites were decided to be Paranal, Chile in the South and La Palma, Spain in the North, after detailed investigation and discussions at several candidate sites. The design study and development of the first Large Size Telescope had already been well matured even before this decision in 2016.

The construction of LST1 has started at ORM on La Palma Spain after receiving the construction license from the local government in the summer of 2017. After two year construction period, we will complete the construction in the fall of 2018. The local computing system of CTA North to take data from 4 LSTs and 15 MSTs was installed in 2018. We can develop the end to end system of data taking, data reduction, online calibration and online data analysis with LST1 and this computing system. This computing system will mitigate the problem of huge data rates from CTA telescopes, and relatively poor internet connections between La Palma and European countries and very poor connections between Europe and Japan.

LST2-4 will be constructed in the next three years in 2019-2022 and already tendering of the foundation and telescopes mechanics are ongoing in Spain. CTA-Japan has produced all responsible elements for LST2-4 and quality control of products and assembly of elements are ongoing. LST1-4 will be operated as a stereoscopic system in 2022. CTA Japan has already produced mirrors, photo-sensors and readout electronics for LST2-4. For the full construction (four LSTs in north and another four in south), we need more efforts to secure the finance and manpower.

Table 1. Timeline for the LST construction. LST1 related events have been almost done / performed. We learned all necessary procedures with this construction. LST2-4 schedule is estimated from the experience of LST1 construction. Their financial resources are almost secured. The possible schedule of LST5-8 in CTA South is also shown at the bottom, highly depending on the future funding.

Time	Decision making Organization	Telescopes	Events / Actions / Schedule
2014 Q3	CTAC, LST	LST1	**Agreement for the construction of LST1 on the CTA site**
2015 Q2	LST	LST1	**Tendering Telescope mechanics**
2015 Q4	LST	LST1	Decision on the LST1 construction at ORM, La Palma, Spain
2016 Q1	CTAO	LST, MST	Decision of La Palma as the CTA-North site
2016 Q3	Cabildo, LST	LST1	**Start the construction of concrete foundation**
2017 Q3	Cablido, LST	LST1	**License for the construction of Telescope mechanics**
2018 Q4	LST	LST1	**First Light**, Commissioning and engineering run of LST1
2019 Q2	CTAO	LST1	Review of LST1
2018 Q2	CTAO, LST	LST2-4	**Tendering foundations and mechanics**
2019 Q3	Cabildo, CTAO	LST2-4	License for the construction of infrastructure
2020 Q2	Cabildo, LST	LST2-4	**Start construction of telescopes**
2021 —	LST	LST2-4	Continue construction
2022 Q4	LST	LST1-4	**First light**, Commissioning and Engineering run as LST-array
2023 Q1	CTAO, LST	LST1-4	Acceptance Review of LST array
2023 Q3	CTAO, LST	LST1-4	**In-kind Contribution, Operate CTA North as an observatory**
2022 —	LST	LST5-8	*Start the installation of CTA South and Tendering ?*
2025 —	LST	LST5-8	*Commissioning and Engineering run of LST5-8 ?*

Summary from 2012 to 2018

- The optimisation of CTA array telescope configuration and the parameters of large size telescopes was done with Monte Carlo simulation, and the requirements and specifications for the large size telescopes were defined.
- The Baseline Design Document (BDD) and Technical Design Report (TDR) for the Large Size Telescope (LST) were documented and included in the TDR of CTA.
- The first stone ceremony for LST1-4 was held in October 2015.
- After successful prototyping of segmented mirrors, 900 mirrors were produced and qualified. The high reflectivity of 92%, small point spread function($\leq 16mm$), high durability, and light weight ($\leq 50kg$) were achieved.
- The 1.5 inch size hemispherical shape photomultiplier for CTA LSTs had been designed and developed with specification of the peak quantum efficiency of 42% and low after pulse rate of 10^{-4}. With this specification, 10,000 photomultipliers are produced by Hamamatsu.
- The 10,000 preamplifier boards with specification of low noise ($\sim 10^4 e$), a few GHz bandwidth and high/low dual gain were produced using PACTA Chip, the ASIC developed in the IEEC, the University of Barcelona.
- 1,100 units of the GHz sampling fast 7ch readout system Dragon boards were produced. The wide dynamic range is achieved with the high and low gain dual gain waveform readout system to measure high energy gamma rays from 20GeV to 3 TeV.
- The first telescope LST1 was inaugurated in October 2018 at CTA North site on La Palma.
- The very fast large flare from radio galaxy IC310 was observed with the MAGIC telescope. The variability of minutes scale is observed from the blackhole with the light crossing time of 50 mins.
- The extension of the energy spectrum up to 1TeV in the pulsed component from Crab pulsar was observed with the MAGIC telescope.
- The observation of 100GeV gamma rays from the possible PeV neutrino source TXS 0506+056.

CTA

Institute	Country	(*)
ICRR, Univ. of Tokyo	Japan	38
Aoyama Univ.	Japan	4
Ibaraki Univ.	Japan	5
Osaka Univ.	Japan	2
Kitasato Univ.	Japan	1
Kyoto Univ.	Japan	10
Yukawa Institute	Japan	1
Kinki Univ.	Japan	3
Kumamoto Univ.	Japan	1
KEK	Japan	3
Konan Univ.	Japan	4
Saitama Univ.	Japan	5
Tokai Univ.	Japan	7
Univ. of Tokyo	Japan	4
Tohoku Univ.	Japan	1
Tokushima Univ.	Japan	1
Nagoya Univ.	Japan	9
ISEE, Nagoya Univ.	Japan	8
Hiroshima Univ.	Japan	3
Miyazaki Univ.	Japan	1
Yamagata Univ.	Japan	4
Yamamashi Gakuin Univ.	Japan	2
RIKEN	Japan	7
Rikkyo Univ.	Japan	1
Waseda Univ.	Japan	1
Total		126

(*) Number of participants as of August 2018.

Members in ICRR

There are 126 collaborators in CTA-Japan consortium. Here we only list members in ICRR, the University of Tokyo.

Staffs

Masahiro Teshima, Professor, 2010 to the present
Takanori Yoshikoshi, Assoc. Professor, 2010 to the present
Koji Noda, Assoc. Professor, 2018 to the present
Daniel Mazin, Research Assoc. Professor, 2014 to the present
Michiko Ohishi, Assist. Professor, 2010 to the present
Takayuki Saito, Research Assist. Professor, 2017 to the present
Daniela Hadasch, Research Assist. Professor, 2014 to the present

Postdoctoral Fellows

Mitsunari Takahashi, 2018 to the present
Masaaki Hayashida, 2011 to 2016
Daisuke Nakajima, 2011 to 2016

Technical Staff and Secretary

Hideyuki Ohoka, 2010 to the present
Kyosuke Awai, 2018 to the present
Nao Okazaki, 2016 to the present
Yusuke Inome, 2018 to the present
Midori Sugahara, 2011 to the present

Graduate Students

Satoshi Fukami (D3)
Yuki Iwamura (D2)
Tomohiro Inada (D2)
Shunsuke Sakurai (D1)
Taku Kumon (M2)
Yukiho Kobayashi (M1)
Yoshiki Otani (M1)

One student was awarded doctor degrees and 9 students earned master degrees during 2013–2018, supervised by ICRR staff members.

List of Publications

[1] **Multimessenger observations of a flaring blazar coincident with high-energy neutrino IceCube-170922A,** IceCube, Fermi and MAGIC Collaborations, M. M. Aartsen, H.Kubo, D. Mazin, D. Hadasch, M. Hayashida, K. Noda, T. Saito, M.Takahashi, M. Teshima, *et al.*, Science **361** (2018) no.6398, eaat1378.

[2] **A technique for estimating the absolute gain of a photomultiplier tube,** M. Takahashi, *et al.*, Nucl.Instrum.Meth. **A894** (2018) 1-7.

[3] **Science with the Cherenkov Telescope Array,** arXiv:1709.07997 **(56 Cited)**

[4] **Prospects for Cherenkov Telescope Array Observations of the Young Supernova Remnant RX J1713.7−3946,** CTA Consortium, Astrophys.J. **840** (2017) no.2, 74.

[5] **Evaluation of novel PMTs of worldwide best parameters for the CTA project** R. Mirzoyan, D. Nakajima, M. Takahashi, M. Teshima, T. Yamamoto it et al., Nucl.Instrum.Meth. A845 (2017) 603-606

[6] **Large size telescope report**, D. Mazin, J. Cortina and M. Teshima, AIP Conf.Proc. **1792** (2017) no.1, 080001

[7] **Status of the Cherenkov Telescope Array's Large Size Telescopes,** J. Cortina and M. Teshima, Proc. of ICRC2015 at Hague, Netherlands. arXiv:1508.06438.

[8] **The Optical System for the Large Size Telescope of the Cherenkov Telescope Array,** M. Hayashida *et al.*, PoS ICRC2015 (2016) 927.

[9] **Development of the photomultiplier tube readout system for the first Large-Sized Telescope of the Cherenkov Telescope Array**, S. Masuda *et al.*, PoS ICRC2015 (2016) 1003.

[10] **Development of Slow Control Boards for the Large Size Telescopes of the Cherenkov Telescope Array**, D. Hadasch *et* al., PoS ICRC2015 (2016) 1024.

[11] **Limits to dark matter annihilation cross-section from a combined analysis of MAGIC and Fermi-LAT observations of dwarf satellite galaxies**, MAGIC Collaboration, M.L. Ahnen *et al.*, JCAP **1602** (2016) no.02, 039.

[12] **Black hole lightning due to particle acceleration at subhorizon scales**, J. Aleksic, D. Hadasch, M. Hayashida, H. Kubo, D.Mazin, K. Noda, K. Saito, T. Saito, M. Teshima *et* al., Science **346** (2014) 1080-1084. **(74 cited)**

[13] **Introducing the CTA concept**, B.S. Acharya *et al.*, Astropart. Phys. 43 (2013) 3-18. **(396 cited)**

[14] **Design concepts for the Cherenkov Telescope Array CTA: An advanced facility for ground-based high-energy gamma-ray astronomy,** CTA Consortium (M. Actis, K. Ioka, H.Kubo, R. Orito, H. Tajima, M. Teshima, T. Totani, T. Yoshida, T. Yoshikoshi, 60 other CTA-Japan members *et al.*). Exper.Astron. **32**, 193 (2011).

[15] **Design Study of a CTA Large Size Telescope,** M. Teshima *et al.*, *Proc. of ICRC2012 at Beijing China,* arXiv:1111.2183

[16] **Development of PMT Clusters for CTA-LST Camera,** R. Orito *et al.*, *Proc. of ICRC2012 at Beijing China,* arXiv:1111.2183

[17] **Development of the Readout System for CTA Using the DRS4 Waveform Digitizing Chip,** H. Kubo *et al.*, *Proc. of ICRC2012 at Beijing China,* arXiv:1111.2183

HIGH ENERGY ASTROPHYSICS GROUP

High-Energy Astrophysics Group Introduction

The high energy astrophysics group aims at making theoretical studies of violent astrophysical phenomena, in which cosmic-rays (nonthermal particles) are being accelerated. Targets of the group's study include high energy astrophysical objects such as supernova explosions/shocks, neutron stars (NSs) and their nebulae, merger of binary stars, and relativistic jets launched from active galactic nuclei (AGNs) and gamma-ray bursts (GRBs). The standard theory of cosmic ray acceleration process invokes effective diffusive-shock-acceleration (DSA) mechanism working around collisionless astrophysical shocks and their turbulent environment. The magnetic reconnection mechanism is another candidate for effective particle acceleration processes. Understanding of transport processes involved in the DSA and magnetic reconnection mechanisms requires deep consideration based on microscopic plasma physics.

The open problems in high-energy astrophysics are not only the acceleration mechanism of cosmic rays. How are relativistic jets from AGNs accelerated? How are very bright gamma-ray emissions emitted in GRBs? How is the magnetic energy of the pulsar winds converted into the kinetic energy to form ultra-relativistic outflows? How are magnetic fields amplified in shocks in supernova remnants (SNRs) or afterglows of GRBs? How do relativistic particles propagate in interstellar space and escape from the galactic plane? Those problems remain unsolved, and are our research themes [5].

In addition, studies have been made also for nonthermal phenomena within the heliosphere, such as interplanetary shocks and the earth's bow shock, magnetic reconnection, the interaction processes between the solar wind and the lunar surface.

We also have carried out observational studies. Analysing a large set of the radio data taken with Japanese telescopes, we have studied giant radio pulses (GRPs) of pulsars to obtain the hint of the emission mechanism. Our group has joined CALET, CALorimetric Electron Telescope, which is a mission for the Japanese Experiment Module-Exposed Facility (JEM-EF) on the International Space Station. The CALET mission carries out accurate measurements of high energy spectra of electrons, gammarays and nuclei.

Summary from 2012 to 2018

Our representative results are as follows:

- Based on the turbulence acceleration model, we have reproduced photon spectra of blazars, gamma-ray bursts, the Fermi bubble, and pulsar wind nebulae.
- We have discussed production of ultra high-energy cosmic-rays and high-energy neutrinos from gamma-ray bursts.
- We estimated the detection rate of GW events for the BH–BH or BH–NS binary mergers especially originated from the Pop Ⅲ stars. We also proposed the binary merger progenitor model to be the long gamma-ray burst progenitor. The GRB rate we obtained is consistent with the observed GRB rate evolution.
- We carried out a detailed radiative transfer simulation in ejecta at the NS–NS binary merger. Our model succeeded in reproducing the complex evolution of the kilonova spectrum in GW170817.
- We operated simultaneous multi-frequency observations of the Crab giant radio pulses with four radio telescopes. Most of spectra can be fitted with a signle power-law between 0.3–2.2 GHz. Our results suggest an anti-correlation between the total energy release and spectral hardness.
- The CALET mission succeeded in obtaining the electron+positron spectrum from 10 GeV to 5 TeV.

Non-thermal Phenomena and Multi-messenger Astronomy

Our main research interest is the emission mechanism of the non-thermal photons in SNRs [41], GRBs [7, 9, 10, 14, 22, 34, 36, 43, 51, 57], blazars (jets from AGNs) [12, 19, 21, 27, 53], pulsars [13, 16, 17, 20, 29, 32, 35], pulsar wind nebulae (PWNe) [8, 11, 40, 42], merger of binary stars [26, 30, 49], and huge gamma-ray bubbles above our galactic plane (Fermi bubble) [25].

A unique point in our study is a proposal of an alternative particle acceleration mechanism, the turbulence acceleration model. Differently from DSA, particle acceleration via scattering by electromagnetic waves induced by turbulence can produce curved energy spectrum as shown in Figure 1, which agrees with the observed blazar spectra [12, 19, 53] (see Figure 2). Our results suggest that the acceleration timescale is independent of the particle energy, which is different assumption from previous studies. We have proposed a model, in which particles are accelerated via interaction with fast mode waves so called transit time damping.

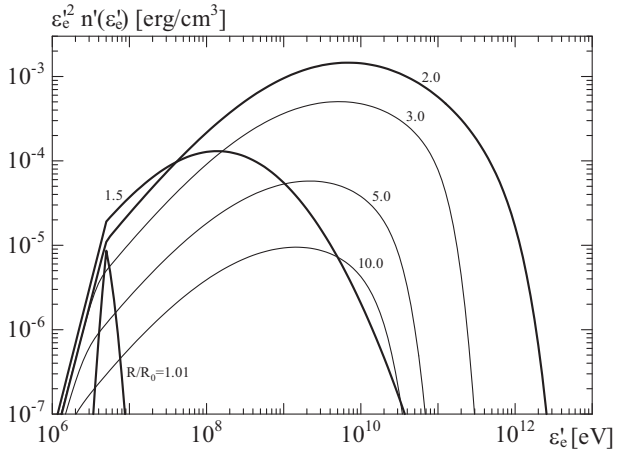

Fig. 1. The evolution of the electron energy spectrum in our turbulence acceleration model for a blazar Mrk 421[53]. While a power-law energy distribution is predicted in the DSA model, our spectra shows curved feature.

This naturally leads to a energy-independent acceleration timescale. With this idea, our model is the first one to succeed in reproducing broadband spectra of blazars with the turbulence acceleration model [53]. We have tested the turbulence acceleration model for GRB [22], the Fermi bubble [25], and PWN [42] as well.

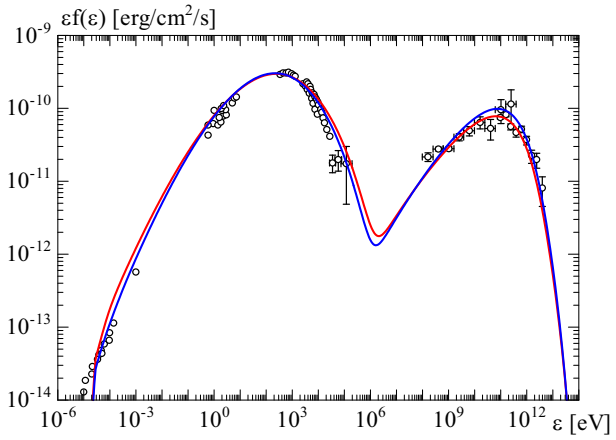

Fig. 2. Photon spectra for Mrk 421[53]. Our turbulence acceleration models (red and blue lines, slightly diffenrent parameter sets) reproduce the curved photon spectra.

Especially in the gamma-ray band, the possible emission mechanisms are divided into two models: leptonic and hadronic models. In the leptonic model, gamma-rays are emitted via inverse Compton (IC) scattering of electrons interacting with low-energy photons. The seed photons for IC scattering are synchrotron photons emitted by the same electron population or external photons such as thermal radiation from hot plasma. The DSA predicts the acceleration of not only electrons but also protons. High-energy protons collide with low-energy photons or background protons, and produce pions. The secondary photons from decay of neutral pions or secondary muons/electrons/positrons are responsible for gamma-ray emission in hadronic models.

In most of high-energy objects, there is no consensus on the gamma-ray emission mechanism. Possible way to determine the emission mechanism is detection of neutrinos from secondary pions in the hadronic model. We have discussed production of ultra high-energy cosmic-rays (UHECRs) and high-energy neutrinos from GRBs [9, 15, 22, 28, 51]. Our model of UHECR production in GRBs [28] is unique one, which is based on the turbulence acceleration model. We expect that the predicted UHECR and neutrino spectra (Figure 3) will be confirmed in near future.

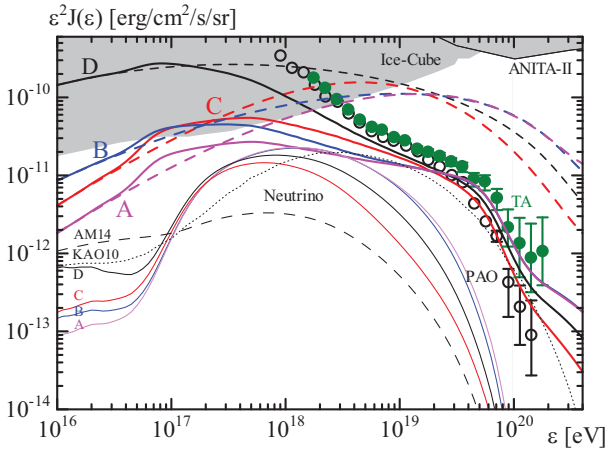

Fig. 3. The diffuse UHECR spectra from GRBs in our model [28] (thick solid lines, different parameter sets for A–D). The thick dashed lines are spectra neglecting the effects of photomeson production and Bethe-Heitler pair production during propagation. The observed data for the UHECR by the Pierre Auger Observatory (open circles) and the Telescope Array (green filled circles) are shown. The thin lines show the all-flavor cosmogenic neutrino intensities, which are below the upper limits (gray shaded area) by IceCube and ANITA-II. For comparison, we also plot the model spectra of the cosmogenic neutrinos by Kotera et al. (JCAP **10**, 013 2010, thin dotted line, denoted as KAO10) and prompt plus cosmogenic neutrinos by Asano and Mészáros [15] (thin dashed line, denoted as AM14).

Recently, IceCube reported a detection of a high-energy neutrino from the direction of the blazar TXS 0506+056[1]. Although this success in the multi-messenger astronomy seems to support the hadronic model, most of interpretations based on the gamma-ray spectrum disagree the hadronic origin for the gamma-ray emission itself[2]. Actually, the hadronic model requires a huge jet luminosity, and the spectral shape in blazars favors the leptonic model [53]. The leptonic model implies that the magnetic field is subdominant component in the jet energy density, while the Poynting flux dominated jet seems consistent with the radio observations of the M87 jet[3]. This discrepancy strongly

*1 Aartsen et al., Science, **361**, 1378 (2018).
*2 see e.g., Murase et al., arXiv:1807.04748 (2018).
*3 Asada & Nakamura, ApJ, **745**, L28 (2012).

motivates us to study blazars. Rich and complex structure may be hidden in relativistic jets, which may relate to the jet launching mechanism.

We have studied mechanisms of the energy transfer to non-thermal particles and photon and neutrino emissions, which are main targets for the next generation astronomy, the multi-messenger astronomy. To develop such a new field in astronomy, deep understanding of plasma physics could be a key. For example, the X-ray PWN profiles disagree with the classical model based on fluid dynamics [40]. We need to incorporate particle diffusion [58], which is an effect beyond the fluid picture. There are non-trivial mechanisms of interaction between particles, waves, photons, and magnetic field [2, 20, 24, 32], which cannot be described by only fluid dynamics. Such fundamental studies are also in our research field.

Merger of Binary Stars

Advanced-LIGO, a ground-based detector in USA, achieved the first detection of a gravitational-wave (GW) event from a merger of binary black holes (BHs) on 14th of September 2015[4]. This ignited the astronomy based on the GW observations. The star formation rate (SFR) peaks at a redshift ~ 2, but the SFR in the universe above $z = 2$ is still uncertain. In the very early universe, gasses were not yet polluted by metals such as C, O, Fe, etc., which act as coolant. In such environment, very massive stars so called Pop Ⅲ stars tend to be produced. A direct observation of Pop Ⅲ stars at very high redshift is almost impossible. GW observations of BH binaries, which are remnants of massive stars, provide clue to revealing the SFR in early universe. The BH formation also relates to high-energy phenomena such as GRBs. Following the history of the SFR, we estimated the detection rate of GW events for the BH–BH or BH–NS binary mergers especially originated from the Pop Ⅲ stars [31, 33, 37, 39, 45] (see Figure 4).

We also considered the binary merger progenitor model to be the long GRB progenitor. A Wolf–Rayet star and a giant star system or two giant stars merge during the common-envelope phase. When a star in a close binary system becomes a red giant, the companion star spirals into the core of the giant owing to the orbital energy loss by the friction. The envelope of the giant is evaporated and the binary separation becomes so close that they merge. After the merger, a rapidly rotating naked helium star remains. Such a compact and highly rotating star is ideal to induce a GRB. Following this scenario, we estimated the GRB rate, and we found the rate is consistent with the observed GRB rate evolution. Future projects to detect high-redshict GRBs such as High-Z GUNDAM may cerify the progenitors of GRBs.

*4 Abbott et al., PRL, **116**, 061102 (2016).

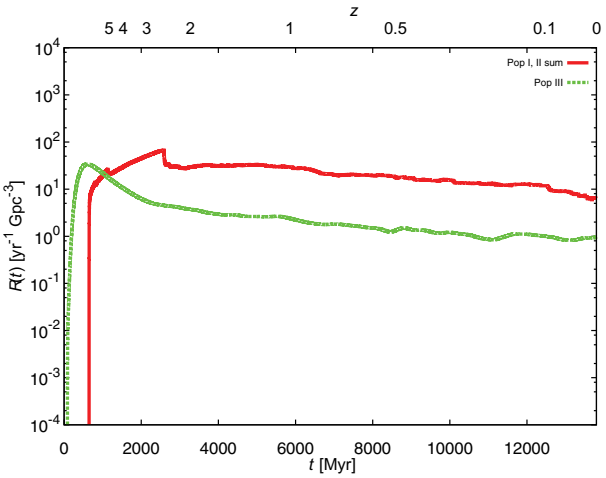

Fig. 4. NS-BH merger rate densities of summation of Pop Ⅰ and Ⅱ, and Pop Ⅲ origins [37]. A significant fraction of Pop Ⅲ NS-BH merger events is expected to be detected.

The detections of GW from a NS-NS merger by Advanced LIGO and Advanced Virgo, an accompanying short GRB, and its optical/radio counterparts [46, 49] are the most exciting news in 2017. Heavy nuclei are produced in the neutron-rich ejecta, and the succeeding decay of the unstable nuclei heats the material. The optical/IR counter part from this heated material showed a different evolution from the expected one. We carried out a detailed radiative transfer simulation taking into account the stuructured ejecta based on hydrodynamical simulations [56]. Our advanced model succeeded in reproducing the complex evolution of the photon spectrum.

Radio Observation of Crab Pulsar

Crab pulsar, the remnant of the supernova explosion in 1054 A.D., is one of the well-known neutron stars. While its physical properties have been studied for more than 40 years since its discovery, there remains an enigma about the origin of giant radio pulses (GRPs). Radio observation of Crab GRPs and its data analysis have been a major project in our group. Huge data sets sampled with high temporal resolution are affected by the dispersion effect due to inter stellar plasma. We have developed technique to carry out dedispersion of radio data.

We operated simultaneous multi-frequency observations of the Crab GRPs at 0.3, 1.6, 2.2, 6.7, and 8.4 GHz with the four radio telescopes (Iitate Planetary Radio Telescope, the 34m telescope at the Kashima Space Technology Center, the 64m telescope at the Usuda Deep Space Center of ISAS, and the Takahagi 32m antenna of Mizusawa VLBI observatory of NAOJ) [35], which is the widest frequency range ever observed simultaneously. In the frequency range in 0.3–2.2 GHz, 70% or more of the spectra in our GRPs are consistent with single power-laws (see Figure 5). We do not

find strong evidence that the majority of GRPs disagree with single power-law spectra, whose spectral index is widely distributed from approximately −4 to −1. Our results suggest an anti-correlation between the total energy release and spectral hardness. Those new discoveries provide constraint on not only the GRP models, but also models of another sporadic phenomenon, fast radio bursts (FRBs). Huge GRPs from young pulsars are possible sources of FRBs. Future FRB observations may find common or different properties with our data.

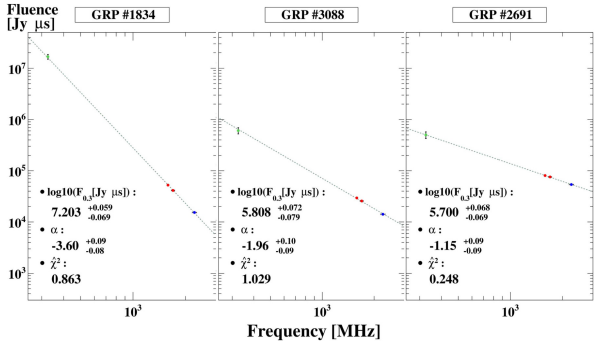

Fig. 5. Some examples of Crab GRP spectra observed by us [35].

R/D Studies on UHECRs and Extraterrestrial Grains

As the next generation technique to detect UHECRs, a space mission EUSO [6, 23, 54] and radio techniques have been proposed. EUSO will detect the UV light emitted by cosmic-ray generated air-showers in the earth's atmosphere. On the other hand, a radio array will measure the coherent radio signal emitted by the electromagnetic air shower component. Collaborating with the TA group of the high energy cosmic ray division of the ICRR, we have made a R/D study of the active method, namely, the detection of radar echoes from extensive air showers of UHECRs. Using the same radar echo technique, we have also joined a radar research project for extraterrestrial grains (meteors) [1, 4], which is also a research target for EUSO [44].

CALET

The CALET mission aims at revealing unsolved problems in high energy phenomena of the Universe by carrying out accurate measurements of high energy spectra of electrons, gamma-rays and nuclei [18, 38, 50]. HTV5 equipped with CALET was successfully launched by the H-IIB at 8:50:49 p.m. on August 19 2015 (JST) from the Tanegashima Space Center, and CALET is observeing cosmic rays without apparent problems.

Major scientific objectives are to search nearby cosmic-ray sources, such as NSs [3] or PWNe [40], and dark matter signatures by carrying out accurate measurements of cosmic ray electrons in 1 GeV - 20 TeV and gamma-rays in 4 GeV - 10 TeV. We succeeded in obtaining the electron–positron spectrum from 10 GeV to 5 TeV [47, 52], which agrees with the result obatained with AMS-02, but does not agree with the DAMPE result, in which a spectral cutoff is claimed.

The recent confirmation of the largely extended gamma-ray halo around the Geminga pulsar by HAWC[5] suggests the suppresion of the particle diffusion around the pulsar. The CALET and HAWC results provide constraint on the electron–positron diffusion in the interstellar medium. Starting from our study of PWNe [40, 42, 58], we are aiming at establishing a consistent model of production and propagation of electron–positron cosmic-rays.

Using the instruments onboard CALET, we set upper-limits of the gamma-ray fluxes for the GW events (see Figure 6) [30, 55]. The upper-limits correspond to a luminosity of 10^{49}–10^{53} erg s^{-1} in the GeV energy band, which is approximately the order of luminosity of typical short GRBs. This implies there will be a favorable opportunity to detect high-energy gamma-ray emission in further observations if events with favorable geometry will occur within our field-of-view.

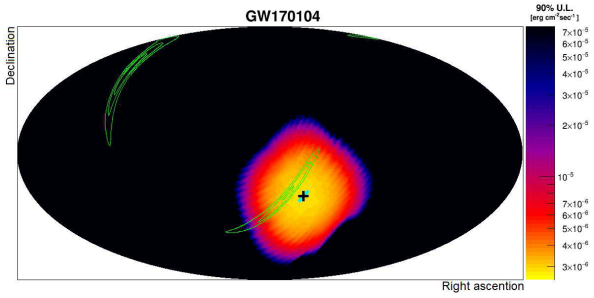

Fig. 6. 90% C.L. upper limit on GW170104 energy flux in the energy region 10–100 GeV shown in the equatorial coordinates [55]. Also shown by green contours is the localization significance map of the GW170104 signal reported by advanced LIGO.

Collaboration with other Projects

Our research fields closely relates to research targets in the other groups in the ICRR, TA, Tibet (cosmic-ray physics), CTA (gamma-ray emission mechanism), Super Kamiokande (extragalactic neutrinos), Observational Cosmology (GRB and star formation rate), and KAGRA (binary mergers). Actually our group has collaborated with the TA group (R/D study radar echoe technique of the UHECR detection) and the CTA group (several collaborating papers [21, 27, 53] have been published). Some of the CTA members join MAGIC team, which operates imaging atmospheric Cherenkov telescopes situated at La Palma, where the first large size

*5 Abeysekara et al. 2017, Science, **358**, 911 (2017).

telescope of CTA is now constructed. Now one of our members has contributes to writing MAGIC papers by interpreting the observation data. Those will be published in one year.

We also frequently teach and advise students in the other groups, especially the CTA and TA group, for promoting their study and writing papers or thesis. Gamma-ray detections from GRB 160509A with the Fermi Large Area Telescope were analysed by a student in the CTA group, and the results were summarized as a doctoral thesis. The results will be published with our interpretation based on our paper [43], which is also based on a master thesis of a student in Osaka university. Thus, we contribute to education for students even in other groups or universities. Now we are preparing a paper on the high redshift GRB rate collaborating with a student of the Observational Cosmology group. A new assistant professor joined 2018 concurrently belongs to the KAGRA group to analyse GW date with general relativistic numerical simulations. When the KAGRA starts its operation, he will greatly contribute to interpretation of the observation data.

Workshops

As a group in one of Joint Usage/Research Centers, we have held workshops on high-energy astrophysics every year. The list of the workshops is as follows:

- "Space Particle Acceleration: Elementary Processes in Relativistic Plasma and Magnetopshere of Pulsar/Magnetar", Jun. 2012
- "Physics for the Electron Energy Distribution", Nov. 2012
- "Particle Acceleration and Radiation in Pulsar Magnetosphere", Mar. 2013
- "Sturucture of Strongly Magnetized Neutron Star and Physical Processes of Particle Acceleration and Photon Emission", Oct. 2013
- "Particle Acceleration in the Universe and Transient Phenomena in Radio Band", Mar. 2014
- "Cosmic-ray Research in the next 10 years", Nov. 2014
- "Root of Relativistic Jet and Particle Acceleration", Feb. 2016
- "High Energy Phenomena in Compact Objects", Oct. 2016
- "Next Step with Gamma-ray Bursts", Nov. 2017

In most of the workshops, we have assured one or two hours for each lecturer. So the audience could hear details in latest topics. Our workshops have provided valuable opportunity to learn studies in unfamiliar fields for astronomical community.

Members

Staff

Toshio Terasawa, Professor, Dec. 2009–Mar. 2016
Katsuaki Asano, Assoc. Professor, Apr. 2013–present
Kyohei Kawaguchi, Assis. Professor, Mar. 2018–present

Postdoctoral Fellows

Shota Kisaka, ICRR researcher, Apr. 2012–Mar. 2014
Yosui Akaike, JSPS fellow, Apr. 2012–Mar. 2015
Shuta J. Tanaka, JSPS fellow, Apr. 2013–Mar. 2016
Ryo Mikami, JSPS fellow, Apr. 2016–Sep. 2016
Tomoya Kinugawa, ICRR researcher, Apr. 2016–Mar. 2018

Collaboration Researcher

Hideaki Miyamoto, Apr. 2012–Mar. 2014
Toshio Terasawa, Apr. 2016–Mar. 2018

Graduate Students

Ryo Mikami, Apr. 2011–Mar. 2016
Ryuji Takeishi, Apr. 2011–Mar. 2013
Kento Sasaki, Apr. 2013–Mar. 2015
Sho To, Apr. 2013–present
Nagisa Hiroshima, Apr. 2014–Mar. 2016
Wataru Ishizaki, Apr. 2014–present

List of Publications

Papers in Refereed Journals

[1] J. Kero, C. Szasz, T. Nakamura, T. Terasawa, H. Miyamoto, & K. Nishimura "A Meteor Head Echo Analysis Algorithm for the Lower VHF Band", Ann. Geophys. **30**, 639-659 (2012)

[2] Yasufumi Kojima, & Shota Kisaka "Magnetic Field Decay with Hall Drift in Neutron Star Crusts", Mon. Not. R. Astron. Soc. **421**, 2722-2730 (2012)

[3] Shota Kisaka, & Norita Kawanaka, "TeV Cosmic-ray Electrons from Millisecond Pulsars", Mon. Not. R. Astron. Soc. **421**, 3543-3549 (2012)

[4] J. Kero, C. Szasz, T. Nakamura, D. D. Meisel, M. Ueda, Y. Fujiwara, T. Terasawa, K. Nishimura, & J. Watanabe, "The 2009–2010 MU Radar Head Echo Observation Programme for Sporadic and Shower Meteors: Radiant Densities and Diurnal Rates", Mon. Not. R. Astron. Soc. **425**, 135-146 (2012)

[5] Toshio Terasawa, & Shuichi Matsukiyo, "Cyclotron Resonant Interactions in Cosmic Particle Accelerators", Space Sci. Rev. **173**, 623-640 (2012)

[6] J.H. Adams Jr., S. Ahmad, J.-N. Albert, et al., "An Evaluation of the Exposure in Nadir Observation of the JEM-EUSO Mission", Astro. Part. Phys. **44**, 76-90 (2013)

[7] Katsuaki Asano, "Wide-band Spectra of Prompt Emission" EAS Publications Series **61**, 115-122 (2013)

[8] Yoichi Yatsu, Katsuaki Asano, Nobuyuki Kawai, Yuki Yano, & Takeshi Nakamori, "Spatially Resolved Spectroscopy of a Pulsar Wind Nebula in MSH 15–56", Astrophys. J. **773**, 25(14pp) (2013)

[9] Katsuaki Asano, & Peter Mészáros, "Photon and Neutrino Spectra of Time-dependent Photospheric Models of Gamma-ray Bursts", J. Cos. Astropart. Phys. **09**, 008 (2013)

[10] M. Ackermann, M. Ajello, K. Asano et al., "The First Fermi LAT Gamma-ray Burst Catalog", Astrophys. J. Supp. **209**, 11(90pp) (2013)

[11] Shuta J. Tanaka, & Fumio Takahara, "Constraint on Pulsar Wind Properties from Induced Compton Scattering off Radio Pulses", Prog. Theor. Exp. Phys. **2013**, 123E01(24pp) (2013)

[12] Katsuaki Asano, Fumio Takahara, Masaaki Kusunose, Kenji Toma, & Jun Kakuwa, "Time-dependent Models for Blazar Emissions with the Second-order Fermi Acceleration", Planet. Space Sci. **59**, 378-386 Astrophys. J. **780**, 64(12pp) (2014)

[13] R. Mikami, T. Terasawa, S. Kisaka, H. Miyamoto, K. Asano, N. Kawai, Y. Yamakoshi, K. Nagata, R. Kataoka, K. Takefuji, M. Sekido, H. Takeuchi, H. Odaka, T. Sato, & Y. T. Tanaka, "Search for a Correlation between Giant Radio Pulses and Hard X-ray Emissions in the Crab Pulsar", JPS Conf. Proc. **1**, 015106(4pp) (2014)

[14] M. Ackermann, M. Ajello, Katsuaki Asano et al., "Fermi-LAT Observations of the Gamma-ray Burst GRB 130427A", Scinece **343**, 42-47 (2014)

[15] Katsuaki Asano, & Peter Mészáros, "Neutrino and Cosmic-ray Release from Gamma-ray Bursts: Time-dependent Simulations", Astrophys. J. **785**, 54(5pp) (2014)

[16] Makoto Takamoto, Shota Kisaka, Takeru Suzuki, & Toshio Terasawa, "The Evolution of High Temperature Plasma in Magnetar Magnetospheres and its Implications for Giant Flares", Astrophys. J. **787**, 84(13pp) (2014)

[17] Shota Kisaka, & Shuta J. Tanaka, "Synchrotron X-ray Emission from Old Pulsars", Mon. Not. R. Astron. Soc. **443**, 2063-2076 (2014)

[18] Tae Niita, Shoji Torii, Katsuaki Kasahara, Hiroyuki Murakami, Shunsuke Ozawa, Yoshitaka Ueyama, Yosui Akaike, Tadahisa Tamura, Kenji Yoshida, Yusaku Katayose, Yuki Shimizu, & Hideyuki Fuke, "A Balloon Experiment Using CALET Prototype (bCALET-2)", Adv. Space Res. **55**, 753-760 (2015)

[19] Jun Kakuwa, Kenji Toma, Katsuaki Asano, Masaaki Kusunose, & Fumio Takahara, "Synchrotron Self-Compton Emission by Relativistic Electrons under Stochastic Acceleration: Application to Mrk 421 and Mrk 501", Mon. Not. R. Astron. Soc. **449**, 551-558 (2015)

[20] Shuta J. Tanaka, Katsuaki Asano, & Toshio Terasawa, "Avalanche Photon Cooling by Induced Compton Scattering: Higher-order Kompaneets Equation", Prog. Theor. Exp. Phys. **2015**, 073E01(14pp) (2015)

[21] Katsuaki Asano, & Masaaki Hayashida, "The Most Intensive Gamma-ray Flare of Quasar 3C 279 with the Second-order Fermi Acceleration", Astrophys. J. Lett. **808**, L18(5pp) (2015)

[22] Katsuaki Asano, & Kohta Murase, "Gamma-ray Bursts as Multienergy Neutrino Sources", Adv. Astron. **2015**, 568516(10pp) (2015)

[23] J.H. Adams Jr., S. Ahmad, J.-N. Albert, D. Allard, L. Anchordoqui, V. Andreev, A. Anzalone, Y. Arai, K. Asano et al., "Special Issue on the JEM-EUSO Mission", Exp. Astron. **40**, 3-326 (2015)

[24] Katsuaki Asano, & Toshio Terasawa, "Stochastic Acceleration Model of Gamma-ray Burst with Decaying Turbulence", Mon. Not. R. Astron. Soc. **454**, 2242-2248 (2015)

[25] Kento Sasaki, Katsuaki Asano, & Toshio Terasawa, "Time-dependent Stochastic Acceleration Model for the Fermi Bubbles", Astrophys. J. **814**, 93(9pp) (2015)

[26] Ryo Yamazaki, Katsuaki Asano, & Yutaka Ohira, "Electromagnetic Afterglows Associated with Gamma-ray Emission Coincident with Binary Black Hole Merger Event GW150914", Prog. Theor. Exp. Phys. **2016**, 051E01(7pp) (2016)

[27] M. Ackermann, R. Anantua, K. Asano, et al., "Minute-timescale > 100 MeV γ-ray Variability during the Giant Outburst of Quasar 3C 279 Observed by Fermi-LAT in 2015 June", Astrophys. J. Lett. **824**, L20(8pp) (2016)

[28] Katsuaki Asano, & Peter Mészáros, "Ultrahigh-energy Cosmic Ray Production by Turbulence in Gamma-ray Burst Jets and Cosmogenic Neutrinos", Phys. Rev. D **94**, 023005(10pp) (2016)

[29] Kazuhiro Takefuji, Toshio Terasawa, Tetsuro Kondo, Ryo Mikami, Hiroshi Takeuchi, Hiroaki Misawa, Fuminori Tsuchiya, Hajime Kita, & Mamoru Sekido, "Very Long Baseline Interferometry Experiment on Giant Radio Pulses of Crab Pulsar toward Fast Radio Burst Detection", Pub. Astron. Soc. Pac. **128**, 084502(6pp) (2016)

[30] O. Adriani, Y. Akaike, K. Asano, et al., "CALET Upper Limits on X-ray and Gamma-ray Counterparts of GW 151226", Astrophys. J. Lett. **829**, L20(5pp) (2016)

[31] Takashi Nakamura, Masaki Ando, Tomoya Kinugawa, Hiroyuki Nakano, Kazunari Eda, Shuichi Sato, Mitsuru Musha, Tomotada Akutsu, Takahiro Tanaka, Naoki Seto, Nobuyuki Kanda, & Yousuke Itoh, "Pre-DECIGO can Get the Smoking Gun to Decide the Astrophysical or Cosmological Origin of GW150914-like Binary Black Holes", Prog. Theor. Exp. Phys. **2016**, 093E01(16pp) (2016)

[32] Shota Kisaka, Katsuaki Asano, & Toshio Terasawa, "Electric Field Screening with Backflow at Pulsar Polar Cap", Astrophys. J. **829**, 12(14pp) (2016)

[33] Tomoya Kinugawa, Hiroyuki Nakano, & Takashi Nakamura, "Gravitational Wave Quasinormal Mode from Population Ⅲ Massive Black Hole Binaries in Various Models of Population Synthesis", Prog. Theor. Exp. Phys. **2016**, 103E01(21pp) (2016)

[34] S. Guiriec, C. Kouveliotou, D. H. Hartmann, J. Granot, K. Asano, P. Meszaros, R. Gill, N. Gehrels, & J. McEnery, "A Unified Model for GRB Prompt Emission from Optical to γ-rays; Exploring GRBs as Standard Candles", Astrophys. J. Lett. **831**, L8(6pp) (2016)

[35] Ryo Mikami, Katsuaki Asano, Shuta J. Tanaka, Shota Kisaka, Mamoru Sekido, Kazuhiro Takefuji, Hiroshi Takeuchi, Hiroaki Misawa, Fuminori Tsuchiya, Hajime Kita, Yoshinori Yonekura, & Toshio Terasawa, "Wide-band Spectra of Giant Radio Pulses from the Crab Pulsar", Astrophys. J. **832**, 212(25pp) (2016)

[36] Makoto Arimoto, Katsuaki Asano, Masanori Ohno, Peter Veres, Magnus Axelsson, Elisabetta Bissaldi, Yutaro Tachibana, & Nobuyuki Kawai, "High-energy Non-thermal and Thermal Emission from GRB 141207A Detected by Fermi", Astrophys. J. **833**, 139(13pp) (2016)

[37] Tomoya Kinugawa, Takashi Nakamura, & Hiroyuki Nakano, "The Possible Existence of Pop Ⅲ NS–BH Binary and its Detectability", Prog. Theor. Exp. Phys. **2017**, 021E01(9pp) (2017)

[38] Y. Asaoka, Y. Akaike, Y. Komiya, R. Miyata, S. Torii, O. Adriani, K. Asano, et al., "Energy Calibration of CALET Onboard the International Space Station", Astro. Part. Phys. **91**, 1-10 (2017)

[39] Kohei Inayoshi, Ryosuke Hirai, Tomoya Kinugawa, & Kenta Hotokezaka, "Formation Pathway of Population Ⅲ Coalescing Binary Black Holes through Stable Mass Transfer", Mon. Not. R. Astron. Soc. **468**, 5020-5032 (2017)

[40] Wataru Ishizaki, Shuta J. Tanaka, Katsuaki Asano, & Toshio Terasawa, "Broadband Photon Spectrum and its Radial Profile of Pulsar Wind Nebulae", Astrophys. J. **838**, 142(14pp) (2017)

[41] F. Acero, R. Aloisio, J. Amans, et al., "Prospects for CTA Observations of the Young SNR RX J1713.7–3946", Astrophys. J. **840**, 74(14pp) (2017)

[42] Shuta J. Tanaka, & Katsuaki Asano, "On the Radio-emitting Particles of the Crab Nebula: Stochastic Acceleration Model", Astrophys. J. **841**, 78(11pp) (2017)

[43] Takuma Fukushima, Sho To, Katsuaki Asano, & Yutaka Fujita, "Temporal Evolution of the Gamma-ray Burst Afterglow Spectrum for an Observer: GeV–TeV Synchrotron Self-Compton Light Curve", Astrophys. J. **844**, 92(11pp) (2017)

[44] G. Abdellaoui, S. Abe, A. Acheli, et al., "Meteor Studies in the Framework of the JEM-EUSO Program", Planet. Space Sci. **143**, 245-255 (2017)

[45] Akinobu Miyamoto, Tomoya Kinugawa, Takashi Nakamura, & Nobuyuki Kanda, "How to Confirm the Existence of Population Ⅲ Stars by Observations of Gravitational Waves", Phys. Rev. D **96**, 064025(10pp) (2017)

[46] B. P. Abbott, et al., "Multi-messenger Observations of a Binary Neutron Star Merger", Astrophys. J. Lett. **848**, L12(59pp) (2017)

[47] O. Adriani, Y. Akaike, K. Asano, et al., "Energy Spectrum of Cosmic-ray Electron and Positron from 10 GeV to 3 TeV Observed with the Calorimetric Electron Telescope on the International Space Station", Phys. Rev. Lett. **119**, 181101(6pp) (2017)

[48] Tomoya Kinugawa, & Katsuaki Asano, "Long Gamma-ray Burst Rate in the Binary Merger Progenitor Model", Astrophys. J. Lett. **849**, L29(5pp) (2017)

[49] Katsuaki Asano, & Sho To, "Subsequent Non-thermal Emission due to the Kilonova Ejecta in GW170817", Astrophys. J. **852**, 105(5pp) (2018)

[50] Y. Asaoka, S. Ozawa, S. Torii, O. Adriani, Y. Akaike, K. Asano, et al., "On-orbit Operations and Offline Data Processing of CALET onboard the ISS", Astro. Part. Phys. **100**, 29-37 (2018)

[51] Kai Wang, Ruo-Yu Liu, Zi-Gao Dai, & Katsuaki Asano, "Hadronic Origin of Prompt High-energy Emission of Gamma-ray Bursts Revisited: In the Case of a Limited Maximum Proton Energy", Astrophys. J. **857**, 24(12pp) (2018)

[52] O. Adriani, Y. Akaike, K. Asano, et al., "Extended Measurement of the Cosmic-Ray Electron and Positron Spectrum from 11 GeV to 4.8 TeV with the Calorimetric Electron Telescope on the International Space Station", Phys. Rev. Lett. **120**, 261102(7pp) (2018)

[53] Katsuaki Asano, & Masaaki Hayashida, "Blazar Spectra with Hard-sphere-like Acceleration of Electrons", Astrophys. J. **861**, 31(7pp) (2018)

[54] G. Abdellaoui, et al., "EUSO–TA — First Results from a Ground-based EUSO Telescope", Astro. Part. Phys. **102**, 98-111 (2018)

[55] O. Adriani, Y. Akaike, K. Asano, et al., "Search for GeV Gamma-ray Counterparts of Gravitational Wave Events by CALET", Astrophys. J. **863**, 160(9pp) (2018)

[56] Kyohei Kawaguchi, Masaru Shibata, & Masaomi Tanaka, "Radiative Transfer Simulation for the Optical and Near-infrared Electromagnetic Counterparts to GW170817", Astrophys. J. Lett. **865**, L21(6pp) (2018)

[57] Yutaro Tachibana, Makoto Arimoto, Katsuaki Asano, et al., "Late Engine Activity of GRB 161017A Revealed by Early Optical Observations", Pub. Astron. Soc. Pac. **70**, 92(9pp) (2018)

[58] Wataru Ishizaki, Katsuaki Asano, & Kyohei Kawaguchi, "Self-Consistent 1–D Model of Pulsar Wind Nebulae with Particle Diffusion", Accepted for ApJ, arXiv:1809.09054

ASHRA (R&D)

In 2002, Sasaki *et al.* presented the distinctive detecting potential of the Earth-skimming tau neutrino (ES-ν_τ) technique with air-shower (AS) telescope array detector [2], which can enjoy a large target mass by imaging ASs produced by τ decays in the air. The method has come to be used as a powerful tool to promote multi-astroparticle astrophysics including very-high energy (VHE) neutrino search [1, 7, 10, 11, 31, 32] [1] [2]. Along with that, Sasaki *et al.* advocated the design of high resolution (1 arcmin) wide field of view (FOV) (50°) AS telescope based on the modified Baker-Nunn optics [3], which can watch such a large air volume keeping the astrometrical advantage of cosmic νs in a cost effective way. The camera mounted on such a high resolution and wide telescope is expected to efficiently trigger and read out images with pixels of orders of million at least at the video rate. The only readout that meets the requirement seemed a CMOS sensor but not a conventional PMT array camera. In 2002, Sasaki *et al.* developed a prototype demonstrating the principle with the light and electron optics transporting images to a fine CMOS sensor to realize a high resolution over a wide FOV [8, 12]. In 2003, Ashra-1 (*All-sky Survey High Resolution Air-shower detector Phase-1*) was funded to start the collaboration. [3]

Ashra-1 [4] [7, 14, 23] is a project to build an unconventional optical telescope complex on Mauna Loa (3,300 m asl.) on Hawaii Island as shown in Fig.1 (*top*), that images very wide FOV, covering most of the whole half sky, yet with the angle resolution of a few arcmin. The project aims to observe Cherenkov (CE) and fluorescence (FL) light from the AS developments induced by the primaries of ES-ν_τ's as well as gamma-rays (γs) and cosmic-ray (CR) nucleons.

The key technical feature of the Ashra-1 detector rests on the use of electrostatic lenses to generate convergent beams rather than optical lens system. This electron optics requires: *photoelectric lens imaging-tube* [18, 30]; the world's largest imaging-tube uses electrostatic lens in addition to an optical system to generate convergent beams from photocathode of 20-in. diameter to output phospher window of 1-in. diameter, enabling a very low cost and high performance image sensor providing a high resolution over a wide FOV, and *image pipeline* [8]; the image transportation from imaging-tube (image intensifier) to a trigger device and image sensors of fine pixels (CMOS), with high gain and resolution, enabling very fine images with parallel self-trigger systems that trigger separately for optical flash, atmospheric CE and FL lights.

Fig. 1. Ashra-1 Mauna Loa Observation Site (*top*), photo-electric lens imaging tube (*bottom left*) photoelectric image pipeline (*bottom middle*) and local exposure/readout fine sensor with trigger (FST) (*bottom right*)

We succeeded in realizing the modified Baker-Nunn optics light collector (LC) cost-effectively by combining three 1 m diameter acrylic aspherical lenses and seven 0.8 m diameter thin (∼1 cm) spherical float glass segment mirrors. In 2004-2006, we made test observations with a prototype of the Ashra-1 LC at Haleakala Observatory on Maui Island, which is owned by University of Hawaii. We searched for optical flash in the field covering the WXM error box of GRB041211 with the prototype [13]. The Ashra-1 wide FOV allows us search for light or/and particle emission both before and after rapid transients such as GRBs covering the starting time [15, 16, 17, 26, 29, 31, 39].

The Ashra-1 has been partly operated since 2008 at the Mauna Loa observation site at 3300 m asl. on Hawaii Island. The LC optics and the readout system as the detector unit (Fig. 1) were confirmed to achieve a total resolution of ~ 3 arcminutes covering 42° FOV with star light images 2 (*left*). Following the alert for GRB081203A given by the SWIFT satellite, Ashra-1 succeeded in the first search for PeV-EeV ν_τ's originating from a GRB with the ES-ν_τ technique setting stringent fluence limits [31]. Furthermore, with detailed Monte Carlo simulation, we performed systematic studies on the detection performance for ES-ν_τ ASs by the Ashra-1 CE mode, confirming the good detection sensitivity due to the large angle method for quasi-horizontal ASs with almost free CR background and very accurate pointing accuracy of less than 0.2° even in the case of the monostatic observation [32]. In the third

*1 M. Ahnen *et al.*(MAGIC Collab.), Astropart. Phys, 102, 77–8 (2018).
*2 J. Alvarez-Muñiz *et al.*, Phys. Rev. D, 97(2), 1–1 (2018).
*3 supported by Coordination Fund for Promoting Science and Technology (157-20004100) from MEXT of Japan.
*4 http://www.icrr.u-tokyo.ac.jp/∼ashra

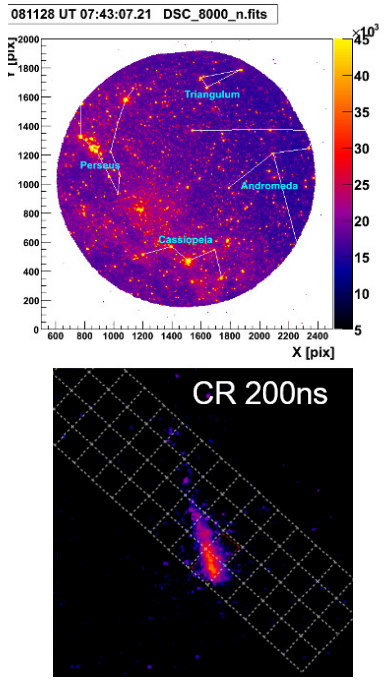

Fig. 2. A real star image taken by Ashra-1 with 1 sec exposure time without trigger (*left*), where big constellations are indicated on it as guiding eyes. A real air-shower image triggered and read out by Ashra-1 with 200 ns exposure time (*right*).

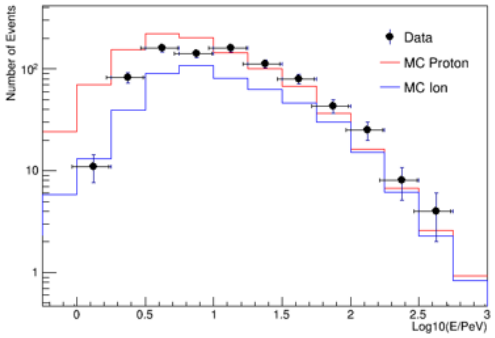

Fig. 3. CR spectrum observed with Ashra-1 LC CE mode.

observation period (Obs3) in 2012-2013, we arranged four sets of trigger pixels toward the 2.6° × 2.6° area around the center of 14.6° in altitude and 22.0° in azumuth to check the sensitivity for the background CR CE ASs. From the analysis of the triggered events like Fig. 2 (*right*), we measured CR flux spectrum which is consistent with conventional measurements [41], as shown in Fig. 3 (*left*) where the MC predictions are normalized by the fluxes from conventional CR observations assuming the primary proton or iron.

Since 2013, we have proposed and prepared for the stage of Obs4, whereas the observation is still not funded. The remaining element to be demonstrated is a fast fine sensor with trigger (FST) to be served as readout of the Ashra-1 FL mode. The observed FL AS trajectories could have various time structure up to their own energies and geometrical conditions. The readout FST is supposed to have the functions of local exposure and local readout corresponding to fast addressing signals indicating when and which pixel groups on the sensor to be exposed by the signal light. We developed FST and performed careful tests so that we confirmed such functions well as the readout of the FL signals. Fig. 1 shows a picture of FST under testing it. Adding that, automatic operation of the detector system is useful and important improvement for the stage of more systematic operation. We have successfully developed a short pulse uniform LED flasher to be equipped at the center of the main mirror of LC to check the total gain and the non-uniformity of the trigger readout system composed of PLI and PIP by counting photons flash by flash. It provides us periodically high-quality gain calibration easily merged into the available data flow without any specific data taking system. Adding to demonstrating the FL AS trigger readout as described above, we have planned to observe at every night the ridge of our Galaxy within the wide FOV combined with six Ashra-1 LCs aligned along the tragectory of the Galactic center. The wide FOV composed of six Ashra-1 LCs can efficiently cover the Galactic ridge region simultaneously [36]. HESS observation of the hard γ-ray spectra from the Galactic Center suggesting a Pevatron candidate is one of fascinating physics motivation. [5]

Based on Ashra-1 performance, we have planned a new extention, i.g. Ashra Neutrino Telescope Array (NTA) [6], which is an AS imaging ν and γ observation system for the aim or scientific goal [33]: *Clear Discovery and Identification of Nonthermal Hadronic Processes in the Universe, be it Galactic, Extragalatic, or Cosmogenic.* By optimizing the layout of the NTA stations to enhance the detection sensitivity for ES-ν_τ's around 1 PeV from the detailed simulation studies [32, 33], four NTA stations are to be deployed on Mauna Loa at 3000 - 3500 m asl. (NTA Summit Array), watching the air volume surrounding Mauna Loa including the surface of Mauna Loa, the largest volcano, to efficiently detect CE and FL light generated from τ ASs with both short and long decay lengths and γ ASs. The reconstructed AS images with fine resolution is powerful not only in the determination of point sources of PeV ν_τ's but also FL observation for γ ASs above PeV with the large effective area. Fig. 4 shows NTA achieves the effective area similar with that of IceCube at 3 PeV and larger than it above 30 PeV by 10-100 times and larger than either of IceCube Gen2 or ARA-100 in the 30 PeV-30 EeV region. The sensitivity for ES-ν_τ's with observing CE light can enhance more the discovery potential around PeV or lower energy region. Fig. 4 shows the integral flux sensitivity limits for γ's with NTA for one year observation time comparing

*5 HESS Collaboration, Nature **531**, 476 (2016).
*6 http://asrws300.icrr.u-tokyo.ac.jp/nta/

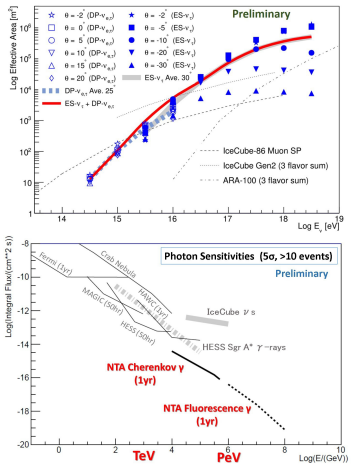

Fig. 4. Effective area for ES-ν_τ's and DP-$\nu_{e,\tau}$'s as changing the energies with NTA in comparison with those for all flavor νs with IceCube, IceCube Gen2, and ARA-100 (*left*). Integral flux sensitivity limits (5σ or more than 10 events) for γ's versus the energies with NTA (1yr observation) and other detectors (*right*).

with those of other detectors. The unique combination among CE and FL observations for both ES-ν_τ's and γ with NTA will truly identify Pevatron(s) and open up new types of search for ν's and γ's in the wide energy range.

A Letter of Intent for NTA has been published since 2013 [33, 34]. In 2014, a preliminary workshop (VHEPA2014) [37, 36, 38] was held at Kashiwa campus of the University of Tokyo to discuss the design of the project and plans with the colleagues who share common interests. After a workshop in Taipei and an informal meeting to discuss the next post-IceCube detector project at the 34th International Cosmic Ray Conference in The Hague in 2015 [40, 41], we held a workshop as VHEPA2016 at the University of Hawaii Manoa in January, 2016 [42] to discuss more detailed physics and NTA potential performance, as well as funding requests in each country. We have set up a Promotion Working Group and our proto-collaboration to reconfirm the basic design of NTA, discuss strategies in the multi-messenger era [43], and publish White Paper and Technical Design Report.

Members

[Spokesperson: Makoto Sasaki]

ICRR, Univ. of Tokyo, Kashiwa, Chiba 277-8582

In collaboration with the members of: T. Aoki[a], P. Binder[d], T. Browder[c], P. Doetinchem[c], Y. Fukasaku[b], J. Goldman[d], J. Hamilton[d], A. Hirose[a], S. Haino[k], Y.B. Hsiung[l], H.A. Huang[N], T. Kimura[g], K. Kohri[i], H. Kuze[f], J. Learned[c], G.-L. Lin[m], H. Mashiyama[a], S. Matsuno[c], R. Mussa[j], H. Oshima[b], S. Ogawa[b], M. Sasaki[a], H. Shibuya[b], N. Sugiyama[e], M. Tanaka[i], M.-Z. Wangr[l], Y. Watanabe[h] K. Yoshimura[o]

(a) ICRR, Univ. Tokyo; (b) Toho Univ.; (c) Univ. Hawaii Manoa; (d) Univ. Hawaii Hilo; (e) Nagoya Univ; (f) Chiba Univ.; (g) Ibaraki Univ.; (h) Kanagawa Univ. (i) KEK (j) Univ. Torino (k) Academia Sinica (l) National Taiwan Univ. (m) National Chiao Tung Univ. (n) Univ.Immersion Program (o) Okayama Univ.

List of Publications

2000–2012

[1] M. Sasaki, in *Proc. ICRR2000 Satellite Symposium: Workshop of Comprehensive Study of the High Energy Universe*, edited by T. Kifune, J. Okada, T. Kajita, and M. Sasaki (ICRR, the University of Tokyo, Kashiwa, 2000), p. 110.

[2] Sasaki, M., Asaoka, Y., Jobashi, M. "Detecting very high energy neutrinos by the telescope array". *Astroparticle Phys.*, 19(1), 37–46 (2003). https://doi.org/10.1016/S0927-6505(02)00191-3. **[41]**

[3] M. Sasaki, A. Kusaka and Y. Asaoka, "Design of UHECR telescope with 1 arcmin resolution and 50° field of view", *Nucl. Instrum. Methods* A **492**, 49 (2002). **[34]**

[4] Aita, Y., et al., "The ASHRA Detector", *ibid.*, pp. 1061-1064 (2003).

[5] Kohri, K., et al., "Particle Physics in ASHRA", *ibid.*, pp. 1747-1750 (2003).

[6] Aita, Y., et al., "High Energy Astrophysics by ASHRA", *ibid.*, pp. 2991-2994 (2003).

[7] Sasaki, M., "Very High Energy Particle Astronomy with All-sky Survey High Resolution Air-shower Detector (Ashra)", *Progress of Theoretical Physics Supplement*, **151**, 192 (2003). **[13]**

[8] M. Sasaki, Y. Asaoka and M. Jobashi, "Self-triggered image intensifier tube for high resolution UHECR imaging detector", *Nucl. Instrum. Methods* A **501**, 359 (2003). **[29]**

[9] Kuze, H., Fukagawa, S., Takeuchi, N., Asaoka, Y., and Sasaki, M., "Development of a wide-area imaging lidar for atmospheric monitoring", *29th SICE Remote Sensing Symposium (Tsukuba)*, 61-64 (2003).

[10] Sasaki, M., "Very High Energy Particle Astronomy with All-Sky Survey High Resolution Air-shower Detector (Ashra)", *Modern Physics Letters* A 19, 1107-1115, 2004. **[13]**

[11] P. Yeh *et al.*, "PeV cosmic neutrinos from the mountains", *Modern Physics Letters A* Vol. 19, Nos. 13-16 (2004) 1117-1124. [**14**]

[12] Arai, Y., et al., "ASHRA Trigger and Readout Pixel Sensors", *Proc. 28th Intl. Cosmic Ray Conf. (Tsukuba),* pp. 961–964, 2003.

[13] Sasaki, M., et al., "GRB041211: Ashra Prototype optical observation", *GCN Circ.* 2846, (2004).

[14] Sasaki, M., et al., "Ashra-1 Analysis", *Proc. 29th Int. Cosmic Ray Conf.* (Pune, India), Vol. 8, 197-200, (2005).

[15] Sasaki, M., et al., "Observation of Optical Transients with the Ashra prototype", *ibid.*, Vol. 5, 319-322, 2005.

[16] Sasaki, M., et al., "GRB050504: Ashra-P2/3 monitor and Ashra-AFT response", *GCN Circ.* 3499, 2005.

[17] Sasaki, M., Manago, N., Noda, K., Asaoka, Y., "GRB050502b: Early Observation", *GCN Circ.* 3421, 2005.

[18] Asaoka.Y., Aita.Y., Aoki.T., and Sasaki.M., "Development of a 16-inch UV-Ray Image Intensifier Tube," *IEEE Transactions on Nuclear Science*, 52, num 5, 1773-1778 (2005).

[19] Fukagawa, S., Kouga, I., Kuze, H., Takeuchi, N., Sasaki, M., Asaoka, Y., Ogawa, S., "Simulation study for aerosol distribution retrieval from bistatic, imaging lidar data", *Conference on Laser and Electro Optics / Pacific Rim* 2005, C15, July 14, 2005.

[20] Fukagawa, S., Kouga, I., Kuze, H., Takeuchi, N., Sasaki, M., Asaoka, Y. and Ogawa, S., "Simulation study for aerosol distribution retrieval from bistatic, imaging lidar data", *Conference on Quantum Electronics 2005 and the Pacific Rim Conference on Lasers and Electro-Optics 2005 (IQEC/CLEO-PR 2005)*, Tokyo, Japan (July 11-15, 2005).

[21] Fukagawa, S., Koga, I., Kuze, H., Takeuchi, N., Sasaki, M., Asaoka, Y., Ogawa, S., "Environmental application of the all-sky survey high-resolution air-shower (Ashra) telescope - aerosol distribution measurement using a bistatic, imaging lidar", *Proceedings of the CEReS international symposium on radiation budget and atmospheric parameters studied by satellite and ground observation data*, P-3, pp.196-199 (2005.2).

[22] Katsuta.T., Yokomizo.S., Sasaki.M., "Study on Machining of Large Acrylic Lens," *Japan Society of Precision Engineering*, 73, No.2, 215-219, (2007).

[23] M. Sasaki, "The Ashra Project", *30th Intl. Cosmic Ray Conf.* (Merida), ID1232, 2007.

[24] Y. Aita *et al.*, "Ashra Mauna Loa Observatory and Slow Control System", *ibid.*, ID684.

[25] Y. Aita *et al.*, "Hybrid Photo Detector as the Ashra Trigger Sensor", *ibid.*, ID1279.

[26] Y. Aita *et al.*, "GRB081203A: Ashra-1 observation of early optical and VHE-neutrino emission", *GCN Circ.*, 8632 (2008).

[27] Y. Aita *et al.*, "VHE neutrino pilot observation with the Ashra detector", *31th Intl. Cosmic Ray Conf. (Lodz)*, ID313, 2009.

[28] Y. Aita *et al.*, "Ashra Optical Transient Observation", *ibid.*, ID1410.

[29] Y. Asaoka *et al.*, "GRB100906A: Ashra-1 observation of early optical emission", *GCN Circ.*, 11291 (2010).

[30] Y. Asaoka and M. Sasaki, "Performance of a 20-in. photoelectric lens image intensifier tube", Nucl. Instrum. Methods Phys. Res. A **647**, 34 (2011). [**18**]

[31] Y. Aita *et al.*, "Observational Search for PeV-EeV Tau Neutrino from GRB081203A", *Ap. J.* Lett. **736**, L12 (2011). [**25**]

2013–2018

[32] Y. Asaoka, M. Sasaki, "Cherenkov τ shower earth-skimming method for PeV-EeV ν_τ observation with Ashra", *Astroparticle Phys.* **41**, 7 (2013). [**19**]

[33] Sasaki, M., Hou, G. W.-S. "Neutrino Telescope Array Letter of Intent: A Large Array of High Resolution Imaging Atmospheric Cherenkov and Fluorescence Detectors for Survey of Air-showers from Cosmic Tau Neutrinos in the PeV-EeV Energy Range", arXiv:1408.6244 (2014). [**10**]

[34] George W.-S. Hou, Makoto Sasaki, "Prospect towards Survey of Astronomical ν_τ Sources", THE UNIVERS EVol. 2, No. 4 October-December 2014, Pages 15-26, ISSN:2309-852X.

[35] S. Ogawa (Ashra-1 Collaboration), *Proceedings of the 12th Asia Pacific Physics Conference*, JPS Conf. Proc. , 013111 (2014).

[36] Sasaki, M., Kifune, T., "Ashra Neutrino Telescope Array (NTA): Combined Imaging Observation of Astroparticles — For Clear Identification of Cosmic Accelerators and Fundamental Physics Using Cosmic Beams —", *Proc. of the 7th International Workshop on Very High Energy Particle Astronomy in 2014 (VHEPA2014)*, 2014,1–8 (2017). https://doi.org/10.7566/JPSCP.15.011013

[37] G. W.-S. Hou (Taiwan), S. Ogawa (Toho) (Chair), M. Sasaki (Tokyo), N. Sugiyama (Nagoya), "Proceedings of the 7th International Workshop on Very High Energy Particle Astronomy in 2014 (VHEPA2014)", *JPS Conference Proceedings* Volume 15 (June 2, 2017), e-ISBN: 978-4-89027-120-7.

[38] Y. Aita *et al.* (Ashra NTA Collaboration),"Ashra NTA: Towards Survey of Astronomical Tau Neutrino Sources" *JPS Conference Proceedings*, 2014, 3095-3098 (2017). http://dx.doi.org/10.7566/JPSCP.1.013095,

[39] M. Sasaki, "Search for PeV-EeV Tau Neutrinos and Optical Transients from Violent Objects with Ashra-1," *Astroparticle, Particle, Space Physics and Detectors for Physics Applications - Proceedings of the 14th ICATPP Conference on Astroparticle,Particle,Space Physics and Detectors for Physics Applications (Villa Olmo,Como 2014)*, 112-119, DOI:10.1142/9789814603164-0018.

[40] G. W.-S. Hou, "Towards survey of astronomical ν_τ source",. *PoS* (ICRC2015) 1167 (2015).

[41] Sasaki, M. *et al.*, "Status of Ashra project", *34th Int. Cosmic Ray Conf. (Hague, Netherlands)*, 2015.

[42] *9th International Workshop on Very High Energy Particle Astronomy Workshop (VHEPA 2016)* 07-09 Jan 2016. Honolulu, HI, USA CNUM: C16-01-07. https://indico.phys.hawaii.edu/event/896/

[43] Sasaki, M., "Neutrino Telescope Array (NTA): Multi-Astroparticle Explorer for PeV-EeV Universe — For Clear Identification of Cosmic Accelerators and Cosmic Beam Physics ",— *PoS* (ICRC2017) 941 (2017).

ALPACA (R&D)

Fig. 1. From Ref.[2]. Experimental site for the ALPACA experiment, Cerro Estuqueria (4,740 m above see level, 16°23' S, 68°08' W), near Mount Chacaltaya, in Bolivia.

Introduction

We have started up the ALPACA (Andes Large area PArticle detector for Cosmic ray physics and Astronomy) project. The ALPACA experiment is composed of an 83,000 m^2 air shower array and a 5,400 m^2 underground muon detector array to make wide field-of-view high-sensitivity observation of high-energy cosmic rays/cosmic gamma rays on the Cerro Estuqueria highland, 4,740 m above sea level around Mount Chacaltaya, Bolivia.

Experiment

The ALPACA[2],[3] is a cosmic-ray experiment with a large surface air shower array with a large underground muon detector array. The experimental site (approximately 500 m×500 m ∼250,000 m^2 in total area) is located on a flat high land called Cerro Estuqueria (4,740 m above sea level, 16°23' S, 68°08' W), as shown in Fig. 1, around Mount Chacaltaya, near La Paz, Bolivia. In some part in this area, our detectors will be set up.

We plan to set up a 5,400 m^2 underground (approximately one to a few meters) muon detector array (MD) and an 83,000 m^2 air shower array (AS), shown in Fig. 2. MD of water Cherenkov type is composed of eight pools with each pool (approximately 1 m deep) containing twelve 56 m^2 unit detectors. AS is made up of 401 1-m^2 plastic scintillation counters at 15 m spacing.

The AS field of view is roughly 2 steradian. The expected angular resolution of AS is approximately 1 degree at 5 TeV and 0.2 degrees around 100 TeV for gamma rays. For 100 TeV gamma rays, the AS energy resolution is estimated to be ∼20-25 %. The hadron

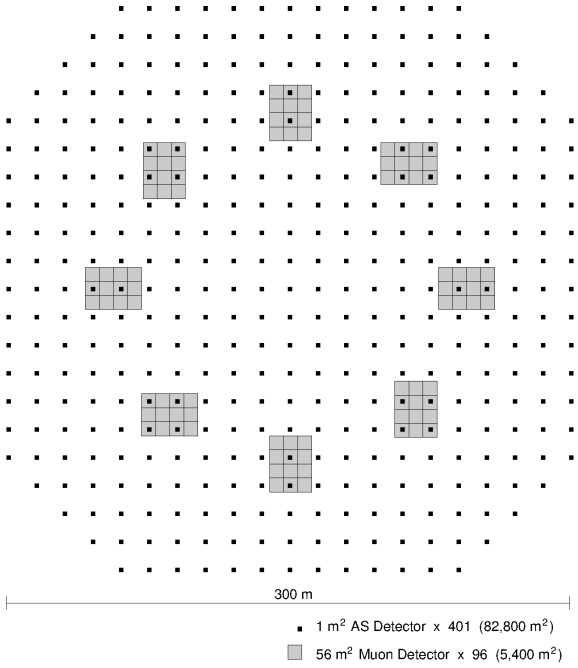

Fig. 2. From Ref.[2]. Schematic view of the ALPACA experiment. The small black squares indicate 401 1 m^2 plastic scintillarion detectors, forming an air shower array with 83,000 m^2 in area.The grey rectangles indicate eight underground muon detector pools, each of which contains twelve 56 m^2 muon detector units. The total area of the underground muon detector array is 5,400 m^2.

rejection power of MD is more than 99.9 % at 100 TeV, while keeping most of gamma-ray events. Long-term detector stability, angular resolution, pointing accuracy and energy scale can be calibrated by the cosmic-ray shadow in the Moon as well as by some of the bright stable TeV gamma ray sources in the southern sky.

Covered Physics

Our reserch target is divided into four in ALPACA:

1. Measurement of high-energy (5 TeV – 1 PeV) cosmic gamma rays.

2. Measurement of cosmic ray energy spectra around the Knee energy region (100 TeV – 100 PeV)

3. Measurement of cosmic ray anisotropy $>$ 5 TeV at sidereal time frame.

4. Measurement of the Sun shadow in cosmic rays $>$ 5 TeV.

We aim at low-background detection of celestial gamma rays in the 100 TeV region with the world-best sensitivity (an order of magnitude better than any pre-

vious/existing experiments) and at locating the origins of cosmic rays accelerated up to the knee energy region in the southern sky. Presuming a Crab-like gamma-ray source extending up with power-law index -2.6 located in the southern sky, the ALPACA experiment is sensitive to the source with ∼15 % Crab intensity during one calendar year, as is demonstrated in Fig. 3.

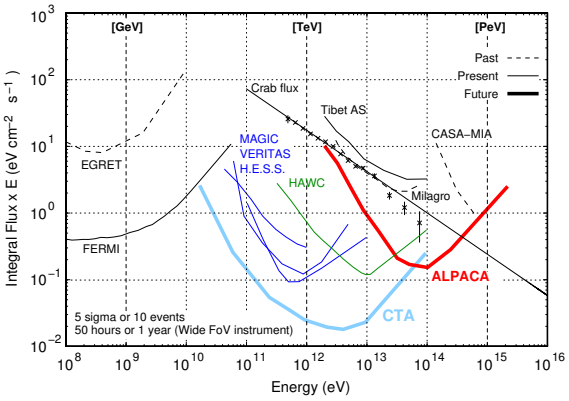

Fig. 3. Sensitivity of ALPACA to high-energy gamma-ray point source. Experimental data points are from HEGRA. The ALPACA sensitivity is evaluated from Ref.[1].

The AS + MD in the southern hemisphere will be a unique/complementary experiment to on-going experiments (FERMI, HESS, VERITAS, MAGIC, CALET, Tibet ASγ, HAWC) and future projects (LHAASO, CTA) in this field, which are either located in the northern hemisphere or aiming at gamma-ray astronomy below 10 TeV region, or having narrow field-of-view. Thus, the new energy window in the 100 TeV region observing gamma rays with wide field-of-view will be opened first in the southern sky by the ALPACA experiment. We expect to detect more than a dozen of established TeV gamma-ray sources, i.e., young SNRs (SN1006, RX J1713.7-3946, RX J0852.0-4622), Pulsar Wind Nebulae, the galactic center, etc) in the 100 TeV region, some of which may be cosmic-ray PeVatron candidates. Furthermore, our wide field-of-view sensitivity to diffuse gamma rays allows us to study extremely diffuse gamma-ray sources which are difficult to detect by imaging air Cherenkov telescopes. The diffuse gamma rays from the Fermi bubbles recently reported by the Fermi-LAT group may be clearly detected, if they extend up to the 100 TeV region. Similarly, detection of diffuse gamma rays above 100 TeV from the extended region around the galactic center is promising, where the gamma-ray energy spectrum strongly suggests existence of PeVatron. Detection and spectral measurement of gamma rays in the 100 TeV region from these celestial sources, together with multi-wavelength (radio, X-ray, gamma-ray) observations, are key points enabling us to discriminate between the two processes (cosmic-ray/electron origins), and to locate the acceleration site of cosmic rays and to examine the standard acceleration model of cosmic rays. From the astronomical point of view, we pioneer the ultra-high energy (above 100 TeV) gamma-astronomy in the southern sky. Besides, gamma-ray emission from near-by extragalactic sources, e.g. M87, Cen A, gamma rays of dark matter origin, those from the Sun disk recently obseved by Fermi may be interesting subjects.

We also aim at measuring energy spectra of proton, helium and iron components separately around the knee energy region with the new AS + MD. The standard cosmic-ray acceleration model at SNR predicts the knee energy of each nucleus component being proportional to Z (atomic number). We can discriminate proton and iron components by MD, as an iron nucleus produces approximately 2 times more muons than a proton with the same energy. Thus, the cosmic-ray acceleration scenario (SNR shock acceleration) will be verified by observing the linearly Z(atomic number)-dependent knee(=bent) positions of proton, helium, iron components around the knee energy region.

Precise cosmic-ray anisotropy measurement at sidereal time frame in the TeV energy region in the southern sky provides unique data for the community to understand the magnetic field structure in the heliosphere. The ALPACA experiment gives complementary data in the TeV region to those from IceCube above a few tens of TeV.

Furthermore, measurement of the Sun shadow in cosmic rays above the TeV energy region in the southern hemisphere also helps understand the modeling of the magnetic fields between the Sun and the Earth, complementary to the observations in the northern hemisphere.

ALPAQUITA

As a proto-type experiment, the ALPAQUITA[4] air shower array without MD, which is ∼20 % of the ALPACA air shower array in area will be constructed at the experimental site, Cerro Estuqueria, in 2018.

THE ALPACAγ COLLABORATION

Institute	Country	(*)
ICRR, Univ. of Tokyo	Japan	5
Universidad Mayor de San Andres	Bolivia	5
Yachay Tech.	Ecuador	1
Kanagawa Univ.	Japan	2
Utsunomiya Univ.	Japan	1
Yokohama National Univ.	Japan	7
Shinshu Univ.	Japan	3
Osaka City Univ.	Japan	3
Chubu Univ.	Japan	2
National Institute of Informatics	Japan	1
Osaka Electro-Communicatoin Univ.	Japan	1
Tokyo Metropolitan College of Industrial Technology	Japan	1
Japan Atomic Energy Agency	Japan	1
Nihon Univ.	Japan	1
Aichi Institute of Technology	Japan	1
RIKEN	Japan	1
Hiroshima City Univ.	Japan	1
Total		37

(*) Number of participants as of April 2018.

Members

Staffs

Masato Takita, Associate Professor (February 2001 to November 2016), Professor (November 2016 to the present)
Takashi Sako, Associate Professer (TA/Tibet), October 2017 to the present
Munehiro Ohnishi, Assistant Professor, April 1993 to the present
Kazumasa Kawata, Specially Appointed Assistant Professor (April 2013 to March 2018), Assistant Professor (Tibet/TA, April 2018 to the present)
Takahide Kobayashi, Technical Staff, from 1967 to March 2013

Postdoctoral Fellows

Takashi Sako, from April 2010 to March 2017 and from June 2018 to the present

Graduate Students

Two graduate students obtained the master degrees during 2012–2018, supervised by ICRR staff members.

List of Publications

Basically after Year 2012

Papers in Refereed Journals

[1] "Exploration of a 100 TeV gamma-ray northern sky using the Tibet air-shower array combined with an underground water-Cherenkov muon-detector array", T.K. Sako et al., Astroparticle Physics 32, (2009) 177.

Papers in International Conference Proceedings

[2] "The ALPACA Project", M. Takita for the ALPACA Collaboration, THE EUROPEAN PHYSICAL JOURNAL, **145**, 01002-1-3, (2017).

[3] "The overview of the ALPACA Experiment", T. Asaba et al, Proc. of ICRC2017, ID=827, Busan, Korea, July 12-20, (2017).

[4] "ALPAQUITA Array in the ALPACA Project", T. Asaba et al, Proc. of ICRC2017, ID=437, Busan, Korea, July 12-20, (2017).

Presentations in Internatinal Conference

[5] "The ALPACA Project", M. Takita, ISVHECRI2016, Moscow, Russia, August 22 - August 27, 2016.

[6] "The overview of the ALPACA Experiment", M. Ohnishi for the ALPACA Collaboration, The 35th International Cosmic Ray Conference, Busan, Korea, July 12 - July 20, 2017.

[7] "ALPAQUITA Array in the ALPACA Project", K. Kawata for the ALPACA Collaboration, The 35th International Cosmic Ray Conference, Busan, Korea, July 12 - July 20, 2017.

[8] "Overview and current status of the ALPACA experiment", T. Sako for the ALPACA Collaboration, TeVPA2017, Colombus, Ohio, U.S.A., August 7 - August 11, 2017.

[9] "ALPACA experiment", T. Sako for the ALPACA Collaboration, The VII School on Cosmic Rays and Astrophysics, Escuela Politecnica Nacional, Quito, Ecuador, August 21 - September 1, 2017.

ASTROPHYSICS AND GRAVITY DIVISION

KAGRA GROUP

Introduction

KAGRA, Large-scale Cryogenic Gravitational wave Telescope, aims at detecting gravitational waves and developing gravitational wave astronomy, which was initiated by the first detection of gravitational waves by LIGO. KAGRA employs a 3 km L-shaped laser interferometer. KAGRA uses an optical configuration which is similar to advanced LIGO and advance Virgo. However, there are some major differences. KAGRA uses cryogenic sapphire mirrors as main test masses of the interferometers, while advanced LIGO and advanced Virgo use room-temperature fused silica mirrors. An another major difference is its site; KAGRA is located in the underground site of the Kamioka mine, while LIGO and Virgo are located on the surface. In the Kamioka mine, two prototype detectors, LISM (a 20-m scale interferometer, ran from 1999 to 2002) and CLIO (a 100-m scale interferometer, started in 2002), were constructed and operated to show the advantages of an underground site. With these achievements and experiences, KAGRA was funded in 2010 and the excavation of the tunnel was started in May 2012.

The construction of the KAGRA detector is divided into two stages: the initial KAGRA (iKAGRA) and baseline KAGRA (bKAGRA). The iKAGRA detector is a simple Michelson interferometer with a 2-Watt laser, room-temperature mirrors, and a simple seismic isolation system. The bKAGRA detector with final configuration will be a Power Recycling, Fabry-Perot Michelson interferometer with a Resonant Sideband Extraction. It uses 180-Watt laser, cryogenic Sapphire mirrors, and an advanced Seismic Attenuation System (SAS).

Figure 2 shows the estimated ultimate sensitivity limits of KAGRA. Observation range for an inspiral and merger of neutron-star binary with the ultimate sensitivity of KAGRA is about 152 Mpc with the same definition of the observation range as LIGO and Virgo.

In October 2015, most of the installation activities for the initial KAGRA interferometer had been completed, and after commissioning work, the interferometer was operated for the first time in March 2016. Though the interferometer configuration at that time was simplified from the final KAGRA design, KAGRA was operated for the first time as a full 3-km-scale interferometer connected to the data acquisition, transfer, and storage system. With that configuration, we carried out a three-week test operation (iKAGRA operation) to check the overall performance as an interferometric gravitational wave antenna system.

Immediately after the end of the iKAGRA operation, installation of bKAGRA configuration started. In the first stage of installation of bKAGRA (Phase 1), a 3 km Michelson interferometer with cryogenic mirrors were constructed. A test operation with this configuration (bKAGRA phase 1 operation) was performed in May 2018.

In this report, we review the progress of the construction of KAGRA during 2012 and 2018. We also summarize the iKAGRA operation and the bKAGRA phase 1 operation. Finally, we explain the plan of the installation toward the final configuration of KAGRA, and the plan of observation which will be done jointly with LIGO and Virgo.

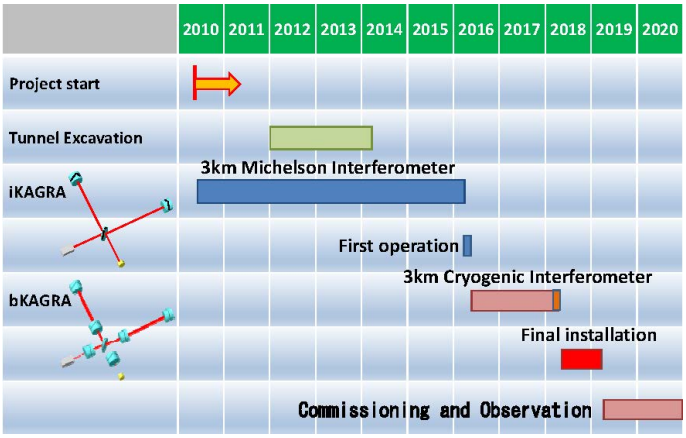

Fig. 1. KAGRA's schedule

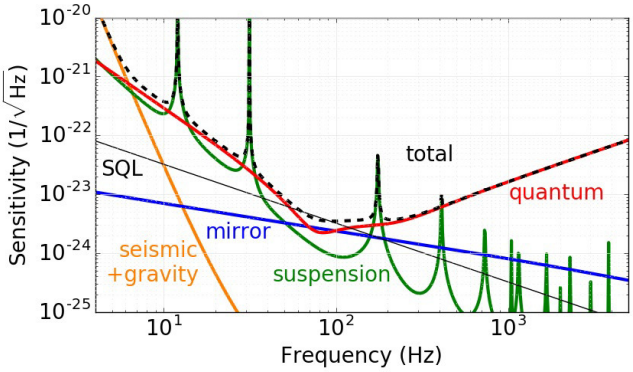

Fig. 2. Ultimate sensitivity limit of KAGRA. "SQL", "seismic+gravity", "mirror", "suspension", "quantum" and "total" mean standard quantum limit, seismic noise and gravity gradient noise, mirror thermal noise, suspension thermal noise, quantum noise and sum of all noises respectively. Observation range for an in-spiral and merger of neutron-star binary with the ultimate sensitivity limit of KAGRA is about 152 Mpc with the same definition of the observation range as LIGO and Virgo.

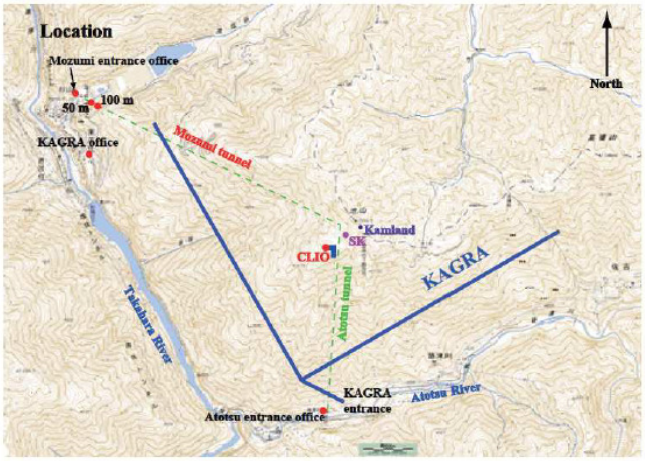

Fig. 3. A map of the Kamioka mine. The blue thick lines are baselines of the KAGRA interferometer.

Summary of construction from 2012 to 2018

The excavation of the tunnel of KAGRA was started in May 2012 after one year delay due to the Great East Japan Earthquake occurred on March 11, 2011. Figure 3 shows a map around the Kamioka mine. The geographical coordinates of the beamsplitter are 36.41 degrees North and 137.31 degrees East. The Y-arm is in the direction 28.31 degrees west of north. Though the central station and the end stations are rather close to the foot of the 1300-m high mountain, they are still at least 200 m below the ground surface. The X and Y arms are 3-km long. Access tunnels lead to the central station and to the Y-arm end station. The excavation of the tunnel was finished in May 2014. Installation of the facilities proceeded in parallel with the excavation. This included electricity, air conditioning, water supply, anti-dust wall painting, floor treatment, crane setup, anchors, spiral steps, networks, telecommunication, laser clean room, etc. Soon after the tunnel and facility neared completion in March 2014, installation of the vacuum system and interferometer components (the vibration-isolation systems, the laser source, the optics for the interferometer, the digital control system, and so on) were started.

iKAGRA operation

By February 2016, we had completed the installation of the vacuum systems, clean booths, seismic isolation systems, and digital control systems to control the interferometer. In March 2016, we aligned the optics to make a 3-km Michelson interferometer, and started the test run operation. The test run was split into two periods, from March 25 to March 31 and from April 11 to April 25. Between the first and the second half of the test run, we had a little interval to improve the sensitivity and the stability of the interferometer.

The interferometer configuration of iKAGRA is shown in Fig. 4. We used a single-frequency laser source with a wavelength of 1064 nm. The laser beam was first

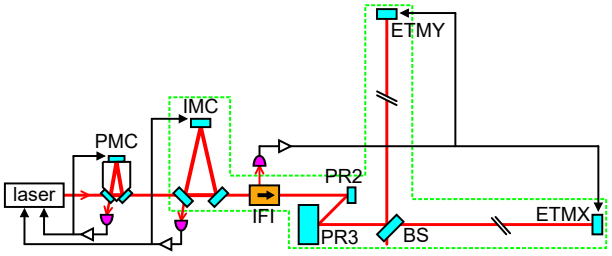

Fig. 4. Interferometer configuration of iKAGRA.

injected into a triangular cavity called the pre-mode cleaner (PMC) and then to the suspended input mode cleaner (IMC), to suppress unwanted spatial higher order modes. The PMC was constructed from three mirrors rigidly attached to an Invar spacer. It has a round-trip length of 0.4 m and a finesse of 197. The IMC was constructed from three mirrors suspended by a double pendulum on a vacuum-compatible vibration isolation stack table. It has a round-trip length of 53.3 m and finesse of 540. The frequency of the laser was stabilized to the PMC length below 0.3 mHz and the IMC length above 30 Hz. The beam at IMC and the main interferometer is s-polarized. The incident power before the IMC was 270mW.

The beam transmitted by the IMC is then sent to an input faraday isolator (IFI), after which the beam radius is expanded by the mirrors called PR2 and PR3. PR2 and PR3 stand for power recycling 2 and 3, and will be used for the folding mirrors of the power recycling cavity in the bKAGRA phase. The main 3-km Michelson interferometer consists of the beam splitter (BS) and two end test masses (ETMX and ETMY). The designed distance between BS and ETMX is 2991.6 m, and that between BS and ETMY is 2988.3 m. The IFI was put on a vibration isolation stack table, and PR2 was fixed on a non-isolated table. PR3, BS, ETMX and ETMY are suspended by double pendula. Of all these suspended mirrors, PR3 was the largest (250 mm diameter and 100 mm thick) mirror, and was the only one with a full-sized suspension, which will also be used in the bKAGRA phase with minor modifications.

All of the optics downstream of the IMC, including the IMC, were placed inside vacuum chambers, but most of the parts were left at atmospheric pressure to allow for easier maintenance of the optics during the test run. Only the IMC and the two 3-km arm ducts are evacuated, to a pressure of $\sim 10^2$ Pa. The differential length signal of the Michelson interferometer was obtained from the reflected beam picked off by the IFI with a photo-diode in air.

The differential length signal was fed back to the ETMs via 3-km reflective memory network to lock the interferometer fringe. During the first half of the test run, we used the DC signal from the photo-diode and locked the interferometer at the mid-fringe. During the

second half, we used the pre-modulation technique to lock the interferometer at the dark fringe. The dark-fringe locking resulted in a lower coupling of laser intensity noise. We also increased the bandwidth of the servo from 8 Hz to 94 Hz by avoiding parasitic resonances of the ETMs. In the first half of the test run, we did not have enough balancing of the mirror actuators, which resulted in the excitation of the suspension pitch modes at around 15 Hz. Moreover, the servo bandwidth was automatically adjusted by monitoring the loop gain using calibration lines in the second test run. These improvements contributed to the high stability of the interferometer. The duty factor during the first half was 85.2 %, whereas that during the second half was 90.4 %. The longest lock stretch was 3.6 hours for the first half, and that for the second half was 21.3 hours. The high duty factor compared to other gravitational wave telescopes is mainly due to the simple configuration of the interferometer, but the state machine automaton *Guardian* also helped recovering lock quickly after lock losses.

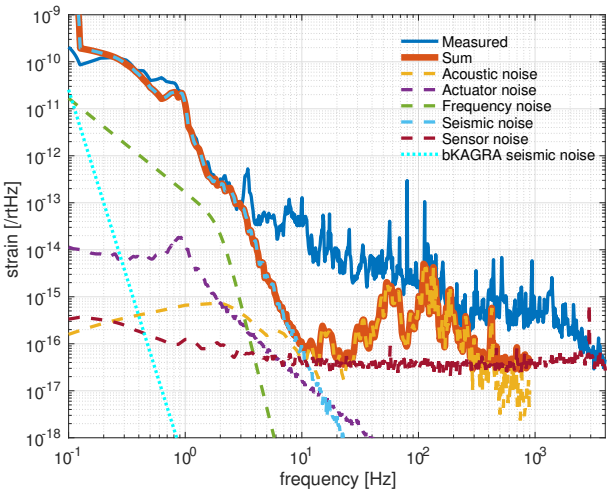

Fig. 5. The strain sensitivity of iKAGRA during the second run. An expected seismic noise level in bKAGRA is also plotted as a reference. (The noise level is about one order of magnitude smaller than other sites such as LIGO and Virgo.) The peaks at 80 Hz and 113 Hz for the measured spectrum are from the calibration lines. The acoustic noise plotted here only shows the acoustic noise coupled via the BS chamber, but it is likely that the acoustic noise is the sensitivity limiting noise source also at neighboring frequencies. Actuator noise is the sum of the displacements of the mirrors from electronics noise for the actuation. Frequency noise is the estimated laser frequency noise suppressed through laser frequency stabilization using PMC and IMC. Seismic noise is the ground displacement attenuated by the mirror suspensions. Sensor noise is the sum of the ADC noise, the dark noise of the photo-diode, and the shot noise.

A typical sensitivity curve for iKAGRA during the second run is shown in Fig. 5. Below 3 Hz, the sensitivity is limited by seismic noise. Over 100 Hz to 3 kHz, the sensitivity is likely to be limited by acoustic noise, mainly from the fans of the clean booths. The acoustic noise in iKAGRA was high because main mirrors were inside the vacuum chambers but at atmospheric pressure. Note that the acoustic noise curve in Fig. 5 only shows the acoustic noise coupled via the BS chamber. We turned off all the fans in the clean booths to confirm that the sensitivity of the frequency regions where the measured spectrum and the sum of all the known noise sources do not match is also limited by acoustic noise. However, the detailed coupling mechanism still needs further investigation. At 3-4 kHz, the sensitivity was limited by sensor noise, which mainly comes from the analog-to-digital conversion of the photo-diode output. These noise contributions will be further reduced in the bKAGRA phase by using better vibration isolation systems, a high vacuum system, and better whitening filters.

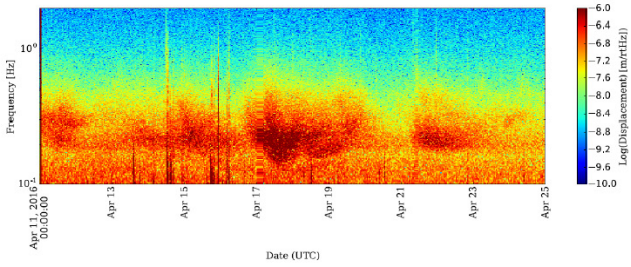

Fig. 6. Spectrogram of seismic noise in the 0.1 Hz∼2 Hz band during the second run. One can see large spikes on April 14th and 16th due to a series of large earthquakes in Kumamoto. Some data on April 17th and 21st is missing due to an issue in our data taking system.

Figure 6 shows a spectrogram of seismic noise in the 0.1 Hz∼2 Hz band during the second run. In this period, a series of large earthquakes hit Kumamoto Prefecture that is about 700 km from KAGRA. According to the United States Geological Survey, the foreshock with a magnitude 6.5 hit Kumamoto at 12:26 UTC on April 14 (2016) and the mainshock with a magnitude 7.3 hit the same area at 16:25 UTC on April 16 (2016). The peak ground acceleration (PGA) levels in the horizontal direction measured at various points in KAGRA are as follows. For the foreshock, PGAs at BS, ETMX, and ETMY were 20 mGal, 30 mGal, and 25 mGal, respectively. For the mainshock, the PGA at BS was not measured as the seismometer was saturated (i.e. over 95 mGal) as the sensor gain had been set higher than the other two. PGAs at ETMX and ETMY were 306 mGal and 298 mGal, respectively. After the mainshock, the suspension system of BS was in trouble and it took half a day to fix it. The earthquake shook the BS suspension and a screw to support a mirror before releasing touched one of the suspension fibers of the BS. The interferometer was not in operation during the time when several aftershock earthquakes hit Kumamoto.

During the test run, 65 people in total participated in shifts to monitor the interferometer conditions. The

interferometer was monitored by at least three people on eight-hour shifts. A cumulative total of 186 people from 35 institutes contributed. The members of the shift monitored the status of the interferometer lock, mirror suspensions, data acquisition system and data transfer system to ensure that the interferometer data was properly transferred.

The data including the gravitational wave signal and environmental monitor signals were transferred to the data center at ICRR in Kashiwa and Osaka City University with latency of about 3 seconds. The amount of data was 7.5 TB in total. We also did a hardware injection test right after the test run. The data management system and the results of the data analysis and the detector characterization will be published in separate papers.

bKAGRA phase 1 operation

After the iKAGRA test operation, we immediately started the installation process toward bKAGRA configuration. In the phase 1 period, a simple Michelson interferometer with cryogenic sapphire mirrors as main test masses was constructed.

A key feature of KAGRA is to cool sapphire mirrors. Sapphire mirrors of KAGRA is suspended by 9-stage suspension. The bottom 4 stages which include a sapphire mirror is called cryogenic payload. The first cryogenic payload with a sapphire mirror was installed at Kamioka in November, 2017. Figure 7 shows the cryogenic payload installed at KAGRA site. This payload was cooled down after installation and reached about 18 K, which is below the target temperature of KAGRA, 20 K.

Performance evaluation of sensors and actuators was performed at the site after cooling. It was then confirmed that all sensors and actuators on the cryogenic payload worked even at cryogenic temperature. Damping feedback system for the suspension eigenmode was also implemented, which is significant to operate KAGRA as an interferometer.

Major development of input and output optics were also done. All mirrors between the input laser to the beam splitter were installed. They are hanged with various types of vibration isolation systems, and are placed in the vacuum chambers.

bKAGRA phase 1 operation was done during April 28th and May 7th in 2018. In the operation, ETMY mirror was 20 K, but ETMX mirror was room temperature. Duty cycle was about 80-90 % during April 28th and May 2nd, but is was about 20-60 % during May 3rd - 7th. The low duty cycle during the last 4 days was caused by several distant major earthquakes and bad weather condition (This is a very rare case in the undergroun site). Total amount of data taken was 8.875 days, and amount of data when the interferometer was operational was 6.731 days. The longest continuous operation was about 11 hours. Figure 14 is the noise spectrum of iKAGRA and bKAGRA-1 and it shows the improvement by 1-2 orders of magnitude. The observable range for binary neutron star was around $15-20$ pc.

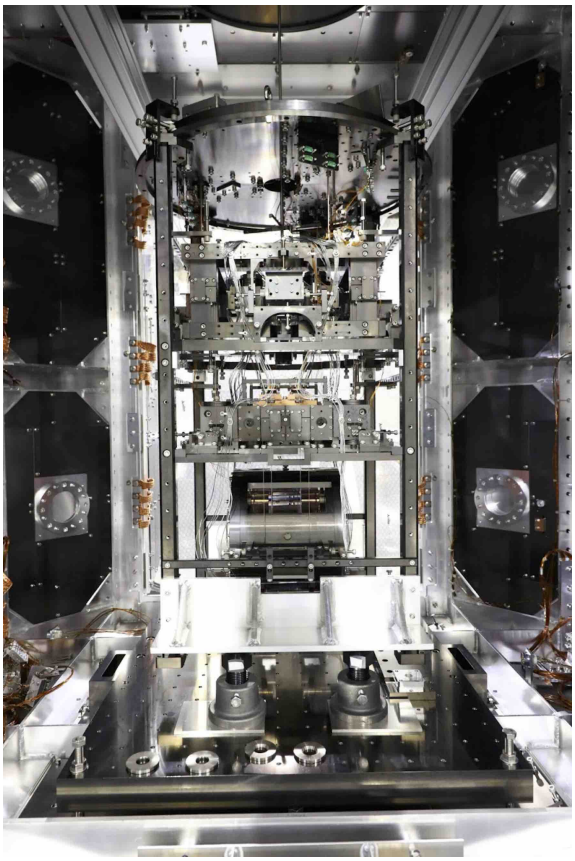

Fig. 7. Cryogenic payload installed into the cryostat at KAGRA site

In February 2017, KAGRA's main data server was introduced in the main ICRR building at Kashiwa. The main role of this system is to store all data produced by KAGRA detector, and it has 2.5 PB storage. It also has 12 computing nodes, and total number of cores is 334. Now, data taken by the digital system of KAGRA detector is continuously transferred to the main data server and stored. By using this data, during the phase 1 operation, an attempt of the low latency data analysis targeting coalescing compact binaries was performed by using low latency data analysis pipeline, gstlal-inspiral which has been developed and used by LIGO collaboration.

Future plan

So far, 7 gravitational wave events (6 binary black holes and one binary neutron star) have been observed. Next scientific observation by LIGO and Virgo (which is called "O3") is planned to start from February 2019, and is expected to continue for about one year. We understand that the most important thing for KAGRA

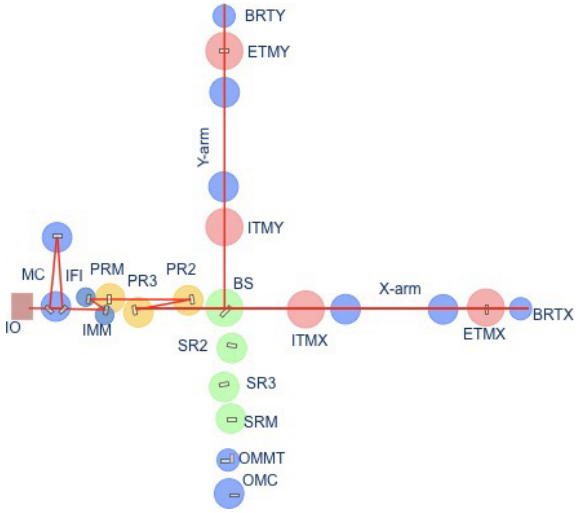

Fig. 8. Optical configuration of bKAGRA phase 1. This is a Michelson interferometer. A laser source is placed in IO and laser beam is input into vacuum systems from MC. Each mirror is suspended by a vibration isolation system. Solid lines indicate laser beams. Both ETMY and ETMX mirrors are sapphire mirrors. Only ETMY was cooled down to cryogenic temperature.

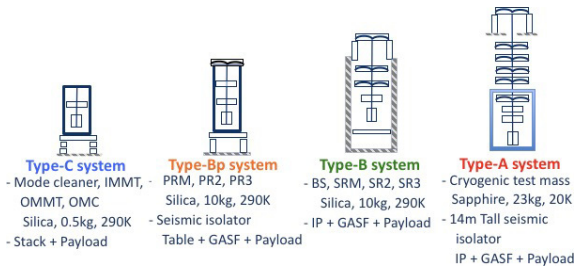

Fig. 9. Vibration isolation systems of KAGRA. KAGRA equips four kinds of vibration isolation systems such as Type-A, Type-B, and Type-Bp. We have installed PRM, PR2, BS, ETMX, and ETMY in 2017. PR3 was upgraded to Type-Bp.

is to operate the interferometer as soon as possible, and to join the observation of LIGO and Virgo, and to contribute to the observation of gravitational wave signals. Now we are planning to join O3 at around autumn 2019. When we perform coincident observation, we jointly analyze data from LIGO, Virgo and KAGRA detectors with LIGO and Virgo Collaborations. In order to realize that, we reformed the organization of data analysis and related subgroups. Since the new organization structure is quite similar to that of LIGO Scientific Collaboration, it will become easy to perform collaboration between LIGO and Virgo.

Summary

The construction of the KAGRA detector has been progressed rapidly since the start of the tunnel excavation in May 2012. We have performed test operation of the detector twice: iKAGRA operation with a room temperature Michelson interferometer, and bKAGRA

Fig. 10. Type-B vibration isolation system for beam splitter.

phase 1 operation with a cryogenic mirror. We are now making great efforts to install various components necessary to achieve good sensitivity and to perform an observation run during LIGO and Virgo's third observation run which is planned during February 2019 and January 2020. It is expected that when KAGRA joins a world-wide network of gravitational wave detectors, KAGRA can contribute greatly to gravitational wave astronomy and astrophysics.

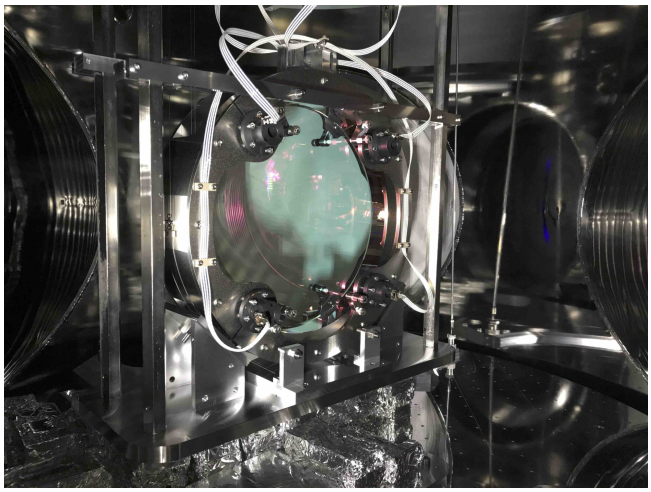

Fig. 11. Beam splitter suspended in a vacuum chamber.

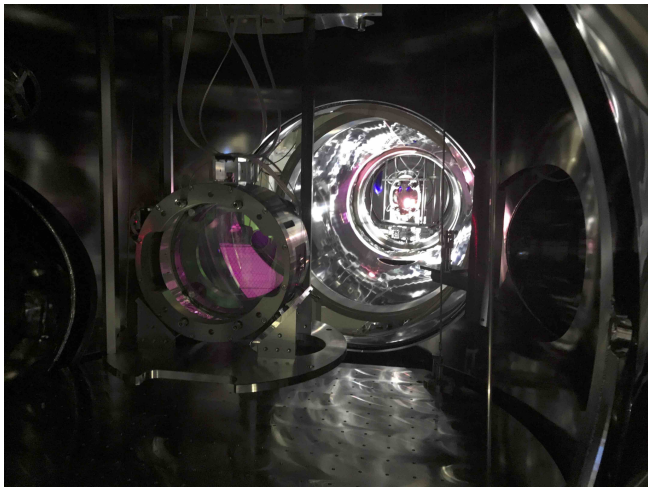

Fig. 12. PR2 mirror suspended in a vacuum chamber. There is beam splitter behind the PR2 mirror.

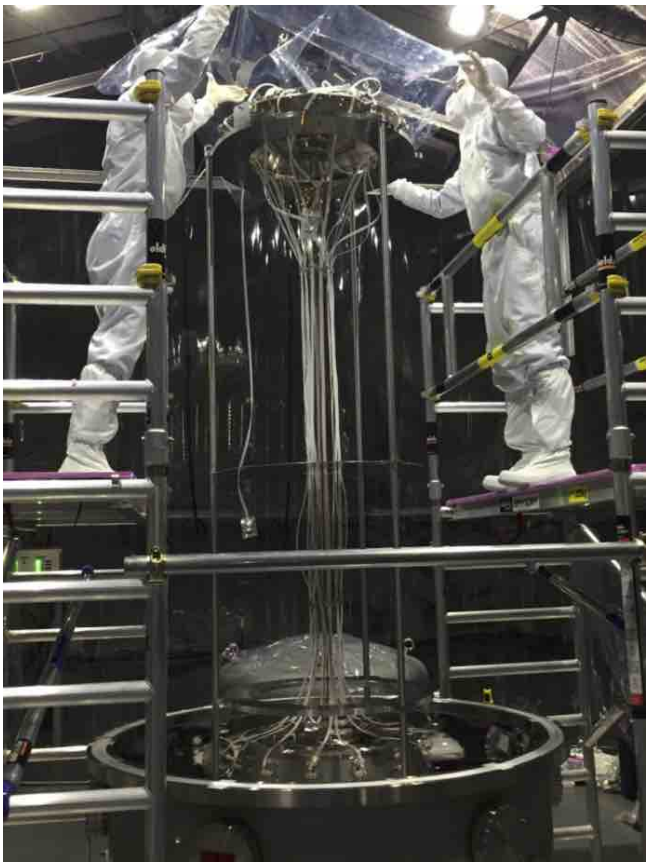

Fig. 13. A part of Type-A vibration isolation system.

KAGRA Collaboration

Institute	Country	(*)
ICRR, Univ. of Tokyo	Japan	34
NAOJ	Japan	29
KEK	Japan	10
School of Sci., Univ. of Tokyo	Japan	17
School of Eng., Univ. of Tokyo	Japan	3
Tokyo Tech	Japan	8
Osaka City Univ.	Japan	13
Kyoto Univ.	Japan	12
Univ. of Electro-Communications	Japan	5
ERI, Univ. of Tokyo	Japan	2
Hosei Univ.	Japan	8
AIST	Japan	3
NICT	Japan	1
Osaka Univ.	Japan	1
Kyushu Univ.	Japan	1
Niigata Univ.	Japan	6
Nagaoka Univ. of Technology	Japan	4
Rikkyo Univ.	Japan	1
Hiroshima Univ.	Japan	1
Ryukyu Univ.	Japan	2
Waseda Univ.	Japan	2
Toyama Univ.	Japan	19
Yokohama City Univ.	Japan	1
Fukuoka Univ.	Japan	1
Aichi Univ. of Technology	Japan	1
Inst. for Molecular Science	Japan	1
Kavli IPMU, Univ. of Tokyo	Japan	1
National Defense Academy	Japan	1
Inst. of Statistical Mathematics	Japan	1
National Inst. for Fusion Science	Japan	1
Toho Univ.	Japan	2
Max-Planck Institutes	Germany	1
Caltech	USA	4
Univ. of Mississippi	USA	4
Univ. of Western Australia	Australia	5
Louisiana State Univ.	USA	1
Beijing Normal Univ.	China	8
IUCAA	India	2
Moscow Univ.	Russia	1
LATMOS, CNRS	France	1
Univ. of Science and Technology of China	China	1
Tsinghua Univ.	China	1

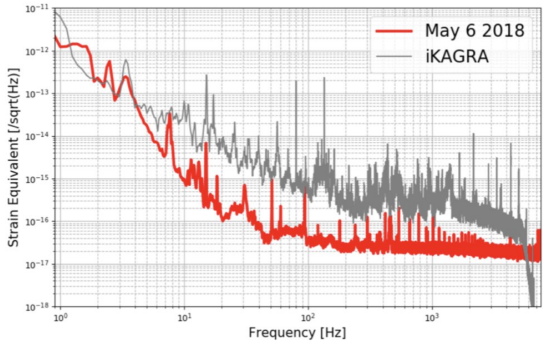

Fig. 14. Average amplitude spectrum density of noise during bKAGRA phase 1 and iKAGRA. Red line (May 6 2018) was measured during phase 1 operation.

Korea Univ.	Korea	1
Inje Univ.	Korea	3
Seoul National Univ.	Korea	2
Korea Astronomy and Space Science Inst.	Korea	1
Myongji University	Korea	1
Hanyang University	Korea	1
Pusan National University	Korea	1
Korea Inst. of Science and Technology Information	Korea	1
National Inst. for Mathematical Sciences	Korea	4
Kyungpook National Univ.	Korea	1
Kunsan National Univ.	Korea	1
Sejong Univ.	Korea	1
Sogang Univ.	Korea	2
Tongji Univ.	Korea	1
Chinese Academy of Science	China	2
Univ. of California Berkeley	USA	1
Princeton University	USA	1
IISER-TVM	India	1
NIKHEF	Netherlands	1
RIKEN	Japan	1
Osaka Inst. of Technology	Japan	2
Warsaw University of Technology	Poland	2
Univ. of Wisconsin-Milwaukee	USA	1
Academia Sinica	Taiwan	3
National Applied Research Lab.	Taiwan	1
University of Perugia	Italy	2
Chinese Univ. of Hong Kong	China	2
Total		288

(*) Number of participants as of 2018.

Members

Staffs

Kazuaki Kuroda, Prof., to Mar.2015
Seiji Kawamura, Prof., to Dec.2017
Masatake Ohashi, Prof.
Hideyuki Tagoshi, Prof., May 2017 to present
Yoshio Saito, Proj. Prof., Apr.2014 to present
Norikatsu Mio, Proj. Prof., Apr.2018 to present
Yuzuru Yoshii, Proj. Prof., Dec.2017 to present
Shinji Miyoki, Assoc. Prof.
Takashi Uchiyama, Assoc. Prof.
Kazuhiro Yamamoto, Assist. Prof., to Feb.2017
Osamu Miyakawa, Assist. Prof., Apr.2013 to present
Keiko Kokeyama, Assist. Prof., Feb.2015 to present
Kyohei Kawaguchi, Assist. Prof., Mar.2018 to present
Ryutaro Takahashi, Proj. Assist. Prof., to Oct.2013
Kazuhiro Hayama, Proj. Assist. Prof., to Mar.2018
Naoko Ohishi, Proj. Assist. Prof., Sep.2012 to Mar.2015
Eiichi Hirose, Proj. Assist. Prof., Sep.2013 to present
Takafumi Ushiba, Proj. Assist. Prof., May 2018 to present

Senior Fellows

Toshikazu Suzuki, Senior Fellow, Apr.2017 to present

Postdoctoral Fellows

Eiichi Hirose, to Mar.2013
Kieran Craig, Aug.2015 to Jul. 2017
Takafumi Ushiba, Apr.2017 to Feb.2018
Takahiro Yamamoto, Jul.2016 to present
Tatsuya Narikawa, to Mar.2018
Nami Uchikata, to Mar.2018
Takaaki Yokozawa, Dec.2017 to present
Hirotaka Yuzurihara, Jan.2017 to Present
Fabian Pena Arellano, Jul.2018 to Present
Lucia Trozzo, Jul.2018 to Present
Shoichi Oshino, Sep.2018 to Present

Graduate Students

2 students were awarded doctor degrees and 20 students earned master degrees during 2012–2017, supervised by ICRR staff members.

List of Publications

[1] "Reduction of thermal fluctuations in a cryogenic laser interferometric gravitational wave detectord", T. Uchiyama, S. Miyoki, S. Telada, K. Yamamoto, M. Ohashi, K. Agatsuma, K. Arai, M.-K. Fujimoto, T. Haruyama, S. Kawamura, O. Miyakawa, N. Ohishi, T. Saito, T. Shintomi, T. Suzuki, R. Takahashi, D. Tatsumi, Physical Review Letters, Vol.108, No.14, (2012)

[2] "Calculation of thermal radiation input via funneling through a duct shield with baffles for KAGRA", Y. Sakakibara, N. Kimura, K. Yamamoto, T. Suzuki, T. Tomaru, S. Miyoki, T. Uchiyama, K. Kuroda, Class. Quantum Grav., 29 (2012) 205019.

[3] "Sapphire mirror for the KAGRA gravitational wave detector", E. Hirose, D. Bajuk, G. Billingsley, T. Kajita, B. Kestner, N. Mio, M. Ohashi, B. Reichman, H. Yamamoto, and L. Zhang, Phys. Rev. D 89, 062003 (2014).

[4] "Mechanical loss of a multilayer tantala/silica coating on a sapphire disk at cryogenic temperatures: Toward the KAGRA gravitational wave detector", E. Hirose, K. Craig, H.i Ishitsuka, I. W. Martin, N. Mio, S. Moriwaki, P. G. Murray, M. Ohashi, S. Rowan, Y. Sakakibara, T. Suzuki, K. Waseda, K. Watanabe, and K. Yamamoto, Phys. Rev. D 90, 102004 (2014)

Y. Sakakibara, N. Kimura, T. Suzuki, K. Yamamoto, D. Chen, S. Koike, C. Tokoku, T. Uchiyama, M. Ohashi, K. Kuroda, Advances in Cryogenic Engineering, 59, 11761183 (2014),

[5] "Progress on the Cryogenic System for the KAGRA Cryogenic Interferometric Gravitational Wave Telescope", Sakakibara, T. Akutsu, D. Chen, A. Khalaidovski, N. Kimura, S. Koike, T. Kume, K. Kuroda, T. Suzuki, C. Tokoku and K. Yamamoto, Classical and Quantum Gravity, 31, 224003, (2014)

[6] "Excavation of an underground site for a km-scale laser interferometric gravitational-wave detector", T. Uchiyama, K. Furuta, M. Ohashi, S. Miyoki, O. Miyakawa and Y. Saito, Classical and Quantum Gravity, 31, 224005, (2014)

[7] "Sapphire screws and strength test on them at liquid nitrogen temperature", Eiichi Hirose, Yusuke Sakakibara, Yukihiko Igarashi and Takashi Ishii, Review of Scientific Instruments, 85, 104503, (2014)

[8] "Vibration measurement in the KAGRA cryostat", D Chen, L Naticchioni, A Khalaidovski, K Yamamoto, E Majorana, Y Sakakibara, C Tokoku, T Suzuki, N Kimura, S Koike, T Uchiyama and S Kawamura, CLASSICAL AND QUANTUM GRAVITY, 31, 224001, (2014)

[9] "Update on development of cryogenic sapphire mirrors and their seismic attenuation system for KAGRA", E Hirose,T Sekiguchi, R Kumar, R Takahashi, CLASSICAL AND QUANTUM GRAVITY, 31, 224004, (2014)

[10] "Evaluation of heat extraction through sapphire fibers for the GW observatory KAGRA", A Khalaidovski, G Hofmann, D Chen, J Komma, C Schwarz, C Tokoku, N Kimura, T Suzuki, AO Scheie, E Majorana, R Nawrodt, K Yamamoto, CLASSICAL AND QUANTUM GRAVITY, 31, 105004, (2014)

[11] "Method to reduce excess noise of a detuned cavity for application in KAGRA", S. Ueda, N. Saito, D. Friedrich, Y. Aso, K. Somiya for the KAGRA Collaboration, Classical and Quantum Gravity, 31, 095003, (2014)

[12] "Design study of the KAGRA output modecleaner", A. Kumeta, C.Bond, and K.Somiya, Optical Review, 22, 149-152, (2015)

[13] "Gravitational waves:classification, methods of detection, sensitivities and sources", Kazuaki Kuroda, Wei-Tou Ni and Wei-Ping Pan, International Journal of Modern Physics D, 24, 1530031, (2015)

[14] "Ground- based Gravitational-wave detectors", Kazuaki Kuroda, International Journal of Modern Physics D, 24, 1530032, (2015)

[15] "Realistic loss estimation due to mirror surfaces in a 10 meters-long high finesse Fabry-Perot filtercavity", Nicolas Straniero, Jérôme Degallaix, Raffaele Flaminio, Laurent Pinard, and Gianpietro Cagnoli, Optics Express, 23, 21455-21476, (2015)

[16] "Gravitational wave astronomy: the current status", David Blair , Li Ju, ChunNong Zhao, LinQing Wen, Qi Chu, Qi Fang, RongGen Cai, JiangRui Gao, XueChun Lin, Dong Liu, Ling-An Wu, ZongHong Zhu, David H. Reitze , Koji Arai, Fan Zhang, Raffaele Flaminio, XingJiang Zhu , George Hobbs, Richard N. Manchester, Ryan M. Shannon, Carlo Baccigalupi, Wei Gao, Peng Xu, Xing Bian, ZhouJian Cao, ZiJing Chang, Peng Dong, XueFei Gong, ShuangLin Huang, Science China-Physics Mechanics and Astronomy, 58, 120402, (2015)

[17] "Mechanical loss in state-of-the-art amorphous optical coatings", Massimo Granata, Emeline Saracco, Nazario Morgado, Alix Cajgfinger, Gianpietro Cagnoli, Jérôme Degallaix, Vincent Dolique, Danièle Forest, Janyce Franc, Christophe Michel,

Laurent Pinard, and Raffaele Flaminio, Physical Review D, 93, 12007, (2016)

[18] "Characterization of the room temperature payload prototype for the cryogenic interferometric gravitational wave detector KAGRA", Fabián Erasmo Peña Arellano, Takanori Sekiguchi, Yoshinori Fujii, Ryutaro Takahashi, Mark Barton, Naoatsu Hirata, Ayaka Shoda, Joris van Heijningen, Raffaele Flaminio, Riccardo DeSalvo, Koki Okutumi, Tomotada Akutsu, Yoichi Aso, Hideharu Ishizaki, Takashi Uchiyama, Osamu Miyakawa, Masahiro Kamiizumi, Akiteru Takamori, Ettore Majorana, Jo van den Brand and Alessandro Bertolini, Review of Scientific Instruments, 87, 34501, (2016)

[19] "5mg Suspended Mirror Driven by Measurement-Induced Backaction", N. Matsumoto, K. Komori, Y. Michimura, G. Hayase, Y. Aso and K. Tsubono, Physical Review A, 9, 33825, (2016)

[20] "Performance test of pipe-shaped radiation shields for cryogenic interferometric gravitational-wave detectors", Y. Sakaibara, N. Kimura, A. Akutsu, T. Suzuki and K. Kuroda, Classical and Quantum Gravity, 32, 155011, (2015)

[21] "An experiment to distinguish between diffusive and specular surfaces for thermal radiation in cryogenic gravitational-wave detectors", Y. Sakaibara, N. Kimura, T. Suzuki, K. Yamamoto, C. Tokoku, T. Uchiyama and K. Kuroda, Prog. Theor. Exp. Phys., Volume 2015, 073F01,(2015)

[22] "The effect of crystal orientation on the cryogenic strength of hydroxide catalysis bonded sapphire", K. Haughian, R. Douglas, A. A. van Veggel, J. Hough, A. Khalaidovski, S. Rowan, T. Suzuki and K. Yamamoto, Classical and Quantum Gravity, 32, 75013, (2015)

[23] "Vacuum and cryogenic compatible black surface for large optical baffles in advanced gravitational-wave telescopes", Tomotada Akutsu, Yoshio Saito, Yusuke Sakakibara, Yoshihiro Sato, Yoshito Niwa, Nobuhiro Kimura, Toshikazu Suzuki, Kazuhiro Yamamoto, Chihiro Tokoku, Shigeaki Koike, Dan Chen, Simon Zeidler, Optical Materials Express, 6, 1613-1626, (2016)

[24] "Calculation method for light scattering caused by multilayer coated mirrors in gravitational wave detectors", Simon Zeidler, Tomotada Akutsu, Yasuo Torii, Eiichi Hirose, Yoichi Aso, and Raffaele Flaminio, Optics express, 25, 4741-4760, (2017)

[25] "Characterization of non-Gaussianity in gravitational wave detector noise", Takahiro Yamamoto, Kazuhiro Hayama, Shuhei Mano, Yousuke Itoh, and Nobuyuki Kanda, Physical Review D, 93, 82005, (2016)

[26] "Observation of reduction of radiation-pressure-induced rotational anti-spring effect on a 23 mg mirror in a Fabry-Perot cavity", Yutaro Enomoto, Koji Nagano, Masayuki Nakano, Akira Furusawa and Seiji Kawamura, Classical and Quantum Gravity, 33, 145002, (2016)

[27] "Standard quantum limit of angular motion of a suspended mirror and homodyne detection of a ponderomotively squeezed vacuum field", Yutaro Enomoto, Koji Nagano, and Seiji Kawamura, Physical Review A, 97, 12115, (2016)

[28] "Mitigation of radiation-pressure-induced angular instability of a Fabry-Perot cavity consisting of suspended mirrors", Koji Nagano, Yutaro Enomoto, Masayuki Nakano, Akira Furusawa, Seiji Kawamura, Physics Letters A, 380, 3871-3875, (2016)

[29] "Design study and prototype experiment of the KAGRA output mode-cleaner", Kazushiro Yano, Ayaka Kumeta, Kentaro Somiya, Journal of Physics: Conference Series, 716, 12032, (2016)

[30] "Measurement of Schumann Resonance at Kamioka", S. Atsuta, T. Ogawa, S. Yamaguchi, K. Hayama, A. Araya, N. Kanda, O. Miyakawa, S. Miyoki, A. Nishizawa, K. Ono, Y. Saito, K. Somiya, T. Uchiyama, M. Uyeshima and K. Yano, Journal of Physics: Conference Series, 716, 12020, (2016)

[31] "The cryogenic challenge: status of the KAGRA project", Raffaele Flaminio and KAGRA collaboration, Journal of Physics: Conference Series, 716, 012034, (2016)

[32] "Active damping performance of the KAGRA seismic attenuation system prototype", Yoshinori Fujii, Takanori Sekiguchi, Ryutaro Takahashi, Yoichi Aso, Mark Barton, Fabián Erasmo Peña Arellano, Ayaka Shoda, Tomotada Akutsu, Osamu Miyakawa, Masahiro Kamiizumi, Hideharu Ishizaki, Daisuke Tatsumi, Naoatsu Hirata, Kazuhiro Hayama, Koki Okutomi, Takahiro Miyamoto, Hideki Ishizuka, Riccardo DeSalvo and Raffaele Flaminio, Journal of Physics: Conference Series, 716, 012022, (2016)

[33] "Design and operation of a 1500-m laser strainmeter installed at underground site in Kamioka", Akito Araya, Akiteru Takamori, Wataru Morii, Kouseki Miyo, Masatake Ohashi, Kazuhiro Hayama, Takashi Uchiyama, Shinji Miyoki and Yoshio Saito, Earth, Planets and Space 69, 77 (2017)

[34] "Mirror actuation design for the interferometer control of the KAGRA gravitational wave telescope", Yuta Michimura, Tomofumi Shimoda, Takahiro Miyamoto, Ayaka Shoda, Koki Okutomi, Yoshinori Fujii, Hiroki Tanaka, Mark A. Barton, Ryutaro Takahashi, Yoichi Aso, Tomotada Akutsu, Masaki Ando, Yutaro Enomoto, Raffaele Flaminio, Kazuhiro Hayama, Eiichi Hirose, Yuki Inoue, Takaaki Kajita, Masahiro Kamiizumi, Seiji Kawamura, Keiko Kokeyama, Kentaro Komori, Rahul Kumar, Osamu Miyakawa, Koji Nagano, Masayuki Nakano, Naoko Ohishi, Ching Pin Ooi, Fabian Erasmo Pena Arellano, Yoshio Saito, Katsuhiko Shimode, Kentaro Somiya, Hiroki Takeda, Takayuki Tomaru, Takashi Uchiyama, Takafumi Ushiba, Kazuhiro Yamamoto, Takaaki Yokozawa, Hirotaka Yuzurihara, Classical and Quantum Gravity 34, 225001(2017)

[35] "Construction of KAGRA: an underground gravitational-wave observatory", The KAGRA collaboration, Prog. Theor. Exp. Phys. 2018, 013F01 (2018)

[36] http://gwcenter.icrr.u-tokyo.ac.jp/en/

OBSERVATIONAL COSMOLOGY GROUP

Summary from 2012 to 2018

We study cosmic reionization and early galaxy formation that are missing pieces of our understanding of cosmic history. The outstanding scientific questions are the unknown reionization physical process, the missing ionizing photon problem, the formation of first stars, and the structural/dynamical/chemical evolutions of galaxies at the early epoch of cosmic history. Our basic strategy is to carry out deep surveys with largest telescope facilities such as Subaru, *Hubble*, and ALMA, that have a sensitivity good enough for probing the distant universe. The main results based on our research activities from April 2012 to March 2018 are summarized as follows.

1. Based on the on-going Subaru Hyper Suprime-Cam (HSC) survey, we have constructed unprecedentedly large samples of luminous galaxies at high redshifts, which enable us to investigate their physical properties with great statistical accuracy. We have revealed a significant excess of their number densities at the bright end compared to the Schechter functional form, suggestive of inefficient AGN feedback for star formation in massive galaxies at redshift $z \sim 4-7$. We have also found a tight correlation between galaxy halo mass and the ratio of star formation rate to the dark matter accretion rate with no significant change (evolution) at $z \sim 4-7$, suggesting that it is a fundamental relation in high-z galaxy formation whose star formation is regulated by the dark matter mass assembly.
2. We have analyzed the deep Hubble Space Telescope (HST) legacy survey data and found that the galaxy half-light radius at a given luminosity significantly decreases toward high z, and their size distribution is well represented by log-normal functions whose standard deviation does not significantly change at $z \sim 0-6$. In addition, we have analyzed the deep HST data targeting six massive galaxy cluster fields and detected intrinsically very faint high-z galaxies thanks to the gravitational lensing effect. We have found that the slopes of the UV luminosity functions (LFs) at $z \sim 6-8$ are very steep and are even steeper at $z \sim 9-10$. We have also found that reionization scenarios exist that consistently explain all the observational measurements.

The details are described in the following section.

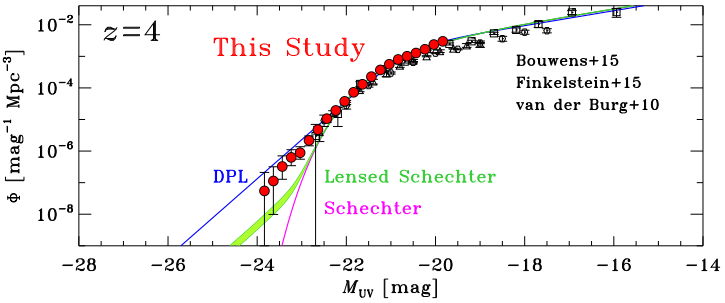

Fig. 1. Rest-frame UV LFs (i.e., differential number densities as a function of rest-frame UV magnitude) of galaxies that take into account quasar contamination correction at $z \sim 4$. The green shaded region corresponds to the best-fit Schechter functions that take into account the effect of gravitational lensing with the two cases of the optical depth estimates. The magenta curve is the best-fit Schechter function without considering the lensing effect and the blue curve is the best-fit double power law (DPL) function. For comparison, we also show previous results for galaxies taken from the literature.

Research Activities

Subaru Hyper Suprime-Cam Survey

We are working on a large-area survey project with Subaru HSC. This survey was awarded 300 nights of Subaru observing time as a Subaru Strategic Program (SSP) [102, 103]. The HSC SSP survey began in 2014 and will last until 2019. This survey will cover 1400 deg^2 with five optical broadband filters of g, r, i, z and y down to 26 mag in g, r, and i band images and $24-25$ mag in z and y band images. This wide field survey will enable us to cover an unprecedentedly large cosmic volume at $z \gtrsim 4$ and to investigate very rare sources such as luminous galaxies and galaxy overdense regions. From early survey data products that were internally released in the HSC collaboration team in August 2016, we have constructed enormous samples of high-redshift galaxy candidates at $z \sim 4-7$, i.e., more than 0.5 million Lyman-break galaxies (LBGs) selected by the standard color selection technique, 358 out of which are spectroscopically confirmed by our follow-up spectroscopy and other studies [104]. We are also carrying out a large-area narrowband (NB) survey in the HSC SSP [107]. The survey area of the latest HSC-NB data reaches $\simeq 21$ deg^2, which is more than four times larger than previous Subaru Suprime-Cam NB fields. Based on the HSC NB data, we have constructed a large sample of 2230 Lyman-α emitters (LAEs) at $z \simeq 5.7-6.6$ [108].

Based on the HSC SSP LBG samples, we have studied the UV LFs at $z \sim 4$, 5, 6, and 7 [104]. We have obtained UV LFs at $z \sim 4-7$ that span a very wide UV luminosity range of ~ 0.002 – $100 L^*_{\rm UV}$ ($-26 < M_{\rm UV} < -14$

mag), where $L^*_{\rm UV}$ denotes the typical luminosity of high-z galaxies, by combining LFs from our program and the ultra-deep HST legacy surveys. Because our HSC SSP data bridge the LFs of galaxies and active galactic nuclei (AGNs) with great statistical accuracy, we have carefully investigated the bright end of the galaxy UV LFs that are estimated by the subtraction of the AGN contribution either aided with spectroscopy or the best-fit AGN UV LFs (Figure 1). We have found that the bright end of the galaxy UV LFs cannot be explained by the Schechter function forms, which can explain the UV LFs of low-z galaxies, at $> 2\sigma$ significance, and require either double power-law functions or modified Schechter functions that consider a magnification bias due to gravitational lensing. Our results indicate that AGN feedback for star formation in massive galaxies would be more inefficient compared to lower redshifts where galaxy LFs are consistent with Schechter functions.

We have also presented clustering properties of LBGs at $z\sim4-6$ over the 100 deg^2 sky (corresponding to a 1.4 Gpc^3 volume) identified in the early data of the HSC SSP [105]. We have derived angular correlation functions (ACFs) for the HSC LBGs with unprecedentedly high statistical accuracies at $z\sim4-6$, and compared them with the halo occupation distribution (HOD) models. We have clearly identified significant ACF excesses in $10''<\theta<90''$, the transition scale between one- and two-halo terms, suggestive of the existence of the non-linear halo bias effect. Combining the HOD models and previous clustering measurements of faint LBGs at $z\sim4-7$, we have investigated the dark matter halo mass ($M_{\rm h}$) of the $z\sim4-7$ LBGs and its correlation with various physical properties including the star formation rate (SFR), the stellar-to-halo mass ratio (SHMR), and the dark matter accretion rate ($\dot{M}_{\rm h}$) over a wide mass range of $M_{\rm h}/M_\odot=4\times10^{10}-4\times10^{12}$. We have found that the SHMR increases from $z\sim4$ to 7 by a factor of ~4 at $M_{\rm h}\simeq1\times10^{11}M_\odot$, while the SHMR shows no strong evolution in the similar redshift range at $M_{\rm h}\simeq1\times10^{12}M_\odot$. Interestingly, we have identified a tight relation of ${\rm SFR}/\dot{M}_{\rm h}-M_{\rm h}$ showing no significant evolution beyond 0.15 dex in this wide mass range over $z\sim4-7$ (Figure 2). This weak evolution suggests that the ${\rm SFR}/\dot{M}_{\rm h}-M_{\rm h}$ relation is a fundamental relation in high-redshift galaxy formation whose star formation activities are regulated by the dark matter mass assembly. Assuming this fundamental relation, we have calculated the cosmic star formation rate densities (SFRDs) over $z=0-10$ (a.k.a. the Madau–Lilly plot). The cosmic SFRD evolution based on the fundamental relation agrees with the one obtained by observations, suggesting that the cosmic SFRD increase from $z\sim10$ to $4-2$ (decrease from $z\sim4-2$ to 0) is mainly driven by the increase of the halo abundance (the decrease of the accretion rate).

In [107], we have presented our NB survey strategy and clustering properties investigated with ~2000 Lyα emitters at $z=5.7$ and 6.6 found in the early data of the HSC SSP survey exploiting the carefully designed narrowband filters. One of the NB filters whose central wavelength is around 0.9 μm, NB921, was created with a support of KAKENHI (23244025; PI: M. Ouchi) Grant-in-Aid for Scientific Research (A) through JSPS. We have derived angular correlation functions with the unprecedentedly large samples of LAEs at $z=6-7$ over the large total area of $14-21$ deg^2 corresponding to $0.3-0.5$ comoving Gpc^2. We have compared the LAE clustering results with two independent theoretical models that suggest an increase of an LAE clustering signal by the patchy ionized bubbles at the epoch of reionization (EoR), and estimate the neutral hydrogen fraction of the intergalactic medium (IGM) to be $x_{\rm HI}=0.15^{+0.15}_{-0.15}$ at $z=6.6$. Based on the halo occupation distribution models, we have found that the $\gtrsim L^*$ LAEs are hosted by the dark-matter halos with an average mass of $\log(\langle M_{\rm h}\rangle/M_\odot)=11.1^{+0.2}_{-0.4}$ $(10.8^{+0.3}_{-0.5})$ at $z=5.7$ (6.6) with a Lyα duty cycle (an abundance ratio of LAEs to dark-matter haloes) of 1 % or less, where the results of $z=6.6$ LAEs may be slightly biased, due to the increase of the clustering signal at the EoR. Our clustering analysis reveals the low-mass nature of $\gtrsim L^*$ LAEs at $z=6-7$, and that these LAEs probably evolve into massive super-L^* galaxies in the present-day universe.

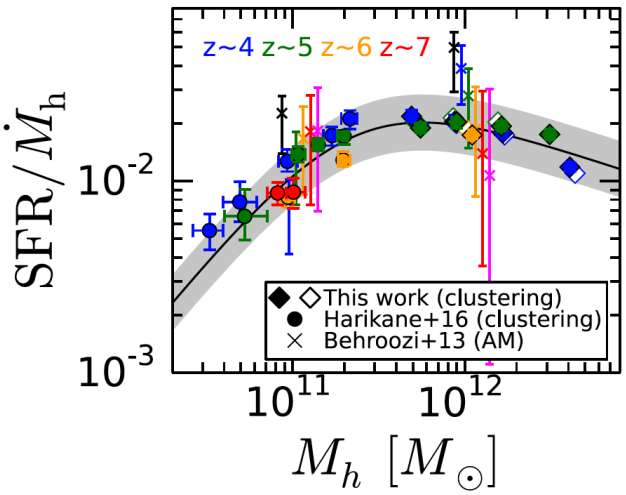

Fig. 2. ${\rm SFR}/\dot{M}_{\rm h}$ as a function of the halo mass. The filled blue, green, orange, and red diamonds (circles) denote the ratio of the extinction-corrected SFR to the dark matter accretion rate at $z\sim4$, 5, 6, and 7, respectively, in this work The statistical errors for our data are smaller than the symbols (diamonds). We also plot ${\rm SFR}/\dot{M}_{\rm h}$ at $z\sim0$, 4, 5, 6, 7, and 8 in the literature with the black, blue, green, orange, red, and magenta crosses for comparison. The black solid curve is the fitting formula for the ${\rm SFR}/\dot{M}_{\rm h}-M_{\rm h}$ relation for $z\sim4-7$, and the gray shaded region represents the typical scatter (0.15 dex) of the data points. For reference, we also plot the results for the subsamples with the magnitude cut of $m^{\rm cut}_{\rm UV}=20.0$ mag with the open diamonds.

We worked on the UDF12 project of ultra-deep imaging with HST at the near-infrared wavelengths with the US, UK, and French colleagues (PI: R. Ellis). In [9], we have presented the results of the deepest search to date for star-forming galaxies beyond a redshift $z \simeq 8.5$ utilizing a new sequence of near-infrared Wide Field Camera 3 (WFC3) images of the Hubble Ultra Deep Field. This UDF12 campaign completed in September 2012 doubles the earlier exposures with WFC3 in this field and quadruples the exposure in the key F105W filter at $\lambda \simeq 1.05\mu$m used to locate such distant galaxies. Combined with additional imaging in the F140W filter at $\simeq 1.4\mu$m, the fidelity of high-z galaxy candidates is greatly improved. Using spectral energy distribution fitting techniques on objects selected from a deep multi-band near-infrared stack we have found 7 promising galaxy candidates at $z > 8.5$. As none of the previously claimed galaxy candidates with $8.5 < z < 10$ is confirmed by our deeper multi-band imaging, our campaign has transformed the measured abundance of galaxies in this redshift range. Although we have recovered the galaxy candidate UDFj-39546284 (previously proposed at $z = 10.3$), it is undetected in the newly added F140W image, implying it lies at $z = 11.9$ or is an intense emission line galaxy at $z \simeq 2.4$. Although no physically-plausible model can explain the required line intensity given the lack of Lyman α or broad-band UV signal, without an infrared spectrum we cannot rule out an exotic interloper. Regardless, our robust $z \simeq 8.5-10$ sample demonstrates a luminosity density that continues the smooth decline observed over $6 < z < 8$. Such continuity has important implications for models of cosmic reionization and future searches for $z > 10$ galaxies with James Webb Space Telescope (JWST). Further details of the UDF12 survey are provided in [27] and catalogs of $z \sim 7-8$ sources used to estimate the UV luminosity function are provided in [17] and [20]. The spectral properties and sizes of the high-z UDF12 sources and measured and analyzed in [19] and [28], respectively. A review of the overall implications of the survey in the context of cosmic reionization is presented in [16].

By extending these studies, we have exploited the deep HST data of extragalactic legacy surveys to systematically investigate the redshift evolution of the galaxy half-light radius r_e obtained from the HST samples of ~ 190000 galaxies at $z = 0-10$ [62]. Our HST samples consist of 176152 photo-z galaxies at $z = 0-6$ from the 3D-HST+CANDELS catalog and 10454 LBGs at $z = 4-10$ identified in the CANDELS, HUDF09, HUDF12, and HFF parallel fields, providing the largest data set to date for galaxy size evolution studies. We have derived r_e with the *same* technique over the wide redshift range of $z = 0-10$, evaluating the effects of the use of images at different wavelengths and the selection bias of photo-z galaxies+LBGs as well as the cosmological surface brightness dimming effect. We have found that r_e values at a given luminosity significantly decrease toward high z (Figure 3), regardless of statistics choices (e.g., $r_e \propto (1+z)^{-1.10\pm0.06}$ for median). For star-forming galaxies, there is no evolution of the power-law slope of the size–luminosity relation and the median Sérsic index ($n \sim 1.5$). Moreover, the r_e distribution is well represented by log-normal functions whose standard deviation $\sigma_{\ln r_e}$ does not show significant evolution within the range of $\sigma_{\ln r_e} \sim 0.45-0.75$. We have calculated the stellar-to-halo size ratio from our r_e measurements and the dark-matter halo masses estimated from the abundance matching study, and obtain a nearly constant value of $r_e/r_{vir} = 1.0-3.5\%$ at $z = 0-8$, where r_{vir} is the virial radius of their host dark matter halos. The combination of the r_e-distribution shape+standard deviation, the constant r_e/r_{vir}, and $n \sim 1.5$ suggests a picture in which typical high-z star-forming galaxies have disk-like stellar components in a sense of dynamics and morphology over cosmic time of $z \sim 0-6$. If high-z star-forming galaxies are truly dominated by disks, the r_e/r_{vir} value and the disk formation model indicate that the specific angular momentum of the disk normalized by the host halo is $\simeq 0.5-1$. These are statistical results for major stellar components of galaxies, and the detailed study of clumpy sub-components is presented in [76]. In addition, we have presented clustering anal-

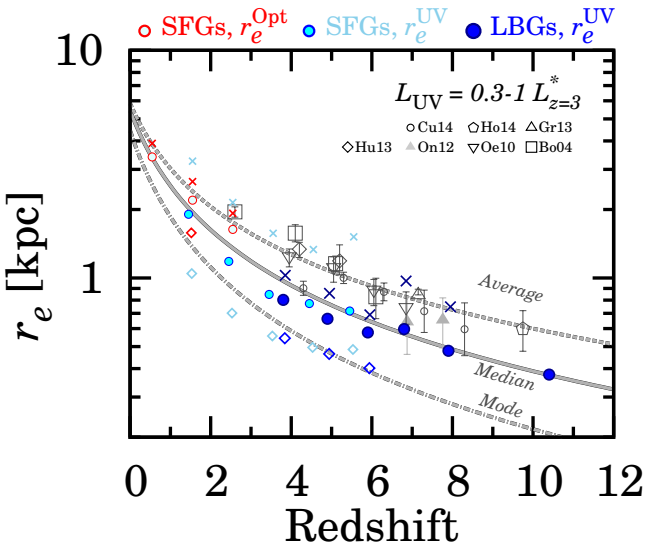

Fig. 3. Difference of the size evolution results based on the average (crosses), median (filled circles), and modal (open diamonds) values of r_e in the bin of $L_{UV} = 0.3-1L^*_{z=3}$. The red, cyan, and blue filled symbols indicate r_e^{Opt} (r_e in the rest-frame optical) and r_e^{UV} (r_e in the rest-frame UV) for the star-forming galaxies (SFGs) and r_e^{UV} for the LBGs, respectively. The error bars for our r_e are not plotted for clarity. The solid, dashed, and dot-dashed curves denote the best-fit size evolution for the average, median, and modal r_e values, respectively, in the linear space. Note that these differences of the statistical results are found in the linear space of r_e, because the r_e-distributions follow the log-normal functions. The r_e values for LBGs in the literature are plotted with gray symbols.

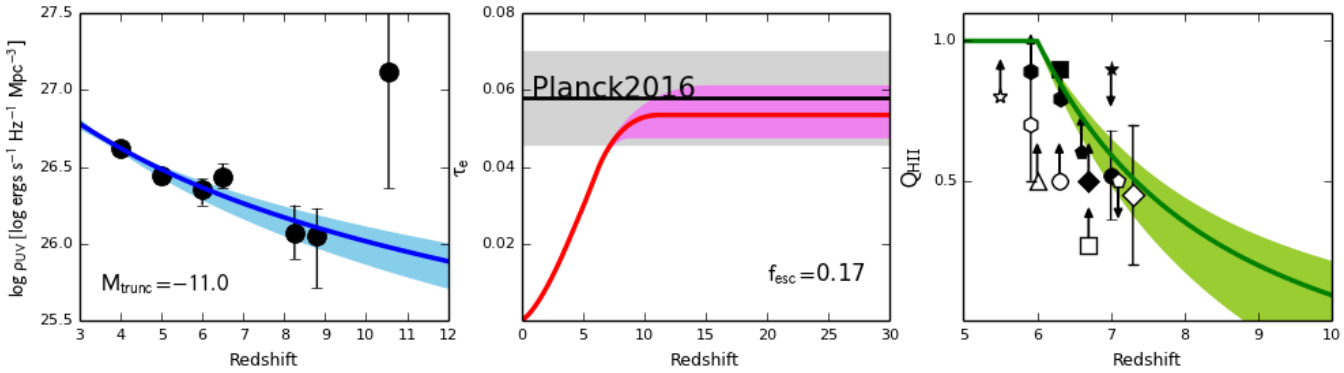

Fig. 4. Left panel: $\rho_{\rm UV}$ calculated with $M_{\rm trunc}=-11.0$. The black circles present $\rho_{\rm UV}$ from the best-fit luminosity functions at $z\sim7-10$ (this work) and those at $z\sim4-6$ in the literature. The blue line and the light blue shade denote the best-fit function of $\rho_{\rm UV}$ and the 1σ error, respectively. The up-scattering $\rho_{\rm UV}(z)$ at $z\sim10$ due to the large uncertainty in α does not affect the fitting result, because the uncertainty in $\rho_{\rm UV}(z)$ is also large. Middle panel: $\tau_{\rm e}$ integrating from $z=0$ to a redshift z. The red line and the magenta shade represent $\tau_{\rm e}(z)$ and the 1σ error, respectively, that are consistent with $\rho_{\rm UV}(z)$ shown with the blue line in the left panel. The black line and the gray region show the values of $\tau_{\rm e}$ and its 1σ error, respectively, obtained by *Planck*. Right panel: evolution of $Q_{\rm HII}$. The green line and the light green shade present $Q_{\rm HII}$ and the 1σ error, respectively, that agree with $\rho_{\rm UV}(z)$ shown with the blue line in the left panel. The symbols denote constraints of $Q_{\rm HII}$ obtained in the literature.

ysis results from the LBGs at $z\sim4-7$ identified in the *Hubble* legacy deep imaging data [74].

Another program with HST, the Hubble Frontier Fields (HFF; PI: J. Lotz), observed six massive clusters down to ~29 mag at the 5σ level, which allows us to detect background high-z sources with intrinsic magnitudes of $\gtrsim30$ mag by lensing magnification [52]. By exploiting the HFF data, we have presented UV luminosity functions of LBGs at $z\sim6-10$ with the complete Hubble Frontier Fields data [119, 73]. We obtain a catalog of ~450 LBG candidates (350, 66, and 40 at $z\sim6-7$, 8, and 9, respectively) with UV absolute magnitudes that reach ~-14 mag, ~2 mag deeper than the Hubble Ultra Deep Field detection limits. We carefully evaluate number densities of the LBGs by Monte Carlo simulations, including all lensing effects such as magnification, distortion, and multiplication of images as well as detection completeness and contamination effects in a self-consistent manner. We find that UV luminosity functions at $z\sim6-8$ have steep faint-end slopes, $\alpha\sim-2$, and likely steeper slopes, $\alpha\lesssim-2$ at $z\sim9-10$. We also find that the evolution of UV luminosity densities shows a non-accelerated decline beyond $z\sim8$ in the case of $M_{\rm trunc}=-15$, while an accelerated in the case of $M_{\rm trunc}=-17$, where $M_{\rm trunc}$ is the faint limit of the UV luminosity function. We examine whether our results are consistent with the Thomson scattering optical depth from the *Planck* satellite and the ionized hydrogen fraction $Q_{\rm HII}$ at $z\lesssim7$ based on the standard analytic reionization model (Figure 4). We find that reionization scenarios exist that consistently explain all the observational measurements with the allowed parameters of $f_{\rm esc}=0.17^{+0.07}_{-0.03}$ and $M_{\rm trunc}>-14.0$ for $\log\xi_{\rm ion}/[{\rm erg^{-1}\ Hz}]=25.34$, where $f_{\rm esc}$ is the escape fraction, and $\xi_{\rm ion}$ is the conversion factor of the UV luminosity to the ionizing photon emission rate. The length of the reionization period is estimated to be $\Delta z=3.9^{+2.0}_{-1.6}$ (for $0.1<Q_{\rm HII}<0.99$), consistent with the recent estimate from *Planck*. In addition, we have presented the results of size measurements for the $z\sim6-9$ LBGs identified in the HFF data and investigated their size-luminosity relation [60, 120].

Programs with ALMA

We have reported deep ALMA observations complemented by associated HST imaging for a luminous ($m_{\rm UV}=25$) galaxy, "Himiko", at $z=6.595$ [29]. The galaxy is remarkable for its high star formation rate, $100M_\odot{\rm yr}^{-1}$, which has been securely estimated from our deep HST and Spitzer photometry, and the absence of any evidence for strong AGN activity or gravitational lensing magnification. Our ALMA observations probe an order of magnitude deeper than previous IRAM observations, yet fail to detect a 1.2 mm dust continuum, indicating a flux of $<52\mu$Jy, which is comparable to or weaker than that of local dwarf irregulars with much lower star formation rates. We have likewise provided a strong upper limit for the flux of [CII] 158μm, $L_{\rm [CII]}<5.4\times10^7L_\odot$, which is a diagnostic of the hot interstellar gas that is often described as a valuable probe for early galaxies. In fact, our observations indicate that Himiko lies off the local $L_{\rm [CII]}$–star formation rate scaling relation by a factor of more than 30. Both aspects of our ALMA observations suggest Himiko is a unique object with a very low dust content and perhaps nearly primordial interstellar gas. Our HST images provide unique insight into the morphology of this remarkable source, highlighting an extremely blue core of activity and two less extreme associated clumps. Himiko is undergoing a triple major merger event whose extensive ionized nebula of Lyα

emitting gas, discovered in our earlier work with Subaru, is powered by star formation and the dense circumgalactic gas. We are likely witnessing an early massive galaxy during a key period of its mass assembly close to the end of the reionization era.

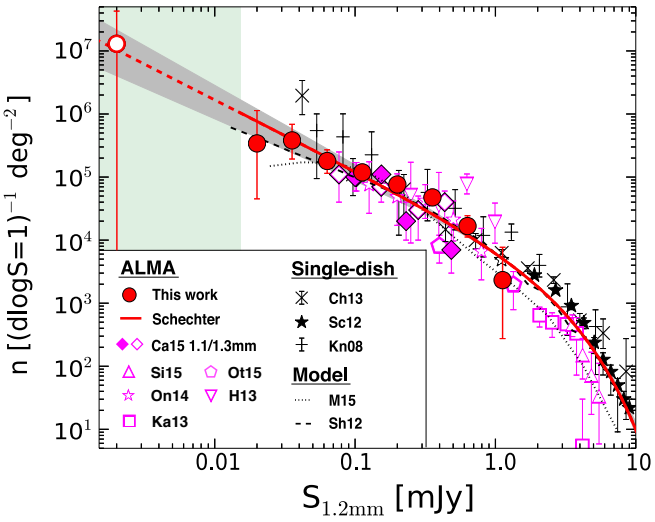

Fig. 5. Differential number counts at 1.2 mm. The red filled circles are our number counts derived from our faint ALMA sources. The red curve and the gray region denote the best-fit Schechter function and the associated 1σ error. In the Schechter function fitting, we use our number counts and the previous measurements shown with the black filled stars and the magenta filled diamonds. Note that the faintest data point of our study (red open circle) is removed from the sample of our Schether function fitting, due to the possible large systematic uncertainties. The pale-green region presents a flux range where no reliable number-count data bin exists (see text). The dashed and dotted curves show the model predictions for number counts based on cosmological hydrodynamic simulations with GADGET-3 and semi-analytic models, respectively. These model predictions are roughly consistent with our results. For the previous measurements of the number counts at 1.1 mm and 1.3 mm different from our 1.2 mm band, we scale the flux densities.

We have also made use of deep ALMA data including archival ones to investigate statistical properties of faint dust continuum sources such as number densities and clustering strengths [49]. In [71], we have presented statistics of 133 faint 1.2 mm continuum sources detected in about 120 deep ALMA pointing data that include all the archival deep data available by 2015 June. We have derived number counts of 1.2 mm continuum sources down to 0.02 mJy partly with the assistance of gravitational lensing (Figure 5), and find that the total integrated 1.2 mm flux of the securely identified sources is $22.9^{+6.7}_{-5.6}$ Jy deg^{-2} that corresponds to 104^{+31}_{-25}% of the extragalactic background light (EBL) measured by *COBE* observations. These results suggest that the major 1.2 mm EBL contributors are sources with 0.02 mJy, and that very faint 1.2 mm sources with $\lesssim$0.02 mJy contribute negligibly to the EBL with the possible flattening and/or truncation of number counts in this very faint flux regime. To understand the physical origin of our faint ALMA sources, we have measured the galaxy bias b_g by the counts-in-cells technique, which is the relation of clustering strengths between galaxies and underlying dark matter, and place a stringent upper limit of $b_g < 3.5$ that is not similar to b_g values of massive distant red galaxies and submillimeter galaxies but comparable to those of UV-bright star-forming BzK galaxies (sBzKs) and LBGs. Moreover, in the optical and near-infrared (NIR) deep fields, we have identified optical-NIR counterparts for 59% of our faint ALMA sources, the majority of which have luminosities, colors, and the IRX-β relation the same as sBzKs and LBGs. We have thus concluded that about a half of our faint ALMA sources are dust-poor high-z galaxies, and that these faint ALMA sources are not miniature (ultra-)luminous infrared galaxies simply scaled down with the infrared brightness.

Programs with Optical Spectroscopy

We have conducted a systematic study of galactic outflows in star-forming galaxies at $z \sim 0$–2 based on the absorption lines of optical spectra taken from SDSS DR7, DEEP2 DR4, and Keck [100]. We have carefully made stacked spectra of homogeneous galaxy samples with similar stellar mass distributions at $z \sim 0$–2, and perform the multi-component fitting of model absorption lines and stellar continua to the stacked spectra. We have obtained the maximum (v_{max}) and central (v_{out}) outflow velocities, and estimate the mass loading factors (η), a ratio of the mass outflow rate to the star formation rate (SFR). Investigating the redshift evolution of the outflow velocities measured with the absorption lines whose depths and ionization energies are similar (Na ID and Mg I at $z \sim 0$–1; Mg II and C II at $z \sim 1$–2), we have identified, for the first time, that the average value of v_{max} (v_{out}) significantly increases by 0.05–0.3 dex from $z \sim 0$ to 2 at a given SFR (Figure 6). Moreover, we have found that the value of η increases from $z \sim 0$ to 2 by $\eta \propto (1+z)^{1.2\pm0.3}$ at a given halo circular velocity v_{cir}, albeit with a potential systematics caused by model parameter choices. The redshift evolution of v_{max} (v_{out}) and η is consistent with the galaxy-size evolution and the local velocity-SFR surface density relation, and explained by high-gas fractions in high-redshift massive galaxies, which is supported by recent radio observations. We have obtained a scaling relation of $\eta \propto v_{cir}^{a}$ for $a = -0.2 \pm 1.1$ in our $z \sim 0$ galaxies that agrees with the momentum-driven outflow model ($a = -1$) within the uncertainty.

On-Going Projects and Future Prospects

Although our previous work provides various implications about the early epoch of cosmic history, large uncertainties raised by the small statistics and systematics do not allow us to obtain conclusive results. One example is shown in Figure 7 that presents the current measurements of UV LFs of galaxies at $z = 5$ and 7. It is

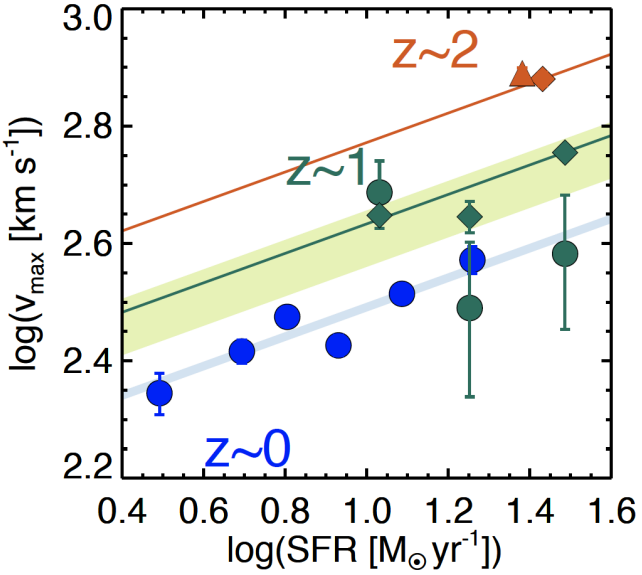

Fig. 6. Maximum outflow velocities as a function of SFRs. Each symbol corresponds to the elements of the absorption lines: Na ID (blue circle), Mg I (green circle), Mg II (green diamond), C II (orange diamond), and C IV (orange triangle). The circles, diamonds, and triangle indicate the velocities of elements, which have the low (5–7 eV), medium (15–24 eV), and high (48 eV) ionization energy, respectively. Error bars denote the 1σ fitting errors. The light blue and green shades describe the result of the power-law fitting to Na ID and Mg I, respectively, with vertical 1σ fitting error range. The green and orange lines denote the best-fitting power-law function of Mg II and C II, respectively.

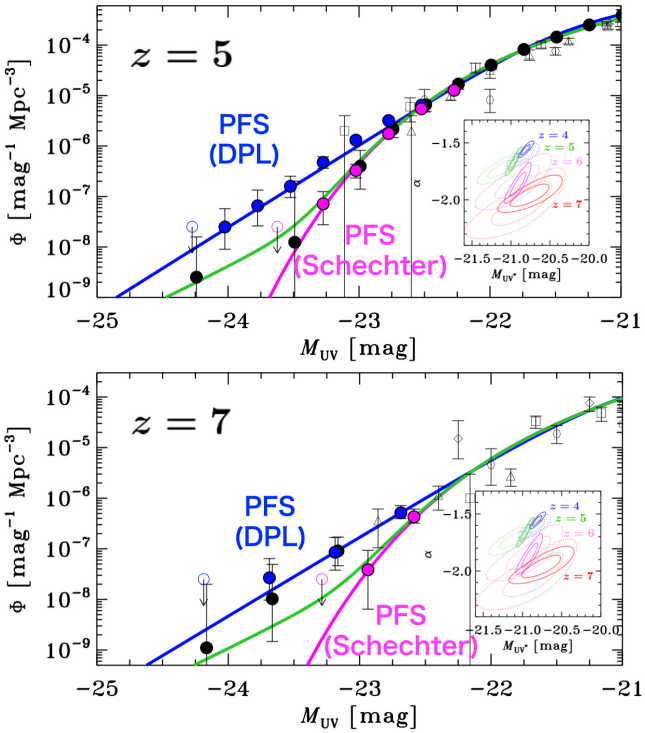

Fig. 7. Bright-end of UV LF at $z=5$ and $z=7$. The magenta and blue circles indicate the expected PFS measurements (plus best-fit functions - curves) and uncertainties for the two cases with LFs having a functional shape of either a Schechter or double-power law model. The green curve shows the Schechter function including the effect of gravitational lensing. The black filled circles represent the current LF at $z=5$ and 7 [104] based on HSC imaging and spectroscopic follow-up that cannot distinguish between Schechter and DPL functions due to uncertainties, contamination, and errors on the AGN fraction. Black open symbols are observational data from the literature. The inset panel shows the error contours of the best-fit parameters of the Schechter function. Solid-line contours are the expected PFS measurements, while the dotted-line contours are the current observational results.

unclear whether the LF follows a Schechter function or has a bright-end excess at the $>5\sigma$ level that is perhaps the result of a heightened AGN population that may be providing considerable feedback effects [104]. Another example is presented in Figure 6. Outflows are a key ingredient in the modeling of galaxies to regulate their stellar mass growth. An open question is how the properties of outflows may vary with SFR and AGN luminosity at a given redshift. Theoretical models predict that the outflow velocity (or the mass loading factor) increases towards high-z thus preventing the production of too many stars at early epochs. Recent observational studies do show indications of strong outflow activity in galaxies up to $z\sim2-3$ through UV metal absorption lines and broad emission-line components [100]. Although, large statistical uncertainties preclude any definitive conclusion. Moreover, no statistical measure of outflows have been obtained at $z>3$ to date.

First of all, the HSC SSP survey is ongoing and promising to extend our previous work with better statistics. Recently, we are also carrying out a multiple HSC NB survey, Cosmic HydrOgen Reionization Unveiled with Subaru (CHORUS), which has been approved as a Subaru intensive program under the collaboration of Osaka Sangyo University, NAOJ, Ehime University, and The University of Tokyo etc. Our contribution to the CHORUS project is to supply one of the NB filters, NB973, which is created for identifying high-z galaxies with a support of KAKENHI (23244025; PI: M. Ouchi) Grant-in-Aid for Scientific Research (A) through JSPS. Although our approved intensive program is a 2-year observation project which will be completed in 2018, some of our observing time was lost due to bad weather. To complete our observations, we have applied for additional observing time for the next semester until January 2019. In addition to the HSC SSP survey, we will work on the CHORUS project and plan to publish our scientific results by 2020.

Moreover, to address the open questions described above, we have started to work on the next generation Subaru wide-field spectrograph, the Prime Focus Spectrograph (PFS) project [36]. After PFS starts science operations planned in 2021, we will start the PFS survey under the large collaboration of The University of Tokyo, NAOJ, Princeton University and Taiwanese institutes etc. Our current contribution to the PFS project is to prepare for an SSP proposal particularly for the section related to high-z galaxy studies. For

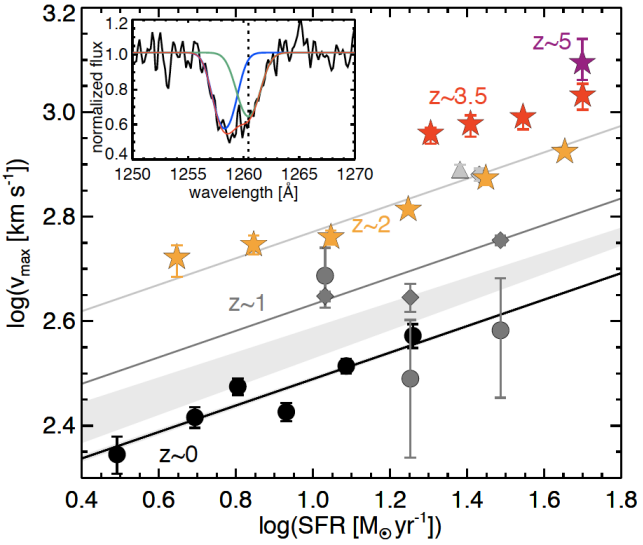

Fig. 8. Maximum outflow velocity $v_{\rm max}$ as a function of SFR. Yellow, red, and purple stars represent the average $v_{\rm max}$ values with errors at $z\sim2$, 3.5, and 5, respectively, based on simulated co-added PFS spectra. The black, dark-gray, and light gray data points (lines) are the average $v_{\rm max}$ values (best-fit linear function) obtained from the SDSS at $z\sim0$, DEEP2 at $z\sim1$, and a Keck survey at $z\sim2$. To illustrate an average measurement at a given redshift and SFR, the inset panel shows the Si II1260 absorption line in a stacked spectrum based on simulated PFS spectra ($t_{\rm exp}=6$ hr each) of 191 galaxies ($23.4<y_{\rm AB}<24$) at $z\sim3.5$. The black and red line represent the stacked PFS spectrum and the best-fit model, respectively. The blue and green lines are the wind and systemic components of the best-fit model. The vertical dotted lines indicates the rest wavelength of Si II1260.

example, we propose to provide a definitive answer to the open question on the shape of the bright-end of the galaxy UV LF at $z\sim4-7$ (Figure 7) by combining the spectral analysis of high-z galaxies (AGN vs. star formation and outflows) and the precise spectroscopic redshifts. With PFS spectra, we will identify and remove foreground contamination to accurately measure the bright-end LF with lessened systematics. The bright-end luminosity function will allow us to determine the Schechter function parameters of M^* and ϕ^*, critical for obtaining the faint-end slope α (Figure 7; see inset panel) that is key to understanding the global evolution of galaxies, i.e. UV luminosity density, for the cosmic star-formation density and the ionizing photon production rate connected to the cosmic reionization photon budget. We also propose to measure maximum outflow velocities of high-z galaxies. With PFS, we will use Mg II2796, 2804, C II1335, and Si II absorption lines as indicators of outflows for galaxies at $2.1<z<2.4$ where [O II] emission detected in the IR arm of PFS provides the systemic velocity. At higher redshift $z\sim3-6$, we will use the strong UV emission lines (e.g. C III]) to indicate the systemic velocity. In Figure 8, we show the expected PFS measurements of the maximum outflow velocity as estimated from stacked simulated spectra. While this analysis is limited to galaxies with measured systemic velocity, we can further determine the maximum outflow velocity at $z\sim2-6$ and relations to galactic properties including starburst and AGN events through spectral emission-line diagnostics.

Subaru Hyper Suprime-Cam Survey

Institute	Country	(*)
ICRR, Univ. of Tokyo	Japan	15
Kavli IPMU, U. of Tokyo	Japan	24
School of Science, U. of Tokyo	Japan	28
NAOJ	Japan	47
JAXA	Japan	6
Tohoku Univ.	Japan	10
Tsukuba Univ.	Japan	1
Kyoto Univ.	Japan	1
Osaka Univ.	Japan	2
Nagoya Univ.	Japan	8
Hokkaido Univ.	Japan	1
Hiroshima Univ.	Japan	4
Ehime Univ.	Japan	12
Tokyo Univ. of Science	Japan	3
Others	Japan	17
ASIAA	Taiwan	23
NCU	Taiwan	9
NTHU	Taiwan	6
Princeton Univ.	USA	27
Stanford Univ.	USA	1
JHU	USA	1
Univ. of Penn.	USA	1
Univ. of Geneva	Switzerland	1
ETH Zurich	Switzerland	1
SJTU	China	1
KIAA	China	1
Saint Mary's Univ.	Canada	1
ESO	Germany	1
SRON	Netherlands	1
Total		254

(*) Number of participants as of April 2018.

Members

Staffs

Masami Ouchi, Assoc. Professor, July 2010 to the present
Yoshiaki Ono, Assist. Professor, April 2012 to the present

Postdoctoral Fellows

Rieko Momose, April 2012 to March 2015
Suraphong Yuma, May 2012 to March 2015
Masao Hayashi, April 2013 to March 2014
Takatoshi Shibuya, April 2013 to February 2018

Tomoki Saito, April 2014 to March 2015
Mariko Kubo, April 2014 to March 2016
Florent Duval, April 2015 to March 2016
Yi-Kuan Chiang, June 2016 to September 2016
Jun Toshikawa, April 2017 to the present
Ken Mawatari, April 2018 to the present

Graduate Students

One student was awarded a doctor degree and ten students earned a master degree during 2014–2018, supervised by Masami Ouchi.

List of Publications

After Year 2012

Papers in Refereed Journals

[1] "The First Systematic Survey for Lyα Emitters at $z = 7.3$ with Red-sensitive Subaru/SuprimeCam"
T. Shibuya *et al.*, The Astrophysical Journal, **752**, 114 (2012). **Cited 95 times**.

[2] "Evidence for Low Extinction in Actively Star-forming Galaxies at $z > 6.5$"
F. Walter *et al.*, The Astrophysical Journal, **752**, 93 (2012). **Cited 42 times**.

[3] "The Spitzer Extragalactic Representative Volume Survey (SERVS): Survey Definition and Goals"
J.-C. Mauduit *et al.*, Publications of the Astronomical Society of the Pacific, **124**, 714 (2012). **Cited 68 times**.

[4] "A Dual-Narrowband Survey for Hα Emitters at Redshift of 2.2: Demonstration of the Technique and Constraints on the Hα Luminosity Function"
J. C. Lee *et al.*, Publications of the Astronomical Society of the Pacific, **124**, 782 (2012). **Cited 36 times**.

[5] "Diffuse Lyα haloes around Lyα emitters at $z = 3$: do dark matter distributions determine the Lyα spatial extents?"
Y. Matsuda *et al.*, Monthly Notices of the Royal Astronomical Society, **425**, 878-883 (2012). **Cited 75 times**.

[6] "Physical Conditions in Molecular Clouds in the Arm and Interarm Regions of M51"
J. Koda *et al.*, The Astrophysical Journal, **761**, 41 (2012). **Cited 33 times**.

[7] "Black Hole Mass and Eddington Ratio Distribution Functions of X-Ray-selected Broad-line AGNs at $z \sim 1.4$ in the Subaru XMM-Newton Deep Field"
K. Nobuta *et al.*, The Astrophysical Journal, **761**, 143 (2012). **Cited 30 times**.

[8] "Intrinsic Shape of Star-forming BzK Galaxies. II. Rest-frame Ultraviolet and Optical Structures in GOODS-South and SXDS"
S. Yuma *et al.*, The Astrophysical Journal, **761**, 19 (2012). **Cited 13 times**.

[9] "The Abundance of Star-forming Galaxies in the Redshift Range $8.5 - 12$: New Results from the 2012 Hubble Ultra Deep Field Campaign"
R. S. Ellis *et al.*, The Astrophysical Journal Letters, **763**, L7 (2013). **Cited 297 times**.

[10] "A Water Maser and NH_3 Survey of GLIMPSE Extended Green Objects"
C. J. Cyganowski *et al.*, The Astrophysical Journal, **764**, 61 (2013). **Cited 28 times**.

[11] "Nebular Attenuation in Hα-selected Star-forming Galaxies at $z = 0.8$ from the NewHα Survey"
I. G. Momcheva *et al.*, The Astronomical Journal, **145**, 47 (2013). **Cited 27 times**.

[12] "Gas Motion Study of Lyα Emitters at $z \sim 2$ Using FUV and Optical Spectral Lines"
T. Hashimoto *et al.*, The Astrophysical Journal, **765**, 70 (2013). **Cited 84 times**.

[13] "Calibrating [O II] star formation rates at $z < 1$ from dual Hα-[O II] imaging from HiZELS"
M. Hayashi *et al.*, Monthly Notices of the Royal Astronomical Society, **430**, 1042-1050 (2013). **Cited 22 times**.

[14] "SEDS: The Spitzer Extended Deep Survey. Survey Design, Photometry, and Deep IRAC Source Counts"
M. L. N. Ashby *et al.*, The Astrophysical Journal, **769**, 80 (2013). **Cited 130 times**.

[15] "First Spectroscopic Evidence for High Ionization State and Low Oxygen Abundance in Lyα Emitters"
K. Nakajima *et al.*, The Astrophysical Journal, **769**, 3 (2013). **Cited 70 times**.

[16] "New Constraints on Cosmic Reionization from the 2012 Hubble Ultra Deep Field Campaign"
B. E. Robertson *et al.*, The Astrophysical Journal, **768**, 71 (2013). **Cited 290 times**.

[17] "The UV Luminosity Function of Star-forming Galaxies via Dropout Selection at Redshifts $z \sim 7$ and 8 from the 2012 Ultra Deep Field Campaign"
M. A. Schenker *et al.*, The Astrophysical Journal, **768**, 196 (2013). **Cited 163 times**.

[18] "Evolution of star formation in the UKIDSS Ultra Deep Survey field - I. Luminosity functions and cosmic star formation rate out to $z = 1.6$"
A. B. Drake *et al.*, Monthly Notices of the Royal Astronomical Society, **433**, 796-811 (2013). **Cited 29 times**.

[19] "The UV continua and inferred stellar populations of galaxies at $z \simeq 7-9$ revealed by the Hubble Ultra-Deep Field 2012 campaign"
J. S. Dunlop *et al.*, Monthly Notices of the Royal Astronomical Society, **432**, 3520-3533 (2013). **Cited 108 times**.

[20] "A new multifield determination of the galaxy luminosity function at $z = 7-9$ incorporating the 2012 Hubble Ultra-Deep Field imaging"
R. J. McLure *et al.*, Monthly Notices of the Royal Astronomical Society, **432**, 2696-2716 (2013). **Cited 234 times**.

[21] "Star Formation on Subkiloparsec Scale Triggered by Non-linear Processes in Nearby Spiral Galaxies"
R. Momose *et al.*, The Astrophysical Journal Letters, **772**, L13 (2013). **Cited 30 times**.

[22] "The Galaxy Environment of a QSO at $z \sim 5.7$"
E. Bañados *et al.*, The Astrophysical Journal, **773**, 178 (2013). **Cited 27 times**.

[23] "Resolved Giant Molecular Clouds in Nearby Spiral Galaxies: Insights from the CANON CO (1–0) Survey"
J. Donovan Meyer *et al.*, The Astrophysical Journal, **772**, 107 (2013). **Cited 44 times**.

[24] "Physical Properties of Spectroscopically Confirmed Galaxies at $z \geq 6$. I. Basic Characteristics of the Rest-frame UV Continuum and Lyα Emission"
L. Jiang *et al.*, The Astrophysical Journal, **772**, 99 (2013). **Cited 46 times**.

[25] "Physical Properties of Spectroscopically Confirmed Galaxies at $z \geq 6$. II. Morphology of the Rest-frame UV Continuum and Lyα Emission"
L. Jiang *et al.*, The Astrophysical Journal, **773**, 153 (2013). **Cited 42 times**.

[26] "On the evolution and environmental dependence of the star formation rate versus stellar mass relation since $z \sim 2$"
Y. Koyama *et al.*, Monthly Notices of the Royal Astronomical Society, **434**, 423-436 (2013). **Cited 90 times**.

[27] "The 2012 Hubble Ultra Deep Field (UDF12): Observational Overview"
A. M. Koekemoer *et al.*, The Astrophysical Journal Supplement Series, **209**, 3 (2013). **Cited 104 times**.

[28] "Evolution of the Sizes of Galaxies over $7 < z < 12$ Revealed by the 2012 Hubble Ultra Deep Field Campaign"
Y. Ono *et al.*, The Astrophysical Journal, **777**, 155 (2013). **Cited 86 times**.

[29] "An Intensely Star-forming Galaxy at $z \sim 7$ with Low Dust and Metal Content Revealed by Deep ALMA and HST Observations"
M. Ouchi *et al.*, The Astrophysical Journal, **778**, 102 (2013). **Cited 123 times**.

[30] "A fundamental metallicity relation for galaxies at $z = 0.84-1.47$ from HiZELS"
J. P. Stott *et al.*, Monthly Notices of the Royal Astronomical Society, **436**, 1130-1141 (2013). **Cited 63 times**.

[31] "Nature of Hα Selected Galaxies at $z > 2$. I. Main-sequence and Dusty Star-forming Galaxies"
K.-i. Tadaki *et al.*, The Astrophysical Journal, **778**, 114 (2013). **Cited 25 times**.

[32] "First Systematic Search for Oxygen-line Blobs at High Redshift: Uncovering AGN Feedback and Star Formation Quenching"
S. Yuma *et al.*, The Astrophysical Journal, **779**, 53 (2013). **Cited 13 times**.

[33] ""Direct" Gas-phase Metallicities, Stellar Properties, and Local Environments of Emission-line Galaxies at Redshifts below 0.90"
C. Ly *et al.*, The Astrophysical Journal, **780**, 122 (2014). **Cited 44 times**.

[34] "The Nature of Hα-selected Galaxies at $z > 2$. II. Clumpy Galaxies and Compact Star-forming Galaxies"
K.-i. Tadaki *et al.*, The Astrophysical Journal, **780**, 77 (2014). **Cited 25 times**.

[35] "The mass-metallicity relation at $z \sim 1.4$ revealed with Subaru/FMOS"
K. Yabe *et al.*, Monthly Notices of the Royal Astronomical Society, **437**, 3647-3663 (2014). **Cited 48 times**.

[36] "Extragalactic science, cosmology, and Galactic archaeology with the Subaru Prime Focus Spectrograph"
M. Takada *et al.*, Publications of the Astronomical Society of Japan, **66**, R1 (2014). **Cited 183 times**.

[37] "Mapping the large-scale structure around a $z = 1.46$ galaxy cluster in 3D using two adjacent narrow-band filters"

M. Hayashi *et al.*, Monthly Notices of the Royal Astronomical Society, **439**, 2571-2583 (2014). **Cited 16 times**.

[38] "AzTEC/ASTE 1.1-mm survey of SSA22: Counterpart identification and photometric redshift survey of submillimetre galaxies"
H. Umehata *et al.*, Monthly Notices of the Royal Astronomical Society, **440**, 3462-3478 (2014). **Cited 23 times**.

[39] "What is the Physical Origin of Strong Lyα Emission? I. Demographics of Lyα Emitter Structures"
T. Shibuya *et al.*, The Astrophysical Journal, **785**, 64 (2014). **Cited 26 times**.

[40] "What is the Physical Origin of Strong Lyα Emission? II. Gas Kinematics and Distribution of Lyα Emitters"
T. Shibuya *et al.*, The Astrophysical Journal, **788**, 74 (2014). **Cited 67 times**.

[41] "Identification of the progenitors of rich clusters and member galaxies in rapid formation at $z > 2$"
R. Shimakawa *et al.*, Monthly Notices of the Royal Astronomical Society, **441**, L1-L5 (2014). **Cited 28 times**.

[42] "Evidence for a Gas-rich Major Merger in a Proto-cluster at $z = 2.5$"
K.-i. Tadaki *et al.*, The Astrophysical Journal Letters, **788**, L23 (2014). **Cited 14 times**.

[43] "Diffuse Lyα haloes around galaxies at $z = 2.2 - 6.6$: implications for galaxy formation and cosmic reionization"
R. Momose *et al.*, Monthly Notices of the Royal Astronomical Society, **442**, 110-120 (2014). **Cited 70 times**.

[44] "Ionization state of inter-stellar medium in galaxies: evolution, SFR-M_*-Z dependence, and ionizing photon escape"
K. Nakajima *et al.*, Monthly Notices of the Royal Astronomical Society, **442**, 900-916 (2014). **Cited 128 times**.

[45] "Large-scale environment of $z \sim 5.7$ C IV absorption systems - I. Projected distribution of galaxies"
C. G. Díaz *et al.*, Monthly Notices of the Royal Astronomical Society, **442**, 946-978 (2014). **Cited 15 times**.

[46] "Constraining dust formation in high-redshift young galaxies"
H. Hirashita *et al.*, Monthly Notices of the Royal Astronomical Society, **443**, 1704-1712 (2014). **Cited 17 times**.

[47] "A First Site of Galaxy Cluster Formation: Complete Spectroscopy of a Protocluster at $z = 6.01$"
J. Toshikawa *et al.*, The Astrophysical Journal, **792**, 15 (2014). **Cited 23 times**.

[48] "MOSFIRE and LDSS3 Spectroscopy for an [O II] Blob at $z = 1.18$: Gas Outflow and Energy Source"
Y. Harikane *et al.*, The Astrophysical Journal, **794**, 129 (2014). **Cited 7 times**.

[49] "Faint Submillimeter Galaxies Revealed by Multifield Deep ALMA Observations: Number Counts, Spatial Clustering, and a Dark Submillimeter Line Emitter"
Y. Ono *et al.*, The Astrophysical Journal, **795**, 5 (2014). **Cited 47 times**.

[50] "Accelerated Evolution of the Lyα Luminosity Function at $z \gtrsim 7$ Revealed by the Subaru Ultra-deep Survey for Lyα Emitters at $z = 7.3$"
A. Konno *et al.*, The Astrophysical Journal, **797**, 16 (2014). **Cited 78 times**.

[51] "NIR Spectroscopic Observation of Massive Galaxies in the Protocluster at $z = 3.09$"
M. Kubo *et al.*, The Astrophysical Journal, **799**, 38 (2015). **Cited 21 times**.

[52] "Hubble Frontier Fields First Complete Cluster Data: Faint Galaxies at $z \sim 5 - 10$ for UV Luminosity Functions and Cosmic Reionization"
M. Ishigaki *et al.*, The Astrophysical Journal, **799**, 12 (2015). **Cited 120 times**.

[53] "The Subaru High-z Quasar Survey: Discovery of Faint $z \sim 6$ Quasars"
N. Kashikawa *et al.*, The Astrophysical Journal, **798**, 28 (2015). **Cited 45 times**.

[54] "The Gas Inflow and Outflow Rate in Star-forming Galaxies at $z \sim 1.4$"
K. Yabe *et al.*, The Astrophysical Journal, **798**, 45 (2015). **Cited 13 times**.

[55] "First Infrared-Based Implications for the Dust Attenuation and Star Formation of Typical Lyα Emitters"
H. Kusakabe *et al.*, The Astrophysical Journal Letters, **800**, L29 (2015). **Cited 17 times**.

[56] "The Relationship between Stellar Mass, Gas Metallicity, and Star Formation Rate for Hα-Selected Galaxies at $z \approx 0.8$ from the NewHα Survey"
M. A. de los Reyes *et al.*, The Astronomical Journal, **149**, 79 (2015). **Cited 31 times**.

[57] "The spectral energy distribution of the redshift 7.1 quasar ULAS J1120+0641"
R. Barnett *et al.*, Astronomy & Astrophysics, **575**, A31 (2015). **Cited 19 times**.

[58] "When did Round Disk Galaxies Form?"
T. M. Takeuchi *et al.*, The Astrophysical Journal, **801**, 2 (2015). **Cited 1 times**.

[59] "Large-scale environment of $z \sim 5.7$ C IV absorption systems -II. Spectroscopy of Lyman α emitters"
C. G. Díaz *et al.*, Monthly Notices of the Royal Astronomical Society, **448**, 1240-1270 (2015). **Cited 11 times**.

[60] "The Sizes of $z \sim 6-8$ Lensed Galaxies from the Hubble Frontier Fields Abell 2744 Data"
R. Kawamata *et al.*, The Astrophysical Journal, **804**, 103 (2015). **Cited 62 times**.

[61] "On the Diffuse Lyα Halo around Lyα Emitting Galaxies"
E. Lake *et al.*, The Astrophysical Journal, **806**, 46 (2015). **Cited 22 times**.

[62] "Morphologies of $\sim$190,000 Galaxies at $z = 0-10$ Revealed with HST Legacy Data. I. Size Evolution"
T. Shibuya *et al.*, The Astrophysical Journal Supplement Series, **219**, 15 (2015). **Cited 112 times**.

[63] "Deep rest-frame far-UV spectroscopy of the giant Lyman α emitter 'Himiko"'
J. Zabl *et al.*, Monthly Notices of the Royal Astronomical Society, **451**, 2050-2070 (2015). **Cited 17 times**.

[64] "The Subaru-XMM-Newton Deep Survey (SXDS). VIII. Multi-wavelength identification, optical/NIR spectroscopic properties, and photometric redshifts of X-ray sources"
M. Akiyama *et al.*, Publications of the Astronomical Society of Japan, **67**, 82 (2015). **Cited 11 times**.

[65] "A Close Comparison between Observed and Modeled Lyα Lines for $z \sim 2.2$ Lyα Emitters"
T. Hashimoto *et al.*, The Astrophysical Journal, **812**, 157 (2015). **Cited 42 times**.

[66] "Physical conditions of the interstellar medium in star-forming galaxies at $z \sim 1.5$"
M. Hayashi *et al.*, Publications of the Astronomical Society of Japan, **67**, 80 (2015). **Cited 17 times**.

[67] "Evolution of star formation in the UKIDSS Ultra Deep Survey Field - II. Star formation as a function of stellar mass between $z = 1.46$ and 0.63"
A. B. Drake *et al.*, Monthly Notices of the Royal Astronomical Society, **454**, 2015-2025 (2015). **Cited 6 times**.

[68] "Thirty Meter Telescope Detailed Science Case: 2015"
W. Skidmore *et al.*, Research in Astronomy and Astrophysics, **15**, 1945 (2015). **Cited 30 times**.

[69] "ALMA Deep Field in SSA22: A Concentration of Dusty Starbursts in a $z = 3.09$ Protocluster Core"
H. Umehata *et al.*, The Astrophysical Journal Letters, **815**, L8 (2015). **Cited 34 times**.

[70] "Physical Properties of Spectroscopically Confirmed Galaxies at $z \geq 6$. III. Stellar Populations from SED Modeling with Secure Lyα Emission and Redshifts"
L. Jiang *et al.*, The Astrophysical Journal, **816**, 16 (2016). **Cited 18 times**.

[71] "ALMA Census of Faint 1.2 mm Sources Down to $\sim$0.02 mJy: Extragalactic Background Light and Dust-poor, High-z Galaxies"
S. Fujimoto *et al.*, The Astrophysical Journal Letters, **222**, 1 (2016). **Cited 50 times**.

[72] "An extremely dense group of massive galaxies at the centre of the protocluster at $z = 3.09$ in the SSA22 field"
M. Kubo *et al.*, Monthly Notices of the Royal Astronomical Society, **455**, 3333-3344 (2016). **Cited 13 times**.

[73] "Precise Strong Lensing Mass Modeling of Four Hubble Frontier Field Clusters and a Sample of Magnified High-redshift Galaxies"
R. Kawamata *et al.*, The Astrophysical Journal, **819**, 114 (2016). **Cited 75 times**.

[74] "Evolution of Stellar-to-Halo Mass Ratio at $z = 0-7$ Identified by Clustering Analysis with the Hubble Legacy Imaging and Early Subaru/Hyper Suprime-Cam Survey Data"
Y. Harikane *et al.*, The Astrophysical Journal, **821**, 123 (2016). **Cited 40 times**.

[75] "Statistical properties of diffuse Lyα haloes around star-forming galaxies at $z \sim 2$"
R. Momose *et al.*, Monthly Notices of the Royal Astronomical Society, **457**, 2318-2330 (2016). **Cited 26 times**.

[76] "Morphologies of $\sim$190,000 Galaxies at $z = 0-10$ Revealed with HST Legacy Data. II. Evolution of Clumpy Galaxies"
T. Shibuya *et al.*, The Astrophysical Journal, **821**, 72 (2016). **Cited 32 times**.

[77] "A New Constraint on the Lyα Fraction of UV Very Bright Galaxies at Redshift 7"
H. Furusawa *et al.*, The Astrophysical Journal, **822**, 46 (2016). **Cited 23 times**.

[78] "A Very Compact Dense Galaxy Overdensity with $\delta \simeq 130$ Identified at $z \sim 8$: Implications for Early Protocluster and Cluster Core Formation"
M. Ishigaki *et al.*, The Astrophysical Journal, **822**, 5 (2016). **Cited 10 times**.

[79] "Bright and Faint Ends of Lyα Luminosity Functions at $z = 2$ Determined by the Subaru Survey: Implications for AGNs, Magnification Bias, and ISM H I Evolution"
A. Konno *et al.*, The Astrophysical Journal, **823**, 20 (2016). **Cited 38 times**.

[80] "Detection of an oxygen emission line from a high-redshift galaxy in the reionization epoch"
A. K. Inoue *et al.*, Science, **352**, 1559-1562 (2016). **Cited 41 times**.

[81] "A Spectroscopically Confirmed Double Source Plane Lens System in the Hyper Suprime-Cam Subaru Strategic Program"
M. Tanaka *et al.*, The Astrophysical Journal Letters, **826**, L19 (2016). **Cited 4 times**.

[82] "Subaru High-z Exploration of Low-luminosity Quasars (SHELLQs). I. Discovery of 15 Quasars and Bright Galaxies at $5.7 < z < 6.9$"
Y. Matsuoka *et al.*, The Astrophysical Journal, **828**, 26 (2016). **Cited 59 times**.

[83] "A Hard Ionizing Spectrum in $z = 3-4$ Lyα Emitters with Intense [O III] Emission: Analogs of Galaxies in the Reionization Era?"
K. Nakajima *et al.*, The Astrophysical Journal Letters, **831**, L9 (2016). **Cited 32 times**.

[84] "ALMA Reveals Strong [C II] Emission in a Galaxy Embedded in a Giant Lyα Blob at $z = 3.1$"
H. Umehata *et al.*, The Astrophysical Journal Letters, **834**, L16 (2017). **Cited 5 times**.

[85] "Lyα emitters with very large Lyα equivalent widths, $\mathrm{EW_0(Ly\alpha)} \simeq 200-400$Å, at $z \sim 2$"
T. Hashimoto *et al.*, Monthly Notices of the Royal Astronomical Society, **465**, 1543-1562 (2017). **Cited 12 times**.

[86] "A new quadruple gravitational lens from the Hyper Suprime-Cam Survey: the puzzle of HSC J115252+004733"
A. More *et al.*, Monthly Notices of the Royal Astronomical Society, **465**, 2411-2419 (2017). **Cited 10 times**.

[87] "Cosmic Galaxy-IGM H I Relation at $z \sim 2-3$ Probed in the COSMOS/UltraVISTA 1.6 Deg^2 Field"
S. Mukae *et al.*, The Astrophysical Journal, **835**, 281 (2017). **Cited 6 times**.

[88] "The redshift-selected sample of long gamma-ray burst host galaxies: The overall metallicity distribution at $z < 0.4$"
Y. Niino *et al.*, Publications of the Astronomical Society of Japan, **69**, 27 (2017). **Cited 2 times**.

[89] "The Galaxy-Halo Connection in High-redshift Universe: Details and Evolution of Stellar-to-halo Mass Ratios of Lyman Break Galaxies on CFHTLS Deep Fields"
S. Ishikawa *et al.*, The Astrophysical Journal, **841**, 8 (2017). **Cited 7 times**.

[90] "Small-scale Intensity Mapping: Extended Lyα, Hα, and Continuum Emission as a Probe of Halo Star Formation in High-redshift Galaxies"
L. Mas-Ribas *et al.*, The Astrophysical Journal, **841**, 19 (2017). **Cited 13 times**.

[91] "Evolution of N/O abundance ratios and ionization parameters from $z \sim 0$ to 2 investigated by the direct temperature method"
T. Kojima *et al.*, Publications of the Astronomical Society of Japan, **69**, 44 (2017). **Cited 14 times**.

[92] "Imaging of diffuse H I absorption structure in the SSA22 protocluster region at $z = 3.1$"
K. Mawatari *et al.*, Monthly Notices of the Royal Astronomical Society, **467**, 3951-3962 (2017). **Cited 2 times**.

[93] "Direct evidence for Lyα depletion in the protocluster core"
R. Shimakawa *et al.*, Monthly Notices of the Royal Astronomical Society, **468**, L21-L25 (2017). **Cited 4 times**.

[94] "Similarities and uniqueness of Ly α emitters among star-forming galaxies at $z = 2.5$"
R. Shimakawa *et al.*, Monthly Notices of the Royal Astronomical Society, **468**, 1123-1141 (2017). **Cited 7 times**.

[95] "Systematic Survey for [O II], [O III], and Hα Blobs at $z = 0.1-1.5$: The Implication for Evolution of Galactic-scale Outflow"
S. Yuma *et al.*, The Astrophysical Journal, **841**, 93 (2017). **Cited 5 times**.

[96] "A New Constraint on Reionization from the Evolution of the Lyα Luminosity Function at $z \sim 6-7$ Probed by a Deep Census of $z = 7.0$ Lyα Emitter Candidates to $0.3L^*$"
K. Ota *et al.*, The Astrophysical Journal, **844**, 85 (2017). **Cited 27 times**.

[97] "Minor Contribution of Quasars to Ionizing Photon Budget at $z \sim 6$: Update on Quasar Luminosity Function at the Faint End with Subaru/Suprime-Cam"

M. Onoue *et al.*, The Astrophysical Journal Letters, **847**, L15 (2017). **Cited 12 times**.

[98] "The infrared-dark dust content of high redshift galaxies"
A. Ferrara *et al.*, Monthly Notices of the Royal Astronomical Society, **471**, 5018-5024 (2017). **Cited 9 times**.

[99] "Demonstrating a New Census of Infrared Galaxies with ALMA (DANCING-ALMA). I. FIR Size and Luminosity Relation at $z = 0-6$ Revealed with 1034 ALMA Sources"
S. Fujimoto *et al.*, The Astrophysical Journal, **850**, 83 (2017). **Cited 13 times**.

[100] "Evolution of Galactic Outflows at $z \sim 0-2$ Revealed with SDSS, DEEP2, and Keck Spectra"
Y. Sugahara *et al.*, The Astrophysical Journal, **850**, 51 (2017). **Cited 4 times**.

[101] "Deep Submillimeter and Radio Observations in the SSA22 Field. I. Powering Sources and the Lyα Escape Fraction of Lyα Blobs"
Y. Ao *et al.*, The Astrophysical Journal, **850**, 178 (2017). **Cited 3 times**.

[102] "The Hyper Suprime-Cam SSP Survey: Overview and survey design"
H. Aihara *et al.*, Publications of the Astronomical Society of Japan, **70**, S4 (2018). **Cited 108 times**.

[103] "First data release of the Hyper Suprime-Cam Subaru Strategic Program"
H. Aihara *et al.*, Publications of the Astronomical Society of Japan, **70**, S8 (2018). **Cited 117 times**.

[104] "Great Optically Luminous Dropout Research Using Subaru HSC (GOLDRUSH). I. UV luminosity functions at $z \sim 4-7$ derived with the half-million dropouts on the 100 deg^2 sky"
Y. Ono *et al.*, Publications of the Astronomical Society of Japan, **70**, S10 (2018). **Cited 38 times**.

[105] "GOLDRUSH. II. Clustering of galaxies at $z \sim 4-6$ revealed with the half-million dropouts over the 100 deg^2 area corresponding to 1 Gpc^3"
Y. Harikane *et al.*, Publications of the Astronomical Society of Japan, **70**, S11 (2018). **Cited 32 times**.

[106] "GOLDRUSH. III. A systematic search for protoclusters at $z \sim 4$ based on the >100 deg^2 area"
J. Toshikawa *et al.*, Publications of the Astronomical Society of Japan, **70**, S12 (2018). **Cited 12 times**.

[107] "Systematic Identification of LAEs for Visible Exploration and Reionization Research Using Subaru HSC (SILVERRUSH). I. Program strategy and clustering properties of ~ 2000 Lyα emitters at $z = 6-7$ over the $0.3-0.5$ Gpc^2 survey area"
M. Ouchi *et al.*, Publications of the Astronomical Society of Japan, **70**, S13 (2018). **Cited 42 times**.

[108] "SILVERRUSH. II. First catalogs and properties of ~ 2000 Lyα emitters and blobs at $z \sim 6-7$ identified over the $14-21$ deg^2 sky"
T. Shibuya *et al.*, Publications of the Astronomical Society of Japan, **70**, S14 (2018). **Cited 24 times**.

[109] "SILVERRUSH. III. Deep optical and near-infrared spectroscopy for Lyα and UV-nebular lines of bright Lyα emitters at $z = 6-7$"
T. Shibuya *et al.*, Publications of the Astronomical Society of Japan, **70**, S15 (2018). **Cited 35 times**.

[110] "SILVERRUSH. IV. Lyα luminosity functions at $z = 5.7$ and 6.6 studied with ~ 1300 Lyα emitters on the $14-21$ deg^2 sky"
A. Konno *et al.*, Publications of the Astronomical Society of Japan, **70**, S16 (2018). **Cited 32 times**.

[111] "A 16 deg^2 survey of emission-line galaxies at $z < 1.5$ in HSC-SSP Public Data Release 1"
M. Hayashi *et al.*, Publications of the Astronomical Society of Japan, **70**, S17 (2018). **Cited 4 times**.

[112] "Enhancement of galaxy overdensity around quasar pairs at $z < 3.6$ based on the Hyper Suprime-Cam Subaru Strategic Program Survey"
M. Onoue *et al.*, Publications of the Astronomical Society of Japan, **70**, S31 (2018). **Cited 5 times**.

[113] "Luminous quasars do not live in the most overdense regions of galaxies at $z \sim 4$"
H. Uchiyama *et al.*, Publications of the Astronomical Society of Japan, **70**, S32 (2018). **Cited 8 times**.

[114] "Clustering of quasars in a wide luminosity range at redshift 4 with Subaru Hyper Suprime-Cam Wide-field imaging"
W. He *et al.*, Publications of the Astronomical Society of Japan, **70**, S33 (2018). **Cited 6 times**.

[115] "The quasar luminosity function at redshift 4 with the Hyper Suprime-Cam Wide Survey"
M. Akiyama *et al.*, Publications of the Astronomical Society of Japan, **70**, S34 (2018). **Cited 15 times**.

[116] "Subaru High-z Exploration of Low-Luminosity Quasars (SHELLQs). II. Discovery of 32 quasars and luminous galaxies at $5.7 < z < 6.8$"
Y. Matsuoka *et al.*, Publications of the Astronomical Society of Japan, **70**, S35 (2018). **Cited 21 times**.

[117] "The stellar mass, star formation rate and dark matter halo properties of LAEs at $z \sim 2$"
H. Kusakabe *et al.*, Publications of the Astronomical Society of Japan, **70**, 4 (2018). **Cited 4 times**.

[118] "ALMA 26 arcmin^2 Survey of GOODS-S at One-millimeter (ASAGAO): X-Ray AGN Properties of Millimeter-selected Galaxies"
Y. Ueda *et al.*, The Astrophysical Journal, **853**, 24 (2018). **Cited 8 times**.

[119] "Full-data Results of Hubble Frontier Fields: UV Luminosity Functions at $z \sim 6-10$ and a Consistent Picture of Cosmic Reionization"
M. Ishigaki *et al.*, The Astrophysical Journal, **854**, 73 (2018). **Cited 49 times**.

[120] "Size-Luminosity Relations and UV Luminosity Functions at $z = 6-9$ Simultaneously Derived from the Complete Hubble Frontier Fields Data"
R. Kawamata *et al.*, The Astrophysical Journal, **855**, 4 (2018). **Cited 18 times**.

Papers in Conference Proceedings

[121] "Spectroscopic confirmation of three z-dropout galaxies at $z = 6.844-7.213$: Demographics of Lyα emission in $z \sim 7$ galaxies"
Y. Ono, AIP Conference Proceedings, **1480**, 277-280 (2012).

[122] "The Resolved Kennicutt-Schmidt Law in Nearby Galaxies"
R. Momose *et al.*, Molecular Gas, Dust, and Star Formation in Galaxies, **292**, 335-335 (2013).

[123] "Early Galaxies and Reionization: Implications from Recent Observations"
M. Ouchi, The First Billion Years of Galaxies and Black Holes, 3 (2014).

[124] "TMT Synergies with Subaru HSC+PFS and Other Facilities"
M. Ouchi, Thirty Meter Telescope Science Forum, 62 (2014).

[125] "Evolution and Feedback Effects of High-z Star-Forming Galaxies"
M. Ouchi, IAU General Assembly, **29**, 2254171 (2015).

[126] "Statistical Study of Stellar/AGN Feedback Evolution at High Redshifts"
S. Yuma *et al.*, IAU General Assembly, **29**, 2254547 (2015).

[127] "Resolving the Extragalactic Background Light with Multi-field Deep ALMA Data"
S. Fujimoto *et al.*, Astronomical Society of the Pacific Conference Series, **499**, 21 (2015).

[128] "Evolution and Feedback Effects of High-z Star-Forming Galaxies"
M. Ouchi, IAU Focus Meeting, **29B**, 228-228 (2016).

[129] "Redshift Evolution of Galactic Outflows Revealed with Spectra of Large Surveys"
Y. Sugahara, The Galaxy Ecosystem: Flow of Baryons through Galaxies, 23 (2017).

THEORY GROUP

Introduction

The primary interests of the theory group are particle physics phenomenology and particle cosmology. The collaborative effort in cosmology and particle physics provides synergy effects in understanding the fundamental law of the Universe.

The theory group has been led by Kawasaki and Ibe. After 2012, the group hosted twelve PDs. The research led to the publications of 194 papers in refereed journals, and 5 papers under referee. The group also conducted the education in the graduate school in collaboration with the Department of Physics. The group accepted twenty-seven graduate-school students after 2012, and ten of them have acquired Ph.D.

Research Highlights

The research activities of the theory group cover a broad range of particle physics and cosmology. Research highlights of the theory group after 2012 are;

- A full two-loop calculation of the mass splitting of the neutral and the charged winos in [164].
- The dark matter detection rates taking into account the final state ionization/excitation of the atoms caused by the nucleus recoil by dark matter (the Migdal effect) [19].
- Spontaneous suppression of the tensor-to-scalar ratio r of the minimal chaotic inflation in the presence of a scalar field which takes a large expectation value during inflation [74].
- Improved analysis of effects of long-lived massive particles decaying during the BBN epoch on the primordial abundances of light elements [16].
- Field-theoretic lattice simulations of the axion abundance produced by the string and the domain-wall network [93].
- Primordial black hole formation in a double inflation model and axion curvaton models [42, 34, 31, 14, 10, 9, 198].

Research Activities: Particle Phenomenology

The Standard Model of particle physics has been confirmed by the discovery of the Higgs boson at the LHC experiments in 2012. Particle physics has entered a new era for discovering new physics beyond the Standard Model.

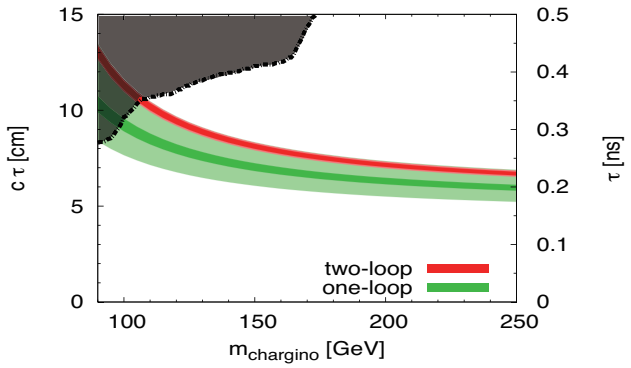

Fig. 1. The lifetime of charged wino evaluated by using δm at the one-loop (green band) and two-loop (red band). The dark shaded region is excluded by the ATLAS collaboration at 95%CL ($\sqrt{s} = 7\,\text{TeV}$, $\mathscr{L} = 4.7\,\text{fb}^{-1}$).

Supersymmetry

For decades, supersymmetry has been widely studied as one of the top candidates for physics beyond the Standard Model which allows a large separation of low energy scales from high energy scales such as the Planck scale. The precise unification of the gauge coupling constants at the scale of the grand unified theory (GUT) also strongly supports the minimal supersymmetric standard model (MSSM). The supersymmetric standard model is entirely consistent with the feature of the elementary scalar field of the discovered Higgs boson.

The pure gravity mediation model proposed by M. Ibe in a collaboration with T. Yanagida is one of the most attractive models which explains the observed Higgs boson mass, i.e. 125 GeV. We study various aspects of the pure gravity mediation model (see e.g. [186, 155, 148, 145, 139, 130, 125, 97, 92, 76]).

In particular, we performed a full two-loop calculation of the mass splitting of the neutral and the charged winos in [164]. The wino (the superpartner of the weak gauge boson) is the lightest supersymmetric particle (LSP) in the pure gravity mediation model, and the neutral wino is a good candidate for dark matter. Due to a tiny mass difference, the charged wino has a long lifetime and can be searched for the disappearing charged tracks inside the detectors at the LHC experiments. Our two-loop calculation shows that the splitting is reduced by a few MeV compared to the one-loop calculation, which leads to about a 30% longer lifetime of the charged wino (Fig. 1). Our results are used in analyses of the wino searches by the ATLAS/CMS experiments.

In the theory group, we also studied various models

of the supersymmetric Standard Model which address phenomenological and cosmological aspects such as the gravitino dark matter, the muon anomalous magnetic moments [194, 193, 175, 160, 158, 152, 150, 149, 124, 65, 62, 39, 37].

Strong CP problem

The strong CP problem is longstanding and probably one of the most puzzling issues of the Standard Model. Although the Peccei-Quinn (PQ) mechanism provides a successful solution to the problem, it is not very satisfactory from various theoretical points of view, as it relies on a global PQ U(1) symmetry. An even tiny explicit breaking of the PQ symmetry spoils the PQ mechanism, while it is conceived that any global symmetries are broken by quantum gravitational effects.

In theory group, we are intensively pursuing theoretical framework which leads to the global PQ symmetry as an accidental symmetry of gauge symmetries [27, 5, 142, 77, 22]. As the gauge symmetries are not broken by quantum gravity effects, such construction makes the PQ mechanism more plausible. For example, we propose a general prescription to achieve the global PQ symmetry which originates from a gauged U(1) symmetry, $U(1)_{gPQ}$ [27]. This mechanism is a generalization of the mechanisms which achieve the PQ symmetry as an accidental symmetry resulting from (discrete) gauge symmetries in the literature.

We also proposed a model of axion where the PQ breaking scale is in the TeV range [82, 29]. With such a low scale PQ breaking, the PQ breaking by quantum gravitational effects do not spoil the PQ mechanism. By introducing a mirror copied sector of the Standard Model with the larger mass scales, the QCD axion is made heavy so that the axion evades experimental constraints. The Peccei-Quinn mechanism still solves the strong CP-problem due to spontaneously broken $\mathbb{Z}_2$ exchanging symmetry between the Standard Model and its mirror copy. Due to its rather low mass scale, this model can be tested in collider experiments.

Dark Matter

The existence of dark matter has been established by a wide range of cosmological and astrophysical observations. Nevertheless, its nature remains elusive. Identification of the nature of DM is one of the most important challenges of modern particle physics. In theory group, we have proposed many new models of dark matter which are interrelated to physics beyond the Standard Model. We are also studying how to identify dark matter experimentally through direct/indirect detection experiments.

Among various candidates for dark matter, thermal relic dark matter is one of the most attractive candidates. The beauty of thermal relic dark matter is that the resultant density is determined by the size of the annihilation cross section of dark matter and does not depend on the initial condition. As the annihilation cross section of dark matter cannot exceed the so-called unitarity limit, the mass of thermal relic dark matter is constrained to be less than a few hundreds TeV. In Ref. [43], we challenged the unitarity limit and proposed a model of thermal relic dark matter where the annihilation cross section effectively exceeds the unitarity limit. As a result, we showed that thermal relic dark matter can be in the PeV range, which, for example, allows a new interpretation of the flux of extraterrestrial neutrinos in the PeV range observed by the IceCube experiment.

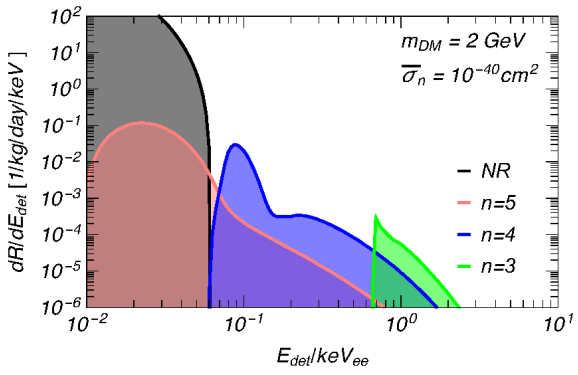

Fig. 2. The event rates at the single-phase experiments with liquid Xe target for 2 GeV dark matter. The green, blue, and pink lines show the ionization rates from $n = 3$, 4, and 5, respectively. Here, we do not take the energy resolution into account.

The direct detection experiment of dark matter is obviously the most important channel to identify its nature, where it is detected by searching for its scattering with the atomic nuclei. In Ref. [19], we provide a coherent formalism of the dark matter detection rates which takes into account the final state ionization/excitation of the atoms caused by the nucleus recoil by dark matter (the Migdal effect). We found that the final state ionization/excitation can enhance the detectability of rather light dark matter in the GeV mass range via the nuclear scattering (Fig. 2).

Collider Phenomenology

Collider phenomenology has been providing many important data on the standard model (SM) and physics beyond the SM. In ICRR, theory group is also studying physics beyond the SM by utilizing new data from the collider experiments [71, 52, 50, 41, 33].

The search for high-mass diphoton resonance is ongoing at the LHC, as it provides a definite evidence of physics beyond the Standard Model. Along with the diphoton resonance, many theoretical models also predict resonances decaying not into a pair of photons but into a pair of highly collimated photon-jets. In Ref. [41], we studied how well we can distinguish such diphoton resonance imposters, i.e. diphoton-jet resonances, from diphoton resonances by examining detector responses to the photon-jets. We find that the sum of p_T of the

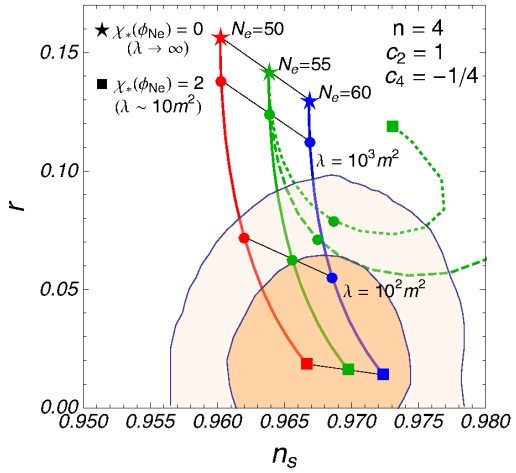

Fig. 3. Predictions on the spectral index n_s and the tensor-to-scalar ratio r of the minimal chaotic inflation model with spontaneous suppression. The solid lines show the predictions when we change the model parameters of the additional scalar field.

first $e^+ + e^-$ pair from the photon conversion provides strong discrimination power. For example, it is possible to discriminate the diphoton-jet resonance from the diphoton resonance at around the 5σ level with an integrated luminosity of $\mathscr{L} = 100\,\mathrm{fb}^{-1}$ for a signal cross section after the cut of 1 fb and $m_s = 750\,\mathrm{GeV}$.

Higgs Properties

The discovery of the Higgs boson and precision measurement of the top quark mass at the LHC and Tevatron now allow us to study the detailed shape of the Higgs potential by extrapolating the Higgs coupling constants according to the renormalization group running. In fact, it has been shown that the electroweak vacuum is not absolutely stable if the Standard Model is valid up to $\mathscr{O}(10^{10})\,\mathrm{GeV}$ or higher. The lifetime of the electroweak vacuum has been one of the important topics in particle physics and cosmology.

In Ref. [26, 25, 18, 4], we performed a precise calculation of the decay rate of the electroweak vacuum in the Standard Model using a gauge invariant calculation of the decay rate at the one-loop level. The decay rate of the electroweak vacuum in the standard model is estimated to be $\log\gamma\times\mathrm{Gyr}\,\mathrm{Gpc}^3 = -582^{+40\,+184\,+144\,+2}_{-45\,-329\,-218\,-1}$, where the 1st, 2nd, 3rd, and 4th errors are due to the uncertainties of the Higgs mass, the top quark mass, the strong coupling constant and the choice of the renormalization scale, respectively.

We also studied high energy behaviors of the Higgs potential in conjunction to physics beyond the Standard Mode and implications on cosmology [129, 109, 100].

Inflation Model Building

Cosmic inflation provides a compelling explanation for why our universe is so huge, which is now considered as an important pillar of big bang cosmology. However, it is not known how inflation occurred and how the Universe was reheated after inflation. In the theory group, we are extensively studying models of cosmic inflation as well as the thermal history of the Universe after inflation including the origin of the asymmetry of the matter-anti-matter in the Universe [168, 132, 122, 119, 115, 105, 103, 99, 85, 74].

Among slow-roll inflation models, chaotic inflation is the most attractive model, since it is free from the initial condition problem. The recent observations of the cosmic microwave background, however, disfavors the chaotic inflation model with a quadratic scalar potential. In Ref. [74], we pointed out that the prediction of the minimal chaotic inflation model can be altered if a scalar field other than the inflaton field takes a large field value close to the Planck scale during inflation. With such effects, we find that the minimal chaotic inflation model, especially the model with a quadratic potential, is still consistent with recent observations of the cosmic microwave background fluctuation without modifying the inflation model itself (Fig. 3).

Research Activities: Astroparticle Physics

The progress in particle physics beyond the Standard Model leads us to more insight into the fundamental aspects of the early universe. At the same time, cosmology and astrophysics are used to test new theories in particle physics. Such particle cosmology is one of main subjects of the theory group.

Big Bang Nucleosynthesis

The predicted abundances of the light elements in Big Bang Nucleosynthesis (BBN) are sensitive to the cosmological scenario of the early universe. Exotic cosmological scenarios based on physics beyond the standard model would modify the light-element abundances too much to be consistent with the observations. Thus, the BBN provides significant constraints on the new particles which change the cosmological evolution at the cosmic time $t \sim 10^{-2} - 10^{12}$sec. In 2005 we derived general constraints on the relic abundances of long-lived particles with hadronic decay modes as well as radiative decay modes.[1] Since no reliable BBN constraints on unstable particles which decay into hadron had not been obtained, our work attracted much attention. The paper gets more than 700 citations as of this writing. Since our previous analysis, we have been updating constrains and applying to decay and annihilation processes of exotic particles at the BBN epoch.

In Ref. [16] we investigated effects of long-lived massive particles, which decay during the BBN epoch, on the primordial abundances of light elements by improving the previous studies. Improvement includes upadate of the reaction rates of the standard BBN reactions, use of the most recent observational data of light

*1 Phys. Rev. D **71**, 083502 (2005) by M. Kawasaki*, K. Kohri and T. Moroi

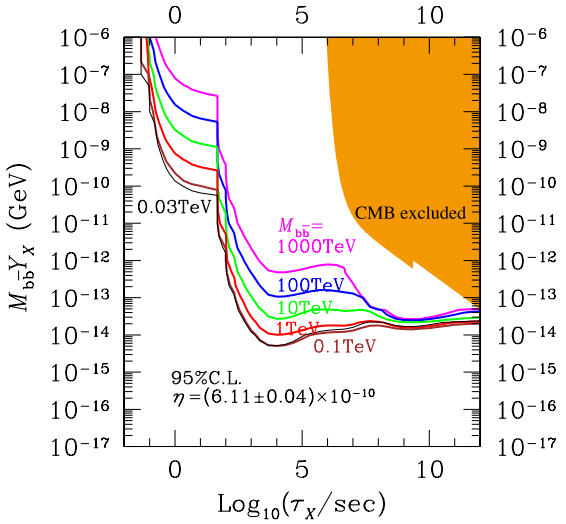

Fig. 4. Constraints on the abundance $m_X Y_X$ and lifetime τ_X of long-lived particles which mainly decay into $b\bar{b}$. Here $m_X (= M_{b\bar{b}})$ is the mass of the decaying particle and Y_X is the ratio of the decaying particle number density to entropy density. The black, red, green, blue and magenta solid lines denote the BBN constraints for $m_X = 0.03,\ 0.1,\ 1,\ 10,\ 100$ and 1000 TeV, respectively. The orange shaded regions are excluded by the constraint from the CMB spectral distortion.

element abundances, effects of the interconversion of energetic nucleons at the time of inelastic scatterings with background nuclei, and effects of the hadronic shower induced by high energy anti-nucleons. Using the improved calculation we derived upper bounds on relic abundance of the decaying particle as a function of its lifetime (Fig. 4). We also applied our analysis to unstable gravitino, the superpartner of the graviton in supersymmetric theories, and obtained constraints on the reheating temperature after inflation. It was found that the upper bound on the reheating temperature T_R is $10^5 - 10^6$ GeV for relatively light gravitino mass i.e., for $m_{3/2} \lesssim$ a few TeV. In Ref. [67] we studied the effects of dark-matter annihilation during the BBN epoch on the BBN and derived upper bounds on the dark-matter pair-annihilation cross section.

The BBN also gives constraints on small-scale density perturbations. We derived the constraints on the adiabatic density perturbations with scale $\sim 10^{4-5}$ Mpc^{-1} [46] and baryonic isocurvature perturbations with scale $\gtrsim 4 \times 10^8$ Mpc^{-1} [196].

Axion Cosmology

The axion is a pseudo Nambu-Goldstone boson of the PQ symmetry, which is introduced to the standard model as a solution to the Strong CP problem. The axion has rich implications for astrophysics and cosmology.

When the spontaneous breaking of the PQ $U(1)$ occurs after inflation, a cosmological network of axionic strings is formed. The produced axionic strings lose their energy by emitting axions and follow the so-called scaling solution. How much the emitted axions contribute to the present dark matter density crucially depends on their energy spectrum. We estimated the energy spectrum precisely by using field-theoretic lattice simulations in a box of 512^3 grids and found that the spectrum has a sharp peak at the horizon scale. From our spectrum we obtained constraint on the axion decay constant $F_a < 2 \times 10^{11}$ GeV [93]. Recently, in Ref. [1] we upgraded our simulation in our previous study in terms of the number of grids (4096^3) as well as the suite of analysis methods. The improved simulation revealed that global strings do not evolve according to the scaling solution but its scaling parameter, or the number of long strings per horizon, increases logarithmically in time. We also computed the spectrum of the axion radiated from the axion strings. The result was in agreement with the previous studies. Our results indicates the abundance of axion can be enhanced by a factor of two or three.

Axion models also predict a formation of domain walls, when the temperature of the universe becomes comparable to $\sim$ GeV. At that time, $N_{\rm DW}$ domain walls are attached to strings, where $N_{\rm DW}$ is an integer number whose value depends on axion models. The subsequent history of the universe is different between models with $N_{\rm DW} = 1$ and $N_{\rm DW} > 1$.

In Ref. [93],[2] we studied the scenario with $N_{\rm DW} = 1$ where domain walls are bounded by strings and they immediately collapse due to the tension of walls. We investigated the formation and annihilation of string-wall networks by performing field-theoretic lattice simulations. We analyzed the spectrum of axions radiated from collapse of domain walls and found that axions produced by the decay of domain walls give a significant contribution to the cold dark matter abundance. Together with contributions from coherent oscillation and emission from strings, axions can account for all dark matter of the universe for $F_a \simeq (4-7) \times 10^{10}$ GeV (Fig. 5).

On the other hand, for the models with $N_{\rm DW} > 1$ the string-wall networks become long-lived, which leads to a serious problem in the standard cosmology. The problem can be avoided by introducing the explicit PQ symmetry breaking term, which leads to the annihilation of string-wall networks at a late time. In Ref. [187, 93], we investigated the evolution of such long-lived domain walls and estimated their decay rate. We found that if we allow the mild tuning on the model parameters the axion can be dark matter for $F_a = \mathcal{O}(10^8 - 10^{10})$ GeV (Fig. 5).

When the PQ symmetry is broken during inflation, the axionic strings and domain walls are diluted away by inflation. However, in this case the axion field acquires fluctuations with amplitude given by the Hubble

[*2] See also Phys. Rev. D **85**, 105020 (2012) by T. Hiramatsu, M. Kawasaki*, K. Saikawa* and T. Sekiguchi.

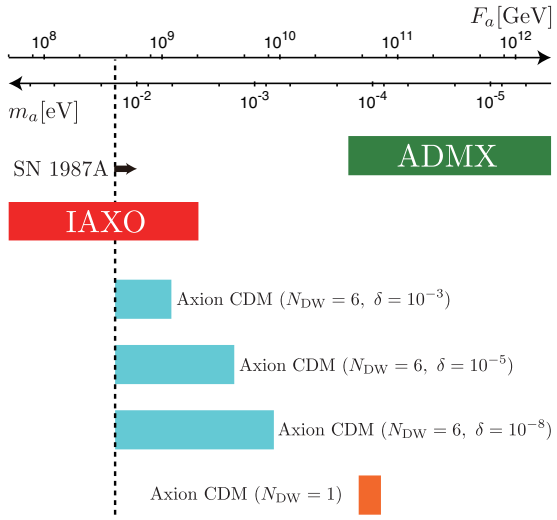

Fig. 5. The schematics of the parameter ranges where the axion becomes cold dark matter for the models with $N_{\rm DW} = 1$ (orange interval) and $N_{\rm DW} = 6$ (light blue interval). The blue intervals represent the allowed region for $\delta = 10^{-8}$, 10^{-5}, and 10^{-3} (δ: phase of the explicit $U(1)_{\rm PQ}$ breaking term). The vertical dotted line corresponds to the bound from the observation of SN1987A. Red and green intervals represent the regions that will be covered by the axion search experiments, IAXO and ADMX, respectively

parameter during inflation, which leads to isocurvature density perturbations. Since the isocurvature perturbations are stringently constrained by observations of the cosmic microwave background (CMB), the Hubble parameter during inflation should be small. This problem is ameliorated if the PQ field has a larger expectation value during inflation. However, in this case the PQ field starts to oscillate after inflation and induces large field fluctuations through parametric resonance, which restores the PQ symmetry and leads to formation of strings and domain walls. In Ref. [146] we performed lattice simulations and obtained the condition for the PQ symmetry not to be restored. Furthermore we proposed models where the parametric resonance is ineffective and hence domain walls are not formed [72, 13]. We pointed out that the allowed region of the decay constant F_a is reduced to a rather narrow region for a given tensor-to-scalar ration r. Thus, if r is determined in the near future we can predict the axion decay constant F_a [7].

Baryogenesis and Q-ball

Baryogenesis is one of the main issues in the theories of the early universe. Among many baryogenesis scenarios proposed so far, the mechanism proposed by Affleck and Dine is a promising candidate since it can be realized in the SUSY standard model. It is known that the Affleck-Dine mechanism is complicated by the formation of Q-balls which is a non-topological solution in the SUSY standard model.

In Ref. [116] we investigated the Affleck-Dine baryogenesis in high-scale inflation models. High-scale inflation is observationally favored because gravitational waves produced during inflation can be detected in future. We found that successful baryogenesis requires too low reheating temperature to produce dark matter particles thermally. Using the non-thermal dark matter production mechanism [127] and Q-balls we constructed consistent scenarios to account for the observed baryon and dark matter densities. In Ref. [20] we studied accidental suppression of the baryon asymmetry due to oscillation of the Affleck-Dine field after inflation.

In Ref. [179] we reexamined the decay rate of a Q-ball. We applied the results to a realistic model in the gauge-mediated supersymmetry breaking and found the branching ratio of the Q-ball decay into the gravitino much smaller than the one estimated in the previous analysis. Based on this analysis, we reinvestigate the cogenesis scenario that the abundances of the baryons and the gravitino dark matter is naturally explained by the decay of the Q-balls, and found that the scenario works well [170]. Furthermore we revisited the scenario of baryon and dark matter cogenesis from Q-balls in gravity mediation in respect of the improved Q-ball decay rates, and found that the successful cogenesis takes place [166, 110].

If a Q-ball is stable, it can account for dark matter of the universe. We studied Q-ball dark matter in gauge-mediated supersymmetry breaking. It was found that the Q-ball is a good dark matter candidate and dark matter Q-balls are detectable by IceCube-like experiments in the future [101, 91].

It is possible that Q-alls are electrically charged. Such Q-balls are called gauged Q-balls. In Refs. [79, 47, 28, 23] we studied the evolution of Q-balls with both baryon and lepton numbers and found that they can evolve into gauged Q-balls by emitting charged leptons. Those Q-balls are stable and can be charged dark matter of the universe.

Formation of Primordial Black Holes

In September 2015, for the first time in history, gravitational waves from the coalescence of binary black holes were detected by the Laser Interferometer Gravitational-Wave Observatory (LIGO). This event, GW150914, comes from the merger of black holes (BHs) with $\sim 30 M_\odot$. Afterward, more gravitational wave events caused by the merger of BHs with similar masses were reported. One of the promising candidates for BHs causing the LIGO GW events is primordial black holes (PBHs). PBHs are considered as a good candidate for dark matter of the universe. Although various observations give stringent constraints on the DM PBH mass, there remains a window between $10^{-13} M_\odot - 10^{-10} M_\odot$. Therefore, we studied formation of PBHs which account for the LIGO events and/or dark matter.

In Refs. [42, 34, 31, 14, 10] we studied PBH formation in a double inflation model which has two stages of inflation, pre-inflation and new inflation. The new in-

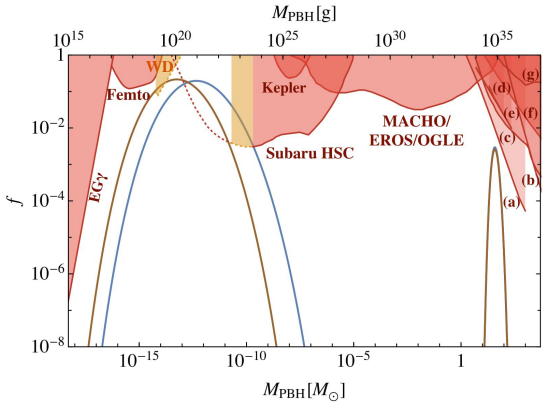

Fig. 6. PBH mass spectra for appropriate sets of model parameters (blue solid and brown lines). The red shaded regions show the observational constraints on the monochromatic mass function. The orange shaded regions are observational constraints which we neglect due to uncertainties.

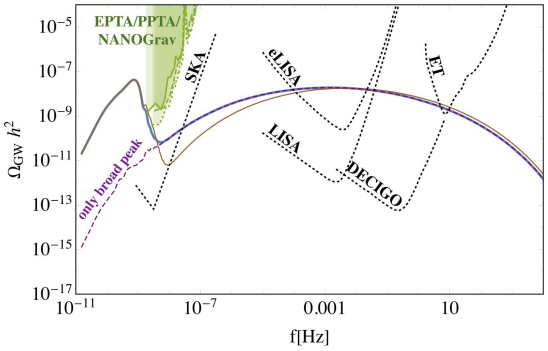

Fig. 7. The induced gravitational wave spectra for the same parameter set as Fig. 6. Green shaded region is excluded by the pulsar timing array experiments. The black dotted lines show the prospects of the future experiments; SKA, eLISA, LISA and DECIGO.

flation can yield small scale perturbations large enough for PBH formation, while the pre-inflation accounts for the scalar perturbations at the large scale observed by Planck. We found that the large density perturbations necessary for the LIGO PBHs produce secondary gravitational waves on which the pulsar timing array experiments put severe constraints. To avoid the stringent constraints the power spectrum has a sharp peak at the scale $k \sim 10^6 \mathrm{Mpc}^{-1}$. We showed that such a peak can be realized in the double inflation model[34]. We also showed that the double inflation model produce PBHs with mass function peak at $\sim 10^{-13} M_\odot$ which account for all dark matter without conflicting with observational constraints [31]. Furthermore, in Ref. [10] we showed that the double inflation can realize a power spectrum with two peaks and hence can simultaneously produce PBHs for all DM in a broad mass spectrum around $\mathcal{O}(10^{-13})M_\odot$ and PBHs for the LIGO events in a sharp mass spectrum at $\mathcal{O}(10)M_\odot$ (Fig. 6). We also showed that the energy density of the secondary gravitational waves is large enough to be detected by future detectors.

In Ref. [9] we investigated the axion curvaton model for PBH formation. The model realizes the highly blue-tilted power spectrum of primordial curvature perturbations, which leads to large perturbation amplitude at small scales. We showed that this model can produce PBHs for the LIGO events and the stringent constraints from pulsar timing array experiments can be avoided owing to non-Gaussianity. We also built another axion curvaton model [198].

In Refs. [11, 195] we proposed a novel PBH formation scenario based on the Affleck-Dine mechanism for baryogenesis. In this scenario, $\mathcal{O}(10)M_\odot$ PBHs and Q-balls are formed from high baryon-density bubbles produced by the Affleck-Dine mechanism. The former account for the LIGO events and the latter explain the dark matter of the universe.

Members

Staffs

Masahiro Kawasaki, Professor, 2004–present
Masahiro Ibe, Assoc. Professor, 2011–present

Postdoctoral Fellows

Motohiko Kusakabe, 2009–2012
Shuichiro Yokoyama, 2012–2014
Shohei Sugiyama, 2011–2013
Daisuke Yamauchi, 2011–2013
Etsuko Kawakami, 2014-2015
Kunio Kaneta, 2014-2015
Keisuke Harigaya, 2015-2015
Ryo Saito, 2015-2015
Yoshihiko Oyama, 2015-2017
Yutaro Shoj, 2016-2018
Kohei Hayashi, 2018-present
Ippei Obata, 2018-present

Graduate Students

Ten students were awarded doctor degrees and fifteen students earned master degrees during 2012–2018, supervised by ICRR staff members.

List of Publications

(The symbol ∗ indicates the authors belonging to ICRR.)
Seventeen papers, [52] [155], [164], [187] [190], [186], are cited more than fifty times. One papers, [93], [161] are cited more than a hundred times.

Papers in Refereed Journals (after April 2012)

[1] Long-term dynamics of cosmological axion strings
M. Kawasaki, T. Sekiguchi, M. Yamaguchi and J. Yokoyama, PTEP (2018) **2018**, no. 9, 091E01 (2018) [arXiv:1806.05566 [hep-ph]].

[2] $B-L$ as a Gauged Peccei-Quinn Symmetry
M. Ibe*, M. Suzuki and T. T. Yanagida
JHEP **1808**, 049 (2018) [arXiv:1805.10029 [hep-ph]].

[3] Exploring compensated isocurvature perturbations with CMB spectral distortion anisotropies
T. Haga, K. Inomata*, A. Ota and A. Ravenni
JCAP **1808**, no. 08, 036 (2018) [arXiv:1805.08773 [astro-ph.CO]].

[4] Decay Rate of Electroweak Vacuum in the Standard Model and Beyond
S. Chigusa, T. Moroi and Y. Shoji*
Phys. Rev. D **97**, no. 11, 116012 (2018) [arXiv:1803.03902 [hep-ph]].

[5] Gauged Peccei-Quinn symmetry – A case of simultaneous breaking of SUSY and PQ symmetry
H. Fukuda, M. Ibe*, M. Suzuki* and T. T. Yanagida
JHEP **1807**, 128 (2018) [arXiv:1803.00759 [hep-ph]].

[6] Primordial black holes and uncertainties in the choice of the window function
K. Ando*, K. Inomata* and M. Kawasak*i
Phys. Rev. D **97**, no. 10, 103528 (2018) [arXiv:1802.06393 [astro-ph.CO]].

[7] Cosmologically allowed regions for the axion decay constant F_a
M. Kawasaki*, E. Sonomoto* and T. T. Yanagida
Phys. Lett. B **782**, 181 (2018) [arXiv:1801.07409 [hep-ph]].

[8] Oscillons from Pure Natural Inflation
J. P. Hong*, M. Kawasaki* and M. Yamazaki
Phys. Rev. D **98**, no. 4, 043531 (2018) [arXiv:1711.10496 [astro-ph.CO]].

[9] Primordial black holes for the LIGO events in the axionlike curvaton model
K. Ando*, K. Inomata*, M. Kawasaki*, K. Mukaida and T. T. Yanagida, Phys. Rev. D **97**, no. 12, 123512 (2018) [arXiv:1711.08956 [astro-ph.CO]].

[10] Double inflation as a single origin of primordial black holes for all dark matter and LIGO observations
K. Inomata*, M. Kawasaki*, K. Mukaida and T. T. Yanagida
Phys. Rev. D **97**, no. 4, 043514 (2018) [arXiv:1711.06129 [astro-ph.CO]].

[11] Cogenesis of LIGO Primordial Black Holes and Dark Matter
F. Hasegawa* and M. Kawasaki*
Phys. Rev. D **98**, no. 4, 043514 (2018) [arXiv:1711.00990 [astro-ph.CO]].

[12] Inflaton fragmentation in E-models of cosmological α-attractors
' F. Hasegawa* and J. P. Hong*
Phys. Rev. D **97**, no. 8, 083514 (2018) [arXiv:1710.07487 [astro-ph.CO]].

[13] Domain wall and isocurvature perturbation problems in a supersymmetric axion model
M. Kawasaki* and E. Sonomoto*
Phys. Rev. D **97**, no. 8, 083507 (2018) [arXiv:1710.07269 [hep-ph]].

[14] $\mathcal{O}(10)M_\odot$ primordial black holes and string axion dark matter
K. Inomata*, M. Kawasaki*, K. Mukaida, Y. Tada* and T. T. Yanagida
Phys. Rev. D **96**, no. 12, 123527 (2017) doi:10.1103/PhysRevD.96.123527 [arXiv:1709.07865 [astro-ph.CO]].

[15] Gravitino problem in inflation driven by inflaton-polonyi Kähler coupling
F. Hasegawa*, K. Nakayama, T. Terada and Y. Yamada
Phys. Lett. B **777**, 270 (2018) doi:10.1016/j.physletb.2017.12.038 [arXiv:1709.01246 [hep-ph]].

[16] Revisiting Big-Bang Nucleosynthesis Constraints on Long-Lived Decaying Particles
M. Kawasaki*, K. Kohri, T. Moroi and Y. Takaesu
Phys. Rev. D **97**, no. 2, 023502 (2018) [arXiv:1709.01211 [hep-ph]].

[17] Adiabatic suppression of the axion abundance and isocurvature due to coupling to hidden monopoles
M. Kawasaki*, F. Takahashi and M. Yamada
JHEP **1801**, 053 (2018) [arXiv:1708.06047 [hep-ph]].

[18] State-of-the-Art Calculation of the Decay Rate of Electroweak Vacuum in the Standard Model
S. Chigusa, T. Moroi and Y. Shoji
Phys. Rev. Lett. **119**, no. 21, 211801 (2017) [arXiv:1707.09301 [hep-ph]].

[19] Migdal Effect in Dark Matter Direct Detection Experiments
M. Ibe*, W. Nakano*, Y. Shoji* and K. Suzuki*
JHEP **1803**, 194 (2018) [arXiv:1707.07258 [hep-ph]].

[20] Oscillating Affleck-Dine condensate and its cosmological implications
F. Hasegawa* and M. Kawasaki*
Phys. Rev. D **96**, no. 6, 063518 (2017) [arXiv:1706.08659 [hep-ph]].

[21] Foreground effect on the J-factor estimation of ultra-faint dwarf spheroidal galaxies
K. Ichikawa, S. i. Horigome, M. N. Ishigaki, S. Matsumoto, M. Ibe*, H. Sugai and K. Hayashi
Mon. Not. Roy. Astron. Soc. **479**, no. 1, 64 (2018) [arXiv:1706.05481 [astro-ph.GA]].

[22] Dynamical Clockwork Axions
R. Coy, M. Frigerio and M. Ibe*
JHEP **1710**, 002 (2017) [arXiv:1706.04529 [hep-ph]].

[23] Gauged Q-ball Decay Rates into Fermions
J. P. Hong* and M. Kawasaki*
Phys. Rev. D **96**, no. 10, 103526 (2017) [arXiv:1706.01651 [hep-ph]].

[24] Does the detection of primordial gravitational waves exclude low energy inflation?
T. Fujita, R. Namba and Y. Tada*
Phys. Lett. B **778**, 17 (2018) [arXiv:1705.01533 [astro-ph.CO]].

[25] False Vacuum Decay in Gauge Theory
M. Endo, T. Moroi, M. M. Nojiri and Y. Shoji*
JHEP **1711**, 074 (2017) [arXiv:1704.03492 [hep-ph]].

[26] On the Gauge Invariance of the Decay Rate of False Vacuum
M. Endo, T. Moroi, M. M. Nojiri and Y. Shoji*
Phys. Lett. B **771**, 281 (2017) [arXiv:1703.09304 [hep-ph]].

[27] A "gauged" $U(1)$ Peccei-Quinn symmetry
H. Fukuda, M. Ibe*, M. Suzuki* and T. T. Yanagida
Phys. Lett. B **771**, 327 (2017) doi:10.1016/j.physletb.2017.05.071 [arXiv:1703.01112 [hep-ph]].

[28] New type of charged Q -ball dark matter in gauge mediated SUSY breaking models
J. P. Hong* and M. Kawasaki*
Phys. Rev. D **95**, no. 12, 123532 (2017) [arXiv:1702.00889 [hep-ph]].

[29] Dark Matter Candidates in a Visible Heavy QCD Axion Model
H. Fukuda, M. Ibe* and T. T. Yanagida
Phys. Rev. D **95**, no. 9, 095017 (2017) [arXiv:1702.00227 [hep-ph]].

[30] Gravitino Problem in Minimal Supergravity Inflation
F. Hasegawa*, K. Mukaida, K. Nakayama, T. Terada and Y. Yamada
Phys. Lett. B **767**, 392 (2017) doi:10.1016/j.physletb.2017.02.030 [arXiv:1701.03106 [hep-ph]].

[31] Inflationary Primordial Black Holes as All Dark Matter
K. Inomata*, M. Kawasaki*, K. Mukaida, Y. Tada and T. T. Yanagida
Phys. Rev. D **96**, no. 4, 043504 (2017) [arXiv:1701.02544 [astro-ph.CO]].

[32] Relaxation leptogenesis, isocurvature perturbations, and the cosmic infrared background
M. Kawasaki*, L. Pearce, L. Yang and A. Kusenko
Phys. Rev. D **95**, no. 10, 103006 (2017) [arXiv:1701.02175 [hep-ph]].

[33] Constraints on $L_\mu - L_\tau$ gauge interactions from rare kaon decay
M. Ibe*, W. Nakano* and M. Suzuki*
Phys. Rev. D **95**, no. 5, 055022 (2017) [arXiv:1611.08460 [hep-ph]].

[34] Inflationary primordial black holes for the LIGO gravitational wave events and pulsar timing array experiments
K. Inomata*, M. Kawasaki*, K. Mukaida, Y. Tada* and T. T. Yanagida
Phys. Rev. D **95**, no. 12, 123510 (2017) [arXiv:1611.06130 [astro-ph.CO]].

[35] A map of the non-thermal WIMP
H. Kim, J. P. Hong* and C. S. Shin
Phys. Lett. B **768**, 292 (2017) doi:10.1016/j.physletb.2017.03.005 [arXiv:1611.02287 [hep-ph]].

[36] Squeezed bispectrum in the δN formalism: local observer effect in field space
Y. Tada* and V. Vennin
JCAP **1702**, no. 02, 021 (2017) [arXiv:1609.08876 [astro-ph.CO]].

[37] Revisiting gravitino dark matter in thermal leptogenesis
M. Ibe*, M. Suzuki and T. T. Yanagida
JHEP **1702**, 063 (2017) [arXiv:1609.06834 [hep-ph]].

[38] Foreground effect on the J-factor estimation of classical dwarf spheroidal galaxies
K. Ichikawa, M. N. Ishigaki, S. Matsumoto,

M. Ibe*, H. Sugai, K. Hayashi and S. i. Horigome
Mon. Not. Roy. Astron. Soc. **468**, no. 3, 2884 (2017) [arXiv:1608.01749 [astro-ph.GA]].

[39] Lower limit on the gravitino mass in low-scale gauge mediation with $m_H \simeq 125$ GeV
M. Ibe* and T. T. Yanagida
Phys. Lett. B **764**, 260 (2017) [arXiv:1608.01610 [hep-ph]].

[40] Elucidating Dark Energy with Future 21 cm Observations at the Epoch of Reionization
K. Kohri, Y. Oyama*, T. Sekiguchi and T. Takahashi
JCAP **1702**, no. 02, 024 (2017) [arXiv:1608.01601 [astro-ph.CO]].

[41] Cracking down on fake photons: Cases of diphoton resonance imposters
H. Fukuda, M. Ibe, O. Jinnouchi and M. Nojiri
PTEP **2017**, no. 3, 033B05 (2017) doi:10.1093/ptep/ptx019 [arXiv:1607.01936 [hep-ph]].

[42] Primordial black holes as dark matter in supergravity inflation models
M. Kawasaki*, A. Kusenko, Y. Tada* and T. T. Yanagida
Phys. Rev. D **94**, no. 8, 083523 (2016) [arXiv:1606.07631 [astro-ph.CO]].

[43] Thermal Relic Dark Matter Beyond the Unitarity Limit
K. Harigaya, M. Ibe*, K. Kaneta, W. Nakano* and M. Suzuki*
JHEP **1608**, 151 (2016) [arXiv:1606.00159 [hep-ph]].

[44] Simple cosmological solution to the Higgs field instability problem in chaotic inflation and the formation of primordial black holes
M. Kawasaki*, K. Mukaida and T. T. Yanagida
Phys. Rev. D **94**, no. 6, 063509 (2016) [arXiv:1605.04974 [hep-ph]].

[45] Revisiting constraints on small scale perturbations from big-bang nucleosynthesis
K. Inomata*, M. Kawasaki* and Y. Tada*
Phys. Rev. D **94**, no. 4, 043527 (2016) [arXiv:1605.04646 [astro-ph.CO]].

[46] Revisiting constraints on small scale perturbations from big-bang nucleosynthesis
K. Inomata*, M. Kawasaki* and Y. Tada*
Phys. Rev. D **94**, no. 4, 043527 (2016) [arXiv:1605.04646 [astro-ph.CO]].

[47] Charged Q-ball Dark Matter from B and L direction
J. P. Hong*, M. Kawasaki* and M. Yamada*
JCAP **1608**, no. 08, 053 (2016) [arXiv:1604.04352 [hep-ph]].

[48] Dark matter annihilation and decay from non-spherical dark halos in galactic dwarf satellites
K. Hayashi, K. Ichikawa, S. Matsumoto, M. Ibe*, M. N. Ishigaki and H. Sugai
Mon. Not. Roy. Astron. Soc. **461**, no. 3, 2914 (2016) [arXiv:1603.08046 [astro-ph.GA]].

[49] Cosmology with the Square Kilometre Array by SKA-Japan
D. Yamauchi *et al. including Y. Oyama** [SKA-Japan Consortium Cosmology Science Working Group]
Publ. Astron. Soc. Jap. **68**, no. 6, R2 (2016) [arXiv:1603.01959 [astro-ph.CO]].

[50] 750 GeV diphoton resonance in a visible heavy QCD axion model
C. W. Chiang, H. Fukuda, M. Ibe* and T. T. Yanagida
Phys. Rev. D **93**, no. 9, 095016 (2016) [arXiv:1602.07909 [hep-ph]].

[51] Why three generations?
M. Ibe*, A. Kusenko and T. T. Yanagida
Phys. Lett. B **758**, 365 (2016) [arXiv:1602.03003 [hep-ph]].

[52] Revisiting Scalar Quark Hidden Sector in Light of 750-GeV Diphoton Resonance
C. W. Chiang, M. Ibe* and T. T. Yanagida
JHEP **1605**, 084 (2016) [arXiv:1512.08895 [hep-ph]], 61 citations counted in INSPIRE as of Nov 2018.

[53] CMB Constraint on Dark Matter Annihilation after Planck 2015
M. Kawasaki*, K. Nakayama and T. Sekiguchi
Phys. Lett. B **756**, 212 (2016) [arXiv:1512.08015 [astro-ph.CO]].

[54] High-scale SUSY from an R-invariant New Inflation in the Landscape
M. Kawasaki*, M. Yamada*, T. T. Yanagida and N. Yokozaki
Phys. Rev. D **93**, no. 5, 055022 (2016) [arXiv:1512.04259 [hep-ph]].

[55] Can massive primordial black holes be produced in mild waterfall hybrid inflation?
M. Kawasaki* and Y. Tada*
JCAP **1608**, no. 08, 041 (2016) [arXiv:1512.03515 [astro-ph.CO]].

[56] Affleck-Dine baryogenesis just after inflation
M. Yamada*
Phys. Rev. D **93**, no. 8, 083516 (2016) [arXiv:1511.05974 [hep-ph]].

[57] Axino dark matter and baryon number asymmetry production by the Q-ball decay in gauge mediation
S. Kasuya, E. Kawakami* and M. Kawasaki*
JCAP **1603**, no. 03, 011 (2016) [arXiv:1511.05655 [hep-ph]].

[58] Suppressing the QCD Axion Abundance by Hidden Monopoles
M. Kawasaki*, F. Takahashi and M. Yamada*
Phys. Lett. B **753**, 677 (2016) [arXiv:1511.05030 [hep-ph]].

[59] The two-field regime of natural inflation
A. Achúcarro, V. Atal, M. Kawasaki* and F. Takahashi
JCAP **1512**, no. 12, 044 (2015) [arXiv:1510.08775 [astro-ph.CO]].

[60] Affleck-Dine leptogenesis and its backreaction to inflaton dynamics
M. Yamada*
Phys. Lett. B **754**, 208 (2016) [arXiv:1510.08514 [hep-ph]].

[61] ,"Spontaneous Baryogenesis from Asymmetric Inflaton
F. Takahashi and M. Yamada*
Phys. Lett. B **756**, 216 (2016) [arXiv:1510.07822 [hep-ph]].

[62] ATLAS on-Z Excess via gluino-Higgsino-singlino decay chains in the NMSSM
K. Harigaya, M. Ibe and T. Kitahara
JHEP **1601**, 030 (2016) [arXiv:1510.07691 [hep-ph]].

[63] Cosmologically safe QCD axion without fine-tuning
M. Yamada, T. T. Yanagida and K. Yonekura
Phys. Rev. Lett. **116**, no. 5, 051801 (2016) [arXiv:1510.06504 [hep-ph]].

[64] Cosmological problems of the string axion alleviated by high scale SUSY of $m_{3/2} \simeq$10-100TeV
M. Kawasaki*, T. T. Yanagida and N. Yokozaki
Phys. Lett. B **753**, 389 (2016) [arXiv:1510.04171 [hep-ph]].

[65] Revisiting R-invariant Direct Gauge Mediation
C. W. Chiang, K. Harigaya*, M. Ibe* and T. T. Yanagida
JHEP **1603**, 145 (2016) [arXiv:1510.04047 [hep-ph]].

[66] Constraints on the neutrino parameters by future cosmological 21 cm line and precise CMB polarization observations
Y. Oyama*, K. Kohri and M. Hazumi
JCAP **1602**, no. 02, 008 (2016) [arXiv:1510.03806 [astro-ph.CO]].

[67] Revisiting Big-Bang Nucleosynthesis Constraints on Dark-Matter Annihilation
M. Kawasaki*, K. Kohri, T. Moroi and Y. Takaesu
Phys. Lett. B **751**, 246 (2015) [arXiv:1509.03665 [hep-ph]].

[68] Can thermal inflation be consistent with baryogenesis in gauge-mediated SUSY breaking models?
T. Hayakawa*, M. Kawasaki* and M. Yamada*
Phys. Rev. D **93**, no. 6, 063529 (2016) [arXiv:1508.03409 [hep-ph]].

[69] Adiabatic Invariance of Oscillons/I-balls
M. Kawasaki*, F. Takahashi and N. Takeda*,
Phys. Rev. D **92**, no. 10, 105024 (2015) [arXiv:1508.01028 [hep-th]].

[70] Strongly broken Peccei-Quinn symmetry in the early Universe
F. Takahashi and M. Yamada*
JCAP **1510**, no. 10, 010 (2015) [arXiv:1507.06387 [hep-ph]].

[71] ,"Diboson Resonance as a Portal to Hidden Strong Dynamics
C. W. Chiang, H. Fukuda, K. Harigaya*, M. Ibe* and T. T. Yanagida
JHEP **1511**, 015 (2015) [arXiv:1507.02483 [hep-ph]].

[72] Dynamics of Peccei-Quinn Breaking Field after Inflation and Axion Isocurvature Perturbations
K. Harigaya*, M. Ibe*, M. Kawasaki* and T. T. Yanagida
JCAP **1511**, no. 11, 003 (2015) [arXiv:1507.00119 [hep-ph]].

[73] Thermalization Process after Inflation and Effective Potential of Scalar Field
K. Mukaida and M. Yamada*
JCAP **1602**, no. 02, 003 (2016) [arXiv:1506.07661 [hep-ph]].

[74] Revisiting the Minimal Chaotic Inflation Model
K. Harigaya*, M. Ibe*, M. Kawasaki* and T. T. Yanagida
Phys. Lett. B **756**, 113 (2016) [arXiv:1506.05250 [hep-ph]].

[75] Cosmologically safe QCD axion as a present from extra dimension
M. Kawasaki*, M. Yamada* and T. T. Yanagida,
Phys. Lett. B **750**, 12 (2015) [arXiv:1506.05214 [hep-ph]].

[76] Cosmological Selection of Multi-TeV Supersymmetry
K. Harigaya*, M. Ibe*, K. Schmitz and T. T. Yanagida
Phys. Lett. B **749**, 298 (2015) [arXiv:1506.00426 [hep-ph]].

[77] Peccei-Quinn Symmetry from Dynamical Supersymmetry Breaking
K. Harigaya*, M. Ibe*, K. Schmitz and T. T. Yanagida
Phys. Rev. D **92**, no. 7, 075003 (2015) [arXiv:1505.07388 [hep-ph]].

[78] K. Harigaya*, M. Ibe* and M. Suzuki*
JHEP **1509**, 155 (2015) doi:10.1007/JHEP09(2015)155 [arXiv:1505.05024 [hep-ph]].

[79] Charged Q-balls in gauge mediated SUSY breaking models
J. P. Hong*, M. Kawasak*, and M. Yamada*
Phys. Rev. D **92**, no. 6, 063521 (2015) [arXiv:1505.02594 [hep-ph]].

[80] Muon g-2 in focus point SUSY
K. Harigaya*, T. T. Yanagida and N. Yokozaki
Phys. Rev. D **92**, no. 3, 035011 (2015) [arXiv:1505.01987 [hep-ph]].

[81] Gravitational wave signals from short-lived topological defects in the MSSM
A. Kamada and M. Yamada
JCAP **1510**, no. 10, 021 (2015) [arXiv:1505.01167 [hep-ph]].

[82] Model of visible QCD axion
H. Fukuda, K. Harigaya*, M. Ibe* and T. T. Yanagida
Phys. Rev. D **92**, no. 1, 015021 (2015) [arXiv:1504.06084 [hep-ph]].

[83] k
,"Wino Dark Matter in light of the AMS-02 2015 Data
M. Ibe*, S. Matsumoto, S. Shirai and T. T. Yanagida
Phys. Rev. D **91**, no. 11, 111701 (2015) [arXiv:1504.05554 [hep-ph]].

[84] Observable dark radiation from a cosmologically safe QCD axion
M. Kawasaki*, M. Yamada*, and T. T. Yanagida
Phys. Rev. D **91**, no. 12, 125018 (2015) [arXiv:1504.04126 [hep-ph]].

[85] Spontaneous thermal Leptogenesis via Majoron oscillation
M. Ibe* and K. Kaneta*
Phys. Rev. D **92**, no. 3, 035019 (2015) [arXiv:1504.04125 [hep-ph]].

[86] Indirect Probe of Electroweak-Interacting Particles at Future Lepton Colliders
K. Harigaya*, K. Ichikawa, A. Kundu, S. Matsumoto and S. Shirai
JHEP **1509**, 105 (2015) [arXiv:1504.03402 [hep-ph]].

[87] Seminatural SUSY from the E_7 nonlinear sigma model
K. Harigaya*, T. T. Yanagida and N. Yokozaki
PTEP **2015**, no. 8, 083B03 (2015) [arXiv:1504.02266 [hep-ph]].

[88] Gravitational waves from domain walls in the next-to-minimal supersymmetric standard model
K. Kadota, M. Kawasaki*, and K. Saikawa*
JCAP **1510**, no. 10, 041 (2015) [arXiv:1503.06998 [hep-ph]].

[89] IceCube potential for detecting Q-ball dark matter in gauge mediation
S. Kasuya, M. Kawasaki*, and T. T. Yanagida
PTEP **2015**, no. 5, 053B02 (2015) doi:10.1093/ptep/ptv056 [arXiv:1502.00715 [hep-ph]].

[90] Affleck-Dine baryogenesis after D-term inflation and solutions to the baryon-dark matter coincidence problem M. Kawasaki*, and M. Yamada*
Phys. Rev. D **91**, no. 8, 083512 (2015) [arXiv:1502.03550 [hep-ph]].

[91] IceCube potential for detecting Q-ball dark matter in gauge mediation
S. Kasuya, M. Kawasaki*, and T. T. Yanagida
PTEP **2015**, no. 5, 053B02 (2015) doi:10.1093/ptep/ptv056 [arXiv:1502.00715 [hep-ph]].

[92] Light Higgsinos in Pure Gravity Mediation
J. L. Evans, M. Ibe*, K. A. Olive and T. T. Yanagida
Phys. Rev. D **91**, 055008 (2015) [arXiv:1412.3403 [hep-ph]].

[93] Axion dark matter from topological defects
M. Kawasaki*, K. Saikawa and T. Sekiguchi
Phys. Rev. D **91**, no. 6, 065014 (2015) [arXiv:1412.0789 [hep-ph]], 106 citations counted in INSPIRE as of Nov 2018.

[94] Coupling Unification and Dark Matter in a Standard Model Extension with Adjoint Majorana Fermions
T. Aizawa*, M. Ibe* and K. Kaneta*
Phys. Rev. D **91**, no. 7, 075012 (2015) [arXiv:1411.6044 [hep-ph]].

[95] New resonance scale and fingerprint identification in minimal composite Higgs models
S. Kanemura, K. Kaneta*, N. Machida and T. Shindou
Phys. Rev. D **91**, 115016 (2015) [arXiv:1410.8413 [hep-ph]].

[96] Mass of Decaying Wino from AMS-02 2014
M. Ibe*, S. Matsumoto, S. Shirai and

T. T. Yanagida
Phys. Lett. B **741**, 134 (2015) [arXiv:1409.6920 [hep-ph]].

[97] Anomaly Mediated Gaugino Mass and Path-Integral Measure
K. Harigaya and M. Ibe*
Phys. Rev. D **90**, no. 8, 085028 (2014) [arXiv:1409.5029 [hep-th]].

[98] CDM/baryon isocurvature perturbations in a sneutrino curvaton model
K. Harigaya, T. Hayakawa*, M. Kawasaki* and S. Yokoyama*
JCAP **1410**, no. 10, 068 (2014) [arXiv:1409.1669 [hep-ph]].

[99] R-symmetric Axion/Natural Inflation in Supergravity via Deformed Moduli Dynamics
K. Harigaya, M. Ibe* and T. T. Yanagida
Phys. Lett. B **739**, 352 (2014) [arXiv:1409.0330 [hep-ph]].

[100] Gravitational effects on vanishing Higgs potential at the Planck scale
N. Haba, K. Kaneta*, R. Takahashi and Y. Yamaguchi
Phys. Rev. D **91**, no. 1, 016004 (2015) [arXiv:1408.5548 [hep-ph]].

[101] Q-ball dark matter and baryogenesis in high-scale inflation
S. Kasuya and M. Kawasaki*
Phys. Lett. B **739**, 174 (2014) [arXiv:1408.1176 [hep-ph]].

[102] Thermal Effects and Sudden Decay Approximation in the Curvaton Scenario
N. Kitajima* D. Langlois, T. Takahashi, T. Takesako* and S. Yokoyama*
JCAP **1410**, no. 10, 032 (2014) [arXiv:1407.5148 [astro-ph.CO]].

[103] Phase Locked Inflation – Effectively Trans-Planckian Natural Inflation
K. Harigaya and M. Ibe*
JHEP **1411**, 147 (2014) [arXiv:1407.4893 [hep-ph]].

[104] Blue-tilted Tensor Spectrum and Thermal History of the Universe
S. Kuroyanagi, T. Takahashi and S. Yokoyama*
JCAP **1502**, 003 (2015) doi:10.1088/1475-7516/2015/02/003 [arXiv:1407.4785 [astro-ph.CO]].

[105] Dynamical fractional chaotic inflation
K. Harigaya, M. Ibe*, K. Schmitz and T. T. Yanagida
Phys. Rev. D **90**, no. 12, 123524 (2014) [arXiv:1407.3084 [hep-ph]].

[106] Gravitational waves as a probe of the SUSY scale
A. Kamada and M. Yamada*
Phys. Rev. D **91**, 063529 (2015) [arXiv:1407.2882 [hep-ph]].

[107] Cosmic neutrino background absorption line in the neutrino spectrum at IceCube
M. Ibe* and K. Kaneta*
Phys. Rev. D **90**, no. 5, 053011 (2014) [arXiv:1407.2848 [hep-ph]].

[108] Relaxing Isocurvature Bounds on String Axion Dark Matter
M. Kawasaki*, N. Kitajima and F. Takahashi
Phys. Lett. B **737**, 178 (2014) [arXiv:1406.0660 [hep-ph]].

[109] Vanishing Higgs potential at the Planck scale in a singlet extension of the standard model
N. Haba, H. Ishida, K. Kaneta* and R. Takahashi
Phys. Rev. D **90**, 036006 (2014) [arXiv:1406.0158 [hep-ph]].

[110] Solution to the baryon-dark-matter coincidence problem in the constrained minimal supersymmetric model with a 126-GeV Higgs boson A. Kamada, M. Kawasaki*, and M. Yamada*
Phys. Rev. D **91**, no. 8, 081301 (2015) [arXiv:1405.6577 [hep-ph]].

[111] Wino Dark Matter and Future dSph Observations
B. Bhattacherjee, M. Ibe*, K. Ichikawa, S. Matsumoto and K. Nishiyama
JHEP **1407**, 080 (2014) [arXiv:1405.4914 [hep-ph]].

[112] No quasistable scalaron lump forms after R^2 inflation
N. Takeda* and Y. Watanabe
Phys. Rev. D **90**, no. 2, 023519 (2014) [arXiv:1405.3830 [astro-ph.CO]].

[113] Non-perturbative approach for curvature perturbations in stochastic δN formalism
T. Fujita, M. Kawasaki and Y. Tada
JCAP **1410**, no. 10, 030 (2014) [arXiv:1405.2187 [astro-ph.CO]].

[114] "Inflatonic baryogenesis with large tensor mode
N. Takeda*
Phys. Lett. B **746**, 368 (2015) [arXiv:1405.1959 [astro-ph.CO]].

[115] Simple realization of inflaton potential on a Riemann surface
K. Harigaya and M. Ibe*
Phys. Lett. B **738**, 301 (2014) [arXiv:1404.3511 [hep-ph]].

[116] Affleck-Dine Baryogenesis and Dark Matter Production after High-scale Inflation

K. Harigaya, A. Kamada, M. Kawasaki*, K. Mukaida and M. Yamada*, Phys. Rev. D **90**, no. 4, 043510 (2014) doi:10.1103/PhysRevD.90.043510 [arXiv:1404.3138 [hep-ph]].

[117] Isocurvature perturbations and tensor mode in light of Planck and BICEP2
M. Kawasaki*, T. Sekiguchi, T. Takahashi and S. Yokoyama*
JCAP **1408**, 043 (2014) [arXiv:1404.2175 [astro-ph.CO]].

[118] Curvaton in large field inflation
T. Fujita, M. Kawasaki and S. Yokoyama*
JCAP **1409**, 015 (2014) [arXiv:1404.0951 [astro-ph.CO]].

[119] High-Scale SUSY Breaking Models in light of the BICEP2 Result
K. Harigaya, M. Ibe*, K. Ichikawa, K. Kaneta and S. Matsumoto
JHEP **1407**, 093 (2014) [arXiv:1403.5880 [hep-ph]].

[120] Compensation for large tensor modes with isocurvature perturbations in CMB anisotropies
M. Kawasaki* and S. Yokoyama*
JCAP **1405** (2014) 046 [arXiv:1403.5823 [astro-ph.CO]].

[121] Neutrino masses, leptogenesis, and sterile neutrino dark matter
T. Tsuyuki*
Phys. Rev. D **90**, 013007 (2014) [arXiv:1403.5053 [hep-ph]].

[122] Dynamical Chaotic Inflation in the Light of BICEP2
K. Harigaya, M. Ibe*, K. Schmitz and T. T. Yanagida
Phys. Lett. B **733**, 283 (2014) doi:10.1016/j.physletb.2014.04.057 [arXiv:1403.4536 [hep-ph]].

[123] Probing small-scale cosmological fluctuations with the 21 cm forest: Effects of neutrino mass, running spectral index, and warm dark matter
H. Shimabukuro, K. Ichiki, S. Inoue and S. Yokoyama*
Phys. Rev. D **90**, no. 8, 083003 (2014) [arXiv:1403.1605 [astro-ph.CO]].

[124] Testing the Minimal Direct Gauge Mediation at the LHC
K. Hamaguchi, M. Ibe*, T. T. Yanagida and N. Yokozaki
Phys. Rev. D **90**, no. 1, 015027 (2014) [arXiv:1403.1398 [hep-ph]].

[125] Peccei-Quinn Symmetric Pure Gravity Mediation
J. L. Evans, M. Ibe*, K. A. Olive and T. T. Yanagida
Eur. Phys. J. C **74**, 2931 (2014) [arXiv:1402.5989 [hep-ph]].

[126] Baryogenesis from the gauge-mediation type Q-ball and the new type of Q-ball as the dark matter
S. Kasuya and M. Kawasaki*
Phys. Rev. D **89**, no. 10, 103534 (2014) [arXiv:1402.4546 [hep-ph]].

[127] Dark Matter Production in Late Time Reheating
K. Harigaya, M. Kawasaki*, K. Mukaida and M. Yamada*, Phys. Rev. D **89**, no. 8, 083532 (2014) doi:10.1103/PhysRevD.89.083532 [arXiv:1402.2846 [hep-ph]].

[128] Critical constraint on inflationary magnetogenesis
T. Fujita and S. Yokoyama*
JCAP **1403**, 013 (2014) Erratum: [JCAP **1405**, E02 (2014)] [arXiv:1402.0596 [astro-ph.CO]].

[129] Flat Higgs Potential from Planck Scale Supersymmetry Breaking
M. Ibe*, S. Matsumoto and T. T. Yanagida
Phys. Lett. B **732**, 214 (2014) [arXiv:1312.7108 [hep-ph]].

[130] One-loop anomaly mediated scalar masses and $(g-2)_m u$ in pure gravity mediation
J. L. Evans, M. Ibe*, K. A. Olive and T. T. Yanagida
Eur. Phys. J. C **74**, no. 2, 2775 (2014) [arXiv:1312.1984 [hep-ph]].

[131] Mixed (cold+warm) dark matter in the bino-wino coannihilation scenario
M. Ibe*, A. Kamada and S. Matsumoto
Phys. Rev. D **89**, no. 12, 123506 (2014) [arXiv:1311.2162 [hep-ph]].

[132] Lower Bound on the Garvitino Mass $m_{3/2} > O(100)$ TeV in R-Symmetry Breaking New Inflation
K. Harigaya, M. Ibe and T. T. Yanagida
Phys. Rev. D **89**, no. 5, 055014 (2014) [arXiv:1311.1898 [hep-ph]].

[133] Decay rates of Gaussian-type I-balls and Bose-enhancement effects in 3+1 dimensions
M. Kawasaki*, and M. Yamada*
JCAP **1402**, 001 (2014) [arXiv:1311.0985 [hep-ph]].

[134] Hypercharged Dark Matter and Direct Detection as a Probe of Reheating
B. Feldstein, M. Ibe* and T. T. Yanagida
Phys. Rev. Lett. **112**, no. 10, 101301 (2014) [arXiv:1310.7495 [hep-ph]].

[135] Halo/galaxy bispectrum with primordial non-Gaussianity from integrated perturbation theory
S. Yokoyama*, T. Matsubara and A. Taruya
Phys. Rev. D **89**, no. 4, 043524 (2014) [arXiv:1310.4925 [astro-ph.CO]].

[136] I-ball formation with logarithmic potential
M. Kawasaki* and N. Takeda*
JCAP **1407**, 038 (2014) [arXiv:1310.4615 [astro-ph.CO]].

[137] CMB distortion anisotropies due to the decay of primordial magnetic fields
K. Miyamoto*, T. Sekiguchi, H. Tashiro and S. Yokoyama*
Phys. Rev. D **89**, no. 6, 063508 (2014) doi:10.1103/PhysRevD.89.063508 [arXiv:1310.3886 [astro-ph.CO]].

[138] Axions as Hot and Cold Dark Matter
K. S. Jeong*, M. Kawasaki*, and F. Takahashi
JCAP **1402**, 046 (2014) [arXiv:1310.1774 [hep-ph]].

[139] A Closer Look at Gaugino Masses in Pure Gravity Mediation Model/Minimal Split SUSY Model
K. Harigaya, M. Ibe* and T. T. Yanagida
JHEP **1312**, 016 (2013) [arXiv:1310.0643 [hep-ph]].

[140] On the estimation of gravitational wave spectrum from cosmic domain walls
T. Hiramatsu, M. Kawasaki*, and K. Saikawa
JCAP **1402**, 031 (2014) [arXiv:1309.5001 [astro-ph.CO]].

[141] ,"A new algorithm for calculating the curvature perturbations in stochastic inflation
T. Fujita, M. Kawasaki*, Y. Tada and T. Takesako*
JCAP **1312**, 036 (2013) [arXiv:1308.4754 [astro-ph.CO]].

[142] Peccei-Quinn symmetry from a gauged discrete R symmetry
K. Harigaya, M. Ibe*, K. Schmitz and T. T. Yanagida
Phys. Rev. D **88**, no. 7, 075022 (2013) doi:10.1103/PhysRevD.88.075022 [arXiv:1308.1227 [hep-ph]].

[143] Type-I cosmic string network
T. Hiramatsu, Y. Sendouda, K. Takahashi, D. Yamauchi* and C. M. Yoo
Phys. Rev. D **88**, no. 8, 085021 (2013) [arXiv:1307.0308 [astro-ph.CO]].

[144] Higher order statistics of curvature perturbations in IFF model and its Planck constraints
T. Fujita* and S. Yokoyama*
JCAP **1309**, 009 (2013) [arXiv:1306.2992 [astro-ph.CO]].

[145] Non-Universalities in Pure Gravity Mediation
J. L. Evans, K. A. Olive, M. Ibe* and T. T. Yanagida
Eur. Phys. J. C **73**, no. 10, 2611 (2013) [arXiv:1305.7461 [hep-ph]].

[146] Domain wall and isocurvature perturbation problems in axion models
M. Kawasaki*, T. T. Yanagida and K. Yoshino*
JCAP **1311**, 030 (2013) [arXiv:1305.5338 [hep-ph]].

[147] Gravitational waves from a curvaton model with blue spectrum M. Kawasaki*, N. Kitajima* and S. Yokoyama*
JCAP **1308**, 042 (2013) doi:10.1088/1475-7516/2013/08/042 [arXiv:1305.4464 [astro-ph.CO]].

[148] AMS-02 Positrons from Decaying Wino in the Pure Gravity Mediation Model
M. Ibe*, S. Matsumoto, S. Shirai and T. T. Yanagida
JHEP **1307**, 063 (2013) [arXiv:1305.0084 [hep-ph]].

[149] Recent Result of the AMS-02 Experiment and Decaying Gravitino Dark Matter in Gauge Mediation
M. Ibe*, S. Iwamoto, S. Matsumoto, T. Moroi and N. Yokozaki
JHEP **1308**, 029 (2013) [arXiv:1304.1483 [hep-ph]].

[150] Muon g-2 and 125 GeV Higgs in Split-Family Supersymmetry
M. Ibe*, T. T. Yanagida and N. Yokozaki
JHEP **1308**, 067 (2013) [arXiv:1303.6995 [hep-ph]].

[151] Implications of Planck results for models with local type non-Gaussianity
T. Suyama, T. Takahashi, M. Yamaguchi and S. Yokoyama*
JCAP **1306**, 012 (2013) [arXiv:1303.5374 [astro-ph.CO]].

[152] Focus point gauge mediation in product group unification
F. Brümmer, M. Ibe and T. T. Yanagida
Phys. Lett. B **726**, 364 (2013) [arXiv:1303.1622 [hep-ph]].

[153] Statistics of general functions of a Gaussian field -application to non-Gaussianity from preheating
T. Suyama and S. Yokoyama*
JCAP **1306**, 018 (2013)

doi:10.1088/1475-7516/2013/06/018 [arXiv:1303.1254 [astro-ph.CO]].

[154] T. Abe, R. Kitano, Y. Konishi, K. y. Oda, J. Sato and S. Sugiyama, EPJ Web Conf. **49**, 15018 (2013) [arXiv:1303.0935 [hep-ph]].

[155] Universality in Pure Gravity Mediation
J. L. Evans, M. Ibe*, K. A. Olive and T. T. Yanagida
Eur. Phys. J. C **73**, 2468 (2013) doi:10.1140/epjc/s10052-013-2468-9 [arXiv:1302.5346 [hep-ph]], 51 citations counted in INSPIRE as of Nov 2018.

[156] "Testing general scalar-tensor gravity and massive gravity with cluster lensing
T. Narikawa, T. Kobayashi, D. Yamauchi* and R. Saito
Phys. Rev. D **87**, 124006 (2013) doi:10.1103/PhysRevD.87.124006 [arXiv:1302.2311 [astro-ph.CO]].

[157] Heavy gravitino in hybrid inflation
M. Kawasaki*, N. Kitajima*, K. Nakayama and T. T. Yanagida
JCAP **1306**, 037 (2013) [arXiv:1301.6281 [hep-ph]].

[158] A Simple Solution to the Polonyi Problem in Gravity Mediation
K. Harigaya, M. Ibe*, K. Schmitz and T. T. Yanagida
Phys. Lett. B **721**, 86 (2013) [arXiv:1301.3685 [hep-ph]].

[159] Scale-dependent bias due to primordial vector field
M. Shiraishi, S. Yokoyama*, K. Ichiki and T. Matsubara
Mon. Not. Roy. Astron. Soc. **432**, no. 3, 2331 (2013) doi:10.1093/mnras/stt594 [arXiv:1301.2778 [astro-ph.CO]].

[160] Natural supersymmetry's last hope: R-parity violation via UDD operators
B. Bhattacherjee, J. L. Evans, M. Ibe*, S. Matsumoto and T. T. Yanagida
Phys. Rev. D **87**, no. 11, 115002 (2013) [arXiv:1301.2336 [hep-ph]].

[161] Axions: Theory and Cosmological Role
M. Kawasaki*, and K. Nakayama
Ann. Rev. Nucl. Part. Sci. **63**, 69 (2013) [arXiv:1301.1123 [hep-ph]], 129 citations counted in INSPIRE as of Nov 2018.

[162] Cosmological and astrophysical constraints on superconducting cosmic strings
K. Miyamoto* and K. Nakayama
JCAP **1307**, 012 (2013) [arXiv:1212.6687 [astro-ph.CO]].

[163] Extended analysis of CMB constraints on non-Gaussianity in isocurvature perturbations
C. Hikage, M. Kawasaki*, T. Sekiguchi and T. Takahashi, JCAP **1303** (2013) 020 [arXiv:1212.6001 [astro-ph.CO]].

[164] Mass Splitting between Charged and Neutral Winos at Two-Loop Level
M. Ibe*, S. Matsumoto and R. Sato
Phys. Lett. B **721**, 252 (2013) [arXiv:1212.5989 [hep-ph]], 96 citations counted in INSPIRE as of Nov 2018.

[165] Effects of power law primordial magnetic field on big bang nucleosynthesis
D. G. Yamazaki and M. Kusakabe*
Phys. Rev. D **86**, 123006 (2012) [arXiv:1212.2968 [astro-ph.CO]].

[166] Opening the window to the cogenesis with Affleck-Dine mechanism in gravity mediation
A. Kamada, M. Kawasaki*, and M. Yamada*
Phys. Lett. B **719**, 9 (2013) [arXiv:1211.6813 [hep-ph]].

[167] Smooth hybrid inflation in a supersymmetric axion model
M. Kawasaki*, N. Kitajima*, and K. Nakayama
Phys. Rev. D **87**, no. 3, 035010 (2013) [arXiv:1211.6516 [hep-ph]].

[168] Chaotic Inflation with a Fractional Power-Law Potential in Strongly Coupled Gauge Theories
K. Harigaya, M. Ibe*, K. Schmitz and T. T. Yanagida
Phys. Lett. B **720**, 125 (2013) doi:10.1016/j.physletb.2013.01.058 [arXiv:1211.6241 [hep-ph]].

[169] Hubble-induced mass from MSSM plasma
M. Kawasaki*, F. Takahashi and T. Takesako*
JCAP **1304**, 008 (2013) doi:10.1088/1475-7516/2013/04/008 [arXiv:1211.4921 [hep-ph]].

[170] Revisiting the gravitino dark matter and baryon asymmetry from Q-ball decay in gauge mediation
S. Kasuya, M. Kawasaki*, and M. Yamada*
Phys. Lett. B **726**, 1 (2013) [arXiv:1211.4743 [hep-ph]].

[171] Non-Gaussianity from Attractor Curvaton
K. Harigaya, M. Ibe*, M. Kawasaki* and T. T. Yanagida
Phys. Rev. D **87**, no. 6, 063514 (2013) [arXiv:1211.3535 [hep-ph]].

[172] CMB constraint on non-Gaussianity in isocurvature perturbations
C. Hikage, M. Kawasaki*, T. Sekiguchi and

T. Takahashi
JCAP **1307**, 007 (2013) [arXiv:1211.1095 [astro-ph.CO]].

[173] Evolution and thermalization of dark matter axions in the condensed regime
K. Saikawa* and M. Yamaguchi
Phys. Rev. D **87**, no. 8, 085010 (2013) [arXiv:1210.7080 [hep-ph]].

[174] "Non-Gaussianity from Axionic Curvaton
M. Kawasaki*, T. Kobayashi and F. Takahashi
JCAP **1303**, 016 (2013) [arXiv:1210.6595 [astro-ph.CO]].

[175] Heavy Squarks and Light Sleptons in Gauge Mediation From the viewpoint of 125 GeV Higgs Boson and Muon g-2
M. Ibe*, S. Matsumoto, T. T. Yanagida and N. Yokozaki
JHEP **1303**, 078 (2013) [arXiv:1210.3122 [hep-ph]].

[176] Forecast constraints on cosmic strings from future CMB, pulsar timing and gravitational wave direct detection experiments
S. Kuroyanagi, K. Miyamoto*, T. Sekiguchi, K. Takahashi and J. Silk
Phys. Rev. D **87**, no. 2, 023522 (2013) Erratum: [Phys. Rev. D **87**, no. 6, 069903 (2013)] [arXiv:1210.2829 [astro-ph.CO]].

[177] Scale-dependent bias with higher order primordial non-Gaussianity: Use of the Integrated Perturbation Theory
S. Yokoyama* and T. Matsubara
Phys. Rev. D **87**, 023525 (2013) [arXiv:1210.2495 [astro-ph.CO]].

[178] Imprints of nonthermal Wino dark matter on small-scale structure
M. Ibe*, A. Kamada and S. Matsumoto
Phys. Rev. D **87**, no. 6, 063511 (2013) [arXiv:1210.0191 [hep-ph]].

[179] Q ball Decay Rates into Gravitinos and Quarks
M. Kawasaki* and M. Yamada* Phys. Rev. D **87**, no. 2, 023517 (2013) [arXiv:1209.5781 [hep-ph]].

[180] Minimal Dilaton Model
T. Abe, R. Kitano, Y. Konishi, K. y. Oda, J. Sato and S. Sugiyama*
, Phys. Rev. D **86**, 115016 (2012) [arXiv:1209.4544 [hep-ph]].

[181] CMB power spectra induced by primordial cross-bispectra between metric perturbations and vector fields
M. Shiraishi, S. Saga and S. Yokoyama*
JCAP **1211**, 046 (2012) [arXiv:1209.3384 [astro-ph.CO]].

[182] Production of 9Be through alpha-fusion reaction of metal-poor cosmic ray and stellar flare
' M. Kusakabe* and M. Kawasaki*
Astrophys. J. **767**, 5 (2013) [arXiv:1208.4210 [astro-ph.CO]].

[183] Gravitational waves from smooth hybrid new inflation
M. Kawasaki*, K. Saikawa* and N. Takeda*
Phys. Rev. D **87**, no. 10, 103521 (2013) [arXiv:1208.4160 [astro-ph.CO]].

[184] Non-Gaussian bubbles in the sky
K. Sugimura, D. Yamauchi* and M. Sasaki
EPL **100**, no. 2, 29004 (2012) [arXiv:1208.3937 [astro-ph.CO]].

[185] Remarks on Hubble Induced Mass from Fermion Kinetic Term
M. Kawasaki* and T. Takesako*
Phys. Lett. B **718**, 522 (2012) [arXiv:1208.1323 [hep-ph]].

[186] Pure gravity mediation of supersymmetry breaking at the Large Hadron Collider
B. Bhattacherjee, B. Feldstein, M. Ibe*, S. Matsumoto and T. T. Yanagida
Phys. Rev. D **87**, no. 1, 015028 (2013) [arXiv:1207.5453 [hep-ph]], 73 citations counted in INSPIRE as of Nov 2018.

[187] Axion cosmology with long-lived domain walls
T. Hiramatsu, M. Kawasaki*, K. Saikawa* and T. Sekiguchi
JCAP **1301**, 001 (2013) [arXiv:1207.3166 [hep-ph]], 62 citations counted in INSPIRE as of Nov 2018.

[188] Stochastic Approach to Flat Direction during Inflation
M. Kawasaki* and T. Takesako*
JCAP **1208**, 031 (2012) [arXiv:1207.1165 [hep-ph]].

[189] Full bispectra from primordial scalar and tensor perturbations in the most general single-field inflation model
X. Gao, T. Kobayashi, M. Shiraishi, M. Yamaguchi, J. Yokoyama and S. Yokoyama*
PTEP **2013**, 053E03 (2013) [arXiv:1207.0588 [astro-ph.CO]].

[190] Seesaw Mechanism with Occam's Razor
K. Harigaya, M. Ibe* and T. T. Yanagida
Phys. Rev. D **86**, 013002 (2012) [arXiv:1205.2198 [hep-ph]], 56 citations counted in INSPIRE as of Nov 2018.

[191] Weak lensing generated by vector perturbations and detectability of cosmic strings

D. Yamauchi*, T. Namikawa and A. Taruya
JCAP **1210**, 030 (2012) [arXiv:1205.2139 [astro-ph.CO]].

[192] Updated constraint on a primordial magnetic field during big bang nucleosynthesis and a formulation of field effects
M. Kawasaki* and M. Kusakabe*
Phys. Rev. D **86**, 063003 (2012) [arXiv:1204.6164 [astro-ph.CO]].

[193] The Lightest Higgs Boson Mass in the MSSM with Strongly Interacting Spectators
J. L. Evans, M. Ibe* and T. T. Yanagida
Phys. Rev. D **86**, 015017 (2012) [arXiv:1204.6085 [hep-ph]].

[194] A 125 GeV Higgs Boson Mass and Gravitino Dark Matter in R-invariant Direct Gauge Mediation
M. Ibe* and R. Sato
Phys. Lett. B **717**, 197 (2012) [arXiv:1204.3499 [hep-ph]].

Papers under referee

[195] Primordial Black Holes from Affleck-Dine Mechanism
F. Hasegawa* and M. Kawasaki*
arXiv:1807.00463 [astro-ph.CO].

[196] Big Bang Nucleosynthesis Constraint on Baryonic Isocurvature Perturbations
K. Inomata*, M. Kawasaki*, A. Kusenko and L. Yang
arXiv:1806.00123 [astro-ph.CO].

[197] Optical Ring Cavity Search for Axion Dark Matter
I. Obata*, T. Fujita and Y. Michimura
arXiv:1805.11753 [astro-ph.CO].

[198] "Formation of primordial black holes as dark matter or LIGO black hole binaries in an axion-like curvaton model
K. Ando*, M. Kawasaki* and H. Nakatsuka*
arXiv:1805.07757 [astro-ph.CO].

[199] A Model of Composite $B-L$ Asymmetric Dark Matter
M. Ibe*, A. Kamada, S. Kobayashi* and W. Nakano*
arXiv:1805.06876 [hep-ph].

FACILITIES

KAMIOKA OBSERVATORY

Kamioka Observatory

1. Introduction

There are four operating bodies for the underground site in Kamioka: 1) Kamioka Observatory, Institute for Cosmic Ray Research (ICRR), the University of Tokyo; 2) Tohoku University Research Center for Neutrino Science; 3) Kamioka Satellite, Kavli Institute for the Physics and Mathematics of the Universe (Kavli IPMU), the University of Tokyo; 4) KAGRA Observatory, ICRR, the University of Tokyo; (in order of foundation). They are cooperating each other in many aspects. They work together for safety issues and some of the maintenance costs for the underground environments in common area are shared. But they are independent and operating different facilities and have separate budgets.

Kamioka Observatory is located at 1000 m underground (2,700 meter water equivalent) of the Kamioka Mine, Gifu prefecture, about 200 km west of Tokyo. Kamioka Observatory was established in 1995, initially to house and operate the Super-Kamiokande (SK) detector. Kamioka Observatory has expanded its role in order to operate XMASS: the direct dark matter search experiment. Kamioka Observatory also accepts experiments to use underground spaces by external research institutions based on the proposals: CANDLES is a double beta decay experiment using ^{48}Ca led by Osaka University and NewAGE is a dark matter experiment led by Kobe University to detect directions of recoil nucleus. There are also experiments to measure precise value of the vertical gravity by a super-conductive gravity meter and to measure the earth's horizontal crustal strain to the level of 10^{-12} by a laser displacement meter.

2. Brief History and Major Achievements

In 1991, the construction budget for SK was approved and the 5 year construction project had started. SK is a 50, 000 ton water Cherenkov detector, and the inner 32,000 tons of water are optically separated from the outer-layer, anti-counters, of 2m thickness on an average. One year after the construction had started, the US group joined and they bore a responsibility to construct and operate anti-counters. The SK detector was built to resolve the remaining problems from Kamiokande, namely the solar neutrino problems and the atmospheric neutrino anomaly. Detection of neutrino bursts from supernovae and proton decay were also very interesting subjects.

In 1995, the Kamioka Observatory was officially founded to operate the SK detector. One year before that, in 1994, the computer building was constructed and the computer system was installed.

In 1996, the detector construction was completed and started data taking. Two years later, in 1998, SK found the up-down asymmetry of the μ-like events in the zenith angle distribution of the atmospheric neutrinos, which provided a clear evidence for neutrino oscillation independent of the flux calculation.

In 1999, the first long baseline neutrino oscillation experiment of the earth scale, K2K, had started, injecting man-made neutrinos produced at KEK PS to SK, 250 km away from the neutrino source. The experiment was completed in 2004 observing 112 μ-like events whereas 156 such events were expected without oscillation. This confirmed the neutrino oscillation observed in atmospheric neutrinos.

In June 2001, SK published the 1256 days of data for solar neutrino observations. On the same day, SNO announced their first result on charged current interactions. They have concluded 3.6σ effect by comparing the SK electron scattering data and the SNO charged current data that there are non-electron type neutrinos in the solar neutrinos detected on the earth. This was the first evidence for solar neutrino oscillation.

In 2009, the new long baseline oscillation experiment called T2K was started to look for as yet undetermined mixing angle of θ_{13}. The intense neutrino beam from JPARC was directed to the SK detector 295 km away. In 2011, T2K presented the first evidence for non-zero θ_{13}, namely observation of electron-like events in muon-neutrino beam.

3. Operation

In Kamioka Observatory we have two technical staffs who work for the daily maintenance of the underground laboratory. Another technical staff works for safety issues such as management of chemicals. The experiments and related equipments are basically operated by the scientists from each collaboration.

The number of full-time scientific staff of Kamioka Observatory is 24 (3 professors, 5 associate professors and 16 research associates) and there are three staffs in administration office. These scientific personnel are conducting researches using SK and XMASS and have responsibilities to operate these detectors. In addition, they have responsibilities on the matters related to the facilities of the underground laboratory and on the supports for about 5000 person$\times$day visiting scientists per year, especially for those taking SK shifts and analyzing the data. The safety issues are one of the

important subjects.

4. Procedure of approving experiments in Kamioka Observatory

Once every year, ICRR receive experimental proposals not only for underground experiments but also for all the relevant experiments to ICRR. And the program assessment committee including some members from outside of ICRR decides if the proposals to be approved or not. This judgement is mostly done based on the scientific point of view. Following this approval, the Kamioka steering committee discusses and decides if the approved proposals would fit to the underground laboratories. Basically, the Observatory provides the space and facility like electricity, water and so on and the user will bring all the necessary equipments. Practically before any decision is made, the experimental collaboration would negotiate with the Observatory if their experiment would fit in the underground or to judge if the experiment needs a new cavity or not.

After the approval, the observatory manages their activities in a point of view for safety. For example, if one uses liquid scintillator, one needs to get permission to use liquid scintillator from the local fire department and there are many rules and regulations to follow. Then the Observatory sometimes ask the experimental group to change a design by taking into account those regulations.

5. Facilities

5.1. Underground Facilities

The entrance of the underground facilities is located at the distance about 10 minutes drive from the ground office buildings. A horizontal access of a few minutes drive of 1.7 km drift brings users to the area where undergrounds facilities are located. The Kamioka mine is no more operating and therefore users can access to the facilities 24 hours a day by just driving a car. The map of the facility area is shown in Fig. 5.1.

SK and KamLAND (Tohoku University) are shown in circle. CLIO and Laser strain meter are placed at the L-shape laboratory and the length of each arm is 100 m. Labs A to G are under the supervision by Kamioka Observatory and Labs 1 and 2 are the Kavli IPMU laboratories. Lab.A is a back yard of SK, where we have the electron LINAC for the calibration for SK and low background test equipments. Lab. B is a L-shape laboratory; the length of each arm is 20 m. NewAGE is operating at the end of one arm and the other arm was used by the Super-Conductive Gravity meter until 2016. The crossing area is used for various test experiments and preparations. Lab.C (15 m wide and 20 m long) is a hall for XMASS and Lab.D houses CANDLES, the double beta decay experiment using ^{48}Ca. Lab.E is hosting 200 ton EGADS water tank, which was built for testing the feasibility of the SK-Gd project. Lab.G area was newly excavated in 2015 and a Gd dissolving system and a Gd-loaded water recirculation system have been constructed since then. Lab.1 has various devices to detect radio-active contaminations, impurities and so on. Among them are two high purity Germanium detectors, Gas analyzer, Particle counters, Scanning Electron Microscope and so on. Lab.2 is used for computer clusters. All the laboratories are within 400 m distances.

5.2. Environmental Backgrounds

The deep underground provides the low radioactive and low seismic noise environment and gives good opportunities to perform physics experiments requiring such experimental conditions.

At the depth of 2,700 m water equivalence, the cosmic ray muon flux, about 250 muons/m^2/day, is $\sim$1/100,000 of the surface flux.

The environmental gamma ray backgrounds from the wall depend upon locations and energy. It ranges from 0.1$\sim$0.2 /MeV/cm^2/sec at around 1 MeV and 0.01$\sim$0.02 /MeV/cm^2/sec at around 2 MeV.

The thermal and non-thermal neutron fluxes in Kamioka Observatory are measured to be

$$\phi_n^{thermal} = 8.3\pm0.6\times10^{-6}\mathrm{cm}^{-2}\mathrm{s}^{-1} \quad \text{and}$$
$$\phi_n^{non-thermal} = 1.2\pm0.1\times10^{-5}\mathrm{cm}^{-2}\mathrm{s}^{-1} \quad ,$$

respectively. In order to reduce those environmental γ and neutron backgrounds, water shields are most effective and commonly used in Kamioka. There are 2 to 3 m water layers surrounding the inner volume of SK which would effectively reduce those backgrounds. The 800 tons water tank for the XMASS experiment provides 10^{-7} reduction for neutrons.

The Rn concentration of the mine air varies $\sim$100 Bq/m^3 to $\sim$2000 Bq/m^3 depending on the season of the year. To reduce the exposure of workers and experiments, fresh air from outside of the mine is brought into the experimental areas. 100 m^3 of fresh air per minutes is brought through a 1.8 km pipe. Rn concentration of the fresh air is $\leq$50 Bq/m^3 and the Rn concentration of the experimental areas are always kept $<$ 100 Bq/m^3. To further reduce the effects of Rn for experiments, so called "Rn-free air" generation system which is based on charcoal filters is installed in the mine. The Rn concentration of "Rn-free air" is $<$ 1 mBq/m^3 and 18 m^3 per hour of flow is available for purging detectors and buffer tanks for the ultra pure water system. The U/Th and K contamination in the rocks in the mine are $\sim$1.0 ppm for U, $\sim$3.2 ppm for Th and 1.6% for K at a typical location.

To study and establish low background environment, we have ICP-MASS spectrometer, GAS MASS spectrometer, and low background Ge detectors in the underground laboratory. Those are available for the users of the underground observatory.

An electron LINAC of which energy ranges 5 MeV to

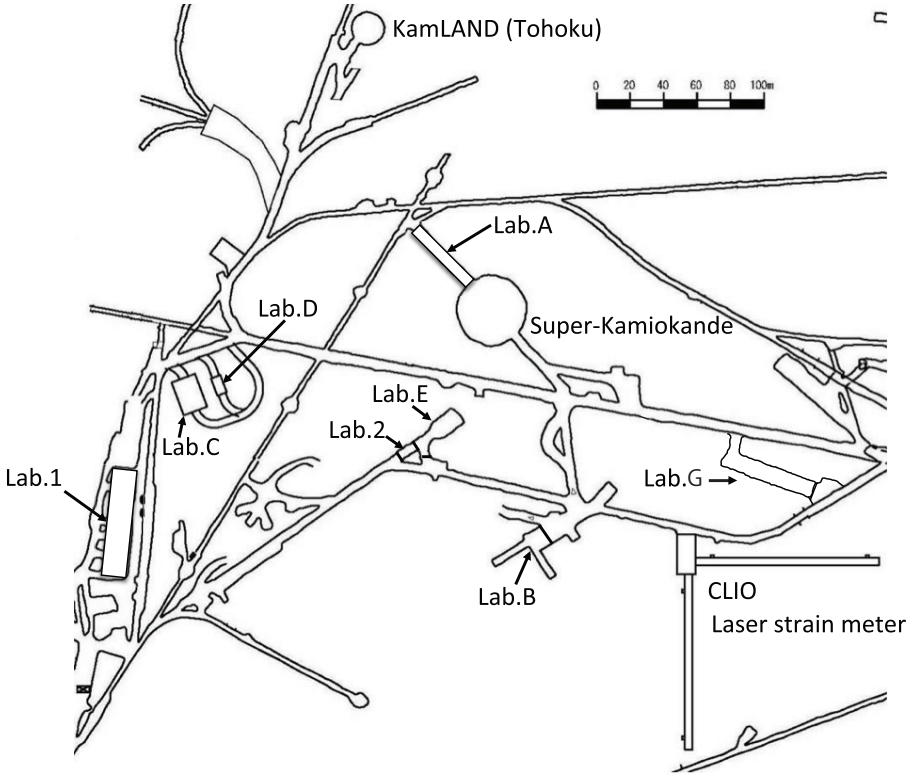

Fig. 1. Layout of Kamioka Observatory

15 MeV is set up near the SK detector for the purpose of the low energy calibration. The energy of the LINAC covers exactly the energy range of the detectable solar neutrinos in SK. The DT neutron generator can also be used to produce ^{16}N in the water as a calibration source. Other radio-active calibration sources are available in the underground laboratory.

5.3. Ground Facilities

The office building for Kamioka Observatory (ICRR) and Kamioka Satellite (Kavli IPMU) are built close each other and actually connected by passage. Kamioka Observatory operates dormitory where we have 18 single rooms and 1 twin room and 1 Japanese style tatami room. Three meals are served at the dormitory, but need reservation. Kamioka Observatory operates computer system, electronics workshop and chemical workshop in the office building. The computer system consists of 2380 cores with 2.40 GHz and the memory size is 4 GB/core. Disk space available is 9 PB and the access speed is greater than 2.5 GB/s in total. We also have a tape backup system with 4.2 PB. The system is mostly used for the SK experiment. All the data from SK are stored in this system and accessed also from abroad.

AKENO OBSERVATORY

Introduction

The Akeno Observatory is situated in Akeno of Hokuto-city situated 20 km northwest of Kofu and 130 km west of metropolitan Tokyo. The location is at the longitude of 138.5°E and the latitude of 35.8°N. The altitude is ∼900 m above sea level. It was established in 1977 as a research center for air shower studies in the very high energy region, and it has been administered by the ICRR as a facility of the joint research of ICRR.

The Akeno Air Shower Experiment started in 1979 with an array covering 1 km^2 area. The array was enlarged to 20 km^2 in 1984 and was gradually expanded to Akeno Giant Air Shower Array (AGASA) of approximately 100 km^2 area by 1990. The AGASA was built to detect Ultra-High Energy Cosmic Rays (UHECRs) in the energy range of 10^{20} eV.

The 40th anniversary of the Akeno Observatory

The ceremony of the 40th anniversary of the Akeno Observatory was held at a hotel in Kofu in Yamanashi Prefecture on September 8th in 2017. Before the ceremony, a tour of the observatory was held. The lectures and ceremony were performed with about 120 participants, followed by the celebration party.

Scientific Activities since 2012

The study of UHECRs by AGASA in Akeno was succeeded by the Telescope Array (TA) experiment in Utah, USA since 2008. After the shutdown of AGASA in 2004, all the AGASA detectors were dismantled and the Akeno Observatory has been used for small-scale cosmic-ray experiments, astrophysical observations and as a test/assembly/R&D facility of TA and other experiments by the ICRR and university researchers[1]. As of 2018, there are the main campus of approximately ten thousand square meters (Fig. 1), one small site of the MITSuME telescope, three small sites each of a muon house, and one small site of an unused muon house. One assistant technical staff works twice per week in order to maintain the Akeno Observatory.

Research and development for the Telescope Array observation in Utah by the TA collaboration: In 2016 and 2017, plastic scintillator counters for the TA extensions[2] were assembled (Fig. 2). The assembly work of the surface detector electronics for the TA extensions was also performed.

Fig. 1. The main campus of the Akeno Observatory. There are the movable tent for a small atmospheric Cherenkov telescope, the large experimental hall, the research building and the lodging facility from the left to the right.

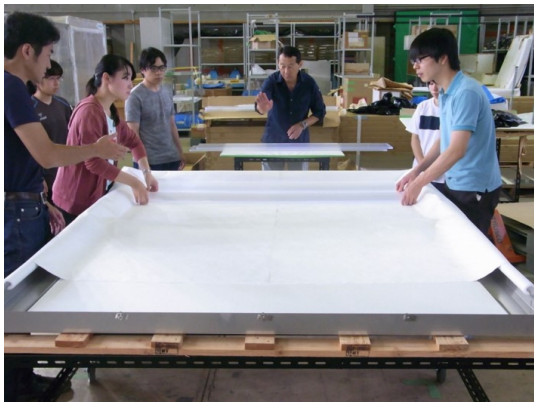

Fig. 2. Assembly of a plastic scintillator counter at the large experimantal hall of the Akeno Observatory

Observation by the multi-color imager for transients, survey and monstrous explosions (MITSuME) by N. Kawai (Tokyo Institute of Technology), et al.: One of the three MITSuME robotic telescopes was installed in the Akeno Observatory in 2003 on the roof of the unused concrete muon house (Fig. 3). The telescope has an aperture of 50 cm, an FOV of 28' × 28' and is equipped with a tricolor CCD camera capable of $g'R_CI_C$-bands photometry. It is operated remotely from the Tokyo Tech. Upon receiving a GRB alert from Swift or Fermi satellite, it quickly directs the telescope (9°/s maneuverability) toward the GRB direction, and makes a prompt observation of the GRB and its afterglow. Since its commissioning in 2004, the MITSuME telescope in Akeno has been

*1 In Japanese Fiscal Year (JFY) 2017, 14 proposals that included the usage of the Akeno Observatory were accepted for the ICRR joint research program.

*2 E. Kido et al., "The TAx4 experiment", CRI199 and S. Udo et al., "The Telescope Array Low-energy Extension", CRI069, 35th ICRC (Busan) 2017

making more than ∼10 GRB follow-up observations every year, and detected GRB afterglows. It has been also joining the multi-wavelength campaign for observing AGNs and other transient objects. The MITSuME telescope joined J-GEM and GROTH[3], and performed follow-up observation of gravitational wave events for GW 170104[4] and GW 170817A with visible light. In November of 2017, the two MITSuME telescopes at the Akeno Observatory and the Okayama Astrophysical Observatory did cooperative follow-up observation of burst phenonmena.

Fig. 3. The dome in which the MITSuME telescope was installed in Akeno.

Observation of galactic cosmic rays by large area muon telescope by A. Oshima (Chubu University), et al.: Four layers of proportional counter telescopes, each with 25 m^2 area, were installed in each of three muon houses in Akeno (Fig.4) and the cosmic ray muons have been measured since 2003. The mode energy of the primary cosmic rays is approximately 25 GeV corresponding to 2-m thick concrete ceiling of the muon house and the latitude of Akeno Observatory. It is also aimed that the measurement in Akeno is combined with a simultaneous measurement with GRAPES-3 in Ooty, India, and the modulation effects of galactic cosmic rays by the solar activity such as the Forbush decrease and its precursor are monitored. The instruments are now under redevelopment in accordance with the upgrade for the GRAPES-3 muon telescope. The analysis of the data with the Akeno muon telescope was carried out and clear solar time variation of muon flux was reported in the annual report of ICRR 2015.

Research and development for a small atmospheric Cherenkov telescope by T. Yoshikoshi (ICRR), et al.: A small alt-azimuth telescope with an aperture of three meters was setup at the main campus of the Akeno Observatory (Fig. 5) for prototype tests with atmospheric Cherenkov observations of gamma rays [5]. This telescope is the only telescope to

Fig. 4. One of the three muon detector housings with concrete shielding.

observe atmospheric Cherenkov light emitted from air showers induced by TeV gamma rays in Japan. Refurbishing of the telescope control system, the unit mirror and optics were assembled in 2010 and 2011. In JFY 2016, an atmospheric Cherenkov light event was firstly observed with this telescope. By the observation in JFY 2017, the data of the Crab Nebula were taken.

Fig. 5. The Cherenkov telescope at the tour of the 40th anniversary of the Akeno Observatory

Research of ultra-low frequency anti-vibration system for KAGRA by R. Takahashi (NAOJ), et al.: Since 2011, the large experimental hall of the Akeno Observatory has been partially utilized for the evaluation of the performance of ultra-low frequency anti-vibration system and advance check of fitting of the system at the installation site of the KAGRA Observatory.

*3 Kawai et al., "MITSuME, Murikabushi and Subaru Telescopes", GROWTH Conference 2016, 2016/07/25-27, Caltech

*4 LVC-GCN #20430

*5 T. Yoshikoshi et al., "A 3-Meter Atmospheric Cherenkov Telescope as a Test Bench for Very High Energy Gamma-Ray Astrophysics Projects", 34th ICRC (The Hague), 887 (2015)

NORIKURA OBSERVATORY

Introduction

Norikura Observatory (36.10°N and 137.55°E) was founded in 1953 and attached to ICRR in 1976. It is located at 2770 m above sea level, and is the highest altitude manned laboratory in Japan (Fig. 1). Experimental facilities of the laboratory are made available to all the qualified scientists in the field of cosmic ray research and associated subjects. The AC electric power is generated by the dynamo and supplied throughout the observatory. The observatory can be accessed easily by car and public bus in summer (July-September). The 60th anniversary of Norikura Observatory was celebrated in 2013.

Fig. 1. Norikura Observatory

Norikura Observatory gave manned operation to the observations by the qualified scientists all the year until the year 2003. However, the feasibility of the automatic operation of Norikura Observatory during winter period has been tested since winter 2004 in order to study the possibilities to reduce maintenance and labor costs without causing serious inconveniences for the researches. A long-distance (∼40km) wireless LAN system (11M bps) was set up in 2003. Two new easy-to-handle and easy-to-maintain dynamos of 115 KVA each, as shown in Fig. 2 were installed in 2004 as well. The unmanned operation of Norikura Observatory has been mostly successful in winter, during which the battery backed-up solar panels and/or wind power generators kept supplying the electricity to the wireless LAN and on-going cosmic-ray experiments.

Present major scientific interests of the laboratory is focused on the modulation of high energy cosmic rays in the interplanetary space associated with the solar activity, the generation of energetic particles by the solar flares, and the particle acceleration mechanism in

Fig. 2. A dynamo of 115KV.

thunderclouds, all of which require long-term observation. These researches have been carried out by the group of user universities, where ICRR provides them with laboratory facility. A part of the facility has been open for the environmental study at high altitude such as aerosol-related mechanism in the atmosphere, observation of total ozone and UV solar radiation, for botanical study in the high-altitude environment, etc..

Cosmic Ray Physics

Space weather observation [represented by Kazuoki Munakata, Shinshu University]

Space weather observation is actively made by a 25 m^2 muon hodoscope at Norikura Observatory. Mt. Norikura muon hodoscope has started operation in May, 1998 and successfully observed a clear precursory signature of the interplanetary shock arrival at Earth. With its improved angular resolution of muon incident direction, the detector succeeded for the first time to observe a loss-cone signature which is an intensity deficit within a narrow cone around the interplanetary magnetic field (IMF). The observation of the loss-cone precursor gives us unique information for the space weather forecast and for understanding the interplanetary disturbances in near Earth space.

Following this successful observation, we installed a small muon hodoscope in Kuwait City, Kuwait as the fourth detector in our Global Muon Detector Network (GMDN) with other three multidirectional muon detectors in Nagoya (Japan), Hobart (Australia), and São Martinho (Brazil). The GMDN has started operation in March, 2006 monitoring the intensity of ~ 50 GeV cosmic rays over an entire sky around Earth. The cosmic ray observations using muon detector are

complementary to observations with neutron monitors monitoring a lower energy range below ~ 10 GeV and the observations with GMDN have a great advantage particularly in precise measurement of the cosmic ray anisotropy, i.e. the dependence of intensity on incident direction in space, which gives us valuable information of the spatial distribution of the cosmic ray density in three dimensions. The Mt. Norikura muon hodoscope and GMDN have revealed the dynamic variations of the anisotropy which give us important information of the space weather. It has been already confirmed that the GMDN can measure the rapid variation of the anisotropy in the "cosmic ray burst" observed in June 2015 in 10 minute time resolution. The Kuwait muon hodoscope was enlarged three times in March 2016 and one minute data are now available from all of four detectors in the GMDN enabling us to analyze the anisotropy in 1 minute time resolution.

Recently, we also developed the method of the correction of the atmospheric temperature effect on muon count rate by using the GMDN data. This is a significant step, because it makes possible for the first time the analysis of the long-term variation of ~ 50 GeV cosmic ray density (i.e. isotropic intensity) which was possible so far only for cosmic ray below ~ 10 GeV using the neutron monitor data nearly free from the temperature effect. We have already published the long-term variation of the anisotropy observed by Nagoya muon detector.[1] [2] [3] [4] [5] [6] [7] [8] [9] [10]

Solar neutron observation [represented by Yutaka Matsubara, Nagoya University]

Observation of solar neutrons in solar cycle 24 has continued at Norikura Observatory of ICRR since fiscal 2007 to understand the acceleration mechanism of high energy (>100 MeV) ions associated with solar flares. These neutrons are produced by the interaction between accelerated ions and the solar atmosphere. Neutrons are not reflected by the interplanetary magnetic field, and thought to be more informative than accelerated ions themselves to study the acceleration mechanism at the solar surface. Solar neutron events detected

*1 " Solar neutron events in association with large solar flares in November 2003", Watanabe, K. *et al.*, Adv. Space Res., **38**, 425–430, 2006.

*2 K. Munakata, M. Kozai, P. Evenson, T. Kuwabara, C. Kato, M. Tokumaru, M. Rockenbach, A. Dal Lago, R. R. S. Mendonca, C. R. Braga, N. J. Schuch, H. K. Al Jassar, M. M. Sharma, M. L. Duldig, J. E. Humble, I. Sabbah, and J. Kota, "Cosmic Ray Short Burst Observed with the Global Muon Detector Network (GMDN) on June 22, 2015", Astrophys. J., 862:170 (9pp), 2018 (August 1).

*3 R. R. S. Mendonca, C. R. Braga, E. Echer, A. Dal Lago, M. Rockenbach, N. J. Schuch,, K. Munakata, "Deriving the solar activity cycle modulation on cosmic ray intensity observed by Nagoya muon detector from October 1970 until December 2012", Proc. IAU Sympo., 328, 1-4 (IAU-16-IAUS328-0453), 2016 (October 20).

*4 R. R. S. Mendonca, C. R. Braga, E. Echer, A. Dal Lago, K. Munakata, T. Kuwabara, M. Kozai, C. Kato, M. Rockenbach, N. J. Schuch, H. K. Al Jassar, M. M. Sharma, M. Tokumaru, M. L. Duldig, J. E. Humble, P. Evenson, I. Sabbah, "Temperature effect in secondary cosmic rays (muons) observed at ground: analysis of the global muon detector network data", Astrophys. J., 830:88 (25pp), 2016 (October 20). Cited by 2

*5 M. Kozai, K. Munakata, C. Kato, T. Kuwabara, M. Rockenbach, A. Dal Lago, N. J. Schuch, C. R. Braga, R. R. S. Mendon, H. K. Al Jassar, M. M. Sharma, M. L. Duldig, J. E. Humble, P. Evenson, I. Sabbah, and M. Tokumaru, "Average spatial distribution of cosmic rays behind the interplanetary shock– Global Muon Detector Network observations", Astrophys. J., 825:100 (19pp), 2016 (July 10). Cited by 7

*6 D. Ruffolo1, A. Saiz, P.-S. Mangeard, N. Kamyan, P. Muangha, T. Nutaro, S. Sumran, C. Chaiwattana, N. Gasiprong, C. Channok, C. Wuttiya, M. Rujiwarodom, P. Tooprakai, B. Asavapibhop, J. W. Bieber, J. Clem, P. Evenson, and K. Munakata, "Monitoring short-term cosmic-ray spectral variations using neutron monitor time-delay measurements", Astrophys. J., 817:38 (12pp), 2016 (January 20). Cited by 8

*7 M. Kozai, K. Munakata, C. Kato, T. Kuwabara, J. W. Bieber, P. Evenson, M. Rockenbach, A. Dal Lago, N. J. Schuch, M. Tokumaru, M. L. Duldig, J. E. Humble, I. Sabbah, H. K. Al Jassar, M. M. Sharma, J. Kota, "The spatial density gradient of galactic cosmic rays and its solar cycle variation observed with the Global Muon Detector Network", Earth, Planets and Space, 66, 151-158, 2014 (November 14). Cited by 12

*8 K. Munakata, M. Kozai, C. Kato, J. Kota, "Long term variation of the solar diurnal anisotropy of galactic cosmic rays observed with the Nagoya multi-directional muon detector", Astrophys. J., 791:22, 1-16, 2014 (August 10). Cited by 19

*9 M. Rockenbach, A. Dal Lago, N. J. Schuch, K. Munakata, T. Kuwabara, A. G. Oliveira, E. Echer, C. R. Braga, R. R. S. Mendonca, C. Kato, M. Kozai, M. Tokumaru, J. W. Bieber, P. Evenson, M. L. Duldig, J. E. Humble, H. K. Al Jassar, M. M. Sharma, I. Sabbah, "Global muon detector network use d for space weather applications", Space Sci. Rev., 182, 1-18, 2014 (May 9). Cited by 18

*10 K. Munakata"For space weather applications", Space Sci. Rev., 182, 1-18, 2014 (May 9).

on the ground are rare, and about 10 events were reported before solar cycle 24. The group led by Institute for Space-Earth Environmental Research, Nagoya University has operated a world-wide network of 7 solar neutron telescopes in the world. The solar neutron telescope operated at Norikura Observatory has an area of 64 m^2, which is largest among the 7 stations. The solar neutron telescope at Norikura consists of plastic scintillation detector and proportional counters. The neutron is detected when a recoil proton is produced in the scintillator, and the energy of the recoil proton is measures. Proportional counters are used both to veto charged particles and measure the direction of recoil protons. The telescope is operated by solar power during the winter period when the Norikura observatory is closed.

Solar cycle 24 was its maximum in February 2014 and has decreased its activity since then. We searched for solar neutron signals from the world-wide network of the solar neutron telescopes between January 2010 and December 2014 when the large ($\geq$X1.0 class) solar flare occurred. No solar neutron event was detected by this search. We statistically studied the relation between upper limits of the neutron flux and the energy of soft X-rays during the solar flare. This comparison was also made for the successful detections of solar neutrons before solar cycle 24. The conclusion from this study is that the total energy obtained by neutrons during solar flare does not exceed 0.1 % of the total energy of soft X-rays.[11]

Relativistic electron acceleration in thunderstorm electric field and high-energy atmospheric phenomena at lightning [represented by Teruaki Enoto, Kyoto University, for GROWTH Collaboration]

The Gamma-Ray Observation of Winter THundercloud (GROWTH) collaboration is aiming at revealing high-energy atmospheric phenomena occurring at lightning and in thunderstorms. The project started in 2006 and has detected bremsstrahlung gamma rays from relativistic electrons accelerated by strong electric fields in winter thunderstorms. This gamma-ray radiation events were named "long burst" by our group (as known as gamma-ray glow), which lasts for a minute time-scale corresponding with passage of a thundercloud above our detectors. Winter thunderstorms observed along the Japan sea are ideal targets for our observation campaigns thanks to its low altitude of the cloud base and frequent energetic lightning, while observations of summer thunderclouds at mountain tops are also important to measure the phenomena very close to or even inside thunderstorms. Our collaboration has used the Mount Norikura cosmic ray observatory to study the long bursts, and successfully recorded events.

The GROWTH collaboration newly launched multipoint mapping observation campaigns in 2015. The primary purpose is to study life cycle of the electron acceleration sites in thunderstorms comparing with weather-monitoring data. Another purpose of the project is to reveal mysterious "short burst" events, which have been sometimes detected in our past observations, associated with lightning discharges with its duration shorter than a second. Financially supported by the ICRR joint research programme, academic crowdfunding "academist", and JSPS/MEXT KAKENHI grant, we have developed portable and high-performance radiation detectors. In FY2016 and FY2017, the collaboration deployed radiation detectors at the Mt. Norikura cosmic ray observatory. So far, there is no detection of "long burst" nor "short burst" events from summer thunderclouds during the two years. However, we successfully used these summer campaigns as pilot observations toward the winter campaigns to check our operation and capability of the detectors. The Norikura observations are also educationally important as a training yard for Ph.D students in the team. In 2017 winter, our new mapping system at Kashiwazaki, Niigata, provided us a chance to solve the mystery of the short burst. This phenomena is revealed to be photonuclear reaction triggered by gamma rays from a lightning discharge. This discovery was selected, by the Physics World, as one of the top 10 breakthrough in the physics field in 2017.[12] We are now trying to develop the "high-energy atmospheric physics" of lightning and thunderstorms, a new interdisciplinary field combining the gamma-ray and radio observations.[13] [14] [15] [16]

*[11] D. Lopez et al., Estimates of the neutron emission during solar flares in the rising and maximum period of solar cycle 24, Astroparticle Physics, 76 (2016) 19-28.

*[12] Enoto, T. and Wada, Y. and Furuta, Y. and Nakazawa, K. and Yuasa, T. and Okuda, K. and Makishima, K. and Sato, M. and Sato, Y. and Nakano, T. and Umemoto, D. and Tsuchiya, H, "Photonuclear reactions triggered by lightning discharge", Nature 551, (2017) 481-484.

*[13] Dwyer, J. R. and Smith, D. M. and Cummer, S. A., "High-Energy Atmospheric Physics: Terrestrial Gamma-Ray Flashes and Related Phenomena", 173 (2012) 133-196.

*[14] Tsuchiya, H. and Enoto, T. and Torii, T. and Nakazawa, K. and Yuasa, T. and Torii, S. and Fukuyama, T. and Yamaguchi, T. and Kato, H. and Okano, M. and Takita, M. and Makishima, K., "Observation of an Energetic Radiation Burst from Mountain-Top Thunderclouds", Physical Review Letters, 102, (2009) 255003.

*[15] Wada, Y. and Bowers, G. S. and Enoto, T. and Kamogawa, M. and Nakamura, Y. and Morimoto, T. and Smith, D. M. and Furuta, Y. and Nakazawa, K. and Yuasa, T. and Matsuki, A. and Kubo, M. and Tamagawa, T. and Makishima, K. and Tsuchiya, H., "Termination of Electron Acceleration in Thundercloud by Intracloud/Intercloud Discharge", Geophysical Research Journal 45, (2018) 5700-5707.

*[16] Tsuchiya, H. and Enoto, T. and Yamada, S. and Yuasa, T. and Kawaharada, M. and Kitaguchi, T. and Kokubun, M. and Kato, H. and Okano, M. and Nakamura, S. and Makishima, K., "Detection of High-Energy Gamma Rays from Winter Thunderclouds", Physical Review Letters, 99, (2007) 165002.

Study of Secondary Cosmic Rays from Thundercloud at Mt. Norikura [represented by Atsushi Shiomi, Nihon University]

In order to study the relativistic electron acceleration mechanism by thundercloud-derived electric field and the relation between thunder and cosmic-ray air shower, we started an experiment in 2015, mainly using gamma-ray detectors at Norikura Observatory of Institute for Cosnic Ray Research, the University of Tokyo. This experiment consists of gamma-ray detectors, a lightning sensor, an electric field meter, a weather monitor, and an air shower array. Gamma-ray detectors using three crystals, NaI, CsI, and BGO respectively, cover the energy range over 3 orders of magnitude from 70 keV to 120 MeV as a whole.

Observation period: 22 days from August 24 to September 14, 2015
During this time, the thundercloud did not pass, and no gamma-ray burst derived from thundercloud was detected. However, the gamma ray detector was able to observe gamma rays derived from radon of less than 3 MeV as expected during rainfall. Also, gamma ray detectors using CsI and BGO for detecting gamma rays of 3 MeV or more did not observe an increase in gamma rays of 3 MeV or more. This means that gamma rays from radon can be distinguished from contributions from other gamma rays not derived from radon, and it can be expected that these detectors can operate normally even when they are installed at an altitude about 4000 m for a certain future project.

Observation period: 30 days from July 19 to September 16, 2016 (excluding the summer season)
No direct lightning strike event occurred during the observation period, but 6 atmospheric electric field fluctuations exceeding 30 kV/m, which seemed to be an influence of thunder cloud passage, were observed. In one of the events, it seems there was a lightning strike in the vicinity.

Observation period: 41 days from July 31 to September 9, 2017
Unfortunately, during this observation period there was no lightning strike nearby, but it was observed that the thundercloud passed several times. Currently, the data at the time of the thundercloud passing is being analyzed in detail (Fig. 3).

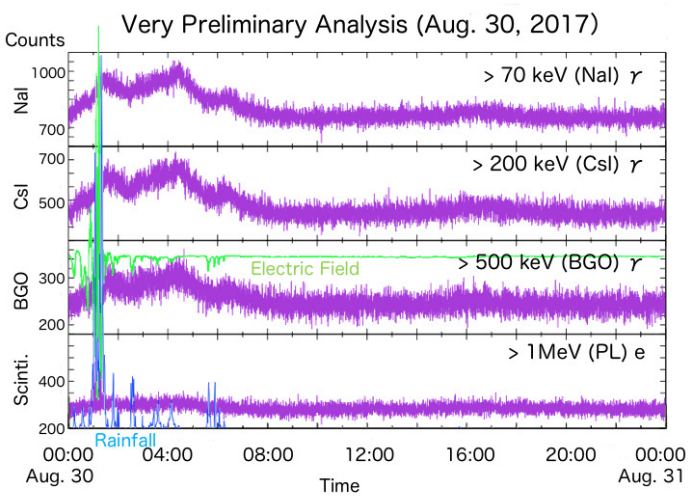

Fig. 3. Electric field (green), rainfall (blue), count value (purple) of each detector at the time of thundercloud passing.

Study of gamma ray bursts from mountain-top thunderclouds [represented by Makoto Minowa, The University of Tokyo]

We observed gamma ray bursts that arise in relation to thunderclouds at the Norikura Observatory of ICRR(2,770 m above sea level). Measurement was carried out by placing PANDA64 detector outdoors of the observatory. The detector is made of 64-module plastic scintillators(total mass about 640 kg) developed for reactor operation monitoring. Our measurement has unprecedented features including high statistics, good energy response, direction sensitivity and neutron identification.

Long-duration persistent bursts were observed 12 times in 54 days from July to September 2014 and their energy spectrum extended up to 25 MeV in the largest burst. The duration of the bursts ranged from a few to ten minutes. Since these bursts were found in the energy range higher than 3 MeV, they were not attributed to the rain fallout of radon and its daughter nuclei.

According to the thundercloud information provided by the Japan Meteorological Agency, the bursts were observed when there was thunder activity near the observatory. The observation is qualitatively in good agreement with thundercloud radiation bursts previously observed in mountain areas or coastal areas of the Sea of Japan.

Monte Carlo simulation showed that the bremsstrahlung γ-rays by source electrons with monochromatic energy of 40–80 MeV falling downwards from altitude of 400–1000 m produced the observed total energy spectra of the bursts well. It is supposed that secondary cosmic ray electrons, which act as seed, were accelerated in electric field of thunderclouds and multiplied by relativistic runaway electron avalanche.

The estimated energy of the source electrons was higher than that of the bursts we previously observed at Ohi Power Station at sea level. Additionally, estimated electron flux at the estimated source height was remarkably lower than that of the Ohi site. These results give new restrictions to the model of electron acceleration and multiplication process in electric field of

thunderclouds.[17] [18] [19] [20]

Development of high energy proton irradiation technique for devices used in spaceship [represented by Kyo Kume, The Wakasa Wan Eenergy Research Center]

Space exploration is presently interesting in business field. Ion beam irradiation verification for devices to be mounted on spaceships is required to simulate cosmic rays expected in the universe to estimate lifetime of these devices.

Flux estimation technique of primary ion beam in wide range from an accelerator is needed In this kind of cosmic ray simulation field. The desired flux of the ion beam for this kind of field is between 10^2 and 10^6 protons·cm^{-2} ·s^{-1} in typical proton cases. Plastic scintillators can be used in lower intense region to count direct primary ions, while ionization chambers can be used in higher intense region to count ionization caused by primary ions. But there have been no definite modalities available to measure throughout this whole intensity region.

One of the candidate techniques is to measure secondary γ-ray intensity emitted through a beam transport, which has nearly a maximum energy of the primary ion beam around 100 MeV for this kind of simulation field. This technique has a feature that detector components do not occupy the beam path and the presence of the detector do not influence the main simulation field at all.

NaI(Tl) scintillator system for high energetic γ-ray measurement which had been used in previous thunder lightning γ-ray measurement was used. This system has a 5-inch NaI(Tl) scintillator with NT100GPS pulse hight analysis system of Laboratory Equipment. Ion beam accelerator experiments using 100 MeV proton beam were carried out at the Wakasa Wan Energy Research Center (WERC). Background measurements were carried out at Norikura Observatory of ICRR in summer, where one can expect high energetic γ-ray, which has the similar energy region compared to the accelerator field of this study. EFM100 atmospheric electric field monitor system of Boltek was added at Norikura to measure accidental high energetic γ-rays caused by thunder lightning.

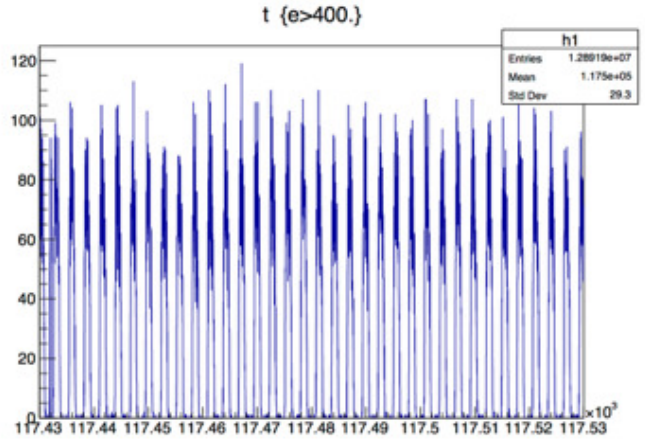

Fig. 4. Time structure of γ-ray above 3 MeV at WERC 100 MeV proton beam delivery. Vertical axis shows γ intensity (events/ms) while horizontal shows time after beginning of the operation (s).

As shown in Fig.4 of a time structure of γ-ray during 100 MeV proton beam delivery duration obtained at WERC, the result clearly shows that this measurement system can distinguish the beam ON/Off, while this system is still in verification for a quantitative discussion. The dead time of the system should be defined.

In the meantime, thunder lightning events were searched using data obtained at Norikura. No events have been distinguished. The whole data at Norikura show a stable condition of the whole system for a couple of months.

With the help of this study, the trial to carry out cosmic ray simulation at the ion beam accelerator facility (WERC) has been successfully carried out. One will keep trying to estimate the quantitative property of the system in ion beam environment.[21] [22] [23] [24]

Development of high energy proton irradiation technique for devices used in spaceship [represented by Kazuaki Yajima, National Institute of Radiological Sciences, National Institutes for Quantum and Radiological Sciences and Technology]

Aircraft crew are exposed to elevated levels of cosmic rays at aviation since the dose rate of cosmic rays increases with altitude. The occupational doses of air-

*[17] Yo Kato, "Observational study of thundercloud radiation bursts using a segmented organic scintillator installed at a mounaintop", Ph.D. thesis, The University of Tokyo, September, 2015.

*[18] Y. Kato, "Thundercloud-related radiation bursts observed at a coastal area and a mountaintop using segmented organic scintillators", Thunderstorms and Elementary Particle Acceleration (TEPA-2015), 5-9 October 2015, Yerevan, Armenia.

*[19] Y. Kato, "Development of Plastic Anti-neutrino Detector Array (PANDA)", Applied Antineutrino Physics(AAP) 2015, 7-8 December 2015, Virginia Tech Research Center, United States.

*[20] Y. Kato "Observation of thundercloud radiation bursts using segmented plastic scintillators", European Geosciences Union General Assembly (EGU), 8-13 April 2018, Austria Center Vienna, Austria.

*[21] T. Torii *et al*., "Gradual increase of energetic radiation associated with thunderstorm activity at the top of Mt. Fuji", Geophys. Res. Lett 36(13) , 2009.

*[22] T. Kuritai *et al*., "The Status of the synchrotron of the Wakasa Wan Energy Research Center", Proc. 12th Annual Meeting of the Particle Accelerator Societ of Japan, 288, 2015.

*[23] K. Kume, T. Torii, M. Takita and T. Hasegawa, "Development of a beam fluence measurement technique at atmosphere", Igaku Butsuri, Vol.36 Suppl.3 178, 2016 (in Japanese).

*[24] K. Kume, T. Hasegawa, S. Hatori, M. Takita and H. Tsuji, "Space engineering application of therapeutic broad beam for cosmic rai simulation", Igaku Butsuri, Vol.37 Suppl. 112, 2017 (in Japanese).

craft crew have generally been evaluated by model calculation. It is necessary to verify the calculation with measurements to maintain accuracy and credibility of dose assessment. The purposes of this study were to construct a compact and inexpensive cosmic-ray neutron monitoring system which was based on a rem-counter at Norikura Observatory (2770 m above sea level), and to examine the feasibility of it. The monitoring system was installed in the Norikura Observatory in 2014. It consisted of an extended-energy neutron rem counter with wide energy range from 25 meV to 5 GeV, a custom-made data logger connected to LAN, and a battery power unit. The measured data was received in National Institute of Radiological Science in Chiba-city via the ICRR network. This monitoring system succeeded in continuous monitoring more than ten months twice during 2014 to 2016. The averaged counting rate was about 1 count per minute, which was equivalent to neutron ambient dose equivalent rate of about 15 nSv/h by the preliminary evaluation. It is a future problem to reveal the cause of the reduction in counting rate seen over from November to April.

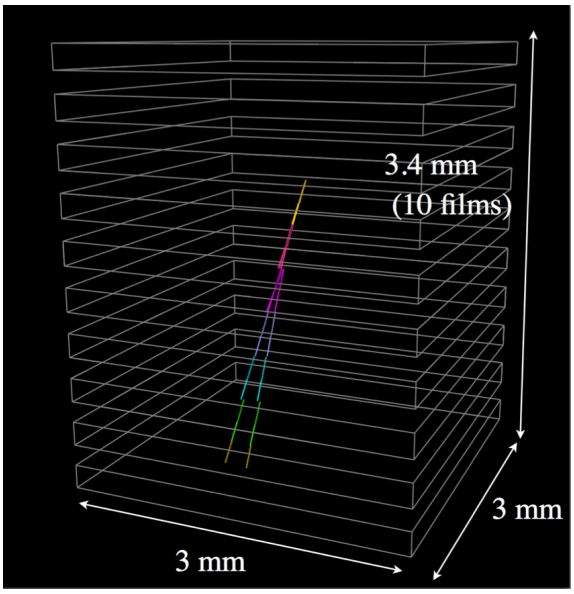

Fig. 5. 3-D view of $\gamma \rightarrow e^+ + e^-$ detected in the chamber employed in the obseration test at Norikura Observatory. The reconstructed energy of this event was 160 MeV.

Evaluation of Response to the Gamma-ray of the Emulsion Telescope (2007, 2013 [represented by Shigeki Aoki for GRAINE collaboration, Kobe University]

GRAINE project (Gamma-Ray Astro-Imager with Nuclear Emulsion) has been developing the observation of cosmic γ-ray in the energy range 10 MeV–100 GeV with precise (0.08° at 1–2 GeV), polarization-sensitive, large-aperture-area ($\sim$10 m^2) balloon-borne telescope using nuclear emulsion film. Under the development of the telescope, we performed test observation at Norikura Observatory (2770 m a.s.l.) in 2007 and 2013 using prototype emulsion telescope in order to confirm detection performance using atmospheric γ-ray.

2007 test was the first trial of the detection to the γ-ray spread wide incoming angle. We established configuration of the telescope and its analysis scheme. Based on this experience, we finalized the design of the first balloon-borne emulsion telescope and performed 1st balloon experiment (GRAINE 2011) at the Taiki Aerospace Research Field of JAXA in June 2011.

In 2013 test, we introduced self-produced nuclear emulsion gel film with higher volume occupancy of silver bromide crystals with respect to conventional ordinary gel in order to improve track finding efficiency as well as signal-to-noise ratio. We obtained high ($> 97\%$) track finding efficiency in a single film and confirmed γ-ray detection capability at 100 MeV energy region (Figure 5).

Based on this experience, we performed 2nd balloon experiment (GRAINE 2015) in Japan-Australia JAXA collaborative balloon experiment at the Alice Springs balloon-launching station in May 2015. [25] [26] [27] [28] [29] [30] [31]

Environmental Study

Aerosol sampling at Mt. Norikura [represented by Fuyuki Tokanai, Yamagata University]

Aerosol in the atmosphere has been sampled since 2013 at the Norikura observing site using air-samplers to investigate the production of cosmogenic nuclide ^{7}Be in a free troposphere above 2 km in the altitude. The aerosol size distribution of ^{7}Be was measured for the aerosols sampled by an Andersen sampler enable to separate aerosols to nine classes from 0.43 μm to 11 μm. The 81.7% of ^{7}Be was covered with the aerosol sizes less than 1.1 μm and the ^{7}Be with the aerosol sizes above 1.1 μm decrease with an exponential function. The ^{7}Be concentration at Mt. Norikura was approximately 9.4 times greater than that at the ground level

*25 Satoru Takahashi,Ph.D Thesis (2011) Nagoya University, http://hdl.handle.net/2237/14900.

*26 Hiroaki Kawahara, Master Thesis (2015), Nagoya University

*27 "GRAINE project: gamma-ray observation with a balloon-borne emulsion telescope", Hiroki Rokujo on behalf of GRAINE Collaboration, Proceeding of Science KMI2013 (2014) 042.

*28 "GRAINE project: The first balloon-borne, emulsion gamma-ray telescope experiment", S. Takahashi, S. Aoki, K. Kamada, S. Mizutani, R. Nakagawa, K. Ozaki and H. Rokujo, PTEP 2015 (2015) no.4, 043H01.

*29 "Gamma-Ray Astro-Imager with Nuclear Emulsion, GRAINE (in Japanese)", Satoru Takahashi, Shigeki Aoki for GRAINE collaboration, Journal of the SPSTJ, Vol,78(2015) No.4, pp.228-234.

*30 "GRAINE 2015, a balloon-borne emulsion γ-ray telescope experiment in Australia", Satoru Takahashi et al. (GRAINE collaboration), PTEP 2016 (2016) no.7, 073F01.

*31 "GRAINE project, prospects for scientific balloon-borne experiments", Satoru Takahashi, Shigeki Aoki for GRAINE collaboration, Advances in Space Research, Articles in press.

in Yamagata-city (Fig.6.). Its ratio is almost consistent to a simulated ratio 8.8 of ^{7}Be productions due to secondary cosmic rays in the atmosphere by EXPACS. This experimental result is useful for an estimation of altitude distribution of cosmogenic nuclide.

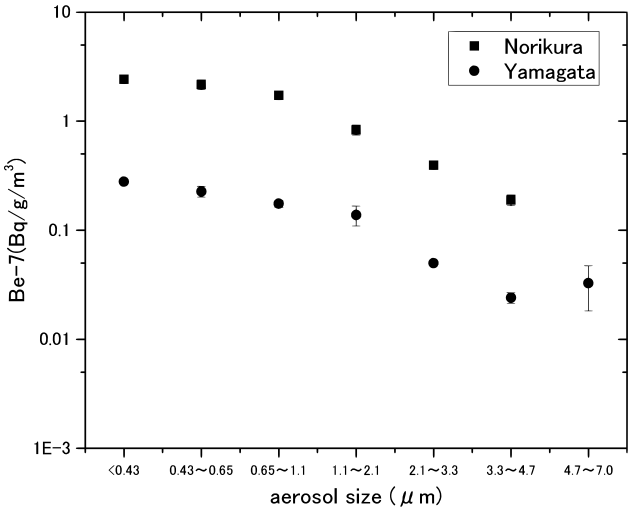

Fig. 6. ^{7}Be concentration as a function of aerosol size

Adaptation of alpine plants to severe environmental conditions [represented by Emiko Maruta, Kanagawa University]

Trees in the alpine regions experience harsh conditions including strong winds, low temperatures, desiccation, and heavy snow. Thus, plants growing in such regions are predicted to have adaptations to these environmental stressors. Through the inter-university research of ICRR, we obtained an opportunity to intensively study plant responses to environmental factors. We identified several characteristics unique to alpine plants, some of which contradict conventional knowledges.

1. Adaptation of leaf cuticles in sub-alpine fir (Abies mariessii) at the alpine tree-line

Leaf browning and death are frequently observed in evergreen conifers at the alpine tree-line. These are thought to due to increased transpiration caused by a thinner cuticle and/or mechanical damage to the cuticle by wind-blown snow and ice particles. However, in the sub-alpine fir (Abies mariessii) at Mt. Norikura, mechanical damage was not observed, and the cuticle was rather thick, which may be an adaptation against overwintering at the alpine regions.

2. Embolism of sub-alpine fir (Abies mariessii) at the alpine tree-line

Trees at high altitudes experience severe embolism (loss of xylem conductivity for water) during winters, which is attributed to the entrapment of air in xylem conduits during frost-drought. However, in the sub-alpine fir (Abies mariessii) at Mt. Norikura, air-filled conduits were not observed even in severely-embolized (complete loss of conductivity) shoots. Rather, the pits (valves of partitions inter-conduits) closed before the severe frost-drought in mid-winter, thereby resulting in severe-embolism (complete loss of conductivity). Thus, by pit (valve) cloure, shoots could maintain water in the xylem throughout the winter, which is thought to be an adaptation against lethal filling of air in the conduits during severe frost-drought.

3. Photosynthesis of Haimatsu (Pinus pumila)

At wind-exposed sites on Mt. Norikura, photosynthesis in Haimatsu was suppressed by lower mesophyll CO_2 conductance, and not by stomatal closure. [32] [33] [34]

Investigation of alpine plants on Mt. Norikura [represented by Koichi Takahashi, Shinshu University]

We studied mainly the following three researches on Mt. Norikura after 2012.

1) Long-term monitoring and community assembly of alpine plants

We made 40 plots for long-term monitoring of alpine vegetation because climate change possibly affects distributions of alpine plants. We also examined the community assembly process of alpine plants at the 40 plots from the view points of habitat filtering and limiting similarity. Habitat filtering and limiting similarity relate environmental conditions and interspecific competition, respectively. It is suggested that habitat filtering is more important than limiting similarity for the community assembly of alpine plants.

2) Soil respiration rates along an altitudinal gradient

This study investigated seasonal changes of soil respiration rates from forest soil along an altitudinal gradient (1600 m to 2800 m above sea level). The soil respiration rate positively correlated with soil temperatures and forest biomass. It is suggested that forest productivity is an important factor for soil respiration rates.

3) Genetic differentiation of Solidago virgaurea complex

Plant species distributed along wide altitudinal or latitudinal gradients show phenotypic variation due to their heterogeneous habitats. This study investigated whether phenotypic variation in populations of the Solidago virgaurea complex along an altitudinal gradient is caused by genetic differentiation. Population genetic

*32 Nakamoto A., Ikeda T., Maruta E. (2013) Needle browning and death in the flagged crown of Abies mariesii in the timberline ecotone of the alpine region in central Japan. Trees 27:815-825.

*33 Maruta E., Yazaki K.(submitted) Mechanism of embolism as induced by pit closure during winter in sub-alpine fir (Abies mariesii)on Mt. Norikura.

*34 Nagano S., Nakano T., Hikosaka K., Maruta E. (2013) Pinus pumila photosynthesis is suppressed by water stress in a wind-exposed mountain site. Arctic, Antarctic, and Alpine Research 45:229-237.

analyses with microsatellite markers were used to infer the genetic structure and levels of gene flow between populations. However, the population genetic analysis suggested an extremely low level of genetic differentiation of neutral genes among the nine populations. This study suggests that genome regions responsible for adaptive traits may differ among the populations despite the existence of gene flow and that phenotypic variation of the S. virgaurea complex along the altitudinal gradient is maintained by strong selection pressure.
35 36 37 38 39 40 41 42 43 44 45 46 47 48 49

*35 Takahashi, K., Hirosawa, T. and Morishima, R. (2012) How the timberline formed: altitudinal changes in stand structure and dynamics around the timberline in central Japan. Annals of Botany 109: 1165-1174.

*36 Takahashi, K. and Okuhara, I. (2013) Forecasting the effects of global warming on radial growth of subalpine trees at the upper and lower distribution limits in central Japan. Climatic Change 117: 278-287.

*37 Takahashi, K. and Obata, Y. (2014) Growth, allometry and shade tolerance of understory saplings of four subalpine conifers in central Japan. Journal of Plant Research127: 329-338.

*38 Takahashi, K. (2014) Effects of wind and thermal conditions on timberline formation in central Japan: a lattice model. Ecological Research 29:121-131.

*39 Takahashi, K. and Koike, S. (2014) Altitudinal differences in bud burst and onset and cessation of cambial activity of four subalpine tree species. Landscape and Ecological Engineering 10:349-354.

*40 Takahashi, K. and Murayama, Y. (2014) Effects of topographic and edaphic conditions on alpine plant species distribution along a slope gradient on Mount Norikura, central Japan. Ecological Research 29: 823-833.

*41 Singh, D., Takahashi, K., Park, J. and Adams, J. M. (2016) Similarities and contrasts in the archaeal community of two Japanese mountains: Mt Norikura compared to Mt Fuji. Microbial Ecology 71: 428-441.

*42 Takahashi, K. and Furuhata, K. (2016) Shoot growth and seasonal changes of non-structural carbohydrate concentrations at the upper and lower distribution limits of three conifers. Landscape and Ecological Engineering 12: 239-245.

*43 Takahashi, K. and Tanaka, S. (2016) Relative importance of habitat filtering and limiting similarity on species assemblages of alpine and subalpine plant communities. Journal of Plant Research 129: 1041-1049.

*44 Takahashi, K. and Matsuki, S. (2017) Morphological variations of the Solidago virgaurea L. complex along an elevational gradient on Mt. Norikura, central Japan. Plant Species Biology 32: 238-246.

*45 Kerfahi, D., Tateno, R., Takahashi, K., Cho, H., Kim, H. and Adams, J. M. (2017) Development of soil bacterial communities on volcanic ash microcosms in a range of climates. Microbial Ecology 73: 775-790.

*46 Sakurai, A. and Takahashi, K. (2017) Flowering phenology and reproduction of the Solidago virgaurea L. complex along an elevational gradient on Mt. Norikura, central Japan. Plant Species Biology 32: 270-278.

*47 Dong, K., Moroenyane, I., Tripathi, B., Kerfahi, D., Takahashi, K., Yamamoto, N., An, C., Cho, H., and Adams, J. (2017) Soil nematodes show a mid-elevation diversity maximum and elevational zonation on Mt. Norikura, Japan. Scientific Reports 7: 3028.

*48 Hirano, M., Sakaguchi, S. and Takahashi, K. (2017) Phenotypic differentiation of the Solidago virgaurea complex along an elevational gradient: Insights from a common garden experiment and population genetics. Ecology and Evolution 7: 6949-6962.

*49 Takahashi, K., Otsubo, S. and Kobayashi, H. (2017) Comparison of photosynthetic traits of codominating subalpine conifers Abies veitchii and A. mariesii in central Japan. Landscape and Ecological Engineering 14: 91-97.

KAGRA Observatory

Introduction

KAGRA observatory is located in the Ikenoyama-mountain on the border between Gifu and Toyama prefecture, about 35 km south of Toyama city in Japan. The observatory was established in 2016 in order to operate Large-scale Cryogenic Gravitational Wave Telescope (nicknamed "KAGRA"). KAGRA itself has a L-shape tunnel facility, and it is located more than 200 m under Ikenoyama-mountain. The corner station of the L-shape tunnel is accessible through a 500 m horizontal access tunnel from Atotsu area. The observatory has its own surface research buildings and rental space in the community center of Hida city located about 5 km away from the Atotsu entrance of KAGRA.

Scientific Goal

KAGRA aims to observe several gravitational waves (GWs) per year with its designed sensitivity as one of observatories of the world GW detection network including Advanced-LIGO, Advanced-Virgo and planned LIGO-India. KAGRA project (formerly named LCGT) was partially approved in 2010 as one of Leading-edge Research Infrastructure Program, and also supported by Program for Promoting Large-scale Science Projects, Subsidy for Facilities Expense and Grants-in-Aid for Scientific Research from Ministry of Education, Culture, Sports, Science and Technology (MEXT).

KAGRA Collaboration

In KAGRA project, Institute for Cosmic Ray Research plays a role of a host promoting institute, and National Astronomical Observatory in Japan (NAOJ) and High Energy Accelerator Research Organization (KEK) are the main support organizations, then more than 280 researchers in 87 institutes and universities in the world are collaborating for construction and data analysis of KAGRA.

Construction Status

The tunnel excavation started in May 2012, and finished in March 2014. After that, the basic laboratory environment was prepared until September 2015. A Michelson interferometer with 3km arm (iKAGRA) was demonstrated in March 2016, and the first engineering run was performed until May 2016. At present (June 2018) all interferometer components are being installed to complete KAGRA observatory that adopts a power recycled Fabry-Perot Michelson type interferometer with resonant sideband extraction technique. We hope to start KAGRA observatory operation around March 2019 and start joint observation with LIGO and Virgo within 2019.

Fig. 1. Surface Research Building.

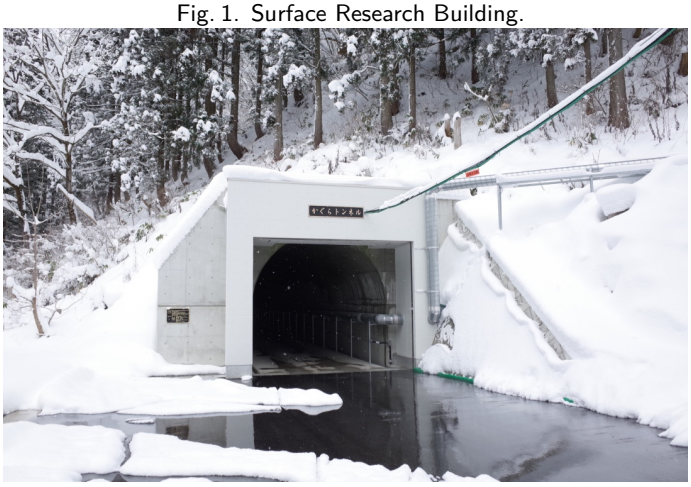

Fig. 2. Atotsu Entrance of KAGRA.

RESEARCH CENTER FOR COSMIC NEUTRINOS

Research Center for Cosmic Neutrinos (RCCN) was established in 1999 in order to promote the activities of neutrino researches. The center belongs to the Cosmic Neutrino Research Division, and the scientific staffs of the center have been working mainly for several research projects of the division such as Super-Kamiokande, T2K, Hyper-Kamiokande. The research activities, that these staffs have been made, are already included in the corresponding sections of these projects. This section describes other RCCN activities which have been made as a role of the inter-university joint-use research institution.

RCCN is in charge of the management of the ICRR main computing system, which is also provided as a service of the joint-use research program. Every researchers, who are accepted for the research program, are able to have the computing account and utilize the computing resources. The system is managed under the ICRR computer committee, which is composed of ICRR staffs. The main part of the system consists of the computing clusters containing about 2000 CPU cores, and the file system of 4 Petabyte (PB) disk space. A high-speed network is connected in-between them, which enables users to read/write the large size of the files speedy and analyze the data efficiently. The system also provides several servers of system control, networking, internet services such as web, mail, online storage, etc. The system has been upgraded in every 5∼6 years in order to have the benefits of the evolution of the latest computer performance. The current system was renewed in January 2014 (Fig. 1). It has been running stably without any serious trouble. The overall efficiency of providing the computing resources is greater than 95% at present (as of year 2018). The next upgrade of the system is planned in 2020.

RCCN has been organizing the series of the domestic workshop since 2000, in order to stimulate the activities of the neutrino research. The workshop have been accepted as one of ICRR joint-use research program, with the external members of other universities. The workshop has been held every year, and focused on the several topics related to neutrino physics, which are listed in Table 1. The photo of the latest workshop held in 2018 is shown in Fig. 2.

RCCN is also contributing to the outreach of the scientific research results. RCCN and the Public Relation Office of ICRR have been performing the public lectures every year, which are co-sponsored by ICRR and the Kavli IPMU (Institute for the Physics and Mathematics of the Universe). The list of the public lectures, held between 2013 and 2018, is shown in Table 2.

RCCN has been accepting several applications of the joint-use research programs of ICRR, especially for the low background radioisotope measurement in the underground laboratory of the Kashiwa campus, and the simulation researches using the ICRR computing system. The underground laboratory is equipped with four Germanium detectors (Fig. 3), mainly utilized for the measurements of cosmic radioactive isotopes. The scientific activities which have been made by using this laboratory are described in other section.

Fig. 1. ICRR computering system managed by RCCN and ICRR computer committee.

Fig. 2. Domestic neutrino workshop held in February 2018.

Table 1. Series of the domestic neutrino workshop organized by RCCN between 2013 and 2018.

	Date	Main topic(s)
1	March 15, 2013	θ_{13} and high energy cosmic neutrino
2	January 20, 2014	Absolute mass of neutrino measured from cosmology and ground experiment
3	February 21, 2015	Non-standard framework of neutrino mixing – sterile neutrino and nonstandard interaction
4	February 20, 2016	Atmospheric neutrino
5	February 4, 2017	Physics of neutrino interaction
6	February 24 2018	High energy neutrino and CP

Table 2. List of public lectures organized by RCCN and ICRR Public Relation Office. These lectures are co-hosted by ICRR and Kavli IPMU.

	Date	Lecturers
1	April 13, 2013	Ouchi Masami (ICRR)
		Nojiri Mihoko (KEK, Kavli IPMU)
2	April 14, 2014	Terasawa Toshio (ICRR)
		Kouno Toshitake (Kavli IPMU)
3	April 18, 2015	Nomura Yasuki (UC Berkley, Kavli IPMU)
		Miyoki Shinji (ICRR)
4	April 16, 2016	Hayato Yoshinari (ICRR)
		Nishimichi Akihiro (Kavli IPMU)
5	April 15, 2017	Sagawa Hiroyuki (ICRR)
		Toda Yukinobu (Kavli IPMU)
6	April 14, 2018	Nakahata Masayuki (ICRR)
		Shrai Satoshi (Kavli IPMU)

Fig. 3. Low-background underground laboratory in Kashiwa campus.

LOW-LEVEL RADIOISOTOPE MEASUREMENT FACILITY

Low-level radioisotope measurement facility was built at Kashiwa campus in 2000 with the relocation of ICRR from Tanashi campus in Tokyo. Historically, the facilities originated in Nokogiri-yama laboratory set up under Mt. Nokogiri-yama approximately 45 years ago, and the initial objectives were low-level counting to investigate cosmogenic nuclides in extraterrestrial materials such as cosmic dust falling down to the earth surface and/or the ocean. The new laboratory at Kashiwa is located in a basement 23 m from the surface. The floor space is approximately 47 m^2 and all of the walls are painted by "MINEGUARD" which is a special paint to block radon gas from the reinforced concrete.

In this laboratory, four High-Purity Germanium (HPGe) detectors are installed to measure natural radioactivity of various kinds of samples by gamma ray spectroscopy (Fig. 1).

Fig. 1. High-Purity Germanium (HPGe) detectors installed in Kashiwa Underground Laboratory

All of HPGe detectors are well type with U-style cryostats. Each HPGe detector is surrounded by an ultra low-background shield with 15 cm thick low background lead. The specifications of these detectors are shown in Tab.1. The data acquisition for the HPGe detector are computer controlled, and the identification of the radioisotopes is automated. In addition, environmental data of the laboratory such as temperature, humidity, atmospheric pressure, radon concentration, weights of liquid nitrogen vessel for cooling HPGe detectors, are monitored and logged by the network data logging system as shown in Fig.2. Oxygen-density-meter is continuously monitored by a TV camera, and is displayed at the entrance level floor. Before entering the underground laboratory, we are obliged to check if (1) Ventilator is working, and (2) Oxygen density is not lower than 20.9%. This facility has been utilized for low-level counting of the cosmogenic and environmental radioisotopes in a variety of samples.

Table 1. Specifications of HPGe detectors.

Det. No.	Well Dia.(mm)	Vol.(cc)	Manu. Year
1	10	190	1997
2	16	170	1997
3	16	116	1986
4	16	160	2005

Theme 1: Detection of time variation of cosmogenic ^{7}Be by Fuyuki Tokanai (Yamagata Univ.) et al.: The temporal variation of the ^{7}Be concentrations in atmosphere has been measured during 18 years since 2000 at Yamagata [1]. This corresponds to the period from the solar maximum of the 23th solar cycle to almost the end of the 24th cycle. The yearly profile of the ^{7}Be concentration indicates the variation in galactic cosmic rays owing to solar modulation because ^{7}Be is produced by spallation of the air elements due to cosmic rays. The yearly profile of the ^{7}Be concentration showed a clear anticorrelation with that of the number of sunspots. Corresponding to the 41% reduction in the number of sunspots from the 23th cycle to the 24th cycle, the ^{7}Be concentration increased by 39.5%, indicating that the variation in the ^{7}Be concentration can quantitatively reflect the variability of solar activity, even in different solar cycles. The daily variation of the concentrations of ^{7}Be has been measured since June 2014 at Bangkok in Thailand (13.45°N, 100.19°E) to observe the variations in the concentration of cosmogenic nuclides at low latitudes. The ^{7}Be concentration shows a clear seasonal variation with high and low concentrations from January to May and from June to December, respectively, in each year, with the highest ^{7}Be concentration 2.3 times larger than the lowest ^{7}Be concentration. From an analysis of air-mass trajectories, it was found that the high and low ^{7}Be concentrations approximately correspond to "Continental and Pacific Ocean trajectories" and "Indian Ocean trajectories", respectively.

Theme 2: Evaluation and monitoring of radioactive Cs released from the TEPCO Nuclear Power Plant since the 2011 Tohoku earthquake by Kotaro Shirai (Univ. Tokyo) et al: The 2011 earthquake and associated tsunami disrupted the operation of the Fukushima Daiichi Nuclear Power Plant (FDNPP), which resulted in the widespread release of large amounts of radio- cesium (^{134}Cs and ^{137}Cs) into the local environment during the period 12-23 March 2011. Understanding of the dy-

*1 S. Suzuki, H. Sakurai, F. Tokanai et al., "Observation of cosmogenic nuclide Be-7 concentrations in the air at Bangkok and trajectory analysis of global air-mass motion", 35th International Cosmic Ray Conference (ICRC2017): Bexco, Busan, Korea, July 12-20, 2017, Proceedings of Science (ICRC2017) 070 (2017) 1-8.

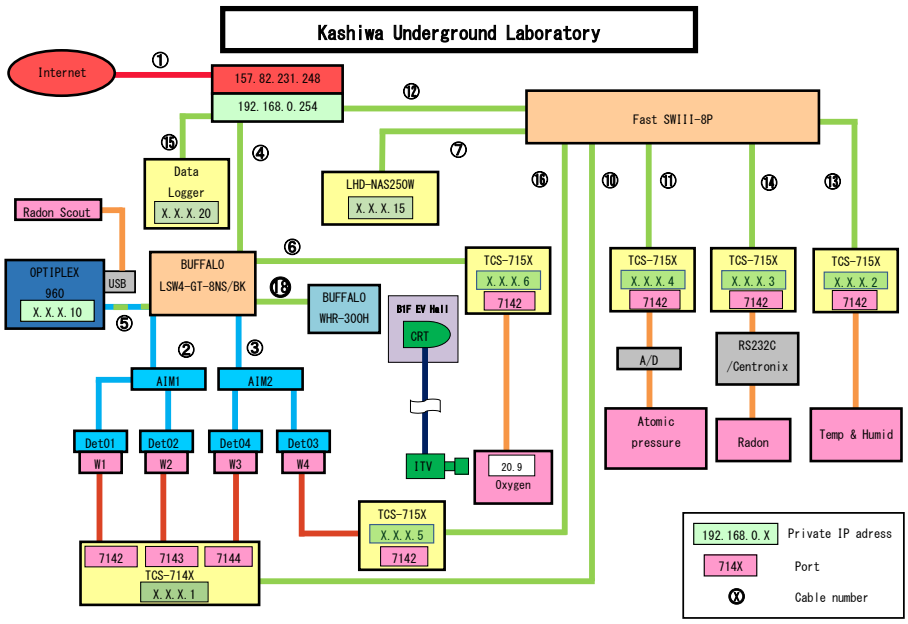

Fig. 2. Data acquisition and monitoring of Kashiwa Underground Laboratory

namics of radioactive Cs is scientifically important as well as socially important. Two topics have been studied to solve the query, (1) the behavior of radioactive Cs in a coastal marine environment and (2) the coastal monitoring of radioactive Cs through the observation of mussels.

(1) Vertical profiles of the ^{137}Cs activity in coastal sandy sediment from Funakoshi bay, Iwate, were determined. The depth of ^{137}Cs intrusion was estimated to be 10-15 cm, where ^{137}Cs was initially deposited on the surface layer of the sandy bottom. In combination with the observation of bioturbation structures based on a view of burrows using a CT scanner, the main driver of ^{137}Cs redistribution was identified as bioturbation by Echinocardium cordatum[2]. (2) Since sessile bivalves such as mussels and oysters are filter feeders and accumulate heavy metals and organic pollutants in their bodies, monitoring of the contaminant concentration in their soft tissue is one of the most common methods of environmental monitoring and is used in the Mussel Watch Program. Radioactive Cs has also been measured at various locations for monitoring purposes. Thus, mussels were collected along the Pacific coast of Japan from Iwate to Fukushima from 2011 to 2015, and the radioactive Cs in the soft tissue was measured to clarify the temporal and spatial changes in radioactive Cs released from FDNPP. For the 2011 samples, ^{137}Cs was above the detection limit at all the sampling points with the coast to the south of FDNPP showing higher concentrations than the northern coast. In addition, the ^{137}Cs level has been decreasing since 2011. Since mussels feed particulate organic materials, quantitative value of radioactivity obtained from these mussels can be used as baseline data for ecosystems.

Theme 3: Evaluation of the erupted radioactivities into the environment by Hisayuki Arakawa (Tokyo Univ. of Marine Sci. and Tech. et al.: As a result of the Great East Japan Earthquake and associated tsunami in March 2011, the Fukushima Daiichi Nuclear Power Plant (FDNPP) released a large amount of radioactive materials into the environment, resulting in the contamination of many marine organisms. Marine plants of various species were collected from the Iwaki coast of Fukushima Prefecture from May 2012 to June 2015 and analyzed to determine variations in ^{110m}Ag, ^{134}Cs, and ^{137}Cs with time. The results indicated that (1)^{110m}Ag was present in all seaweed and seagrass collected in May 2012. (2) The concentration of ^{110m}Ag in the sea grass *Phyllospadix iwatensis* decreased significantly with time, while the ecological half-life of^{110m}Ag in *P. iwatensis* was longer at locations nearer to FDNPP.

*2 Koji Seike, Kotaro Shirai, Naoko Murakami-Sugihara, "Using tsunami deposits to determine the maximum depth of benthic burrowing", PLOS ONE. 12 (8) e0182753, DOI:10.1371/journal.pone.(2017) 0182753

APPENDIX

A.1: ORGANIZATION

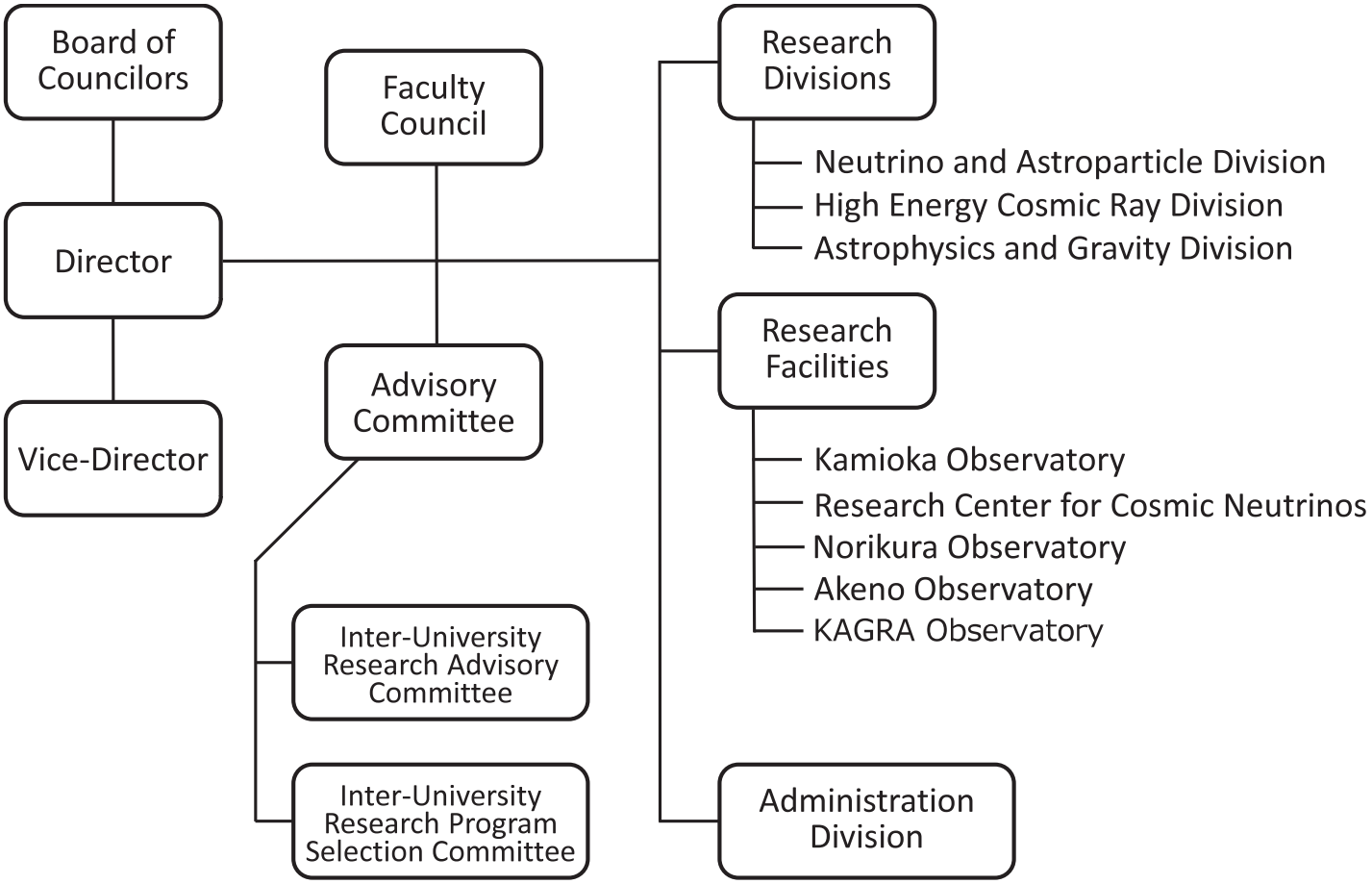

Fig. A.1-1 Organization of the Institute for Cosmic Ray Research as of April 2018.

A.2: ICRR STAFFS (2018)

The number of tenured researchers (Professors, Associate Professors, and Research Associates) in ICRR was slightly increased; it is 42 in 2018. Essentially, there is the balance between newly allocated posts by the University of Tokyo, and the un-filled posts (after retirement or departure of the staff) under a general rule in the University of Tokyo, which is based on a law to restrict the total number of employees in the governmental agency.

The University of Tokyo established the post re-allocation system to assign new posts to departments and institutes. Under this system, each department or institute submits a post re-allocation proposal to the University of Tokyo. Then the posts might be re-allocated to them after the evaluation of the proposal. In 6 years, ICRR got some re-allocations.

The Table below summarizes staffs of ICRR in 2018. In FY2018, ICRR accepted one visiting professors and two visiting associate professors, which are not shown in this table.

Table A.2-1 Numbers of ICRR staffs as of May 2018.

Professors	Associate Professors	Research Associates	Technical Staffs	Project Professors[1]	Project Associate Professors[1]	Project Research Associates[1]	Post-Doctoral Fellows	Total
9	15	18	13	1	1	13	9+4[2]	79

*1 Project Associate Professors and Project Research Associates have fixed terms.
*2 3 JSPS Post-Doctoral Fellows studying in ICRR.

A.3: BUDGET (FY2012–2017)

After the restructuring of national universities in 2004, the same level of government revenue funding as of FY2004 has been maintained for each fiscal year with a limited amount of yearly cut due to the government's general saving policy (Table A.3-1). Funding for specific research projects, designated as "Promotion of Science" in Table A.3-2, changes depending on the project status. KAGRA construction started in FY2010 and finished in FY2016. An increase of the total annual budget in FY 2016 is due to CTA construction. Other sources of research fund are listed in Table A.3-3.

Table A.3-1 Government Revenue Funding (in thousand yen).

	2012	2013	2014	2015	2016	2017
Personnel Expenses	658,000	687,000	706,000	684,000	683,000	779,000
Supplies and Facilities	1,172,000	1,095,000	1,282,000	1,595,000	1,288,000	1,514,000
Total	1,830,000	1,782,000	1,988,000	2,279,000	1,971,000	2,293,000

Table A.3-2 Research Grant for Promotion of Sciences (in thousand yen).

	2012	2013	2014	2015	2016	2017
KAKENHI	305,100	282,600	328,400	499,787	626,100	475,800
KAGRA Construction Budget	5,956,579	725,670	468,400	674,000	576,000	0
CTA Construction Budget	0	0	0	0	1,346,000	0
Total	6,261,679	1,008,270	796,800	1,173,787	2,548,100	475,800

Table A.3-3 Other research funds (in thousand yen).

	2012	2013	2014	2015	2016	2017
Trust Fund	0	36,321	38,250	13,500	0	0
Private Scholarship	85	364	181	0	0	17,765
Others	0	3,000	300	201	300	130
Foundation	–	–	–	–	18,182	62,421
Total	85	39,685	38,731	13,701	18,482	80,316

B.1: AGREEMENTS OF INTERNATIONAL ACADEMIC COOPERATION

Table B.1-1 Agreements of academic cooperation with the ICRR, or the University of Tokyo, and overseas universities and research organizations.

Country	University/Institute	Year of Agreement
Bolivia	Universidad Mayor de 'San Andres'	1981
China	The institute of High Energy Physics, Chinese Academy of Sciences	1995
USA	College of Science, University of Utah	1995
USA	School of Physical Science, the University of California, Irvine	1995
USA	Graduate School of Arts and Sciences, Boston University	1995
Russia	Institute for Nuclear Research, Russian Academy of Science	2001
Australia	Faculty of Life and Physical Sciences, University of Western Australia	2001
Korea	College of Natural Science, Seoul National University	2009
USA	CIT LIGO Laboratory, California Institute of Technology	2009
Italy	European Gravitational Observatory/ Virgo Collaboration	2011
China	Shanghai United Center for Astrophysics, Shanghai Normal University	2011
UK	Institute for Gravitational Research, University of Glasgow	2011
Taiwan	College of Science, National Tsing Hua University	2011
China	SICCAS-GCL Research & Development Center, Shanghai Institute of Ceramics, Chinese Academy of Sciences	2012
USA	College of Science, Louisiana State University	2012
Italy	University of Sannio at Benevento Department of Engineering	2012
China	National Astronomical Observatories, Chinese Academy of Sciences	2012
Spain	The Faculty Sciences, Autonomous University of Madrid	2013
Taiwan	Institute of Physics Academia Sinia	2017
Germany	Max Plank Institute for Physics	2017
Korea	Sungkyunkwan University, College of Science, Center for Cosmic Ray Research	2017
Poland	National Centre for Nuclear Research	2018
Spain	Instituto de Astrofisica de Canarias	2018
Canada	TRIUMF	2018

B.2: INTERNATIONAL MEETINGS

Table B.2-1 List of international meetings hosted or co-hosted by ICRR.

Date	Place	Symposium/Workshop Title	Participants
May 28–29, 2012	Kashiwa	2nd Japan Korea workshop on KAGRA	26
Oct. 3–4, 2012	Tokyo	1st EliTES General Meeting	80
Dec. 21–22, 2012	Korea	3rd Japan Korea workshop on KAGRA	20
Jun. 10–11, 2013	Osaka	4th Japan Korea workshop on KAGRA	34
Nov. 29–30, 2013	Korea	5th Japan Korea workshop on KAGRA	36
Dec. 4–5, 2013	Tokyo	2nd EliTES General Meeting	80
Jan. 14–17, 2014	Kashiwa	CTA LST General Meeting	83
Jun. 20–21, 2014	Tokyo	6th Japan Korea workshop on KAGRA	49
Dec. 19–20, 2014	Toyama	7th Japan Korea workshop on KAGRA	34
Jan. 31, 2015	Kashiwa	The Inaugural Symposium of the Hyper-Kamiokande Proto-Collaboration and Signing Ceremony	108
Feb. 9–10, 2015	Tokyo	3rd EliTES General Meeting	42
Jun. 17–20, 2015	Osaka	Gravitational Wave Physics and Astronomy Workshop (GWPAW) 2015	133
Oct. 26–30, 2015	Kashiwa	Tev Particle Astrophysics (TeVPA) 2015	169
Nov. 16–21, 2015	Osaka	10th International Workshop on Neutrino-Nucleus Interactions in the Few-GeV Region	109
Dec. 2–3, 2015	Tokyo	4th EliTES General Meeting	38
Jan. 13–14, 2016	Kashiwa	The extreme Universe viewed in very-high-energy gamma rays	68
May 30–Jun. 1, 2016	Ibaraki	Third International Meeting for Large Neutrino Infrastructures	80
May 30–Jun. 1, 2016	Kashiwa	PhyStat-ν Workshop on Statistical Issues in Experimental Neutrino Physics	90
Jun. 16–20, 2016	Kashiwa	CTA Consortium Meeting Kashiwa	170
Nov. 11–14, 2016	Kyoto	International Conference on Ultra-Hgh Energy Cosmic Rays (UHECR2016)	100
Sep. 6–9, 2017	Kashiwa	5th Hyper-Kamiokande Proto-Collaboration Meeting	82
Mar. 5–7, 2018	Kashiwa	The first annual symposium innovative area "Gravitational Wave Physics and Astronomy: Genesis"	99
Mar. 26–30, 2018	Tokyo	Tokyo Spring Cosmic Lyman Alpha Workshop	120

B.3: INTER-UNIVERSITY COLLABORATIVE RESEARCHES

As one of the "Joint Usage/Research Centers" in Japan, ICRR has been supporting inter-university collaborative researches. Annually ICRR issues calls for applications of collaborative researches. The following tables summarize the annual numbers of the applications after selection.

Table B.3-1 Annual numbers of applications for collaborative research programs.

Facilities	2012	2013	2014	2015	2016	2017	Subtotal
Kamioka Observatory	33	33	38	39	39	42	224
Akeno Observatory	4	4	5	7	4	4	28
Norikura Observatory	7	9	10	11	12	10	59
Low-Level Radioisotope Measurement Facility	6	5	4	3	4	4	26
KAGRA Observatory[1]	15	21	22	19	17	14	108
Laboratorial Facility in Kashiwa	10	9	5	9	3	3	39
Computer Facility in Kashiwa	12	17	14	12	12	12	79
Conference Facility in Kashiwa	7	7	10	10	11	13	58
Overseas Facilities[2]	11	12	11	13	23	26	96
Annual Sums	105	117	119	123	125	128	717

*1 The first laser interferometer using cryogenic mirrors developed in Kashiwa. KAGRA Observatory was established in 2016.
*2 The Tibet ASγ Observatory, Observatory for Highest Energy Cosmic Rays in Utah, Chacaltaya Observatory of Cosmic Physics, and The Cherenkov Telescope Array in La Palma. Applications for domestic activities corresponding to these overseas works are included here.

Research Project Titles

1. Study of simulation for atmospheric neutrino
2. Study of atmospheric neutrino flux and neutrino oscillations
3. Studying the Neutrino Mass Hierarchy With Atmospheric Neutrinos
4. Study of flavor identification of atmospheric and beam neutrinos
5. Study of solar neutrino energy spectrum
6. Precise measurement of Day/Night effect for B8 solar neutrinos
7. Study for Supernova monitor
8. Improved measurement of solar neutrino at Super-Kamiokande and SK-Gd
9. Study of Supernova Relic Neutrinos
10. Search for proton decay via $e^+\pi^0$ mode
11. Study of proton decay p$\rightarrow\nu K^+$
12. Study in upward-going muons and high energy neutrinos
13. Sidereal daily variation of ~10TeV galactic cosmic ray intensity observed by the Super-Kamiokande
14. Tokai to Kamioka Long Baseline Experiment T2K
15. Neutrino interaction study using accelerator data

16. Study of the electron neutrino appearance measurement in the T2K experiment
17. Study to improve sensitivity of neutrino oscillation measurement in T2K experiment
18. Joint Oscillation Analysis With the T2K and Super-Kamiokande Experiments
19. Energy cailbration for Super-Kamiokande
20. Research and development of computer simulation of Super-Kamiokande detector.
21. Development of low concentration radon detection system
22. R&D of Megaton scale water Cherenkov Detector Hyper-Kamiokande
23. Development of the Large Aperture Photodetector for a next-generation neutrino detector
24. Development of software for the next generation neutrino detector
25. A Search for Dark Matter using Liquid Xenon Detector
26. Study of annual modulation for dark matter search with XMASS
27. Study for future XMASS detector
28. Development of calibration system for XMASS detector
29. Micro-analysis of gaserous cantamination in Xe
30. Study on neutrino physics using liquid xenon
31. Radon emanation measurement from material using dark matter search experiment.(2)
32. A study on scattering processes of scintillation photons in liquid xenon
33. Study on surface background removal in the dark matter search
34. Study of Double beta decay of 48Ca
35. Direction-sensitive dark matter search
36. Study for lowering backgrounds of radioisotopes in large volume detectors
37. Studies on the background evaluation using laser spectroscopy analysis
38. Development of a radioactivity assay system for underground experiments
39. Dark Matter Search with double-phase Argon detector
40. Integration of crustal activity observation around the Atotsugawa fault
41. Strain, tilt, seismic measurement in Kamioka-mine
42. Keeping neuclear emulsion plates in a box made of lead blacks at Kamioka Underground Lab
43. R&D for a Small Atmospheric Cherenkov Telescope in Akeno Observatory
44. Development of new surface detector for observation of ultra high energy cosmic ray at Telescope Array site
45. Development of the national control station for the fully remote operation of TA-FD
46. Multi-Color Imager for Transients, Survey and Monstrous Explosions
47. Observation of Galactic Cosmic Ray Intensities using Large Area Muon Telescopes
48. Study for cosmic ray detector with capability of indivisual particle identification and particle tracking
49. The development for the platform of advanced field measurement

50. Observation of solar neutrons in solar cycle 24
51. Space weather observation using muon hodoscope at Mt. Norikura
52. Observation of cosmogenic nuclides concentrations at Mt. Norikura
53. Study of secondary cosmic rays from Thundercloud at Mt. Norikura
54. Relativistic Electron Acceleraton in Thunderstorm Eelectric Field
55. Observational study of electron acceleration mechanism in thunderclouds
56. High-energy phenomena via interaction between cosmic-rays and thunderstorms
57. Development of high energy proton irradiation technique for devices used in spaceship
58. Investigation of alpine plants on Mt. Norikura
59. Effect of forest fragmentation on the belowground microorganisms
60. Symbiosis betweem Pinus pumila and Nucifraga caryocatactes on Mt. Norikura
61. The CTA Project
62. CTA-Japan Physics Research
63. Development of Focal Plane Instruments for the CTA Large Sized Telescope
64. Development of the readout system for the CTA large sized telescopes
65. Installation and commissioning of the first Large Size Telescope of CTA in La Palma, Canary Islands, Spain
66. Integration & Commissioning of the Slow Control Program for the Camera of the first Large Size Telescope of CTA in La Palma, Spain
67. Development of the optical system for CTA Large size telescopes
68. Development of a calibration system of the CTA-LST PMT modules
69. Development of camera for CTA small-sized telescopes
70. CTA Monte Carlo Simulation
71. Development of advanced photon counter for the future IACT
72. Study of High Energy Gamma-ray Objects with the MAGIC telescope
73. The study on simultaneous observations of gamma ray bursts by CTA and LEAP
74. Study of Extremely-high Energy Cosmic Rays by Telescope Array
75. Observation of Ultra High Energy Cosmic-Ray with New Fluorescence Detector at the Telescope Array Site
76. Timing and position calibration of surface detectors of TA×4 and TALE experiment
77. Research and development of the surface detectors for the TALE experiment
78. Study of radio detection of highest energy cosmic rays
79. Research and development of a Fresnel lens air fluorescence telescope for the next generation UHECR observation
80. The observation of abnormal shower event with lightning by TA surface particle detector
81. Development of solar power system and detector protection system for the new-type fluorescent detector

82. Calibration of fluorescence detector responce and optical system with standard light source mounted on UAV
83. Development and analysis of night cloud observation by CCD camera for automatic observation of air fluorescence detector
84. Study of absolute energy calibration of air shower by a compact electron linac
85. Observation of airshower fluorescence light at the TA FD site by using an Imaging UV telescope
86. Experimental Study of High-energy Cosmic Rays in the Tibet ASγ experiment
87. Study of High Enegitic Radiation from Thundercloud in Tibet
88. Sidereal daily variation of ~10TeV galactic cosmic ray intensity observed by the Tibet air shower array
89. Study of the composition of cosmic-rays at the Knee
90. A study on variation of interplanetary magnetic field with the cosmic-ray shadow by the sun.
91. Air shower observation for high-energy gamma ray and cosmic ray detections at the Chacaltaya Cosmic Ray Observatory
92. Study on High Energy Cosmic Ray Sources by Observation in Spac with CALET
93. Design study of a Compton camera for study of cosmic rays
94. Observation with Ahsra
95. Integration of the optical fiber trigger system for Ashra
96. Comparative study of astrophysical particle acceleration processes
97. The extreme Universe viewed in very-high-energy gamma rays 2017
98. Development of a new code for cosmic-ray air shower simulation
99. Cosmic ray interactions in the knee and the highest energy regions
100. YMAP symposium 2017 (Basic Part)
101. Research of Large-scale Gravitational wave Telescope (VII)
102. Research on ultra-low frequency anti-vibration system for KAGRA
103. Development of High Performance Cryogenic Mirror Control System
104. Research on cryogenic payload for KAGRA
105. Study for improving a curing time of silicate bonding by controlling gas environment.
106. Development of Very Low Vibration CryoCooler System
107. Development of ultra-low loss coating for the KAGRA sapphire mirror - 2
108. Numerical Simulation of Electro-Magnetic Wave Propagation in Gravitational wave Detector V
109. Control and automatic operation for KAGRA
110. Construction of KAGRA data transfer and storage system (3)
111. Data analysis of KAGRA detector (III)
112. R&D for the intensity stabilization of the laser system in KAGRA
113. Technical development for effects on high optical power for bKAGRA mode cleaner

114. Precise geophysical observation at the Kamioka underground site and modeling of crustal activities
115. Study of Gravitational-wave by cryogenic laser interferometer CLIO in KAMIOKA Mine
116. Development of precision profiler for mirrors of LCGT interferometer 7
117. Development of optical cavity for ultranarrow stable lasers
118. Research and development on advanced gravitational wave observatory network for KAGRA
119. Cosmic Reionization and Galaxy Formation Probed with Large Optical Near-Infrared Telescope
120. Evolution of the universe and particle physics
121. Detection of time variations for cosmogenic nucleid Be-7
122. Evaluation of the erupted radioactivities into the environment
123. Frontier of the planetary material science
124. Time profile of radioactive Cs concentration and its aerosol size distribution in local area
125. Continuous Measurement of Underground Laboratory Environment
126. Precise calculation of the atmospheric neutrino flux
127. Neutrino Workshop
128. CRC workshop for future plans in cosmic ray research

B.4: EDUCATIONAL ACTIVITIES

One of the important functions of ICRR is to educate graduate students directly at ICRR as a part of the Graduate School of Science, the University of Tokyo, and indirectly at graduate schools of domestic/foreign universities through collaborative research programs.

Table B.4-1 Annual numbers of accepted master/doctor theses.

	2012	2013	2014	2015	2016	2017	Subtotal
Master theses at ICRR	9	9	18	12	16	13	77
Master theses at domestic universities	15	9	8	10	14	10	66
Total numbers of master theses in Japan[1]	24	18	26	22	30	23	143
Doctor theses at ICRR	5	3	3	8	4	3	26
Doctor theses at domestic universities	4	2	5	5	10	7	33
Doctor theses at foreign universities	19	14	10	9	1	17	70
Total numbers of doctor theses	28	19	18	22	15	27	129

*1 Since the numbers of master theses are not available for all the collaborating foreign universities, only the domestic numbers are tabulated.

B.5: PUBLIC RELATIONS

6. Overview

Four staffs take charge of public relations; two of them are assigned in Kashiwa ICRR headquarters and each one in both Kamioka Observatory and KAGRA Observatory. Under the supervision of ICRR director, Public Relations Committee, organized by the 4 members, create and manage following public relations activities.

1. Publications
2. Multimedia Contents
3. Exhibitions
4. Original Goods
5. Interactive Events

7. Publications

2.1 News Letter

ICRR News is published quarterly and provides summary of the seasonal news topics and photos.

2.2 Brochure

ICRR Brochure, published annually, offers a basic overview of the entire ICRR research activities.

2.3 Annual Report

ICRR Annual Report provides detailed information on scientific outcomes of every research group in ICRR.

8. Multimedia Contents

3.1 Websites

Not only PR office in Kashiwa ICRR headquarters, but also every research group such as Super Kamiokande (SK) and KAGRA, create their original websites to introduce a series of topics. In the summer of 2018, SK detector was opened for the first time in 12 years because of the refurbishment. ICRR posted a feature of 9 questions and answers on SK refurbishment on the ICRR website. [Find more on http://www.icrr.u-tokyo.ac.jp/sk_open/]

3.2 Videos

An 8-minutes-video which is edited in English with Japanese subtitles, introduces ICRR experimental facilities all over the world. [Find more on http://www.icrr.u-tokyo.ac.jp/beta/movie.html]

3.3 The 360° Panoramic Video for Virtual Reality(VR)

A goggle with a smartphone display on its glass top provides a chance to explore Super-Kamiokande, XMASS and KAGRA observatory as a VR experience. [Find more on http://www.icrr.u-tokyo.ac.jp/panorama/index.html]

9. Exhibitions

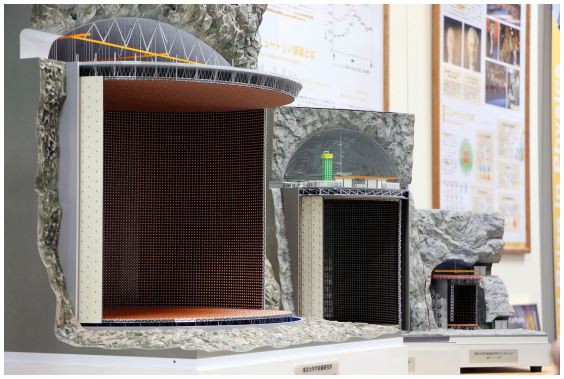

ICRR collaborates with other organizations to create new type of exhibitions. Main collaborators are as follows:

- National Museum of Nature and Science, Tokyo
- National Museum of Emerging Science and Innovation (Mirailan)
- Local government and universities located near ICRR experimental facilities

10. Original Goods

ICRR creates several kinds of original goods for sale: jigsaw puzzle featuring SK, note, mug, calendar and so on. The purpose is to promote public relations and to

support research activities in ICRR: for example, employing young researchers who already have promising results.

11. Interactive Events

6.1 Open Campus

Several thousand people visit ICRR headquarters every year on the Kashiwa Open Campus days. They are attracted by science cafe, workshops, original goods sale and other entertainments the PR Committee created with many students and researchers.

6.2 ICRR x Kavli IPMU Public Lecture

ICRR collaborates with Kavli Institute for the Physics and Mathematics of the Universe (Kavli IPMU) to organize public lectures in both spring and fall every year. The number of people wishing to attend the lecture largely exceeds the quota. In the spring of 2018, four hundred people who won the lottery enjoyed the lecture.

6.3 Spring School

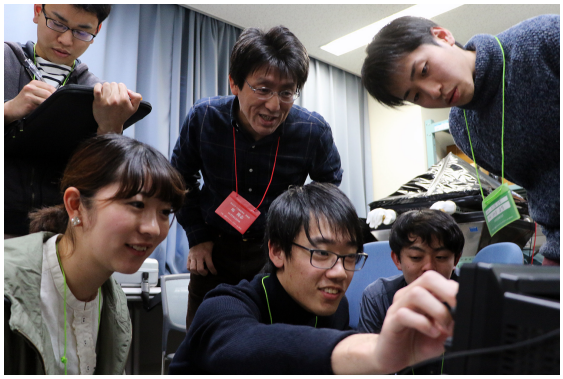

ICRR offers 30 university students from all over Japan, sometimes from overseas, to spend in ICRR for 5 days and 4 nights in March every year from 2012. This program, called “Spring School,” provides lectures, experiments, data analysis, and presentation to researchers and colleagues. Students, tutors and also the ICRR director who never met before get along with each other soon and have a profitable experience under one roof.

C: REPORT FROM THE FUTURE PLANNING COMMITTEE (2013 and 2017)

Report from the University of Tokyo, Institute for Cosmic Ray Research (ICRR), Future Planning Committee

September 26, 2013

History and Objective Behind the Establishment of the Committee

The University of Tokyo, Institute for Cosmic Ray Research (ICRR), has organized Future Planning (Sub-) Committee meetings on three occasions since 1987. At the subcommittee, future plans for the institute, especially large-scale projects that could serve as a pillar for the institute's future research, were evaluated and recommendations were made. The institute has been striving to realize these plans. The Kamioka Gravitational Wave Detector (KAGRA) project that was recommended at the 2nd (1993) and the 3rd (2007) committee meeting, has moved onto the construction phase after being chosen as a state-of-the art research project, and has been allocated a budget for the cavity excavation needed for detector construction. The ICRR decided that the time has come for considering a new future project that can follow Super-Kamiokande and KAGRA, and this committee was established in January 2012 to provide recommendations for a way forward for the ICRR and its in-house projects.

Also, the ICRR has restructured its organization by terminating projects such as the CANGAROO experiment and SDSS experiment, and establishing new research groups such as the Cherenkov Cosmic Gamma-ray Group, the Observational Cosmology Group, and the High Energy Astrophysics Group. It also conducts relatively small scale research on such areas as primary cosmic rays (studying topics including changes in cosmic-ray intensity and the relation with the climate) and Ashra (All-sky Survey High Resolution Air-shower detector). The role of evaluating and providing recommendations on the directionality, scientific significance, and human resource allocation for these research projects was assigned to the Committee.

The Committee invited advocates from each future plan to the meeting to conduct hearings on the details of each plans. In 2012, the Cosmic Ray Conference (CRC) held a town hall meeting discussing future research plans in the field of cosmic rays. To efficiently obtain information on each experiment plan, the Committee has co-hosted events, beginning with the 3rd CRC Town Hall Meeting (2012, June 30). (Members of the Committee coordinated and attended the 2nd CRC Town Hall Meeting (2012, January 22) as well, but did not take the form of co-sponsorship.) However, it should be noted that while the Town Hall Meeting examined mainly the scientific significance of the proposed plans, including future plans from outside the ICRR, the Committee evaluates projects that the ICRR has assumed to implement, which sets it aside from the future plan discussions with the CRC and its aims.

Committee Members

K. Saito (Chairperson) Director, National Institutes of Natural Sciences
H. Aihara, Professor, Graduate School of Science, the University of Tokyo
Y. Ito, Professor, Institute for Space-Earth Environmental Research, Nagoya University
K. Inoue Professor, Research Center for Neutrino Science, Tohoku University
N. Kanda, Professor, Osaka City University Graduate School of Science
T. Kishimoto, Professor, Osaka University Graduate School of Science
N. Sugiyama, Professor, Nagoya University Graduate School of Science
Y. Mizumoto, Professor, National Astronomical Observatory of Japan
T. Terasawa, (Secretary) Professor, The University of Tokyo, Institute for Cosmic Ray Research
K. Okumura, (Vice secretary, clerk) Associate professor, The University of Tokyo, Institute for Cosmic Ray Research
T. Kajita, (Observer) Director, The University of Tokyo, Institute for Cosmic Ray Research

Committee History

・ 1st Meeting (January 25, 2012)
  － On the establishment of the Committee and items requested for evaluation
  － Discussion on future policies
・ 2nd Meeting (February 21, 2012)
  － Hearing on Cherenkov Telescope Array (CTA) from two project members
  － Discussion within the Committee on the hearings
  [Follow-up questions from the Committee were sent to the group from the Secretariat on a later date.]

・ 3rd Meeting (April 10, 2012)
  － Continued the previous hearings on the CTA from two project members
  － Discussion within the Committee on the hearings
・ 4th Meeting (May 29, 2012)
  － About cohosting the town hall meeting with CRC
  － Discussion based on the response from the CTA group
・ 5th Meeting (July 17, 2012)
  － Hearing on Telescope Array (TA) from one project member
  － Discussion on personnel matters of the High-Energy Astrophysics Group
  [Follow-up questions from the Committee were sent to the TA group from the Secretariat on a later date.]
・ 6th Meeting (August 7, 2012)
  － Hearing on the Tibet Experiment from one project member
  － Discussion on the Tibet Experiment within the Committee
  － Discussion based on the response from the TA group
・ 7th Meeting (November 1, 2012)
  － Hearing on the Hyper-Kamiokande from one project member
  － Hearing on the XMASS Experiment from one project member
  － Hearing on the Ashra Experiment from one project member
・ 8th Meeting (December 21, 2012)
  － Discussion on the Hyper-Kamiokande, XMASS, and Ashra
  － Discussion on the interim report
・ 9th Meeting (February 26, 2013)
  － Discussion on the interim report
・ 10th Meeting (April 19, 2013)
  － Hearing on the joining of TA group to EUSO, and details on TA×4 Plan from one project member
  － Discussion on the interim report

About Cherenkov Telescope Array (CTA) Experiment

Project Outline

Much of the rapid advancement in the understanding of the origin of cosmic rays in the past decade is attributed to the development of observations in the energy regions of several dozen GeV to several TeV by HESS, MAGIC, and VERITAS, which stemmed from the pioneering ground-based high energy gamma-ray observations, such as Whipple, HEGRA, and CANGAROO. The next generation, ground-based high energy gamma-ray experiment, Cherenkov Telescope Array (CTA), aims to maintain this momentum of research—and advance it further. In fact, CTA plans to increase the sensitivity of the conventional ground-level gamma-ray experiment by approximately 10 times, and expand the target energy region in both ends of the spectrum by nearly an order of magnitude. Astronomical and astrophysical themes in which progress can be expected by the experiment are as follows:

1. The origin, acceleration, and propagation of cosmic rays
2. Galactic high energy astronomical objects (Pulsar, Magnetar, Pulsar wind nebula, Supernova remnant (SNR), X-ray Binaries, Globular clusters).
3. The origin, acceleration, and propagation of extra-galactic high-energy cosmic rays
4. Extra-galactic high energy astronomical objects (active galactic nucleus (AGN), gamma-ray bursts (GRB), nearby galaxy clusters, nearby starburst galaxies, etc).
5. Cosmological studies using gamma-rays from active galactic nuclei (AGN) and gamma-ray bursts (GRB)
6. Dark matter annihilation in a Galactic Center, dwarf galaxies, galactic halos, galaxy clusters, and search for gamma-ray decay
7. Tests for Lorentz invariance at the Planck scale

In this way, the scientific perspective of CTA extends not only to each field of high energy astrophysics, but also cosmology and particle physics; that the list of participants of this project encompasses nearly all researchers in the world involved with high energy gamma-ray astronomy. In response to these trends internationally, Japan's high energy gamma-ray astronomy community has organized the CTA-Japan Consortium, which has been examining future plans. The following is the summary of the hearings on the plans.

There are three kinds of telescope: LST (Large Size Telescope), MST, and SST, having a 23-meter, 12-meter, and 6-meter diameter, respectively. The northern and southern hemispheres are being considered for the site, and at each site, 4 LSTs, 23 MSTs, and 32 SSTs are planned to be set up. (SSTs

are not planned for the northern hemisphere.) Japan's core responsibilities are the LST, the mirror and the imaging camera, and the camera module (the photomultipier and the electronics part), and Germany (MPI, Munich) is to be responsible for the structuring, such as the gantry. Mr. Teshima from ICRR is managing the LST Project. LST is an important telescope in filling the gap in the energy range between Fermi and currently working IACT. The low energy threshold target is at 10 GeV. Also, the requirements specifications for LST is the most stringent out of the three telescopes, and Japan's technical contribution is expected by the world's experiment teams in this regard. If Japan is able make a significant contribution to LST, we can expect to obtain a drastic increase in observation time in the Core Programme. Regarding the development of the mirror, which is Japan's main contribution to LST, the aim is to extend the equipment life by multilayer coating (sputtering) and to achieve high reflectance of 95% or more. In addition, in order for fast GRB follow-up observation to be possible, it is necessary to drive the telescope at high speed, so measures are being taken to reduce the weight. As for the imaging camera module, the photomultiplier tubes are made by Hamamatsu Photonics. The electronics is able to secure 3-digit dynamic range with 2 gains, achieving pulse height sampling and high speed readings at 2 gigahertz. There are some issues to be solved including the trigger system between modules and the cooling system that uses a camera box to cool the heat generated from the electronics. Going forward, the plan is to build a camera prototype with the Kakenhi scientific research grants, and test the MST prototype in Germany. There is no major technical development factor in producing the mirror, so it is thought that the remaining developmental factors can be sufficiently accomplished by Japanese technology. The overall production of the mirror is planned at 1,600 mirrors, the photomultiplier at 16,000 tubes, and the electronics at 16,000 channels.

In addition to the ICRR-led group of researchers responsible for LST, members of CTA-Japan from Nagoya University Solar-Terrestrial Environment (STE) Laboratory are to be in charge of MST and SST. In order to secure financial resources for these, separately from the funding for the LST plan, measures to obtain competitive funding have already been put in place.

Based on the CTA experiment time schedule, by 2010 the design (LOI and documents on the design concept) has been completed, and from 2010 to 2014, preliminary studies are to begin. Construction is to start in 2015, and partial observation is scheduled to commence in 2017. The overall budget that includes both the northern and the southern hemisphere sites is 190 million euros (totalling about 20 billion yen, as of 2012), and Japan is aiming for about 20% for the cost allocation, which is 4 billion yen. The breakdown is about 1.3 billion yen for the mirror, 0.9 billion yen for the photomultiplier, 1.4 billion yen for the electronics, 0.3 billion for the camera box, and 0.1 billion yen for the personnel expenses. As the host institution of CTA-Japan, the ICRR needs to secure observation time, operate the experiment, and become the point-of-contact for providing observation data and analysis tools. In addition to the approximately 4 billion yen for construction, about 0.2 billion yen must be secured annually for maintenance, so the ICRR needs to submit a budget request.

The total number of CTA-Japan members is 84 (as of October 2012). Besides those responsible for equipment development, there is a science group composed of about 35 individuals, whose main research topics are AGN, GRB, and SNR. (The breakdown for the 35 members is: about 20 theoretical researchers and 15 experimental researchers. To organize headcount by each research topic, with some duplications, there are 10 members for AGN, 12 members for GRB, and 20 members for SNR). At the same time, by using the author list from the Task-B paper (a report on the study to quantify scientific progress under each scientific theme) CTA-Japan's contribution to the world—for GRB, AGN, and SNR—is found to be 11/20 (out of 20 authors, 11 people are from CTA-Japan), 5/28, and 1/ 14, respectively. As a strategy to lead the course of future research topics, the group plans to compile observation proposal papers, give presentations at general meetings, and target new themes like Fermi Bubbles. Also, the CTA group made a request for collaboration with X-rays and radio observation groups, wishing to have a connection especially with the X-ray observation group, so a joint meeting is to be organized with the X-ray group in 2013.

As preparation for the CTA-Japan data analysis, the group acquired Monte Carlo (MC) simulation code, analyzed MC summary data, and based on the summary data, reproduced the CTA sensitivity curve. Currently, there are 13 members in CTA-Japan MC team, which is too small of a team to thoroughly investigate all physics, calling for expansion of the scale of activities. As the future course of action for the analysis group, the group

cites, in preparation for the launch of CTA operation, aims to set up the environment necessary for analysis, improve the MC team's activity scope, and cooperate with the science group in the future. Also, the group will investigate the possibilities such as using the ICRR as the data center to secure sufficient storage and participating in the European group's grid system. The development items for the analysis method include: an expansion of the field-of-view for GRB follow-up observations by improving the methodology of the stereo observation, and increasing the rate of GRB detection. In addition, there is an issue with the network speed for transferring data from the Europe region to the ICRR, (3 -terabyte data requires over 1 month to be sent) that going forward, measures need to be taken to reinforce the network and/or to secure a different method for transferring data.

Committee Evaluation

CTA's plan was evaluated highly by the Committee for its scientific achievement goals, breadth of research topics, high-level technology and experience in the production of the CTA-Japan telescope and detectors, that it was concluded that it could be a candidate for the next large-scale project for the ICRR. The CTA plan is anticipated to make a significant contribution to the elucidation of the origin of cosmic rays, which is an important subject in cosmic ray research. In Japan, the ICRR should take the lead in promotion of the plan. A discussion was made on the issue of having a project, unlike Super Kamiokande and KAGRA, that is not hosted by Japan, become the pillar of ICRR researches. However, the consensus was that considering the current globalization trend where countries are collaborating without borders, the plan was only following those norms.

At the same time, the shortage of manpower in construction of telescopes and detectors, mass production of detector parts, and in the data analysis in general, is a concern. There is a shortage of personnel who can concentrate solely on the construction. Therefore, it is necessary to ensure such talent is arranged, by leveraging posts such as project assistant professors who have longer office terms than the regular postdoctoral researchers. Particularly, in order to become one of the first to achieve results in international projects, it is vital to allocate more human resources and expand the scale of activities in data and simulation analyses. Also, if only calibrated and already reduced summary data is sent from Europe, it becomes impossible to carry out detailed analyses on the whole observation data. Taking into consideration also the problem of data transfer, there was an opinion that it may be necessary to establish a system within the ICRR where analytic processes such as calibration can be carried out. As for graduate students who can take an active part in observation shifts and analyzing data, cooperation with university laboratories that conduct CTA experiments, such as those at Kyoto University, Nagoya University and Ibaraki University, is necessary. Moreover, the Committee expects the team to investigate measures to be taken in order to jointly acquire budgets with these laboratories and universities.

In particular, building the workforce structure in the ICRR is believed to be an urgent task. The CTA experiment is planned to be conducted over the long-term, over a 10-year span. Thus, a system must be in place to stably provide experimental operation and data distribution and observation shifts for the duration of the term. Furthermore, to be able to announce the latest results from the ICRR at any time, talented people who are knowledgeable of the experiment and well-versed in relevant theories need to be posted at the institute. In particular, in order to promptly release scientific achievements and other experimental results immediately after the onset of the research, a plan that shows scientific strategies and expected achievements at each experimental phase needs to be prepared in advance.

Telescope Array (TA) Project

Research Results and Future Project Outline

The TA experiment is an experiment aiming to elucidate extreme phenomena of the universe by measuring the energy spectrum, arrival directions, mass composition of ultra-high-energy cosmic rays (UHECR) with energies greater than 10^{18} eV. The experimental site is located in Utah, United States (at an altitude of 1,400 meters); 507 surface detectors (SD) and 3 stations of atmospheric fluorescence telescope (FD) are installed in the area of approximately 700 square kilometers.

The breaks in the cosmic energy spectrum were observed at $10^{18.7}$ eV and $10^{19.7}$ eV. The significance of the cutoff above $10^{19.7}$ eV is 3.9 sigma. Taking into account the systematic error of energy

determination, it was confirmed that the shape of the spectrum obtained from TA and all other experiments agreed well below $10^{19.5}$ eV. The analysis of the mass composition of the cosmic rays investigated from the distribution of maximum of air-shower profiles (Xmax) provides the result that the TA data are consistent with protons in the energy region above $10^{18.2}$ eV. On the other hand, the results at Pierre Auger Observatory (PAO) showed the transition to iron towards high energy side, so that there is inconsistency in the two experimental data.

An analysis is underway on the autocorrelation of arrival directions of cosmic rays and on the correlations with active galactic nuclei (AGN), astronomical objects, and large scale structures (LSS). There is no contradiction with the assumption that these are ultra-high-energy protons generated in LSS. However, the probability is 2% that this correlation occurs in the isotropic distribution. The probability is low but it is not sufficient to exclude isotropic assumption completely. Also, the clusters detected by AGASA were not reproduced in the autocorrelation analysis.

As the next plan for the TA experiment, the TA Low Energy Extension (TALE) is currently in progress. In this experiment, the plan is to conduct precise measurements on the mass composition, which be an indicator of the transition from galactic source cosmic rays to extragalactic cosmic rays in the energy region from $10^{16.5}$ eV up to $10^{20.5}$ eV with the TALE and TA. For this project, we will add the high-density SD array and relocate and enhance the FD that was used in the HiRes experiment. The FD, under the responsibility of the United States, is already under construction, and as for the SD, which Japan is in charge of, the scale of the budget is approximately 100 million yen. In the fiscal year 2013, we plan to construct the SD and start its observations. In order to verify the differences in results such as cosmic-ray energy scales and mass composition obtained by PAO and TA, a number of steps are being planned, such as exchanging light intensity calibration data and atmospheric data between the experimental groups, making analysis programs public, organizing collaborative analyses, and exchanging FDs and SDs. The exchange of light intensity calibration data has already begun, in 2012, and it can continue until 2018.

TA×4 is a plan to deploy 500 SDs at 3 different sites with 2-kim spacing. The plan is to quadruple the total area including the current TA, and to install an additional FD at one site. It is possible to acquire over 20 years of the current TA's data within the first 5 years—that is, a 2-year construction period followed by a 3-year observation period. It is hoped that the question of anisotropy of the highest energy cosmic rays will be settled with sufficient statistical accuracy.

Also, the central figures of the TA experiment in Japan, such as the TA team from the ICRR, is participating in the RIKEN-led, The groups from the TA experiment in Japan including the TA team in ICRR participate in the highest-energy cosmic-ray observation project, JEM-EUSO, which is led by RIKEN and will be mounted on the International Space Station (ISS). And the TA group supports the test observations of JEM-EUSO prototype at a TA site.

TA2 is the next generation air shower experimental plan, aiming to elucidate the origin of UHECR and to limit cosmic ray source density, and to identify chemical compositions, by expanding the detection area by 60 times compared to TA. Approximately 10 thousand SDs are placed at 2 km intervals, and the total area is 39,200 square kilometers (60 times the TA). The estimated budget is about 100 million dollars (approx. 10,000 dollars per unit, for 10,000 SDs) but the specifics of the plan will be finalized in the future based on the comparison results between PAO and TA, as well as results from TA×4 and JEM-EUSO.

Committee Evaluation

Regarding the TA experiment, the research achievements such as the construction and operation of the experimental equipment, observations, energy spectrum measurements, chemical composition of cosmic rays, and correlation analysis of cosmic ray arrival directions were highly commended within the Committee. However, in terms of the discrepancies in the energy scale and the chemical compositions with the data from PAO, it is not clear whether these are ascribed to systematic errors such as from the calibration, or from simulations, and the Committee recognized it was important to identify the cause and resolve the issue before proceeding to the next plan. Therefore, it is essential to deepen the understanding of the observation data, by performing energy calibration with LINAC and carry out comparative verification with PAO.

With regards to the TALE experiment, it is expected that it will contribute to a greater

understanding of the cosmic ray spectrum and the chemical composition in a wider energy range, and by expanding to the low energy end to fill the gap between the observed energy region of the Tibet experiment, a more comprehensive understanding can be expected about cosmic ray generation and propagation.

TA×4 plan aims to accumulate data equivalent of 20 years of the TA data in total, in the short period of the next five years. The Committee appreciates that it is a realistic plan that saves resources. However, the TA×4 plan was submitted during the Committee discussion, giving the impression that the concrete planning of this experiment started later compared to other projects. The Committee expects the planning be expedited and the project be implemented as soon as possible.

With regard to TA group members such as those from the ICRR participating in JEM-EUSO, and each aiming to make contributions via their own capacities, the Committee believes that the diverse experiences of the members related to the highest energy cosmic rays will be advantageous in JEM-EUSO, and concludes that this situation is appropriate.

With the TA2 Project, in accordance with the current policy of the TA group, it is desired that the discussions based on PAO and TA comparison results, and results from TA×4 and JEM-EUSO should be continued.

The Next Term Tibet Experiment

Hitherto Research Results and Future Project Outline

The Tibet experiment, conducted on a highland at an altitude of 4,300 meters, aims to study the energy spectrum, the chemical composition and anisotropy observation of cosmic ray particles (nucleons) from several TeV to the "knee" region (10^{15}—10^{16} eV), and to conduct a high energy celestial gamma-ray observation in the regions from several TeV to over 100 TeV. As for the achievements of the Tibet experiment, there are a few events detected for the first time. These include: the deficit of the cosmic ray intensity due to the shielding effect of the sun and the moon, the Compton-Getting effect associated with the revolution of the earth, change in the structure of magnetic field near the sun that is dependent on solar activities, and the cosmic ray anisotropy in the regions of a few TeV that provide information on the interstellar magnetic field structure in the vicinity of the solar system.

The ongoing expansion work and the next term plan for the Tibet experiment are described below. With the conventionally used AS array (having the effective surface area of approximately 37,000 square meters by the counter array consisting of plastic scintillators and photomultiplier tubes), it was difficult to distinguish between gamma rays and nucleons. For that reason, currently there is a plan underway to expand the facility by building muon detectors (MD) under the AS array~~s~~. MD is a water tank installed 2.5 meters underground, and is designed to detect muon Cherenkov light generated by cosmic ray particle events, and with anti-coincidence, it is aimed to significantly improve the S/N of gamma-ray observation. As a result, meaningful gamma-ray observation can be expected in the energy region over 10 TeV up to regions exceeding 100 TeV. The prototype for MD was constructed in 2007, and for the most part confirmed the performance expected from the simulations. Currently, there are 5 MDs being constructed (the final target is 12). Moreover, 100 counters (with 1.5 meter-intervals) consisting of lead, iron and plastic scintillators are currently being built in the 160-square meter area, at the center of the AS array (YAC-II). With these in place, the energy spectrum and composition ratio of protons and helium in the "knee" region are expected to be determined.

The construction of the remaining seven MDs, the expansion of the AS array~~s~~ (37,000square meters → 83,000 square meters), and the construction of YAC-III are being considered, as the next term plan of the Tibet experiment. YAC-III plans to build 400 detectors at the center of the AS array, in an area of 5,000 square meters, aiming to determine the energy spectrum and the composition ratio of the iron component in the "knee" region. The budget is 400 million yen for the MD, 150 million yen for the AS expansion, and 250 million yen for the YAC-III, totalling 800 million yen. It is a 6-year plan, which breaks down to 3 years of construction and 3 years of observation. Kakenhi scientific research grant is being considered for the budget acquisition, and in f~~or~~ the fiscal year 2012, and Grant-In-Aid for Scientific Research (A) was adopted. The budget allocation is planned to be 3:1 for Japan and China, respectively.

Committee Evaluation

Knowing the cosmic ray chemical composition in

the "knee" region is important in investigating the origin, acceleration, and propagation issues of galactic cosmic rays. At present, the composition model that is considered standard is based on the KASCADE observation, but muons are the main component of the air shower at KASCADE, (1 atm altitude) and its development heavily depends on hadronic interaction models. On the other hand, the altitude at the maximum development of air showers generated by cosmic ray particles in the "knee" region almost equals that of the Tibetan altitude (X=600 grams). The main component of the air showers detected at this altitude is electromagnetic, and their model dependence is low, which is advantageous for determining the chemical composition.

Meanwhile, HESS, MAGIC, and VERITAS, which are international gamma-ray observation projects that employ Cherenkov light detectors, are fiercely competing for results. Also, as the next term plan, CTA is starting to take form. However, as it was pointed out at the 2007 Future Planning Committee, CTA has a narrow field of view, and as the scale of its budget is large, it may take years to materialize. Complementarily, the Tibet observation has a wide field of view and requires a small-scale budget, and a quick implementation of the plan is expected to achieve reasonable scientific results. Considering the construction for the North American experiment HAWC—that has similar scientific objectives and is already in progress—a prompt implementation of the plan is extremely important if they are to achieve pioneering results with the Tibet MD plan.

Finally, the relationship between the Tibet experiment group and the TA group is described here. Although the observation altitude is different, as the TALE experiment starts, having both the Tibet and the TALE experiments will enable a wide and continuous measurement of energy in higher regions than the "knee" region. Both are groups within the ICRR, and as such:

○ Unified research on cosmic-ray energy spectrum/chemical composition,

○ Efficient use of human resources drawing on the similarities of technologies used (detectors, simulations etc.), training students and postdoctoral fellows, facilitating acquisition of external funds, and other possibilities that can be utilized to strengthen the mutual collaboration in advancing the research must be considered.

Comments on Hyper-Kamiokande (Hyper-K)

Project Outline

Hyper-Kamiokande (Hyper-K) is a third-generation proton decay/neutrino experimental plan using a water Cherenkov detector, following the previous Kamiokande and Super-K projects. A wide range of physics is envisaged from this plan, including measurements of charged parity (CP) asymmetry in lepton by accelerator neutrinos, determination of neutrino mass hierarchy in atmospheric neutrinos, nucleon decay search, study of solar neutrinos, supernova burst neutrinos, supernova relic neutrinos, and solar flare neutrinos.

The ability of the water Cherenkov detector has already been demonstrated with Kamiokande and Super-Kamiokande, and its excellent scalability is notable. Hyper-K detector consists of two sets of tanks 54 meters high and 250 meters long, with a total mass of 1 million tons (of which the effective volume is 560,000 tons, resulting in a 25-fold increase from Super-K), 20% photo-sensitive area, and about 100,000 photosensors in total. Tochibora mine (650m-deep underground located about 10 kilometers away from Super-K) in Kamioka Town, Hida City, Gifu Prefecture is being considered as a candidate site for the detector. Cavern analysis and design for the detector are nearly complete, and the detector design is almost finalized. Either 20-inch photomultiplier tubes (PMT) or the hybrid photodetector (HPD), a new model that is designed to improve performance and costs, is considered as the photosensor. A prototype of the 20-inch HPD is to be completed in 2013, and its feasibility test is scheduled to be conducted in a water tank with 200 tons of gadolinium water in Kamioka. In addition, the designing of the plastic liner shielding, which is used as the outer wall of the water tank and the development of DAQ are ongoing.

In order to form a collaborative body through international cooperation, in August 2012, an Open Meeting was held at the Kavli IPMU of the University of Tokyo at Kashiwa Campus, and about 100 people from 35 different research facilities from 9 different countries came together to participate in. At the meeting, the participants reviewed projects, formed working groups, and assigned conveners to accelerate the detector R&D.

The estimated cost of the construction is about 80 billion (with an error of 25%) of which 30 billion is for the cavern excavation, 30 billion for the water tank construction, and 20 billion for the photo-sensors (assuming highly photoelectric efficient HPD is to be deployed), however, further cost reduction is recognized as an issue to be solved. Although it is

contingent upon the budget acquisition period, the construction is scheduled to start in 2016, and the operation is to start in 2023.

One of the most anticipated physics topics with accelerator neutrinos is the search for the CP asymmetry in the lepton sector. If the CP symmetry is violated, the probability of occurrence of electron neutrinos from muon neutrinos for neutrino and antineutrino beams are different and thus, it is possible to check whether there are differences in the probability of occurrence for each or not. Assuming the beam power of neutrino is 750kW and the experiment period is 10 years, about 4000 electron neutrino events and about 2000 anti-electron neutrino events are expected to be detected, and assuming the systematic error to be 5% or less, it will be possible to detect CP violation with the confidence level of over 3 sigma. The systematic errors are expected to be further reduced with the advancement of the currently ongoing T2K experiment. With atmospheric neutrinos, it is anticipated that the mass hierarchy of neutrinos can be determined by measuring the matter effect of neutrino oscillations in the Earth's interior. The oscillation between muon neutrino and electron neutrino is amplified by neutrinos in the several GeV region passing through the Earth. However, the amplitude differs depending on the mass hierarchy, so with the Hyper-K detector and the observation period of 10 years, it will be possible to determine the mass hierarchy with over 3 sigma of confidence even taking the uncertainty of the oscillation parameters into account. Regarding the supernova burst neutrinos, it is expected that the verification of the theoretical model of supernova burst mechanism and the measurement of the mass hierarchy of neutrinos will be possible, by measuring the time dependencies of flux, energy and neutrino types. For proton decays, in $p \rightarrow e\pi^0$ decay mode, the search is made possible up to 1.3×10^{35} years of lifetime (90% reliability), and in many other modes, the sensitivity will be improved by an order of magnitude from Super-K that the discovery of nucleon decay is also anticipated.

Other competing experiments include LBNE in the United States, and LBNO in Europe, and these experimental projects are planning to employ liquid argon detectors. LBNE is scheduled to start its experiment in 2022 and is mainly focused on the measurement of CP asymmetry by accelerator based long-baseline neutrino oscillations. LBNO has long-baseline of 2,300km and it has significant sensitivity in identifying mass hierarchy. However, there are only limited precedents of the large-scale liquid argon detectors, unlike the water Cherenkov detector, and thus, it is necessary to demonstrate its performance and capability.

Committee Evaluation

Hyper-K is an experimental plan that uses a large-scale water Cherenkov detector following the previous Kamiokande and Super-Kamiokande. As mentioned above, its technology and analytical methods have been well demonstrated and confirmed. Other than the scale of the budget, there are no other significant concerns with the project. The required person-power has been estimated and it goes beyond that of the Super-Kamiokande project, and thus asking the ICRR alone for contribution is clearly not enough. More human resources must be secured by other means such as leveraging international cooperation.

In terms of the budget, 80 billion yen stands at such a large scale that it has never been requested for before from the ICRR, and therefore, the possibility of a joint budget request with KEK and J-PARC must be examined, also. For the budget request as well as its acquisition to be successful, all neutrino researchers in Japan need to unite to establish a system that can promote Hyper-K plan. In that respect, it is important that the directionality of the future plan is shared and aligned with the KEK group. (Written as of November, 2012. After the above note was made, an agreement was made with KEK group which affirmed Hyper-K project to be Japan's future neutrino plan).

There is no issue with the scientific significance or the employed technology with accelerator neutrinos and atmospheric neutrinos, however, the cosmic ray muon-sourced background level is high in the solar neutrino observation indicating a possible impediment in the research development in the future, so it may be necessary to examine the course of the experimental plan more closely.

In addition, there is a concern about the timing of the acquisition of the budget, as it may be too pressed for time for the construction scheduled to start in 2016 and for the operation scheduled to start in 2023. Therefore, it is necessary to review the budget acquisition plan in detail, and work towards actualizing it. Moreover, reportedly there is still a 25% error in the 80 billion construction cost estimate at present. The Committee urges the group to improve the accuracy of the budget estimate by clarifying each country's cost allocation, and to examine the estimate in depth for a successful acquisition of the budget.

XMASS Experiment

Hitherto Research Results and Future Project Outline

The XMASS project is based on a single-phase detector that uses liquid xenon as target material, and is a multi-purpose cosmic elementary particle experiment that aims for not only the direct search of dark matter (DM) but also observation of solar neutrinos and double-beta decay. At present, as phase 1 of the experiment, XMASS-I (effective volume 100kg, total mass 835kg), is already under operation. For the next phase, XMASS-1.5 (effective volume 1 tons, total mass 5 tons) is in the planning, and XMASS-II (effective volume 10 tons, total mass 25 tons) will be the final phase. With the XMASS detector, it is possible to eliminate the gamma-ray and neutron-induced external background by the self-shielding effect of xenon. Also, as the detector extension is comparatively easy, this project is more advantageous than its competitors, such as Xenon-100, which employ a gas-liquid dual phase detector.

XMASS-I detector is comprized of 630 2-inch photomultiplier tubes (PMT) and 62% of the inner wall is made of a photoelectric surface. As a measure against ambient background, the detector is set up completely submerged in the 800 ton water tank, in order to shield gamma rays and neutrons. The team also developed PMTs with low radioactivity background. In addition, for the xenon internal background, krypton (Kr) and radon (Rn) were eliminated almost to the required target value. The construction was completed in September 2010, and by 2012 May, the commissioning was completed. The photoelectron yield is about 14.7 p.e. per 1 keV, which is 6 times higher than Xenon 100. With the 122 keV gamma-ray calibration using Cobalt 57, the energy resolution is evaluated at 4%. The position resolution of the detector core is 1.4 cm in RMS.

More than expected amount of background was observed from the commissioning data, and the identification of its source was carried out. One of the backgrounds was gamma rays from uranium 238 and lead 210 contained in the aluminum used to compress the quartz window and the metal pipes of the PMT. The radiation measurement using a germanium detector and simulations explain the amount of background energy over 5 keV. The energy below 5 keV is assumed to be background from the carbon contained in Gore-Tex used to fill in the gap between the PMT and the holders. For theses reasons, the background rate is approximately 2 orders of magnitude higher than the target value. Nonetheless, using the 6.7-day observation data from XMASS-I, DM and axions were searched. For DM search, by using the fiducial volume cut analysis, it is expected to be possible to set limits from 2.2×10^{-41} to 10^{-43} cm^2 in scattering cross-sections for the range and from 4.7×10^{-43} to 1.1×10^{-44} cm^2 in cut analyses.

Currently, the detector is being refurbished, and the plan is to cover the aluminum sealing on the PMT with a copper plate, and to further remove the Gore-Tex in order to reduce the background rate down to 1/100th of the current rate. XMASS-1.5 is also in the planning, for fundamental amelioration and sensitivity improvement, as well as to compete with the new project emerging abroad called Xenon-1ton. In order to improve the surface background identification, PMTs with a round shape light receiving surface will be developed, Gore-Tex will be removed, and the background due to the lead on the surface of the detector will be reduced. For the DM search, the expected physics results include the cross-section 10^{-46} cm^2 and less (at an energy range over 5 keV) and for the lower energy range, the sensitivity improvement for the scattering cross section up to a few10^{-42} cm^2, and an improvement by 2 orders of magnitude for the axion search compared to the current capability. The construction is scheduled to start in 2014, and the experiment is to start in 2015.

The main foreign competitor is Xenon-1ton (Gran Sasso, scheduled to start operation in 2015). Similar to XMASS-1.5, they are expected to achieve sensitivity lower than 10^{-46} cm^2, however, there are some technical developmental factors such as high electric pressure, that still remain. Other foreign projects include LUX (Xe 300kg, Homestake), LZ (Xe 7ton), and Super-CDMS. Among these project designs, what characterizes XMASS is its sensitivity to both nuclear recoil and electron/gamma ray.

In terms of manpower, except for the contribution from Korea for the development of calibration sources, it is comprized of personnel from domestic research institutions, and the total number of collaborators is 41. The total budget for XMASS-1.5 is planned to be 1.3 billion yen.

Committee Evaluation

XMASS is an experiment led by a Japanese group that is capable of competing with other experiments overseas, in the area of dark matter search. The expected scientific achievements range widely from

the field of axion dark matter to solar neutrinos. The experiment demonstrates excellent background removal by the detector and the energy threshold etc., and it shows high potential. The members of the experiment group have advanced technical capabilities in areas such as removal of impurities in xenon, and thus, considering the background of the group, there seems to be no issue technologically in terms of detector manufacturing. Also, in terms of the project structure and scale, presently there seem to be no issues. It is considered to be a reasonable experiment to execute at the Kamioka Observatory in the next 10 years, which is when the Hyper-Kamiokande project is planned to start.

The remaining issues are the background and the budget, but the competitor, Xenon-1ton, despite uncertainties in its feasibility, has been approved and budgeted. The Committee urges to resolve the surface background of XMASS-I by upgrading the detector as soon as possible, and to seek various possibilities to acquire a budget for XMASS-1.5, in order to implement the plan.

Ashra Project

Hitherto Research Results and Future Project Outline

For the last decade, the Ashra group has been developing a detector that captures images of air shower by using imaging intensifier, and conducting observations in Mt. Mauna Loa. Ashra has been aiming at very-high energy astronomy, observation of gamma-ray burst (GRB)-origin tau neutrinos, and observation of optical flash from GRB in the visible light region.

In the interview with this Committee, in addition to the details of Ashra, the Neutrino Telescope Array (NTA) project was also reported. The NTA plan is to succeed from the Ashra experiment the air shower imaging technology, and to perform observation on the very-high-energy astronomical-origin neutrinos ranging from 10^6 to 10^9 GeV. The experiment is located on the island of Hawaii, United States, in an area surrounded by three mountains. Very-high-energy events due to air shower of tau neutrinos generated by passing through the mountains will be observed. The observable solid angle is approximately π steradian, and the angular resolution is evaluated at about 0.2°. Currently, there are about 30 collaborators from Japan, Taiwan, and the United States, and the target is to involve over 100 collaborators from 10 different countries. In terms of the timeline, it is planned that the R&D and budget application are to be completed between 2013 and 2014, the construction to start from 2015, and the observation to start from 2018.

Committee Evaluation

The Ashra experiment has been working on the research and development of cosmic ray observation in a very ambitious way, such as wide filed-of-view imaging observation using the image intensifier, and the observation of very-high-energy, earth-skimming tau neutrinos of astronomical origin. Some of the results obtained from this detector development research are quite unique. Also, through a series of development studies, the project attained some physics results such as cosmic ray spectrum measurement in the PeV region, neutrino search, and GRB optical flash search.

However, the Committee must conclude that Ashra is drastically behind its initial plan. The projects abroad that were expected to become competitors while Ashra was still in the planning stage are now delivering some results, so the Committee concludes there is little significance in continuing the verification tests for Ashra for another period of time in the future. Moreover, NTA was suggested as a future plan following Ashra. However, at present, the scale of the joint research organization, especially the manpower within the ICRR, is insufficient to fulfil the proposed plan, and therefore the Committee concludes that it cannot endorse implementing the NTA plan in such a way that the institute acts as the main body of the program.

Finally, the Committee agrees that the results obtained from the Ashra's detector development can be efficiently utilized in some form in the future, and therefore recommends to compile the technical results of the research in detail in papers and so forth.

Gadzooks!

Project Outline

Gadzooks! is a plan that aims to improve physics in supernova background neutrinos and supernova burst neutrinos and other events, by dissolving gadolinium sulphate at 0.1% in pure water in Super-Kamiokande equipment and thereby improving neutron capture efficiency of anti-electron neutrino reactions.

The primary background of the supernova

background neutrino is electron events originating from atmospheric neutrinos that are generated by the decay of muons with energy levels lower than the Cherenkov threshold. By detecting the delayed signal with energy approximately 8 MeV that is released when neutrons are captured by gadolinium, it is possible to reduce this background by about one-fifth, thereby improving the detector sensitivity for the supernova background neutrinos. Also, in the supernova burst neutrinos, electron events are sensitive with respect to the direction of arrival of neutrinos, however, by neutron tagging it is possible to use the sample that excludes anti-neutron events to calculate the direction, which then makes it possible to improve the resolution for the arrival direction by nearly 2-fold. In addition, further development of physics can be expected in areas including verification of supernova burst models such as for neutronization burst and Si burning, and in supernova burst sensitivity in nearby galaxies. Currently, in the Kamioka mine shaft, a 200-ton test tank is constructed and set up, and demonstration tests (EGADS) are being conducted for Gadzooks!, including tests for the Cherenkov radiation transmission, equipment corrosion, and water circulation equipment.

Committee Evaluation

At the Committee, no hearing on the Gadzooks! experiment was conducted with the parties involved, so the discussion on this topic was based on the information obtained at the town hall meeting hosted by the Cosmic Ray Conference. At the Committee, the Gadzooks! project is recognized as a research plan that is a natural extension in the realm of Super-Kamiokande research activities. The Committee highly appreciates its significance in physics, and concludes that it demonstrates high feasibility due to R&D that have been steadily executed. Regarding the transition of Super-Kamiokande detector to Gadzooks!, the Committee shares the opinion that the final decision is dependent of the Super-Kamiokande group, nonetheless, the experiment is considered feasible also in terms of obtaining a large-scale budget. Therefore, the Committee concludes an early realization of the plan is desired.

Other research groups (the Theory Group, the Observational Cosmology Group, and High-Energy Astrophysics Group)

Hitherto Research Results and Future Prospects

The Committee asked the Theory Group, the Observational Cosmology Group, and the High-Energy Astrophysics Group to each submit documents of a few pages reporting research achievements and future prospects. The following is the record of the discussions and evaluations made at the Committee based on these reports.

The Theory Group has been conducting theoretical research on various subjects related to particle physics and cosmology. In the field of particle physics, theories such as the grand unified theory and supersymmetry standard model, which is considered hopeful due to the presence of a candidate for dark matter, are the targets of study. In the field of cosmology, focusing on the particular area called particle cosmology, subjects such as cosmic inflation, baryogenesis, cosmological nucleosynthesis based on the supersymmetry theory, dark matter, and the generation and the evolution of cosmological density perturbation are studied. Over the past 5 years, the group has published 20 to 40 articles per year in peer-reviewed journals. Recent major research achievements include limitations to nucleosysnthesis and gravitino in the early universe, the Axion cosmology, limitations on equal curvature perturbation in inflation, Higgs particles in LHC experiments, and research on the supersymmetry standard model. Going forward, while paying close attention to the latest results from LHC and CMB observations, the group aims to propose a strong physics candidate that surpasses the standard model and to explore cosmological reasoning. Also, the group will accept students and researchers, and maintain activities to contribute to the field of particle physics/cosmology.

The observational cosmology group has gone through an organizational change from the SDSS group, and since 2010 the group has been embarking on preparatory research for deep space exploration using Subaru Telescope Super Wide Camera (Hyper Suprime-Cam: HSC). Using HSC, the deep space visible light imaging survey will be conducted over the next five years from 2013 to 2017, to detect about 10 thousand Lyα spectral lines at z=5~7, and by analyzing the data, the group aims for a unified understanding of the reionization of the universe. After 2018, the group will consider participating in projects such as the infrared spectrum survey using Subaru Prime Focus Spectrograph (PFS) and the

super large-scale, next-generation telescope, the Thirty Meter Telescope (TMT). As a collaboration, the group plans to provide data analysis tools and catalog a database inside and outside of Japan, as well as to host lectures and research workshops on deep imaging data analysis.

The High-Energy Astronomy Group was first established within High-Energy Cosmic Ray Division of ICRR in December 2009, and has been conducting research with an aim to study various high-energy astrophysical events related to the origin of cosmic rays, by employing theoretical and analytical methods. Thus far, the group has achieved results in the area of high-energy astrophysics, such as studies on explosion energy release phenomena and its related research on particle acceleration phenomena. The group has numerous research targets in common with other groups within the ICRR. The subjects that are expected to grow in the future are researches on extragalactic super-high energy cosmic rays, the acceleration mechanism of galactic cosmic rays, anisotropy, propagation, electromagnetic field detection methodologies on ultra-high energy cosmic rays, high energy γ-ray astronomy, and binary neutron start system merger events.

Committee Evaluation

It is noteworthy that two members of the theoretical group comprehensively share and cover a broad field of research, from particle physics to cosmology, and have been delivering numerous research results while maintaining a high level of activities. In addition, many excellent researchers currently active in the field of theoretical research originally resided in this group, that it seems the group has also contributed greatly to educating researchers.

At the ICRR, in addition to the Theoretical Group and Observational Cosmology Group, the High-Energy Astronomy Group was established, and these 3 research groups together resulted in the formation of a researcher's group that covers a wide range of studies including particle physics, cosmic rays, and cosmology. Taking advantage of these characteristics, it is recommended that the group investigate new collaborative research possibilities. Moreover, the Committee expects the 3 groups will not become siloed but, instead, expand their network and interact with other experimental and observational groups. In fact, the Committee encourages the continuation of already active collaborative research with investigators from the KAVLI Institute for the Physics and Mathematics of the Universe (Kavli IPMU), whose building is adjacent to the ICRR building.

Overall Conclusion

Before this Future Planning Committee commenced, the ICRR organized Future Planning Subcommittee meeting on three occasions since the 1980s to examine future plans for the institute. At the 1st committee meeting, Super-Kamiokande plan was recommended with the highest ranking. This plan has since been implemented, has made significant scientific achievements, and continues to produce new results. At the 2nd meeting, the researches on the highest-energy cosmic rays and gravitational waves were strongly recommended. The Telescope Array plan that promotes the studies on the highest energy cosmic rays has since been implemented. Its achievements are materializing at present, and the results have already received high evaluation by the international cosmic-ray community. At the 3rd committee meeting, the subject of gravitational waves was again strongly recommended. The promotion of the plan called KAGRA, which aims to detect gravitational waves, was approved by the Committee, and it is now under construction. In this way, recommendations made by the ICRR Future Plan Discussion (Sub) Committee have greatly influenced the execution of the research plans of the institute, and these researches have made many scientific achievements. Looking back on such history, the conclusion of this Committee, therefore, will have significant weight.

The Committee convened a total of 10 meetings over the period of about one year and a half since the beginning of 2012, and various possibilities for the future plan were discussed. The details of the Committee's evaluation on each future plan have been described in the previous chapters of this report. Although it is extremely difficult to rank these future plans, based on the comprehensive evaluation which takes into account the aspects of its expected scientific achievement, scientific ripple effects, and technical and budgetary feasibility of implementing the plan, the Committee's conclusions are reported below.

For the next plan the ICRR must promptly work towards realizing, the Committee recommends a

focus on CTA experiments that aim at dramatic advancements of gamma-ray astronomy. The CTA plan must be executed through an international collaborative effort. Hence, in order for the Japanese community to make a significant contribution and to actively implement the research, it is important to further reinforce Japan's research team organization comprised of the ICRR and other research groups, for the development of both equipment and software.

Regarding the advancement of neutrino physics such as neutrino oscillation, Japan has been leading the world for more than 10 years. Hyper-Kamiokande is a vital project that the Committee believes will be able to continue such trends, and even further develop it. In particular, the measurement of CP asymmetry and elucidation of mass hierarchy are one of the top-priority issues in particle physics, and their feasibility is considered sufficiently high based on the experiences from the current experiments. The Committee hopes to see a great progress in the research and development of Hyper-Kamiokande, to prepare for its swift implementation when the opportunity arises. At the same time, the budget scale is estimated at approximately 80 billion yen, and therefore it is recommended to those involved to clarify details—such as the cost ratio of each country to improve the accuracy of the budget estimate—in order to go forward with attaining the budget.

Many other future plans of the ICRR that were examined by the Committee can also be expected to demonstrate high scientific significance and sufficient scientific results. As for the XMASS experiment, if the background issue is resolved and the superiority of its methodology can be demonstrated, it can be expected—considering the scalability of the XMAS-1.5 detector—to drastically improve detection sensitivity for dark matter.

Considering their experimental scale, not only budgetary requests but also every other funding possibilities (including competitive funds) must be sought for XMASS-1.5: the next Tibet plan (which conducts gamma-ray observation in the 100TeV region), Gadzooks! (which searches for neutrinos originated from supernovae from the past, and TA×4 (which expands the observational area for the highest energy cosmic-rays by 4 times). The ICRR is also to support these plans and advocate for their speedy implementation. While its scientific significance is recongnized, the impression has been given that the TA×4 experiment's logistics and planning had a slower start compared to other projects. The Committee expects the planning to be expedited and the project be implemented as soon as possible.

Moreover, since XMASS-1.5 and TA×4 are not final plans, but have their next stages already being planned in detail, and hence also from the perspective of setting these future experiments in motion, early realization of these projects is desirable.

As the TALE experiment is to start, having both the Tibet and the TALE experiments will enable a wide and continuous measurement of energy in higher regions than the "knee" region. Such comprehensive implementation of air shower observation in such a wide energy range by one research facility is internationally unique. In order to take advantage of this, it is important for TA and Tibet, as well as for the theoretical groups, to work together and strengthen their cooperation. In terms of joining JEM-EUSO, the Committee expects active contributions from Japan's groups, even while leveraging the TA group's experience.

For the 3 groups of theory, observational cosmology, and high energy astrophysics, the Committee expects the groups to achieve results through implementing each other's collaborative studies, and to promote research exchange with other experiment observational groups.

Still, in order to realize all the large- and medium-size future plans examined this time by the Committee, there is not only the difficulty of financing, but also the difficulty of securing human resources. Therefore, it must be noted that, even for plans that were evaluated highly scientifically by the Committee, research teams must be flexible in their actions—by changing the order of plans, reevaluating research organizational structures, and so on—though the project's prompt implementation has been deemed difficult.

The ICRR has been providing various resources including experiment facilities, computers, and research groups, to support small-scale cosmic-ray research projects at different universities to date, fulfilling the role of Joint Usage/ Research Center (the former Joint Research Laboratories). The Committee hopes to see the institute continue the role of being the base for cosmic-ray studies. Finally, the Committee anticipates KAGRA to make steady progress in its ongoing construction, and to produce scientific results as soon as possible.

The Institute for Cosmic Ray Research of the University of Tokyo
Future Planning Committee Final Report

October 26th, 2017

Background and Objectives of Committee Establishment

The University of Tokyo, Institute for Cosmic Ray Research (ICRR), has coordinated Future Plan Discussion Committees four times since 1987 under the supervision of the organizing Committee. In these committees, discussions and nominations of the research projects of the next generations, especially on the ones, which could be the flagship (projects) of the institute. Based on the recommendations, the institute has strived to realize the plans. At the first committee in 1987, the Super-K was proposed and realized, thereby contributing to immense research progress. The second committee, in 1993, proposed highest-energy cosmic rays research, and this was realized in the form of the Telescope Array (TA) experiments. Furthermore, the gravitational wave telescope KAGRA, proposed in the second and third Committee (2007), has its detector under construction. To succeed Super-K and KAGRA in a timely manner, it was recommended—at the fourth Committee (2013)—that Cherenkov Telescope Array (CTA) experiments were to be prioritized, therefore permitting the construction of the CTA following the 2016 budget request. The Institute is at a point where future plans to follow up KAGRA and CTA must be debated.

In the 2012-2013 Future Plan Review Committee, a large-scale plan, Hyper-Kamiokande (Hyper-K), was also discussed. It was recommended that, "We have high expectations for progress on the development research of Hyper-K so that we are ready to realize the plan whenever the opportunity arises."

Since the budget is estimated to be around 80 billion yen, it is recommended that outstanding details are finalized, such as responsibilities and budget ratios for each participant country, so that the budget request can be moved forward [1].

Subsequently, ICRR and Institute of Particle and Nuclear Studies (IPNS), High Energy Accelerator Research Organization (KEK) have agreed to collaborate regarding Hyper-K. Also, these two institutes have set up an external advisory committee for the further discussion to realize the project.

The ICRR steering committee has decided to appoint a new Future Plan Committee, which focuses its efforts around the Hyper-K plan. This committee examines the work following the 2013 Future Plan Committee Report [1] and evaluate the purpose and the feasibility of the project to determine whether this project is appropriate as the next main project or not. This committee also has decided to discuss new projects which are proposed after the previous Future Plan Discussion Committee.

At the time this Committee commenced, the science council of Japan had been developing master plans for the 23rd large-scale research facility plan. The Ministry of Education, Culture, Sports, Science and Technology (MEXT) had also decided on discussing the reassessment of the roadmap in early 2017. It was projected that Hyper-K would be one of the main topics in this discussions, so this Future Plan Committee held a discussion on Hyper-K prior to the other projects to accommodate the developments that were to happen in the MEXT meetings and, published an interim report on March 24th, 2017.

Regarding the new research plans, proposals were solicited from faculty members of ICRR, from October 8th to November 1st 2016, which resulted in 3 proposals: "ALPACA Experiment Plan," "Proposal for extension of the high-energy cosmic ray observation on the ground," and ""Composite Imaging Observations of Cosmic Elementary Particles."

In addition, on May 1st, 2017, the research representative of the XMASS collaboration requested a discussion on changes to the current plan and it was decided at the 8th committee meeting (May 10th, 2017) that this was to be regarded as a new proposal. This final report is comprised of the discussions on the four new proposals, the summary of the plans and the evaluation of the Committee.

Members

Y. Okada (Chairperson) Director, High-Energy Accelerator Research Organization

H. Aihara Professor, Graduate School of Science, The University of Tokyo
Y. Ito Professor, Institute for Space-Earth Environmental Research, Nagoya University
K. Inoue Professor, Research Center for Neutrino Science, Tohoku University
S. Ogio Professor, Osaka City University Graduate School of Science
T. Kishimoto Professor, Osaka University Graduate School of Science
J. Hisano Professor, Center for Theoretical Studies, Nagoya University
M. Mori Professor, Ritsumeikan University College of Science and Engineering
M. Nakahata (Secretary) Professor, Institute for Cosmic Ray Research, The University of Tokyo
M. Ibe (Vice secretary, clerk) Associate professor, Institute for Cosmic Ray Research, The University of Tokyo
T. Kajita (Observer) Director, Institute for Cosmic Ray Research, The University of Tokyo

Background

- 1st Meeting (October 4th, 2016)
  - Introduction
  - Report from Hyper-K Advisory Committee
  - About Hyper-K Plan
  - On the status of the evaluations by the community
  - Future course of action
    - Discussion procedures for Hyper-K
    - Inviting other project proposals and the review timeframe
- 2nd Meeting (November 14th, 2016)
  - Hearing on Hyper-K Plan
    - On the set-up for promoting Hyper-K
    - Physics of Hyper-K I (solar, supernova neutrino bursts)
    - Physics of Hyper-K II (CPV, Proton decay)
  - Discussions on Hyper-K Plan
  - New proposals
    - Soliciting proposals from faculty members
    - Proposals
    - Discussion procedures for new proposals
- 3rd Meeting (December 13th, 2016)
  - Discussions on interim report
  - Hearings on new projects
- 4th Meeting (February 2nd, 2017)
  - Discussions on interim report
- 5th Meeting (February 21st, 2017)
  - Reports on the submission of the draft interim report to the faculty and the steering committee
  - Hearings on new proposals
- March 6th - March 24th, 2017
  - Discussed revisions via email based on the comments received from the faculty meeting (commenced on Feb. 23rd, Mar. 23rd) and the steering committee (commenced on Mar. 6th)
- March 24th 2017
  - The Institute for Cosmic Ray Research of the University of Tokyo Future Plan Discussion Committee finalized the interim report
- 6th Meeting (April 10th, 2017)
  - Discussions on the new proposal the "ALPACA Project"
  - Discussions on the new proposal "Future Plans on the Ground-level observations of Ultra-High Energy Cosmic Rays"
  - Discussions on the new proposal "Composite Imaging Observations of Cosmic Elementary Particles"
  - Discussions on the final report
- 7th Meeting (April 27th, 2017)
  - Discussions on the draft final report
- 8th Meeting (May 10th, 2017)
  - Discussions on the draft final report
  - Procedures for handling new/revised proposals
- 9th Meeting (June 12th, 2017)
  - Review on the direct search of dark matter
  - A hearing and discussions on the new proposal "A Proposal for the New Development of the Direct Dark Matter Search Experiment with Liquid Xenon"
- 10th Meeting (July 3rd, 2017)
  - Additional hearing and discussions on the new proposal "A Proposal for the New Development of the Direct Dark Matter Search Experiment With Liquid Xenon"
- 11th Meeting (August,18th)
  - Discussions on the new proposal "A Proposal for the New Development of the Direct Dark Matter Search Experiment With Liquid Xenon"
  - Discussions on the final report
- September 19th - 22nd, 2017
  - Based on the comments received from the steering committee (commenced on September 19), revisions were discussed via email.

- 12th Meeting (October 16th, 2017)
  - Discussion on the draft final report based on comments received from the faculty meeting (commenced on September 26).
- October 26th, 2017
  - The Institute for Cosmic Ray Research of the University of Tokyo Future Plan Discussion Committee concluded the final report

Hyper-Kamiokande Plan

Overview of Hyper-K plan and Updates from the Future Planning Committee

Hyper-K is a third-generation nucleon decay/neutrino experimental plan using a water Cherenkov detector, following the previous Kamiokande and Super-K projects. A wide range of physics is envisaged from this plan, including measurements of charged parity (CP) asymmetry in lepton sector by accelerator neutrinos, determination of neutrino mass hierarchy in atmospheric neutrinos, nucleon decay search, studies of solar neutrinos, supernova burst neutrinos, and supernova relic neutrinos. A candidate site for the detector is Tochibora mine (underground, 650m-deep, located about 10 km away from Super-K) in Kamioka Town, Hida City, Gifu Prefecture.

The detector design examined at the previous Future Planning Discussion Committee comprised two sets of cylindrical tanks, 54-meters high and 250-meters long with total mass of 1 million tons (of which the effective volume is 560,000 tons, resulting in a 25-fold increase from Super-K), 20% photo-sensitive coverage with about 100,000 photosensors in total. The detector size was then optimized, and the revised design submitted to this committee consisted of a cylindrical tank of 60 meters in height and 74 meters in diameter (260,000 tons in total mass with an effective volume of 190,000 tons,) with 40,000 ultra-sensitive photosensors (twice the conventional sensitivity) mounted in the inner tank. The production cost is scaled down in the new design by reducing the total mass. Although the effective volume is smaller compared to the former design, the sensitivity in CP asymmetry measurements will not be affected owing to the revised plan of the J-PARC beam power upgrade from the previously expected 0.75 MW to 1.3 MW.

Furthermore, while in the former design the detector was instrumented with photodetectors of regular photon-sensitivity at photocathode coverage of 20%, the new design installs photodetectors with doubled photon-sensitivity and increases the photocathode coverage to 40%. As a result, it is possible to suppress the background of nucleon decay events by neutron tag (simultaneous measurement of 2.2 MeV gamma rays associated with neutron capture by protons), thus maintaining the experimental sensitivity (the discovery capabilities). The Hyper-K group is also considering the possibility of having the second detector in the future.

The total construction cost for one tank is estimated to be 67.5 billion yen, which consists of 16.3 billion yen for excavation, 9.2 billion yen for the disposal of the sludge and the wastewater treatment, 2.4 billion yen for the geological surveys and the design work for construction, 12.5 billion yen for the liner and the structure, 19.6 billion yen and 1.8 billion yen for the optical sensors for the internal and the external tanks respectively, 1.2 billion yen for the electronic circuit, 3.3 billion yen for the pure water system, 100 million yen for the measurement computer, 100 million yen for the calibration equipment, and 100 million yen for the construction management. Out of the total, 12.4 billion yen, which covers a half of the inner tank optical sensors, the whole outer tank optical sensors, the electric circuit, the measurement computer and the calibration equipment, is expected to be contributed from the international collaborators.

The international collaborative research group that officially launched in January 2015 has now grown into an international joint experiment with about 300 members, representing 15 different countries. The research organization is comprised of 10 working groups operating under the project leader with each overseeing a specific experimental component, the International Steering Committee (ISC) that makes decisions on the major policies of the project, and the International Board of Representative (IBR) that consists of the representatives from the member countries.

The construction is expected to be completed in 2025 following 2 years for the access tunnel excavation, 2 years for the experimental cave excavation, 2 years for the tank construction, and 1 year for the photo-sensor and the supporting structure installation, if the construction is budgeted. Then, the detector is filled with pure water and starts its operation from 2026.

Progress in the Research Environment

Until now, the following developments were made in relation to the promotion of Hyper-K:

(1) In the KEK's project implementation plan (KEK-PIP), improving J-PARC performance for Hyper-K was recognized as the most crucial among the other four top-priority research plans that should be implemented by new budgetary requests [2].
(2) Japan Association of High Energy Physicists (JAHEP) made a recommendation in its future plans that the massive neutrino detector be made one of the core large-scale future projects [3].
(3) Cosmic Ray Researchers Congress (CRC) placed Hyper-K as one of the projects of utmost importance [4]. Furthermore, the CRC steering committee submitted a letter "A Request from CRC for the Early Realization of Hyper-Kamiokande Project" to the Chairperson of Particle Physics and Nuclear Physics Sub-committee of the Science Council of Japan (March 31, 2016). The steering committee recognized the project as a super-large scale future plan of utmost importance in the field of cosmic ray research since the completion of KAGRA.
(4) Based on the discussions evolved in the research community, the Hyper-K project was submitted to the Science Council of Japan (SCJ) with the project title "Nucleon decay and neutrino oscillation experiment using a large-scale advanced detector," which was then selected in the Master Plan 2017. The council also acknowledged it as one of the key large-scale research plans.
(5) A memorandum for cooperation was signed by the host institutions (ICRR and KEK-IPNS). The International Advisory Committee was set up, and discussions by the committee members are making progress. The International Advisory Committee concluded Hyper-K is highly competitive internationally, and therefore must be promoted going forward.

Committee Evaluation

The precision measurements of the neutrino oscillation parameters and the search for the nucleon decay lead to elucidation of physics beyond the Standard Model of particle physics, and these play a crucial role in shedding light on the early stages of the universe. In addition, through its unique means to study the internal structure of stars, neutrino astronomy can provide information that cannot be obtained from the other observational methods.

The Committee highly commends Hyper-K, the multipurpose detector, as it is able to contribute to the developments of diverse fields of science, including the precision measurements of neutrino oscillation parameters, the contribution to the neutrino astronomy, and the direct verification of the Grand Unified Theory. Hyper-K is an excellent detector that not only provides a solution to the urgent issue of neutrino CP symmetry violation, but also can serve as a long-term neutrino astronomy observation site. The detector evaluated by this committee is the 260 thousand-ton design that was included in the SCJ Master Plan 2017.

In recent years, it has been known that the neutrino mixing angle θ_{13} has a sufficiently large value that it may lead to the early discovery of the violation of the CP symmetry. Leptogenesis (lepton number generation by the universe) by the seesaw mechanism that incorporates right-handed neutrino is a strong candidate for the origin of the baryon number of the universe. Finding the presence of the CP violation in the lepton sector can mark an important step towards the elucidation of leptogenesis.

Hyper-K is at an advantage internationally in terms of becoming the first to discover the CP violation with the neutrino oscillation, having the most reliable and the matured technology. Hyper-K is capable of searching a wide range of the CP violation parameters, and as the result of the T2K experiment suggests, in cases where the CP violation parameter is at its maximum, its sensitivity exceeds 5 sigma. A way to steadily reduce the systematic errors is outlined—and it indicates a high degree of achievability. Hyper-K's ability to determine the mass hierarchy by using the high statistical observation of atmospheric neutrinos is also commendable.

Discovering nucleon decay is the direct means to verify the Grand Unified Theory (GUT). Hyper-K is the only future plan that is capable of extending the sensitivity of $e^+\pi^0$ mode lifetime to 10^{35} years. $e^+\pi^0$mode is caused by a gauge boson (X Boson) newly introduced in GUT. Based on the measurements of three coupling constants using the Standard Model, it is expected that supersymmetric Grand Unified Theory is being realized at 10^{16}GeV, that if the mass of X Boson is in the vicinity of 10^{16}GeV, there is a high probability Hyper-K is able to detect nucleon decay. Also, vK+ mode that greatly restricts the

model of supersymmetric GUT will be improved in the new design, having 2 to 3 times the current sensitivity. The Committee recognizes Hyper-K as an appropriate project for the next-generation nucleon decay search.

The supernova explosion mechanism and the precise measurements of solar neutrinos are important subjects in neutrino astronomy. With Hyper-K, we can expect about 100,000 neutrino induced events observed from supernova explosions within our galaxy. These events allows us to study the neutralization burst in the initial stage of explosion and the short scale time structure from the shock induced instability during the explosion process and the core rotations. It is anticipated that these new information will be of help in understanding the explosion mechanism. The Committee recognizes Hyper-K as a vital project in promoting neutrino astronomy.

The Committee recognizes the significance in increasing the observational accuracy of solar neutrinos, especially in improving the measurement precision for neutrino mass difference. Currently, there is a discrepancy in 2 sigma level between Δm^2_{21} obtained from solar neutrino observations and the Δm^2_{21} obtained from KamLAND's nuclear reactor neutrino observations, and thus it is important to determine whether this is due to the statistical or systematic errors or due to the unknown new physics. Although the estimation of the cosmic background is in progress, more detailed study based on various simulations is required. In addition, the influence of radon from bedrocks and the reduction of radon due to water flow should also be considered.

As a competing project, there is the LBNF/DUNE project in the United States, measuring CP violation and searching for nucleon decay using a 40,000-ton liquid argon TPC detector, whose construction is already underway and aiming to commence operation from 2026. This project has equivalent sensitivity to Hyper-K in measuring CP violation and it has become an international competition. Against the liquid argon TPC detector, which requires technological development, Hyper-K is in an advantageous position in terms of feasibility because similar type of detector, including Super-K, have been in realized with existing technology and has already proved its capability. Hyper-K is able to accumulate useful data from the onset of the research scheduled in 2026, and deemed likely to discover CP violation ahead of DUNE. It should be noted that the construction of LBNF/DUNE project has already started and it is essential Hyper-K is put into motion as soon as possible.

With regard to proton decay search, the sensitivity of the $e^+\pi^0$ mode is essentially determined by the size of the effective volume. With vK+mode, Hyper-K demonstrates sensitivity close to that of DUNE's. As such, and also for the field of proton decay search, a steady progress can be anticipated by utilizing the existing technology and enlarging the detectors.

Regarding neutrino astronomy/atmospheric neutrino observation, there is the IceCube/DeepCore project that utilizes Antarctic ice sheets, and ANTARES project that uses the water at the Mediterranean Sea, where observations are being conducted for neutrinos over 20GeV. In addition, the PINGU project is in the planning stage, to extend the sensitivity of IceCube to low energy, equal to 10GeV and lower. Hyper-K is able to observe solar neutrinos and supernova neutrinos, which cannot be detected by these projects, and therefore these projects are complementary.

As such, Hyper-K demonstrates uniqueness not seen in its competitors, and due to the urgency in studying the CP violation, which is now a global race, the Committee concludes that an immediate start is highly desired.

It is commendable that, compared to the previous draft plans, cost-saving measures have been taken without compromising the detector sensitivity to CP violation and the nucleon decay search by reexamining the design. Moreover, the Committee acknowledges that the cost uncertainties pointed out at the previous Future Plan Discussion Committee have been reduced. For example, the expenses for the sludge disposal and the wastewater treatment, which were not estimated previously are now included in the cost estimates. Also, for the cost of cavity excavation, which accounts for a major portion of the expenses, a conservative estimate is made based on the boring survey. Progress is also seen in the specific designing of the tank structure (including the surface treatment such as the waterproof sheets and the polyethylene liner), and the designing and the testing of the shockwave prevention cover. For these reasons, it can be concluded that the details of the plan have been improved and the technical feasibility, including expenses is confirmed.
After the last Future Plan Discussion Committee, the International Collaborative Research Group was officially launched in January 2015, paving the way to establish a collaborative system, and the

Committee commends this development. Notably, it is highly evaluated that an agreement on the construction and operational expense allocations is to be signed by foreign delegates in March 2017. The required next step is the further substantiation of the plan.

The Committee applauds that the signing of the memorandum for cooperation was completed by the host institutions (ICRR and KEK-IPNS), and that the International Advisory Committee was subsequently established where discussions by the members are already making progress. The division of responsibility is more clearly defined, where ICRR is to focus on the construction and the operation of Hyper-K, and KEK to focus on the contraction and the operation of the J-PARC beam and the near detector, showing a significant improvement since the last committee meeting. ICRR having the responsibility over the construction and the operation of Hyper-K sends a strong message that this project is a future plan in the field of the cosmic ray research. In fact, it is noteworthy that Hyper-K not only acts as a far detector for long baseline experiments, but also serves as a comprehensive cosmic ray research facility.

However, it is estimated that about 20 personnel, twice the number of staff at Super-K, are required for the internal system of ICRR, indicating that additional six personnel are needed. In cases where securing full-time researchers is deemed to be difficult, the Committee recommends to hire project researchers in order to propel the project, and at the same time to take measures to develop more young researchers. It is commendable that there was a proposal for establishing an organizational structure that accommodates a large-scale budget. Further improvement of the organization is required, however. This includes the setting up of a promotion team lead by the project managers who have responsibility over the implementation of the construction. The Committee urges that ICRR and the international collaboration team cooperate to develop a management system appropriate for the construction and the execution. The Committee views that it is also important to seek advices, as deemed necessary, from a third-party committee of experts who have experience in executing large-scale projects.

The Committee recognizes significant improvements in the budget estimation accuracy that was an issue identified at the last meeting, in the international collaboration formation, and in defining the role-sharing between ICRR and KEK. Based on the points made above and its scientific significance, the Committee recognizes Hyper-K as an appropriate plan for ICRR's next major project, and concludes that its prompt realization is desirable.

The ALPACA Project

Project Outline

ALPACA Project is a collaborative experiment plan by 14 Japanese and Bolivian research institutions, led by the Institute of Cosmic Ray Research (ICRR) of the University of Tokyo and San Andres University. The plan is composed of an air shower array with an effective area of 83,000m^2 and the world's biggest (5,400m^2) muon detector array, set up on a highland in Mt. Chacaltaya in Bolivia (at an altitude of 4,740m). By coupling the two detectors, it aims to make a wide field-of-view imaging in the 100TeV region （10TeV-1000TeV） of ultra-high energy gamma rays, employing the world's highest sensitivity. The two major research objectives for the experiment are as follows:
(1) To become the world's pioneer in probing the acceleration point sources of cosmic rays in the over 100TeV region by detecting the point sources of ultra-high energy gamma rays in the southern sky.
(2)To aim for discovering Galactic PeVatrons by investigating the extended region around the Galactic Center and the diffuse gamma-ray emission in the 100TeV region from Fermi bubbles' diffuse gamma-ray sources.

Furthermore, this experiment will cover various other research themes such as the elucidation of the chemical composition of the primary cosmic-ray nuclei in the cosmic ray "knee" region, precise measurements of the cosmic ray anisotropy above the TeV energy region that is still unobserved in the southern hemisphere, and the elucidation of the general structure of the solar terrestrial magnetic fields by precise measurements of the Sun's shadow against the cosmic ray flux.

The ALPACA experiment consists of an air shower array with 401 1m^2 scintillation detectors deployed at a 15m-apart grid covering 83,000m^2 , and of 96 sets of 56m^2 underground water Cherenkov muon detectors. Regarding the performance of this detector, it is estimated that the primary gamma-ray modal energy detected is 5TeV, the angular

resolution is 0.2° at 100TeV, and the energy resolution is 25% at 100TeV.

The key to this experiment lies in the successful selection of gamma rays by the number of muons in air shower. With the planned detector, by the optimized selection process using muon numbers within 100m of the core, it is estimated that, for the primary energy at 100TeV, the removal rate of primary cosmic-ray nuclei to be 99.9%, while having the gamma-ray survival rate at 90%. For that reason, it is estimated that the world's highest sensitivity can be achieved by this experiment, going beyond the CTA experiment, for gamma-ray sources over 40TeV. Moreover, for more diffused sources, the sensitivity is expected to surpass that of the CTA experiment even at lower energy levels, for example, over 30 TeV for sources extending over 0.1°and over 10 TeV for sources extending over 1.5°.

The necessary cost for the construction is estimated to be approximately 500 million yen, and hence a large-scale Kakenhi (Grants-in-Aid for Scientific Research) is planned to be utilized. After the preparation, the construction is expected to be completed in four years, and the stationary continuous observation to start in the fifth year and to continue for the next 10 years.

The advantage of its implementation in Bolivia is that an easily accessible flat land can be secured, at an altitude of over 4000m where air shower before its attenuation is detectable, and it is in the southern hemisphere where the Galactic Center, the most promising candidate of the galactic cosmic-ray source, can be observed. It is also because the country shares strong rapport with—and a history of—cosmic ray observation research with Japan since the 1960s, and that adequate infrastructures (such as electricity, water supply, roads etc.) are available.

<u>Committee Evaluation</u>

In the southern hemisphere, since there are a number of interesting celestial objects—from the Galactic Center and Fermi bubble to supernova remnants and pulsar wind nebulae—that the discovery of Galactic PeVatrons can be anticipated. As such, the scientific significance of this plan that aims to survey gamma rays in the 100TeV region is very high. The plan demonstrates high feasibility in both technology and budget, and hence the Committee evaluates it as a research that should be promoted.

Tibet ASγ and BASJE members are participating in this project, so Tibet ASγ's technology and the already-established international cooperation system with BASJE can be leveraged. Considering the results from the Tibet ASγ experiment in the northern hemisphere,10 to 20 high-energy gamma-ray point sources are expected to be discovered with the ALPACA experiment. Furthermore, as ALPACA has the angular resolution of 0.2°, which is excellent for an air shower array, a detailed analysis of diffuse gamma-ray sources is possible. The Committee considers that with this experiment it may be possible to also search for electrons and gamma rays that originated from dark matter in the southern hemisphere.

A reasonable cost estimate is made from years of experience and prototype production that implementation of the plan seems feasible with the acquisition of the large-scale science grants.

The South-HAWC plan that aims to carry out a wide-field-view continuous survey of gamma rays in the energy region from 100GeV to 100TeV and ALPACA experiment overlap and compete in the 10TeV region, so it is desired to implement the ALPACA experiment in advance of the South-HAWC plan. Regarding the HAWC experiment and the LHAASO experiment in the north, ALPACA is complementary in its field of observation where observation is made in the south. CTA, an experiment that has a high angular resolution and limited observation time, and ALPACA that employs wide field-of-view and long-term continuous observation, are mutually complementary. ALPACA is to widely survey the southern hemisphere, HAWC/LHAASO to widely survey in the north, and CTA to survey specific areas in detail, which subsequently creates a synergistic effect and utilizes CTA's observation time more efficiently. For this reason, ALPACA should commence its survey in the southern hemisphere in time for the launch of CTA observation in 2021, emphasizing the point that the speedy realization of the plan is essential.

Tibet ASγ experiment has completed the construction of the muon detector, and has entered a stationary observation mode that it can be said that the time is ripe to embark on the ultra-high energy gamma-ray detector in the southern hemisphere. However, there is a concern that human resources may be insufficient to execute two experiments simultaneously. The Committee asks to consider personnel allocation for the steady execution of the project.

Future Plans of Observations of Ultra-High Energy Cosmic Rays on the ground

Project Outline

TA2 project is an air shower detection plan that has detection area 60 times larger than the current TA experiment, having 10,000 ground detectors in an area of 40,000km^2. About 1000 highest energy cosmic rays above 57EeV will be observed annually. The field-of-view is divided into 60 regions, and energy spectrum is measured in each region. The aim is to examine with high statistical precision the source of anisotropy of the highest energy cosmic rays, which is becoming apparent by the TA experiment. For the ground detector, the scintillator is mainly used, but water tanks and lead-plate-type detectors are also being considered as the particle discrimination capability is required. It is also under consideration to carry out chemical composition measurement by deploying the atmospheric fluorescencetelescope, which has been drastically reduced in cost. Total construction cost is estimated to be in the scale of 10 billion yen. It is planned to be realized through a big experimental project under the international collaboration led by researchers from TA and Auger projects. It is estimated that Japan will bear approximately 20% of the total construction cost. The construction is planned to start in 2025, aiming for full-scale operation from 2028.

In proposing the TA2 experiment, regarding the progress of the highest energy cosmic ray research using air shower observation, expected results and the timeline of the currently under construction TAx4 experiment as well as the TALE SD experiment were explained—based on the results from the presently ongoing TA experiment. A holistic roadmap of the highest energy cosmic-ray observations was presented. According to the roadmap, the TAx4 experiment that has the detection surface area four times larger than the current TA experiment, is to be continued with some other funds after its current budget ends in 2020. Within 10 years of observation, it is aimed to obtain six times more data than from the current TA experiment, to affirm the arrival direction of the highest energy cosmic rays claimed by the TA experiment with the statistical significance of 3.4σ (HotSpot) at the 5σ confidence, as well as to probe Hotspot structure and search for other Hotspots. The proposed TA2 experiment aims to elucidate the origin of the highest energy cosmic rays based on the results expected from the TAx4 experiment and the increased data with 16-fold increase from the TAx4, which is to be obtained from the 10-year observation.

As for other future plans concerning the observation of the highest energy cosmic rays, there is the Auger Prime experiment, which is an upgrade from the Auger experiment, as well as the JEM-EUSO experiment, which is a plan to detect cosmic-ray shower from the satellite orbit. Both have their structures for collaboration in place. The joint discussion with the Auger experiment group is at the stage where a WG has been set up. Regarding the JEM-EUSO experiment, it will be succeeded by the Russia-led experiment K-EUSO Project, but the detection aperture remains twice the size of TAx4. TA group will continue to maintain the cooperative framework with other projects, such as TA-EUSO.

Committee Evaluation

Observation of the high-energy cosmic rays is an important research subject with respect to the elucidation of cosmic ray acceleration mechanism over 10^{20} eV and its celestial accelerator, and the propagation mechanism. In the last decade, understanding of the highest-energy cosmic rays has been dramatically advanced by the progress made by the TA and Auger projects. In particular, the discovery of HotSpot by the TA experiment in the northern hemisphere is commendable as it gives an important clue to the origin of high-energy cosmic rays. In addition, the discrepancies between the TA experiment and the Auger experiment in their observation results—such as chemical compositions—are being reconciled through collaborative efforts by the two groups. Attempts to advance the understanding of chemical composition, such as the Auger Prime experiment, are making headway. The Committee commends the results from the current TA experiment and its development into TAx4 regarding highest-energy cosmic-ray observation. At the same time, it also acknowledges that the TA2 plan that can further advance these accomplishments is now being studied. The strategy of the current TA2 plan is mainly to increase the area of ground detectors, and after statistically establishing the HotSpot in the northern hemisphere by the TAx4 experiment, the main focus is on accomplishing even greater statistical accuracy to determine the disparities in the energy spectrum according to the arrival directions. The optimization of these TA2 experiments strongly depends on the results of ongoing TAx4 experiments and Auger

Prime experiments. With other experiments such as GZK neutrino search by the IceCube experiment, the integrity as a multi-messenger observation is questioned such that further evaluation that incorporates these results is necessary.

On the other hand, international cooperation is indispensable to advance a large-scale future plan of this level. The Committee commends that a cooperative framework is being established between the TA and Auger experiments. The Committee recommends continuing further studies toward realization of the high statistical accuracy of highest-energy cosmic-ray observations in future ground-based experiments. At the same time, the Committee also recommends to take specific measures to advance building the structures needed for this large experimental project under international collaboration.

Composite Imaging Observation of Cosmic Elementary Particles

Project Outline

Neutrino Telescope Array (NTA) plan is to install a wide-field observation station equipped with an optical imaging device at four locations in the mountains of Mauna Loa, Hawaii Island at an altitude between 3000 and 3500m. The plan is to carry out observations on the Earth-skimming high-energy tau neutrinos, large zenith-angle high-energy electron neutrinos/tau neutrinos, and high-energy cosmic rays/gamma rays, by utilizing Cherenkov light and atmospheric fluorescence, as an international, collaborative experiment with researchers from the United States and Taiwan. The optical imaging device utilizes the technology developed by Ashra-1, including a condenser, an image intensifier, a trigger sensor circuit, and a CMOS sensor circuit, to achieve high sensitivity, high resolution of 0.1 degrees or less, and a wide field-of-view. If the neutrino observation in the PeV region can be realized, data complementary to other experiments such as the IceCube experiment, can be obtained. It is possible to observe gamma rays in wide field-of-view up to the PeV region. Within fiscal 2017, the Technical Design Report is to be published, and if the plan goes smoothly, the operation is to commence from fiscal 2022.

Committee Evaluation

The Future Plan Discussion Committee of 2012-2013 reported that it could not endorse executing the NTA plan in such a way that the ICRR is positioned as the main body. Taking into consideration the change in the environment since high-energy neutrinos derived from astronomical sources were detected by IceCube, the discussion at this committee was focused on whether there has been a new development that would greatly alter the previous committee's conclusion.

The detection technology for implementing NTA can be described as ambitious, based on technological developments aimed at Ashra-1. There is also progress seen in the forming of the research structure, as a Letter of Intent was issued in 2014 and a subcommittee which promotes international collaborative experiments has been set up.

However, the development of elemental technology has resulted in considerably longer time than the original estimation. There is insufficient material that points to significant progress since the last Future Plan Discussion Committee, in developing the detection technology that can provide basis for realizing the NTA plan. In addition, there are no feasibility studies of the Earth-skimming neutrino observation by means of atmospheric fluorescence that have been published.

The Future Plan Discussion Committee 2012-2013 reported that "The scale of the joint research organization, especially the manpower within the ICRR, is insufficient to fulfil the proposed plan, and therefore the Committee concludes that it cannot endorse implementing the NTA plan in such a way that the institute acts as the main body of the program." The Committee made the discussion on the promotion organization for the plan again, however, the Committee concludes that a project team required to lead the experiments has not been formed domestically yet and the promotion organization remains inadequate.

Based on the above, the Committee has not been able to acknowledge any significant progress being made that would overturn the last Committee's decision. Therefore, the Committee concludes that it cannot endorse the NTA plan as the ICRR's future plan.

A Proposal for the New Development of Direct Dark Matter Search Experiment with Liquid Xenon

Project Outline

There was a new proposal from the current research representative on the proceedings with the XMASS going forward. The Committee conducted a hearing twice to the representative, and based on discussions among the Committee members, the Committee understood the present situation and the future research plan as below.

The XMASS experiment is to search for WIMP, a promising candidate for dark matter, with the world's highest sensitivity and thereby aims for its discovery. It also endeavors to conduct low-energy solar neutrino observation and discover neutrinoless double beta decay. As a pioneer of single-phase experiments using liquid xenon, the team has propelled the construction and experiment of XMASS-I, yielding valuable results with numerous technological developments and new insights into physics. At the same time, further improvement in sensitivity was required for the WIMP search. Based on this, XMASS-1.5 (6 tons of xenon liquid to be used) that has about 10^{-47} cm^2 in sensitivity to the nucleon-WIMP scattering cross-section was proposed as a next generation detector. However, the construction of XMASS-1.5 has not been realized, and in a different direction, projects that are called the second generation (G2), such as the XENONnT experiment and the LZ experiment（10 tons of liquid xenon is to be used each by the 2-phase detector, with search sensitivity of approximately 1048cm2, can improve the sensitivity even further—by one order of magnitude. These experiments are planned to be launched in 2019 and 2020, and will allow searches in a wide parameter area of the supersymmetric model. Moreover, another future experiment, called the third generation (G3), is in the planning. In this type of detector, the ultimate sensitivity, which is restricted by the background of solar and atmospheric neutrinos, can be achieved. Here, high particle discrimination capability is a requirement. While the single-phase XMASS experiment has been dependent on the advantage of easy size enlargement, its particle discrimination capability is too poor to achieve the desired sensitivity. As the problem of enlargement has become less of an issue for the two-phase type—which has higher particle discrimination capabilities—it has become clearer the superiority of the two-phase type, indicating that the time has come to reevaluate the directionality of the next generation experiment of XMASS.

It is assumed that target size will become the decisive factor in the future, creating a situation where a large-scale detector, something that can only be produced singularly in the world, becomes essential, which then leads to the formation of an international collaborative experiments that will have to integrate such initiatives as XMASS. In view of this situation, there was a proposal from the XMASS experiment group to shift the policy from the current one that aims at realizing XMASS-1.5 to forming a research group that participates in overseas G2 experiments and promotes research and development for the future G3 experiment. There are two G2 experiments, LZ and XENONnT, but the research group is already having discussions based on the premise to join XENONnT. Both projects plan to conduct searches on the scattering cross section of 10-48cm2, and their targets are similar. However, XENON1T, which forms the basis for XENONnT, has already yielded superior results compared to LUX, and is one step ahead.

Furthermore, since XENONnT has not finalized the detector design yet, it is possible for Japan to make great contributions with resources such as knowledge and experience gained from the XMASS experiment. Specific contributions that can be expected include (1) research and development of liquid xenon purification technology, (2) low background technology, (3) personnel who will stay at the site and conduct research (4), utilization of Japan's photomultiplier, (5) lending of up to 1.9 tons of xenon gas, (6) adopt XMASS-I at Kamioka's underground laboratory C as a test bench, and leverage the leading edge development and research of dark matter experiments, as well as to form a base that can support these operations.

Committee Evaluation

It has become a common understanding among the Committee members that even with the XMASS-1.5 being realized as an extension of the current single-phase, it remains impossible to keep up with research carried out by other countries. It is appropriate that the research group has proposed to change the research plan. Also, taking part in the ongoing G2 experiment overseas, particularly in the XENONnT project, is a promising plan. The Committee recommends the research group to promptly investigate the possibilities in this direction and work towards its materialization, and to continue the efforts to gain understanding from the researcher community.

In promoting this plan, it is desirable to thoroughly examine the following points.

1. Scientific Rationality
The outline of the proposal consists of: (1) terminate the current XMASS experiment in two years time, and withdraw its next phase, XMASS1.5; (2) participate in overseas G2 experiments. It is an appropriate decision to terminate the current XMASS experiment and withdraw XMASS1.5, considering the competition with the ongoing researches overseas. The Committee recognizes the plan to join overseas G2 experiment to be a promising policy that can initiate cutting edge physics. As G3 is in the planning following G2, it should be noted that consideration must be taken about the transferring of experience gained from G2 and the activities in Kamioka to G3.

2. Development towards international stage
The purpose of XMASS experiment is the search of dark matter, so it appears only natural that a larger scale experiment at an international level becomes more favorable in terms of scientific objectives. By joining the international effort with the resource for the current XMASS experiment, it is expected that the team will be able to make a great contribution to the G2 experiment overseas. At the same time, XMASS experiment is set up as research focused on the low background technology at Kamioka Observatory—with the research and personnel costs funded by the ICRR—that this could possibly restrain some research activities overseas. For example, the researchers for XMASS were hired on the premise that they work in Kamioka, and this could lead to problems as to the researchers' place of employment. It is desirable to compose a research group capable of promoting the research while maintaining consistency with the project at Kamioka Observatory, once the participation requirements for the G2 experiment are clarified.

3. Ownership of the resources
The resources of the XMASS project includes not only those purchased with the ICRR's budget but also with external funding such as the Kakenhi scientific grants. Even if the research group's plan to expand its experiment overseas gains understanding, it is essential to take into account the research representative's intentions, especially regarding the resources purchased with external funding.

4. As a joint research in Kamioka
The XMASS experiment has been positioned as a collaborative research promoted by Laboratory C of Kamioka Observatory. In the proposal, Laboratory C is used as a place for research and development for G3, however, even after joining the international G2 experiment, it is more preferable to provide the facility as a place for substantial research to advance their shared part of the collaborative experiment.

Committee requests the group to continue having dialogue within the community while addressing the aforementioned issues, and to finalize a plan which can lead to the G3 experiment in the future.

References

[1] Institute for Cosmic Ray Research, The University of Tokyo Future Plan Discussion Committee Report (September 26, 2013)
http://www.icrr.u-tokyo.ac.jp/report/futureplan/futureplan2013.pdf

[2] KEK Project Implementation Plan<s0/>(KEK-PIP) (June 30, 2016)
https://www.kek.jp/ja/About/OrganizationOverview/Assessment/Roadmap/KEK-PIP.pdf

[3]<s0/>High Energy Physics Future Plan Discussion Subcommittee <s1/>(February, 11, 2012)
http://www.jahep.org/office/doc/201202_hecsubc_toushin.pdf

[4] CRC Future Plan Discussion Subcommittee Annual Report 2013-2014
http://www.icrr.u-tokyo.ac.jp/CRC/townmeeting/doc/CRC_FPSC_report_2013-14-v3.pdf